Applicability of AREVA NP Containment Response Evaluation Methodology to the U.S. EPR™ for Large Break LOCA Analysis

Technical Report

December 2009

AREVA NP Inc.

Non-Proprietary

Nature of Changes

Rev# Item	Section(s) or Page(s)	Description and Justification
1-1.	3.4	Addition of a link to Appendix A referencing the qualifications of the PIRT Panel
1-2.	4.2	Addition of the results from the scaling analysis for the U.S. EPR during the blowdown phase.
1-3.	5.3	Updated to reflect the use of a Mult-node GOTHIC model
1-4.	6.1.5	Addition of the GOTHIC DLM models and justification for use of the models in a multi-node model.
1-5.	6.2.3	Addition of GOTHIC Benchmarks with Multi-Node and Subdivided nodalization.
1-6.	7.0	Updated uncertainty analysis
1-7.	8.1	Realize hot leg injection at 60 minutes
1-8.	8.3	Section updated to incorporate Multi-Node GOTHIC inputs
1-9.	8.3.2	Enhanced development of vessel mixing relationships
1-10.	9.0	Revised Sample Problem Calculation to include the multi-node GOTHIC model and hot leg injection at 60 minutes.
1-11.	Appendix A	Addition of PIRT panel member qualifications
2-1.	4.2	Removal of prior blowdown phase scaling analysis development
2-2.	4.4	Addition of distortion analysis summary between the U.S. EPR design and the Heissdampfreaktor test facility
2-3.	Appendix B	Addition of development of the scaling analysis governing equations, corresponding Pi groups and resulting distortion analysis
2-4.	Appendix C	Addition of development of the dynamic pressure equations utilized in Appendix B

AREVA NP Inc.

Applicability of AREVA NP Containment Response Evaluation Methodology to the
U.S. EPR™ for Large Break LOCA Analysis

Technical Report

ANP-10299NP

Revision 2

Page ii

Contents

AREVA NP Inc.

ANP-10299NP

Applicability of AREVA NP Containment Response Evaluation Methodology to the
U.S. EPR™ for Large Break LOCA Analysis

Revision 2

Technical Report

Page iv

AREVA NP Inc.

Applicability of AREVA NP Containment Response Evaluation Methodology to the
U.S. EPR™ for Large Break LOCA Analysis
Technical Report

ANP-10299NP
Revision 2

Page vii

List of Tables

AREVA NP Inc.

Applicability of AREVA NP Containment Response Evaluation Methodology to the
U.S. EPR™ for Large Break LOCA Analysis

Technical Report

ANP-10299NP
Revision 2

Page viii

AREVA NP Inc.

Applicability of AREVA NP Containment Response Evaluation Methodology to the
U.S. EPR™ for Large Break LOCA Analysis
Technical Report

ANP-10299NP
Revision 2

Page ix

AREVA NP Inc.   ANP-10299NP

Applicability of AREVA NP Containment Response Evaluation Methodology to the   Revision 2
U.S. EPR™ for Large Break LOCA Analysis

Technical Report   Page x

List of Figures

AREVA NP Inc.

Applicability of AREVA NP Containment Response Evaluation Methodology to the
U.S. EPR™ for Large Break LOCA Analysis

Technical Report

ANP-10299NP

Revision 2

Page xi

AREVA NP Inc.

ANP-10299NP

Applicability of AREVA NP Containment Response Evaluation Methodology to the

Revision 2

U.S. EPR™ for Large Break LOCA Analysis

Technical Report

Page xii

AREVA NP Inc.

ANP-10299NP

Applicability of AREVA NP Containment Response Evaluation Methodology to the

Revision 2

U.S. EPR™ for Large Break LOCA Analysis

Technical Report

Page xiii

AREVA NP Inc.

Applicability of AREVA NP Containment Response Evaluation Methodology to the
U.S. EPR™ for Large Break LOCA Analysis

Technical Report

ANP-10299NP
Revision 2

Page xiv

AREVA NP Inc.

Applicability of AREVA NP Containment Response Evaluation Methodology to the
U.S. EPR™ for Large Break LOCA Analysis

Technical Report

ANP-10299NP
Revision 2

Page xv

AREVA NP Inc.

Applicability of AREVA NP Containment Response Evaluation Methodology to the
U.S. EPR™ for Large Break LOCA Analysis

Technical Report

ANP-10299NP
Revision 2

Page xvii

Nomenclature

Acronym / Initialism	Definition
ACC	Accumulator
AS	Accessible Space
BFMC	Battelle-Frankfurt Model Containment
CHF	Critical Heat Flux
CLPD	Cold Leg Pump Discharge
CLPS	Cold Leg Pump Suction
CVTR	Carolina Virginia Tube Reactor
DBA	Design Basis Accident
DEG	Double Ended Guillotine
DNB	Departure from Nucleate Boiling
ECCS	Emergency Core Cooling System
EDG	Emergency Diesel Generator
EM	Evaluation Model
EMDAP	Evaluation Model Development and Assessment Process
EOB	End of Blowdown
EQ	Equipment Qualification
ER	Equipment Room
FW	Feedwater
GDC	General Design Criteria
GRS	Gesellschaft fur Anlagen- und Reaktorsicherheit
HDR	Heissdampfreaktor
HL	Hot Leg
HLB	Hot Leg Break
HTC	Heat Transfer Coefficient
LBLOCA	Large Break Loss-of-Coolant Accident
LOCA	Loss-of-Coolant Accident
LOOP	Loss Of Offsite Power
LP	Lower Plenum
M&E	Mass and Energy
MDLM	Mist Diffusion Layer Model
MFLB	Main Feedwater Line Break
MFW	Main Feedwater
MSIV	Main Steam Isolation Valve
MSLB	Main Steam Line Break
MSL	Main Steam Line
MSS	Main Steam System
NCG	Non-Condensable Gas
NPSH	Net Positive Suction Head
NRC	United States Nuclear Regulatory Commission
NRCV	Non-Return Check Valve(s)

Acronym / Initialism	Definition
NSSS	Nuclear Steam Supply System
OTSG	Once-Through Steam Generator
PIRT	Phenomena Identification and Ranking Table
PWR	Pressurized Water Reactor
RAS	Recirculation Actuation Signal
RC	Reactor Coolant
RCP	Reactor Coolant Pump
RCS	Reactor Coolant System
RSG	Recirculating Steam Generator
RV	Reactor Vessel
RVVV	Reactor Vessel Vent Valves
SAR	Safety Analysis Report
SBLOCA	Small Break Loss-of-Coolant Accident
SG	Steam Generator
SRP	Standard Review Plan
TSV	Turbine Stop Valve
UPTF	Upper Plenum Test Facility

ABSTRACT

This report to the U.S. NRC supports the U.S. EPR containment design and AREVA NP's deterministic evaluation methodology used to calculate containment pressure and temperature response to a large-break loss-of-coolant accident, per the regulatory requirements in NUREG-0800 and Regulatory Guide 1.203. The methodology described herein is used in the containment response analyses, including quantification of the performance ranges and limits of U.S. EPR containment response design basis events in the U.S. EPR Final Safety Analysis Report (FSAR).

This report addresses the U.S. EPR containment design philosophy, key processes and phenomena, the experimental bases for important containment thermal-hydraulic phenomena, a scaling analysis, the analytical techniques and tools used to assess hypothetical ruptures of high-energy pipes, the major computer code models, analytical verification and validation, an uncertainty analysis, and sample problem analyses. The report also demonstrates that the passive containment heat sinks are sufficient to limit the pressure response, while providing a well-mixed environment to allow containment pressure to decrease to less than one-half the peak pressure in less than 24 hours following a postulated accident.

SUMMARY AND CONCLUSIONS

The material presented in this report was developed to demonstrate the ability of AREVA NP containment analysis methods to analyze the U.S. EPR design for containment cooling following a large break loss of coolant accident (LBLOCA). The following section-by-section summary draws key material from the full report.

Section 1 describes the regulatory framework for the demonstration of methodology applicability and Section 2 reviews the relevant design features of the U.S. EPR. Sections 3 through 9 provide the description of AREVA NP's containment response methodology within the framework of the structured evaluation model development and assessment process (EMDAP) called for in NRC guidance. The conclusions of this work are found at the end of this Summary and Conclusions.

Section 1

Section 1 discusses specific NRC guidance, including the GDCs that form the firm regulatory requirements for containment design. The key regulatory requirements for containment design are General Design Criteria (GDC) 16, 38 and 50. GDC 16 requires that the containment provide an essentially leak-tight barrier against uncontrolled release of radioactivity for as long as postulated accident conditions require. GDC 38 requires that containment pressure be rapidly reduced after a loss of coolant accident (LOCA) and maintained acceptably low. Finally, GDC 50 prescribes that containment design must withstand the calculated LOCA pressure and temperature, with margin:

> *This margin shall reflect consideration of (1) the effects of potential energy sources which have not been included in the determination of the peak conditions, such as energy in steam generators and as required by 50.44 energy from metal-water and other chemical reactions that may result from degradation but not total failure of emergency core cooling functioning, (2) the limited experience and experimental data available for defining accident phenomena*

and containment responses, and (3) the conservatism of the calculational model and input
parameters.

The GDC 50 requirement for margin determination is key to demonstrating the adequacy of containment analysis.

Section 2

Section 2, using material largely drawn from the U.S. EPR FSAR, describes design features important for containment function. For the instantaneous containment response to a high energy line break, the most important features are the massive concrete and steel structures inside the containment and the containment walls. ECCS, consisting of four accumulators, and four sets of medium-head (MHSI) and low-head (LHSI) injection pumps, then replace the reactor coolant system (RCS) water inventory, cooling the core and removing the latent heat of the RCS equipment. The safety injection pumps draw water from the in-containment refueling water storage tank (IRWST), which also collects water spilling from any RCS break as well as the water condensing on the containment structures and walls. Section 2 also describes the system of dampers and foils which open to allow use of the containment structures and walls to absorb energy in the short term and, in the long term, be cooled by air circulation within the 2.8 million cubic foot containment.

Section 3

Section 3 describes the establishment of requirements for the evaluation model capability, the first four steps of the EMDAP. When used with already-developed analysis methodologies, the EMDAP serves both to collect and organize existing material and to identify places where that material needs to be expanded for a specific application. That is the case with AREVA NP's existing containment response methodology and the specific application to the U.S. EPR.

This section notes that the first EMDAP steps, including analysis purpose and figures of merit, have already been presented in the AREVA NP evaluation methodology

AREVA NP Inc.
ANP-10299NP
Applicability of AREVA NP Containment Response Evaluation Methodology to the
Revision 2
U.S. EPR™ for Large Break LOCA Analysis
Technical Report
Page xxiv

description. The section continues with a description of principle phenomena of the five phases of a PWR LBLOCA. The phenomena for blowdown, refill, reflood, and post-reflood phases for the U.S. EPR are essentially the same as those for existing U.S. PWRs. However, for the U.S. EPR, a manual realignment of a significant portion of the safety injection from cold-legs to hot-legs occurs about 60 minutes after the initiating event. This realignment serves as a mechanism for removing core decay heat, leading to complete steam quenching. The phenomena associated with coolant mixing in the upper plenum and in the core region, and condensation from safety injection in the hot legs and upper plenum, are identified as important for the U.S. EPR.

Section 3 continues with a description of containment response phenomena. Phenomena important for the U.S. EPR in the short term are the same as those for existing U.S. PWRs: forced convection and condensation on walls and structures. In the long-term, following complete steam quenching after realignment of ECCS, principle phenomena become those associated with liquid flow into the IRWST. Energy is ultimately removed from the U.S. EPR containment via liquid flow through the core and from condensation on walls and structures, all of which collect in the IRWST and are cooled by the LHSI heat exchanger.

Sub-section 3.4 summarizes the Phenomena Identification and Ranking Table (PIRT) developed for the U.S. EPR. The PIRT process identified the important phenomena impacting both mass and energy release into the containment and containment pressure itself. The process also evaluated the state of knowledge for each important phenomenon. Section 6 reports on additional work done to successfully address the phenomena for which the state of knowledge was originally identified as deficient and by providing the required knowledge.

Sub-section 3.4 also describes the PIRT used for assessment of containment pressure analysis. Because it is largely applicable to the U.S. EPR, AREVA NP started with a PIRT developed by experts from the Organization for Economic Cooperation and Development / Nuclear Energy Agency (OECD/NEA). Two U.S. EPR-specific changes

to the OECD/NEA PIRT were identified. Without containment sprays, structure conduction becomes the principle heat removal mechanism; thus, the ranking was moved from medium-high to high. Also, the ranking of pool free convection was changed to high to reflect the importance of heat removal via the IRWST—not so much by free convection, but by the active cooling systems attached to the IRWST—and to acknowledge the state-of-knowledge of the pool conditions that govern the overall effectiveness of these phenomena and processes.

Section 4

Section 4 describes the validation assessment base and presents the approach to scaling and similarity analysis. It also summarizes the review of previous code assessments and test programs.

AREVA NP's containment analysis evaluation methodology relies upon the RELAP5-BW and GOTHIC codes to predict the physical behavior anticipated during a LOCA. These tools are validated using an appropriate assessment base consisting of both separate and integral effects test program results, standard problems, benchmarks with other codes, and analytical exercises with known solutions.

Section 4 presents the objectives of the assessment base. These include preserving the dominant phenomena, providing a sufficient degree of model resolution that conforms to important design characteristics, and demonstrating that results are insensitive to scale distortion and possible compensating errors. In addition, AREVA NP's containment response evaluation methodology incorporates conservatisms, based on the NRC's guidance described in Section 8, to satisfy the objective of assessing the safety margins for the figures-of-merit

Subsection 4.3 provides a review of test data and previous code assessments. The majority of the code validation performed for RELAP5-BW and GOTHIC is applicable to the thermal-hydraulic phenomena following an LBLOCA in a U.S. EPR. The principle difference between the U.S. EPR and other U.S. PWR containment designs is that

neither containment sprays nor fan-coolers are necessary for the mitigation of containment pressure loads following an LBLOCA. Consequently, the emphasis is on the termination of core steaming through a safety injection switchover from injection in each cold leg to injection in all cold and hot legs. From this point, all the core heat is rejected through the IRWST, which receives the RCS liquid spillage and actively cools it through the LHSI heat exchanger. It is this difference in the long-term mitigation strategy that necessitates additional code assessments reported on in Section 6.

A process for scaling analysis is developed in Subsection 4.2. A cold-leg break scenario is described and "discretized", that is, broken into specific components or elements. Following this, a closed set of equations to conduct scaling analysis is developed. For AREVA NP's containment response evaluation methodology, the scaling analysis methodology described in this subsection and the scalability evaluation (including scale distortion) discussed in Sections 4.4 and 6.4. A confirmatory scaling analysis comparison of the figure-of-merit results between the HDR and the U.S. EPR GOTHIC calculations show that the IET results can scale the behaviors of the U.S. EPR design in non-dimensional space and time. The containment pressure figure-of-merit results show that the HDR test scales well in the Blowdown and Post-HL-Injection phases. For the pre-HL-Injection phase, the HDR dome pressure response was about 25 percent less than that of U.S. EPR design due to lack of decay-heat simulation during this phase.

Section 5

In accordance with the EMDAP, Section 5 presents the structure within which the AREVA NP containment assessment model was developed. This evaluation model is applicable to any pressurized water reactor (PWR) with a large dry containment, including the U.S. EPR.

The adequacy of the RELAP5-BW code has been validated for performing deterministic mass and energy LBLOCA analysis for the U.S. EPR. This effort included a review of code-governing equations and numerics, evaluation of the applicability of code models

and correlations (with an emphasis on code resolution of high rank phenomena), and assessment of code performance for simulating integral effects and separate effects experiments. The existing assessments indicated that the code is capable of adequately predicting all but one medium-rank and one high-rank mass and energy phenomena, as identified by the U.S. EPR PIRT presented in Section 3. Hot leg nozzle bypass, one of the phenomena ranked medium in the PIRT, can be conservatively defined through input. The lack of a multi-dimensional fluid flow model in RELAP5-BW limits its application to only the early LBLOCA phases. To address the multi-dimensional fluid mixing in the upper plenum and core regions, a phenomenon ranked high in the PIRT, an appropriate modeling treatment for the decay heat phase has been developed and is presented in Subsection 6.1.4.

The GOTHIC code has been evaluated to determine its adequacy for performing global pressure and temperature containment response analysis of an LBLOCA in the U.S. EPR. This effort included a review of the code-governing equations and numerics, evaluation of the applicability of code models and correlations with an emphasis on code resolution of high rank phenomena, and assessment of integrated code performance for simulating integral effects and separate effects experiments. The assessments indicated that the code is capable of adequately predicting all medium- and high-rank mass and energy phenomena, except for interfacial heat transfer from the IRWST, which is addressed by assuming no heat transfer, a conservative modeling treatment.

Section 6

Section 6 provides validation and sensitivity analyses of specific interest to the analysis of the U.S. EPR. The process for producing an acceptable analysis code consists of three phases: development, developmental assessment, and independent assessment. Several studies are provided in this section to demonstrate the applicability of both RELAP5-BW and GOTHIC for assessing containment behavior of the U.S. EPR following an LBLOCA.

AREVA NP Inc.

Applicability of AREVA NP Containment Response Evaluation Methodology to the
U.S. EPR™ for Large Break LOCA Analysis

Technical Report

ANP-10299NP
Revision 2

Page xxviii

Subsection 6.1 highlights a suite of separate effects test benchmarks. Three RELAP5-BW studies using FLECHT-SEASET data are reported. Two previously-reported studies highlight core heat transfer and liquid carryout. The results show that core cooling and quench front progression as well as integrated carryout rate fraction (CRF) are well-predicted by RELAP5-BW.

A new study benchmarked the RELAP5-BW computer code against the FLECHT-SEASET steam generator heat transfer tests to predict the heat transfer from the secondary side of the steam generator to the primary side during the reflood and post-reflood phases. The results demonstrate that replacing the Biasi-Zuber CHF model with the Becker CHF model in the tube side of the steam generators improves the prediction of energy transfer to the primary side, yielding results that compare well to the test data. Moreover, using the Becker CHF model also improves the prediction of the quench fronts in the tubes.

Subsection 6.1.4 describes the AREVA NP analytical treatment to predict the efficiency of mixing in the upper plenum between cold ECC water from hot leg injection with rising hot water from the core. This mixing is key to termination of core steaming. The mixing efficiency analysis is based on a plume dynamics model and correlated data from the UPTF, CCTF, and SCTF test facilities. Analyses performed using the STAR-CD computational fluid dynamics (CFD) code provide additional confirmation of effective mixing in the upper plenum. The derived results show that the effective mixing efficiency of the water falling into the core region is at least 50%, even neglecting the additional mixing that occurs in the core region due to vigorous natural circulation driven by core heat and the down-flow of relatively cool ECC water from the upper plenum.

Wall condensation is the principal containment atmosphere heat transfer mechanism for the U.S. EPR following an LBLOCA. As reported in subsection 6.1.5, AREVA NP uses the tandem Tagami-Uchida heat transfer correlation for wall condensation for single node models. This is not appropriate for a multi-node GOTHIC model because of the

formulation of theTagami correlation. The mechanistic Diffusion Layer Model (DLM or DLM-FM) is used instead.

The Diffusion Layer Model calculates the convective heat transfer and the condensation rate at a cold wall surface. The model accounts for the presence of noncondensing gases, the water film resistance, possible mist generation near the wall, and enhancement effects due to film roughening.

Subsection 6.2 presents the results of several GOTHIC assessments for integral-effects tests, which include containment phenomena expected in the U.S. EPR during an LBLOCA. Most of these studies examine the effect of nodalization by comparing both a multi-control-volume model and a single-control-volume model. Assessments were performed with data from the Heissdampfreaktor (HDR) and the Battelle-Frankfurt Model Containment (BFMC). Six HDR and seven BFMC integral tests were examined, covering a wide range of conditions including large and small break LOCAs. Additional studies examine the impact of subdivided nodalization. The subdivided nodalization assessments were performed with data from the Battelle-Frankfurt Model Containment (BFMC), NUPEC, CVTR, TOSQAN, and MISTRA test facilities.

In all LBLOCA assessment tests, both the multi-volume model and the single-volume model show good agreement with test data. While the assessment with the longest duration is only about 2 hours, the phenomenological progression is simple and does not exhibit significant change. Extension of the conclusion that the single-volume model is sufficient to simulate beyond the period considered in the assessed events is appropriate.

The SBLOCA tests illustrate GOTHIC's performance in the long-term with similar phenomena. The slower event progression of the SBLOCA tests in the HDR facility leads to less fully-developed conditions for heat transfer. The assessments performed with the BFMC Biblis atmospheric mixing tests illustrate the benefit of the U.S. EPR CONVECT system of rupture foils and opening dampers to promote atmospheric mixing. The improved mixing improves the ability of GOTHIC to simulate the event.

A few general conclusions are presented from these integral test assessments. When used with a multi-volume model, GOTHIC provides a reliable simulation of both global and local containment thermal-hydraulic phenomena. The single-volume model provides a reliable simulation of global phenomena, particularly when the containment atmosphere is well-mixed, such as during an LBLOCA with the containment design featuring the CONVECT system. The best agreement with test data was generally achieved by models employing a combination of multi-volume and subdivided modeling or only subdivided modeling.

A GASFLOW analysis was performed to assess the atmospheric mixing phenomena. Section 6.3 describes the realistic, three-dimensional, analysis that covered the first hour following LBLOCA initiation. Several observations are made, including that convective flows establish through all steam generator towers, that the highest gas temperature occurs in the central, "non-accessible", area of the containment and that, globally, the released steam is distributed well in the entire containment. The GASFLOW analysis demonstrates the convective flows produce an adequately mixed containment atmosphere, an implicit assumption for the analysis done by the single-volume GOTHIC model.

In accordance with EMDAP Step 19, subsection 6.4 summarizes the scalability of the integral and separate effects test data presented in Section 6. The test facilities supporting the PIRT span a scaling range from full-scale to 1:1500. Collectively, the common trend of good or conservative agreement over this large assessment knowledge base addresses the closure and scalability of models, and thus covers the domain of nuclear power plant operational and accident conditions.

Section 7

Section 7 describes the analytical methodology for preparing the U.S. EPR containment response uncertainty analysis, which is based on Code Scaling, Applicability and Uncertainty (CSAU) methodology. Parameters considered in an uncertainty analysis are defined by a range of values that bound the expected value of the parameter.

The quantification of phenomenological uncertainties began with identifying the important containment phenomena through the PIRT presented in Section 3. For the U.S. EPR containment response uncertainty analysis, the quantification of phenomenological uncertainty also considered the GOTHIC user-specified modeling options and a complete containment response uncertainty analysis and importance study presented by the Gesellschaft fur Anlagen und Reaktorsicherheit (GRS).

The uncertainty analysis confirmed the expert assessment given in Section 3 for the containment PIRT. Specifically, structure conduction and condensation were shown to be the dominant phenomena influencing the containment pressure response. The impact of containment mass and energy uncertainties are addressed in AREVA NP's containment response evaluation methodology by implementing the conservatisms required by the SRP. Section 9 provides an assessment of the impact of containment mass and energy on the containment pressure and on the overall retained margin of AREVA NP's containment response evaluation methodology.

Section 8

Section 8 summarizes the containment response evaluation methodology applied for the U.S. EPR, which is an adaptation of the methodology AREVA NP developed for conventional Westinghouse, Combustion Engineering, and B&W PWRs. This methodology incorporates the guidelines presented in the NRC's Standard Review Plan and ANSI/ANS-56.4 for maximizing coolant mass and energy releases. The technical basis for this methodology is built upon a broad foundation of thermal-hydraulic research and development programs and associated code development activities for RELAP5-BW and GOTHIC and their predecessor code versions.

Subsections 8.1 - 8.3 describe AREVA NP's general approach to performing containment analysis. This general discussion acknowledges that several parametric studies are performed to identify the appropriate modeling prior to finalizing the models and event scenarios. These sections address short-term containment mass and energy release rates using RELAP5-BW, the long-term containment mass and energy release

AREVA NP Inc.

Applicability of AREVA NP Containment Response Evaluation Methodology to the
U.S. EPR™ for Large Break LOCA Analysis
Technical Report

ANP-10299NP
Revision 2

Page xxxii

rates using GOTHIC, and the prediction of containment pressure and temperature using GOTHIC. Section 8.4 summarizes SRP compliance for the U.S. EPR-specific calculations.

Section 9

Section 9 describes the application of the LOCA containment pressure response methodology described in Section 8 to the analysis of a sample problem for the U.S. EPR, a double-ended guillotine break in the cold leg pump suction (CLPS) piping. As conservatively analyzed, it is the limiting containment pressure response scenario for the U.S. EPR.

Figure 9-14, reproduced below, presents the containment pressure result from AREVA NP's containment response evaluation methodology (Figure 9-8 together with the best-estimate plus uncertainty result shown in Figure 7-4).

The second containment pressure peak in the conservative EM analysis is mitigated by the switchover of LHSI safety injection to the hot leg at 60 minutes. The best estimate plus uncertainty response assumes best estimate M&E and a later switchover of LHSI to hot leg injection at 90 minutes.

Given that the uncertainty analysis explicitly addressed containment phenomena uncertainty, the large margin observed in Figure 9-14 is the result of AREVA NP's implementation of the containment mass and energy release conservatism specified in the SRP.

Design Basis Envelope to the Coverage Bands for the US EPR CLPS LOCA Containment Pressure Response
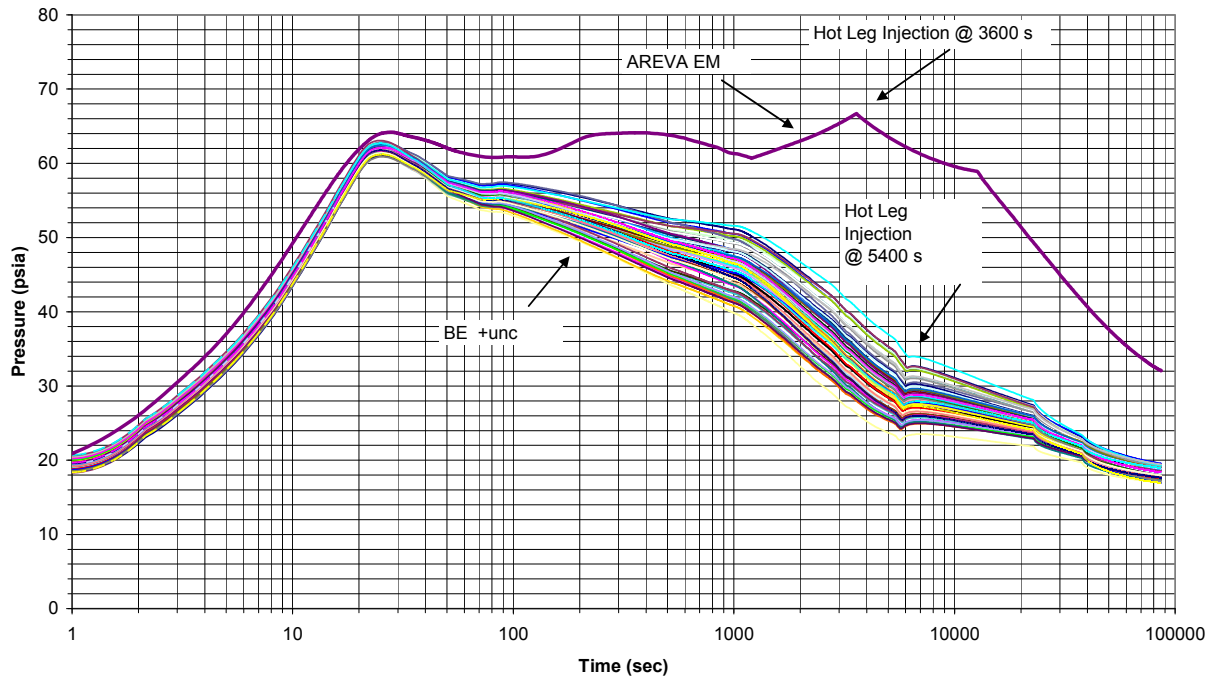
Assessment of Retained Margin in Containment Pressure Calculation

The effects of these conservatisms appear at different periods in the simulation and hence can be distinguished in Figure 9-13. During the blowdown phase (~30 s), the faster rise in containment pressure is evidence of the critical flow model assumption. The decay heat model and the additional lost ECCS train act to slow the cooling process and are reflected in the elevated pressure following the peak. After the transition from RELAP5-BW to GOTHIC, the abrupt increase in containment pressure reflects the accelerated removal of sensible energy from the RCS and steam generators.

CONCLUSIONS

The AREVA NP containment response evaluation methodology, as applied to the U.S. EPR, for LBLOCA analysis has been evaluated in accordance with the structured

evaluation model development and assessment process (EDMAP) called for in NRC guidance.

It has been demonstrated that the AREVA NP methodology is able to reliably analyze the containment response and, when combined with analyses reported on in the U.S. EPR FSAR, confirm that the U.S. EPR containment design will reduce post-LOCA pressure rapidly and maintain it acceptably low for as long as postulated accident conditions require.

1.0   INTRODUCTION

The U.S. EPR is a 4590 MW$_{th}$ evolutionary pressurized water reactor (PWR) that incorporates proven technology with innovative system configurations to enhance safety. The U.S. EPR was developed by AREVA NP and Siemens in the 1990s by incorporating key technological and safety features from the French and German reactor fleets.   Consistent with the 1986 NRC Policy Statement on Advanced Nuclear Power Plants (Reference 1), the U.S. EPR provides enhanced safety margins by utilizing simple and innovative methods to achieve safety and security.

In a nuclear power plant the containment building is part of the defense-in-depth design strategy and serves as the final barrier against the release of radioactive fission products in the event of an accident. The containment structure must be capable of withstanding, without loss of function, the pressure and temperature excursion resulting from loss-of-coolant accidents and steam line, or feedwater line break accidents. The containment structure must also maintain functional integrity in the long term following a postulated accident; i.e., it must remain a leak tight barrier against the release of fission products for as long as postulated accident conditions require.

The objective of this report is to provide technical support for the analysis methods used to evaluate containment response to loss-of-coolant accidents (LOCA) that appear in the U.S. EPR Final Safety Analysis Report (FSAR) (Reference 2). This technical report includes the U.S. EPR containment design philosophy, phenomenological assessment, the experimental bases for design features, analytical techniques, major computer codes and models, and analyses supporting the applicability of the methodology and the validity of the containment design.

1.1   *U.S. EPR Design and Analysis Background*

The U.S. EPR containment and its associated systems are designed to be a leak tight barrier against the release of radioactivity to the environment and to remain functional during a design basis accident (DBA). The containment's structures, systems, and

components (SSC) that are important to safety have been engineered to withstand the anticipated loads from environmental and dynamic effects associated with both normal plant operation, including maintenance and testing, and postulated accidents. The environmental effects include the temperatures, pressures, and fluids encountered during normal and accident conditions.

AREVA NP's containment evaluation methodology described herein has been applied as part of the U.S. EPR design certification effort and complies with the NRC's Standard Review Plan (Reference 3) and Regulatory Guide 1.206 (Reference 4). This generic AREVA NP methodology for large, dry PWR containments was originally submitted and reviewed by the NRC in 2005 (Reference 14). It employs the GOTHIC computer code (Reference 20) to predict the maximum containment pressure and temperature following a high-energy line break. The RELAP5/MOD2-B&W (RELAP5-BW) (Reference 19) code supplies reactor coolant system (RCS) mass and energy releases up to and through the post-reflood phase, which serves as a boundary condition to the GOTHIC calculation. An analytical approximation for mass and energy releases is applied for the period beyond the post-reflood phase.

The containment pressure response to a LOCA in a U.S. EPR is similar to that of a conventional PWR with a large dry containment. The U.S. EPR does not rely on new or unique phenomena to meet established containment integrity acceptance criteria; furthermore, containment sprays are not an engineered safety feature used to mitigate the containment pressure response. Termination of a LOCA event is achieved by quenching core region steaming through pumped safety injection. Following steam quench, hot liquid leaving the reactor coolant system drains to the in-containment refueling water storage tank (IRWST), which is attached to a cooling chain providing the ultimate heat sink.

This report has been prepared adhering to the Evaluation Methodology Development and Assessment Process (EMDAP) of Regulatory Guide 1.203. Detail is provided on containment design features; containment response phenomenology and a complete

phenomenological identification and ranking table (PIRT); relevant test programs and a review of the assessment database; a compilation of new developmental assessment studies; an assessment of analysis uncertainties; a complete description of the analytical methods; and a sample analysis demonstrating the application of this containment evaluation methodology to the U.S. EPR.

1.2   Governing Documents

Regulatory rules regarding the general safety of nuclear power plants and the specific containment design draw on several NRC policy statements, including:

- NRC Policy Statement, "Regulation of Advanced Nuclear Power Plants" (Reference 1)

- NRC Policy Statement, "Nuclear Power Plant Standardization" (Reference 5)

- NRC Policy Statement, "Safety Goals for the Operations of Nuclear Power Plants" (Reference 6).

These NRC Policy Statements set the regulatory expectation for new reactor designs. They build upon the principle that new U.S. nuclear power plant designs will provide enhanced safety margins and utilize simplified, inherent, passive, or other innovative means to accomplish their safety and security functions. Specifically, designs will employ features to prevent loss of containment integrity and to maintain core cooling through reliable, long-term decay heat removal systems.

The principal regulatory document implementing the NRC Policy Statement objectives is the U.S. Code of Federal Regulations (CFR) (Reference 7). The specific parts related to the containment design and the preparation and reporting of design-basis analyses are:

- 10 CFR 50.34(b), Content of Application, technical information, final safety analysis report (see also 10 CFR 52.47)

- 10 CFR 50.44, Combustible Gas Control

- 10 CFR 50 Appendix A General Design Criteria.

The above CFR sections define the analytical evaluation methodologies and the scope of the analysis, in terms of the documents to be presented to the NRC. This includes the following requirements regarding applications for construction permits and licenses to operate a facility:

- Safety analysis reports must analyze the design and performance of structures, systems, and components, and their adequacy to prevent accidents and mitigate the consequences of accidents.

- Analysis and evaluation of emergency core cooling system (ECCS) cooling performance following postulated LOCAs must be performed in accordance with the requirements of 10 CFR 50.46.

- The technical specifications for the facility must be based on the safety analysis and prepared in accordance with the requirements of 10 CFR 50.36.

The General Design Criteria (GDC) refer to specific nuclear power plant design requirements. For containment integrity analysis, the relevant design criteria are described in the following 10 CFR 50 Appendix A sections:

GDC 4, Environmental and dynamic effects of design bases

GDC 13, Instrumentation and control

GDC 16, Containment design

GDC 38, Containment heat removal

GDC 50, Containment design basis

GDC 64, Monitoring radioactivity releases

The regulatory position on the analytical interpretation of the CFR requirements has evolved through revisions of the NRC's Standard Review Plan, beginning with the publication of NUREG-75/087 (Reference 8) in 1975. Before that, individual review plans existed but they were not published in a single authoritative document.   NUREG-75/087 was revised and reissued as NUREG-0800 in 1981. During this period, NUREG 0588 was prepared to address containment analysis questions regarding qualification of safety-related equipment. After public comment and Three Mile Island (TMI) lessons-learned considerations, NUREG-0588 was revised and released coincident with NUREG-0800 in 1981. During the late 1980s and early 1990s, the Electric Power Research Institute (EPRI) and the NRC pursued separate evaluations of plant requirements for advanced light water reactors. EPRI released its Utility Requirements Document in 1992 (Reference 10) and the NRC updated the Standard Review Plan in 1996. In June of 2007, the NRC issued Regulatory Guide 1.206, following a revision to the SRP in March 2007, to specifically address the issuance of combined construction and operation licenses for nuclear power plants.

As a complement to the NRC's Standard Review Plan, industry representatives participated in an ANSI standards development activity endorsed by the American Nuclear Society. That effort produced ANS/ANSI 56.4, released in 1983 and revised in 1988 (Reference 11). The standard was withdrawn in 1998.

The current status of open and resolved generic safety issues are regularly published in NUREG-0933, "A Prioritization of Generic Safety Issues" (Reference 12). According to the September 2007 edition, there are no outstanding safety issues specifically regarding design-basis containment analysis of large, dry PWR containments.

1.3   Applicable Requirements and Acceptance Criteria

The pressure from an LBLOCA is the most significant load for evaluating the integrity of the containment wall and dome to over-pressurization. Procedures for treating the design and analysis input for performing containment analyses within the NRC regulatory framework are generally outlined in the governing documents identified in

Section 1.2. The specific restrictions and requirements are extensive and are presented in Section 8.0, along with an assessment of compliance with each of these requirements.

The analytical restrictions and requirements address the principal uncertainties associated with containment response analysis. The analytical treatment of these phenomenological and process uncertainties is conservative; that is, the modeling characteristics and assumptions, the design input values, and the initial conditions are biased to maximize containment pressure and temperature.

The basic functional design requirements for containment are given in GDC 16 and 50 in Appendix A to 10 CFR Part 50. GDC 50 requires that the potential consequences of degraded engineered safety features—such as the containment heat removal system and the emergency core cooling system, the limitations in defining accident phenomena, and the conservatism of calculational models and input parameters— be considered in assessing containment design margins.

Chapter 6.2.1, "Containment Functional Design," of the SRP delineates the current guidance for demonstrating that a containment design complies with the requirements of GDC 16, 38, and 50. The SRP addresses the acceptance criteria and some specific model assumptions for design-basis LBLOCA and main steam line break (MSLB) analyses for all existing containment types. AREVA NP's evaluation methodology is consistent with these guidelines and with Regulatory Guide 1.203, "Transient and Accident Analysis Methods."

1.3.1 Peak Pressure Criteria (GDC 16 and 50)

The peak pressure requirement is addressed in both GDC 16 and 50; however, GDC 50 is more explicit. It reads as follows:

> *The reactor containment structure, including access openings, penetrations, and the containment heat removal system shall be designed so that the containment structure and its internal compartments can accommodate, without exceeding the design leakage rate and with sufficient margin, the calculated pressure and*

temperature conditions resulting from any loss-of-coolant accident. This margin shall reflect consideration of (1) the effects of potential energy sources which have not been included in the determination of the peak conditions, such as energy in steam generators and as required by § 50.44 energy from metal-water and other chemical reactions that may result from degradation but not total failure of emergency core cooling functioning, (2) the limited experience and experimental data available for defining accident phenomena and containment responses, and (3) the conservatism of the calculational model and input parameters.

AREVA NP's LOCA containment analysis evaluation methodology demonstrates that the calculated peak pressure does not exceed the design pressure using a conservative approach that is consistent with the defined regulatory restrictions and requirements, addresses the principal design and analysis uncertainties, and assures containment integrity with a high degree of confidence. Applying these methods demonstrates that the U.S. EPR meets the following acceptance criteria:

- Peak pressure ≤ maximum allowable pressure

- Peak temperature ≤ maximum allowable temperature.

1.3.2   Long-Term Pressure Criteria (GDC 38)

The objective of GDC 38 is to demonstrate that the containment design provides for the long-term reduction of containment pressure and temperature while accounting for a worst single failure and with the worst electrical power availability situation. Further, it requires establishing a containment heat removal system that will rapidly reduce containment pressure and temperature following any loss-of-coolant accident. The U.S. EPR principally relies on passive heat removal by convection and condensation to the containment steel and concrete structures. The containment design enables condensate coalescing on structural surfaces to drain to the IRWST. Low head safety injection pumps draw liquid from the IRWST, sending it through the LHSI heat exchanger. From there the flow is split to provide for both safety injection to the RCS and direct cooling of the IRWST. Other non-safety systems are also available to keep the containment cool. These containment heat removal systems support the

containment function by minimizing the duration and intensity of the pressure and temperature increase following an LBLOCA, thus lessening the challenge to containment integrity. For the U.S. EPR, these systems demonstrate adherence to the SRP acceptance criteria in the Section 6.2.1.1.A that containment pressure be ≤ 50% of the peak pressure within 24 hours after accident.

1.3.3   10 CFR 50.43 Criteria

Demonstrating the effectiveness and performance of the U.S. EPR's passive containment heat removal strategy requires scaled testing data and mathematical modeling. The unique characteristics of plants using simplified, inherent, passive, or other innovative means to accomplish their safety functions are explicitly recognized in the regulations governing the evaluation of standard plant designs. To successfully demonstrate U.S. EPR containment performance, the testing and modeling data must satisfy the regulations in 10 CFR 50.43(e)(1) that:

- The performance of each safety feature of the design has been demonstrated through analysis, test programs, experience, or a combination thereof.

- Interdependent effects among the safety features of the design have been found acceptable by analysis, appropriate test programs, experience, or a combination thereof.

- Sufficient data exist on the safety features of the design to assess the analytical tools used for safety analysis over a range of normal operating conditions, transient conditions, and specified accident sequences, including equilibrium core conditions.

To satisfy these requirements, relevant test data and analyses must be cited to verify and validate the computer codes used to evaluate the U.S. EPR containment response following a large-break LOCA.

1.4 Definitions

Several technical terms appear throughout this report. Those that frequently occur have been compiled in this section along with appropriate definitions and explanations.

Active Component: A component that has moving parts or that is designed to perform its functions by a change of configuration or properties.

Active System: A system that depends on major active components for operation. For example, active systems depend on pumps, motors, and ac power generators.

Beyond Design Basis Accidents: Hypothesized accidents that bound the consequences of any design-basis events and that are used to test mitigating design features and safety margins.

CFR (Code of Federal Regulations): Written regulations of federal agencies. For example, Chapter 1 of Title 10 of the CFR (10 CFR) contains the regulations of the NRC.

Containment: The structure or vessel that encloses, as a minimum, the components of the reactor coolant pressure boundary and serves as an essentially leak-tight barrier against the uncontrolled release of radioactivity to the environment.

Containment Isolation Valve: Any valve which is relied upon to perform a containment isolation function.

Coolant: The fluid circulated through the reactor core, the primary system pipes and components, which transfers the heat of the fission process to a secondary heat-transfer system.

Core: The central portion of the nuclear reactor containing the fuel elements. Nuclear fission takes place there and neutron flux and heat are generated within the core.

Core Uncovery: A condition in which coolant mixture level in the reactor vessel falls below the top of the active fuel.

Criteria: Safety and licensing specifications defined by licensing and regulatory bodies as acceptable, and augmented by ANS-specific licensing and safety specifications; a measure by which one can determine if a goal is achieved.

Decay Heat: Residual heat generation in nuclear fuel resulting from the decay of fission products.

Defense-in-Depth: The concept of designing nuclear power plants to avoid equipment failure, human error, and severe natural events, and to provide redundant and backup systems so that safety functions can be accomplished even in the event of the most unlikely malfunctions.

Design Basis Accidents (or Design Basis Events): Postulated scenarios used in the design of a facility to establish the performance requirements of the structures, systems, and components. Design basis events that the plant design must accommodate include normal operation, anticipated operational occurrences, postulated accidents, external events, and natural phenomena.

Design Bases: Information that identifies the specific functions to be performed by a structure, system, or component of a facility, and the specific values or ranges of values chosen for controlling parameters as reference bounds for design. These values may be restraints derived from generally accepted ''state of the art'' practices for achieving functional goals, or requirements derived from analysis (based on calculation or experiments) of the effects of a postulated accident for which a structure, system, or component must meet its functional goals.

Design Limit: The boundary value of a parameter for which a design analysis has been performed (e.g., pressure, temperature, flow).

Engineered Safety System: A hardware system designed for preventing or mitigating the consequences of an accident. In contrast to a passive safety feature, active engineered safety systems often require external power and have moving parts.

Limiting Conditions for Operation: The limiting condition for operation refers to the lowest functional capability or performance levels of equipment required for safe operation of the facility (see 10 CFR 50.36).

Loss of Coolant Accidents: Those postulated accidents that result in reactor coolant leaks due to breaks in the reactor coolant pressure boundary up to and including a break equivalent in size to an instantaneous, non-communicative, double-ended rupture of the largest pipe in the reactor coolant system (i.e., 200% of the pipe area).

Reactor Coolant Pressure Boundary: All those pressure-containing components of water-cooled nuclear power reactors, such as pressure vessels, piping, pumps, and valves, which are part of or connected to the reactor coolant system, up to and including any and all of the following:

- The outermost containment isolation valve in system piping that penetrates primary reactor containment

- The second of two valves normally closed during normal reactor operation in system piping that does not penetrate primary reactor containment

- The reactor coolant system safety and relief valves.

Safety Analysis Report (SAR): The part of an application for a construction permit (preliminary safety analysis report) or an operating license (final safety analysis report) that provides technical information concerning the proposed facility, including sitting, design, engineered safety features, construction, quality assurance, operation, control, accident analysis, and technical specifications (see 10 CFR 50.34).

Safety Evaluation Report (SER): A summation of the reviewing body's conclusions concerning action proposed by an applicant. The proposed action is often in the form of a safety analysis report (SAR).

Safety Limits: Bounding values for important process parameters necessary to reasonably protect the integrity of specific physical barriers.

Safety-Related Structures, Systems, and Components: Those structures, systems, and components that are relied upon to remain functional during design basis events to assure:

- The integrity of the reactor coolant pressure boundary

- The capability to shut down the reactor and maintain it in a safe shutdown condition

- The capability to prevent or mitigate the consequences of accidents which could result in potential offsite radiological exposures.

Severe Accident: A severe accident is a category of beyond design basis accidents that result in catastrophic fuel rod failure, degradation of the structural integrity of the reactor core, and release of radioactive fission products into the reactor coolant system (RCS). Such an event can only occur as a result of a sustained loss of adequate core cooling, which leads to a build up of fission product decay heat and elevated core temperatures. The resulting consequence of melting the reactor core (and internals) may lead to the breaching of the reactor pressure vessel and, through the relocation of molten core material into the containment, may potentially compromise the ability of the containment to perform its radionuclide retention function.

Single Failure: A single failure means an occurrence resulting in the loss of capability of a component to perform its intended safety functions. Multiple failures resulting from a single occurrence are considered to be a single failure. Fluid and electric systems are considered to be designed against an assumed single failure if neither a single failure of any active component (assuming passive components function properly) nor a single failure of a passive component (assuming active components function properly), results in a loss of the capability of the system to perform its intended safety function(s).

Technical Specifications: Limits, controls, and surveillance requirements on process variables and equipment in an operating nuclear plant that cannot be changed without prior approval from the regulatory body.

AREVA NP Inc.   ANP-10299NP

Applicability of AREVA NP Containment Response Evaluation Methodology to the   Revision 2
U.S. EPR™ for Large Break LOCA Analysis
Technical Report   Page 2-1

2.0 DESIGN DESCRIPTION OF U.S. EPR CONTAINMENT AND PERIPHERAL SYSTEMS

The containment and its associated systems are part of the defense-in-depth design strategy. They must remain a leak tight barrier against the release of fission products for as long as postulated accident conditions require. The containment structure is designed to withstand, without loss of function, the pressure and temperature conditions resulting from postulated design basis accidents (DBA). The principal elements of the U.S. EPR containment system include the Reactor Building, the containment isolation system, and the containment combustible gas control system.

The containment is designed so that containment pressure and temperature are rapidly reduced and maintained at acceptably low levels following a rupture of any high-energy pipe, thus ensuring that the design leak rate is not exceeded. The design basis accidents (DBA) for the containment systems are defined as the most severe event within a spectrum of postulated loss-of-coolant accidents (LOCA) and main steam line break (MSLB) accidents. DBA mitigation depends upon the high reliability of these containment systems. This section describes the design features and criteria defining the containment's functional requirements.

2.1 Reactor Building

The U.S. EPR Reactor Building (see Figure 2-1) consists of a cylindrical reinforced concrete outer Shield Building, a cylindrical post-tensioned concrete inner Containment Building with a steel liner, and an annular space between the two buildings. The Shield Building protects the Containment Building from external hazards.
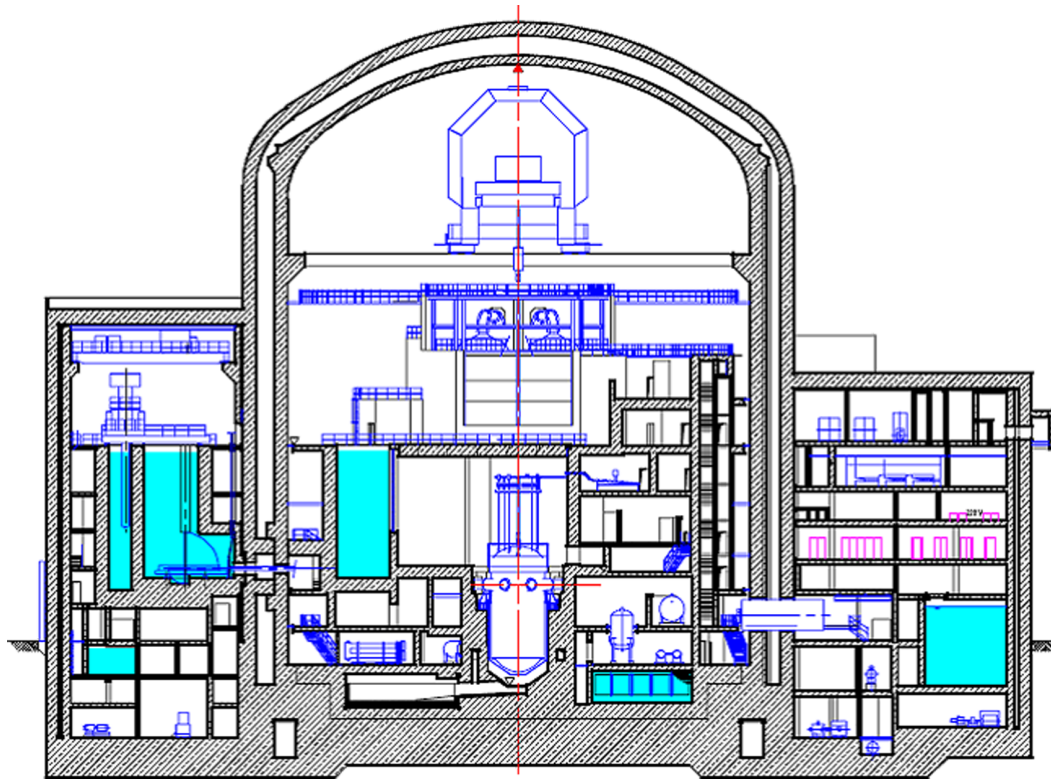
Figure 2-1—U.S. EPR Layout

The containment is designed to withstand the environmental and dynamic effects associated with both normal plant operation and postulated accidents as required in GDC 4. The Containment Building (commonly referred to as simply the "containment") is a pre-stressed concrete shell with a steel liner on its inner surface (including the basemat). It has a free volume of approximately 2.8×10^6 ft^3 and a design pressure of 62 psig. Within the containment are the RCS, the in-containment refueling water storage tank (IRWST), and parts of the main steam and feedwater lines.

2.1.1   General Layout

The U.S. EPR containment is designed with a number of internal subcompartments to protect components and systems against dynamic effects, including the effects of missiles, pipe whipping, and discharging fluids caused by equipment failures and events and conditions outside the containment. The containment internal compartments can

withstand the effects of environmental conditions associated with normal operation, maintenance, testing, and postulated accidents, including LOCAs.

The reactor containment structural design, including the design of access openings and penetrations, allows the containment internal compartments to accommodate the calculated pressures and temperatures resulting from a LOCA without exceeding the design leakage rate requirement, per GDC 50.

The containment is segregated into two zones delineating areas that are accessible during normal operation from those that are inaccessible. Equipment rooms immediately surrounding the RCS are isolated from the rest of the containment during normal operation, while beyond this inner region personnel access can be provided during certain maintenance tasks. Separation is provided by structures and closed portals to minimize radiation exposure in the accessible space areas. During power operation the inaccessible areas inside containment (the "equipment space") experience higher temperatures than the accessible areas because they are exposed to the hot walls of the nuclear steam supply system. The cooler, accessible areas are the "service space."

In the event of an accident, communication is established between these equipment rooms by opening mixing dampers and foil barriers, thereby transforming the containment into a single convective volume.

2.1.2   In-Containment Refueling Water Storage Tank

The function of the IRWST is to maintain a large reserve of borated water at a homogeneous concentration and temperature that is used to flood the refueling cavity during reactor refueling. It is also the safety-related source of water for emergency core cooling in the event of a LOCA, and is a source of water for containment cooling and for core melt cooling in the event of a severe accident. The IRWST constitutes the lowest point in the containment, and communication paths allow any water discharged from the RCS to drain into the IRWST.

Each of the four safety-related safety-injection system (SIS) trains and one non-safety-related severe accident heat removal system (SAHRS) train is provided with a separate sump suction connection to the IRWST. To prevent RCS thermal insulation and other debris from reducing the suction head of the SIS and SAHRS pumps, a series of barriers are used to capture debris that could reach the sumps. The SAHRSs includes a back-flushing function to clear debris from sump drains.

2.1.3   Containment Cooling Systems

In the U.S. EPR, during normal operation or hot shutdown conditions, active systems accomplish containment heat removal; the containment cooling ventilation system (CCVS) removes heat released by the operation of plant components. The CCVS is not a safety-related system, but is designed with sufficient redundancy to ensure reliable operation.

In response to design-basis events, the large free volume and heat capacity of the containment and internal structures means the U.S. EPR does not require active containment heat removal systems to ensure short-term pressure and temperature control. Steam condenses on these surfaces and drains to the IRWST. IRWST heat removal is provided by the low head safety injection (LHSI) heat exchanger located outside containment (see Figure 2-2). Under a design-basis LOCA, safety injection pumps draw water from the IRWST and reject the containment heat to the component cooling water system (CCWS) and the essential service water system (ESWS) through the LHSI/RHR heat exchanger. The cooled LHSI water is then split between safety injection to the RCS and return to the IRWST for direct cooling of the IRWST..
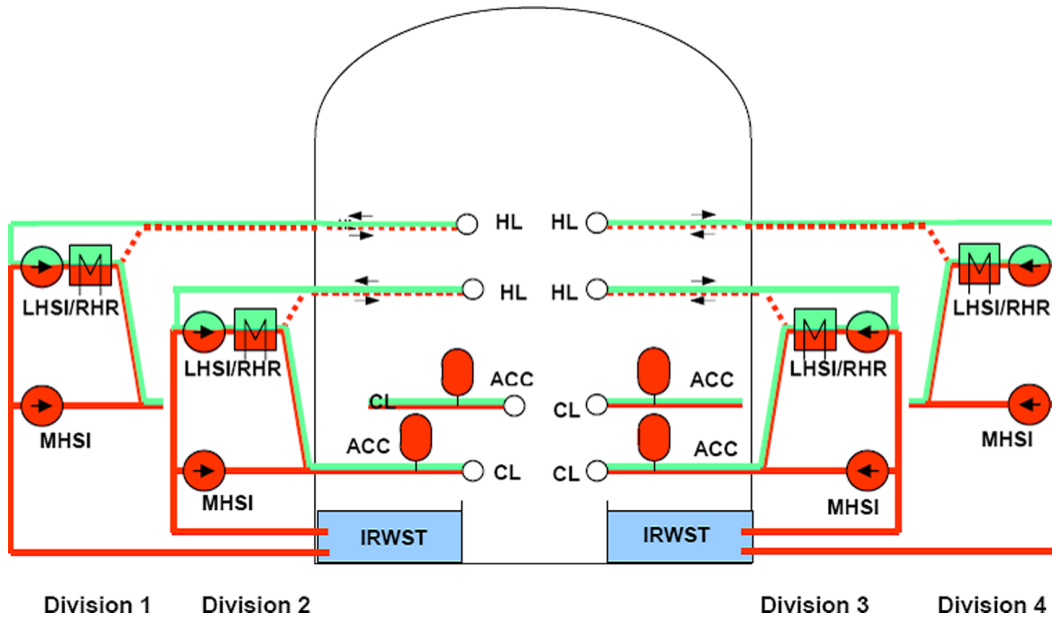
Figure 2-2—Safety Injection Systems

2.1.4 Annulus Ventilation System

The Containment Building and Shield Building are physically independent except at the basemat. The annular space between these structures is maintained at sub-atmospheric pressure by the annulus ventilation system (AVS). The AVS (see Figure 2-3) is a safety-related system used in the event of a design basis or severe accident to filter any leakage from the containment building prior to exhausting it from the plant stack. The AVS provides 2 x 100% extraction capability and consists of high efficiency particulate air (HEPA) filters and charcoal absorbers in series with air handling equipment.
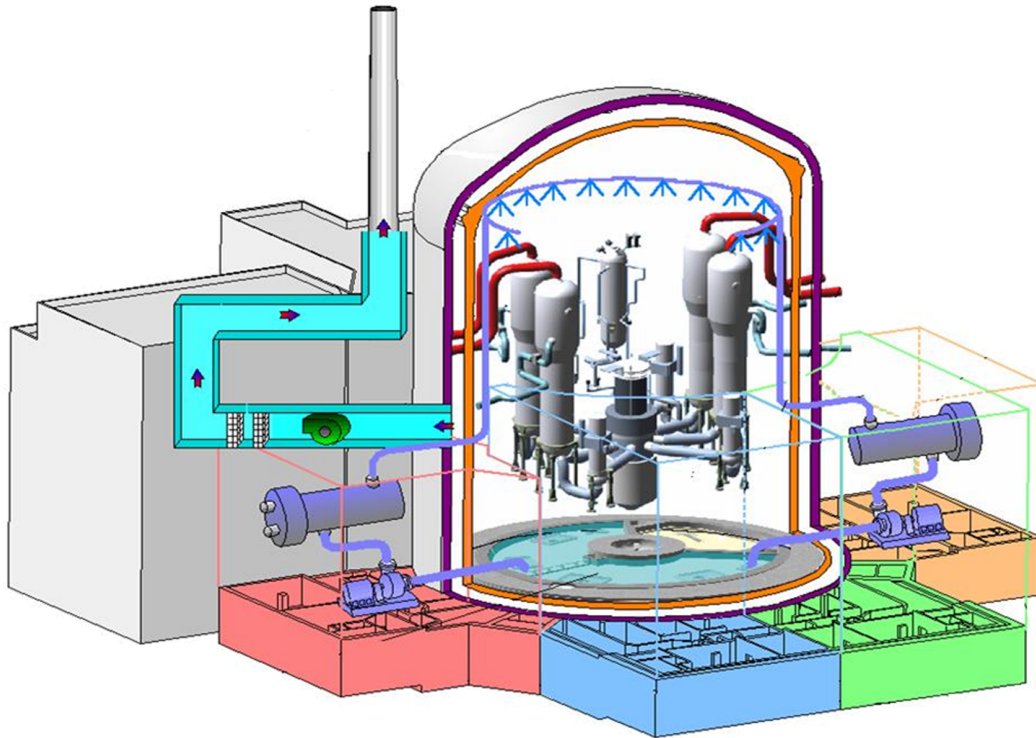
Figure 2-3—Annulus Ventilation System

2.1.5   Containment Monitoring

The containment instrumentation is capable of monitoring variables and systems over their anticipated ranges for all normal operation, for anticipated operational occurrences, and for accident conditions as appropriate to safety, including those variables and systems that can affect the containment and its associated systems. Appropriate controls maintain these variables and systems within prescribed operating ranges (GDC 13).

The containment is provided with the means for monitoring radioactivity in the Reactor Building atmosphere, the compartments containing components for recirculation of LOCA fluids, the effluent discharge paths, and the plant environs. This radioactivity may be released during normal operations, anticipated operational occurrences, and postulated accidents (GDC 64).

2.2   Conversion to a Single Convective Volume – The CONVECT System

During accidents involving a breach of the RCS, pressure and temperature within the inner equipment rooms will increase. To lower pressure and temperature, the U.S. EPR employs a system designed to ensure pressure equalization and atmospheric mixing throughout the containment. Equipment rooms surrounding the RCS are isolated from accessible portions of the containment building during normal operation. In the event of an RCS breach, communication is established between these equipment rooms and the accessible areas, which promotes circulation.

This transformation into a single convective volume is performed by the CONVECT system, which equalizes pressure between the containment compartments and promotes efficient mixing of the atmosphere by establishing a global convective pathway. The CONVECT system of convection foils, rupture foils, and mixing dampers that transforms the two-room containment into a one-room containment is part of the combustible gas control system (CGCS). The CONVECT system rupture foils are currently implemented in German Konvoi plants. The large passive heat sinks with broad surface areas enhance containment atmospheric mixing and pressure equalization during LOCAs by encouraging:

- Buoyancy-driven convective currents between the containment's accessible regions and the equipment rooms

- A uniform steam distribution in LOCA events, which mitigates containment pressure through the condensation of steam on structure surfaces

- Fast pressure equalization between the rooms, thereby limiting the event loads on internal walls

- Good atmospheric convection conditions to limit the peak hydrogen concentration.

AREVA NP Inc.

ANP-10299NP

Applicability of AREVA NP Containment Response Evaluation Methodology to the

Revision 2

U.S. EPR™ for Large Break LOCA Analysis

Technical Report

Page 2-8

To make portions of the containment accessible during plant operation, the U.S. EPR containment is separated into two regions with separate ventilation systems. This separation is delineated by:

- Walls between equipment rooms and annular containment (radiation shield)

- Massive doors providing access between the accessible area and the equipment rooms during outages

- The CONVECT system of rupture and convection foils in the steam generator equipment room ceiling and the mixing dampers in the wall between the lower accessible area and the IRWST air space.

To quickly and efficiently distribute the steam effluent throughout the containment following a LOCA, convection should be established early in the event. This is achieved by the prompt conversion from the two-room to the one-room containment, allowing rapid steam transport to the areas far from the break location. The CONVECT system accomplishes this as follows:

1. At the upper boundary of the equipment rooms, the steam generator (SG) pressure equalization ceiling, the following components are installed (see Figure 2-4).
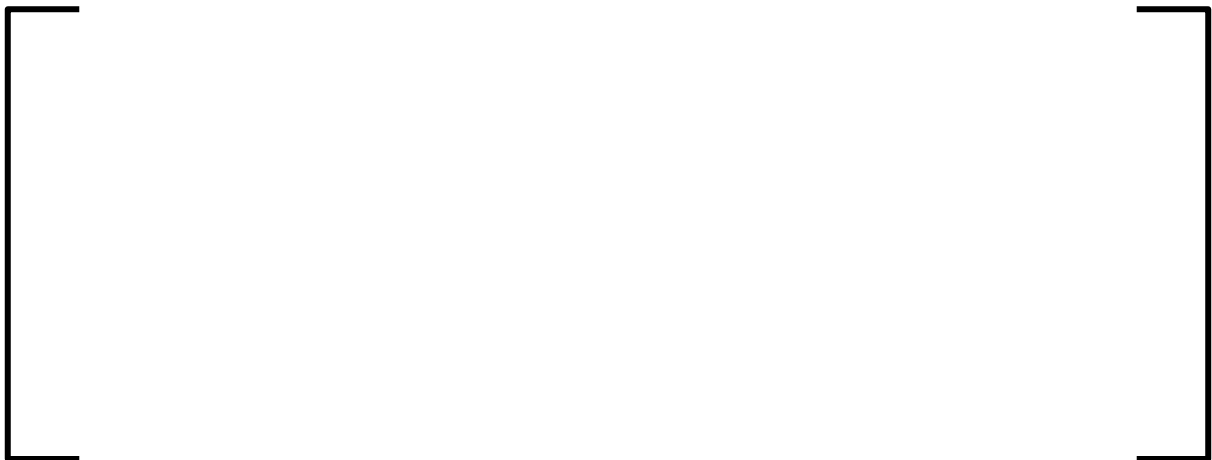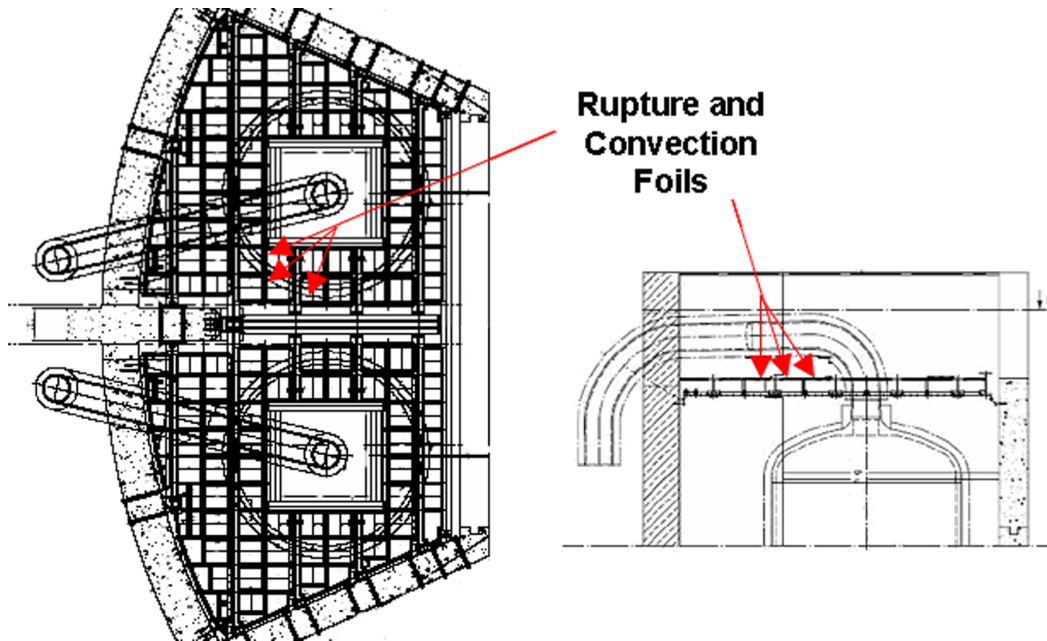
Figure 2-4—Pressure Equalization Ceiling

The rationale for the installation of different components in the upper and lower containment areas is based on the following:

- In the lower part of the containment, high gas temperature cannot be assured for all LOCA events, as it can in the upper SG compartments; hence convection foils activated by temperature are not suitable for the lower containment.

- Activation solely by pressure difference across the SG pressure equalization ceiling in the upper containment is not appropriate for all LOCA events because in some scenarios there is the possibility that the initial rupture of a few foils could equalize the pressure across the foils, thus preventing other rupture foils from opening.

Large break LOCA (LBLOCA) and small break LOCA (SBLOCA) events establish different requirements for flow cross sectional area and the timing of flow path opening, which is achieved by different system components:

- As a consequence of low mass and energy release during a SBLOCA event, opening of all the rupture foils may not occur. For effective steam distribution in the containment, a minimum free-flow cross-sectional area similar to that designed for the mixing dampers provides sufficient atmospheric mixing. This requirement is fulfilled by the convection foil function.

2.2.1   Rupture Foils
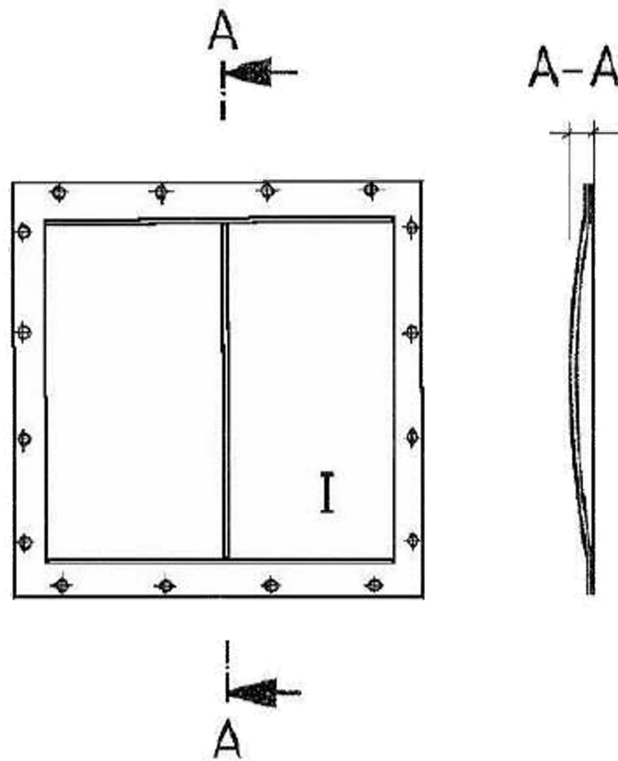
Figure 2-5—Rupture Foil

2.2.2   Convection Foils

A convection foil is essentially a rupture foil combined with a temperature-sensitive opening mechanism. They open passively by exceeding either a setpoint on pressure differential or one on temperature. The opening on differential pressure occurs in the same manner as described for rupture foils in Section 2.2.1. The steel framework is held closed by a thermo-lock which integrates fusible links. The design of the fusible link ensures the opening under gravity at a predefined temperature via a hinge mechanism. [   ] Figure 2-6 illustrates a single convection foil.
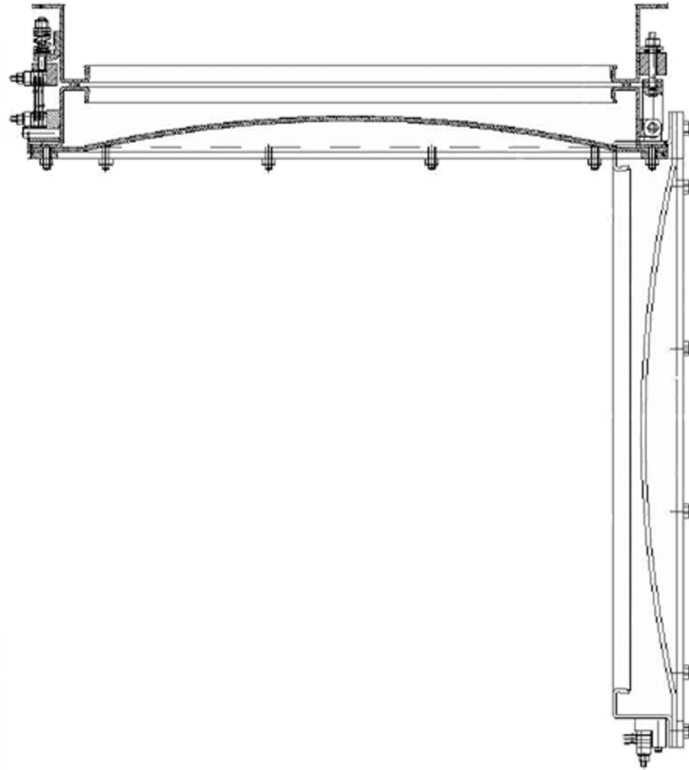
Figure 2-6—Convection Foil

2.2.3 Mixing Dampers

The mixing dampers are equipped with fail-safe-open actuators and LOCA-proofed position indicators. Their design is similar to those used in fire dampers or in heating, ventilating and air-conditioning (HVAC) systems. A motor-driven actuator operates the damper. During closing, a spring is compressed and held in the loaded position by an electro-magnet. In case of power failure to the solenoid of the electro-magnet, the spring will drive the motor-driven actuator and damper to the open position without any external energy supply. When electrical power is restored, the motor-driven actuator is again available for normal operation. A dashpot controls the spring speed.

The mixing dampers (see Figure 2-7) open if sensors indicate a LOCA or severe accident, specifically:

- Manual actuation by an operator is also an option.
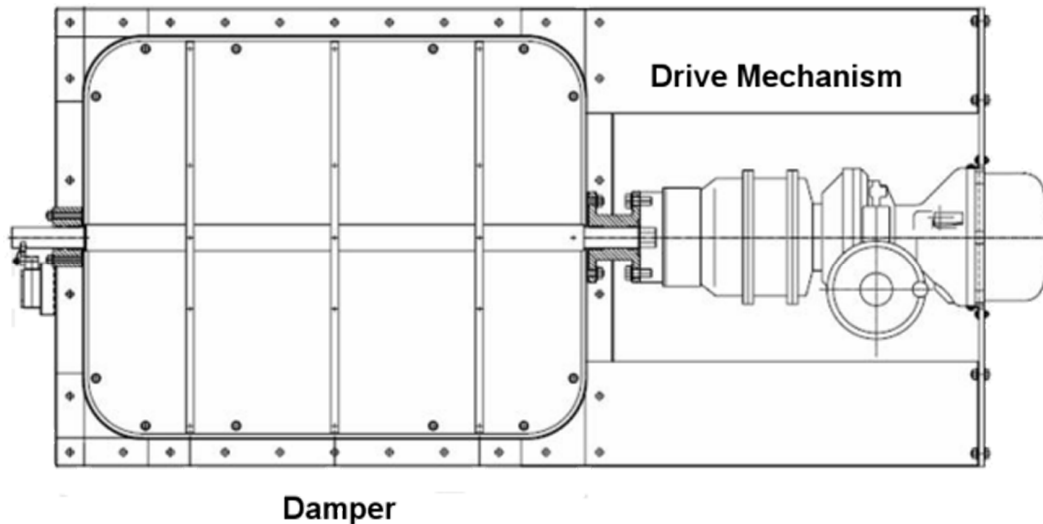
Figure 2-7—Mixing Damper

2.3   Hydrogen Reduction System

The hydrogen reduction system (HRS) consists of 41 large and six small passive autocatalytic recombiners (PARs) installed in various parts of the containment (see Figure 2-8). The two models of PARs used in the U.S. EPR design have been developed by AREVA NP and are currently used in some European operating plants. Each PAR consists of a metal housing designed to promote natural convection with a gas inlet at the bottom and a lateral gas outlet at the top. Numerous parallel plates with a catalytically active coating (Pt/Pd substrate) are arranged vertically in the bottom of the housing with access provided by a removable inspection drawer. The recombiner housing protects the catalyst against direct water spray and aerosol deposition.
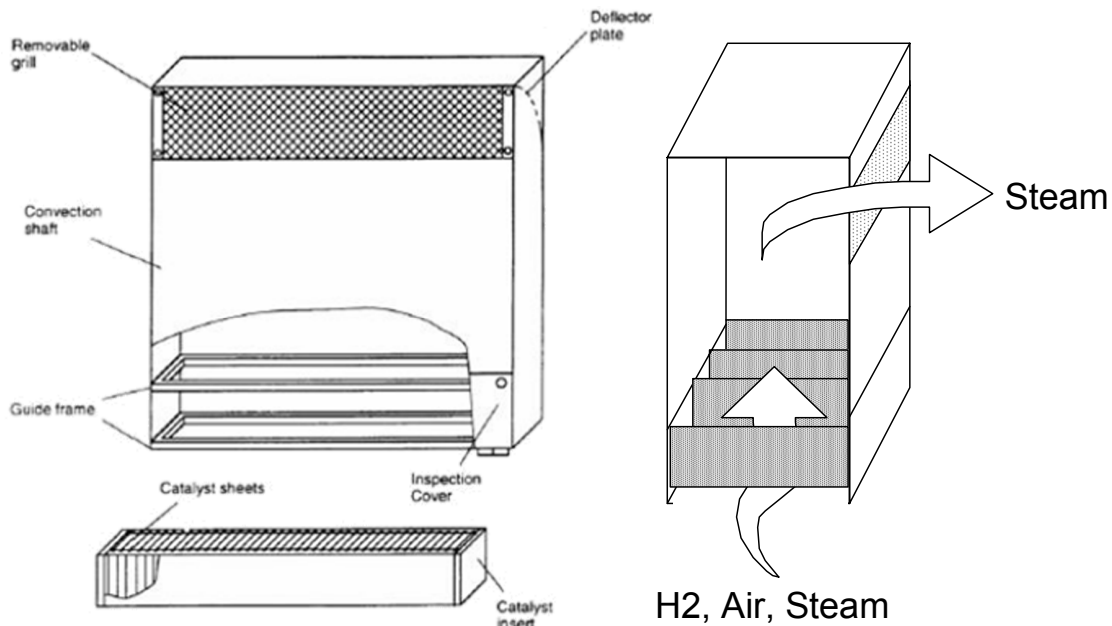
Figure 2-8—Passive Autocatalytic Recombiner

Hydrogen and oxygen in containment gas mixtures are recombined upon contact with the catalyst in the lower part of the housing. The heat from this reaction in the lower part of the recombiner causes a reduction in gas density in this area, promoting natural circulation through the PAR and ensuring high recombination efficiency.

In the presence of oxygen, the PARs will automatically start if the threshold hydrogen concentration is reached at the catalytic surfaces. The recombination rate depends mainly on the hydrogen density seen by the PAR. An increasing hydrogen concentration enhances the removal rate.

The PARs are arranged to support global convection within the containment, and thereby optimize the homogenization of the atmosphere. This strategy ensure that the global concentration of hydrogen in the containment atmosphere is maintained below 10% by volume during a severe accident resulting in oxidation of up to 100% of the zirconium surrounding the reactor fuel. Recombiners are also included in the containment dome to cope with stratification and to improve depletion after atmospheric homogenization. The PARs are installed above the floor to provide unobstructed inflow

and easy access for maintenance. The arrangement of PARs also favors locations that avoid direct contact with spray water (despite their qualification to operate in the presence of water).

2.4   Severe Accident Heat Removal

The severe accident heat removal system (SAHRS) is a dedicated thermal-hydraulic system used to control the environmental conditions within the containment following a severe accident. As such, the SAHRS is a non-safety-related system. Therefore, demonstrating traditional safety-related design criteria, such as single failure considerations or seismic events within the design basis, is not required. Nonetheless, certain conservative principles and guidelines are applied to the system.

The SAHRS has four primary modes of operation, each playing a role in controlling the environmental conditions within the containment. The modes of SAHRS operation include:

- Passive cooling of molten core debris

- Active spray for control of the containment atmosphere

- Active recirculation cooling of the molten core debris and containment atmosphere

- Active back-flush of the IRWST sump strainers.

The SAHRS train is located in a dedicated, radiologically-controlled room within one of the four plant Safeguards Buildings. The SAHRS train includes:

- A dedicated suction line from the IRWST

- Containment isolation valves

- A pump to support active recirculation

- A heat exchanger for containment heat rejection

- Discharge lines to a containment spray header, the spreading room, and sump screen

- Support from a dedicated cooling chain via plant auxiliary systems.

The SAHRS heat exchangers transfer the residual heat from the containment to the ultimate heat sink via dedicated portions of the component cooling water (CCW) and essential service water (ESW) trains. During operation, the three available flow paths downstream of the pump and heat exchanger combination direct flow to:

- A containment spray system with a ring header and spray nozzles

- The spreading area of the core melt stabilization system (CMSS)

- A sump screen flushing device which is used to remove accumulated debris.

The general configuration of the SAHRS train is shown in Figure 2-9.
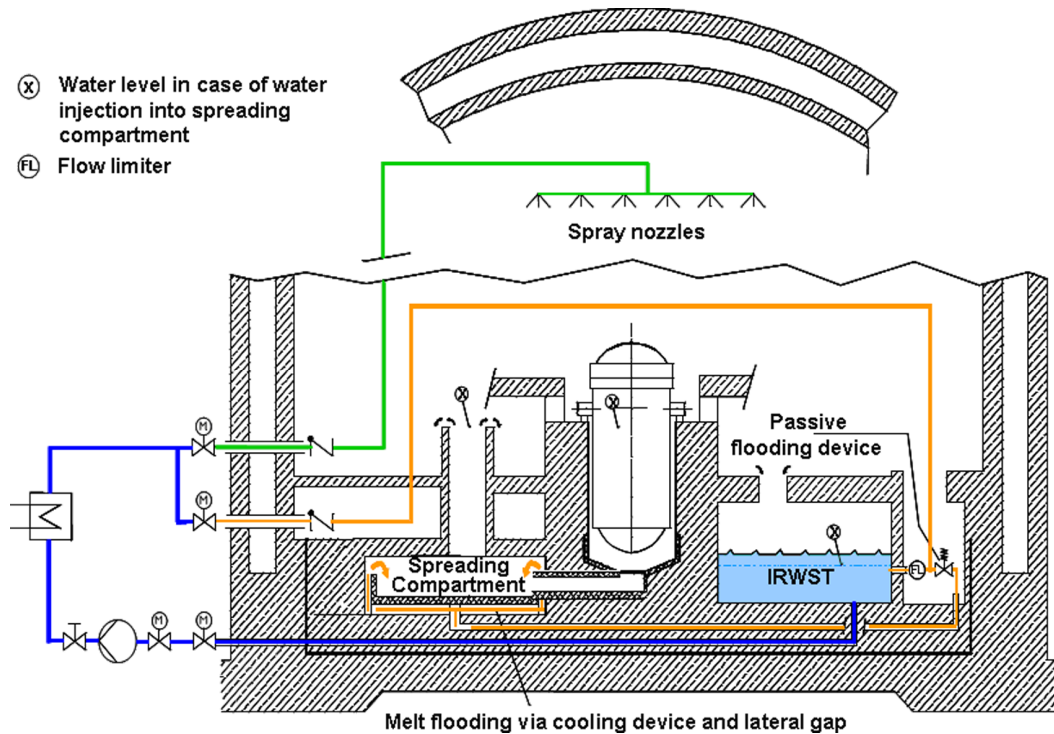
Figure 2-9—Severe Accident Heat Removal System

2.4.1 Active Spray

When operating in the containment spray mode, the SAHRS takes suction from the IRWST; coolant then flows through a heat exchanger outside containment before being routed back to the spray headers located in the upper volume of the containment. The spray water condenses atmospheric steam as the water droplets fall through the containment atmosphere. The resulting condensate then flows along the structural elements of the containment back into the IRWST for continued recirculation.

The U.S. EPR containment spray system is an approximately 1600 gpm system. The capacity is a direct function of the intended use. The containment spray system in the conventional operating fleet and other evolutionary plants is used for environmental control of the containment atmosphere following design basis events, whereas the spray in the U.S. EPR was designed for severe accident mitigation.

2.4.2   IRWST Strainer Backflush

SAHRS operation in back-flushing mode serves to dislodge any debris from the sump strainers that might compromise the ability of the SAHRS to draw water from the IRWST. Only a fraction of the SAHRS capacity is used for back-flushing; therefore, the system can operate in this mode while continuing operation in another containment cooling mode.

2.4.3   SAHRS Dedicated Cooling Chain

To support the active heat removal modes of the SAHRS, dedicated portions of the CCW and ESW systems are used to form a dedicated cooling chain to transfer heat to the ultimate heat sink. These dedicated cooling trains are composed of a non-safety CCW and ESW train for the one SAHRS train. This cooling chain is dedicated to severe accident operation and is not used to support normal plant operations or to mitigate the effects of a design basis event. Both the CCW and ESW are designed to receive power from either emergency diesel generators (EDG) or station blackout (SBO) diesels.

The CCW trains consists of a pump located upstream of a dedicated heat exchanger, a surge tank connected to the pump suction line and, a demineralized water supply line with a pressurizing pump. This portion of the cooling chain feeds water to the shell side of the SAHRS heat exchanger, where containment heat is removed and discharged through the tube side of the CCW heat exchanger interfacing with ESW. The pressurizing pump ensures the demineralized water supply to this CCW train and pressurization of the surge tank. The surge tank allows for pressurization of the dedicated CCW train to ensure an outflow of the system cooling medium in the event of a rupture in the SAHRS heat exchanger. This prevents contamination of the cooling chain by leakage of radioactive water at the SAHRS heat exchanger.

The ESW train essentially consists of a pump whose inlet is separated from the ultimate heat sink by a strainer. This ESW train supplies water to the shell side of the CCW heat

exchanger where it removes transferred heat and rejects it back into the ultimate heat sink.

2.5   Safety Injection System

The safety injection system (SIS) provides emergency coolant injection and recirculation functions to maintain reactor core coolant inventory and adequate decay heat removal following a LOCA. The safety functions of the SIS during an LBLOCA are:

- Rapid reflood of the reactor pressure vessel (RPV) and the reactor core

- Long-term injection of water to the core

- Injection of water to terminate the release of steam to the containment atmosphere as early as possible

- Cooling the IRWST

- Long-term mixing of water that is recirculated to ensure homogeneous boron concentration and temperature.

Safety injection within the U.S. EPR is performed by accumulators, a medium head safety injection (MHSI) system, and a low head safety injection (LHSI) system. These safety-related systems consist of four independent trains that are physically separated and protected. The accumulators are located inside the containment and inject into the RCS cold legs when the RCS pressure falls below the accumulator pressure, using the same injection nozzles as the LHSI and MHSI pumps. In the injection mode, the MHSI and LHSI pumps take suction from the IRWST and inject into the RCS. These pumps are located in the Safeguard Buildings, close to the containment. A heat exchanger is located downstream of each LHSI/RHR pump. These heat exchangers are cooled by the component cooling water system.

Each of the four SIS trains has a separate suction connection to the IRWST. The IRWST includes a series of screens, protecting the SIS pumps against debris entrained with IRWST fluid. Each pump is provided with a miniflow line routed back to the IRWST for cooling and mixing the IRWST.

The MHSI system draws borated water from the IRWST and injects it into the cold leg at a pressure lower than the main steam safety valve setpoints, to ensure that in the event of a steam generator tube rupture, primary inventory cannot be released directly to the environment.

The LHSI pumps and the MHSI pumps normally inject into the cold legs. In the long term following a LOCA, the majority of LHSI discharge is switched over to the hot legs to limit the boron concentration in the core and to terminate core steaming. The switchover to hot leg injection locations recovers a SIS train that might otherwise be delivered directly to the break in the event that the break is in the cold leg pump discharge piping. Impact to a postulated hot leg break is compensated for by ongoing MHSI (and some LHSI) into the cold leg, high efficiency coolant mixing in the RPV, and by the steam generators—a significant source of energy during the post-reflood phase—being segregated from the RCS fluid paths.

3.0   SAFETY ISSUE RESOLUTION METHODOLOGY

3.1   EMDAP

In 2005, the NRC published Regulatory Guide 1.203, describing the structured evaluation model development and assessment process (EMDAP). The EMDAP is considered to be generally applicable to the development of analysis methods for the purpose of evaluating safety issues related to abnormal nuclear power plant states (i.e., unanticipated transients and accidents). EMDAP starts from the definition of the objectives, the functional requirements, and the identification of important phenomena. Guided by these top-level priorities, code development and assessment follow, ultimately leading to the evaluation model adequacy decision. The EMDAP process is depicted in the flowchart of Figure 3-1.
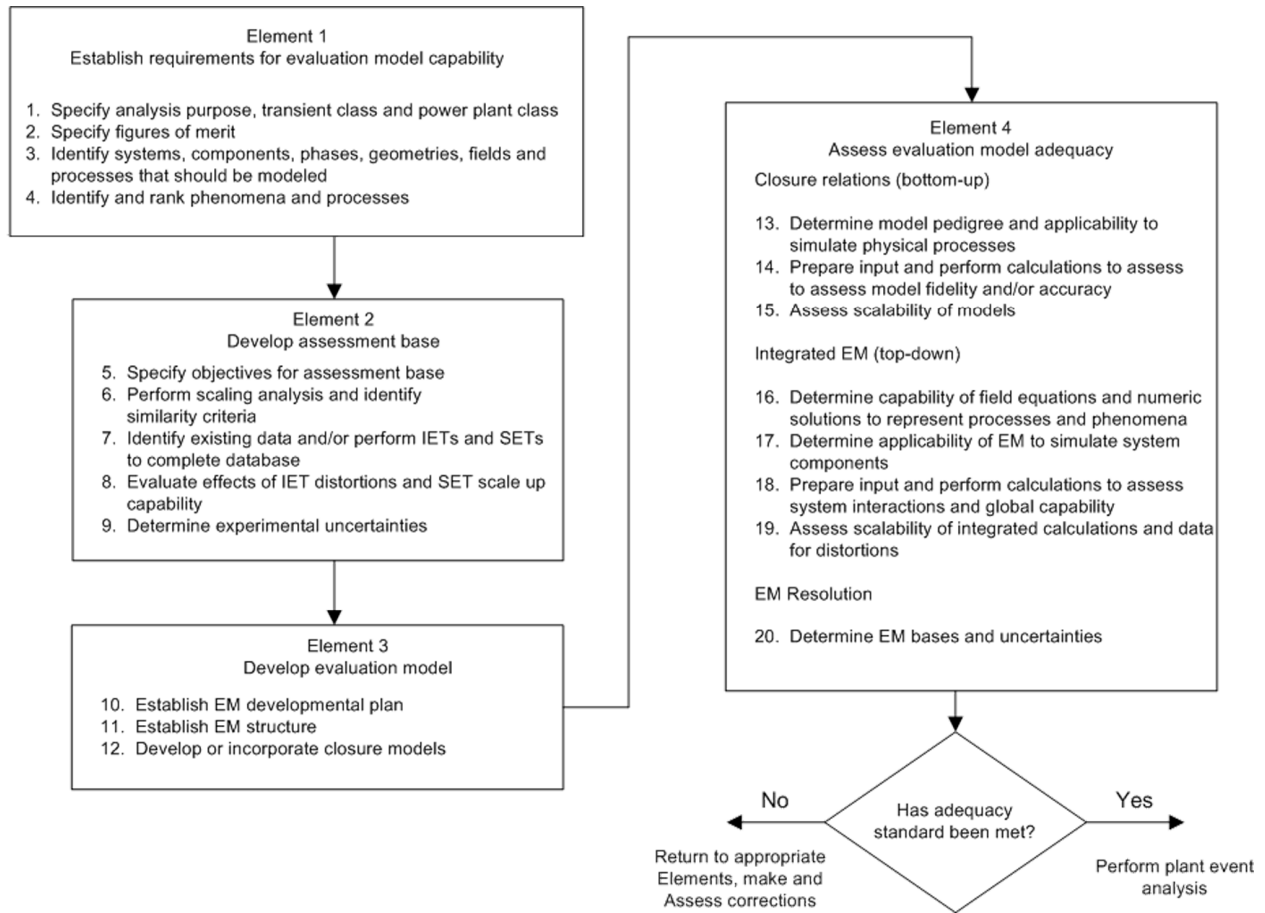
Figure 3-1—EMDAP Process

The EMDAP follows the same principles as the Code Scaling Applicability and Uncertainty (CSAU) roadmap (Reference 13); however, EMDAP was not developed exclusively for statistics-based evaluation methodologies.

3.2 Requirements for Evaluation Model (EMDAP Steps 1 and 2)

AREVA NP's containment analysis methodology for the U.S. EPR presented in this technical report builds on the NRC-approved containment analysis evaluation methodology presented in Reference 14. The generic evaluation methodology was prepared to assess the containment response to design basis LBLOCA and main feedwater and steam line breaks in PWRs. Containment pressure is the principal

figure-of-merit for addressing regulatory compliance. Containment pressure and temperature are used in tandem to address equipment qualification.

3.3 Description of Principal Phenomena (EMDAP Step 3)

The magnitude of the temperature rise and pressure peak resulting from a LOCA or MSLB depends upon the nature, size, and location of the postulated rupture. The U.S. EPR containment is designed to contain the energy released from the RCS in the event of a LOCA or from the steam generator during a MSLB.

The LBLOCA is typically the most limiting event for containment analysis because it adds the greatest mass and energy to the containment in the shortest period of time. This condition leads to a short-term peak in the containment temperature and pressure that is referred to as the blowdown peak.

The course of an LBLOCA is divided into five phases characterized by distinct phenomena:

1. Blowdown (discussed in Section 3.3.1)
2. Refill (discussed in Section 3.3.2)
3. Reflood (discussed in Section 3.3.3)
4. Post-reflood (discussed in Section 3.3.4)
5. Decay heat (discussed in Section 3.3.5).

Containment response phenomena are discussed in Section 3.3.6.

3.3.1 Blowdown

A double-ended guillotine LBLOCA is initiated by a postulated rupture of an RCS primary pipe. The immediate consequence of the LBLOCA is a rapid depressurization of the RCS. Soon after, the reactor protection system (RPS) signals a reactor trip, most likely when the low pressurizer pressure trip setpoint is reached. If the RPS should fail, the reactor is shutdown by coolant voiding in the core region. Active mitigation of the LBLOCA begins when the safety injection system (SIS) actuation signal is generated on

"low-low" pressurizer pressure. The reactor coolant pumps are tripped automatically on coincident low pump differential pressure and begin to coast down during this period. Figure 3-2 illustrates RCS conditions during early blowdown.

The coolant flow rate from the RCS to the containment varies depending upon the nature, size, and location of the break; nevertheless, the break plane is choked during blowdown. While fluid conditions at the break remain subcooled, the mass and energy release from the RCS is at the fastest rate possible. Eventually, the fluid at the break becomes saturated and voiding occurs. This significantly reduces the mass and energy release rate and slows RCS depressurization.

The principal containment energy source during blowdown is coolant stored energy. Decay heat and sensible heat in RCS piping, components, and fuel are also present. However, these sources are relatively small in comparison. Similarly, heat generation from fuel cladding oxidation is possible if fuel rod temperatures get high enough. This also is a relatively small energy source given the low core heat transfer during this LOCA phase.

As the RCS pressure falls, MHSI and the accumulator inventory are added to the RCS cold leg locations downstream of the reactor coolant pumps (RCP). If the break is located in the cold leg, the inventory of one accumulator is likely lost to the break. In addition, the integral effect of several flow phenomena (e.g., entrainment, condensation, etc.) causes a significant amount of accumulator inventory to bypass the reactor vessel downcomer and exit the break.

Significant mixing between liquid and steam occurs because of the high steam velocities and the large volume of accumulator water being ejected. This has two relatively small and competing effects on mass and energy releases: it reduces steam releases to the containment, and lowers liquid subcooling of any liquid that remains in the RCS. The reduction in steam quality of the break effluent leads to a slower rise in containment pressure. The reduction in subcooling of the RCS fluid can lead to an early

onset of nucleate boiling and thus enhanced heat transfer from RCS and reactor pressure vessel (RPV) surfaces.

Coolant released from the primary system causes an increase in containment steam mass, which in turn increases pressure and temperature. In response to the initial pressure wave and increase in temperature, rupture and convection foils located above the U.S. EPR equipment rooms (i.e. compartments containing the steam generators and reactor coolant pumps) burst open, exposing the released mass and energy to the full containment volume. Mixing dampers located low in the containment on the walls separating the containment's accessible area and the IRWST air space also open to complete a flow circuit that allows the air/steam mixture to circulate. Containment pressure rises until pressure between the primary system and the containment equalizes. This is considered the end of the blowdown phase.
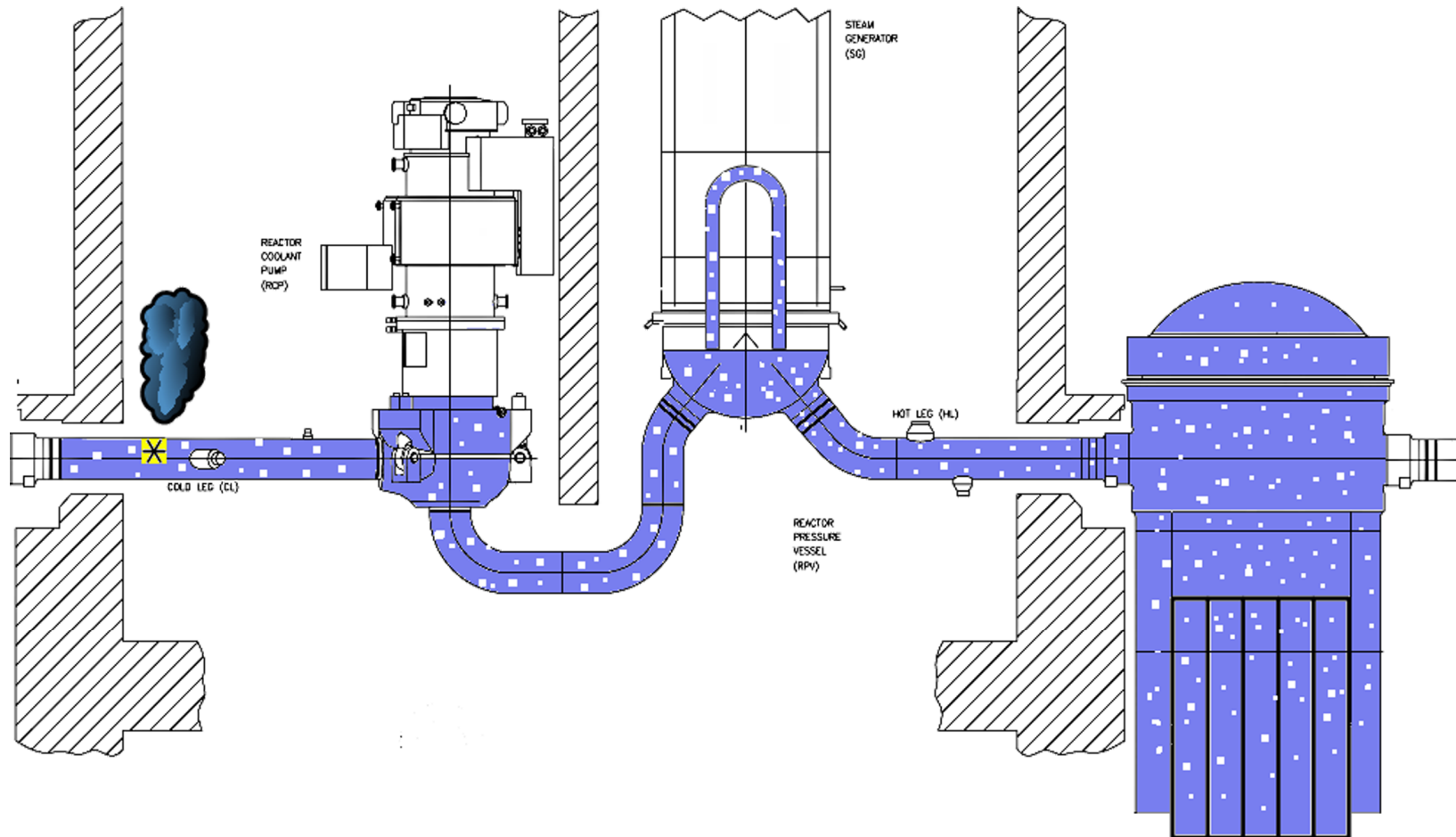
Figure 3-2—RCS Conditions During Blowdown

3.3.2 Refill

Following blowdown from a cold leg break location, the RCS and RPV are expected to be nearly empty of coolant. A period of time is required to refill the reactor vessel lower plenum to the core inlet level. Accumulator flow and MHSI to the cold legs provide ECC water during this period. With the RCS and containment at nearly equal pressure, much of the ECCS coolant is directed to the downcomer. It is possible for the RCS to be at a lower pressure than the containment momentarily, causing a flow reversal at the break. This might introduce air into the RCS that adds to the non-condensable gases evolving out of the reactor coolant during blowdown and affecting mixing and condensation rates. Nonetheless, this phase can be described as "filling a pot." Within the RPV, residual steam and hot wall effects causing steaming in the lower plenum must be displaced during this period.   Some of this steam escapes through the break. The speed with which the lower plenum refills depends on the total coolant delivery rate, the steam/water interfacial interactions, and the break size and location. The refill phase ends when the water level reaches the core inlet elevation. Figure 3-3 illustrates RCS conditions during refill.
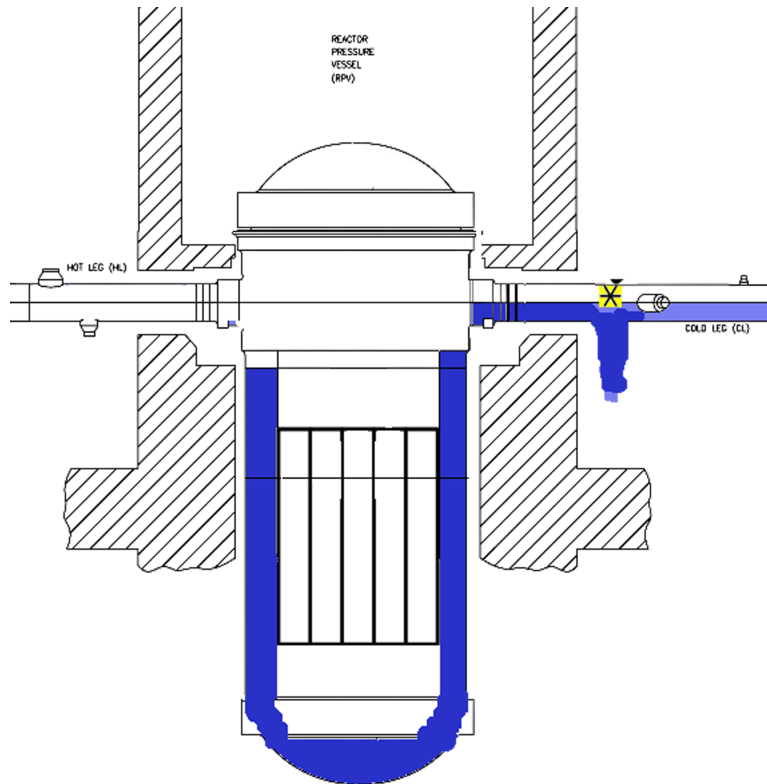
Figure 3-3—RCS Conditions During Refill

3.3.3   Reflood

Core reflood is characterized by emergency core coolant coming into contact with hot structures in the core region and steam generators. The water level in the reactor vessel rises upwards from the bottom of the reactor core. The principal source of mass and energy impacting containment conditions is the progressive quenching in the core. Concurrently, a substantial quantity of liquid is entrained into the rising steam flow and carried out of the core region, through the hot leg, and into the steam generators. This starts the removal of the sensible heat residing in the secondary fluid and adjacent structure. For an RCS cold leg pipe rupture, a two-phase mixture travels through the SGs, where it absorbs energy from the secondary side fluid, thereby becoming superheated steam, before exiting to the containment. Figure 3-4 illustrates the RCS conditions during reflood. If the pipe rupture is in one of the RCS hot legs, the saturated

steam and water mixture partially bypass the steam generators and exits the break directly into the containment.

Simultaneous gravity-driven reflooding of the core and the interaction of cold ECC water (both MHSI and LHSI) with steam in the cold legs and downcomer cause both manometric- and condensation-driven oscillations in flow rate and pressure. High reflood rates from accumulator discharge rapidly drive water toward the hot fuel surface, producing steam. As the steam expands, the water is pushed away from the fuel surface. The gravity head of the water in the downcomer pushes back on the steam, returning coolant to the core where the resident steam can condense. These manometric oscillations slowly dampen as the quench front progresses through the core. Separately, steam leaving the core and traveling through the intact cold legs meets subcooled accumulator and safety injection coolant and the subsequent condensation of the steam decreases the local pressure, which impacts delivery rates into the reactor vessel. These oscillations are generally considered as a heat transfer enhancement; however, there are offsetting effects (e.g., reduced subcooling and counter-current flow) that diminish the overall enhancement on core heat transfer.

During early reflood, while accumulator injection is ongoing, the lower portion of the core is cooled rapidly. High flows and the generation of steam with entrained liquid also effectively remove heat in the upper regions of the core and, to a lesser extent, the steam generator. As some of this liquid comes into contact with component structures, liquid de-entrains and accumulates in the upper plenum, hot legs, and steam generators. This liquid falls back into the core and again contributes to the cooling process.

After the accumulators exhaust their inventory, the nitrogen cover gas escapes and passes through the ECCS, RCS, and RPV before leaving the system. Because this nitrogen gas expands faster than it can escape out the break, RCS downcomer pressure increases. With increased RCS downcomer pressure, liquid in the downcomer surges into the core, enhancing core cooling and liquid entrainment. The stabilization of

this surge decreases liquid subcooling in the downcomer and also can pull steam from the core into the downcomer, thereby momentarily increasing mass and energy release out the break (cold leg break only).

Once the accumulators empty, MHSI and LHSI continue to provide ECC water for core cooling. Reflood rates decrease significantly and are sensitive to steam/water ECC mixing, heat transfer from downcomer structure, and containment pressure. At the lower reflood rates, a progression of heat transfer regimes develops through the core: nucleate boiling in the lower regions and a post-critical heat flux (CHF) region above a frothy liquid level. Reflood rates can be affected by the gap between the hot leg nozzle and core barrel, which varies in size as a consequence of thermal expansion and system pressure. As the gap enlarges reflood rates increase and core heat transfer improves.

Even at the lower reflood rates, some liquid is entrained and delivered to the upper plenum, hot legs, and steam generators, eventually changing to superheated steam before leaving the RCS through the break. The vaporization of entrained liquid in the steam generator causes steam binding. This reduces the reflood rates and slows quenching of the core. The core reflood phase ends when the entire core is quenched. At this point, the peak fuel cladding temperature approaches the peak temperature of the fluid, which is near the saturation temperature corresponding to the containment pressure.

AREVA NP Inc.
ANP-10299NP
Applicability of AREVA NP Containment Response Evaluation Methodology to the
Revision 2
U.S. EPR™ for Large Break LOCA Analysis
Technical Report
Page 3-11
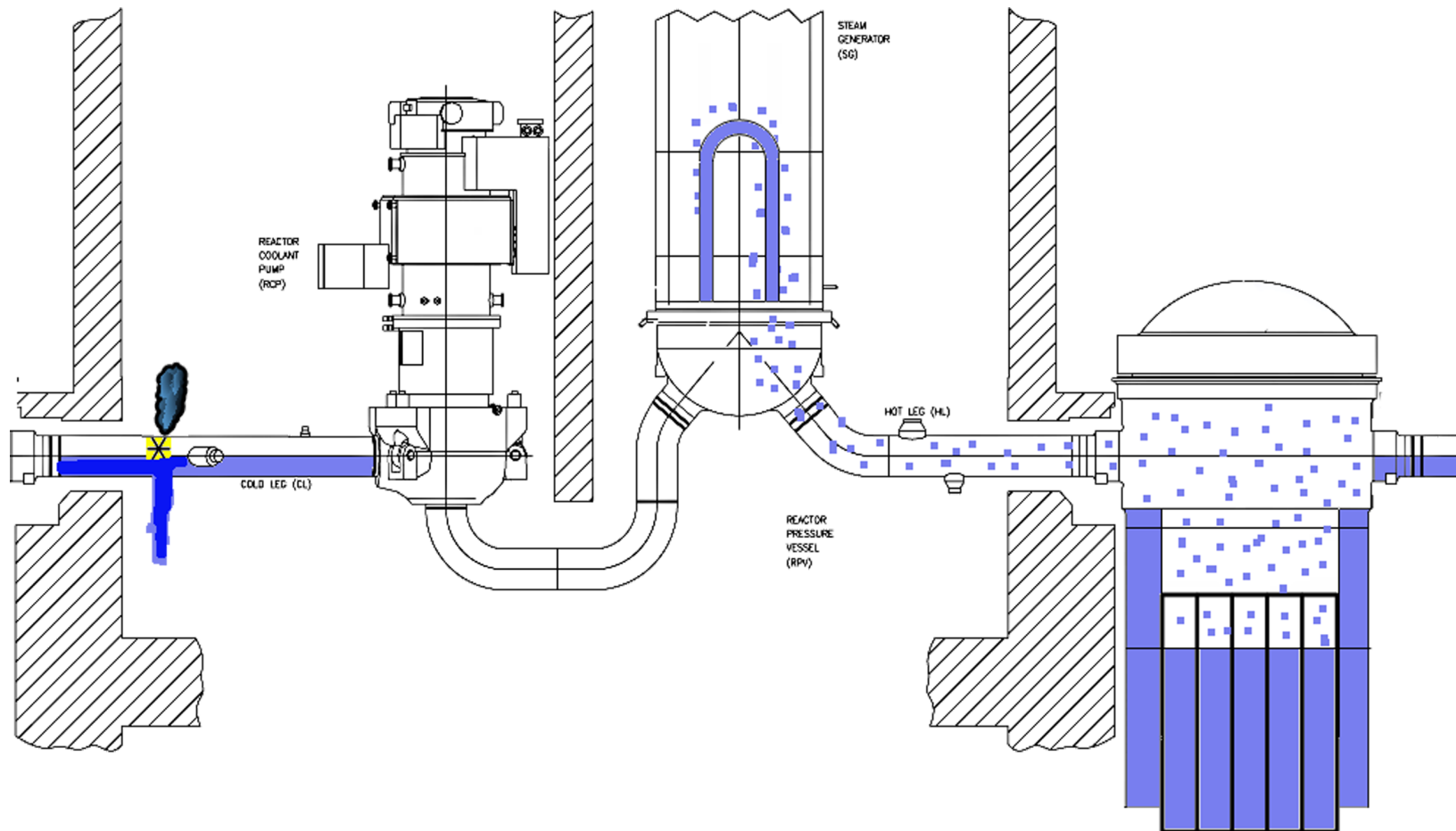
Figure 3-4—RCS Conditions During Reflood

3.3.4   Post-Reflood

The post-reflood phase begins following core quench. LHSI to the cold leg continues to provide cooling for the removal of core decay heat. LHSI coolant temperatures rise while the LHSI heat exchanger works against the increase in the IRWST temperature as hot water leaves the RCS and flows back into this source for LHSI. Nucleate boiling heat transfer in the core causes a two-phase mixture that rises above the core, into the upper plenum, hot legs, and steam generators. For cold leg breaks, the bulk of the remaining fluid sensible heat in the secondary-side of the steam generators is removed by the two-phase mixture residing in the steam generator tubes. This causes superheated steam to exit the steam generator primary side. In addition, the remaining RCS structure sensible heat is released to the circulating coolant and delivered to the containment during this LBLOCA phase. For hot leg breaks, heat removal from these sources can still occur; however, the break location in the hot leg causes a significant bypass of coolant away from the steam generators and intact loop piping. Figure 3-5 illustrates the RCS conditions during post-reflood. The succession of events in crossover legs shown in Figure 3-5 reflects the potential for the loop seal plugging/clearing phenomena.

Subsequent steam flow through the remaining RCS piping is sufficient to keep the piping clear of accumulating liquid, including the horizontal segment approaching the reactor coolant pump suction, i.e., crossover leg. This steam and water mixture is carried to the break location as in the reflood phase, but in a manner best described as "pot boiling." When steam flow decreases to a level at which it no longer can prevent the filling of the crossover leg, the post-reflood phase ends. This occurs when heat transfer from the steam generator secondary to the primary ends, i.e., after the fluid and structure sensible heat from the steam generators is removed, but before the LHSI safety injection is realigned from cold leg injection to hot leg injection.
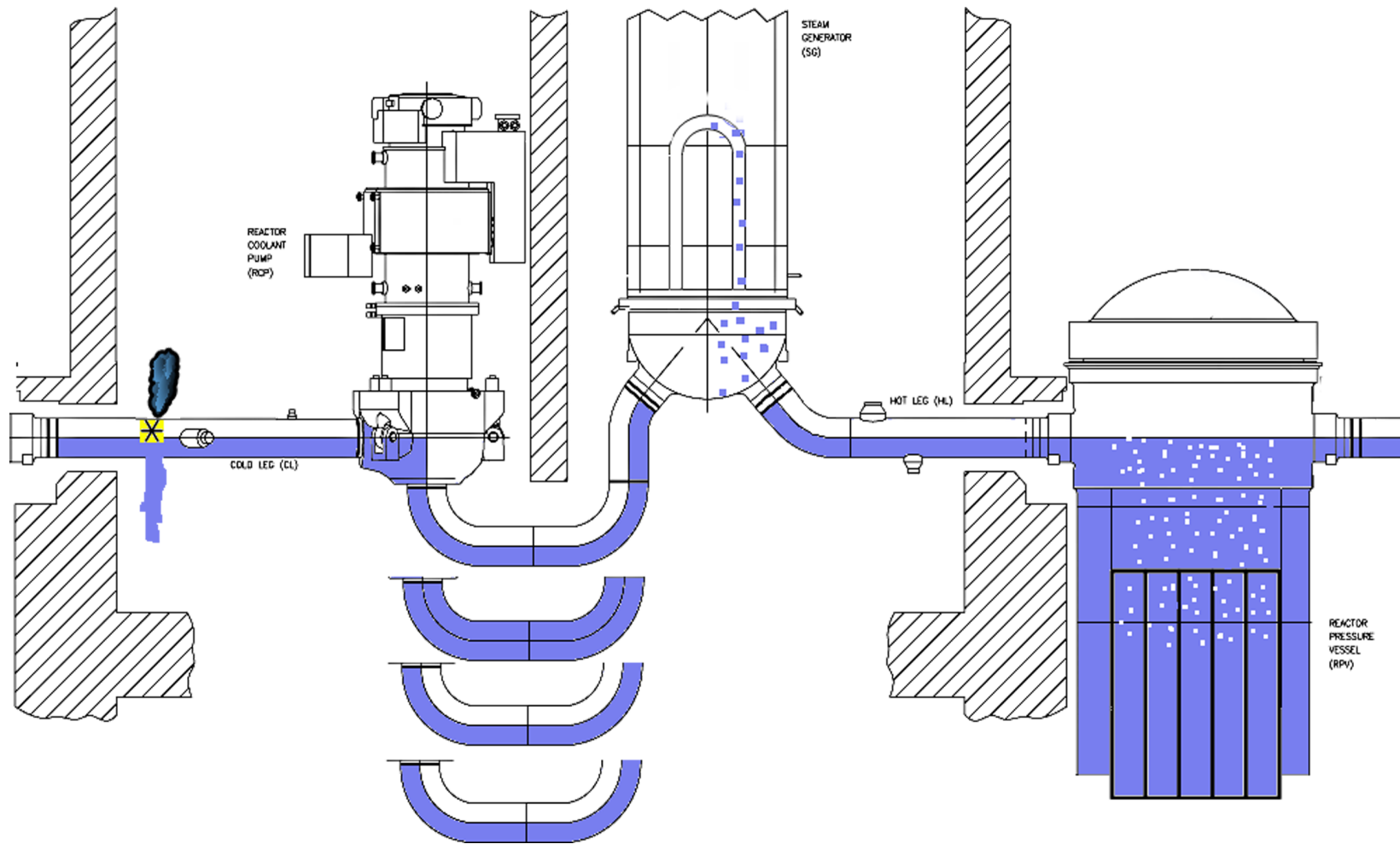
Figure 3-5—RCS Conditions During Post-Reflood

3.3.5   Decay Heat

Like the post-reflood phase, the decay heat phase is characterized as a simple "boiling pot" situation in which decay heat is the only significant heat source remaining in the RCS. In contrast to the post-reflood phase, it is expected that fluid flow through the RCS loops is significantly reduced by lower steam generation coming from the core and the formation of loop seals in the horizontal piping segment near the reactor coolant pump suction. The oscillatory hydraulic behavior in the RCS makes it possible for one or more loop seals to clear, which would perturb mass and energy releases. While the loop seal clearing phenomenon is intermittent, integrated mass and energy flows are not sensitive to loop seal clearing uncertainties. Figure 3-6 illustrates the RCS conditions during the decay heat phase.

For the U.S. EPR, a manual realignment of a majority of the LHSI from the cold leg to the hot leg injection location takes place early in this final LBLOCA phase (about 60 minutes after the initiating event). This realignment serves both as a mechanism for removing core decay heat, leading to complete steam quenching, and for maintaining core boron concentrations below the threshold concentration for precipitation. Only core heat removal phenomena are considered in characterizing mass and energy releases.

Mass and energy releases are impacted in two ways: coolant mixing in the upper plenum and core region and condensation efficiency between steam flows and safety injection in the hot legs and upper plenum. With regard to steam condensation, this phenomenon reduces the overall steam flow through the loops to the break. Safety injection water penetrates the upper plenum and the periphery of the core below the hot leg nozzle, providing emergency core coolant. Mixing of this coolant in the upper plenum and core region is driven by buoyancy processes. Coolant leaving the core towards a cold leg break might be subcooled because of incomplete mixing; however, the realignment provides additional safety injection flow that otherwise could bypass the core during cold leg injection. During this later LBLOCA phase, the hot leg break is

mitigated, such that the reduction in LHSI from the possible loss of one train to the
break is not penalizing to containment pressure (or fuel cladding temperatures). In
addition, there is efficient ECC mixing since the colder safety injection coolant should
fall along the core periphery before flowing back up through hotter fuel assemblies.

The principal phenomena during this phase are driven by decay heat removal and are
related to the effectiveness of coolant mixing, both within the core region and in the hot
leg at the point of safety injection.
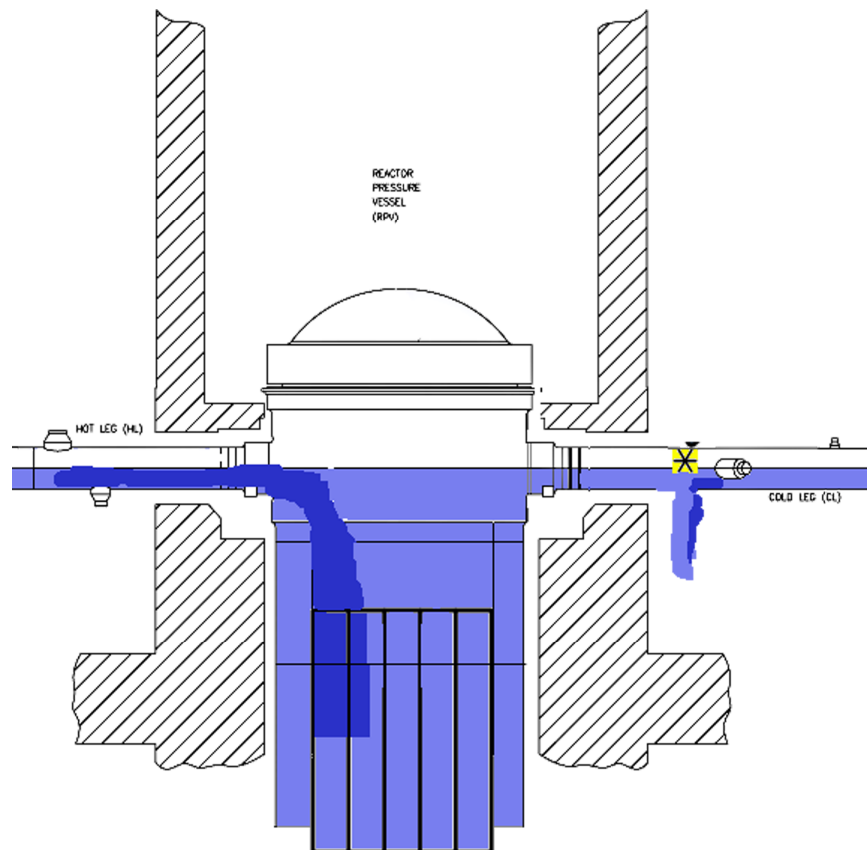
Figure 3-6—RCS Conditions during the Decay Heat Phase

3.3.6   Containment Response

Containment response is characterized by two distinct LBLOCA phases. The first one
(blowdown) is a large injection of hot steam corresponding to RCS depressurization.
The high rate of steam injection during this period rapidly increases containment

temperature and pressure, inducing a turbulent atmosphere. At this stage, forced convection and condensation are the most important heat transfer mechanisms. The second phase (post-blowdown) is distinguished by much less atmospheric turbulence, where natural convection and condensation are the principal heat transfer processes.

At the moment of an LBLOCA in a U.S. EPR, the resulting pressure opens rupture and convection foils above the equipment rooms, thereby providing atmospheric communication between the outer accessible areas and the inner equipment rooms. Shortly thereafter, mixing dampers (connecting the lower portion of the outer accessible region of the containment and the IRWST air space) open on an absolute pressure or pressure differential between the accessible areas and the equipment rooms. At that moment the containment becomes a single convective volume and a highly mixed steam-air mixture is forcibly distributed throughout the containment.

Figure 3-7 illustrates the expected heat and mass transfer mechanisms defining U.S. EPR containment response dynamics. The lowest compartment in this rendering represents the IRWST. The IRWST, with its coupling to the LHSI heat exchanger cooling chain, is the ultimate heat sink for long-term cooling. Before this system becomes the dominant heat removal mechanism in the containment, heat is passively removed from the containment atmosphere by the containment floors, walls, and other structures as the environment is driven to thermal equilibrium. Following the blowdown phase, which forcibly delivers the steam/air mixture throughout the containment, the rate at which the containment achieves thermal equilibrium is a function of buoyancy-driven atmospheric mixing.

In Figure 3-7, $\left.\rho,\overset{\bullet}{m}\right|_{in,g}$ and $\left.\rho,\overset{\bullet}{m}\right|_{in,l}$ represent the density and mass flow for steam and water, respectively, entering the containment from the break in the RCS. The hot water spills on compartment floors and drains to the IRWST which is below the equipment rooms. The high-temperature steam rises, displacing air, and diffusing throughout the containment. Immediately, the containment walls, dome, and internal structures (mostly

concrete and steel) begin to cool (Q) and condense the steam that comes into contact with them ($\dot{m}_c$). The wetting of surfaces by condensation further enhances the heat removal rates. The condensate coalesces and drains to the IRWST.

Following the initial blowdown, the higher temperatures and steam concentrations in the equipment rooms, i.e., areas near the break, cause a buoyancy imbalance between the column of atmosphere within this area and that residing beyond this inner containment region. This imbalance drives a natural circulation flow path characterized by a rising hot steam/air mixture plume in the lower and inner regions of the containment, and a falling cold mixture in the outer regions of the containment (both high and low areas). This circulation is sustained as long as the outer structure effectively cools the steam/air mixture.

Long-term reliance on these natural processes is reduced and eventually eliminated by the termination of core steaming. This is accomplished by the realignment of the ECCS pumped injection at 90 minutes into the event, such that a majority of the core cooling water is delivered to the hot legs. As presented in Section 2.5, the switchover to hot leg injection locations recovers a SIS train that might otherwise be delivered directly to the break if the break is in the cold leg pump discharge piping. Impact to a hypothetical hot leg break is compensated for by ongoing MHSI (and some LHSI) into the cold leg, high efficiency coolant mixing in the RPV, and by the steam generators, a significant source of energy during the post-reflood phase, being segregated from the RCS fluid paths.

Once core steaming has been quenched, RCS effluent entering the containment is liquid only. The liquid drains to the IRWST. The IRWST, with its coupling to the LHSI heat exchanger cooling chain, is the ultimate heat sink for long-term cooling.

For the purposes of identifying evaluation model characteristics and scaling analysis, it is useful to present the containment response phenomena and processes with a hierarchical description. Peterson (Reference 15) previously presented the description shown in Figure 3-8. For in-containment atmospheric mixing, individual enclosures, and

AREVA NP Inc.

ANP-10299NP

Applicability of AREVA NP Containment Response Evaluation Methodology to the
U.S. EPR™ for Large Break LOCA Analysis

Revision 2

Technical Report

Page 3-18

interconnecting channels between enclosures can be grouped as subsystems. The
large enclosures are divided into pool, air space, and structure modules. The
constituent materials of each module are water, non-condensable gases, steel, and
concrete. The fundamental phases are liquid, vapor, and solid. Each phase can exist
in several geometric forms, such as droplets, films, bubbles, jets, etc. Associated with
each geometrical form are fields that describe the distribution of mass, momentum, and
energy.
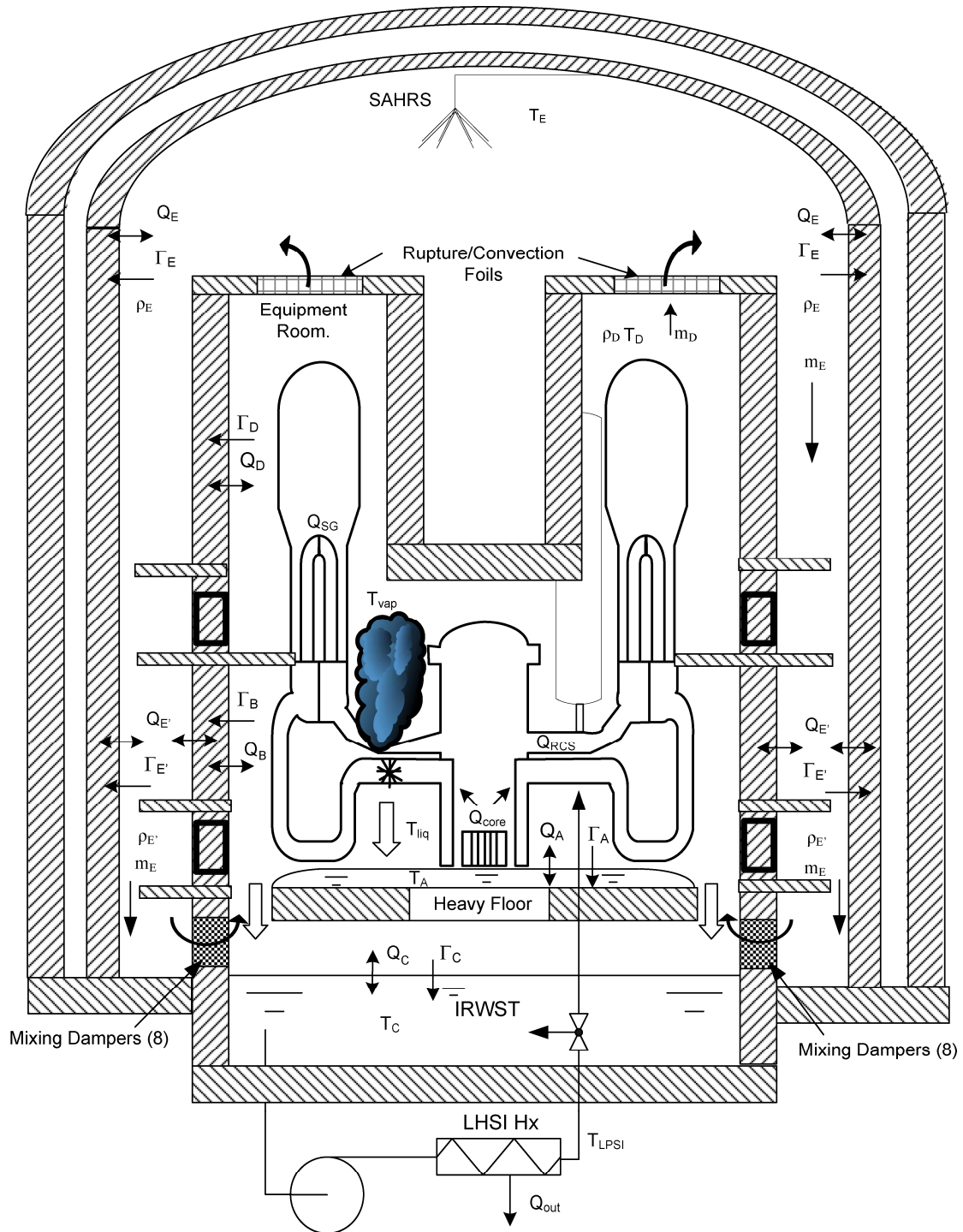
Figure 3-7—Schematic of U.S. EPR Showing Expected Mass and Heat Transfer Mechanisms

AREVA NP Inc.

AREVA NP Inc.
Applicability of AREVA NP Containment Response Evaluation Methodology to the
U.S. EPR™ for Large Break LOCA Analysis
Technical Report

ANP-10299NP
Revision 2

Page 3-20
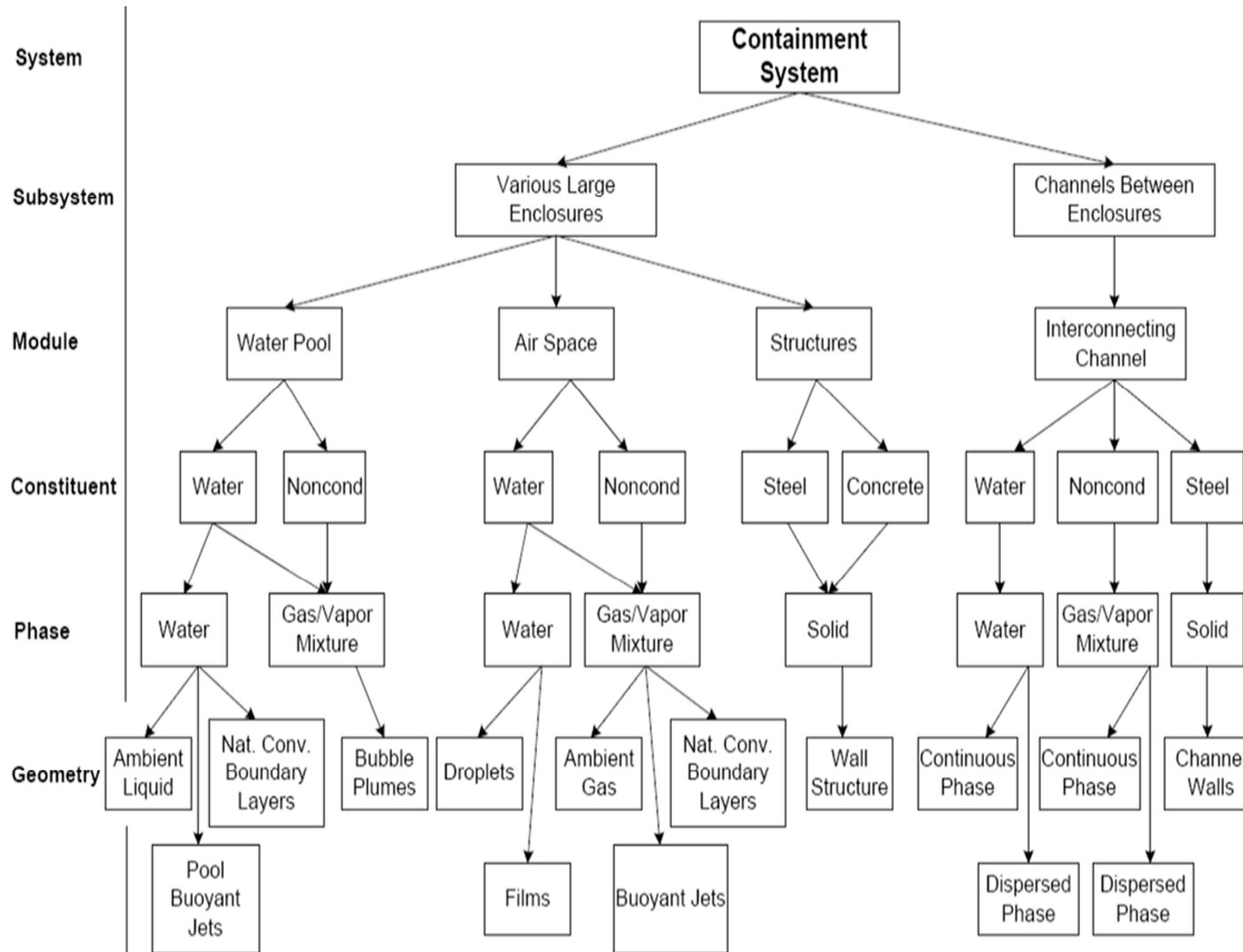
Figure 3-8—Containment Response Hierarchical Description

3.4   PIRT Summaries (EMDAP Step 4)

A ranking procedure similar to that described in Reference 16 is used to determine the phenomena and processes important to evaluating the containment response to an LBLOCA. The objective is to rank the importance by the relative figure-of-merit sensitivity to a particular phenomenon. The collection of this information is referred to as a Phenomena Identification and Ranking Table (PIRT). A PIRT provides the basis for:

- Determining the adequacy of analysis tools (i.e., does the code properly model the important phenomena)

- Establishing the assessment matrix (i.e., identifying test data that contain the appropriate phenomena during each accident phase)

- Identifying phenomenological parameters that can be quantified for evaluating and propagating uncertainties.

AREVA NP sponsored a peer review in July 2008 to develop a PIRT for the U.S. EPR LBLOCA calculations. PIRTs for LBLOCA mass and energy release and containment pressure were prepared and refined through an extended post-meeting review and comment period. These PIRTs are presented in this section, followed by the phenomenological ranking analysis for the phenomena that rank medium or higher.

These ten PIRT participants have an average of 20 years of experience in the area of LOCA and/or containment phenomena. The qualifications of the panel participants are provided in Appendix A.

3.4.1   Mass and Energy (M&E)

The starting point for the peer review was the composite PIRT presented in Reference 17. While the plant design associated with this PIRT is the Westinghouse AP600/1000, many of the phenomena and their importance rankings are applicable to

the U.S. EPR, thus the PIRT benefits from this additional external expertise. Participants thoroughly discussed each itemized entry and changes were made by consensus and recorded.

Phenomenological ranking was determined by majority consensus using a qualitative measure of importance with the following meanings:

- High – Mass and energy releases are strongly influenced by the phenomenon. Phenomenon uncertainties must be characterized and appropriately addressed in the analyses.

- Medium – Mass and energy releases have measurable sensitivity to the phenomenon. Phenomenon uncertainty should be acknowledged (i.e., treated or dispositioned).

- Low – Mass and energy releases have weak or negligible sensitivity to the phenomenon. It is unnecessary to further consider these phenomena in the evaluation methodology development process.

The expected behavioral uncertainty or state-of-knowledge was also assessed separately following the compilation of PIRT entries. A state-of-knowledge statement was not applied to phenomenon with a "Low" importance rank. State-of-knowledge is described and defined by the following terms and associated meanings:

- Good – Phenomenon has been explicitly observed in test programs. Its behavior is well understood and characterized over the expected event conditions.

- OK – Phenomenon has been explicitly observed or inferred in test programs. The phenomenon may be sensitive to subscale phenomenological dynamics or integral effects. Phenomenon characterization is reasonably complete over the expected event conditions.

- Deficient – Phenomenon may or may not have been the subject of explicit test programs. The phenomenon has not been previously characterized over the expected event conditions.

Of particular interest in post-PIRT activities are the phenomena of high rank or deficient characterization. The phenomena identified as such in the following PIRT are explicitly considered in subsequent EMDAP steps.

3.4.1.1   Blowdown

Table 3-1 summarizes the PIRT committee consensus and includes the state-of-knowledge assessment for medium and high rank phenomena during the blowdown phase.

Table 3-1—Consensus Large LOCA M&E Release PIRT: Blowdown

Component / Phenomena	Importance Ranking	State of Knowledge
Global Fluid Conditions (Initial Fluid Stored Energy, RCS Volume)	High	Good
Core		
Stored Energy	Medium	OK
Oxidation	Low	
Decay Heat	Low	
Reactivity-Void	Medium	Good
Reactivity- Boron	Medium	OK
DNB	Medium	Good
Post-CHF	Medium	OK
Rewet	Medium	OK
Reflood Heat Transfer	N/A	
Nucleate Boiling	Medium	Good
Multi-D Flow	Low	
Void generation / distribution/two-phase level	Low	
Entrainment/De-entrainment	Low	
Flow Reversal/Stagnation	Medium	OK
Downcomer		
Entrainment / De-entrainment	Medium	OK
Condensation	Medium	OK
Countercurrent, slug, nonequilibrium	Low	
Hot Wall	Low	
Nucleate Boiling	Low	
Multi-D Effects	Medium	OK
Flashing	Medium	OK
Liquid Level Oscillations	Medium	OK

Table 3-1—Consensus Large LOCA M&E Release PIRT: Blowdown

Component / Phenomena	Importance Ranking	State of Knowledge
Upper Head		
Initial Water Temperature	Medium	Good
Flow Path Area / Flow	Low	
Metal Heat	Low	
Upper Plenum		
Entrainment / De-entrainment	Low	
Phase Separation	Low	
Counter Current Flooding	Low	
Two-Phase Convection	Low	
Bypass	Low	
Lower Plenum		
Sweep-out	Medium	Good
Hot Wall	Low	
Multi-D Effects	Medium	Good
Hot Leg		
Condensation	N/A	
Entrainment / De-entrainment	Medium	OK
Flow Reversal	Low	
Void Distribution	Low	
Two-Phase Convection	Low	
SI Mix	N/A	
Pressurizer		
Early Quench/Flow	Low	
Critical Flow in Surge Line	Low	
Flashing	Low	
Steam Generator		
Initial Fluid Stored Energy (Secondary)	Low	
SG Isolation	Low	
Heat Transfer	Medium	Good
Steam Binding	Low	
Delta-P, Form Losses	Medium	Good
Secondary Stratification	Low	
Feedwater	Low	
Pump		
Two-phase Performance	Medium	Good
Delta-P, Form Losses	Medium	Good
Cold Leg / Accumulator		
Condensation / SI Discharge	Medium	Good
Non-condensable Gases	Low	
Accumulator Discharge (Flow)	High	Good
Flow Asymmetries	Low	
SI Mix	Low	
IRWST Temperature	N/A	
Break		
Flow	High	Good
Flashing	High	Good
Containment Pressure	Low	

Table 3-1—Consensus Large LOCA M&E Release PIRT: Blowdown

Component / Phenomena	Importance Ranking	State of Knowledge
Loop		
2-Phase Delta-P	Medium	Good
Oscillations	Low	
Flow Split	Medium	OK

3.4.1.1.1   High Rank Phenomena

The principal phenomena affecting mass and energy release during blowdown are the initial fluid stored energy and total RCS volume, i.e., global fluid conditions. The rate of mass and energy release is coupled to the critical flow condition at the break plane. Flashing at the break plane causes a reduction in the break flow; however, during blowdown it is closely linked to critical flow and, as such, is ranked similarly. In addition, the introduction of accumulator flow and its subsequent mixing with steam flowing through the RCS will change the fluid conditions at the break.

3.4.1.1.2   Medium Rank Phenomena

Any phenomena clearly contributing to mass and energy transport not appearing as a high rank phenomenon are ranked as medium. The next most important phenomenon influencing mass and energy release dynamics is fluid delivery through the downcomer and lower plenum into the core region. ECCS bypass is not considered to be a unique phenomenon; rather the result of all identified downcomer phenomena. While ECCS bypass is arguably a highly important phenomenon contributing to the end of blowdown time, it is the complex integral effect of many constitutive phenomena with no particularly dominant phenomenon. As such, the related phenomena—pump characteristics, lower plenum/downcomer interfacial effects (e.g., condensation and bypass), core stored energy, core reactivity, and core heat transfer—fall within this category.

Removal of steam generator energy becomes significant as primary coolant is entrained through the steam generator tube side. As RCS pressure becomes lower than the

secondary-side pressure, the secondary transitions from a heat sink to a heat source. Secondary heat transfer to the primary vaporizes droplets and superheat steam. Piping and component flow resistances have a moderate influence on mass and energy released during blowdown.

3.4.1.2   Refill

Table 3-2 summarizes the PIRT committee consensus and includes the state-of-knowledge assessment for medium and high rank phenomena during refill.

Table 3-2—Consensus Large LOCA M&E Release PIRT: Refill

Component / Phenomena	Importance Ranking	State of Knowledge
Global Fluid Conditions (Initial Fluid Stored Energy, RCS Volume)	N/A	
Core		
Stored Energy	Low	
Oxidation	Low	
Decay Heat	Low	
Reactivity-Void	Low	
Reactivity- Boron	Low	
DNB	Low	
Post-CHF	Low	
Rewet	Low	
Reflood Heat Transfer	N/A	
Nucleate Boiling	Low	
Multi-D Flow	Low	
Void generation / distribution/two-phase level	Low	
Entrainment / De-entrainment	Low	
Flow Reversal / Stagnation	Low	
Downcomer		
Entrainment / De-entrainment	Medium	OK
Condensation	Medium	OK
Countercurrent, slug, nonequilibrium	Medium	OK
Hot Wall	Low	
Nucleate Boiling	Low	
Multi-D Effects	Medium	OK
Flashing	Low	
Liquid Level Oscillations	Medium	OK
Upper Head		
Initial Water Temperature	N/A	
Flow Path Area / Flow	Low	
Metal Heat	Low	
Upper Plenum		
Entrainment / De-entrainment	Low	

Table 3-2—Consensus Large LOCA M&E Release PIRT: Refill

Component / Phenomena	Importance Ranking	State of Knowledge
Phase Separation	Low	
Counter Current Flooding	Low	
Two-Phase Convection	Low	
Bypass	Low	
Lower Plenum		
Sweep-out	Low	
Hot Wall	Medium	OK
Multidimensional Effects	Low	
Hot Leg		
Condensation	N/A	
Entrainment / De-entrainment	Low	
Flow Reversal	Low	
Void Distribution	Low	
Two-Phase Convection	Low	
SI Mix	N/A	
Pressurizer		
Early Quench/Flow	Low	
Critical Flow in Surge Line	N/A	
Flashing	N/A	
Steam Generator		
Initial Fluid Stored Energy (Secondary)	N/A	
SG Isolation	Low	
Heat Transfer	Low	
Steam Binding	Low	
Delta-P, Form Losses	Low	
Secondary Stratification	Low	
Feedwater	Low	
Pump		
Two-phase Performance	Low	
Delta-P, Form Losses	Low	
Cold Leg / Accumulator		
Condensation / SI Discharge	High	Good
Non-condensable Gases	Medium	Good
Accumulator Discharge (Flow)	High	Good
Flow Asymmetries	Low	
SI Mix	Low	
IRWST Temperature	Low	
Break		
Flow	Low	
Flashing	N/A	
Containment Pressure	Medium	OK
Loop		
2-Phase Delta-P	Low	
Oscillations	Medium	OK
Flow Split	Low	

3.4.1.2.1   High Rank Phenomena

In the refill phase, the bulk of the mass and energy release from the RCS is the result of accumulator inventory and MHSI, and depends on the break location. For the cold leg pump discharge break, accumulator and pumped injection delivered to the broken loop subsequently escapes out the break. For other break locations, mass and energy release is primarily steam and the refill period does not last as long. As such, the two ECCS delivery mechanisms are the only two phenomena identified as being highly important during refill.

3.4.1.2.2   Medium Rank Phenomena

Fluid flow phenomena contributing to mass and energy transport within the cold legs, downcomer, and lower plenum are identified as having medium influence. In addition, with the possibility of reverse flow at the break, containment pressure and the effects of non-condensable gases are also included. Instabilities in the delivery of safety injection cause oscillations that influence the mass and energy releases during this period.

3.4.1.3   Reflood

Table 3-3 summarizes the PIRT committee consensus and includes the state-of-knowledge assessment for medium and high rank phenomena during reflood.

Table 3-3—Consensus Large LOCA M&E Release PIRT: Reflood

Component / Phenomena	Importance Ranking	State of Knowledge
Global Fluid Conditions| (Initial Fluid Stored Energy, RCS Volume)	N/A	
Core		
Stored Energy	High	OK
Oxidation	Low	
Decay Heat	High	Good
Reactivity-Void	Low	
Reactivity- Boron	Low	
DNB	N/A	
Post-CHF	N/A	
Rewet	N/A	
Reflood Heat Transfer	High	OK
Nucleate Boiling	Medium	Good
Multi-D Flow	Low	
Void generation / distribution / two-phase level	High	OK
Entrainment / De-entrainment	High	OK
Flow Reversal / Stagnation	Low	
Downcomer		
Entrainment/De-entrainment	Medium	OK
Condensation	High	OK
Countercurrent, slug, nonequilibrium	Medium	OK
Hot Wall	Medium	OK
Nucleate Boiling	Medium	OK
Multi-D Effects	Medium	OK
Flashing	Low	
Liquid Level Oscillations	Medium	OK
Upper Head		
Initial Water Temperature	N/A	
Flow Path Area / Flow	Low	
Metal Heat	Low	
Upper Plenum		
Entrainment / De-entrainment	High	OK
Phase Separation	High	OK
Counter Current Flooding	Medium	OK
Two-Phase Convection	Low	
Bypass	Medium	Deficient[*]
Lower Plenum		
Sweep-out	N/A	
Hot Wall	Low	

---

[*] Addressed in subsequent sections

Table 3-3—Consensus Large LOCA M&E Release PIRT: Reflood

Component / Phenomena	Importance Ranking	State of Knowledge
Multidimensional Effects	Low	
Hot Leg		
Condensation	N/A	
Entrainment / De-entrainment	High	OK
Flow Reversal	Low	
Void Distribution	High	Good
Two-Phase Convection	Low	
SI Mix	N/A	
Pressurizer		
Early Quench/Flow	Low	
Critical Flow in Surge Line	N/A	
Flashing	N/A	
Steam Generator		
Initial Fluid Stored Energy (Secondary)	N/A	
SG Isolation	N/A	
Heat Transfer	High	Good
Steam Binding	High	OK
Delta-P, Form Losses	Medium	Good
Secondary Stratification	Medium	Good
Feedwater	Low	
Pump		
Two-phase Performance	N/A	
Delta-P, Form Losses	Medium	Good
Cold Leg / Accumulator		
Condensation / SI Discharge	High	Good
Non-condensable Gases	High	Good
Accumulator Discharge (Flow)	Medium	OK
Flow Asymmetries	Medium	OK
SI Mix	Medium	OK
IRWST Temperature	Medium	OK
Break		
Flow	Medium	Good
Flashing	Low	
Containment Pressure	Medium	Good
Loop		
2-Phase Delta-P	Medium	Good
Oscillations	Medium	OK
Flow Split	Medium	OK

AREVA NP Inc.   ANP-10299NP
Applicability of AREVA NP Containment Response Evaluation Methodology to the   Revision 2
U.S. EPR™ for Large Break LOCA Analysis
Technical Report   Page 3-31

3.4.1.3.1   High Rank Phenomena

High rank phenomena during reflood relate to all processes affecting heat removal from the core and steam generators. Core stored energy, decay heat, and secondary-to-primary heat transfer are the principal energy sources. The dominant phenomena associated with the delivery of coolant to these components are considered most important, including:

- ECCS delivery related phenomena (including, for example, pumped safety injection and steam binding).

- Phenomena that destabilize core reflooding (i.e., oscillations and nitrogen gas).

- Phenomena (such as entrainment) causing primary coolant to be swept into the steam generator primary tube side.

3.4.1.3.2   Medium Rank Phenomena

The reflood phase is very active with many relevant LBLOCA phenomena. All fluid flow phenomena contributing to mass and energy transport within the RCS are considered medium rank. Along with the previously identified high rank phenomena, additional phenomena impacting reflood rates include steam/water ECC mixing, downcomer heat transfer, and containment pressure. Phenomena associated with components having little impact on the mass and energy release dynamics are excluded (i.e., lower plenum, upper head, and pressurizer). Other phenomena not included are core reactivity, fuel oxidation, and two-phase convection from RCS structures (i.e., other than in the core and steam generator regions). Oxidation is of low importance for the U.S. EPR because temperatures are not high enough to cause oxidation.

3.4.1.4   Post-Reflood

Table 3-4 summarizes the PIRT committee consensus and includes the state-of-knowledge assessment for medium and high rank phenomena during the post-reflood phase.

Table 3-4—Consensus Large LOCA M&E Release PIRT: Post-Reflood

Component / Phenomena	Importance Ranking	State of Knowledge
Global Fluid Conditions (Initial Fluid Stored Energy, RCS Volume)	N/A	
Core		
Stored Energy	N/A	
Oxidation	N/A	
Decay Heat	High	Good
Reactivity-Void	Low	
Reactivity- Boron	Low	
DNB	N/A	
Post-CHF	N/A	
Rewet	N/A	
Reflood Heat Transfer	N/A	
Nucleate Boiling	Medium	Good
Multi-D Flow	Medium	Good
Void generation / distribution / two-phase level	Medium	OK
Entrainment / De-entrainment	Low	
Flow Reversal/Stagnation	N/A	
Downcomer		
Entrainment / De-entrainment	Low	
Condensation	Medium	OK
Countercurrent, slug, nonequilibrium	Low	
Hot Wall	Low	
Nucleate Boiling	Low	
Multi-D Effects	Low	
Flashing	N/A	
Liquid Level Oscillations	Low	
Upper Head		
Initial Water Temperature	N/A	
Flow Path Area / Flow	Low	
Two-Phase Convection	Medium	OK
Upper Plenum		
Entrainment / De-entrainment	High	OK
Phase Separation	High	OK
Counter Current Flooding	Low	
Two-Phase Convection	Medium	OK
Bypass	Low	
Lower Plenum		
Sweep-out	N/A	
Hot Wall	Low	

Table 3-4—Consensus Large LOCA M&E Release PIRT: Post-Reflood

Component / Phenomena	Importance Ranking	State of Knowledge
Multidimensional Effects	Low	
Hot Leg		
Condensation	N/A	
Entrainment / De-entrainment	High	OK
Flow Reversal	Medium	Good
Void Distribution	Medium	Good
Two-Phase Convection	Medium	OK
SI Mix	N/A	
Pressurizer		
Early Quench/Flow	N/A	
Critical Flow in Surge Line	N/A	
Flashing	N/A	
Steam Generator		
Initial Fluid Stored Energy (Secondary)	N/A	
SG Isolation	N/A	
Heat Transfer	High	Good
Steam Binding	Medium	OK
Delta-P, Form Losses	Medium	Good
Secondary Stratification	Medium	Good
Feedwater	Low	
Pump		
Two-phase Performance	N/A	
Delta-P, Form Losses	Medium	Good
Cold Leg / Accumulator		
Condensation / SI Discharge	Medium	Good
Non-condensable Gases	Low	
Accumulator Discharge (Flow)	N/A	
Flow Asymmetries	Low	
SI Mix	Low	
IRWST Temperature	Medium	OK
Break		
Flow	Low	
Flashing	Low	
Containment Pressure	Medium	OK
Loop		
2-Phase Delta-P	Medium	Good
Oscillations	Medium	OK
Flow Split	Medium	OK

3.4.1.4.1   High Rank Phenomena

For the simple "boiling pot" that characterizes the post-reflood phase, high rank

phenomena are those affecting core and steam generator heat removal. Decay heat

and secondary fluid sensible heat are the principal energy sources. The high rank phenomena include these heat sources and the phenomena associated with the two-phase mixture state of the coolant neighboring these energy sources (i.e., heat transfer and entrainment / de-entrainment). Heat transfer is primarily by nucleate boiling; however, it is the two-phase condition of the coolant mixture that most affects mass and energy release.

3.4.1.4.2   Medium Rank Phenomena

The fluid flow and heat transfer phenomena not ranked high that affect the coolant mixture condition in the core and steam generator regions are ranked medium. Medium rank fluid flow phenomena exclude phenomena in the cold leg piping and in components between the steam generator and the core region, with the exception of flow resistances in the pumps and loops. Medium rank heat transfer phenomena highlight the importance of RCS structure stored energy removal during this phase (i.e., upper plenum, upper head, and hot legs). Containment pressure is included because it sets the back-pressure, and thereby influences the releases. Containment pressure may span a large range because of the uncertainties in mass and energy release and containment response.

3.4.1.5   Decay Heat

Table 3-5 summarizes the PIRT committee consensus and includes the state-of-knowledge assessment for medium and high rank phenomena during decay heat.

Table 3-5—Consensus Large LOCA M&E Release PIRT: Decay Heat

Component / Phenomena	Importance Ranking	State of Knowledge
Global Fluid Conditions (Initial Fluid Stored Energy, RCS Volume)	N/A	
Core		
Stored Energy	N/A	
Oxidation	N/A	
Decay Heat	High	Good
Reactivity-Void	Low	
Reactivity- Boron	Low	

Table 3-5—Consensus Large LOCA M&E Release PIRT: Decay Heat

Component / Phenomena	Importance Ranking	State of Knowledge
DNB	N/A	
Post-CHF	N/A	
Rewet	N/A	
Reflood Heat Transfer	N/A	
Nucleate Boiling	Medium	Good
Multi-D Flow	High	Good
Void generation / distribution / two-phase level	Low	
Entrainment / De-entrainment	Low	
Flow Reversal/Stagnation	N/A	
Downcomer		
Entrainment / De-entrainment	Low	
Condensation	Medium	OK
Countercurrent, slug, nonequilibrium	N/A	
Hot Wall	Low	
Nucleate Boiling	Low	
Multi-D Effects	Low	
Flashing	N/A	
Liquid Level Oscillations	Low	
Upper Head		
Initial Water Temperature	N/A	
Flow Path Area / Flow	Low	
Metal Heat	Low	
Upper Plenum		
Entrainment / De-entrainment	Low	
Phase Separation	High	Deficient*
Counter Current Flooding	Low	
Two-Phase Convection	Low	
Bypass	Low	
Lower Plenum		
Sweep-out	N/A	
Hot Wall	Low	
Multidimensional Effects	Low	
Hot Leg		
Condensation	High	Deficient*
Entrainment / De-entrainment	Low	
Flow Reversal	Low	
Void Distribution	Low	
Two-Phase Convection	Low	
SI Mix	High	Deficient*
Pressurizer		
Early Quench / Flow	N/A	
Critical Flow in Surge Line	N/A	

---

* Addressed in subsequent sections

AREVA NP Inc.   ANP-10299NP
Applicability of AREVA NP Containment Response Evaluation Methodology to the   Revision 2
U.S. EPR™ for Large Break LOCA Analysis
Technical Report   Page 3-36

Table 3-5—Consensus Large LOCA M&E Release PIRT: Decay Heat

Component / Phenomena	Importance Ranking	State of Knowledge
Flashing	N/A	
Steam Generator		
Initial Fluid Stored Energy (Secondary)	N/A	
SG Isolation	N/A	
Heat Transfer	Low	
Steam Binding	Low	
Delta-P, Form Losses	Low	
Secondary Stratification	Low	
Feedwater	Low	
Pump		
Two-phase Performance	N/A	
Delta-P, Form Losses	Low	
Cold Leg / Accumulator		
Condensation / SI Discharge	Medium	OK
Non-condensable Gases	Low	
Accumulator Discharge (Flow)	N/A	
Flow Asymmetries	Low	
SI Mix	Low	
IRWST Temperature	Medium	OK
Break		
Flow	Low	
Flashing	Low	
Containment Pressure	Medium	OK
Loop		
2-Phase Delta-P	Low	
Oscillations	Medium	OK
Flow Split	Medium	OK

3.4.1.5.1   High Rank Phenomena

Only three phenomena are considered high rank in this simple "boiling pot" scenario: decay heat, coolant mixing in the upper plenum and core (considered separately), and steam condensation in the hot leg and upper plenum.

3.4.1.5.2   Medium Rank Phenomena

Phenomena affecting heat transfer and coolant mixing in the upper plenum and the core and the fluid state upon reaching the core are ranked medium. Since the possibility of some loop flow remains (e.g., loop seal clearing), related phenomena (e.g., cold leg condensation) are also included.

As with the post-reflood phase, containment pressure is included because it represents the back-pressure influencing releases and varies significantly due to continued RCS mass and energy releases and heat transfer in the containment, primarily on the large passive heat sinks.

3.4.2   Containment Pressure

Reference 18 captures the current state-of-the-art understanding of containment phenomena, including the identification and ranking of important containment response phenomena in a large, dry PWR containment. The Organization for Economic Cooperation and Development / Nuclear Energy Agency (OECD/NEA) experts prepared a PIRT that considered an LBLOCA through the "core damage phase of a severe accident." In addition, they considered no delineation of LBLOCA phases and addressed three figures-of-merit: pressure, local temperature, and steam-air-hydrogen composition.

The OECD/NEA PIRT, expressing phenomena ranking for total pressure only, appears in Table 3-6 with some modification to reflect the U.S. EPR-specific application. Among the phenomena listed, only two are identified as being highly important for containment pressure. These are free convection (condensation and evaporation driven) and structure conduction. It is notable that fan and spray cooling are given only a medium importance. This is attributed to a unique assumption considered in the PIRT development in which these systems are degraded as a consequence of a worst single failure. As a result, they have little impact on peak pressure, which is a strong function of containment structure surface area and total volume. Atmospheric buoyancy and stratification phenomena are given low-medium and medium rankings for intra-compartment mixing and inter-compartment transport, respectively. Liquid advection is the only other phenomena receiving a ranking other than low.

AREVA NP Inc.
Applicability of AREVA NP Containment Response Evaluation Methodology to the
U.S. EPR™ for Large Break LOCA Analysis
Technical Report

ANP-10299NP
Revision 2

Page 3-38

Table 3-6—PIRT for Containment Conditions Following an LBLOCA

Component	Process	Phenomena	Rank
			Pressure
Atmosphere	Pressurization / Depressurization	Multi-component gas compression/expansion	M
		Aerosol mass and energy exchange	L
		Spray mass and energy exchange	M
		Volume displacement/pool filling or draining	L
		Atmosphere cooling by fan-cooler	M
	Mixing (intracompartment)	Jet-plume gas interaction/entrainment (localized)	L
		Buoyancy/stratification (regional)	L-M
		Buoyancy/wall interaction (regional)	L
		Diffusion (turbulent)	L
		Spray dynamics	L
		Fan dynamics	L
	Transport (intercompartment)	Buoyancy/stratification	M
		Form and friction losses	L
		Aerosol coupling	L
		Liquid water carryover	L
Structure Interior	Heat Transfer	One-dimensional transient conduction	H
		Two- or three-dimensional transient conduction	L
	Mass Transfer	Outgassing (concrete)	L
Structure: Surface (solid and film)	Sensible Heat Transfer	Spray/aerosol deposition or impingement	L
		Free convection	L
		Forced/mixed convection	L
		Radiation (structure to atmosphere)	L
		Radiation (structure to structure)	L
		Liquid film resistance	L
		Liquid film advection	L
	Latent Heat and Mass Transfer (condensation/ evaporation)	Free convection	H
		Forced/mixed convection	L
	Transport (film flow)	Liquid film advection	L-M
		Interfacial shear (film/gas interaction)	L
Pool: Interior	Mixing	Buoyancy/stratification	L
		Bubble dynamics	L
	Transport	Filling and draining	L
		Displacement (pressure driven)	L
	Heat Transfer	Convection (flooded structures)	L
		Boiling	L
		Steam condensation (bubbles)	L
Pool: Surface	Sensible Heat Transfer	Free convection	L
		Forced/mixed convection	L
		Aerosol/spray deposition	L
	Latent Heat and Mass Transfer (condensation/ evaporation)	Free convection	H
		Forced/mixed convection	L

The OECD PIRT is applicable to the U.S. EPR, with few exceptions. Without safety-grade sprays, structure conduction is the principal heat removal mechanism; thus, the ranking is moved from medium-high to high. The spray phenomenon is assumed to include entrained liquid droplets exiting the RCS and retains the rank of medium importance. The other exception is the role of the in-containment refueling water storage tank. The IRWST is the ultimate heat sink, in that mass and energy transported into the IRWST from RCS spillage and the collection of condensate are then removed by the low head safety injection heat exchanger. The ranking of "Pool free convection" is changed to "High" to reflect the importance of heat removal via the IRWST—not so much by free convection, but by the active cooling systems attached to the IRWST—and to acknowledge the low state-of-knowledge of the pool conditions that govern the overall effectiveness of these phenomena and processes.

In summary, the principal phenomena influencing containment pressure response only, together with their rank, are as follows:

- Structure free convection (condensation/evaporation) – High

- Structure conduction – High

- Pool (IRWST) free convection (condensation/evaporation) – High

- Expansion/compression of multi-component gases – Medium

- Inter-compartmental transport by buoyancy – Medium

- Spray/fans – Medium (U.S. EPR sprays are non-safety)

- Local buoyancy/stratification – Low/Medium

- Liquid advection (transport only) – Low/Medium

4.0   ASSESSMENT OF CONTAINMENT RESPONSE PHENOMENA

The credibility of an evaluation methodology relies on the associated verification and validation. Verification is the confirmation that documented statements accurately reflect the evaluation methodology objectives, while validation is the act of demonstrating or testing. Verification typically takes the form of a line-by-line review of coding and supporting evaluation documentation, and confirmation of compliance with an approved quality assurance plan. As the computational analysis tools used in AREVA NP's containment analysis evaluation methodology, the RELAP5-BW and GOTHIC codes are used to predict the physical behavior anticipated during a LOCA. Therefore, these tools are validated using an appropriate assessment base consisting of both separate and integral effects test program results, standard problems, benchmarks with other codes, or analytical exercises with known solutions. A scaling analysis supports both verification and validation by providing independent insight into the dominant physical processes, as indicated by the relative magnitudes of non-dimensional coefficients modifying terms in the field equations.

4.1   Objectives for Assessment Base (EMDAP Step 5)

The assessment matrix supports the evaluation methodology development in defining the nuclear power plant nodalization, quantifying the code accuracy, and demonstrating any code or model scaling effects. The principal objectives are to demonstrate sufficient accuracy in modeling dominant physical processes (determined from a PIRT), appropriate nodalization, independence of scale effects, and the relative insensitivity of compensating error.

4.1.1   PIRT Considerations

The mass and energy release and containment pressure PIRTs presented in Section 3.4 provide a qualitative expression of the relative importance of key phenomena present in an LBLOCA that impact containment pressure response. The assessment matrix must include experiments that address the important phenomena, defined as those with "High"

rank in Table 3-1 – Table 3-6. For deterministic evaluation methodologies, quantifying phenomenological uncertainty for the dominant phenomena is addressed using a bounding model approach. The PIRT can be used either to establish or confirm the appropriate modeling treatment for code parameters explicitly impacting an important phenomenon. Given the disparity of importance among the various phenomena, the code models that describe these phenomena should be examined to a degree meriting the phenomenological importance.

4.1.2   Nodalization Considerations

To evaluate model nodalization sensitivities, experiments are selected that represent the physical configuration and fluid conditions of the selected scenario. Individual experiments cover one or more of the LBLOCA phases identified in Section 3 (i.e., blowdown, refill, reflood, post-reflood, and decay heat).

Reference 16 makes the following statements regarding nodalization:

> *The plant model must be nodalized finely enough to represent both the important phenomena and design characteristics of the nuclear power plant but coarsely enough to remain economical.*
>
> *Thus, the preferred path is to establish a standard nuclear power plant nodalization for the subsequent analysis. This minimizes or removes nodalization, and the freedom to manipulate noding, as a contributor to uncertainty.*
>
> *Therefore, a nodalization selection procedure defines the minimum noding needed to capture the important phenomena. This procedure starts with analyst experience in previous code assessment and application studies and any documented nodalization studies. Next, nodalization studies are performed during the simulation of separate- and integral-effects code data comparisons. Finally, an iterative process using the nuclear power plant model is employed to determine sufficiency of the nuclear power plant model nodalization.*

Given these general recommendations, the goal of a nodalization methodology is to optimize somewhat independent priorities. These include preserving dominant phenomena, minimizing code uncertainty, conforming to design characteristics, and

minimizing computational expense. The modeling approach developed in AREVA NP's containment analysis evaluation methodology is consistent with the ECCS performance analysis methods or simplified with conservative inputs to remove nodalization as a contributor to uncertainty.

4.1.3   Scaling Considerations

As noted in Appendix C of Reference 16, there are two premises on which the assessment process is based. The first premise is that the tests are scalable to a LBLOCA and the second is that the code models themselves provide code predictions scalability. For the first premise to be true, the selection of tests needs to be such that the important phenomena in a PWR LBLOCA are captured by one or more appropriately scaled tests. For the second premise to be true, the phenomenological models in the computer codes should apply to both the PWR LBLOCA and the scaled test. Generally this is done by selecting a number of assessments in facilities of different scale and demonstrating that the code and nuclear power plant nodalization is capable of consistently predicting the experimental data.

4.1.4   Compensating Errors

Because it is difficult to demonstrate that a code does not contain compensating errors, it should be demonstrated that the compensating errors will not produce erroneous results for the selected scenario and nuclear power plant being analyzed. Thus, an attempt must be made to select experiments that cover the range of each important phenomenon observed in the nuclear power plant analyses. Analysis of these experiments will demonstrate that, even if the code contains compensating errors, the code is still capable of reliably predicting the selected scenario in the selected nuclear power plant.

The issue of compensating errors arises from the use of empirically-derived correlations and closure relations in the code, a reduced set of field equations, or simplified modeling approximations. Compensating errors can result in the code being able to predict specific tests but being incapable of predicting other tests. For the LBLOCA, only those

compensating errors which could function in one manner in the assessments and in an entirely different manner in the LBLOCA are a concern. Thus, the assessment matrix must include tests that can be scaled up and that cover the range of the LBLOCA PIRT phenomena.

4.1.5   Summary

As the computational analysis tools used in AREVA NP's containment response evaluation methodology, the RELAP5-BW and GOTHIC codes can only approximate the physical behavior anticipated during a LOCA. As such, an assessment base is necessary to validate the sufficiency of code models and correlations and the overall code accuracy. The objectives of an appropriate assessment base include preserving the dominant phenomena, providing a sufficient degree of model resolution that conforms to important design characteristics, and demonstrating that results are insensitive to scale distortion and possible compensating errors. In addition, AREVA NP's containment analysis evaluation methodology incorporates conservatisms (based on the NRC's SRP as described in Section 8.0) to satisfy the objective of assessing the safety margins for the figures-of-merit.

A review of the general assessment base for the RELAP5-BW and GOTHIC codes is provided in Section 4.3. Based on the evaluation of high-rank phenomena given in Section 5.0, new assessments have been developed for the U.S. EPR application. These are provided in Section 6.0.

4.2   Scaling Analysis and Similarity Criteria (EMDAP Step 6)

A scaling analysis is performed because all integral and most separate effects tests addressing thermal-hydraulic behavior in nuclear power plants are conducted in scaled-down test facilities. Consequently, it is necessary to assure that the important processes of interest are appropriately scaled and to assess the effects of distortions (if present) on processes and parameters of interest to nuclear power plant accident scenarios. As scaling is relevant not only to experimentation but also to analyses based on code

calculations, an efficient methodology for resolving technical issues must integrate both applications. To provide for sufficiency and efficiency, a scaling analysis features both an inductive approach (i.e., top-down) that considers the whole system, and a deductive approach (i.e., bottom-up) that focuses on the parts.

Top-down scaling entails developing detailed non-dimensional governing equations for the physical processes expected to be encountered during accidents. The coefficients for the terms in the governing equations are referred to as Pi ($\prod$) coefficients. Top-down scaling analysis results can be used to identify which phenomena are important to the system behavior and therefore need to be well-scaled in the test facilities. The equations developed are also useful for identifying distortions in the test facilities. Significant differences between the $\prod$ values for the prototype and a test facility are indicative of distortions in the test. This is discussed further in Section 4.4

Bottom-up scaling examines the individual processes that are identified as important through the top-down scaling, and determines whether the test data cover the appropriate ranges of the key variables. One aspect of the comparison is determining whether the experimental data and the prototype cover the same range of the similarity variables (for example, Reynolds Number, Froude Number, Prandtl Number, and Zuber Number) that govern the important phenomena.

The objective of the scaling analysis is to identify the processes, variables, and parameters that govern the system's response in non-dimensional space. Having determined these, one can validate the containment response PIRTs presented in Section 3.4 generated by expert opinion, relate prototype behavior to small scale experiments, identify potential distortions, evaluate the impact of such distortions, and ultimately determine if the available body of data is sufficient to contain the expected phenomena in the prototype's behavior.

The strategy is to use rigorous analysis, existing data results, and first principles to achieve the objective. These are the specific steps:

- Develop a scenario description

- Discretize the scenario in a manageable set of components or elements

- Develop a closed set of governing equations for these elements based on conservation laws and first principles

- Use the closed set of equations to conduct scaling analysis, as follows:

  - Normalize equations to develop non-dimensional coefficients ($\prod$s)

  - Determine the proper reference parameters according to the time period (phase) of interest

  - Choose a reference time (a potentially recurrent step) according to the time scale of interest

  - Evaluate $\prod$s and establish ranking per component and complete system. The figure of merit or primary safety criterion defines the metric with which to determine what process is more or less important.

  - Compare with the experimental system and identify and evaluate the impact of scaling distortions on the figure of merit (see discussion in Section 4.4)

  - Compare dominant $\prod$s and process ranges with available data and assess data sufficiency (see discussion in Section 4.4).

  - Relate PIRT phenomena with system processes and with $\prod$s to determine if ranges of data are sufficient and complete.

4.2.1 Scenario Description

A schematic of a cold-leg break scenario appears in Figure 3-7, showing the processes and components that may participate in the transient. Mass and energy from the reactor coolant system (RCS) escape through the break into the adjacent equipment rooms (ER)

in the inaccessible space, while the ECCS injects liquid back into the RCS. Steam from the break quickly disperses into the ER and into the accessible space (AS) areas where the cooler steel and concrete structures absorb some of the heat by condensing steam. The liquid from the break and the condensate are channeled down to the IRWST, while the remaining mixture of air and steam circulates throughout the containment, allowing further condensation. Water from the IRWST is drawn by the LHSI pumps and delivered to a heat exchanger. A portion of this flow returns to the IRWST to provide minimum pump flow, and the remaining flow is delivered to the reactor coolant system primary loop. In time, the primary depressurizes and becomes a "boiling pot." The ER gas pressure rises at the beginning of the break from the hot steam released into it by the primary, reaches a maximum, and begins to drop as the steam condenses on the walls and the energy escapes to the structures and the passive heat sink.

4.2.2   Problem Discretization

Three types of components or elements are expected:

- A volume in which fluid enters, is stored, or leaves. The state of the gas volumes is defined by their gas mixture temperature and pressure. The state of liquid volumes (or tanks) is defined by the level or hydrostatic pressure at the lowest exit point and the temperature of the liquid. The reactor vessel can be a special case when it contains a two-phase mixture where the collapsed liquid level and steam quality are directly related. In this case the system state requires temperature or pressure, and quality.

- Masses of structures or components that store and conduct heat. Their state is given by their temperature, as it measures the amount of energy they contain.

- There also might be elements such as pipes or ducts in which momentum gets stored or transferred. Such elements are not present in this application for the U.S. EPR containment design.

AREVA NP Inc.   ANP-10299NP
Applicability of AREVA NP Containment Response Evaluation Methodology to the   Revision 2
U.S. EPR™ for Large Break LOCA Analysis
Technical Report   Page 4-8

Inputs and boundary conditions that have no dynamic contribution to the system, but rather represent algebraic (static) relationships are also considered. For example, heat exchangers or pumps.

Following the flow of energy from the reactor core to the passive heat sink (as illustrated in Figure 4-1), the components of interest are:

The arrows in Figure 4-1 suggest interaction between components. This is important because the governing equations are developed from this schematic of the system interactions.
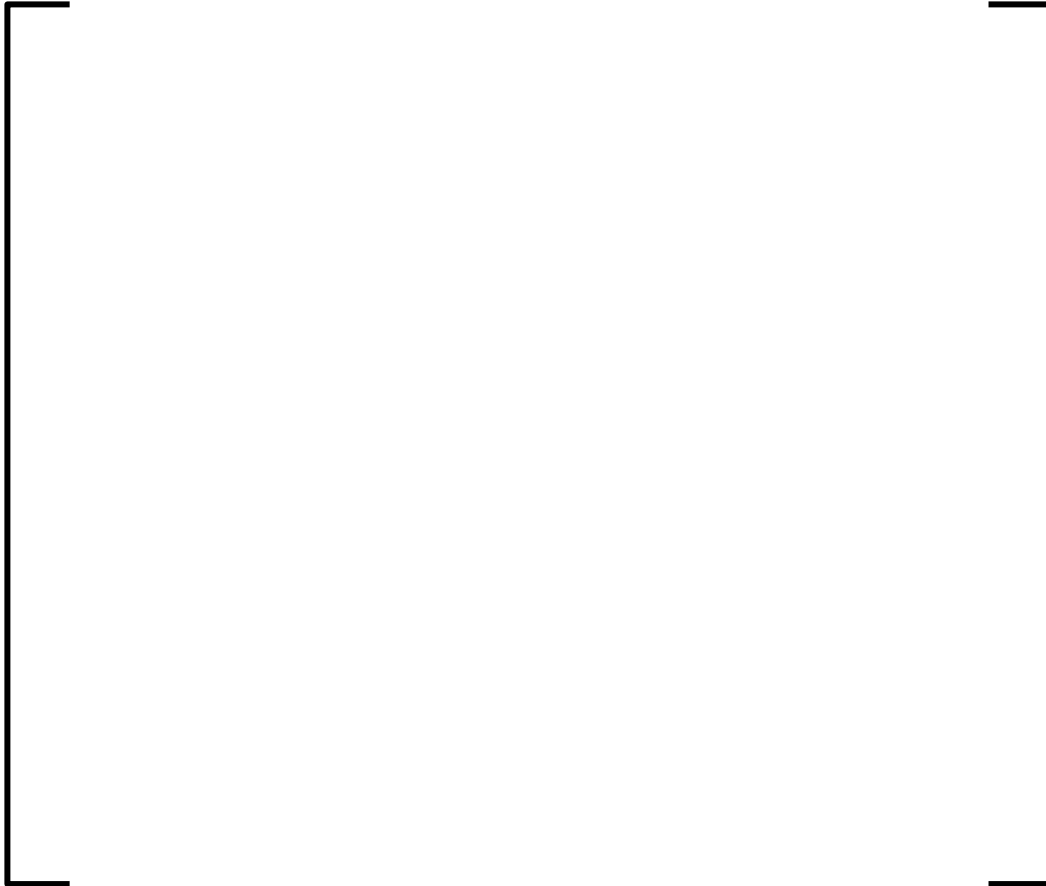
Figure 4-1—System Components

4.2.2.1   Governing Equations

The system governing equations are derived from mass and energy balances on each one of the components listed in Section 4.2.2. This derivation step yields a complete set of state equations that will be used to develop non-dimensional coefficients (∏s). The formal derivation of the governing equations and the development of the non-dimensional coefficients is provided in Appendix B, Subsection 12.4.

4.3 Review of Previous Code Assessments (EMDAP 7)

4.3.1 RELAP5-BW LOCA Assessments

For mass and energy release rates calculations, large best-estimate system thermal-hydraulic codes, such as those based on RELAP5/MOD2 (Reference 21), RELAP5/MOD3 (Reference 22), and TRAC-PF1 (Reference 23), are necessary. AREVA NP has regulatory approval to utilize both the RELAP5-BW and S-RELAP5 thermal-hydraulic analysis codes (References 19 and 24) to predict nuclear power plant response to an LBLOCA for PWRs, in compliance with the 10 CFR 50.46. Both of these codes are derivatives of RELAP5/MOD2 code developed at the Idaho National Engineering Laboratory. Mass and energy release calculations for the U.S. EPR have been evaluated using the RELAP5-BW code. RELAP5-BW maintains much of the original best-estimate models and correlations; however, model refinements and additions were developed by AREVA NP to allow it to be conservatively applied for both fuel cladding and containment response to an LBLOCA.

The RELAP5-BW code has benefited from extensive prior assessments of its ability to predict the accident behavior of existing reactors (References 19, 25, and 26). These prior assessments remain applicable for U.S. EPR LBLOCA calculations. In addition, these assessments build upon the large suite developed originally for the RELAP5/MOD2 code by the Idaho National Engineering Laboratory, the International Code Assessment Program (Reference 27), the Code Applications and Maintenance Program (Reference 28), and also upon the large assessment suite developed for AREVA NP's S-RELAP5 code (Reference 29).

From Section 3.4 the principal phenomena of importance for mass and energy release calculations can be summarized as follows: break discharge model, decay heat, entrainment/de-entrainment, condensation, reflood heat transfer, and upper plenum and core multi-dimensional mixing/void distribution/two-phase liquid level. In considering this subset of phenomena, the principal code assessments performed for RELAP5-BW are Semiscale, FLECHT-SEASET, Cylindrical Core Test Facility (CCTF), Slab Core Test Facility (SCTF), Upper Plenum Test Facility (UPTF), and Loss of Fluid Test (LOFT) Facility. Reference 30 provides a good description of each of these programs and the technical understanding revealed from the individual experiments.

4.3.2   GOTHIC Assessment

The GOTHIC code has also benefited from extensive prior assessments of its ability to predict the accident behavior of existing nuclear power plant containments (Reference 31). These prior assessments remain applicable to the U.S. EPR containment response to an LBLOCA. The GOTHIC code validation and model benchmarks establish the appropriateness of the GOTHIC code and models to predict the containment response to LOCA and main steam line break / feedwater line break (MSLB/FWLB) postulated accidents. The GOTHIC validation base for lumped-parameter and coarsely-meshed distributed parameter models is extensive, with application to several International Standard Problems (ISP) (References 32 – 36); Battelle-Frankfurt Model Containment (BFMC) blowdown tests D-1, D-15, D-16, C-13, and C-15; BFMC hydrogen mixing tests

6, 12, and 20; HEDL hydrogen mixing tests HM-5 and 6; LACE tests LA-5 and 6; Marviken tests 17, 19, 22, and 24; the Carolina Virginia Tube Reactor (CVTR) design-basis accident tests 3, 4, and 5; and the Heissdampfreaktor (HDR) tests V21.1, T31.1, T31.5, and V44. This validation base has also been extended to include the CEC-F2 experiment, VANAM-M2, PAR test MC1 and MC3, all in the BFMC series, and several HDR tests, including simulations of E11.2 and E11.4. Most of these test programs and key results are described in Reference 18.

4.3.3 International Standard Problems - Lessons Learned

International standard problem (ISP) exercises, organized by the OECD, have been conducted specifically for code verification purposes. The main goal has been to increase confidence in the validity and accuracy of codes used in assessing the safety of nuclear installations. These code validation exercises have been formulated to prove simulation accuracy and to quantify uncertainties in simulations. As part of an ISP, several organizations are invited and the participating organizations select the codes and the analysts who will perform the calculations. Information about the test facility and test configuration are provided to the participating organizations, which then develop an independent analysis using their organization's best-practices. Results of these code exercises are provided to the sponsoring organization that, in turn, documents the code comparisons with the experiment data. Typically, a follow-up workshop is held by participants to discuss the results of the code comparisons.

References 18 and 36 provide a synopsis of the current state-of-the-art understanding of containment thermal-hydraulics and the general capability of analytical tools used in containment safety analysis. Much of this understanding has come from the ISP program. Five exercises relevant to thermal-hydraulic and hydrogen distribution have been performed as part of the ISP program to study the performance of both lump parameter and multi-dimensional field codes. These are listed in Table 4-1.

Table 4-1—Relevant International Standard Problems

ISP Name	Facility/Experiment	Description
ISP-23	HDR/T31.5	LBLOCA with natural cooldown
ISP-29	HDR/E11.2	SBLOCA, long-term gas distribution
ISP-35	NUPEC/M-7-1	Gas distribution with containment sprays
ISP-37	BFMC/VANAM M3	Gas distribution with aerosol injection
ISP-47	TOSQAN/ThAI/MISTRA	Both separate and integral effects study of dominant containment phenomena (i.e., wall condensation, buoyancy, stratification, and turbulence)

In each of these ISP exercises, at least one participating organization provided a calculation using a version of the GOTHIC code. As is customary with the ISP program, GOTHIC was not used exclusively. The following discussion highlights the major ISP programs and conclusions.

4.3.3.1   ISP-23 HDR/T31.5

This experiment was performed in the late 1980s in the large, 11,300 m^3 HDR containment. The experiment was designed to emulate the mass and energy contribution of a LBLOCA and the subsequent natural thermal-hydraulic response of a containment. No sprays or fan coolers were involved. As such, the main interest was the thermal loads expected on structures during a large blowdown and the long-term temperature and pressure behavior. Both "blind" and "open" code studies were contributed to the exercise. Overall, the code prediction of the pressure response was good. Specifically, the relatively tight range of results was considered "indicative of the integral capabilities of all involved codes to simulate well the overall heat absorption by the containment structures during the post-blowdown period" (Reference 18).

Assessment of how well the codes capture local phenomena was determined from temperature predictions. A pronounced stable temperature stratification (40 K over total height) preventing convective flows was observed in the measurement results in the late term; however, containment pressures were significantly reduced by that time from heat

absorption into structures (< 50% of the peak). Throughout the long-term phase of the experiment, deviations between locally measured and predicted temperatures were attributable to spatial effects (i.e., elevation and dead-end locations); however, these results were of comparable magnitude. The scatter of temperature predictions correspond to shortcomings in the prediction of heat transfer coefficients and transport processes. Most of the contributed studies (both lump parameter and field codes) predicted higher than measured local flow rates. For lumped parameter codes this translated into over-mixing of the steam-gas mixture and, as a consequence, temperatures were under-predicted in the upper containment region and over-predicted in the lower containment region. Results from field codes were considered equally ineffective at predicting local heat transfer phenomena, however for different reasons.

An overall code result improvement was not observed between the "blind" and "open" studies. Reference 18 concluded that "the state-of-the-art of the codes predictive capabilities to describe the traditional DBA effects had been reached." Further, the analysis of the long-term post-LOCA containment behavior was considered "limited … to simulate the distribution of energy and the heat exchange between the containment atmosphere and … structures." Therefore, it was further concluded that current conservative licensing procedures remain justified for design decisions and safety analysis.

4.3.3.2   ISP-29 HDR/E11.2

The planning of HDR Test E11.2, performed during the early 1990s, was motivated by interest in hydrogen distribution during a severe accident. From the phenomenological point-of-view, this experiment retains similar heatup and cooldown phases. Cooldown was enhanced in Test E11.2 through spray actuation on the outer surface of the steel containment shell. The main concern of this ISP was containment internal natural convection flows, heat absorption by structure, and gas distribution (with the emphasis on hydrogen).

Certain problems with information disseminated about the tests contributed to results that the project leaders considered unsatisfactory. Nonetheless, overall containment peak pressure was predicted within 15% in all code studies and the long-term behavior tended to improve from that maximum deviation. The margins for the observed local temperature simulations consistently indicated energy distribution problems within the containment atmosphere. The comparison of calculated and measured atmosphere temperatures and of the gas concentrations demonstrated that too much energy and gas transport was simulated to have occurred. Thermal non-equilibrium between the containment atmosphere and condensate formed on containment internal structures may have amplified the simulation difficulties. Recalculations with improved facility information subsequently led to improved agreement between the calculated and measured pressure transients. This improvement was essentially related to the application of a realistic energy input function.

Test E11.2 also showed that during accidents with small leaks, at medium or high elevation, pronounced and sustained temperature stratifications can occur. The relative stable separation into "warm" (above the break) and "cold" (below the break) zones caused equally stable thermal and gas stratification. The introduction of low-elevation steam was shown to eventually break up this stratification layer, although not immediately.

Neither lump parameter nor field codes presented a preferred result.

4.3.3.3   ISP-35 NUPEC/M-7-1 and other NUPEC Counterpart Tests

The NUPEC model containment, a Japanese test facility, consisted of a one-quarter linearly scaled PWR dry, insulated steel containment vessel with a free volume of 1300 m^3. It had 25 subcompartments, separated by steel partitions, including a large dome with 70% of the total free volume and an internal containment spray system. The experiment, conducted in 1992, involved 30 minutes of steam/gas injection with simultaneous containment spray. Containment spray assured that the containment atmosphere was well mixed; however, it was delivered at a rate inconsistent with the

facility scaling (too much by a factor of four). Lump parameters and field codes alike showed very good agreement with measured results.

NUPEC Tests M-4-3 and M-8-1 were performed to complement M-7-1. The objective of these tests was to investigate the mixing effect of hot gas and steam being injected at low and high elevations, respectively, without containment spray. Like ISP-29, Test M-8-1 showed a stable stratification. Because of the low elevation of the steam injection in Test M-4-3, stratification was less pronounced (i.e., atmospheric mixing and natural convection flows were reduced), though it was observed. While a formal code study was not performed for these tests within the ISP program, CONTAIN and MELCOR benchmarks have been performed with good prediction of dome pressure and gas temperature stratification.

4.3.3.4   ISP-37 BFMC/VANAM M3, BFMC Test F2 and Biblis Tests

Although the VANAM M3 experiment was primarily an aerosol test, it also included thermal-hydraulic aspects. The main phenomena investigated were the thermal behavior of a multi-compartment containment (i.e., pressure and temperatures) and aerosol transport. The experiment was performed in 1993 at the Battelle Model Containment Test Facility in Germany. The injection phases—both at high (i.e., pressurizer safety valve level) and low (i.e., sump level) elevations—resulted in good atmospheric mixing in these regions; although, this was the result of independent convection loops. As such, stratification was observed.

Overall, codes were able to calculate the thermal-hydraulic containment behavior with reasonable accuracy. In particular, containment pressure was quite well predicted. All calculations simulated both the upper and lower convection loops; but, not all calculations simulated the atmospheric stratification between the dome and the annulus. Prediction of the stratification phenomenon was observed to be particularly sensitive to nodalization.

BFMC Test F2 provided data for a broad spectrum of generic (not accident-specific) thermal-hydraulic conditions, including long-term natural convection from onset to

stagnation, thermal stratification, and local condensation effects. Relevant conclusions were:

- Large-scale mixing can be affected by natural convection, provided that a suitable geometry of walls and openings and steam or heat source in the lower containment region exists

- Steam condensation on structures can result in very distinct local accumulations of non-condensable gases

- Only zones participating in large-scale convection loops show uniform steam-air distribution, different compositions can develop in stagnation zones. No formal code study was performed for this test within the ISP program.

The BFMC Biblis tests examined hydrogen mixing by natural convection in both short- and long-term time domains following a hypothetical LBLOCA. These experiments demonstrated the initiation and stability of an overall natural-convection circulation path under adverse temperature stratification conditions (short-term) and small favorable temperature differences. Following the first 30 minutes, good mixing was observed as a consequence of sump evaporation. Sump evaporation continued to drive good mixing in the long-term as containment structures cool the containment temperature. Circulation was observed with up-flow through the center and down-flow in the annulus; a convection circuit equivalent to that is expected in the U.S. EPR. No formal code study was performed for this test within the ISP program.

4.3.3.5   *ISP-47 TOSQAN, ThAI, and MISTRA*

The main objective of ISP-47 was to assess the capabilities of lumped parameter and field codes in the area of containment thermal-hydraulics. The study referred to field codes as computational fluid dynamic (CFD) codes; however, this term, a misnomer, was not necessarily completely accurate in all instances. The ISP was based on the conclusions derived from the earlier ISPs, with a particular focus was on pressure

transients and gas temperature field. Detailed gas velocity and gas concentration fields were obtained for the first time in an ISP program.

The exercise was separated into two steps. The first was dedicated to the validation of steady-state separate effects models in the TOSQAN and MISTRA facilities. Specifically, wall condensation, buoyancy, stratification, and turbulence and their phenomenological interactions were addressed. In the second step, these phenomena were examined in the complex, multi-compartment geometry at the ThAI test facility. Both "blind" and "open" code calculations were made for both steps.

The surprising result from ISP-47 was that field code results were not substantially better than results from lump parameter codes employing appropriate user modeling for expected phenomena. Concerning the pressure response during the tests, all codes (i.e., both lump parameter and field codes) demonstrated generally good accuracy. In addition, resolution of vertical and radial temperature profiles required attention to compartment nodalization for both lump parameter and field code models. Field codes distinguished themselves in their ability to capture velocity profiles, resulting in a better prediction of vertical temperature profiles; however, field codes did have trouble with bulk and wall condensation and injection jet dynamics. Overall, the use of field codes did not result in substantially improved predictions over the better lump parameter models.

4.3.4   Review Summary of Established Assessment Databases

The majority of the code validation performed for RELAP5-BW and GOTHIC is applicable to the RCS and containment thermal-hydraulic phenomena following a hypothetical LBLOCA in a U.S. EPR. The U.S. EPR RCS design and accident response systems are very similar to conventional PWRs, consequently there are no new or unique thermal-hydraulic phenomena present during an LBLOCA. Likewise, while the U.S. EPR containment is larger than conventional PWR containments, the dominant containment thermal-hydraulic phenomena are consistent with that of other PWR designs. The principal difference between the U.S. EPR and other PWR containment designs is that

neither safety-grade containment sprays nor fan-coolers are necessary for the mitigation of containment pressure loads following an LBLOCA.

4.3.4.1 *Phenomenological Assessment Database*

The role of traditional containment spray or fan-cooler systems is to provide an active system for the long-term rejection of heat released from the RCS, and to create a mixed containment atmosphere. For the short-term response, both conventional PWRs and the U.S. EPR rely on the natural processes of wall condensation and structural conduction. For long-term heat rejection, the U.S. EPR extends reliance on these natural processes. Robust atmospheric mixing becomes less important as the heat removal rate is dominated structure conduction. Rather, the emphasis is on the ultimate termination of core steaming through a safety injection switchover from injection locations in each cold leg to injection locations in all cold and hot legs, with the majority of the safety injection delivered to the hot leg injection locations. The switchover is manual and occurs 90 minutes following accident initiation. Once core steaming is terminated, all the core heat is rejected through the IRWST, which receives the RCS liquid spillage and actively cools it through the LHSI heat exchanger. Additional code assessments are used to address long-term mitigation.

With regard to RELAP5-BW, the assessment database addressing the short-term thermal-hydraulic phenomena has benefited from its dual purpose as a design-basis accident safety analysis tool for evaluating ECCS performance (i.e., peak clad temperatures). Table 4-2 summarizes the test program database supporting the evaluation of high rank LOCA RCS phenomena for all phases of an LBLOCA.

Table 4-2—Summary of High Ranked LOCA RCS Phenomena and Associated Data

Phenomena	Transient Phase	Source of Data
Break: Critical Flow	Blowdown	LOFT, Semiscale
Fuel Rod: Decay Heat	Reflood/Long-Term	ANS 1979 Decay Heat Standard

Phenomena	Transient Phase	Source of Data
Core: Reflood Heat Transfer (includes post-CHF, nucleate boiling, entrainment/de-entrainment, and rewet/quench)	Reflood	FLECHT, FLECHT SEASET, Semiscale, SCTF, CCTF,
Upper Plenum : Entrainment/de-entrainment	Reflood/Long-Term	FLECHT-SEASET, CCTF, SCTF, UPTF
Hot Leg: Condensation	Long-Term	UPTF
Hot Leg: Stratification/entrainment/de-entrainment	Reflood/Long-Term	FLECHT-SEASET, CCTF, SCTF, UPTF
Steam Generator: Heat Transfer (both primary and secondary, includes secondary stratification)	Reflood/Long-Term	FLECHT SEASET, CCTF
Cold Leg/Accum: Condensation	Reflood	UPTF
Downcomer: Condensation	Reflood	UPTF

As noted in Section 4.3.1, assessments for the short-term phenomena have been reported in References 19, 25, and 26. The NRC's Standard Review Plan requires that mass and energy code assessments be provided for critical flow, liquid carryout rate fraction, and long-term steam quenching. Section 6.0 presents code assessment studies demonstrating RELAP5-BW performance for several key phenomena, including liquid carryout rate fraction using FLECHT-SEASET, steam generator heat transfer using FLECHT-SEASET, and steam quenching using UPTF, CCTF, and SCTF. Given the close relationship between liquid carryout and core heat transfer, assessments are also provided on core heat transfer during the early LOCA phases. No new assessments are provided on critical flow since the same Moody critical flow model used in AREVA NP's 10 CFR 50 Appendix K based evaluation methodology is used. This model is considered conservative for safety analysis of ECCS performance and containment mass and energy releases.

Numerical Applications, Inc. (NAI) has conducted an extensive assessment of GOTHIC (Reference 31).

Table 4-3 summarizes NAI's test program database supporting the evaluation of medium- and high-rank containment phenomena during an LBLOCA based on the PIRT given in

AREVA NP Inc.
Applicability of AREVA NP Containment Response Evaluation Methodology to the
U.S. EPR™ for Large Break LOCA Analysis
Technical Report

ANP-10299NP
Revision 2

Page 4-21

Section 3.4.2. The table presents the governing phenomena separated into one or more phenomenological processes.

Table 4-3—Summary of High Ranked Containment RCS Phenomena and Associated Data

Phenomena / Phenomenological Processes / Test Programs	Structure Free Convection				Thermal Conduction in Solids	Pool Free Convection		Expansion/Compression of Multi-Component Gases							Buoyancy Induced Stratification
	Natural Convection	Forced Convection	Mixed Convection	Condensation on Walls		Pool Surface Evaporation	Pool Surface Condensation	Gas Mixing	Flashing	Vapor Compression	Vapor Decompression	Jet Mixing	Mass Diffusion in Vapor	Turbulence	
Battelle-Frankfurt Containment Tests	X	X	X	X	X			X		X	X		X	X	X
HDR Full Scale Containment Tests	X	X	X		X			X		X	X				
Marviken Full-Scale Containment Tests	X	X		X	X	X		X	X	X	X				X
HEDL Hydrogen Mixing Tests	X	X	X	X	X			X				X	X	X	X
CVTR Simulated DBA Tests	X	X	X	X	X	X		X		X	X	X	X		
NUPEC Tests	X			X	X			X		X	X			X	X
TOSQAN/MISTRA	X			X								X			

New code assessments are featured in Section 6.0 which addresses GOTHIC's analysis capability to simulate containment LBLOCA phenomena in the absence of dedicated safety-grade spray or fan-cooler systems. Because of the nature of the containment pressure response to an LBLOCA, large-scale integral-effects tests performed without these systems were selected. Without these systems there is greater reliance on the

natural processes of condensation and structural conduction, which are important LBLOCA containment response phenomena in all large dry PWR containment designs. The specific assessments examined code performance with tests performed at the HDR and BFMC facilities.

4.3.4.2   GOTHIC Model Nodalization

The GOTHIC model of the U.S. EPR containment applies the common lumped-parameter approach, that is, multiple computational control volumes evaluating bulk conditions based on computed heat and mass transfer. The GOTHIC model of the U.S. EPR containment applies the common lumped-parameter approach, that is, multiple computational control volumes evaluating bulk conditions based on computed heat and mass transfer. A three-dimensional, subdivided mesh in the containment dome is used to predict the natural circulation patterns and any potential thermal stratification. The containment has been designed to encourage the natural flow circulation. The RCS is positioned low and central in the containment such that the effluent from an LBLOCA rises through this central region of equipment rooms, each with openings/vents providing separate circulation pathways. Above the equipment rooms, the pressure equalization ceiling (PEC) responds to a relatively small differential pressure by exposing the RCS and adjacent equipment rooms to the full containment volume that encompasses both the equipment rooms and the accessible space regions. The large, cool vertical surface of the steel and concrete structures begins to remove heat from the steam-rich atmosphere through both condensation and convection. The cooldown results in a buoyancy-driven flow along the periphery of the containment structure. The natural circulation pathway is completed by the opening of mixing dampers residing along the walls separating the lowest level of the accessible space regions and the air space above the IRWST.

The short-term event is characterized by a violent rupture of a high-energy RCS pipe, sending its fluid inventory throughout the containment. Natural circulation develops following the blowdown period. While pressure reduction is primarily the consequence of steam condensation, the heat removal rate is ultimately driven by heat conduction

through concrete. The process becomes conduction-limited within an hour. The
conduction-limited condition slows down the containment cooldown rate relative to the
early condensation period. As such, local variations in steam concentration are
significantly attenuated. Similarly, the condensation process itself is self-adjusting. High
steam concentration results in high condensation and, consequently, low steam
concentration results in low condensation.

As highlighted in several ISPs, finer nodalization or subdivision did not necessary improve
code-to-data comparisons. In particular, the participants in ISP 29 observed that the peak
pressure was primarily grouped within the 15% uncertainty band, regardless of
nodalization or code. While this was for the short term peak, no new phenomena are
introduced for the long-term and it is reasonable to extrapolate this relative uncertainty
beyond the testing period of the test. ISP 47 also noted that finer nodalization models
had difficulty with bulk and wall condensation and injection jet dynamics.

Considering the nature of the LBLOCA and the U.S. EPR design features engineered to
produce atmospheric mixing, the natural processes essentially decouple the global
response from local variation. The historical performance of lump parameter computer
codes to predict containment pressure response supports this contention. As such, the
single control volume model assumption is valid for predicting bulk containment pressure
response following an LBLOCA. Code assessments comparing the performance of
single- and multiple-control volume models against test data are given in Section 6.2. A
discussion of the applicability of the single control volume assumption based on those
studies is presented in Section 6.2.6. However, a multi-node model is applied to all of the
U.S. EPR long term containment analyses.

4.4   Evaluate Effects of IET Distortion and SET Scaleup Capability (EMDAP Step 8)

The objectives of the scaling analysis are to identify the processes and parameters that
govern the containment responses in non-dimensional space following a LBLOCA,
validate or reconcile the Phenomena Identification and Ranking Table (PIRT), relate the
plant behavior to a smaller scale test facility, identify potential distortions, evaluate the

impact of such distortions, and determine if the available test data is sufficient to envelope the expected phenomena in the U.S. EPR plant behavior.

A top-down scaling analysis entails developing detailed non-dimensional governing equations for the physical processes. The coefficients for the terms in the governing equations are referred to as Pi (⊓) coefficients. The ideal test would scale 1:1 for all of the prototype components.   However, in practice such scaling is not possible and compromises must be made. These compromises become the source of potential distortions in the scaling analysis.

To identify the distortions, non-dimensional coefficients (⊓s) representing the experiment and the prototype are compared on two levels. First, to determine if the dominant processes for the prototype are the same as those observed in the experiment. On the second level, the processes included in the equation should be in the same phenomenal regime as in the prototype. If they are not, this too introduces a potential distortion. In some instances, the experiment may not exhibit a process that the prototype is designed to exhibit (for example, decay heat); yet, it may be possible for the distorted test component to interact with the rest of the system in a typical way.

The level of a distortion is based on the importance of the Pi groups and the magnitude of the distortion. The result for a low importance Pi group distortion is low regardless of the magnitude of the distortion. Pi groups with medium importance will have a medium level even if there is a high distortion. Pi groups with high importance will have a level proportional to the distortion, highly distorted important Pi groups have a high level and medium distorted important Pi groups will have medium level. The distortion factors for all of the Pi groups identify the significant levels of distortion determined using the reconciled PIRT, summarized in Appendix B, Subsection 12.5. All the highly distorted Pi groups are then identified and analyzed.

The number of highly distorted Pi groups reduces from 10 (or 29 percent of total) in the Blowdown phase, to 5 (or 14 percent of total) in the Pre-HL-Injection phase and to only one (or 10 percent of total) in the Post-HL-Injection phase. Most of the 10 high ranking Pi

groups in the Blowdown phase are due to large break and expansion flow rates in the U.S. EPR results. The remaining distortions are a consequence of a larger relative surface area to volume ratio in the HDR ER volume. The majority of the distortions in the Pre-HL injection phase result from a higher natural circulation flow between the ER and AS volume for the U.S. EPR design. Finally, the lone distortion in the Post-HL injection phase is due to the relatively smaller gas mass and energy remaining in the HDR containment.

A confirmatory scaling analysis comparison (Appendix B, Subsection 12.6.3.6) of the figure-of-merit results between the HDR and U.S. EPR GOTHIC calculations show that the IET results scale the behaviors of the U.S. EPR containment design in non-dimensional space and time. The containment pressure figure-of-merit results show that the HDR test scales well in the Blowdown and Post-HL-Injection phases. For the pre-HL-Injection phase, the HDR dome pressure response was approximately 25 percent less than that of U.S. EPR design due to lack of decay-heat simulation during this phase.

In conclusion, the U.S. EPR scaling analysis results show that:

- All important phenomena have been identified.

- No unexpected phenomena were observed in the IET results.

- All distortions with respect to the HDR test facility have been identified and understood.

- The confirmatory scaling analysis comparisons of the figures-of-merit demonstrate that the HDR IET is adequately scaled for the U.S. EPR design behaviors identified during the Blowdown and Post-HL-Injection phases.

4.5   Experimental Uncertainties (EMDAP Step 9)

As a deterministic evaluation methodology, uncertainties have been addressed through compliance with the Standard Review Plan and the ANSI/ANS 56.4 standard. Section 8.4

presents a compliance matrix listing the Standard Review Plan and ANSI/ANS 56.4 standard modeling expectations, along with an explanation how AREVA NP's containment analysis methodology addresses these expectations.

Section 7.1 presents a discussion of experimental uncertainties associated with containment response. Principal uncertainty contributors to the containment pressure response to an LBLOCA are quantified and total uncertainty is evaluated for a cold leg pump suction break in Section 7.3.

5.0   EVALUATION MODEL

5.1   *Evaluation Model Development Plan (EMDAP 10)*

The evaluation model concept establishes the basis for methods used to analyze a particular event or class of events. AREVA NP's containment analysis evaluation methodology predicts the containment pressure and temperature response for a spectrum of high energy line breaks. It complies with the NRC's evaluation model expectations, as highlighted in NUREG-0800, Standard Review Plan. This evaluation model is applicable to any pressurized water reactor (PWR) with a large dry containment, including the U.S. EPR. It is founded on state-of-the-art thermal-hydraulic codes for the prediction of mass and energy releases and containment pressure and temperature response. Design inputs and other modeling assumptions needed to apply these computer codes must conform to a licensee's plant-specific licensing and design bases.

AREVA NP has formalized software and evaluation methodology development efforts with several guidelines, standards, and procedures that are consistent with 10 CFR Part 50, Appendix B. This formal approach to evaluation model development defines a generic plan that addresses the principal areas highlighted in EMDAP Step 10:

- Design specifications for the computer codes

- Documentation requirements

- Programming standards and procedures

- Transportability requirements

- Quality assurance procedures

- Configuration control procedures.

Both the RELAP5-BW and GOTHIC codes were developed in accordance with a quality assurance program compliant with 10 CFR Part 50, Appendix B. Applying these quality assurance procedures establishes the acceptability of the quality and safety-related functions of AREVA NP's products and services. This enables quality engineering work in the development and maintenance of the engineering software used by AREVA NP. At the initiation of a project, various items must be defined including:

- Functional requirements, including the specific input, processing, and output details

- Performance requirements, design constraints, or particular quality issues

- Any customer- or project-specific requirements, such as external interfaces, quality concerns, project design reviews, etc.

- Potential impact on software interfaces, including identifying upstream and downstream software components that may require modification to accommodate the planned changes

- Acknowledgement of any outstanding code (i.e., software) or guideline (i.e., methodologies) modification requests that are open

- Identification of the certification status of applied software

- Status and location within the access control system (i.e., method by which users are permitted to run software).

When calculations are being performed, procedures for treating code input arising from the plant geometry and the assumed plant state at transient initiation are defined through methodology guidelines (see Section 8.0 for details on the containment analysis evaluation methodology). Similarly, outputs are confirmed for accuracy and relevancy to the analysis objectives, and compared to the inputs for consistency.

During the course of a development project, the cognizant engineer is responsible for documenting software and evaluation methodology details. The documentation supporting the codes and methods are consistent with the approved code version used. AREVA NP procedures require that code modifications to approved licensing topical reports are accompanied by revisions to the affected assessment documents. Formal documentation for evaluation methodologies includes user manuals, user guides, developmental assessment reports, and the models and correlations report (providing information on code closure relations).

5.2   *Evaluation Model Development Structure (EMDAP 11)*

To address the principal containment integrity acceptance criteria specified in GDC 16, 38, and 50, a computational analysis is performed that spans the period from the initiating event out to one day. The computational framework for containment analysis incorporates models based on firmly supported first-principles correlations where possible. Conservative models are employed where the technical basis is less developed. The basic calculational framework is shown in Figure 5-1.
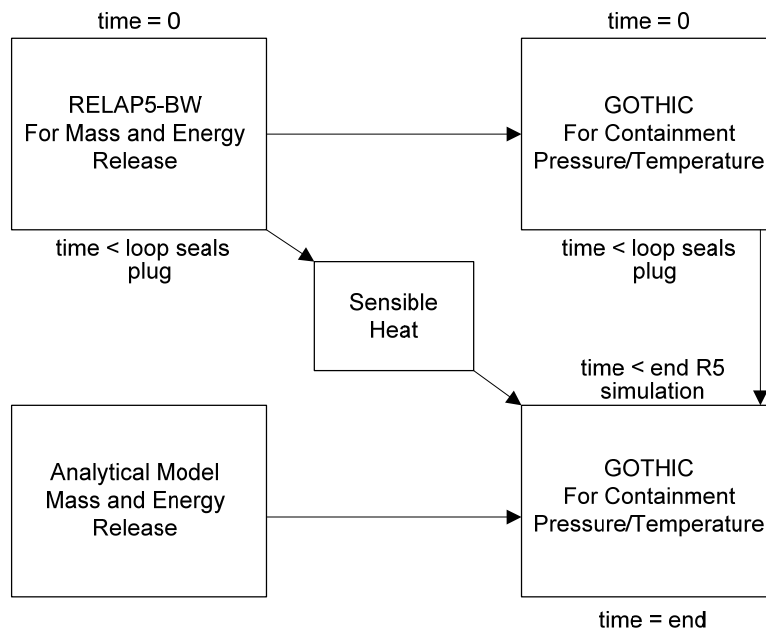
Figure 5-1—Containment Analysis Evaluation Methodology Flowchart

The RELAP5-BW and GOTHIC codes apply models and correlations based on first-principles to the extent practical. RELAP5-BW is used to calculate the mass and energy releases, applied in GOTHIC as a boundary condition, up to and through the post-reflood phase. [

]Following that time, a simplified analytical approach is applied to conservatively estimate RCS mass and energy releases. The mass and energy release rates are then incorporated into GOTHIC in a manner that considers both first-principle models and correlations, and conservative treatments of uncertainties.

Where first-principle models are applied, the computer codes provide the capability to analyze both the top-level behavior of all systems, structures, and components and the lower-level behavior of individual constituents and phases that play a role in the event. The integrity of first-principal models and correlations is a function of the field equations, closure relations, numerics, and model nodalization. A discussion of these topics appears in Section 5.3.

5.3   Code Adequacy and Model Closure (EMDAP Steps 12, 13, 15, 16, 17)

The objective of a code adequacy review is to assess the capability a code to accurately model the phenomena and processes associated with the event scenario of interest, and to provide the flexibility necessary to develop an appropriate evaluation methodology. The code adequacy step considers the code application through the

PIRT assessment of important phenomena; however, it is independent of how the code is used in an application. The assessment is accomplished by comparing the event and important phenomena identified in the PIRT with the models and correlations documents for the selected codes. Four attributes are needed to make this comparison:

- Field equations that address global processes

- Closure (constitutive) equations which support the field equations by modeling specific phenomena or processes

- Code numerics that demonstrate that the code can efficiently and reliably perform the required calculations

- Structure and nodalization, which address the ability of the code to model the nuclear power plant geometry and components, and to provide an accurate prediction of the nuclear power plant response.

These attributes, plus an evaluation of high rank phenomena, are discussed in the following sections. As necessary, the code adequacy determination is supported by calculations to assess the fidelity and accuracy of specific models and correlations (emphasizing PIRT conclusions) and the RELAP5-BW code.

5.3.1 RELAP5-BW

RELAP5-BW is an AREVA NP adaptation of the Idaho National Engineering Laboratory's RELAP5/MOD2. The code was developed for best estimate transient simulation of pressurized water reactors, and modified to include models required for licensing analysis of ECCS performance and containment mass and energy releases. Modeling capabilities include simulation of large and small break loss-of-coolant accidents as well as operational transients, such as anticipated transient without scram, loss of offsite power, loss of feedwater, and loss of flow. The solution technique utilizes two-phase mass, energy, and momentum equations, a gap conductance model, constitutive models, and component and control system models. Control system and

secondary system components were added to permit modeling of plant controls, turbines, condensers, and secondary feedwater conditioning systems.

5.3.1.1 *Field Equations (EMDAP Step 16)*

The thermal-hydraulic field equations must possess the capability of simulating each of the distinct LBLOCA phases. During the refill and reflood phases, counter-current flow occurs at various locations in the RCS, and subcooled liquid coexists with superheated steam in parts of the reactor core. Therefore, the field equations should be non-homogeneous (unequal velocity for each phase) and non-equilibrium (unequal temperature for each phase). The presence of nitrogen in the accumulator requires an additional field equation to model and track the movement of a non-condensable gas. Heat transfer through structures also must also be included and coupled with the hydraulics model. RELAP5-BW satisfies these requirements with a two-fluid non-equilibrium model consisting of two phasic continuity equations, two phasic momentum equations, and two phasic energy equations. An additional equation is provided to address a non-condensable component, if present. The RELAP5-BW field equations have been evaluated against their ability to model the important PIRT phenomena. As shown in Table 5-1, the field equations represented in RELAP5-BW are sufficient.

Table 5-1—Field Equations/Models in RELAP5-BW

Scenario and PIRT Requirements	RELAP5-BW Model	Field Equations/Model
Non-equilibrium two-phase flow	Yes	One-dimensional, six equation unequal velocity, unequal temperature
Non-condensable gas flow	Yes	Gas mass balance in vapor flow field
Solute tracking for boron	Yes	Solute mass balance liquid flow field
Multi-region structure heat flow	Yes	Standard one-dimensional heat conduction model; two-dimensional heat conduction for core region reflood
Separation due to gravity	Yes	Gravity pressure differential in flow field equations
Interphase exchange terms	Yes	Mass and energy transfer between phases, vaporization and condensation

5.3.1.2   Closure Equations

Closure equations (constitutive models and correlations) are required to support the basic field equations. These closure equations are essential for modeling the processes and phenomena given in the PIRT. Closure models are developed to represent these parameters, and the development may include correlation with experimental data. The adequacy of a closure model is assessed by determining if the model reproduces applicable test data. These data are derived from the extensive investigation of LBLOCA phenomena through world-wide test programs in both separate-effects and integral facilities (e.g., LOFT, MIST, UPTF, CCTF, etc.). The adequacy of RELAP5-BW constitutive models and correlations are presented along with description of the verification and validation of these models and correlations in Reference 19.

The capability of the RELAP5-BW code closure equations to meet the requirements of the PIRT is summarized in Table 5-2 and described in Reference 19 (unless otherwise stated in Table 5-2). The closure equations address wall friction, interphase friction, mass transfer (interphase heat transfer), wall-to-fluid heat transfer, form-losses, and similar functions. The various models require flow regime maps, boiling curves, state relationships, and fluid and material properties for completeness. As indicated in Table 5-2, the RELAP5-BW code has the closure equations necessary address the important LBLOCA phenomena.

Application of the RELAP5-BW code is ultimately limited by its inability to resolve a multi-dimensional flow field. As identified in Section 3.4, multi-dimensional flow becomes important only in the decay heat phase of an LBLOCA. In the "boiling pot" mode that characterizes this phase, the RELAP5-BW calculation is replaced by an analytical expression described in the GOTHIC model. This simplification is fundamentally an energy balance, with an assumption defining the thermal mixing efficiency of pumped safety injection and the fluid resident in the core and upper plenum. The mixing efficiency model is described in Section 6.1.4.

5.3.1.3   Code Numerics

The general formulation and structure of RELAP5-BW enable the user to define a generalized nodal finite difference model for system transient predictions. It is essentially unchanged from the original INEL RELAP5/MOD2 code. Coupling of the major system models (hydrodynamics, heat structures, reactor core, and control system) provides the capability to simulate a range of normal and off-normal nuclear power plant conditions and events. The solution control is designed to handle both the semi-implicit and implicit solution options; however, the semi-implicit finite difference technique is preferred for its general applicability.

Table 5-2—Phenomena/Processes in RELAP5-BW

Component	Phenomenon	RELAP5-BW Model	Model
Fuel rod	Stored energy	Yes	TACO fuel model (Reference 37)
	Oxidation	Yes	Baker-Just model
	Decay heat	Yes	ANS 1979 Standard
	Gap conductance	Yes	TACO fuel model
Core	DNB	Yes	Biasi and modified Zuber CHF correlations; product-specific options available
	Post CHF	Yes	Full boiling curve. Code models rod-to-coolant radiation, but does not model rod-to-rod or rod-to-wall radiation.
	Rewet	Yes	Full boiling curve
	Reflood heat transfer plus quench	Yes	Full boiling curve, quench front tracking, 2-D heat conduction
	Multi-D flow, void distribution, generation	No	1-D and cross flow, two-fluid field equations; constitutive models (vaporization, condensation and interphase friction)
	Entrainment/ de-entrainment	Yes	Interphase friction model, countercurrent flow limiting (CCFL) model, upper plenum entrainment model (Wilson, all vertical, slug flow regime)
	Flow reversal, stagnation	Yes	Two-phase flow field equations, critical flow model, mass transfer model (flashing), wall friction, form-loss

Component	Phenomenon	RELAP5-BW Model	Model
Upper Plenum	Entrainment/ de-entrainment	Yes	CCFL model, interphase friction model, upper plenum entrainment model, nodalization (Wallis, product specific)
	Drain, fallback	Yes	CCFL model, interphase friction model, upper plenum entrainment model, nodalization
Upper Head	Initial temperature	Yes	Two-phase flow field equations, mass transfer model (flashing), nodalization
Hot Leg	Entrainment/ de-entrainment	Yes	CCFL model, interphase friction model, mass transfer model, upper plenum entrainment model
Pressurizer	Early quench	Yes	Two-phase flow field equations, mass transfer model (flashing), form-loss, mixture level model, nodalization
	Critical flow in surge line	Yes	Critical flow model (Moody), form-loss, nodalization
Steam Generator	Steam binding	Yes	Primary-secondary heat transfer, interphase friction model, CCFL model, upper plenum entrainment model, mass transfer model (vaporization)
Pump	Two-phase	Yes	Four-quadrant head and torque homologous curves, EPRI data for two-phase degradation model
	Differential pressure form loss	Yes	Pump loss model, nodalization
Cold Leg, Accumulator	Condensation, oscillations	Yes	Mass transfer model (condensation), non-condensable model, Two-phase flow field equations
	Non-condensable gas	Yes	Non-condensable gas continuity field equation, effects of non-condensable gas on condensation
	Accumulator discharge	Yes	Expansion of non-condensable gas, two-phase flow field equations, form-loss, nodalization
Downcomer	Entrainment/ de-entrainment	Yes	Interphase friction model
	Condensation	Yes	Mass transfer model (condensation), wall heat transfer model
	Hot wall	Yes	Wall heat transfer model, heat structure nodalization
	Multi-D	No	1-D and cross flow, two-fluid field equations; constitutive models (vaporization, condensation and interphase friction)

Component	Phenomenon	RELAP5-BW Model	Model
	Countercurrent, slug, non-equilibrium flow	Yes	Interphase friction model, mass transfer model, wall vapor generation
	Liquid level oscillations	Yes	Interphase friction model, two-phase mixture level, two-phase flow field equations
Lower Plenum	Sweep-out	Yes	Interphase friction model, two-phase flow field equations
	Hot wall	Yes	Wall heat transfer model, heat structure nodalization
Break	Critical flow	Yes	Subcooled and two-phase Moody critical flow model, nodalization
	Containment pressure	No	Implicit backpressure calculation (N/A: addressed by GOTHIC calculation)
Loop (Excluding Pump & Steam Generator)	Oscillations	Yes	Mass transfer model (condensation), interphase friction model, two-phase flow field equations, wall heat transfer
	Flow split	Yes	Wall friction model, form-loss, mass transfer model (vaporization and condensation), two-phase flow field equations

The heat conduction solution accounts for internal structure conduction, heat transfer coupling, and source and boundary condition treatments. Special treatments are provided for reactor core modeling including kinetics, decay heat, gap conductance, cladding rupture, and metal-water reaction. The one-dimensional heat conduction can be solved for modeled structures in rectangular, cylindrical, or spherical geometry. Finite differences are used to advance the heat conduction solutions. In one-dimensional problems, an analyst defines boundary conditions through code input identifying the left and right surfaces. The spatial finite-difference approximations use exact expressions for the space and volume factors and simple differences for the gradient terms.

The system of equations is reduced to a matrix describing volume pressure and junction velocities. The numerical solution contained in RELAP5-BW is based on the commonly-

applied Gaussian elimination method. These numerics were improved in RELAP5-BW and are described in Reference 19.

5.3.1.4 *Structure and Nodalization*

To properly model a nuclear power plant, a code must be able to adequately model the hydraulic and conductor contributions of important components and the nuclear power plant control systems for the chosen accident scenario. The modeling of each of the nuclear power plant components is discussed in detail in Reference 26. The RELAP5-BW code has been developed with the capability to specifically address nuclear power plant applications. Table 5-3 summarizes RELAP5-BW's ability to model all the major components and associated control systems of the plant.

Table 5-3—PWR Component Modeling Requirements

Required Component	Component Model Existence	Code Component
Pressure Vessel	Yes	1-D component model of upper head, upper plenum, core, lower plenum, downcomer, structure, flow paths, elevations, resistances, volumes Heat structures: model vessel walls, internal structures, fuel rods
Cold/Hot Leg	Yes	Pipes, volumes, and junctions: model flow areas, lengths, volumes, resistances, elevations Heat structures: model pipe walls
Steam Generator	Yes	Separators, pipes, volumes and junctions: model flow areas, volumes, lengths, resistances, elevations, flow paths, phase separation, recirculation, feedwater, steam flow Heat structures: model generator walls, heat exchange between the primary and secondary system.
Pumps	Yes	Pump: models homologous curves, degradation, flow areas, volumes, losses, suction, discharge flow

Required Component	Component Model Existence	Code Component
Pressurizer	Yes	Pipe: models volumes, flow areas, phase separation, lengths, resistances, elevations Heat structures: model vessel walls and heater
Surge Line	Yes	Pipe and junctions: models volumes, flow areas, lengths, resistances, elevations, choked flow Heat structures: model pipe walls
ECCS	Yes	Pipes, volumes, junctions, valves, and pumps: model flow areas, lengths, volumes, resistances, elevations Heat structures: model pipe walls

5.3.1.5   Evaluation of High Rank Phenomena

This section provides an overview of how RELAP5-BW models the phenomena identified in Table 3-1 – Table 3-5 identified as high-rank or deficient state-of-knowledge. Several of these phenomena are similar over multiple components and event phases, or can be characterized as initial or boundary conditions. This list is simplified to the following phenomena: break discharge model, decay heat, entrainment/de-entrainment, condensation, reflood heat transfer, hot leg nozzle bypass flow, and core multi-dimensional mixing/void distribution/two-phase liquid level. Refer to Table 4-2 for a summary of the test program database supporting the evaluation of high-rank phenomena. The evaluation objective is to present each of the identified phenomena, describe the code's capability and limitations, and discuss whether an appropriate modeling approach can be applied. It is not to present evaluation methodology choices; that is presented in Section 8.0.

5.3.1.5.1   Break Discharge Model

Choking or critical flow is defined as the condition wherein the mass flow rate becomes independent of the downstream conditions (that point at which further reduction in the

downstream pressure does not change the mass flow rate). Two mutually exclusive models are available for calculating choked flow in RELAP5-BW. The first option uses the original RELAP5/MOD2 built-in Ransom-Trapp method. The second option uses a table interpolation with any of the four following critical mass flux tables: Extended Henry-Fauske, Moody, Homogeneous Equilibrium (HEM), or Murdock-Bauman. Whereas the Ransom-Trapp model mechanistically solves for phasic velocities of non-equilibrium, non-homogeneous flow, the table-lookup models consist of tabular critical mass fluxes as a function of upstream volume stagnation pressure and enthalpy. RELAP5-BW translates the critical mass flux from the tables into equivalent liquid and vapor velocities based on the liquid/vapor slip, which is defined by the particular critical flow model chosen.

The ranges of the U.S. EPR application are within valid ranges of these correlations; that is, no extrapolation is necessary from the tabular models. RELAP5-BW developmental assessments performed using the results from the LOFT (1/50 scale W PWR) and Semiscale (1/1500 scale W PWR) (Reference 19) integral test programs indicate successful implementation and comparison to experimental data. The uncertainty in the critical flow model arises primarily because critical flow is sensitive to the geometry near the choking plane, particularly for low-quality flow. Experimental programs addressing the critical flow phenomenon incorporate valves and orifices that modify the geometry and, consequently, the flow conditions. In general, best-estimate critical flow models considering an idealized break plane over-predict test program results. This is an inherent conservatism for mass and energy release evaluations. RELAP5-BW, like other RELAP5 and TRAC based codes, includes code input parameters that allow analysts to develop analysis treatments to address specific application needs, such as NUREG-0800 analysis requirements. As such, the RELAP5-BW code adequately addresses the modeling expectations for break discharge.

5.3.1.5.2   Decay Heat

Decay heat can be prescribed in RELAP5-BW either through specification of a built-in model or through a user-defined table. The built-in models reflect the "Simplified Method for Determining Decay Heat Power and Uncertainty" as specified in the 1973 and 1979 American Nuclear Society standard models (References 38 and 39). RELAP5-BW also provides for a multiplier that can be used to bias the result to accommodate evaluation model requirements (e.g., NUREG-0800 analysis requirements). The ranges of the application of the built-in models as applied to the U.S. EPR are within the valid ranges of the model.   In addition, an assessment of the RELAP5-BW calculated decay heat for the U.S. EPR application conservatively bounds the best-estimate result from the ORIGEN2 code (Reference 40), as presented in Figure 5-2. With this capability, decay heat can be adequately considered in the RELAP5-BW code.
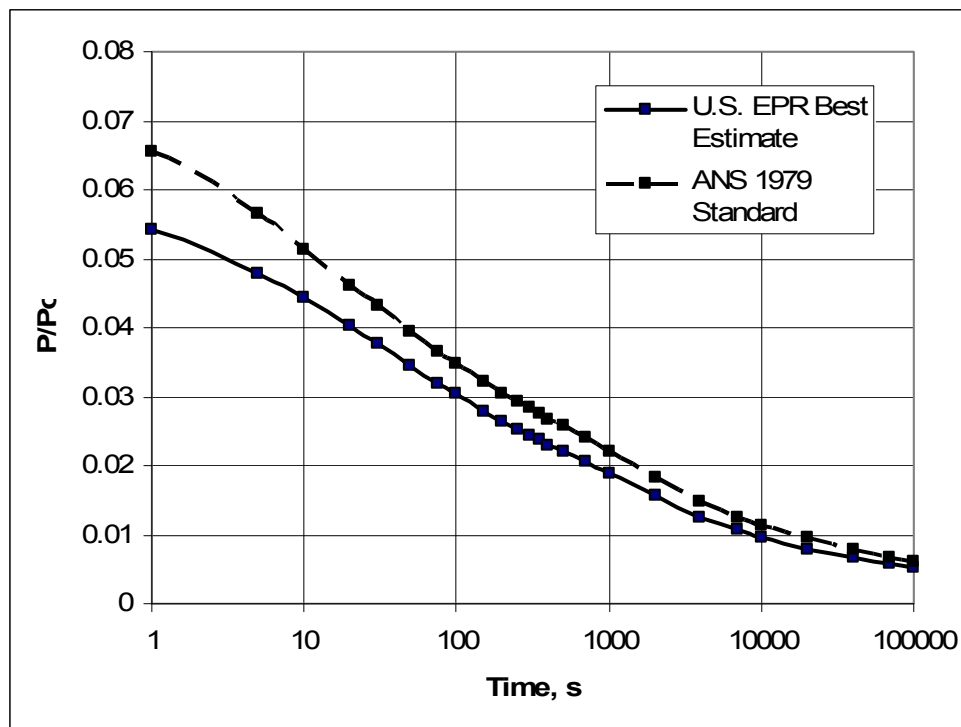
Figure 5-2—U.S. EPR Best-Estimate (ORIGEN2) vs. 1979 ANS Standard Decay Heat

5.3.1.5.3   Entrainment / De-Entrainment

Following RCS blowdown and subsequent refill, water enters the bottom region of the core, contacts hot fuel rods, and boiling occurs. The steam thus formed in the lower region of the core flows up through the core and vents through the reactor coolant loops. Along with the steam, a fraction of the liquid water in the core is entrained and carried out of the RPV. Some liquid is expected to de-entrain and fall back to the core; however, much of the liquid is expected to reach the steam generator. The importance of the core, upper plenum, and hot leg entrainment/de-entrainment phenomena for mass and energy release is attributed to the steam generator heat removal. The liquid content (i.e., droplet densities) in core exit flows is strongly correlated to steam generator heat removal. The prediction of liquid entrainment rates is addressed in the RELAP5-BW code's interfacial drag package.

RELAP5-BW inherits the interfacial drag package from RELAP5/MOD2, with the exception of the slug flow regime. Measurement of interfacial drag phenomena must be inferred from core reflooding test program results. The phenomenon is tightly coupled with core heat transfer; that is, high core temperatures usually imply high liquid entrainment. Also, some tests provide for phase separation and collection such that the integrated effect of liquid entrainment can be measured. From this data, liquid carryout rate fractions can be evaluated.

Because the enhancement in steam generator heat transfer participates in the steam binding phenomena important in ECCS performance analyses, there is significant interest in the fidelity of this model. The RELAP5-BW model is built upon a large body of experience derived from code benchmarks covering the breadth of normal and off-normal conditions anticipated for light water reactors, including the U.S. EPR. The modification of the interfacial drag for slug flow in RELAP5-BW greatly expanded this development assessment database. This modification is based on the Wilson bubble rise model (Reference 41). The INEL drag model was modified by the separate-effects benchmarks to the GE Level Swell Test 1004-3, the Christensen subcooled boiling

tests, and the ORNL bundle dryout tests. The results of these benchmarks (Reference 18) show good agreement with the experimental data.

In addition, the RELAP5-BW code has been benchmarked against data from the FLECHT-SEASET, UPTF, CCTF, and SCTF test program. These bound the range of pressures, power densities, and mass flux typical for an LBLOCA reflood phase (Reference 19). The significant figures-of-merit related to the liquid entrainment phenomenon are: core region void fractions, core temperatures, and carry-out rate fractions. In general, the RELAP5-BW results for cladding temperatures and quench front propagation are in good agreement with these results.

In all these tests liquid carryover was observed under conditions representing the reflood phase of the LBLOCA. While each test by itself may have limitations with instrumentation and scale, the combination of these tests provides a substantial basis for evaluating modeling of the drag between the two phases during reflood at full scale. Given these results from the different test facilities, AREVA NP demonstrated that the RELAP5-BW code prediction of core entrainment is appropriate for the evaluation of mass and energy release calculations. In addition, an assessment of RELAP5-BW's performance with FLECHT-SEASET was performed to address NUREG-0800 expectations. This is given in Section 6.1.2.

5.3.1.5.4   *Condensation*

Interfacial mass transfer is modeled in RELAP5-BW according to the thermodynamic process (i.e., wall vs. phasic mass transfer), interfacial heat transfer regime, and flow regime. After the thermodynamic process is determined, a flow regime map is used to determine the phasic interfacial area and select the interfacial heat transfer correlation. For mass and energy releases, the primary interface mass transfer phenomenon is liquid-vapor direct contact condensation. The interfacial mass transfer in the bulk fluid is modeled according to the flow regime. For condensation processes, the interfacial mass transfer in the bulk fluid on the liquid side is calculated by the Unal bubble collapse model in the bubbly flow regime (Reference 42), by the Theofanous interfacial

condensation model (Reference 43) in the annular mist flow regime, and on the vapor side, a large interfacial heat transfer coefficient is assumed in order to drive the vapor temperature toward saturation.

Measurements allowing direct comparisons of calculated and measured interfacial mass and energy transfer are not available. RELAP5-BW code performance for calculated interfacial heat transfer between the ECCS water and the steam in the cold leg has been assessed against both separate-effects (e.g., UPTF) and integral-effects tests (e.g., Semiscale, CCTF, and SCTF) in which cold water is sprayed into a steam flow stream.

One-dimensional thermal-hydraulic codes have limited ability to accurately predict interfacial condensation with stratified liquid, as a consequence of the assumed homogeneity within each phase. The assumption of homogeneity within each phase implies that all of the liquid within a control volume is at a single temperature. As a result, it is not possible to represent a situation where condensation of steam on a free liquid surface locally warms the liquid at the surface, limiting further condensation. If sufficient steam is available, then condensation is calculated to continue until all subcooling has been removed from the liquid present in the control volume containing the steam/liquid interface. While this is a limitation of RELAP5-BW, the model aligns well for the low flow of pump injection, which is the long-term condition.

5.3.1.5.5   *Reflood Heat Transfer*

When the heat flux from fuel rods exceeds the critical heat flux, heat transfer is calculated using correlations specific to the particular flow and heat transfer regime. RELAP5-BW provides a generalized heat transfer package for identifying and applying convective heat transfer correlations. This package addresses the full spectrum of expected heat transfer regimes, with correlations for single-phase liquid, nucleate boiling, transition boiling, film boiling, and single-phase vapor heat transfer. These heat transfer correlations are consistent with those used in other large system codes, including RELAP5/MOD2, RELAP5/MOD3, and TRAC-PF1. They were developed to

represent both the normal and off-normal conditions expected in current generation PWRs and the U.S. EPR. Extensive information on the scaling dependency and applicability of these correlations is presented in the TRAC-PF1/MOD1 and RELAP5/MOD2 Models and Correlations documents (References 23 and 21).

Core heat transfer during the reflood phase has a distinct profile; a schematic diagram of the boiling curve is shown in Figure 5-3. For this specialized situation, RELAP5-BW establishes a heat transfer regime profile in the reactor core that covers the entire boiling curve. In addition, when the reflood model is activated (through user's input specifications), a fine-mesh rezoning scheme is used to nodalize the core heat structures into two-dimensional (radial and axial) heat conduction nodes. The axial nodes extend from the bottom to the top of active fuel rods. The finest axial nodes are in the regions of nucleate boiling, transition boiling, and film boiling.
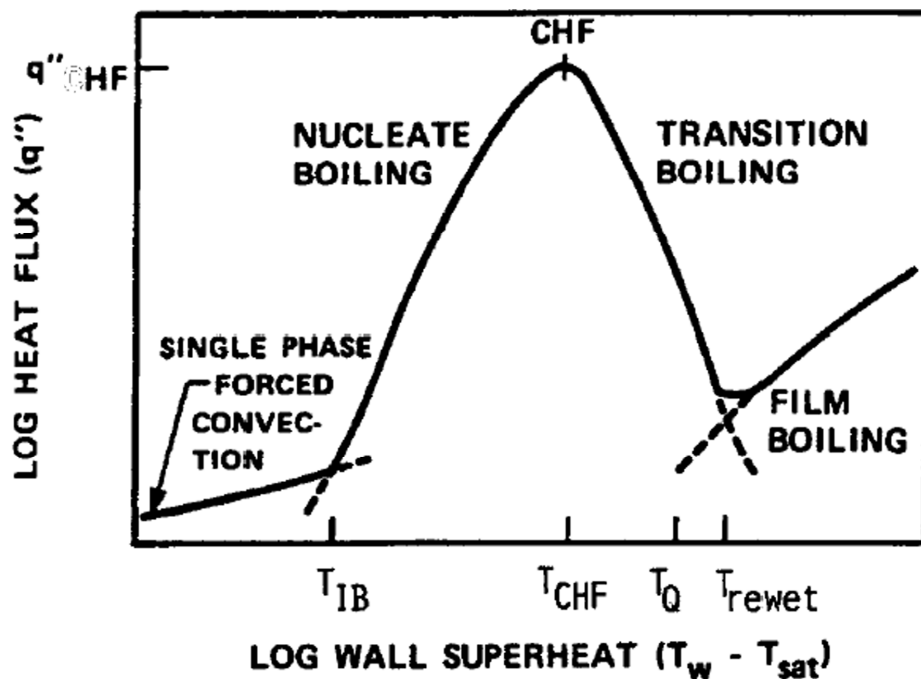
Figure 5-3—Pool Boiling Curve

For mass and energy release calculations, core heat transfer is the dominant heat source during reflood, and the advancement of the reflood phase influences heat

removal from the steam generators. The RELAP5-BW reflood heat transfer package has been assessed against a large suite of separate- and integral-effects tests, including FLECHT-SEASET, CCTF, SCTF, LOFT, and Semiscale.

5.3.1.5.6   Hot Leg Nozzle Bypass

The upper plenum to downcomer bypass around the hot leg nozzles is a medium rank phenomenon. However, the state-of-knowledge of the bypass flow rate is considered deficient because of the complicated nature of nozzle gap expansion and contraction. The overall flow through the nozzle gaps, even at its maximum, is small; however, this small difference can have a noticeable impact on core cooling dynamics.

Nozzle gap dynamics are a function of structural thermal expansion/contraction and RCS pressure. At full power/full pressure, the hot leg nozzle gaps may be slightly open. During the initial blowdown phase the reduced RCS pressure reduces the outward hoop stress on the reactor vessel (RV) and the gaps can close. During the later blowdown, refill, and early reflood phases, the thinner core barrel structure is cooled and the gaps grow to their maximum size. Slower cooling of the RV shell from the accumulator and pump injection during the reflood phase cause the gaps to decrease in size. During the post-reflood phase, the RV shell will cool and approach the pumped ECCS injection temperature. This may take several hours, but as the RV cools below the RCS saturation temperature the gaps can reclose. Based on the timing of hot leg injection, the gaps will likely still be open. Once safety injection is switched to the hot leg, portions of the core barrel will cool faster than the RV shell and this could keep the gaps open longer.

RELAP5-BW does not have a bypass model capable of simulating the expected dynamics. Rather, the best-practice is to estimate the maximum flow rate and tune the steady-state solution to that value. At maximum flow, reflood rates are expected to be conservatively high.

5.3.1.5.7 Core and Upper Plenum Multi-Dimensional Mixing / Void Distribution / Two-Phase Liquid Level

During the reflood phase, multi-dimensional fluid flow behavior in the upper plenum and core becomes important for mass and energy release calculations when core heat transfer is a function of the reflooding rate. Later, following safety injection switchover to the hot leg (i.e., after 90 minutes), the mixing efficiency of the hot fluid residing in the upper plenum and core region with the cold safety injection arriving via the upper plenum is important for determining core steaming rates. It is this realignment of the safety injection that provides the ultimate termination of core steaming.

The ability of RELAP5-BW to calculate flow distributions in the upper plenum and core during reflood is demonstrated in Reference 26 through code assessments against test data from LOFT, CCTF, and SCTF. These assessments demonstrate that the code is capable of modeling and predicting the measured flows in these tests. A simplified analytical model is applied in the GOTHIC model to describe the mixing efficiency in the upper plenum and core during the latter LBLOCA phases. A complete discussion of this model is described in Section 6.1.4.

5.3.1.6 Conclusion

The adequacy of RELAP5-BW code has been validated for performing deterministic mass and energy LBLOCA analysis for the U.S. EPR. This effort included a review of code governing equations and numerics, evaluation of the applicability of code models and correlations (with an emphasis on code resolution of high rank phenomena), and assessment of code performance for simulating integral effects and separate effects experiments. While the developmental assessment database needs to explicitly provide mass and energy assessments for critical flow, liquid carryout, and steam quenching to satisfy a NUREG-0800 requirement, the existing assessments indicated that the code is capable of adequately predicting all but one medium-rank and one high-rank mass and energy phenomena, as identified by the U.S. EPR PIRT. These are hot leg nozzle bypass and decay heat phase multi-dimensional fluid mixing, respectively. Hot leg

nozzle bypass can be conservatively defined through input. The lack of a multi-dimensional fluid flow model in RELAP5-BW limits its application to only the early LBLOCA phases. To address the multi-dimensional fluid mixing in the upper plenum and core regions during the decay heat phase, an appropriate modeling treatment is necessary and has been developed for AREVA NP's containment response evaluation methodology to overcome the limitation with RELAP5-BW (Section 6.1.4).

This assessment demonstrates that the RELAP5-BW computer code is adequate for performing U.S. EPR LBLOCA mass and energy analyses when used with an appropriate modeling approach and guidance.

5.3.2   GOTHIC

AREVA NP uses the GOTHIC computer program to calculate the U.S. EPR containment thermal-hydraulic response to mass, momentum, and energy releases from postulated pipe break scenarios (e.g., design-basis LOCAs and MSLBs). GOTHIC was developed from the public domain containment analysis code, COBRA-NC by Numerical Applications Inc. (NAI), which owns the code together with the Electric Power Research Institute. GOTHIC solves the conservation equations for mass, momentum, and energy for multi-component, multi-phase flow.

Its modeling capabilities address the analysis requirements for both current generation containment designs with active cooling systems, and new containment designs with passive cooling systems. Specifically, GOTHIC calculates both forced and buoyancy-dominated flows, condensation and evaporative heat transfer in the presence of non-condensables, stratification, and any associated control systems. GOTHIC simulations can include models of engineered safety systems, including valves and doors, pumps and fans, cooling sprays, heat exchangers, and hydrogen recombiners. Incorporating these models enables calculating the containment response to both automatic and manual actions. Engineered safety features are activated through trips, which respond to changes in selected variables such as pressure, temperature, and velocity, or on the status of other trips. Trips also are used to control boundary conditions.

GOTHIC's validation base for lumped-parameter and coarsely meshed distributed parameter models is very good. It has been assessed against ISP 29, ISP 35, and ISP 37; BFMC blowdown tests D-1, D-15, D-16, C-13, and C-15; BFMC hydrogen mixing tests 6, 12, and 20; HEDL hydrogen mixing tests HM-5 and 6; LACE tests LA-5 and 6; Marviken tests 17, 19, 22, and 24; CVTR DBA tests 3, 4, and 5; and HDR tests V21.1, T31.1, T31.5, and V44. This validation base has been extended by Battelle's application of GOTHIC to the CEC-F2 experiment, VANAM-M2, PAR test MC1 and MC3, all tests in the BFMC, and several HDR tests, including simulations of E11.2 and E11.4 using a truly two-dimensional six-node region for the dome. (See Reference 18 for summaries and related references.)

5.3.2.1   *Field Equations*

GOTHIC models the containment building as a collection of interconnected volumes. As a lumped-parameter model, GOTHIC treats each building compartment as a single control volume. A more detailed analysis is be obtained by subdividing some or all of the control volumes into one-, two- or three-dimensional Cartesian meshes. Mass, momentum and energy are transferred between control volumes using one-dimensional flow paths. Heat transfer to and from structures is handled using thermal conductor models. The response of a model is calculated by solving a combination of mass, momentum, and energy conservation equations for three phases (vapor, liquid, and droplets), and mechanistic models for interface mass, energy, and momentum transfer. (An ice phase is also included for simulating ice-condensers.)

The thermal-hydraulic field equations must be able to simulate the expected containment response phenomena. GOTHIC solves the conservative equations for a fixed volume that represent either an entire region of interest or a portion of the total volume. The field equation formulation carries the storage, convective, and diffusion terms, as well as additional terms characterizing the contributions from boundary, interface, and equipment sources. The separate sets of mass and energy conservation equations are provided for continuous liquid, continuous vapor, droplet, and mist fields.

This enables the analyst to account for possible thermodynamic and mechanical non-equilibrium between the phases. Heat transfer through structures can be included and coupled with the hydraulics model.

GOTHIC solves the mass and energy conservation equations for five flow fields: steam, liquid, drop, mist, and ice (ice is not applicable to the U.S. EPR), and for each of the pre-selected, non-condensable gas components. By including separate droplet and mist fields, GOTHIC offers expanded code capability and user options. This eliminates the need for ad-hoc liquid-carryover fractions and dropout and flashing models commonly used in similar codes. The steam/air mixture, termed the vapor phase, can take the form of bubbles or a continuous vapor region. The liquid phase can exist as pools, films, or liquid drops. The drop phase results from break discharges, de-entrainment from condensate films, or spray nozzles. The fluid energy equation is solved for enthalpy, so the equation is written in terms of enthalpy rather than internal energy. The phase balance equations are coupled by mechanistic models for interface mass, energy, and momentum transfer that cover the entire flow regime from bubbly flow to film/drop flow, as well as single-phase flows. The interface models enable thermal non-equilibrium between phases and unequal phase velocities, including countercurrent flow.

Reference 44 provides additional details on the field equations in GOTHIC, including the differences between GOTHIC's field equation model for sub-divided, multi-dimensional analysis and for lump parameter analyses. Table 5-4 summarizes how GOTHIC satisfies the field equation requirements.

Table 5-4—Field Equations / Models in GOTHIC

Scenario and PIRT Requirements	GOTHIC Model Existence	Field Equations / Model
Non-equilibrium multi-phase flow	Yes	Energy equation for liquid, droplets, and steam/gas/mist fields; continuity equation for liquid, droplets, and steam; unequal velocity (N/A for single-volume nodalization); unequal temperature
Non-condensable gas flow	Yes	Separate continuity equation for each gas component
Multidimensional flow capability	Yes	Multiple lumped parameter volumes with a three-dimensional subdivided dome
Multi-region structure heat flow	Yes	Standard one-dimensional heat conduction model
Separation due to gravity	Yes	Gravity pressure differential in flow field equations
Interfacial exchange terms	Yes	Mass and energy transfer between flow fields, vaporization and condensation
Spray / fans	Yes, not applied	No safety-grade sprays or fans in U.S. EPR

5.3.2.2 Closure Equations

Closure relationships for heat and mass transfer are necessary even with the simplification of the field equations used to perform global pressure and temperature analysis using a single-volume, lump parameter approach. These closure relationships complete the heat and mass model through correlations describing the particular phenomenon and coupling the phenomenon between the four fluid fields and solid structures inside the containment, as appropriate. These encompass the wall source terms that include convective heat transfer, condensation and boiling (evaporation) at the structural surfaces, friction at walls, and orifice drag in junctions.

The GOTHIC conservation equations do not limit the thermodynamic and mechanical characteristics of the four fields. Closure relationships account for interfacial transitions between all four fields. Table 5-5 summarizes how the GOTHIC closure equations satisfy the requirements of the PIRT. The closure equations address both interfacial

source terms and wall-to-fluid heat transfer. For the interface source terms it is assumed that there is no mass or energy storage at the interface. The various models require flow regime maps, heat transfer correlations, state relationships, and fluid and material properties for completeness.

As indicated in Table 5-5, the GOTHIC code has the required closure equations and the capability through code input to address the important containment phenomena for quantifying the global pressure and temperature response following an LBLOCA.

Table 5-5—Phenomena / Processes in GOTHIC

Component	Phenomenon	GOTHIC Model	Model
Atmosphere	Multi-component gas compression / expansion	Yes	Equation of state
	Inter-compartmental transport by buoyancy	Yes	Multiple volume nodalization
	Spray mass and energy exchange	Yes, not applied	No safety-grade sprays or fans in U.S. EPR
	Atmosphere cooling by fan-cooler	Yes, not applied	No safety-grade sprays or fans in U.S. EPR
	Buoyancy / stratification (regional)	Yes	
Structure	One-dimensional transient conduction	Yes	Standard one-dimensional heat conduction model
	Free convection (wall condensation)	Yes	Diffusion Layer Model (DLM or DLM-FM)
	Liquid film advection	Yes, not applied	Condensate appears immediately in the pool region of lump-parameter volumes and is tracked in subdivided volumes
Pool	Free convection (wall condensation)	Yes	Reynolds analogy

5.3.2.3   Code Numerics

The finite-volume equations for the mass, energy, and momentum balances are written such that they may be solved for either a lump parameter form or for a rectangular mesh (to resolve flow fields in multi-dimensional geometries). Mass and energy balances are maintained for each finite-difference volume. Lumped parameter finite-

difference volumes are defined by the total free volume, height, and hydraulic diameter. The actual shape of a lumped volume is unspecified. All calculated variables are cell-centered except for velocity, which is a function of cell edge velocities. Cell center velocity is zero for a single-volume representation.

The transient, one- or two-dimensional heat conduction equation is solved for all unheated conductors. The geometry can be represented as a flat plate, a solid cylinder, or a cylindrical tube. For plate geometries, the solver calculates the temperature profile through the thickness of the plate and optionally one orthogonal direction. For cylindrical geometries, the radial temperature profile is calculated and optionally the axial temperature profile. The solution is fully implicit in the conductor temperatures. For convective heat transfer, the fluid temperature and the heat transfer coefficient are treated explicitly; except when it is a single-volume representation. In this case the cell-center velocity is zero.

The suite of equations is reduced to a matrix describing volume pressure and junction velocities. Although GOTHIC has several solution algorithm options, Gaussian elimination is generally used for lump parameter models. The GOTHIC numerical solution has been validated through the numerous assessments reported in the GOTHIC qualification document (Reference 31).

5.3.2.4   Structure and Nodalization

The GOTHIC code has the capability to model the necessary components for containment global pressure analysis, including atmosphere, structure, pool, and control systems. Nodalization is flexible, in that control volume and conductor properties are described uniquely for each volume or conductor node. Models applying GOTHIC's lump parameter capability are built with flow paths, network models, and initial/boundary conditions. Flow paths are used for describing both the connections between control volumes and the connections between control volumes and boundary conditions, enabling the addition or removal of mass, momentum, and energy. A separate set of momentum equations (one for each phase) is solved for each flow path. Network

models are applied to model piping systems. These types of hydraulic connections can include multiple branches between control volumes. Initial and boundary conditions specify the state of the fluid and solid structures at the start of a transient. These include the initial temperature and composition of the atmosphere, the location and temperature of liquid pools, the location and amount of liquid components, and the temperatures of solid structures within the building.

GOTHIC includes an extensive set of special process models to describe operating equipment. These items, referred to collectively as components, include pumps and fans, valves and doors, heat exchangers and fan coolers, vacuum breakers, spray nozzles, coolers and heaters, volumetric fans, hydrogen recombiners, igniters, and pressure relief valves.

The level of detail required for numerical analysis depends on the application and the important figure(s)-of-merit. For containment safety analysis, the code must be able to adequately model the thermal-hydraulic behavior of the important components and associated control systems for the chosen event scenario. As discussed in Section 4.3.4.2, for well-mixed environments the behavior of global system variables, like pressure, can be appropriately simulated with coarse, single-volume nodalization. Section 6.2 presents several assessments addressing single-volume vs. multi-volume nodalizations against test program data. Section 6.3.4 provides conclusions about the merits of the single-volume model for LBLOCA analyses.

5.3.2.5   Evaluation of High Rank Phenomena

The GOTHIC code has benefited from extensive assessment, performed over many years, of its capability to determine the response of nuclear power plant containments to a LOCA (Reference 31). Most of these assessments are applicable for U.S. EPR. However, because the U.S. EPR does not use safety-grade spray or fan coolers, additional studies have been performed to expand GOTHIC's assessment database to address this U.S. EPR design element.

This section provides an overview of how GOTHIC simulates the primary mechanism for heat transfer, i.e., to the containment passive heat sinks (the steel shell and concrete Containment Building). This is through condensation on the inside of the shell, conduction through the shell and concrete, and direct condensation on the IRWST surface.

5.3.2.5.1   *Structure Free Convection / Wall Condensation*

Following an LBLOCA, the condensation of steam on containment walls reduces containment pressure and temperature directly through heat transfer from the atmosphere and the removal of steam mass. Condensation is a complex phenomenon influenced by several conditions, including the development of a liquid film layer along the wall surface, the build-up of non-condensable gases outside the film condensate layer, movement or rippling of the film surface, and mist formation. A gas layer adjacent to the film surface can act as a barrier, degrading heat transfer to the wall. The interface temperature and, subsequently, the condensate mass flux decrease as a consequence of the mass diffusion process through the non-condensable gas layer. For large systems however, degradations to heat transfer caused by local non-homogeneity tends to be self-correcting, with the concentration of non-condensable gases on one section of the containment surface offset by other steam-rich sections.

The GOTHIC code includes several models for condensation heat transfer on solid structures. The presence of non-condensable gases strongly influences the condensation and associated heat transfer rate. For solid structures, GOTHIC employs heat transfer correlations that account for the effects of condensing steam and the build-up of non-condensable gases in the boundary layer, reducing the rate of condensation. For single-node GOTHIC LBLOCA analyses, AREVA NP applies the turbulent and direct condensation correlation combination of Tagami and Uchida (References 94 and 95). Both models are empirical correlations based on air-steam mixture data. The Tagami correlation is a strong function of the blowdown energy and containment volume. The Uchida correlation is a function only of the ratio of the steam mass to the

non-condensing gas mass. For the multi-node models, AREVA NP applies the

Diffusion Layer Model to calculate the convective heat transfer and the condensation

rate at a cold wall surface. The model accounts for the presence of noncondensing

gases, the water film resistance, possible mist generation near the wall, and

enhancement effects due to film roughening. The model was validated by comparison

with several experimental test sets.

In the short term, the Tagami correlation is applicable; long-term containment response

is a strong function of the Uchida correlation. The implementation of the Uchida

correlation in GOTHIC has been studied and is documented in Reference 31. While the

GOTHIC studies show that application of the Uchida model exhibits wide scatter in heat

transfer predicted-to-measured results, the results trend the data well. GOTHIC

supports modeling treatments that enable users to address model uncertainty.

Free convection has secondary importance relative to wall condensation. GOTHIC

provides several models. The general correlation for free convection on a vertical plate

(Reference 77) is used, and is based only on fluid and wall properties. Forced

convection can also be modeled. However, as described in Section 4.3.4.2, a single-

volume GOTHIC model is used in AREVA NP's containment response evaluation

methodology. With the single-volume model the containment air/steam flow is always

zero; hence, no heat transfer by forced convection is credited in this approach.

5.3.2.5.2   *Structure Conduction*

All solid structures are referred to in GOTHIC as thermal conductors. Thermal

conductors are modeled as one-dimensional slabs in which heat transfer occurs

between the fluid and the conductor surfaces and within the conductor perpendicular to

the surfaces. Nodalization of a conductor allows variation of material properties in the

direction of heat transfer. Heat generation within thermal conductors may be specified

on a node-by-node basis. In addition, non-flowing fluid gaps can be modeled as a

separate heat conducting region. GOTHIC numerically solves the heat conduction

problem using finite difference. The number and location of temperature nodes through

the conductor needed to obtain an accurate solution depends on the material properties, conductor thickness, heat transfer coefficient, and rate of change in the fluid temperature.

Thermal conductor nodalization may be specified by user input or by GOTHIC's "auto-divide" automatic nodalization feature. Generally, surface nodes should be more closely spaced for materials with low conductivity or in the presence of large heat transfer coefficients and rapidly changing fluid temperature. The auto-divide feature applies this progressive subdivision of the conductor based on a Biot number criterion and a user-selected characterization of the magnitude of the expected heat transfer coefficient on the conductor inner and outer surfaces. The Biot number criterion is

$$Bi = \frac{h\Delta x}{k} = 0.1$$,

where Δx is the mesh spacing, h is the heat transfer coefficient and k is the thermal conductivity. This approach is recommended by the GOTHIC code developers and, therefore, is the approach used by AREVA NP for containment analyses.

5.3.2.5.3   Pool Free Convection/Direct Condensation

Vaporization and condensation can occur on a pool surface, such as the U.S. EPR IRWST. Heat is transferred to or from the interface depending on the relative values of the interface and phase temperatures. Since the interface cannot store any heat, any energy surplus or deficit must be made up by vaporization or condensation at the interface. GOTHIC applies a "Reynolds analogy" to model these pool heat transfer mechanisms. The qualification of this GOTHIC model is weak for applications to the U.S. EPR.

In addition, the lump parameter approach inherits an implicit assumption of homogeneity within each phase; that is, all of the liquid within a control volume is calculated to be at a single temperature. Therefore, it is not possible to represent a situation where condensation of steam on a free liquid surface locally warms the liquid

at the surface, limiting further condensation. If sufficient steam is available, then
condensation is calculated to continue until all subcooling has been removed from the
liquid present in the control volume containing the steam/liquid interface. While this is a
weakness in GOTHIC and the lump parameter model, this phenomenon can be treated
conservatively by neglecting it.

5.3.2.6   *Conclusions*

The GOTHIC code has been evaluated to determine its adequacy for performing global
pressure and temperature containment response analysis of an LBLOCA in the U.S.
EPR. This effort included a review of the code-governing equations and numerics,
evaluation of the applicability of code models and correlations with an emphasis on
code resolution of high rank phenomena, and assessment of integrated code
performance for simulating integral effects and separate effects experiments. The
assessments indicated that the code is capable of adequately predicting nearly all
medium- and high-rank mass and energy phenomena, as defined by both the
containment pressure and temperature PIRT developed for the U.S. EPR. For the
specific application of GOTHIC to the U.S. EPR, there is one exception: interfacial heat
transfer from the IRWST. A conservative modeling treatment is applied to overcome
modeling limitations in this situation (i.e., no heat transfer assumption). As such, when
used with an appropriate modeling approach and guidance, GOTHIC is adequate for
performing U.S. EPR LBLOCA global containment pressure and temperature analyses.

6.0   VALIDATION AND SENSITIVITY ANALYSIS

The process for producing a reliable analysis code consists of three phases: development, developmental assessment, and independent assessment. Both RELAP5-BW and GOTHIC have benefited from extensive development and assessment efforts. For RELAP5-BW, much of the assessment has been performed for applications studying ECCS performance (i.e., peak cladding temperature). While for GOTHIC, much of the assessment has been performed by the code vendor and does not necessarily reflect how the code is applied in containment analyses supporting a plant's licensing basis. Several studies are provided in this section to demonstrate the applicability of both RELAP5-BW and GOTHIC for assessing containment behavior of the U.S. EPR following an LBLOCA.

This section provides a diverse examination of phenomena relevant to containment analysis using data from separate-effects and integral test programs and the RELAP5-BW, GOTHIC, and GASFLOW best-estimate thermal-hydraulic codes. Separate-effects tests, the RELAP5-BW studies, and one GOTHIC study appear in Section 6.1. Integral-effects tests featuring GOTHIC calculations using both single-volume, multi-volume, and sub-divided nodalization models appear in Section 6.2. A GASFLOW computation fluid dynamics analysis of the U.S. EPR's best-estimate response to a LBLOCA is presented in Section 6.3.

6.1   Separate Effects Test Benchmarks (EMDAP 14)

This section presents two RELAP5-BW separate-effects studies highlighting core heat transfer and liquid carryout (Sections 6.1.1 and 6.1.2). These studies were originally developed for validating RELAP5-BW's BEACH heat transfer package for ECCS performance analysis applications (Reference 26). A new RELAP5-BW assessment against test data from the steam generator heat transfer FLECHT-SEASET experimental program is presented in Section 6.1.3. An analytical assessment of upper plenum and core region multi-dimensional fluid flow and mixing is presented in Section 6.1.4. The objective of that assessment is to provide the technical basis for an

analytical model describing the mixing efficiency of pumped safety injection and resident core flow for use in U.S. EPR GOTHIC LBLOCA simulations. One GOTHIC separate-effects study is included in this section to justify applying the Diffusion Layer Model for steam condensation.

6.1.1   Core Heat Transfer

For containment LOCA analysis, the methodology for core heat transfer is described in Section 5.1.2.3 of Reference 14. The analysis tool for this methodology is the RELAP5-BW code (Reference 19). In general, this methodology is the same as that used for peak cladding temperature LOCA analysis (Reference 26), but with exceptions aimed at maximizing the energy removal to containment. These exceptions will be addressed in this section in the course of describing the core heat transfer processes that occur during the short-term LOCA M&E release, which extends into reflood and core quench.

In Section 2.2 of Reference 26 and Section 2.3.3 of Reference 19, the large break core heat transfer models and correlations are reviewed. The methodology applies to all plant recirculating steam generator (RSG) categories with any differences in design—such as RCS geometry, containment pressure suppression features, ECCS design, or fuel design—addressed in each application.

6.1.1.1   Heat Transfer Processes

The blowdown phase is characterized by the rapid depressurization of the reactor coolant system to a condition nearly in pressure equilibrium with the immediate surroundings. Core flow is variable and depends on the size and location of the break. Departure from nucleate boiling (DNB) is generally calculated to occur very quickly, and subsequent core cooling is by film boiling. Subcooled boiling is calculated using the Rohsenow-Choi and Dittus-Boelter correlations and nucleate boiling is based on several correlations depending on local pressure and void fraction. The CHF correlation is specific for the fuel type. After CHF, core heat transfer reduces to film boiling, which

amounts to only a small fraction of the steady-state cooling. The fuel and cladding temperatures can increase by 600 – 800°F during the last phases of blowdown.

For mass and energy release calculations, a return to transition boiling, when predicted, is allowed to enhance the heat transfer rate from the fuel elements.

Following blowdown, a period of time is required for the ECCS to refill the bottom of the reactor vessel to the bottom elevation of the core before core reflood can be established. During this period, core heat transfer is negligible and the fuel rods undergo adiabatic heatup.

As described in Section 8.0, the refill period is shortened for containment mass and energy release calculations because the intent is to transport the core energy to the containment environment as quickly as possible. The refill period is shortened by direct injection of the accumulators into the lower plenum and downcomer.

The reflood heat transfer is computed using the BEACH heat transfer package (Reference 26) in the RELAP5-BW code. These models are designed specifically to calculate heat transferred from the fuel rods to the core hydrodynamic volumes. A fine–mesh rezoning scheme is used to model the rise in the quench front explicitly. The scheme is needed to resolve large axial variations in wall temperature that occurs in the vicinity of the advancing quench front. During this period, there is gravity-driven core reflooding and, simultaneously, cold accumulator/pumped ECC injection in contact with steam in the cold legs and downcomer. These manometric and condensation-driven forcing functions produce oscillatory flow rates and pressures.

As the quench front progresses and the liquid level builds in the downcomer, the manometric oscillations slowly dampen; lower portions of the core become cooled, and additional core cooling occurs in the upper part of the core provided by steam generated from below by the rising water level. At the same time, a fraction of the liquid is entrained and carried out with the steam flow exiting the core. The amount of steam flow and liquid carryout does not exceed the incoming safety injection, so the core

inventory continues to increase. The core is eventually covered by a two-phase mixture. The path to long-term cooling is established through continuing pumped injection.

6.1.1.2 Reflood Heat Transfer Assessments

Appendices C through G of Reference 26 document the benchmark calculations performed by AREVA NP at various stages of the code development to demonstrate its applicability to LBLOCA licensing calculations. BEACH was approved by the NRC to calculate the cladding thermal response during the reflooding phase of a LOCA in both B&W-designed plants and U-tube steam generator plants with cold leg ECCS injection.

Appendix G of Reference 26 presents the benchmark comparisons of BEACH to twelve reflood experiments, at varying conditions, selected to cover the range of expected code applications. The experiments consists of six unblocked FLECHT-SEASET tests, a G-2 test that included a mixing vane grid, two Cylindrical Core Test Facility (CCTF) tests, one Slab Core Test Facility (SCTF), one FLECHT-SEASET test that included blockage, and a REBEKA-6 test that simulated rod swell and rupture. These experiments were well designed, well instrumented, and well documented. The available data are extensive and have undergone sufficient scrutiny to assure a high level of confidence.

Table 6-1 features the test conditions for four of the single-bundle FLECHT SEASET tests and a larger scale SCTF test performed to demonstrate successful code benchmarks for reflood behavior in the core.

Table 6-1—Core Heat Transfer Benchmark Test Conditions

Test	Flooding Rate (in/s)	Pressure (psia)	Initial Temperature (°F)	Rod Power (kW/ft)	Coolant Temperature (°F)
31504	0.97	40	1585	0.7	123
31805	0.81	40	1600	0.7	124
34209	1.07	20	1636	0.72	90
31302	3.01	40	1597	0.69	126

Test	Flooding Rate (in/s)	Pressure (psia)	Initial Temperature (°F)	Rod Power (kW/ft)	Coolant Temperature (°F)
SCTF Test Conditions					
S3-15	Variable	29*	1472	0.59	Variable

* Initial pressure (after reflood initiation, pressure went to approximately 40 psia)

Core mass and energy releases during reflood are strongly correlated to the progression of the quench front. Figure 6-1 - Figure 6-8 show a succession of calculated vs. measured core heat transfer coefficient (at the assembly mid-plane) and quench front for the FLECHT-SEASET tests 31504, 31805, 34209, and 31302. These test illustrate that core cooling and quench front progression is well-predicted by RELAP5-BW for a broad spectrum of initial conditions (i.e., reflood rates, pressures, and rod and liquid temperatures). Similarly, Figure 6-9 shows the quench front progression in SCTF Test S3-15. The larger scale SCTF test included eight heated bundles with a defined hot and average core. The comparison plots that demonstrate effective heat removal are those representing the average channel. The results show that core cooling and quench front progression are well-predicted by RELAP5-BW.
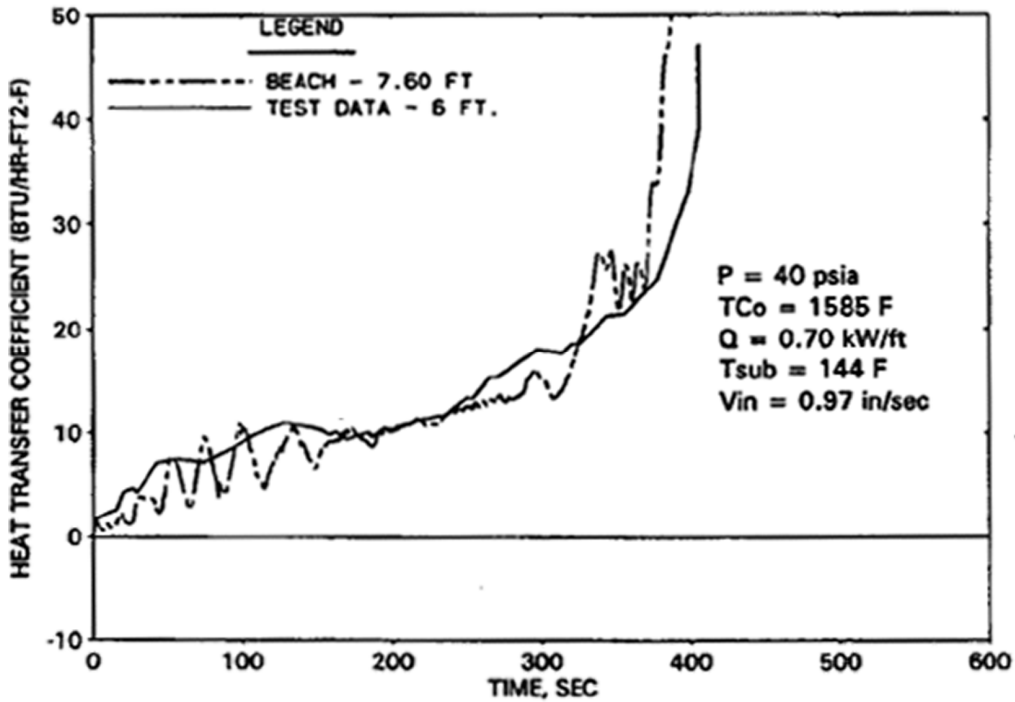
Figure 6-1—Code-to-Data Comparison of Heat Transfer Coefficient in FLECHT-SEASET Test 31504
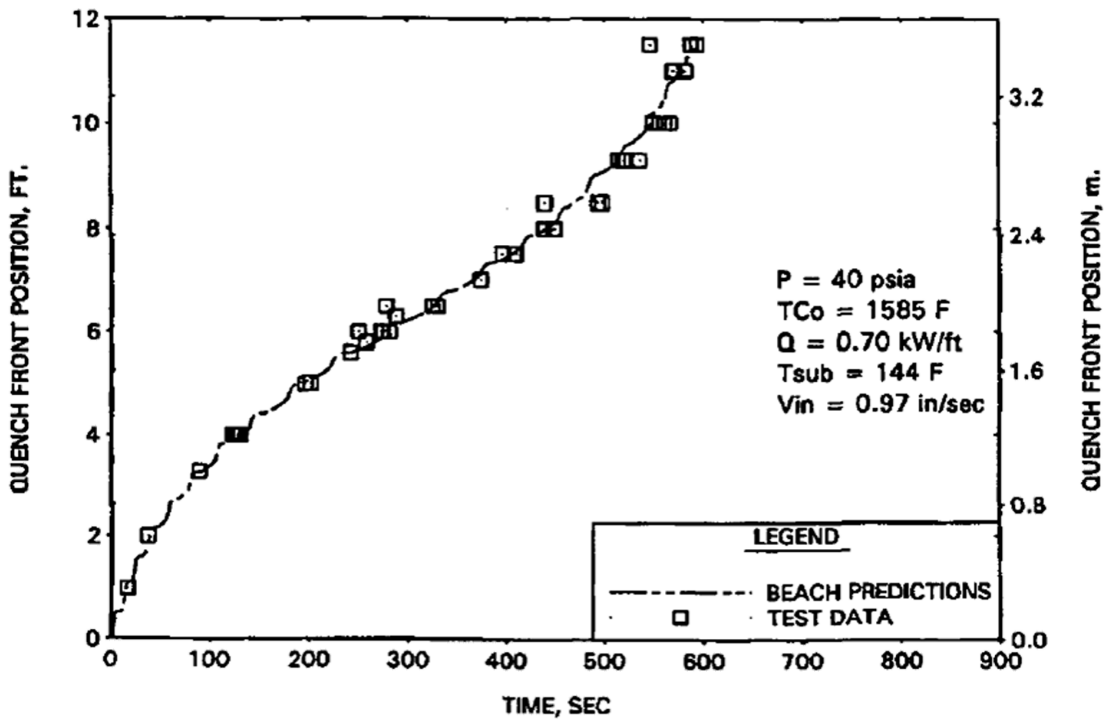
Figure 6-2—FLECHT SEASET Test 31504: Quench Elevations
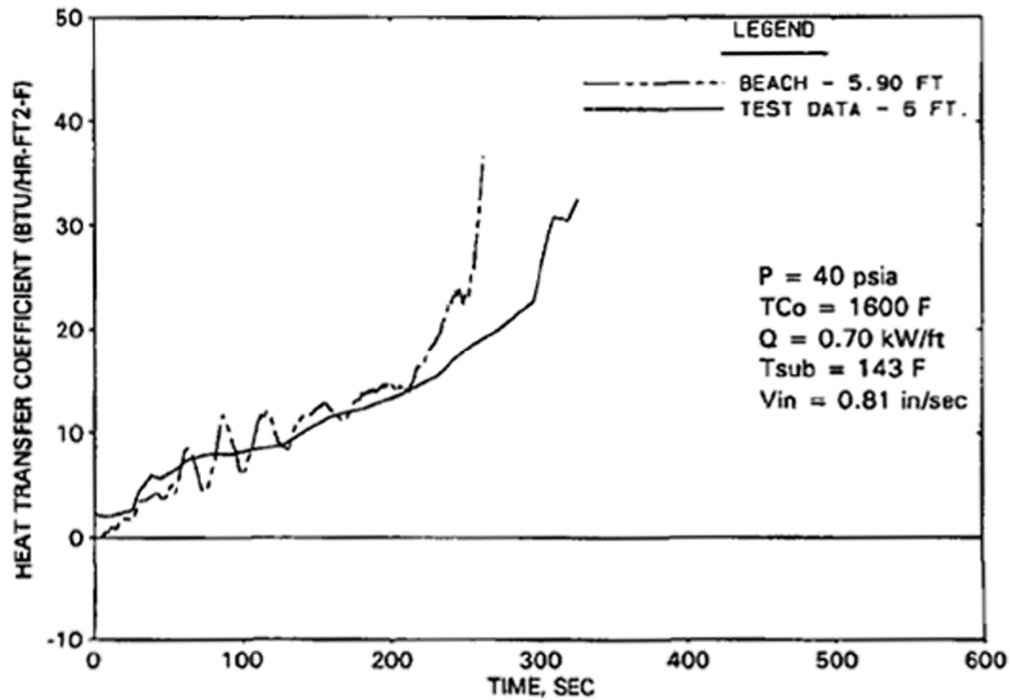
Figure 6-3—Code-to-Data Comparison of Heat Transfer Coefficient in FLECHT-SEASET Test 31805
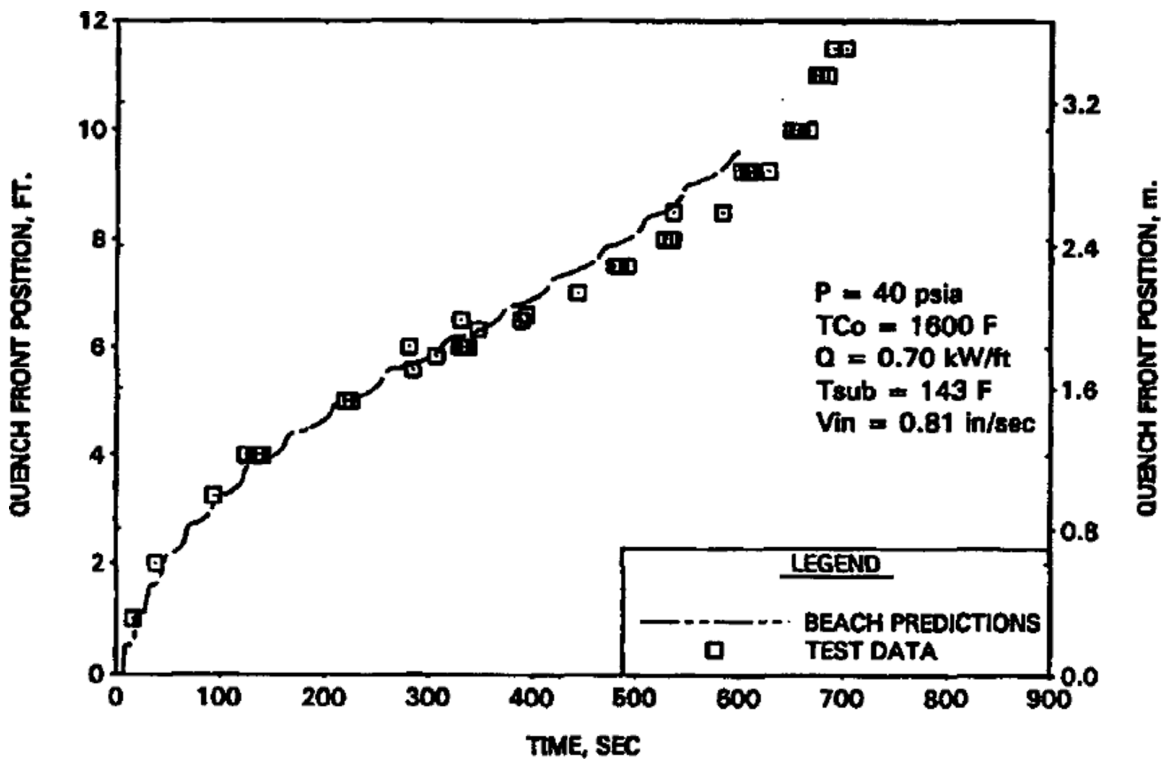
Figure 6-4—FLECHT SEASET Test 31805: Quench Elevations
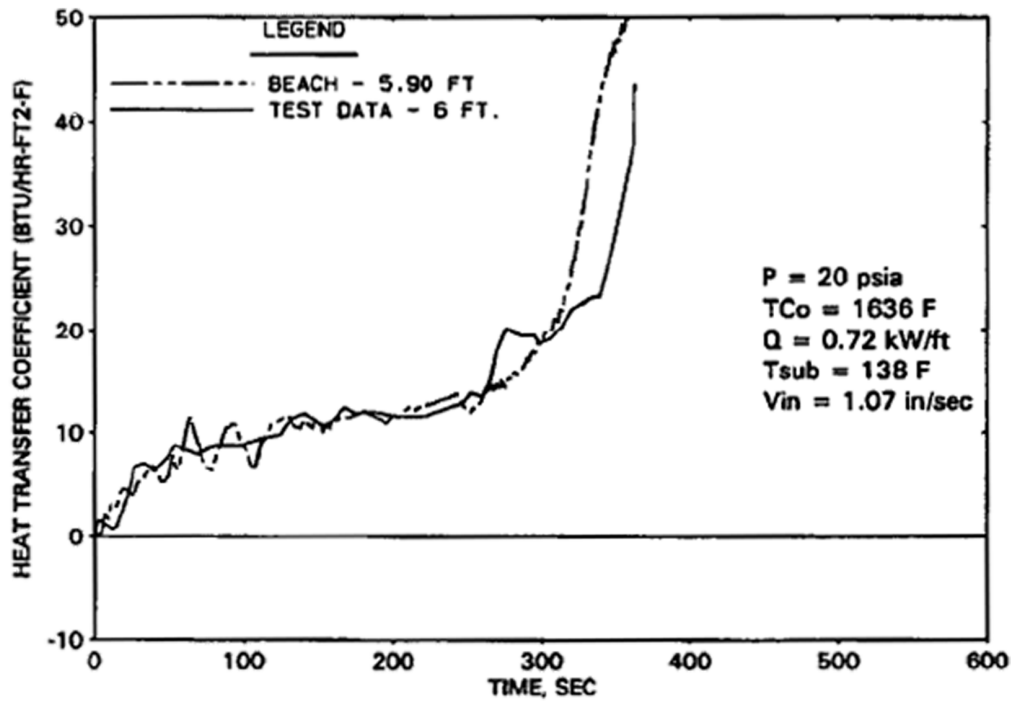
Figure 6-5—Code-to-Data Comparison of Heat Transfer Coefficient in FLECHT-SEASET Test 34209
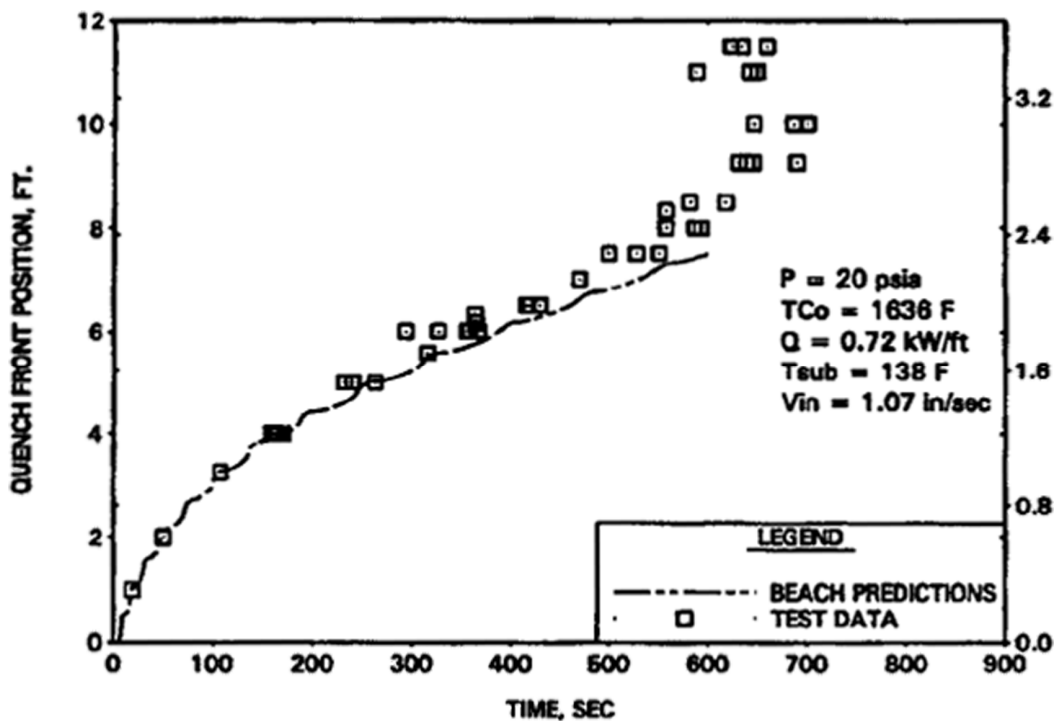
Figure 6-6—FLECHT SEASET Test 34209: Quench Elevations
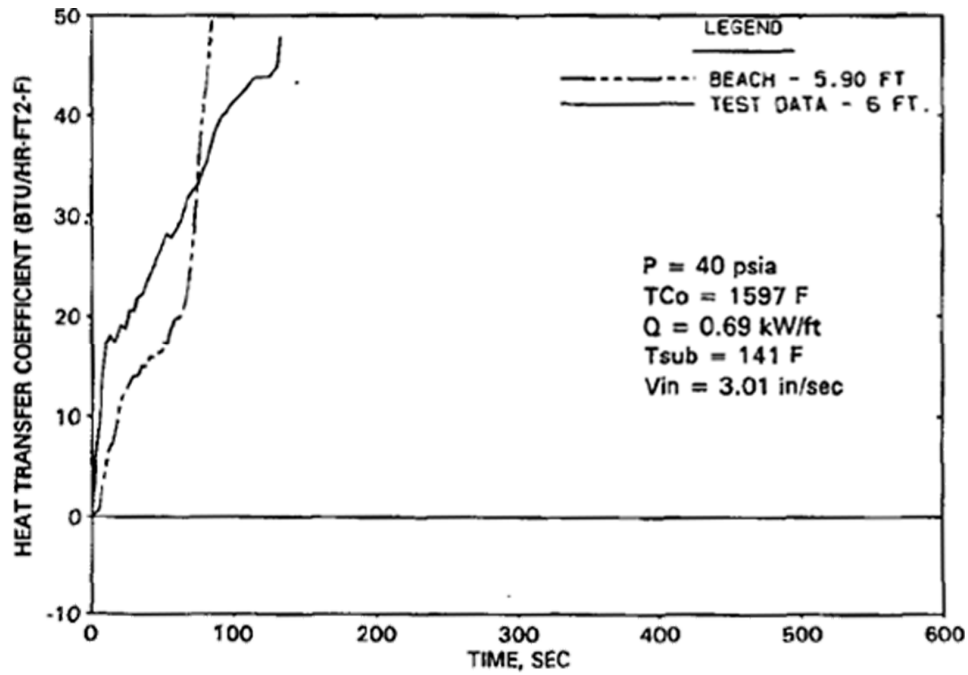
Figure 6-7—Code-to-Data Comparison of Heat Transfer Coefficient in FLECHT-SEASET Test 31302
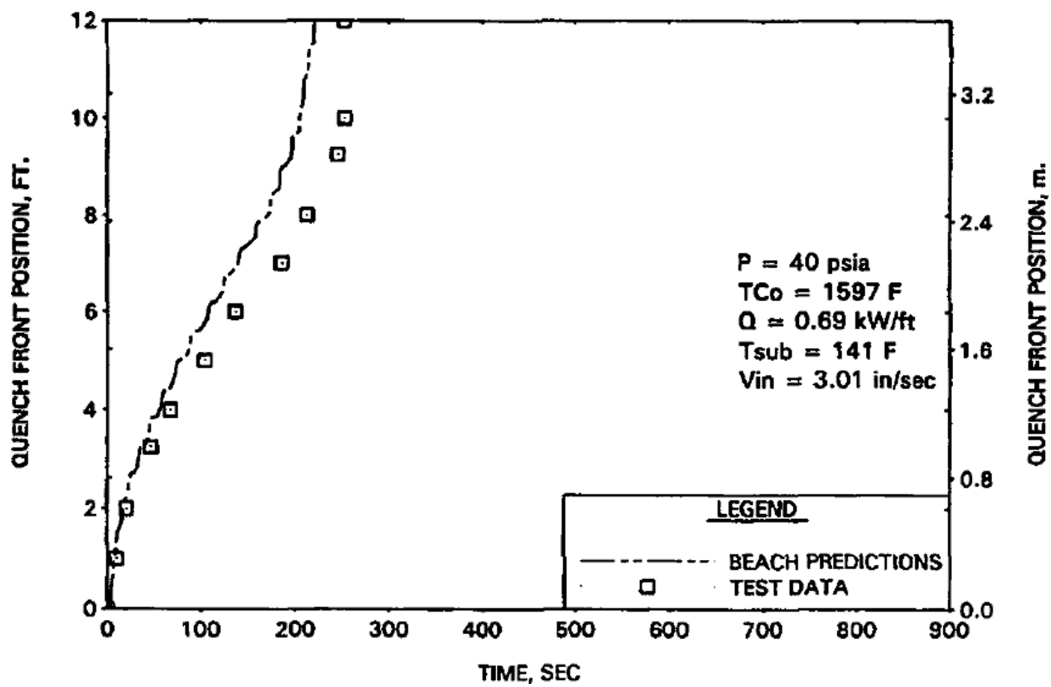
Figure 6-8—FLECHT SEASET Test 31302: Quench Elevations
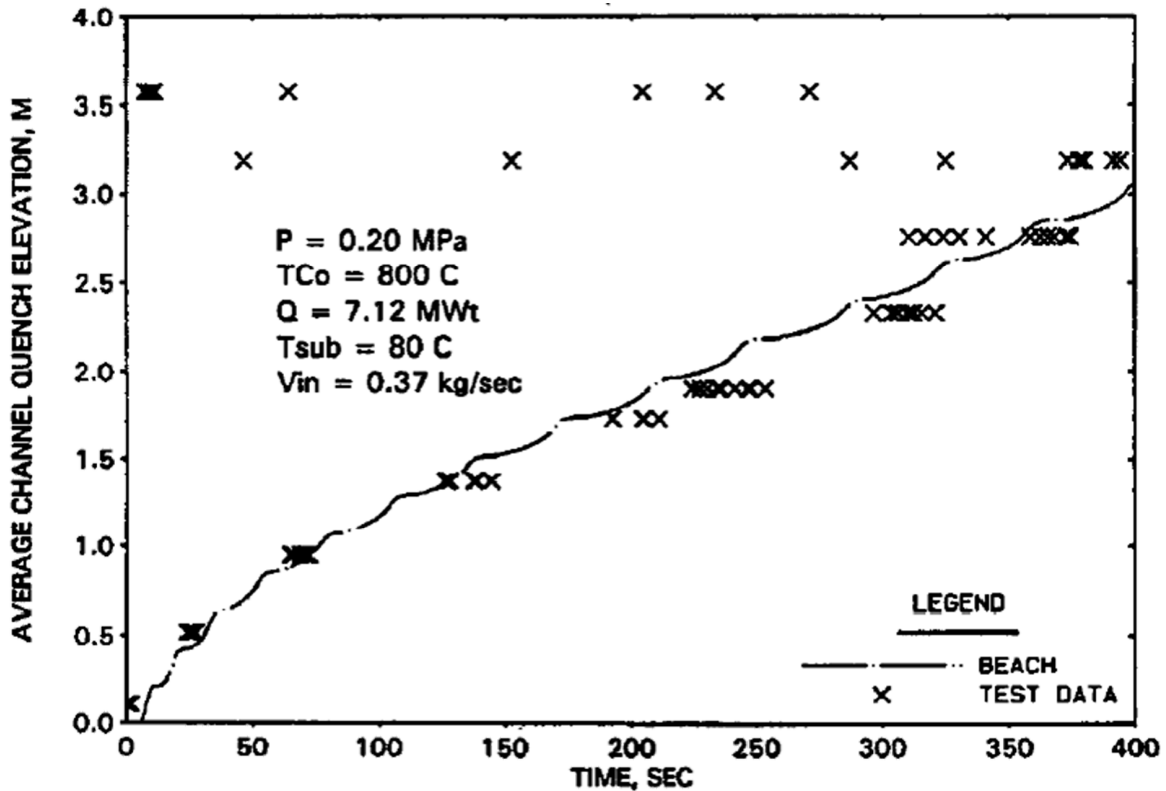
Figure 6-9—SCTF Test S3-15: Quench Elevations

6.1.2 *Carryout Rate Fraction (FLECHT-SEASET)*

As described in Section 6.1.1, the BEACH heat transfer package in the RELAP5-BW code (Reference 26) calculates thermal-hydraulic phenomena during the core reflood phase of an LBLOCA. The BEACH heat transfer package includes AREVA NP-developed code model enhancements in several areas, including the interfacial drag models for the slug and the inverse slug flow regimes. Specifically, the original RELAP5/MOD2 model were replaced by one based on the Wilson phase separation model (Reference 46). These interfacial drag model modifications improve the fluid distribution prediction and reduce numerically-induced oscillations in the core region.

Section 6.1.1.2 describes the many reflood heat transfer tests performed during the development of RELAP5-BW. One of the important parameters deduced from the test measurements was the carryout rate fraction (CRF), which is defined as the ratio of the

mass flow rate at the bundle exit to the mass flow rate at the core inlet. Results from four of the FLECHT-SEASET program tests (Reference 47) discussed in Appendix G of Reference 26 are provided to highlight the performance of RELAP5-BW for carryout rate fraction. Table 6-2 shows the test conditions. Figure 6-10 through Figure 6-13 show the measured and integrated RELAP5-BW-predicted CRF, defined as:

$$Integrated \quad CRF \quad = \quad \int W_{OUT} / \int W_{IN} \, ,$$

where,

W_{IN} = bundle inlet mass flow rates (lbm/s), and

W_{OUT} = bundle outlet mass flow rates (lbm/s).

The integrated CRF is better than the instantaneous CRF in determining the core exit flow rates, because the purpose of CRF is to determine the mass carried out of the core and into the primary side of the steam generator tube regions. The liquid is boiled to steam causing steam binding. The results show that RELAP5-BW predictions match the integrated CRF well.

Table 6-2—FLECHT-SEASET Test Conditions

Test	Flooding Rate (in/s)	Pressure (psia)	Initial Temperature (°F)	Rod Power (kW/ft)	Coolant Temperature (°F)
31504	0.97	40	1585	0.7	123
31805	0.81	40	1600	0.7	124
34209	1.07	20	1636	0.72	90
31302	3.01	40	1597	0.69	126

Figure 6-10—FLECHT-SEASET Test 31504: Integrated CRF
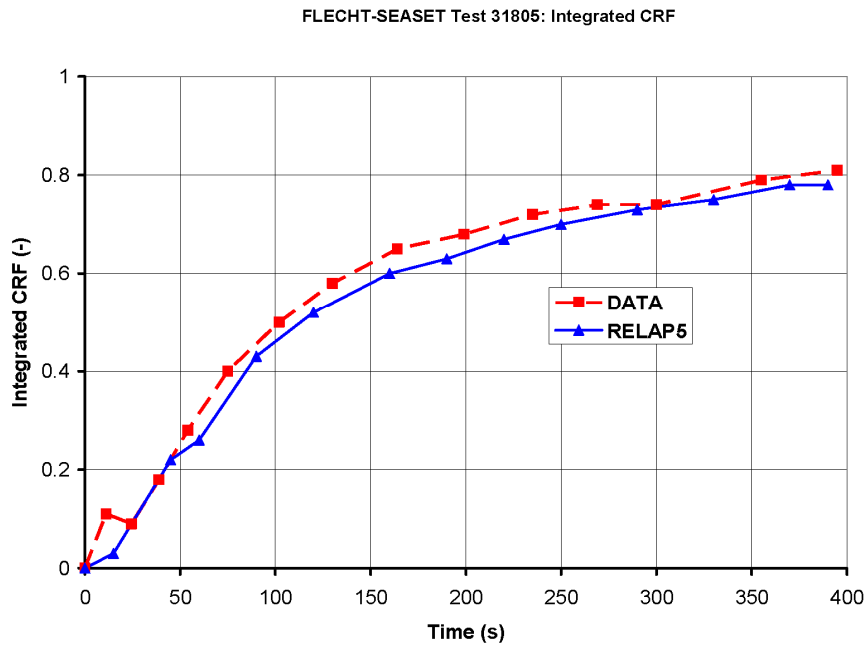
Figure 6-11—FLECHT-SEASET Test 31805: Integrated CRF
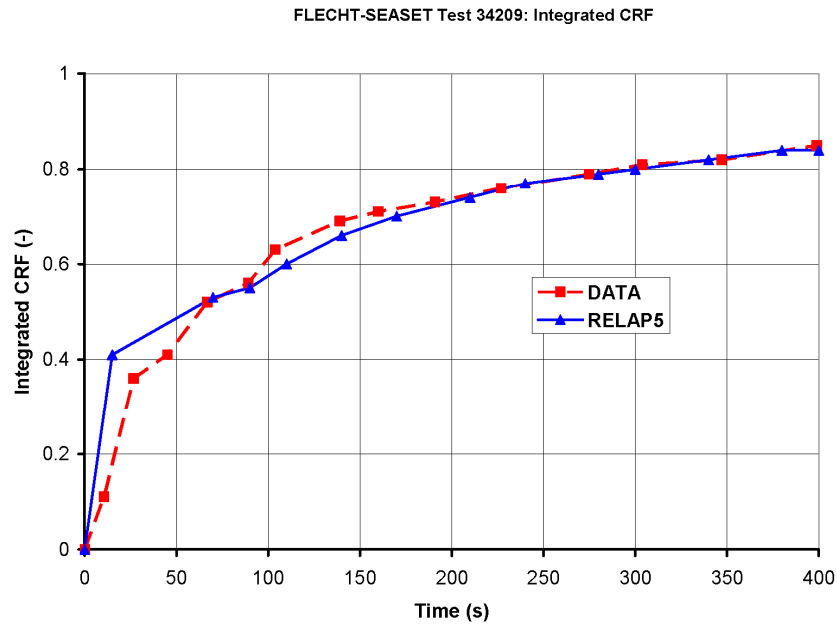
Figure 6-12—FLECHT-SEASET Test 34209: Integrated CRF
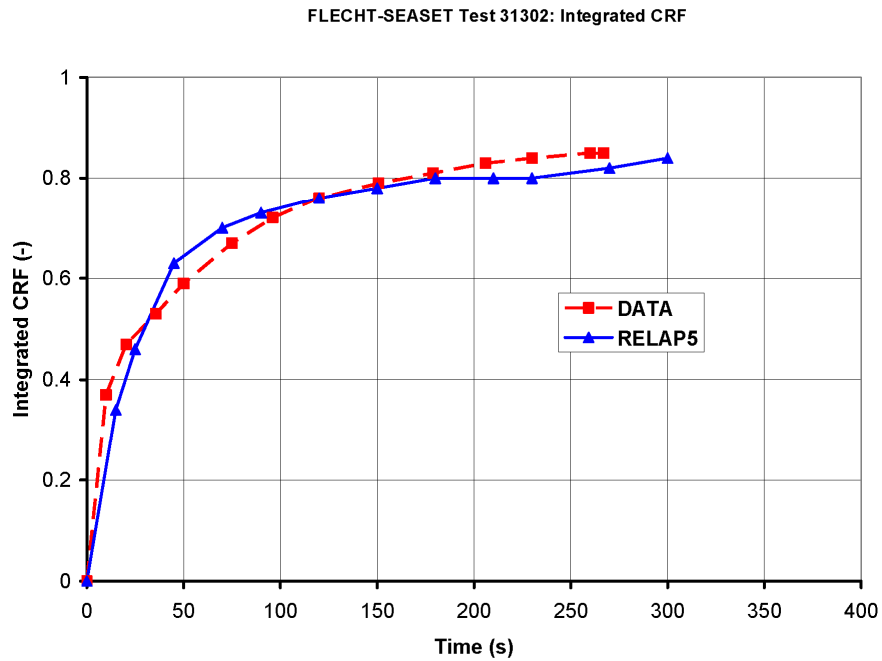
Figure 6-13—FLECHT-SEASET Test 31302: Integrated CRF

6.1.3   Steam Generator Heat Transfer (FLECHT-SEASET)

For LOCAs located downstream of a steam generator, part of the frothy, two-phase mixture from the core is forced into the broken-loop steam generator tubes during the early part of the post-reflood phase. Energy from the hot steam generator secondary fluid and metal is transferred to the froth, causing it to become all steam. The steam exiting the steam generator outlet plenum is initially super-heated, but as the steam generator secondary fluid cools from the bottom up, a two-phase mixture begins to exit the outlet plenum. If the break is in the cross-over leg (i.e., RCP suction), the safety injection flow to that cold leg mixes with the steam and water coming from the intact loops and spills out the pump side of the break. If the break is downstream of the RCP, the safety injection line to that cold leg is assumed to be broken and spilling to containment, in which case the steam and water coming from the intact loops exits the vessel side of the cold leg.

The heat transfer between the secondary side of the steam generators and the primary fluid is important for peak containment pressure calculations. During reflood the secondary side of the steam generators is at a higher pressure than the primary fluid of superheated steam and saturated droplets. The steam-droplet interfacial heat transfer model influences the degree of vapor superheat and the temperature difference between the vapor and the tube wall.

During the reflood portion of a postulated LOCA event, the two-phase mixture is swept into the reactor upper plenum and travels down the hot leg into the steam generator inlet plenum. At the start of reflood, the primary side of the steam generator is dry and the secondary side collapsed level covers the tubes. When the two-phase mixture enters the tubes, additional boiling occurs on the tube walls. As the steam generator cools down, the primary side exit temperature approaches its saturation temperature.

The FLECHT-SEASET tests (Reference 48) measured the energy transfer from the hot steam generator secondary fluid to the cooler two-phase mixture flowing through the steam generator tubes under large-LOCA, post-blowdown conditions. Two-phase

mixtures were forced into the steam generator test assembly at various flow rates and void fractions to measure the transient heat transfer rates and fluid temperature distribution.

The FLECHT-SEASET experimental test results showed the appearance of a quench front inside the steam generator primary side tubes. The dispersed two-phase flow above the quench front provided enough heat transfer and precursory wall cooling so that the quench front advanced up the tubes. An abrupt drop in the temperature at certain times confirms there is active heat transfer inside the tubes.

AREVA NP performed a series of FLECHT SEASET steam generator heat transfer benchmarks using RELAP5-BW to demonstrate that its containment analysis methodology closely predicts the heat transfer from the secondary to the primary side in the post-reflood phase. Tests 21806, 21909, 22314, and 22415 were selected because of the similarity of their initial thermal-hydraulic conditions with those of the U.S. EPR during the reflood and post-reflood phases. Table 6-3 provides the initial and boundary conditions for these tests. Figure 6-14 shows the nodalization diagram for the FLECHT SEASET steam generator heat transfer tests.

Table 6-3—Initial and Boundary Conditions for the FLECHT-SEASET Tests

Test Number	Test 21806	Test 21909	Test 22314	Test 22415
Steam Flow, lb/s	0.100	0.100	0.248	0.213
Water Flow, lb/s	0.400	0.847	0.252	0.402
Steam Temperature, °F	299	309	311	300
Water Temperature, °F	262	264	260	256
Mixer Pressure, psig	29	30	28	29
Outlet Pressure, psig	25	25	25	25
SG Water Level, ft	32.7	34.0	34.3	33.8
SG Dome Temperature, °F	520	525	523	522
Mixer Quality	0.2	0.105	0.495	0.345
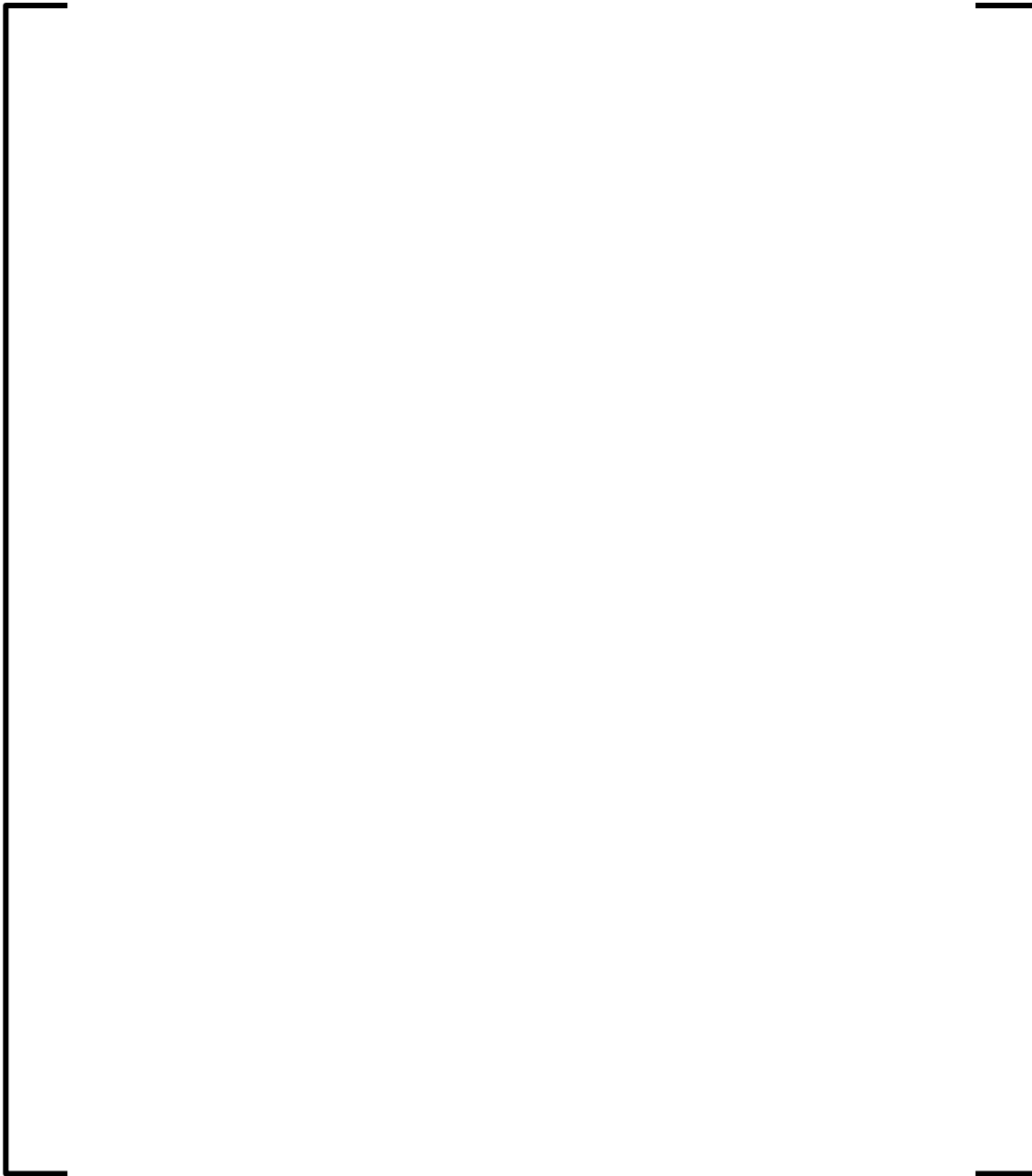
Figure 6-14—FLECHT SEASET Steam Generator Nodalization Diagram

AREVA NP performed a series of sensitivity studies to compare the test results to code predictions. They found that the Biasi-Zuber critical heat flux (CHF) correlation (References 49 and 50) under-predicts the dryout location in the steam generator. The Becker CHF correlation (Reference 51) predicts the dryout location more accurately.

AREVA NP Inc.

Applicability of AREVA NP Containment Response Evaluation Methodology to the
U.S. EPR™ for Large Break LOCA Analysis

Technical Report

ANP-10299NP

Revision 2

Page 6-17

Therefore, the analyses presented in this section for the four FLECHT-SEASET tests use the Becker CHF option for both the tube and shell sides in the steam generators.

Figure 6-15 compares the predicted steam generator (vapor) temperature on the tube side, the tube wall temperature, and the shell (liquid) temperature with the Test 21806 data. Since the test data were for temperatures 10 ft above the inlet to the steam generator, the comparison was made to temperatures at that same elevation in the RELAP5-BW model. The test data show the tubes quench at around 550 seconds into the transient, compared to about 250 seconds for the RELAP5-BW prediction.

Figure 6-16 compares the energy of the shell side for Test 21806 with the RELAP5-BW prediction. The energy content on the shell sides was not obtained directly from the tests, but was calculated based on the initial conditions of the fluid on the shell side. As the figure shows, the rate of heat removal from the shell side predicted by RELAP5-BW is slightly greater than indicated by the test results.
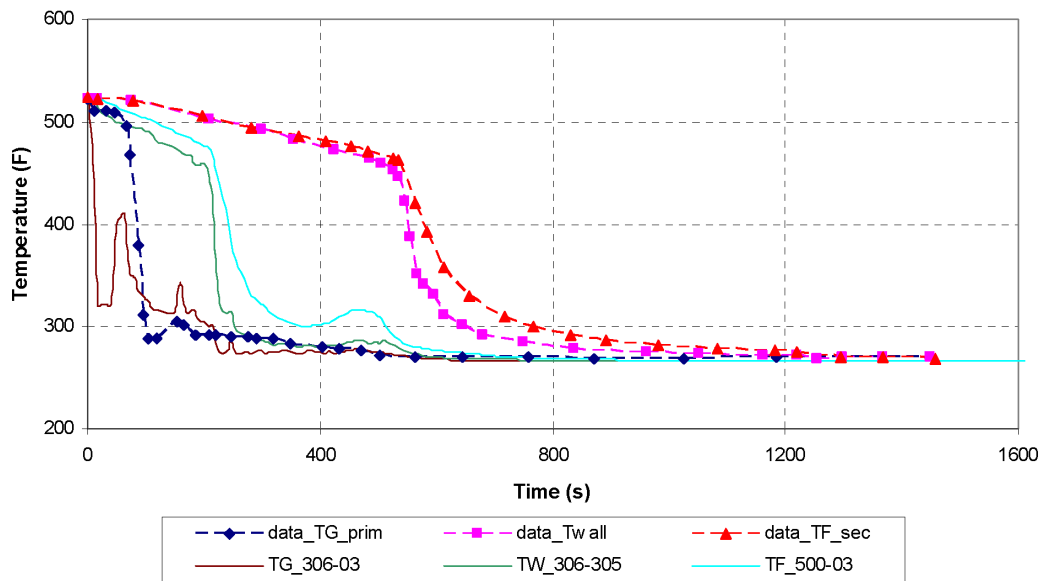
Figure 6-15—Tube, Wall, and Secondary-Side Temperatures, Test 21806 (Becker CHF)
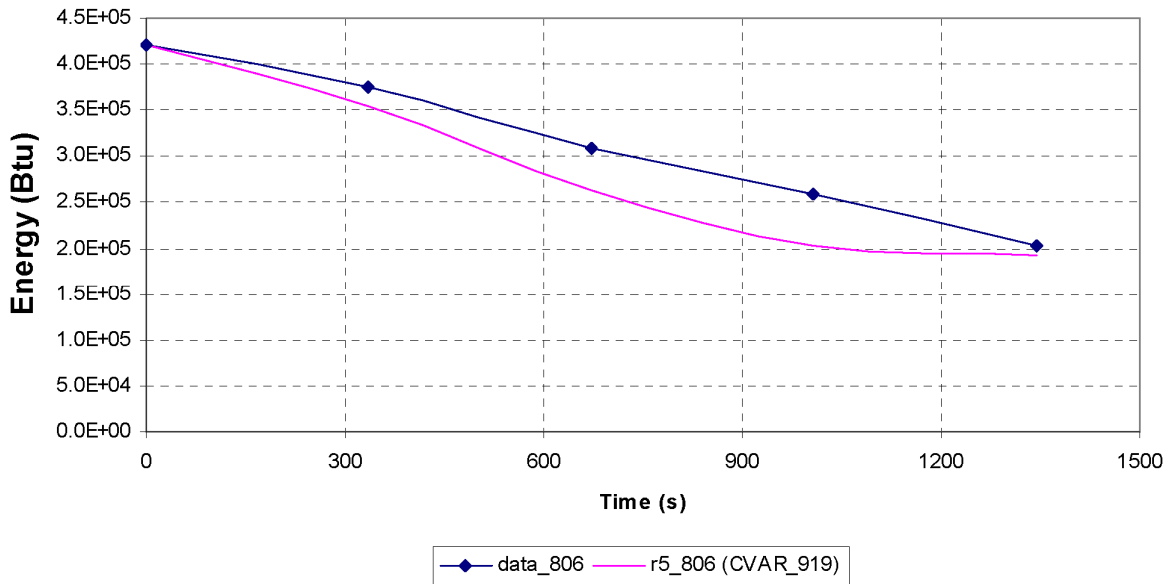
Figure 6-16—Steam Generator Energy, Test 21806 (Becker CHF)

Test 21909 and Test 21806 have the same tube-side steam flow, but the water injection is almost double for Test 21909. Figure 6-17 compares the steam generator (vapor) temperature on the tube side, the tube wall temperature, and the shell (liquid) temperature with the Test 21909 data. Figure 6-18 compares the energy of the shell side for Test 21909 with the RELAP5 prediction. RELAP5-BW very closely predicted the steam generator energy removal.
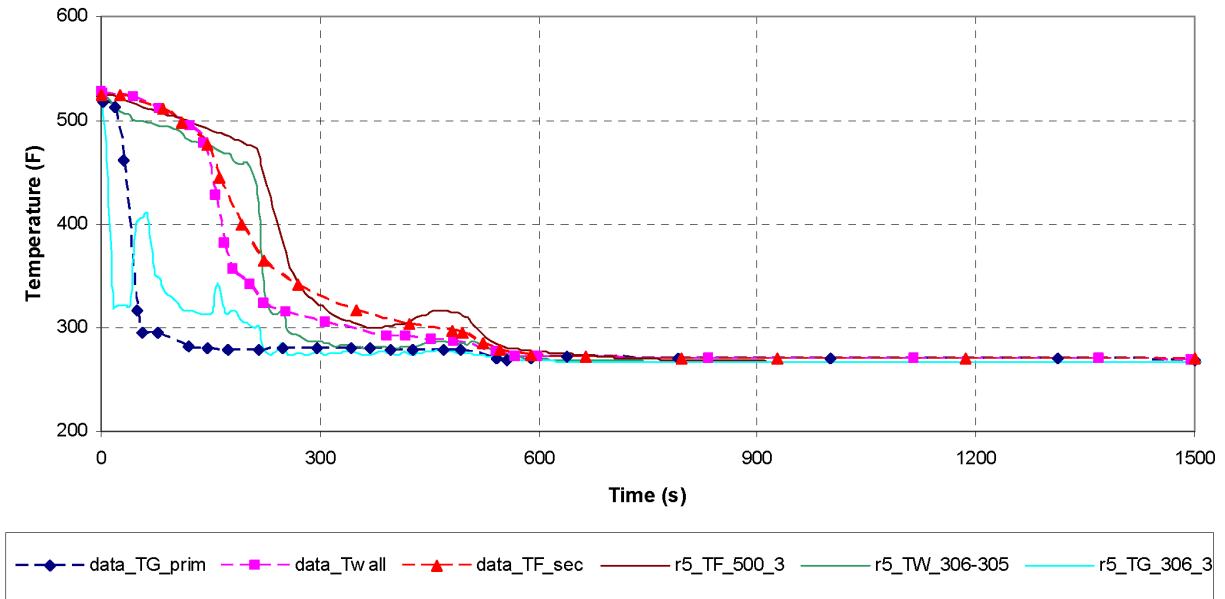
Figure 6-17—Tube, Wall, and Secondary Side Temperatures, Test 21909 (Becker CHF)
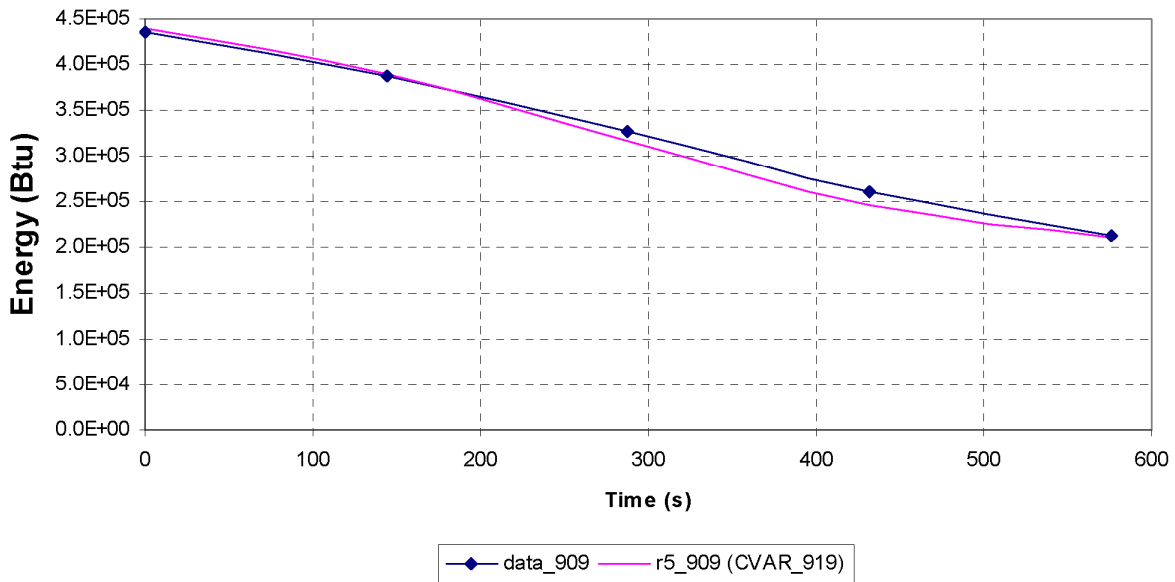
Figure 6-18—Steam Generator Energy, Test 21909 (Becker CHF)

In Test 22314, the steam flow rate corresponds closely to the rate of water injection into the tubes. Figure 6-19 compares the energy of the shell side for Test 22314 with the

RELAP5-BW prediction. RELAP5-BW predicts faster heat removal from the steam generator shell side compared to the test results.
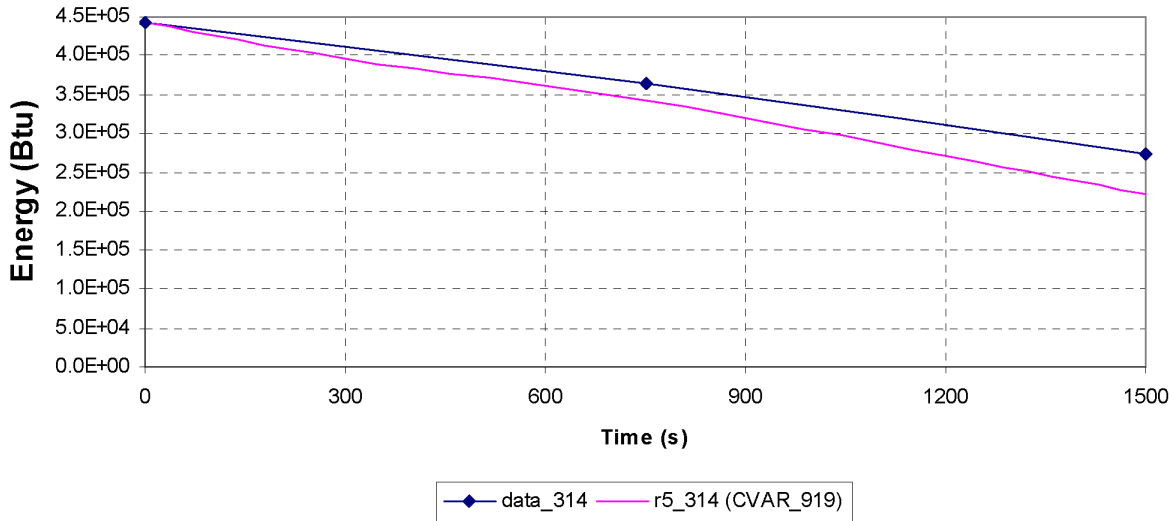
Figure 6-19—Steam Generator Energy, Test 22314 (Becker CHF)

Figure 6-20 compares the energy of the shell side for Test 22415 with the RELAP5-BW prediction; results are similar to those shown for Test 22314.
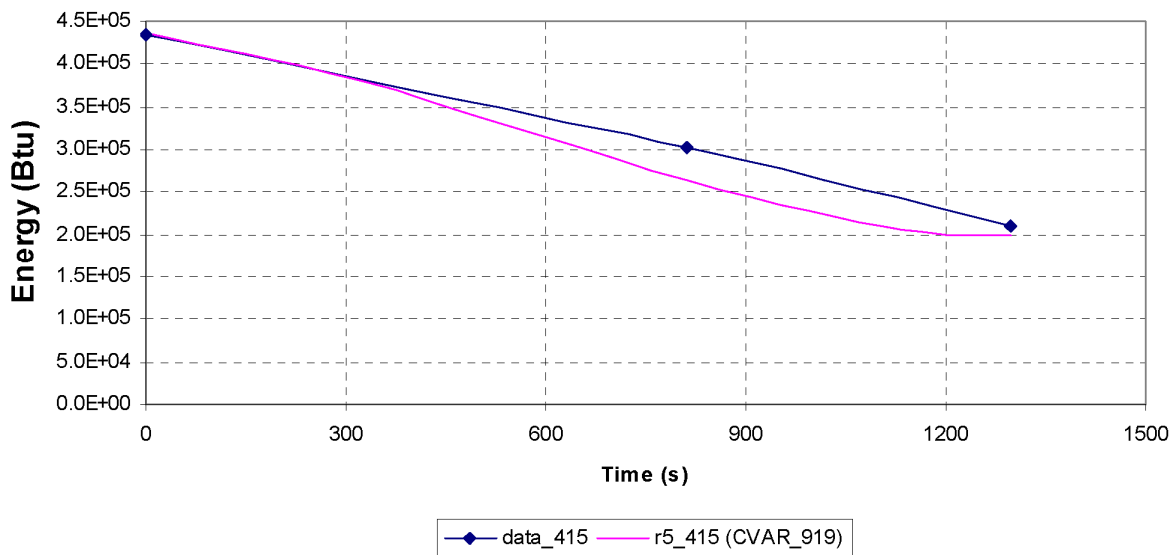
Figure 6-20—Steam Generator Energy, Test 22415 (Becker CHF)

6.1.3.1   Summary of FLECHT SEASET SG Heat Transfer

AREVA NP benchmarked the RELAP5-BW computer code against the FLECHT-SEASET steam generator heat transfer tests to predict the heat transfer from the secondary side of the steam generator to the primary side during the reflood and post reflood phases. The results demonstrate that replacing the Biasi-Zuber CHF model with the Becker CHF model in the tube side of the steam generators improves the prediction of energy transfer to the primary side, yielding results that compare well to the test data. Moreover, using the Becker CHF model also improves the prediction of the quench fronts in the tubes.

6.1.4   Long-Term Reactor Vessel Fluid Mixing

In the U.S. EPR, mitigation of the long-term LOCA containment pressure increase depends on termination of core steaming. To accomplish this, the injection from four LHSI pumps, each with a capacity of 120 kg/s, is aligned to inject ~60°C (140°F) water into hot legs through bottom-entry safety injection nozzles. This injected water flows into the upper plenum, partially condensing any steam in the region. The cooler safety injection water then falls as a plume into the core and passes through several peripheral fuel assemblies located below the hot leg nozzles, quenching steaming from these fuel assemblies.

As this water falls into the core, part of it traverses into the adjacent fuel assemblies and reduces boiling in these adjacent assemblies. The water that is not drawn into the adjacent assemblies continues down into the lower plenum. Some fraction of the remaining safety injection plume participates in the ongoing flow recirculation in the core region, and the balance leaves the RCS via a path leading into the lower head, the downcomer, and to the cold leg break location.

Under perfect mixing conditions, complete post-LOCA steam quenching would occur when the energy to raise the safety injection coolant to saturation exceeds the core decay heat. Because of asymmetry with safety injection delivery and the loss of part of

the safety injection to the break, perfect mixing is not possible. At the time of switchover to hot leg injection, the energy removal potential of the fully mixed ECCS is sufficient—by a significant margin—to quench core steaming. However, the efficiency of mixing the ECCS water with water in the core region must be determined.

Tests performed at the Upper Plenum Test Facility (UPTF), the Cylindrical Core Test Facility (CCTF), and the Slab Core Test Facility (SCTF) tests from the multi-national 2D/3D program (Reference 52) provide insight into the vessel mixing phenomena. The following sections describe the physical phenomena in the reactor vessel during the long-term core cooling, the development of a simple core mixing model using test data from UPTF, CCTF, and SCTF, and analytical validation results using CFD calculations. The derived results show that the effective mixing efficiency of the water falling into the core region is at least 50%.

6.1.4.1　　　*Fluid Mixing Phenomena in the Upper Plenum and Core*

Section 3.3 provides a general description of an LBLOCA. Of particular interest is the upper plenum and core fluid mixing phenomena in response to pumped safety injection delivered via hot leg locations. Following the initiation of the hot leg injection, the cool ECCS water mixes with the steam-water mixture in the hot leg and upper plenum before fluid density differences drive this fluid into the core region.

- There are several opportunities for hot-cold water and steam-water interaction along the path from the hot leg injection location to the upper plenum. If the injection is in a hot leg mostly filled with water, little mixing occurs in the hot leg itself. The cold water flows along the bottom of the hot leg to the upper plenum.

- If the mixture level in the upper plenum is below the bottom of the hot leg, the cold water interacts directly with the steam in the upper plenum and in the hot leg, producing highly efficient steam condensation.

- If the mixture level in the upper plenum and hot legs is above the centerline of the hot leg, then the ECCS water jet might not penetrate the steam-mixture

interface to enable a direct steam-water interaction. Rather, as the water falls into the upper plenum it spreads on top of the upper core plate that covers the tops of the several fuel assemblies that are below the hot leg nozzles. This spreading of the water depends on the ECCS injection rate and the hot water recirculation rate.

– If the cold water spreading is limited to the top of one or two peripheral fuel assemblies, then the ECCS water mixes primarily with the re-circulating hot water (without entrained bubbles) and does not quench much steam before falling into the core.

– If the spreading cold water covers more than the tops of a few outer fuel assembly rows, it will interact with the steam bubbles coming from the core region. This increases the effective condensation efficiency.

Figure 6-21 illustrates this situation for the U.S. EPR. The same mixing phenomena have been observed in tests performed at the UPTF, CCTF, and SCTF facilities. In these tests, cold water flows into the upper plenum and spreads across the upper core support plate before flowing down into the core region through the relatively low-power peripheral fuel assemblies. Boiling in these fuel bundles is suppressed and water cross-flow into the neighboring assemblies occurs.

MHSI
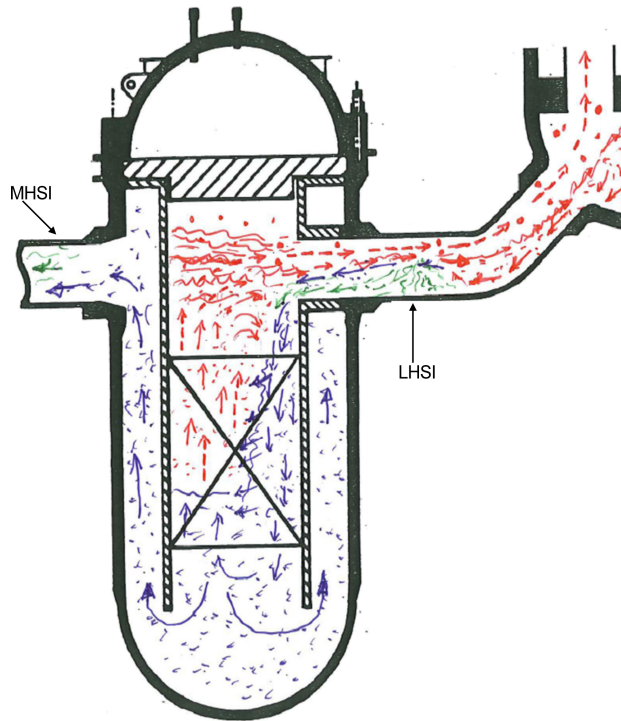
LHSI

Figure 6-21—Vessel and Hot Leg Flow Pattern During Hot Leg LHSI

Figure 6-22 shows a typical progression to steam quench observed in the tests. This illustration represents SCTF CORE-III Test S3-SH1 (Run 703) (Reference 53), which featured combined safety injection. The facility was designed to have a full height, full bundle-width core with eight bundles across. Instrumentation included fluid temperature and horizontal differential pressure (ΔP) to measure the two-dimensionality of the fluid flow in the pressure vessel. A hot leg and downcomer (not shown in Figure 6-22) are attached to the upper and lower plena flanking the simulated core on the right-hand-side of the illustrations. Pumped injection simulating ECCS flow from a hot leg location appears on the right-hand-side of each illustration. As steam production in the adjacent cross-flow bundle decreases, the momentum of the two-phase mixture entering the upper plenum also decreases, causing the migration of the cold water over the top of the bundle. Thus, the down-flowing liquid region continues to grow until the steam production ceases in all bundles.
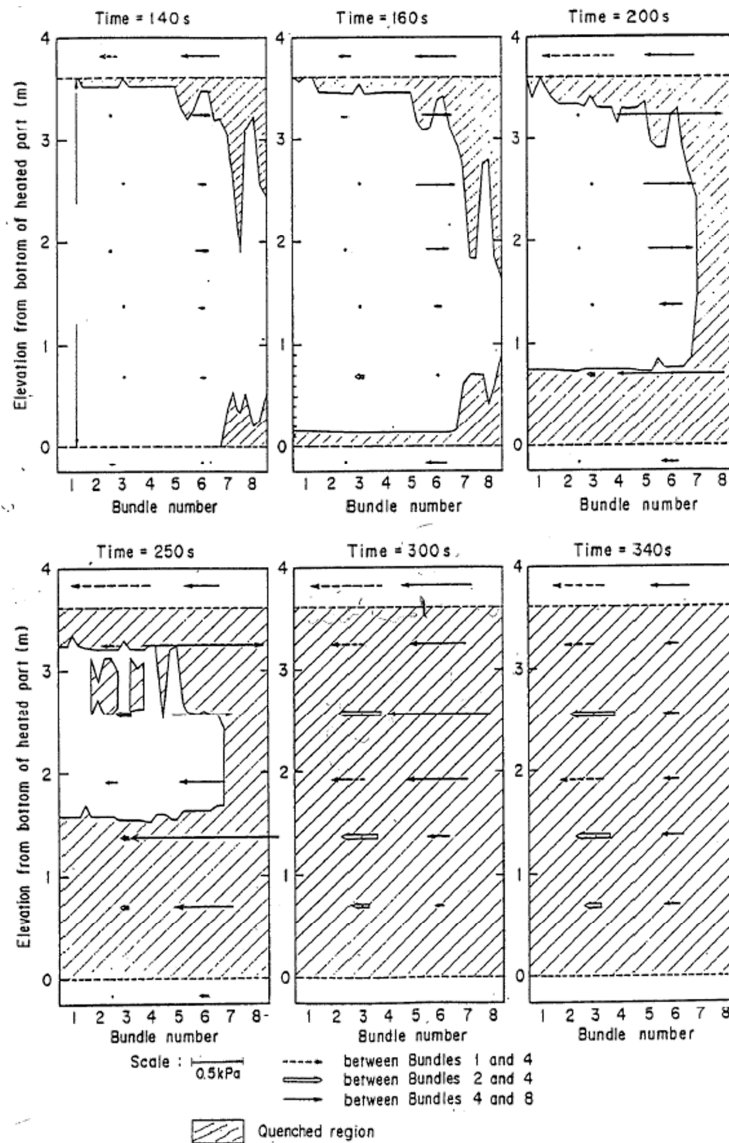
Figure 6-22—SCTF CORE-III Test S3-SH1 (Run 703) Quench Front Propagation

Figure 6-22 shows the horizontal ΔP between assembly 2 (simulating a center core assembly) and assembly 4 (simulating an average core assembly) as a function of void fraction difference for several SCTF Core-III tests, including test S3-SH1 shown in Figure 6-23. The data are a representative sample of elevations and times before local quench. The negative sign indicates flow from assembly 4 to assembly 2 and, as implied in Figure 6-22, the flow is generally negative during the period prior to local steam quench. These SCTF tests represent a spectrum of initial conditions (power

profile, pressure, etc.). The results show that, within the parameter range considered, the distributed mixing behavior along the axial length of the core region is not sensitive to system pressure and the difference in void fraction.
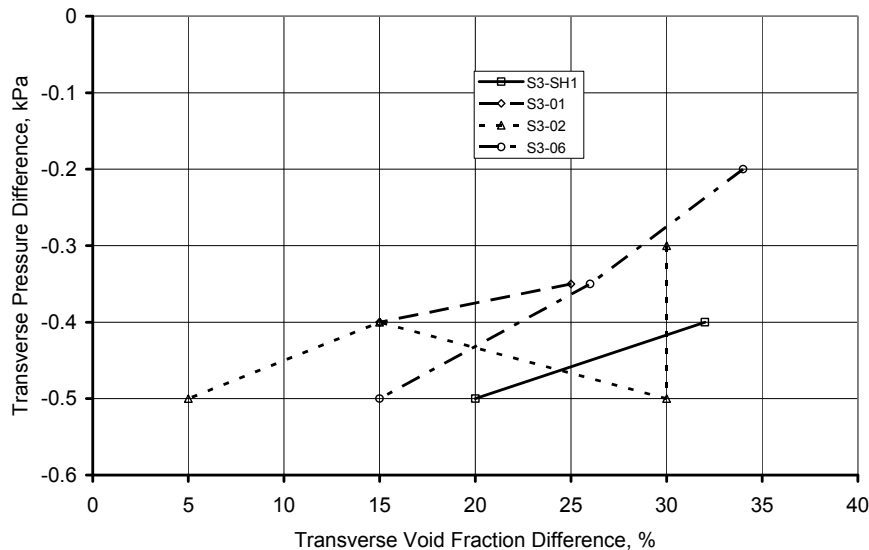
Figure 6-23—Horizontal ΔP Between Bundles 2 and 4 After the Whole Core is Quenched in Several SCTF Core-III Tests

6.1.4.2 *Predictive Model for Upper Plenum Mixing Efficiency*

The development of a simple, yet conservative, predictive model considers the expected flow pattern of the U.S. EPR reactor vessel illustrated in Figure 6-21. In this configuration, interaction between the safety injection from hot leg locations and core steam is minimal; thus, there is no credit for direct contact condensation. The cold ECCS water injected into the hot leg forms a negative-buoyant plume (i.e., heavier than the liquid resident in the core, upper plenum, and hot leg). This plume entrains ambient hotter water on its way from the hot leg to the upper tie plate and into the core. The entrainment transfers heat from the hotter ambient water to the ECCS-water. The resulting heat transfer efficiency is defined as:

$$\eta_{mix} = \frac{h - h_{ECC}}{h_{amb} - h_{ECC}} \approx \frac{t_{mix} - t_{ECC}}{t_{amb} - t_{ECC}}$$ Eqn. 6-1

where,

h_{mix}, (t_{mix}) =   average specific enthalpy (temperature) of the ECCS-water adjacent to the upper tie plate

h_{amb}, (t_{amb}) =   specific enthalpy (temperature) of ambient water in upper plenum

h_{ECC}, (t_{ECC}) =   specific enthalpy (temperature) of ECCS-water in the injection port

6.1.4.2.1   Minimum Mixing Efficiency Based on UPTF TRAM Test A3

The Upper Plenum Test Facility (UPTF) was built and operated by the former Siemens/KWU, now AREVA NP, for German reactor safety research. The UPTF is a geometrically full-scale mock-up of the RPV and the main coolant piping of a typical Western-type PWR (German PWR Grafenrheinfeld, 3782 MW$_{th}$). The facility has a core simulator that injects steam and water from below dummy fuel assemblies. The upper plenum—including internals, the downcomer, the four connected loops, and the pressurizer—are represented at full-scale. The UPTF was designed to perform separate effects tests, focusing on multi-dimensional, thermal-hydraulic phenomena in the upper plenum, across the upper core grid, in the downcomer, and in the loops, as well as in the surge line and the pressurizer. After the UPTF-test program, the UPTF TRAM Program was started to study accident management scenarios. The UPTF TRAM Program was completed in June 1997.

The purpose of UPTF-TRAM Test A3 (Reference 54) was to investigate flow phenomena associated with hot leg injection in the presence of a two-phase mixture flow from the upper plenum to the steam generator. An ECCS-water flow rate of 27.5 kg/s was injected into one hot leg and steam and water near saturation were injected via the core simulator.   This corresponds to an equivalent U.S. EPR mass flow rate of 33.4 kg/s, based on the relative power of the U.S. EPR and Grafenrheinfeld

(4590 MW$_{th}$ and 3782 MW$_{th}$, respectively). The test vessel was filled with water at least up to the upper edge of the hot leg.

Figure 6-24—UPTF-TRAM A3 Run 06a: Assembly Map with Indication of Water Down-Flow

AREVA NP Inc.

ANP-10299NP

Applicability of AREVA NP Containment Response Evaluation Methodology to the

Revision 2

U.S. EPR™ for Large Break LOCA Analysis

Technical Report

Page 6-30

[

]

Table 6-4—UPTF TRAM Test A3—Injection Rates and Water Temperatures

Measured in the Down-Flow Region Adjacent to the Upper Tie Plate

[

]

6.1.4.2.2 *Minimum Mixing Efficiency Based on CCTF II Test 79*

[

]

AREVA NP Inc.   ANP-10299NP

Applicability of AREVA NP Containment Response Evaluation Methodology to the   Revision 2
U.S. EPR™ for Large Break LOCA Analysis
Technical Report   Page 6-32
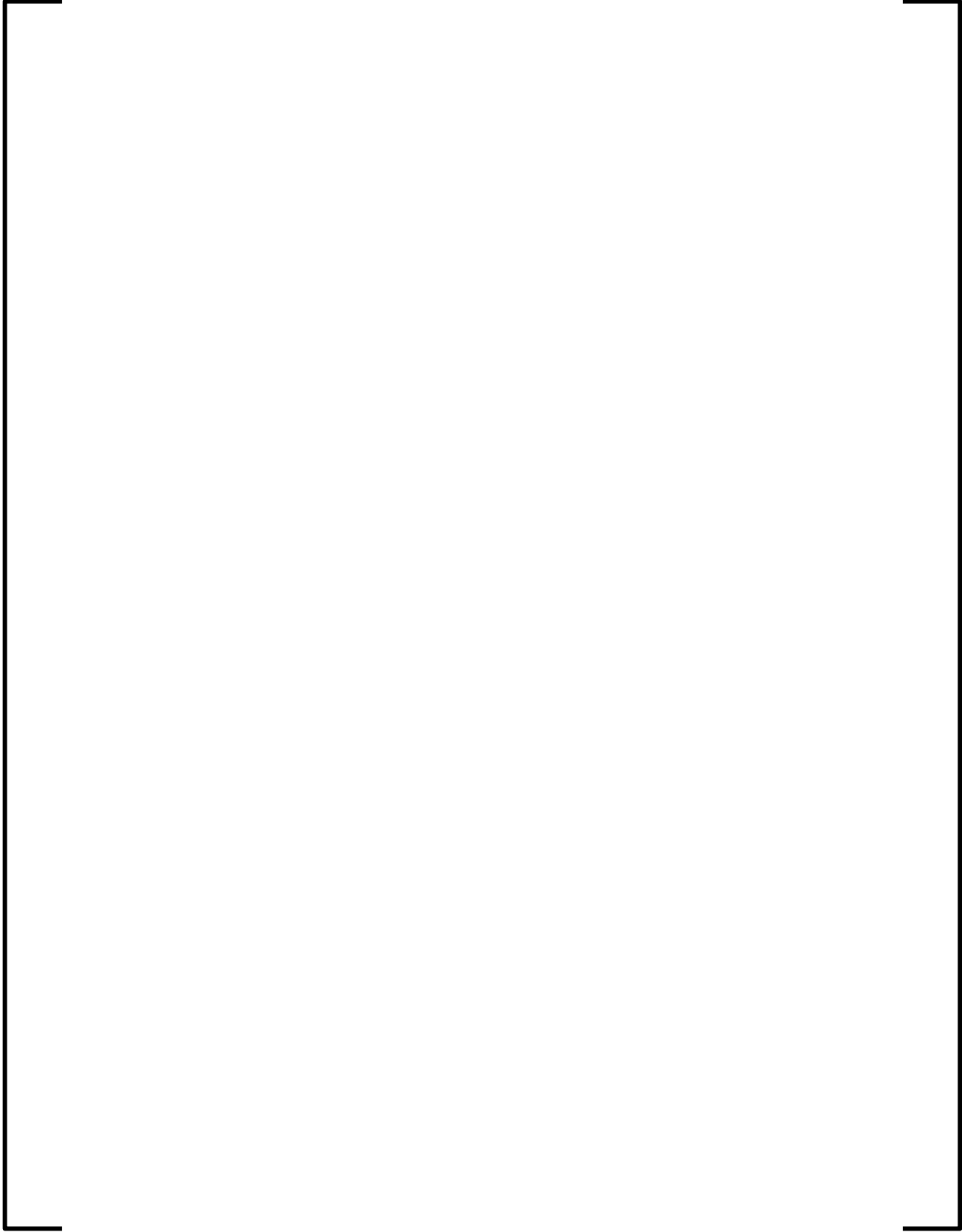
Figure 6-25—CCTF II Test 79: Assembly Map with Indication of Up-Flow Bundles (dark) in the Test Period 250s to 300s

6.1.4.2.3 Mixing Efficiency Correlation

AREVA NP Inc.

Applicability of AREVA NP Containment Response Evaluation Methodology to the
U.S. EPR™ for Large Break LOCA Analysis

Technical Report

ANP-10299NP

Revision 2

Page 6-33

AREVA NP Inc.

Applicability of AREVA NP Containment Response Evaluation Methodology to the
U.S. EPR™ for Large Break LOCA Analysis

Technical Report

ANP-10299NP
Revision 2

Page 6-34
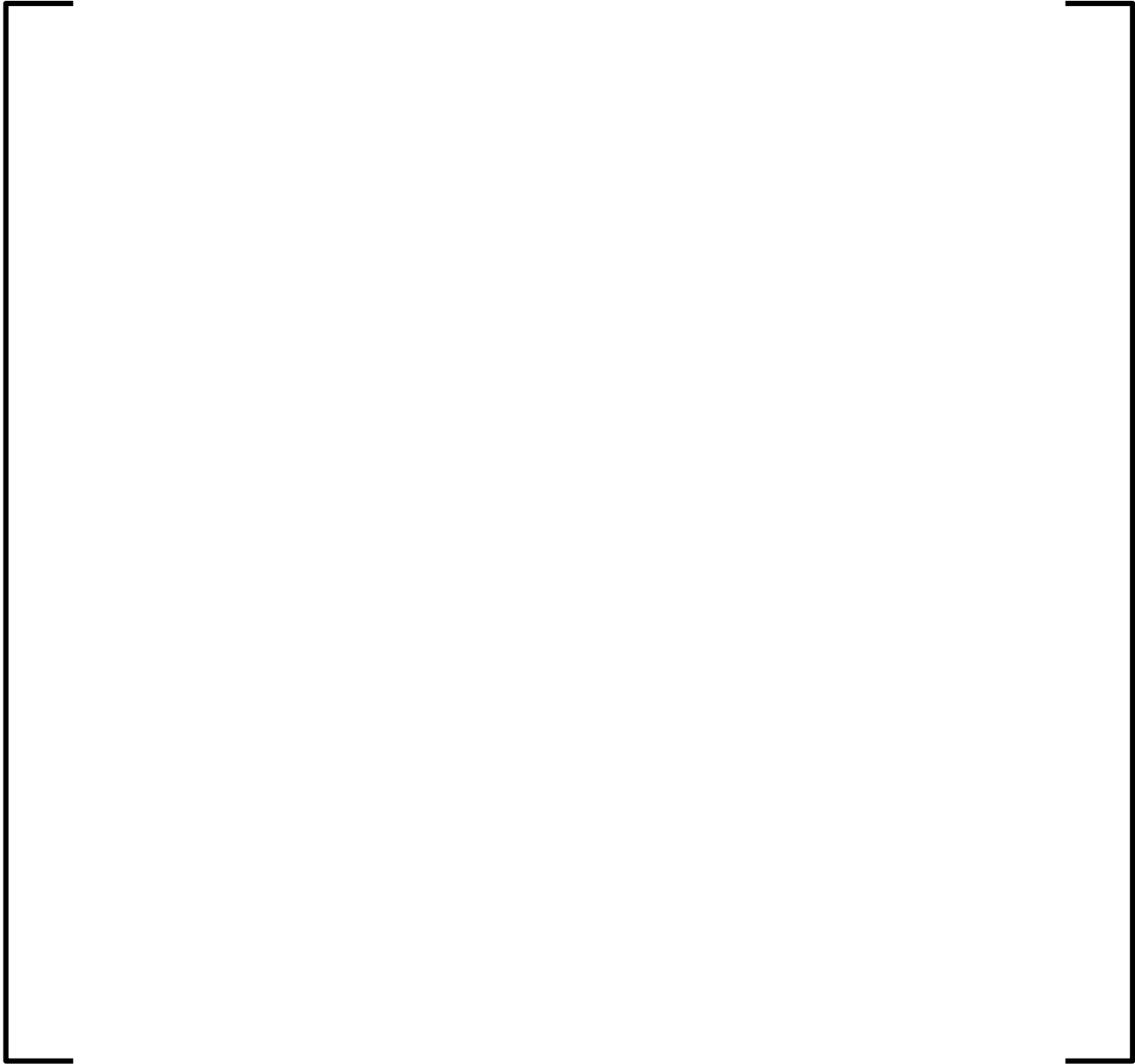
Figure 6-26—Dimensionless Density in the Adiabatic Wall Plume (Reference 57)

Figure 6-27—Minimum Mixing Efficiency η in the Upper Plenum of UPTF TRAM Test A3 Runs 03a, 04a and 05b, CCTF II Test 79, and the Wall Plume Correlation

6.1.4.2.4   Engineering Model for Core Flow Behavior
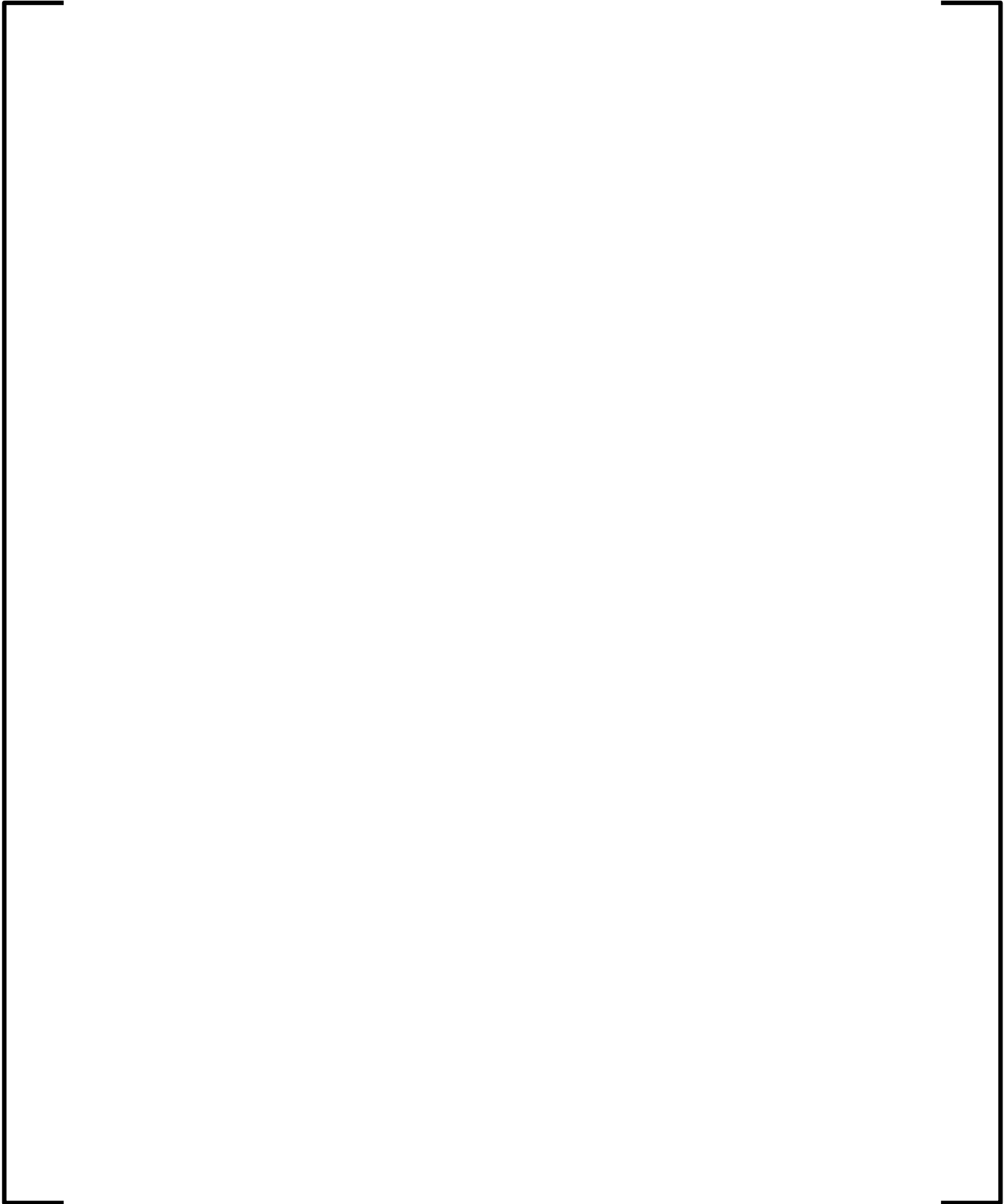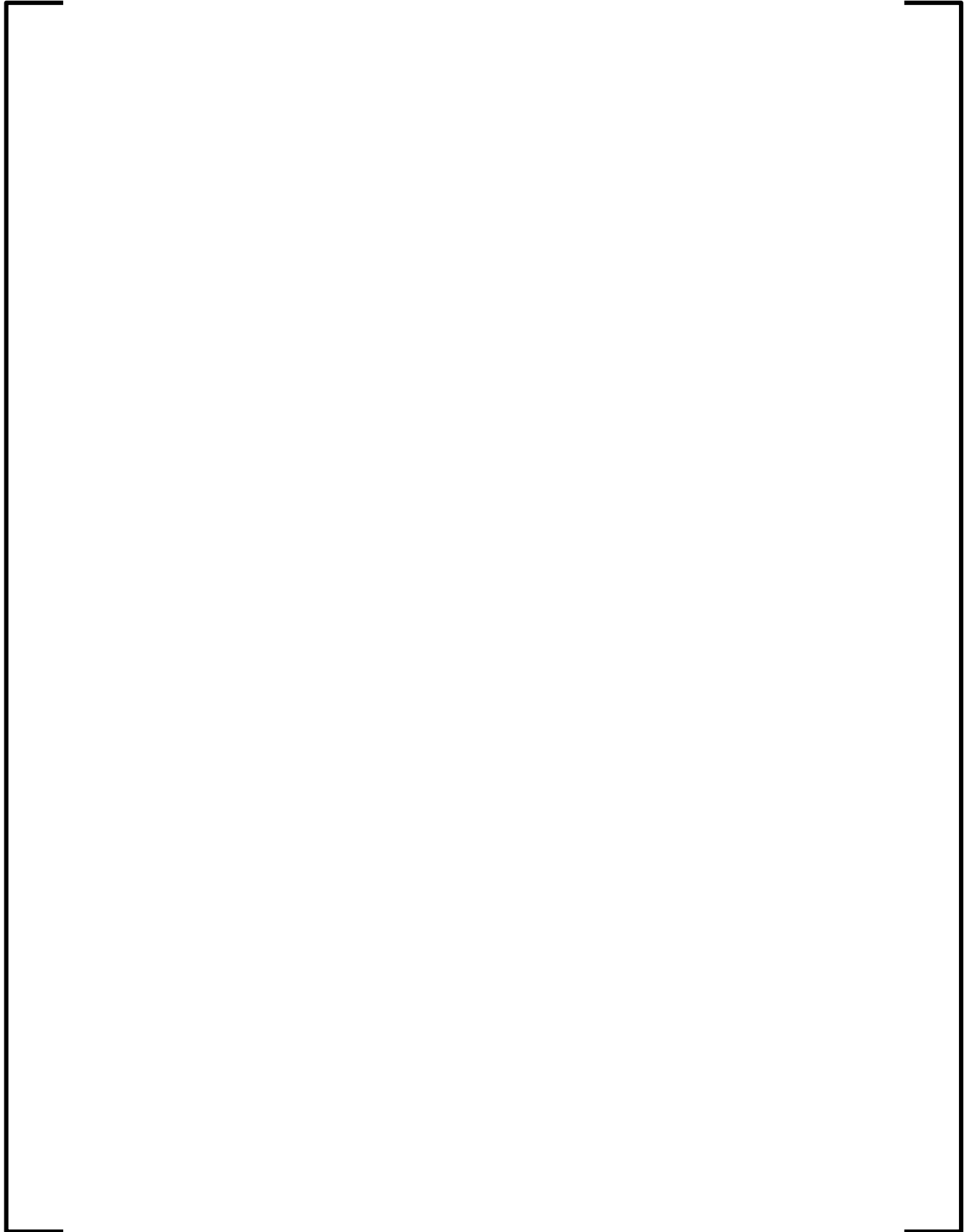
Figure 6-28—Time for Core Steam Production to Become Zero at Different System Pressures for a Mixing Efficiency of 50%

6.1.4.3   *Analytical Validation*

AREVA NP performed two quasi-steady-state, single phase liquid mixing calculations with the CFD code STAR CD (Reference 59) to examine upper plenum flow mixing phenomena during hot leg injection. The model simulates the upper plenum of the U.S. EPR. It contains all the upper plenum structures, including 241 orifices representing the upper core support plate (UCSP). The first case simulates the scaled flow rates used in the UPTF TRAM Test 6A. The second case simulates the typical U.S. EPR condition with LHSI injection rates of 120 kg/s into two adjacent hot legs.

AREVA NP Inc.   ANP-10299NP
Applicability of AREVA NP Containment Response Evaluation Methodology to the   Revision 2
U.S. EPR™ for Large Break LOCA Analysis
Technical Report   Page 6-39

6.1.4.3.1   *Simulation of UPTF Test 6A*

Figure 6-29 shows the CFD model used to simulate the upper plenum mixing phenomena in UPTF Test 6A. This model represents the test facility from above the UCSP to the steam generator inlet plenums. It contains about 1.4 million hexahedral cells.
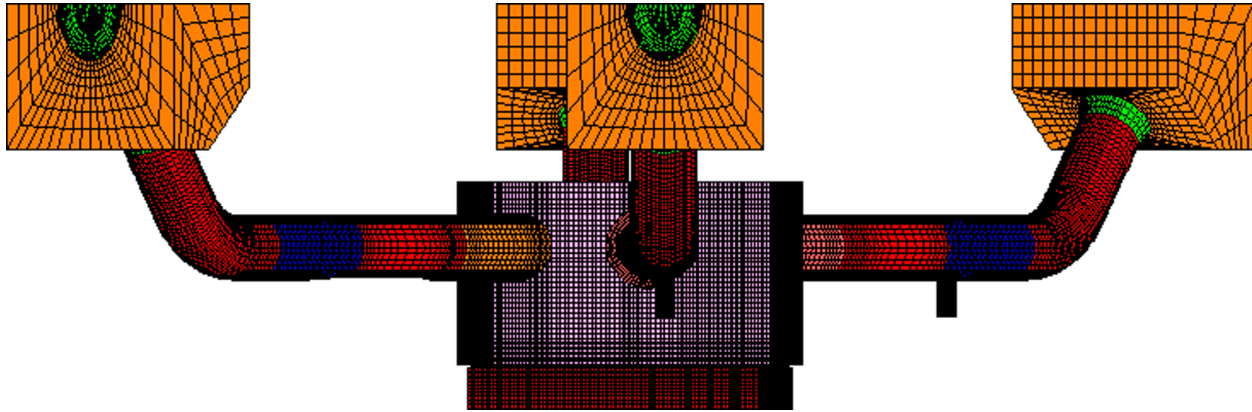
Figure 6-29—CFD Model of UPTF TRAM Test-3 Run-6a

Figure 6-30 shows a snapshot of fluid temperature at 100 seconds of cold flow from the hot leg safety injection location into the upper plenum. The figure shows little mixing in the hot leg. The ECCS water impinges on the control rod guide assemblies (CRGA) as it flows into the upper plenum. Figure 6-31 shows the spreading of the ECCS water on the UCSP. The ECC water spreads over about 15 UCSP holes just below the ECC injected hot leg. This STAR-CD prediction of cold water spreading on the UCSP compares well with the same behavior observed in UPTF TRAM Run 06a (Figure 6-24).

Figure 6-32 shows the fluid temperature in the UCSP holes where the coldest water plume is located. After about 30 seconds, the fluid distribution reaches quasi-steady-state.

These results demonstrate the ability of STAR-CD to calculate the mixing of the hot leg injected water in the U.S. EPR as it reaches the UCSP.
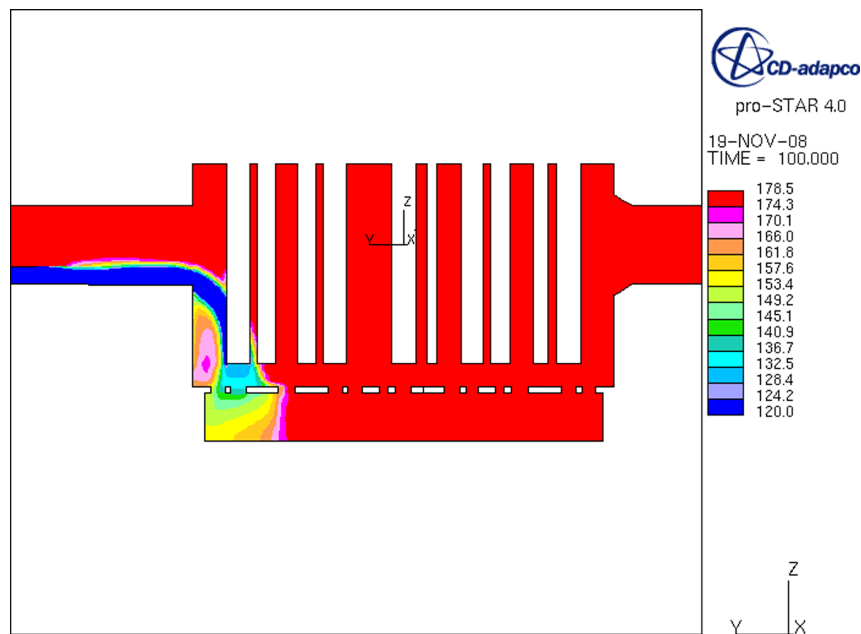
Figure 6-30—UPTF TRAM Test 6A: Thermal Mixing of Injected ECC Water in the Upper Plenum at 100 s

AREVA NP Inc.
ANP-10299NP
Applicability of AREVA NP Containment Response Evaluation Methodology to the
Revision 2
U.S. EPR™ for Large Break LOCA Analysis
Technical Report
Page 6-41
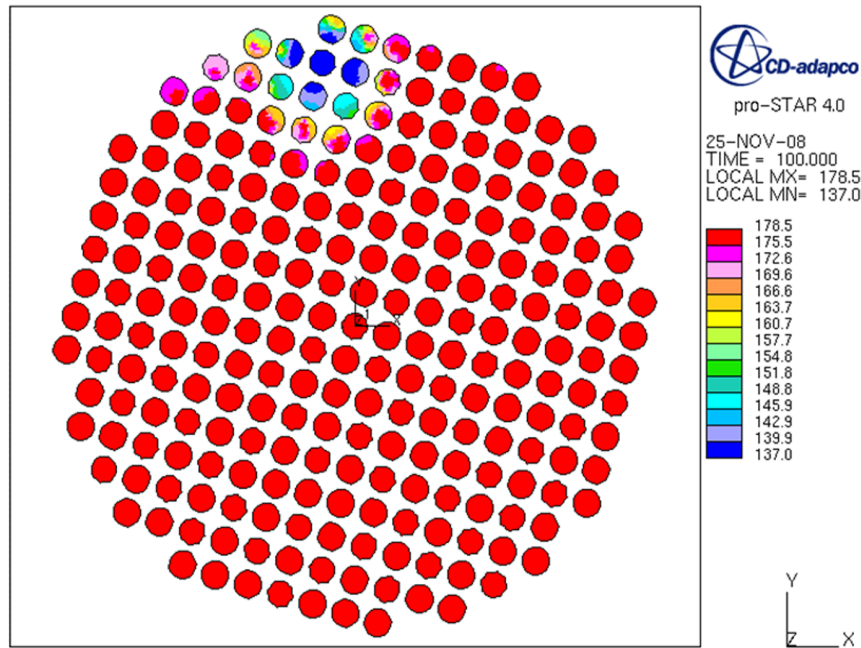
Figure 6-31—UPTF TRAM Test 6A: Thermal Mixing of Injected ECC Water above the UCSP at 100 s
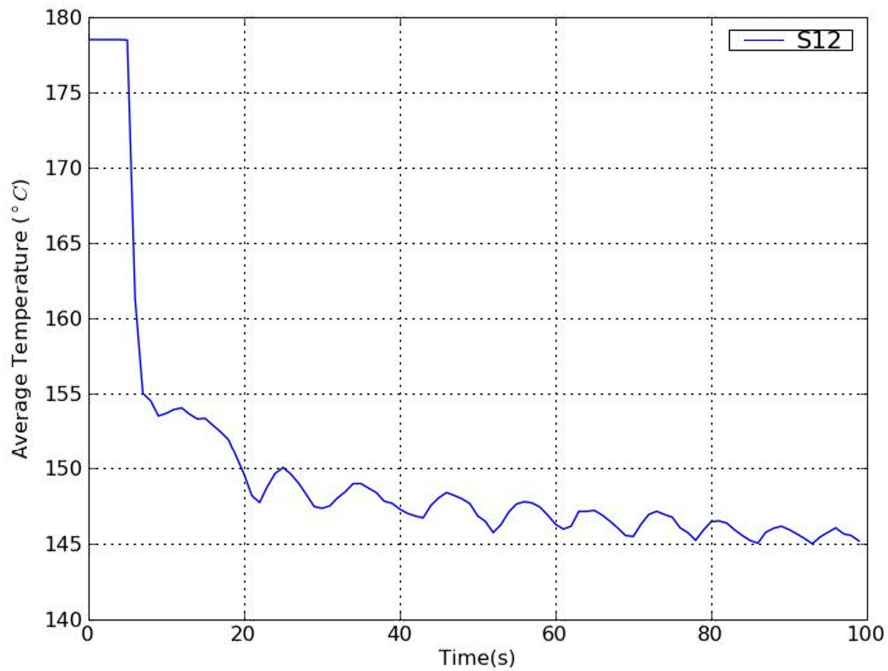
Figure 6-32—UPTF TRAM Test 6A: Temperature in a UCSP Hole below the ECCS Injection Hot Leg Nozzle

6.1.4.3.2   Simulation of U.S. EPR

Figure 6-33 shows the CFD model of the U.S EPR; it contains about 1.5 million hexahedral cells. The model uses the same methodology used to describe the model for the UPTF test. In this model of the U.S. EPR, the initial and boundary conditions are

Figure 6-34 shows the fluid temperature at 60 seconds in both hot legs receiving ECCS water. The mixing zones in both hot legs extend two diameters upstream from the injection nozzle. Thermal stratification occurs as the cold water flows towards the upper plenum. Figure 6-35 shows the temperature distribution at 60 seconds in a cross section plane across the upper plenum that passes through the centerline of one of the hot legs. Figure 6-36 shows the temperature distribution at 60 seconds in an upper plenum cross-sectional plane near the two hot legs receiving ECCS. It shows the interaction with the two cold water plumes as they flow down the hot legs to the upper core support plate.

Figure 6-37 shows that the thermal distribution in the US EPR calculation reaches a quasi-steady-state in about 40 seconds.   The lowest temperature of 96°C is reached in one of the UCSP holes that is just below one of the ECCS injected hot leg nozzles. This corresponds to a minimum mixing efficiency of 56%. Figure 6-38 shows that the cold water spreads from the periphery of the upper plenum on top of more than four rows of fuel assemblies.

In the U.S. EPR just before the hot leg injection initiation, it is expected that the water in the upper plenum region segment will fall on top of the outer two rows of fuel

AREVA NP Inc.

Applicability of AREVA NP Containment Response Evaluation Methodology to the
U.S. EPR™ for Large Break LOCA Analysis
Technical Report

ANP-10299NP
Revision 2

Page 6-43

assemblies. As a result, there will only be a few steam bubbles in this upper plenum segment. Since the cold water spreads over more than this segment of the upper plenum, there will be cold water and steam interaction causing substantial steam condensation.
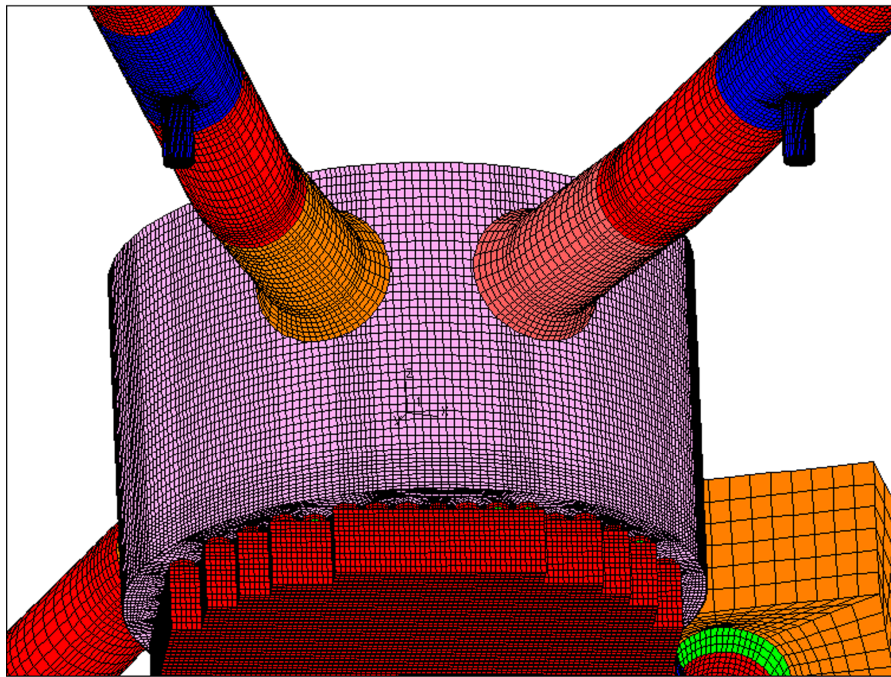
Figure 6-33—STAR-CD Model for the U.S. EPR Upper Plenum Thermal Mixing Calculation
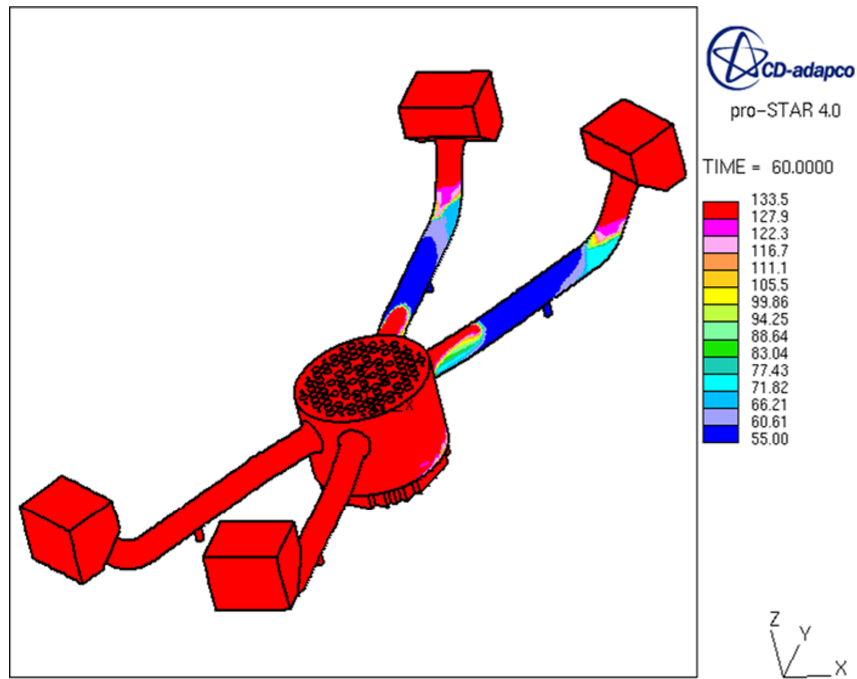
Figure 6-34—U.S. EPR: Thermal Mixing in the ECCS Injected Lot Legs at 60 s
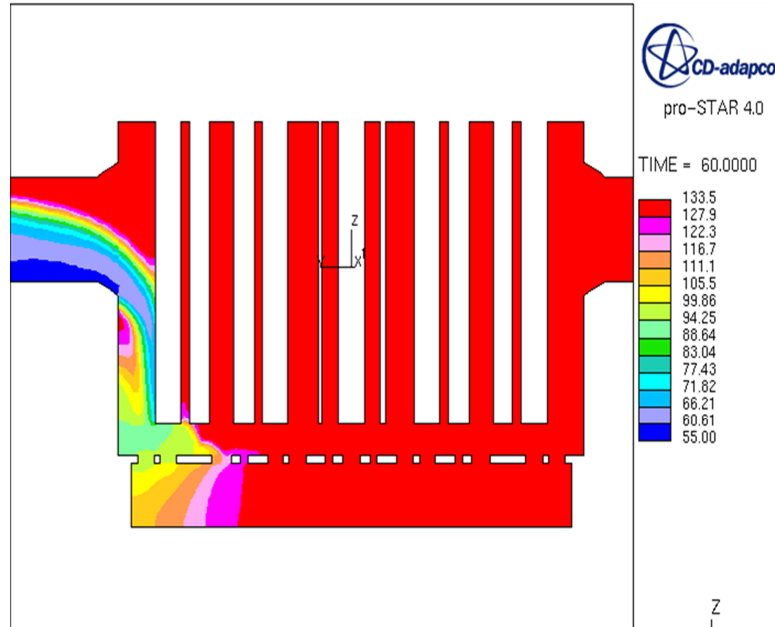
Figure 6-35—U.S. EPR: Thermal Mixing of ECCS Injection in the Upper Plenum at 60 s
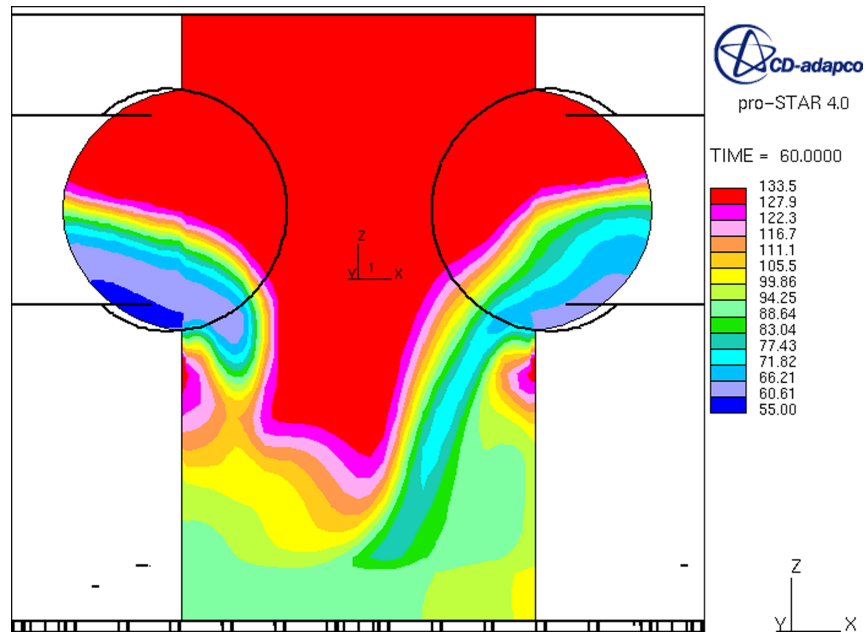
Figure 6-36—U.S. EPR: Thermal Mixing Upper Plenum Temperature Distribution from two ECCS Injected Hot Legs at 60 s
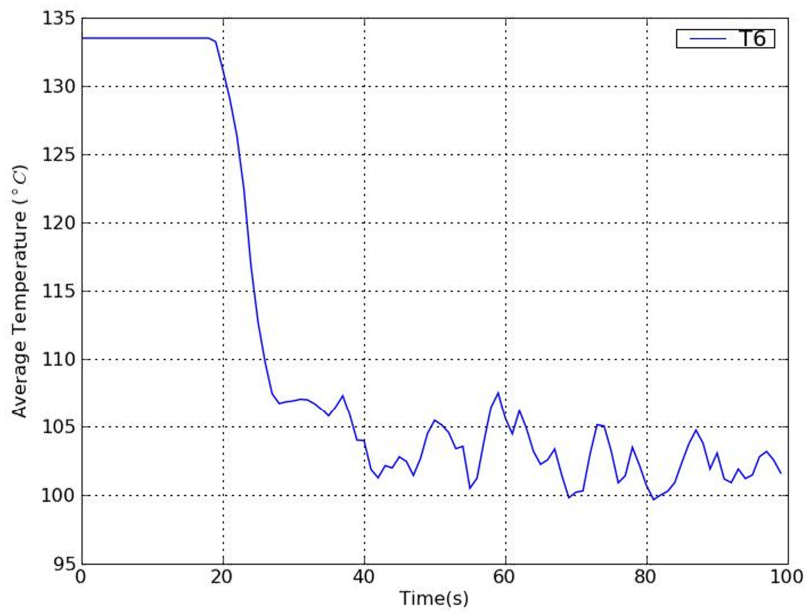
Figure 6-37—Temperature in a UCSP Hole below the ECCS Injection Hot Leg Nozzle
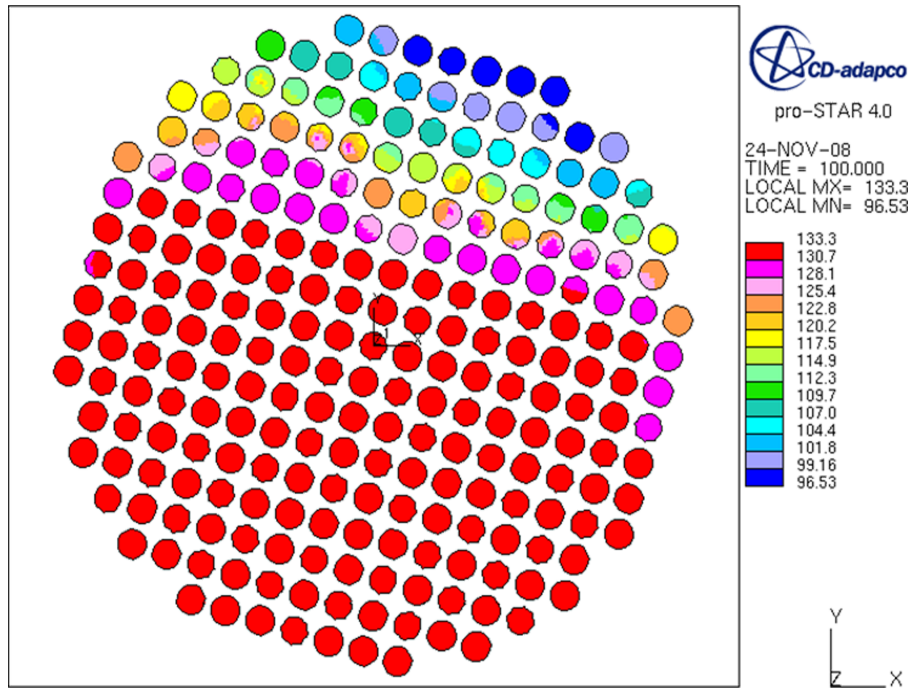
Figure 6-38—U.S. EPR: Thermal Mixing of Injected ECC Water above the UCSP at 100 s

6.1.4.4   Summary

AREVA NP developed an analytical model to predict the efficiency of mixing in the upper plenum between cold ECC water from hot leg injection with rising hot water from the core. It is based on a plume dynamics model and correlated data from the UPTF, CCTF, and SCTF tests. Analyses performed using the STAR-CD CFD code provide additional confirmation of effective mixing in the upper plenum. These studies lead to the following conclusions:

AREVA NP Inc.

Applicability of AREVA NP Containment Response Evaluation Methodology to the
U.S. EPR™ for Large Break LOCA Analysis
Technical Report

ANP-10299NP
Revision 2

Page 6-47
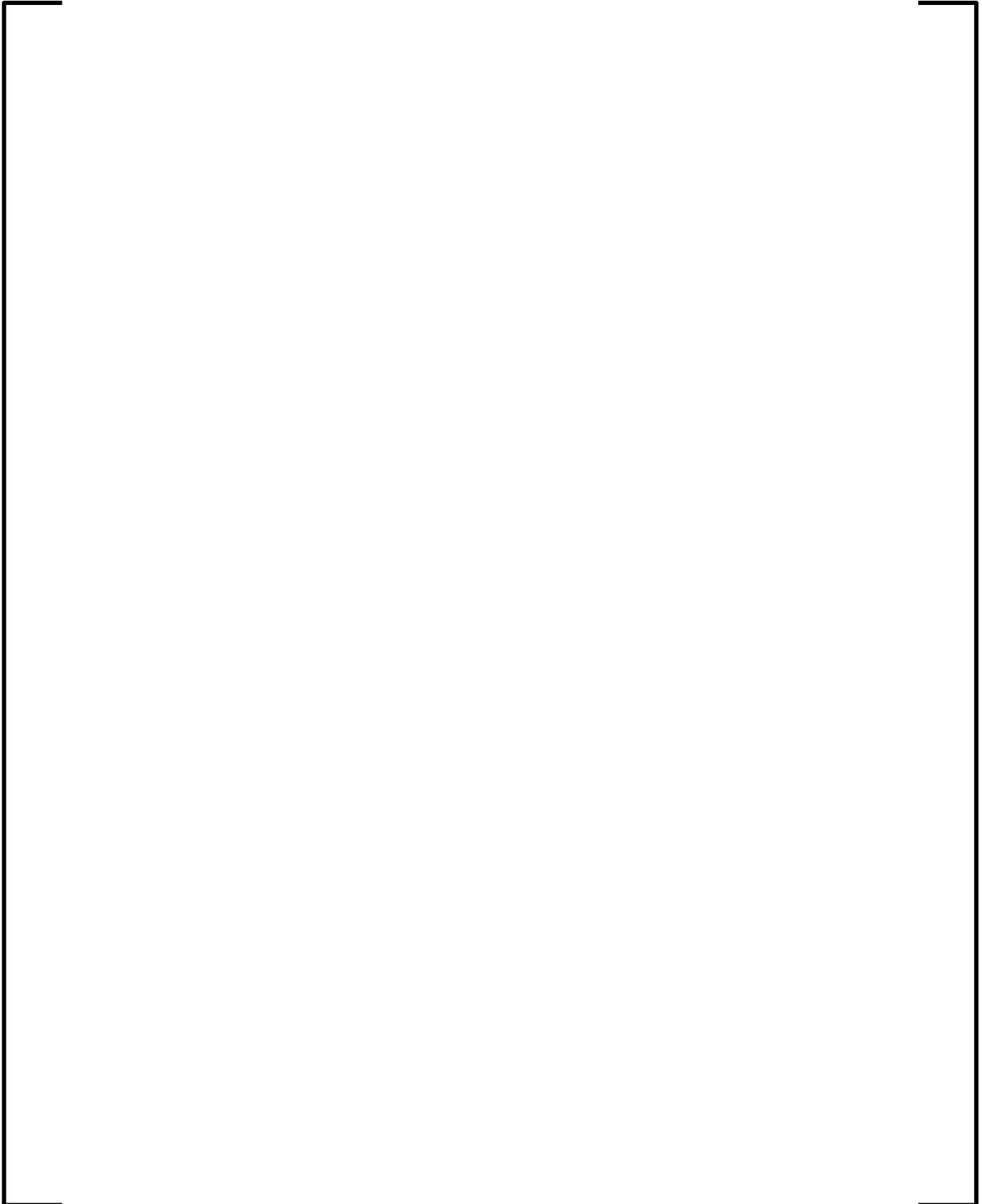
6.1.5   Wall Condensation

Following an LBLOCA, wall condensation is the principal containment atmosphere heat removal mechanism for the U.S. EPR. Forced and free convection are additional containment atmosphere heat transport mechanisms; however, AREVA NP's containment response evaluation methodology neglects forced convection. Additionally, sensible heat transfer by free convection (Reference 77 for a vertical plate) is a small contributor relative to wall condensation.

For wall condensation, AREVA NP has used the tandem Tagami-Uchida heat transfer correlation (References 94 and 95) for single-node models. However, a multi-node GOTHIC model is used for the U.S. EPR design. Because the Tagami correlation includes a term for the total energy release at the end of blowdown, it is not appropriate for use in a multi-node model where the energy needs to be apportioned among the volumes. Using the total energy in each sub-volume overstates the condensation rate, so the mechanistic Diffusion Layer Model (DLM or DLM-FM) is used instead.

A separate-effects assessment study, presented below from Reference 31, shows the DLM-FM model accurately predicts wall condensation for a large suite of test programs and provides better predictions than Uchida. The DLM-FM model was also used for the integral test GOTHIC assessments in Section 6.2.

6.1.5.1   Diffusion Layer Model for Wall Heat and Mass Transfer

The Diffusion Layer Model calculates the convective heat transfer and the condensation rate at a cold wall surface. The model accounts for the presence of noncondensing gases, the water film resistance, possible mist generation near the wall, and enhancement effects due to film roughening. The model was validated by comparison

AREVA NP Inc.

ANP-10299NP

Applicability of AREVA NP Containment Response Evaluation Methodology to the

Revision 2

U.S. EPR™ for Large Break LOCA Analysis

Technical Report

Page 6-49

with several experimental test sets. The tests are first described and the general approach used to model the tests is presented along with the test results.

6.1.5.2   Uchida

The experimental setup and testing are briefly described in Reference 95. The test set includes atmospheric tests with steam mixed with air, nitrogen, or argon. The 0.4 m diameter cylindrical test chamber is 0.3 m high. The experimental results are presented on a small, hand-drawn chart showing an effective heat transfer coefficient as a function of the gas-to-steam mass ratio. The chart can be read with an accuracy of about 10%, and there was no estimate of the experimental error provided.

Peterson (Reference 106) reports that the tests were conducted by injecting steam into a container initially filled with the noncondensing gas at 1 atmosphere. Based on this assumption, Peterson shows in Reference 107 that the fit to the Uchida data over-predicts the heat rate to the wall if the air pressure is less than 1 atmosphere.

However, there is no evidence in the Uchida reference that the tests were performed in this manner. In fact, the Uchida reference clearly states that the total pressure for three of the tests (air, nitrogen, and argon) is 0.098 MPa and that the total pressure for the fourth test with air is 1.27 to 2.74 MPa. This implies that the first three tests were performed in a vented chamber. For the fourth test, if it is assumed that the air/steam mixture is saturated and the container initially contains dry gas at 1 atmosphere, then the calculated total pressure for the reported data falls between 1.1 and 2.7 MPa. (This ignores one possible data point from the pressurized air tests at an air/steam mass fraction of ~0.1, which would require a very high total pressure.)

Based on the information provided in the Uchida reference, AREVA NP has interpreted the data to mean that the low-pressure tests are vented at 1 atmosphere and the high-pressure tests are for a closed container initially filled with air at 1 atmosphere. Further, it is assumed that the air/gas mixture is saturated, the unspecified wall temperature is 30°C, and natural circulation conditions prevail. Corradini (Reference 108) indicates

that there may be some forced convection influence, which would be more likely in the vented test and may explain why the data do not fully agree with the model.

Under the assumption of saturated conditions, the bulk temperature and steam concentration can be deduced from the gas/steam mass ratio. Assuming that the steam and gas each behave as a perfect gas,

$$x_r = \frac{\rho_g}{\rho_s} = \frac{P_g M_g}{P_s M_s}$$

where x_r is the given gas/steam mass ratio, P_g and P_s are the gas and steam partial pressures, and M_g and M_s are the gas and steam molecular weights.

For the vented tests, it is assumed that

$$P_s + P_g = 1\,atm$$

so that

$$P_s = \frac{1\,atm}{1 + x_r \dfrac{M_s}{M_g}}$$

The vapor temperature is assumed to be the saturation temperature at P_s.

For the pressurized test, it is assumed that the container was initially filled with dry air at 1 atmosphere. From the equation for x_r with P_g set to 1 atm,

$$P_s = \frac{P_g M_g}{x_r M_s} = \frac{M_g}{x_r M_s}\,atm$$

Again, the vapor temperature is assumed to be the saturation temperature at P_s.

6.1.5.3   U of W Atmospheric Tests

Anderson (Reference 109) presents data for a steam/air and steam/air/helium test in a vented vessel. Heat transfer to vertical and horizontal surfaces was measured in the 2.44 m high vessel, and steam was injected into a vessel initially filled with gas at 1 atmosphere. Steam and gas were vented from the system until the vessel contents remained saturated at a pressure of 1 atmosphere and the desired bulk temperature.

The heat transfer was measured in two ways: local heat flux meters and a coolant energy balance. The local heat flux meters give the total heat transfer rate in a small region on the plate. Results from several of these meters were averaged to get an average effective heat transfer coefficient. The coolant energy balance was used to deduce the total heat transfer rate from the measured flow rate and temperature rise of the coolant flow across the backside of the condenser plate. Because the heat transfer rate needed in GOTHIC is the plate total, the coolant energy balance is presumed to give the better estimate. The experimental results showed that the coolant energy balance was more consistent with the known heat input for the system and was generally higher than the average from the flux meters. Measured heat transfer rates to the horizontal surface were generally 10 –15% higher than that for the vertical surface. The model is compared only to the experimental results for the vertical surface and, therefore, should conservatively underestimate the heat transfer rates for horizontal surfaces. The estimated error in the data is ±15%.

The bulk temperature, steam pressure, and total pressure are listed for each test. The steam pressure is consistent with the saturation pressure at the specified bulk temperature. The bulk-to-wall surface temperature difference is also listed so that the wall temperature is easily obtained.

6.1.5.4   U of W Pressurized Vessel Tests

Anderson (Reference 109) also presents data for steam/air and steam/air/helium tests in a pressurized vessel. Heat transfer to a vertical surface and a curved surface

representing a containment dome was measured in the 2.94 m high vessel. There were two types of air/steam test in the test vessel: vented and pressurized. The vented tests were conducted as described in Section 6.1.5.3. The pressurized tests were similar except that only condensed steam was vented from the vessel so that the initial gas content was retained in the vessel. Both test sets are referred to as the pressurized vessel tests.

In these tests the heat transfer to the vertical and domed surfaces was combined into a single average value. The measured heat transfer rates from the heat flux meter were generally higher than that from the coolant energy balance and, in some cases, much higher than expected. The values from the coolant energy balance followed expected trends and were selected to compare against the model because they should more closely represent the average heat transfer rate. The new model is compared with all of the data from the unvented tests. All of the vented tests were at bulk temperature near 90°C (±2°C). Five of the tests (representative of the test set) were selected for comparison with the model. The bulk temperature, steam pressure, and total pressure are listed for each test. The steam pressure is consistent with the saturation pressure at the specified bulk temperature. The bulk-to-wall surface temperature difference is also listed so that the wall temperature is easily obtained.

6.1.5.5   U of W Flat Plate Tests

The University of Wisconsin (U of W) flat plate tests (Reference 110) measure heat transfer to cooled plates at various orientations ranging form horizontal to vertical. Tests were carried out with saturated steam/air mixtures flowing through the test chamber at 1, 2 and 3 m/s at atmospheric pressure. Test results for the average effective heat transfer coefficient from the heat flux meter and from the coolant energy balance are presented, along with the experiment parameter values for the steam/gas mass ratio, bulk temperature, wall temperature, bulk velocity, and plate angle. Heat transfer coefficients from the coolant energy balance were generally higher than those from the heat flux meters, and the coolant energy balance values were used for

comparison with the model. To be consistent with the model assumptions, only those tests that were vertical or very near vertical were used for comparison. Measured heat transfer rates for the horizontal tests were typically 20–30% higher than the corresponding vertical tests, and heat transfer rates generally decreased as the angle of inclination increased. No estimate of the experimental error was given.

6.1.5.6   Debhi MIT Tests

Debhi (Reference 111) measured heat transfer to a cooled vertical cylinder 3.2 meters high. The tests were carried out at 1, 3, and 4.5 atmospheres. The data were adjusted so that they could be compared with flat plate correlations. The correction factor was overestimated to ensure that the data fit gave conservative estimates of the heat transfer rate. The data were readjusted to give best estimate flat plate data rather than conservative data. The correction factor is based on boundary layer theory in natural convection, and for this geometry the value is between 0.82 and 0.86. These correction factors do not account for condensation effects. The suction effect caused by the condensation effectively thins the boundary layer, and therefore the effect of curvature is not expected to be as large. In order to compensate for the correction factor of 0.80 used by Debhi, the data are readjusted by a factor of 0.86/0.80. The upper limit (0.86) on the correction factor is used because the influence of curvature is expected to be reduced when suction is included.

6.1.5.7   Nusselt Theory

For condensation of pure steam, the wall heat transfer rate is controlled by the resistance of the liquid film. For condensation of steam at 1 atmosphere, the effective heat transfer coefficient reduces to (Reference 112):

$$\bar{h} = \frac{4000}{H^{1/4} \Delta T^{1/3}} \text{ Btu/hr-ft}^2\text{-R}$$

where H is the wall height in feet and ΔT is the bulk-to-wall surface temperature difference in Rankine. The model is compared to results from the above equation for

wall heights of 1, 10, and 100 meters, and temperature differences of 10, 45, and 80 Kelvin.

6.1.5.8   CVTR

The Carolina-Virginia Tube Reactor (CVTR) facility was instrumented with heat transfer measurement devices on the vertical wall of the full–scale, PWR-type containment (Reference 113). This test was used for validation in two ways: comparison with the measured heat transfer rates as described here, and comparison with the overall containment behavior, including pressure and local atmosphere temperatures, as discussed in Section 6.2.4 with test description. The heat transfer rate was measured at the containment wall at 1.2 and 7.3 meters above the operating deck. The heat transfer rate and the bulk temperature were deduced from temperature readings from thermocouples imbedded in the concrete and the average of readings from thermocouples at 5.1, 3.8, 1.3, and 0.6 cm away from the wall surface. These are local heat transfer readings and may not be representative of the average values for the larger wall areas modeled by GOTHIC. The overall uncertainty in the measured values was not reported.

6.1.5.9   Park Film Tests

Park et al. (Reference 114 and Reference 115) measured the overall heat transfer rate to a vertical wall from a downward flowing steam/air mixture. The test apparatus was 1.5 m high and 24 mm from the cooled wall to the insulated wall. The film flow was a combination of the condensate plus a controlled water flow introduced at the top of the cooled wall. The vapor phase Reynolds number (based on the channel width) ranged from 2,000 to 14,000, while the film Reynolds number ranged from 75 to 14,000. The heat transfer rate was measured towards the bottom of the apparatus, where flow and heat transfer were fully developed. The overall uncertainty of the measurements was not reported.

AREVA NP Inc.

ANP-10299NP

Applicability of AREVA NP Containment Response Evaluation Methodology to the

Revision 2

U.S. EPR™ for Large Break LOCA Analysis

Technical Report

Page 6-55

6.1.5.10   Modeling Approach

For the U of W tests and the Debhi data, the air/gas mixture is saturated, while for the

CVTR and Uchida data it is assumed that the mixture is saturated. Therefore, only two

of the first three parameters listed at the beginning of this section are needed to define

the vapor conditions. The simple model shown in Figure 6-39 can be adjusted to match

all of the experimental conditions. The total pressure is maintained by the pressure

boundary condition. The bulk vapor temperature and velocity are controlled by the flow

boundary condition, with the incoming humidity set to 100% for all cases. The wall

surface temperature is controlled by the back face temperature of a thin conductor, and

the wall height is controlled by the volume height.

Figure 6-39—GOTHIC Model for Wall Heat Transfer Tests

A null transient (100 seconds) was run for each of the experimental conditions to

acquire the steady heat transfer rate. The forced convection heat transfer option was

used only for the U of W forced convection tests and the Park tests.

6.1.5.11   Discussion

The GOTHIC results from all of the above tests using the DLM-FM (Diffusion Layer

Model with enhancement due to film roughening and mist generation in the boundary

layer) heat transfer option are shown in Figure 6-40. This plot compares the measured

heat transfer rate divided by the bulk-to-wall temperature difference against the

predicted value. For most of the data, the predicted value is within the 20% error bands

about the exact 1:1 comparison line. Notable exceptions where the model under-predicts that data are the Uchida nitrogen tests and some of the CVTR data points. The under-predicted CVTR points are for heat plug #2, which is located about 7 meters above the operating deck and may have been influenced by local high velocities induced by the steam diffuser. In these simulations for the CVTR data, the bulk velocity was small, resulting in natural convection heat and mass transfer. In the integrated tests described in Section 6.2.4, calculated local velocities are considered in the evaluation of the heat and mass transfer. For the Uchida data, the uncertainty in the experimental setup and data means that these results must be discounted.

Figure 6-41 shows predicted versus measured heat transfer for the Uchida option for all data sets. Compared with the DLM-FM option, the data vary more widely from the Uchida correlation. The tighter band indicates the DLM-FM is a more accurate model than Uchida for these tests. Also, there is no particular conservative bias in the Uchida results. In many cases, the Uchida correlation substantially over-predicts the condensation rate. The Uchida option, as implemented in GOTHIC, has an upper limit of 278 Btu/hr-ft^2-°F, which explains the constant value for the Nusselt tests. Also, the Uchida model does not account for any velocity or film roughening effects, which results in the near constant values for some of the other test sets. However, the DLM-FM option compares better with the data than the Uchida model, even for the Uchida data itself. Others have noted the shortcomings of the Uchida model on a theoretical basis (refer to Reference 116).

The effective heat transfer coefficient for the DLM option, without the enhancements due to film roughening and mist formation, is compared to the experimental results in Figure 6-42. The film and mist formation effects are substantial in many cases and neglecting them can result in underestimating the effective heat transfer coefficient by a factor of two or more.

These tests demonstrate that the DLM-FM heat and mass transfer option in GOTHIC gives a good estimate of the total heat transfer rate to the wall over a wide range of

conditions, and is an improvement over the Uchida model. Conservatism in the overall energy removal rate from the atmosphere can be realized by ignoring forced convection (retained as an option in the DLM models) and using a low estimate on the total available wall heat capacity and surface area in the model input.
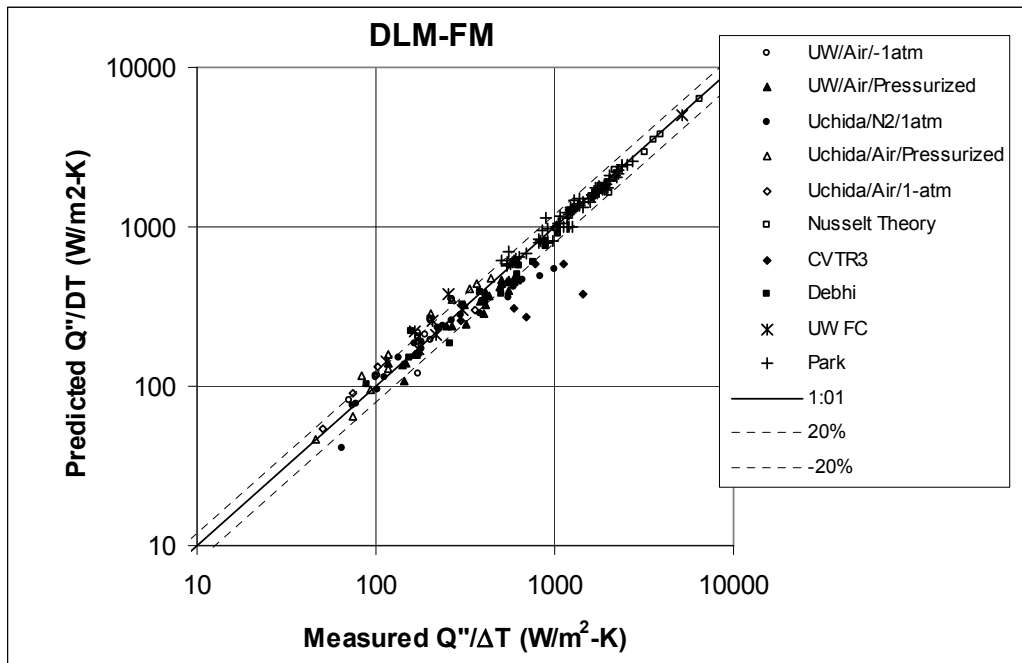
Figure 6-40—Experiment versus DLM-FM Heat and Mass Transfer Option

AREVA NP Inc.

Applicability of AREVA NP Containment Response Evaluation Methodology to the

U.S. EPR™ for Large Break LOCA Analysis

Technical Report

ANP-10299NP

Revision 2

Page 6-58
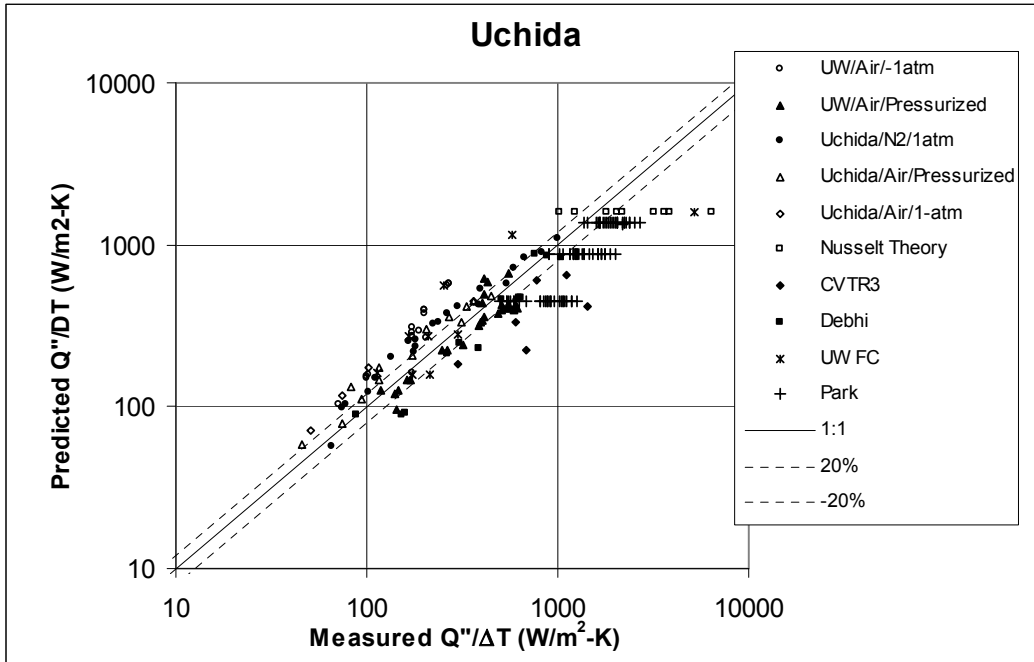
Figure 6-41—Experiment versus Uchida Heat and Mass Transfer Option
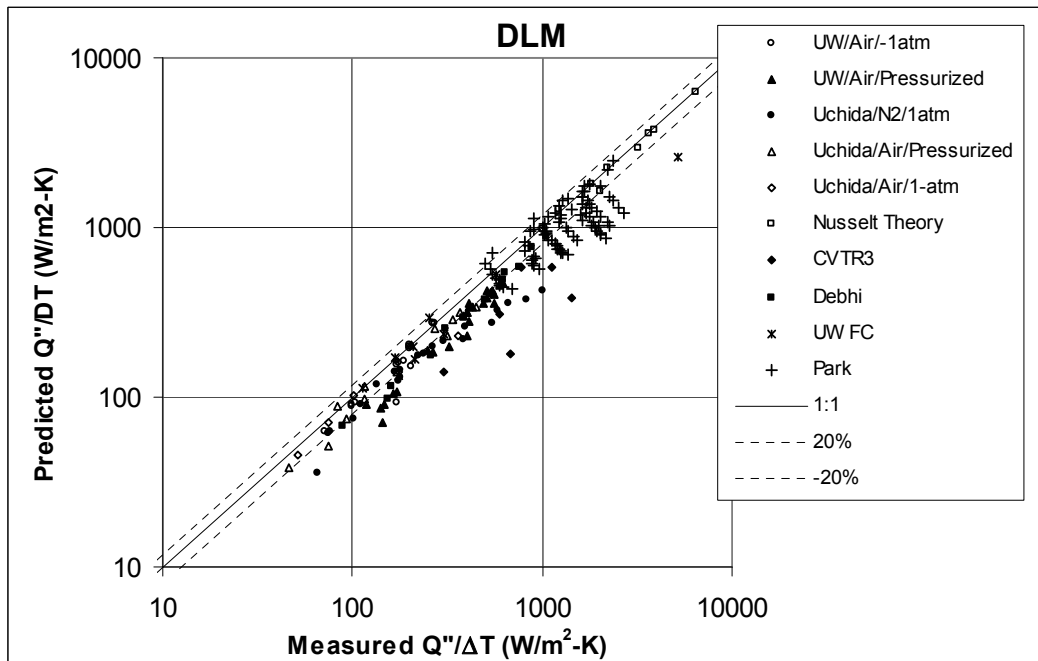
Figure 6-42—Experiment versus DLM Heat and Mass Transfer Option

6.2   Integral Test Benchmarks (EMDAP 18)

This section presents the results of several GOTHIC assessments for integral-effects tests that include containment phenomena expected in the U.S. EPR during an LBLOCA. The assessments build upon GOTHIC's extensive assessment database described in (Reference 31). Most of these studies examine the effect of nodalization by comparing both a multi-control-volume model and a single-control-volume model (as used in AREVA NP's containment response evaluation methodology).

6.2.1   HDR Tests

The Heissdampfreaktor (HDR) is a decommissioned superheated steam reactor in the Federal Republic of Germany (Reference 60). Following its decommissioning, the HDR reactor vessel and containment system were used as an experimental facility called Project HDR. Beginning in the late 1970s, several blowdown and related tests were performed at the site. Comparing GOTHIC predictions to HDR test data demonstrates GOTHIC's ability to predict the thermal-hydraulic response of a full-scale, multi-compartment containment to a water-only or steam/water blowdown from a reactor vessel.

Elevation views of the HDR containment are shown in Figure 6-43 and Figure 6-44. The primary features of the experimental facility are the pressure vessel and the containment structure. Internally, the pressure vessel is approximately 3 m in diameter and 11 m high. Most pressure vessel internals were removed before the blowdown test series was performed to maximize discharge flows. The free volume in the vessel is 75 m³.

The containment is 20 m in diameter and 60 m high, with a total free volume of 11,300 m³. Notable features of the containment include the dome, which is about 42% of the total containment volume, and the spiral stairs and the main stairway. The stairways are significant because they provide the dominant vertical flow paths from the lower portions of the containment to the dome. Rooms in the containment are

AREVA NP Inc.

ANP-10299NP

Applicability of AREVA NP Containment Response Evaluation Methodology to the

Revision 2

U.S. EPR™ for Large Break LOCA Analysis

Technical Report

Page 6-60

interconnected by a large number of openings, and the interconnections are shown schematically in Figure 6-45.

The HDR tests are integral effects tests in which all relevant phenomena are represented and play their respective roles during the various phases of the test transients. Some of the key phenomena addressed in the HDR tests include: drop condensation and evaporation, mist generation and depletion, natural convection, forced convection, mixed convection, thermal conduction in solids, pool surface evaporation, and gas mixing.

The primary difference among the tests is the location of the simulated pipe break. For tests V21.1, T31.1, and V44 (Reference 61), the break is in room 1603. For test T31.5 the break is in room 1704. Another distinction between tests was the vent openings from the break room to adjacent rooms.

HDR Tests V21.1, T31.1, T31.5, and V44 simulate various types of LBLOCAs. Because of the force of the mass and energy releases, the tests all exhibit a significant amount of containment atmosphere mixing. HDR Tests E11.2 and E11.4 represent SBLOCAs, so the containment response is driven primarily by the buoyancy of the steam released from the injection points. This leads to natural circulation within the containment. The HDR containment spray system was not used during any of the tests.

The HDR and U.S. EPR containment buildings have a similar structure, consisting of a steel concrete-backed liner, an air annular space, and a concrete outer building. Both the HDR and U.S. EPR are dry, non-suppression pool type containments, although the U.S. EPR does have an IRWST in the form of a pool located at the bottom of the containment. Because of these similarities, the results of the HDR code qualification cases are directly applicable to the U.S. EPR containment design.

Benchmarks were performed against the HDR test data using both of single-volume and multi-volume GOTHIC models. Results are presented in the following sections.
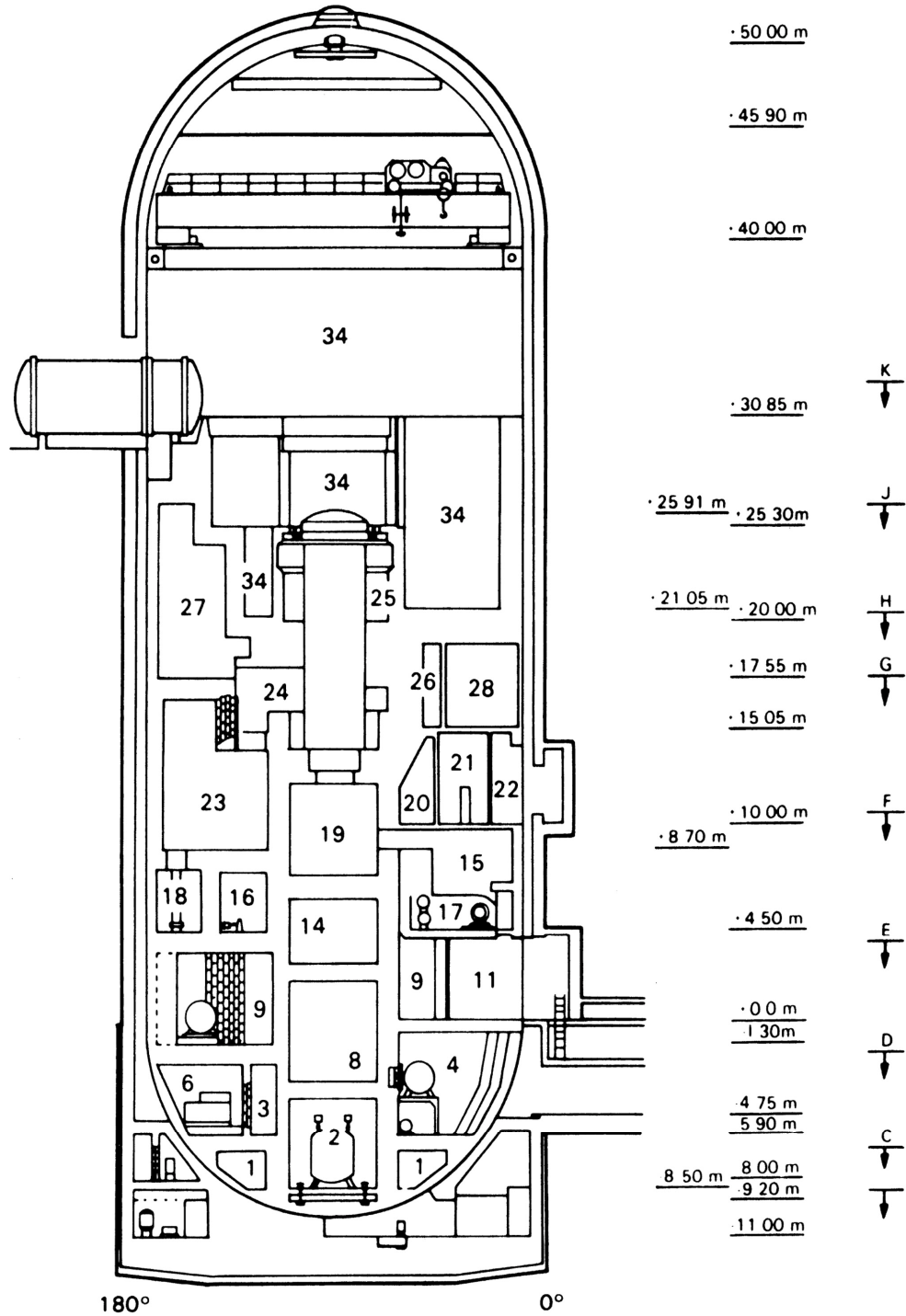
Figure 6-43—Elevation View of HDR (0° – 180°)
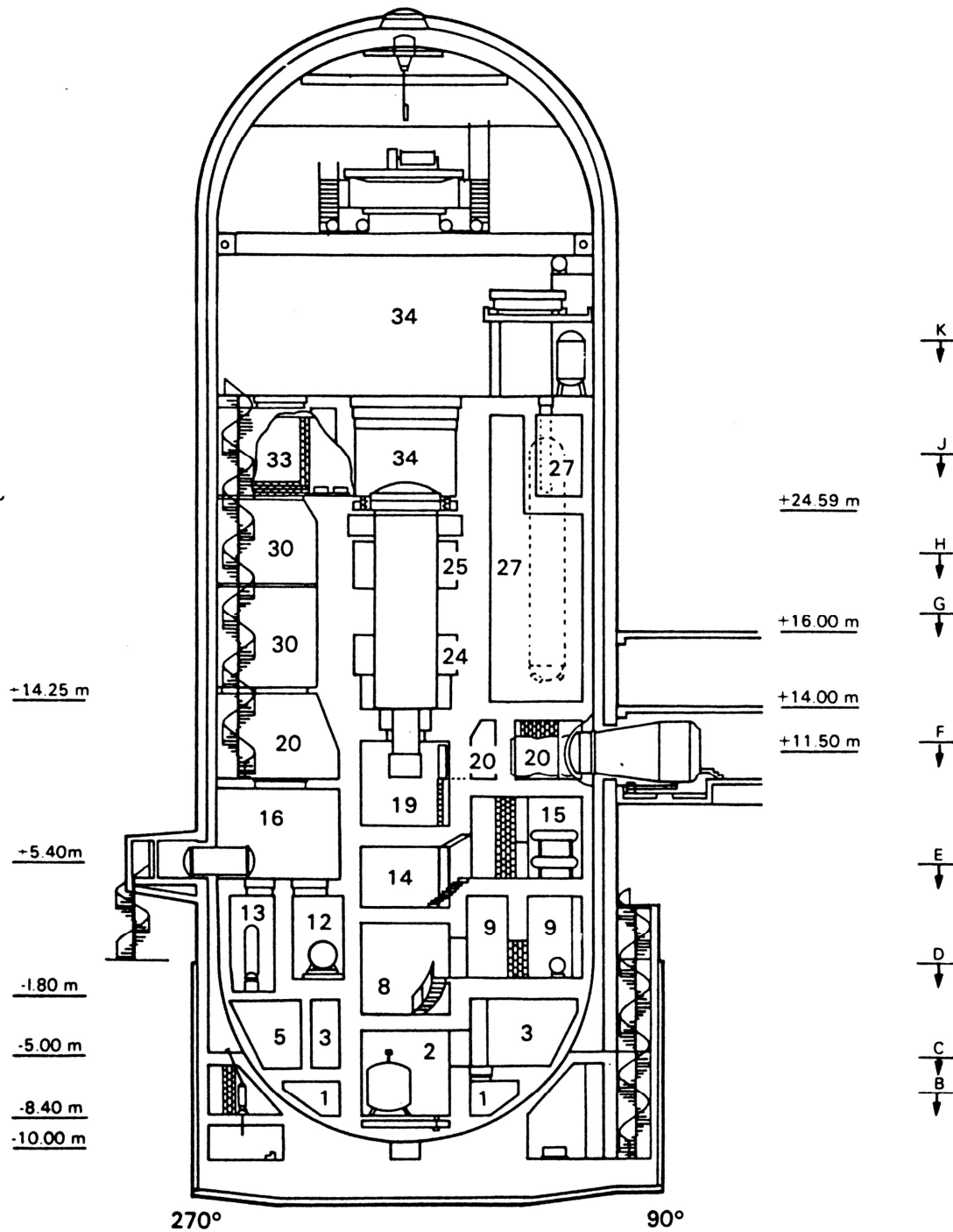
Figure 6-44—Elevation View of HDR (90° – 270°)

AREVA NP Inc.   ANP-10299NP
Applicability of AREVA NP Containment Response Evaluation Methodology to the   Revision 2
U.S. EPR™ for Large Break LOCA Analysis
Technical Report   Page 6-63
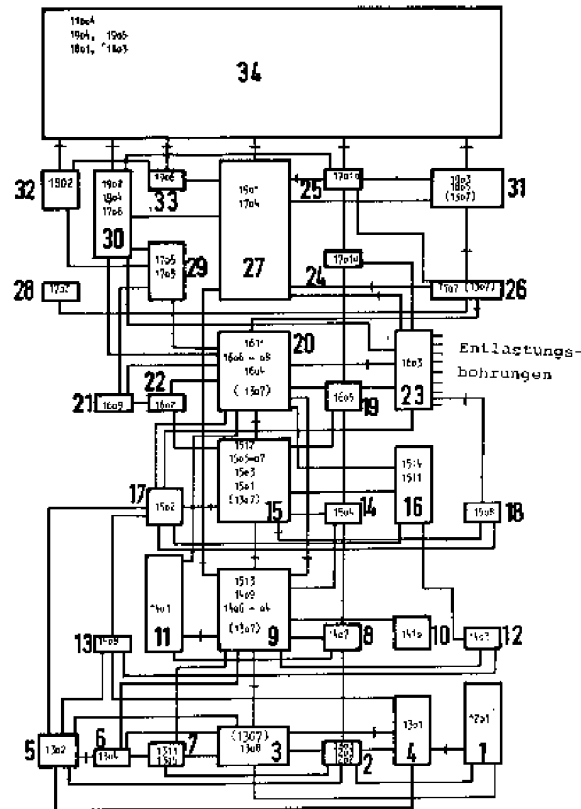
Figure 6-45—HDR Schematic Showing Room Inter-Connections

6.2.1.1 HDR Test V21.1

HDR test V21.1 (References 62 and 63) was a water-only blowdown test in which the break was located near the bottom of the pressure vessel. The main test parameter was the vent openings between the break room and the adjacent rooms. Initial vessel conditions included a pressure of 11.1 MPa and a temperature of 318°C. The vessel was full, with the water level at about 10.5 m. A liquid only break flow was obtained by installing the pipe break at the bottom of the vessel. The blowdown lasted about 25 s and the benchmark calculation was terminated at around 200 s.

Figure 6-46 shows the HDR test V21.1 GOTHIC multi-volume model. (Because the single-volume model for this test is simple, it is not presented in a figure; this is the case

for all the HDR tests that follow.) Figure 6-47 shows the benchmark calculations of containment pressure using these GOTHIC models and the HDR test data. The figure shows that the single-volume GOTHIC model calculates higher containment dome pressures than the multi-volume GOTHIC model over the entire test duration. Moreover, both GOTHIC models produce pressures that are higher than the HDR test data during this relatively short test.

Figure 6-48 compares the containment temperature results. The single-volume GOTHIC model calculates containment dome temperatures that are higher than the multi-volume GOTHIC model. Both GOTHIC models produce peak temperatures that are higher than the peak containment dome temperature. On the other hand, both models produce long-term temperatures that are lower than the test data.

AREVA NP Inc.

Applicability of AREVA NP Containment Response Evaluation Methodology to the
U.S. EPR™ for Large Break LOCA Analysis
Technical Report

ANP-10299NP
Revision 2

Page 6-65
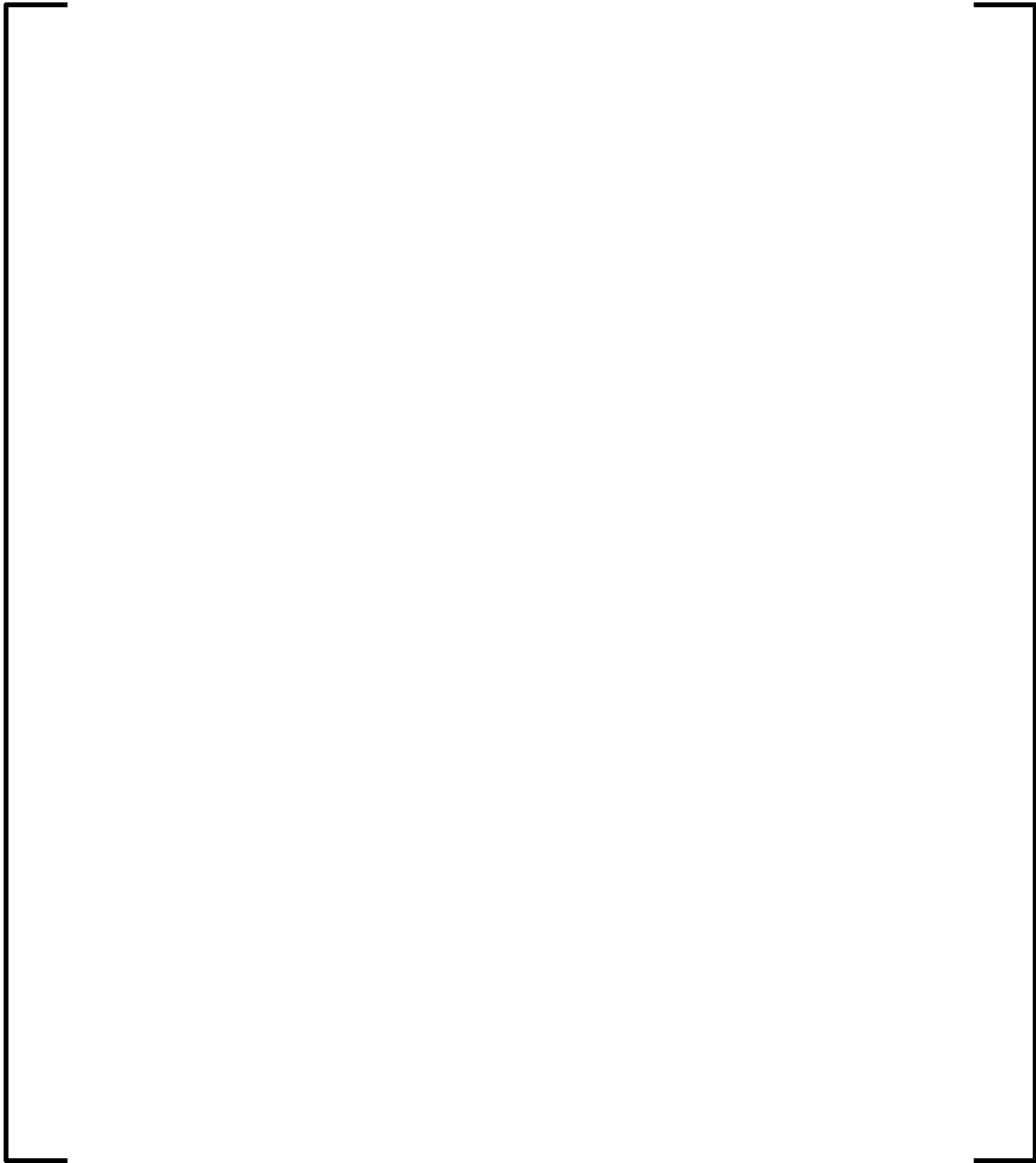
Figure 6-46—HDR Test V21.1 Multi-Volume GOTHIC Model
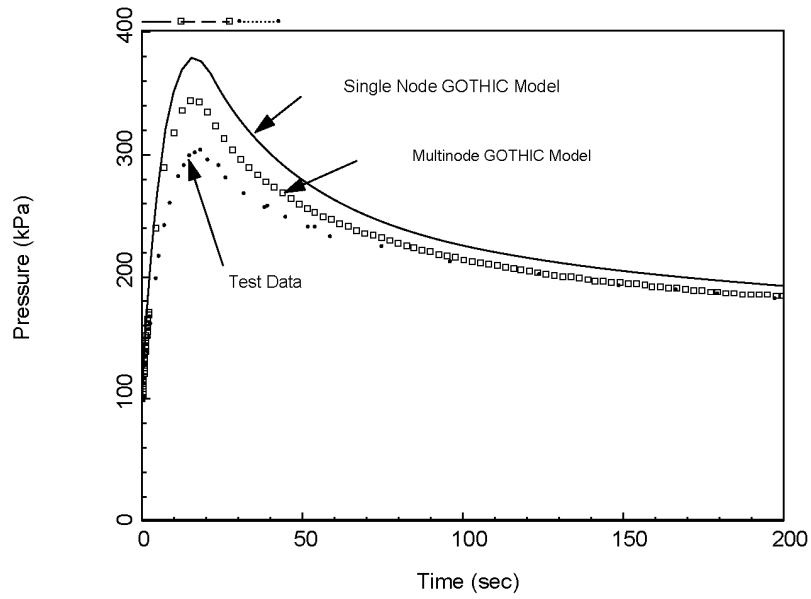
Figure 6-47—HDR Test V21.1 Containment Pressure
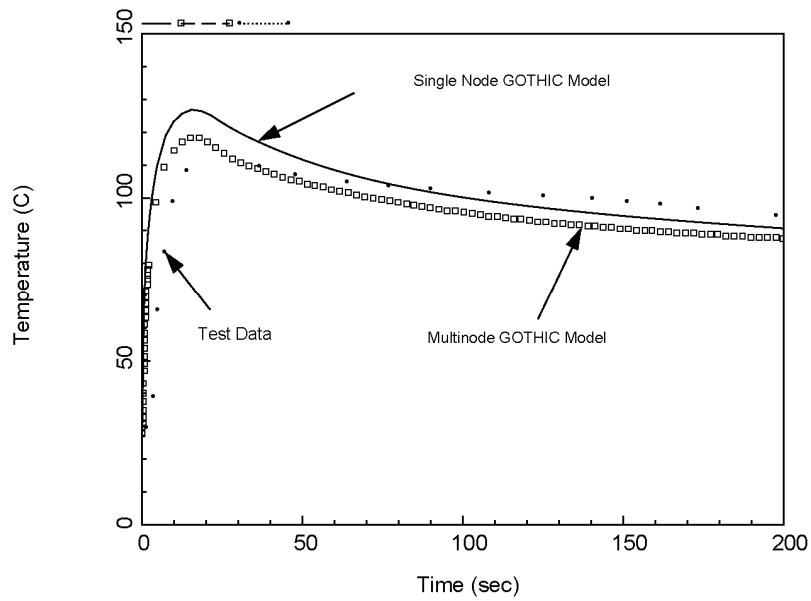
Figure 6-48—HDR Test V21.1 Containment Temperature

6.2.1.2 HDR Test V44

HDR test V44 (References 64 and 65) was performed to evaluate the long-term containment response to an LBLOCA. CSNI-OECD designated test V44 as International Standard Problem 16. The main purpose of test V44 was to compare containment behavior in various compartments after a steam line rupture. The initial conditions were a pressure of 11 MPa and a temperature to 390°C, with a coolant level of 9 m in the pressure vessel. The test parameters were the initial liquid level in the pressure vessel and the vent openings between the break room and the adjacent rooms. Blowdown lasted about 50 s and the benchmark calculations were terminated around 1200 s.

Figure 6-49 shows the GOTHIC multi-volume model for test V44. Figure 6-50 compares the measured containment pressure response to that calculated with the multi-volume and single-volume GOTHIC models. The figure shows the single-volume GOTHIC model produces a higher peak containment pressure than the multi-volume GOTHIC model. Both are higher than the measured peak containment pressure. After the peak, the single-volume GOTHIC model calculates a pressure response that compares well with that of the multi-volume GOTHIC model and the measured containment pressure.

Figure 6-51 compares the containment temperature response for HDR Test V44 with the benchmark calculations. The single-volume GOTHIC model produces a higher peak temperature than the multi-volume GOTHIC model, and both were higher than the test data. After the peak, the single-volume GOTHIC model produced temperatures lower than both the multi-volume GOTHIC model and the test data.
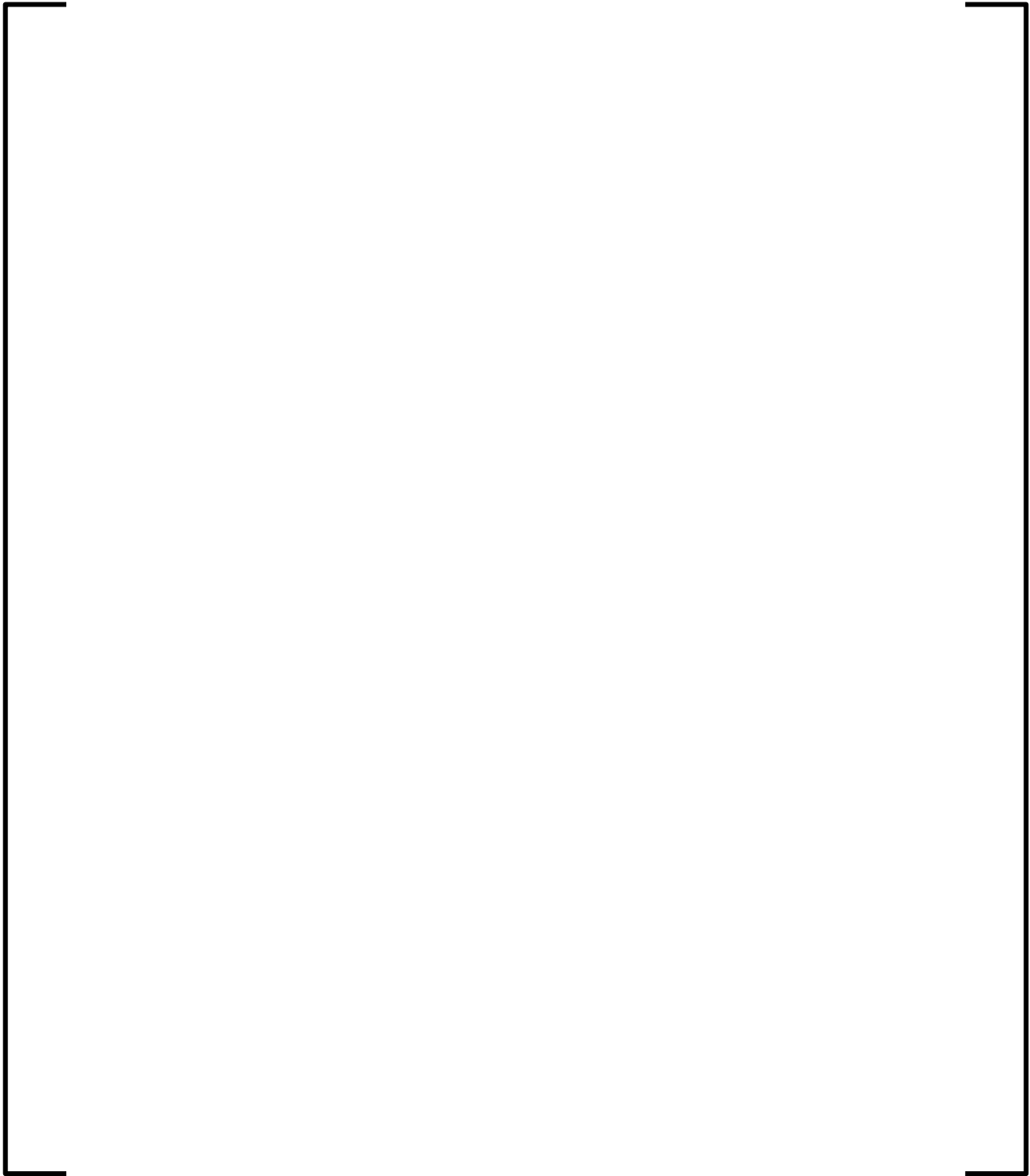
Figure 6-49—HDR Test V44 Multi-Volume GOTHIC Model
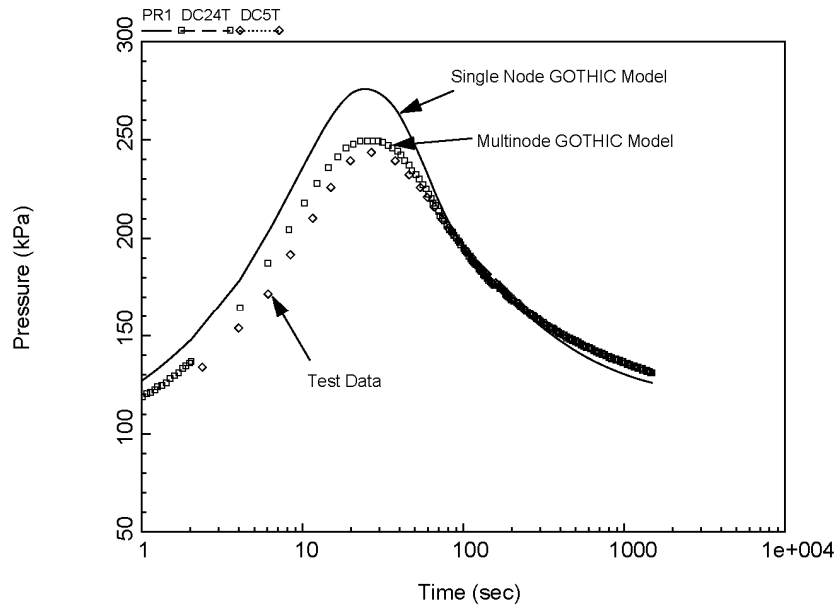
Figure 6-50—HDR Test V44 Containment Pressure
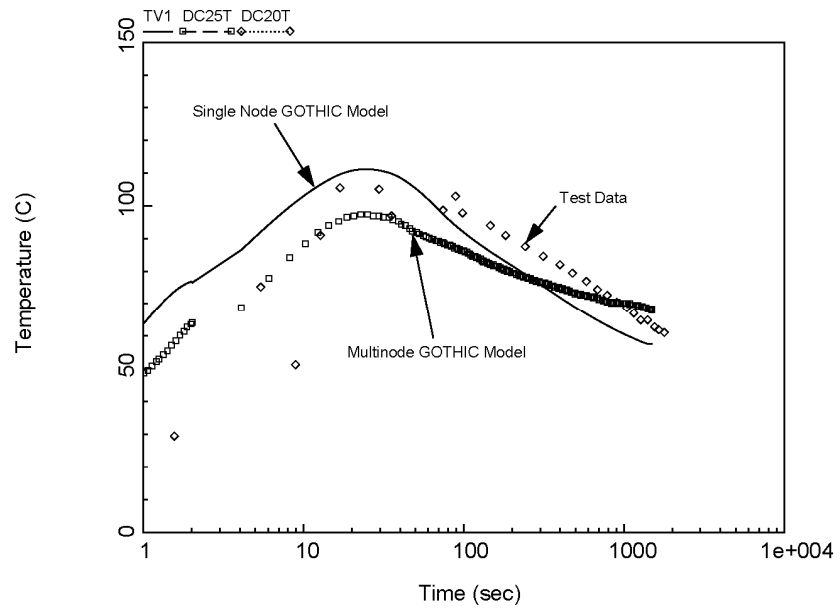
Figure 6-51—HDR Test V44 Containment Temperature

6.2.1.3 HDR Test T31.1

HDR test T31.1 was a short-term LBLOCA steam-water blowdown in which the break is located near the top of the pressure vessel (Reference 66). The initial conditions were 11 MPa and a temperature to 390°C, with a coolant level of 7.8 m in the pressure vessel. The blowdown lasted about 55 s and the benchmark calculation was terminated around 1200 s.

The HDR test T31.1 GOTHIC multi-volume model is shown in Figure 6-52. Figure 6-53 compares the measured containment pressure response with the GOTHIC single-volume and multi-volume calculations. The comparison shows that for the entire duration of the case, the single-volume GOTHIC model calculates containment pressures that are greater than or equal to those for the multi-volume GOTHIC model. Both GOTHIC model produce pressures that compare well with test data in the long term.

Figure 6-54 compares the containment temperatures calculated by the single-volume and multi-volume models with the test data. The single-volume GOTHIC model produced containment temperatures greater than those calculated by the multi-volume model. The single-volume GOTHIC model produced a peak temperature greater than the measured peak temperature, but it under-predicts the long-term containment temperature.
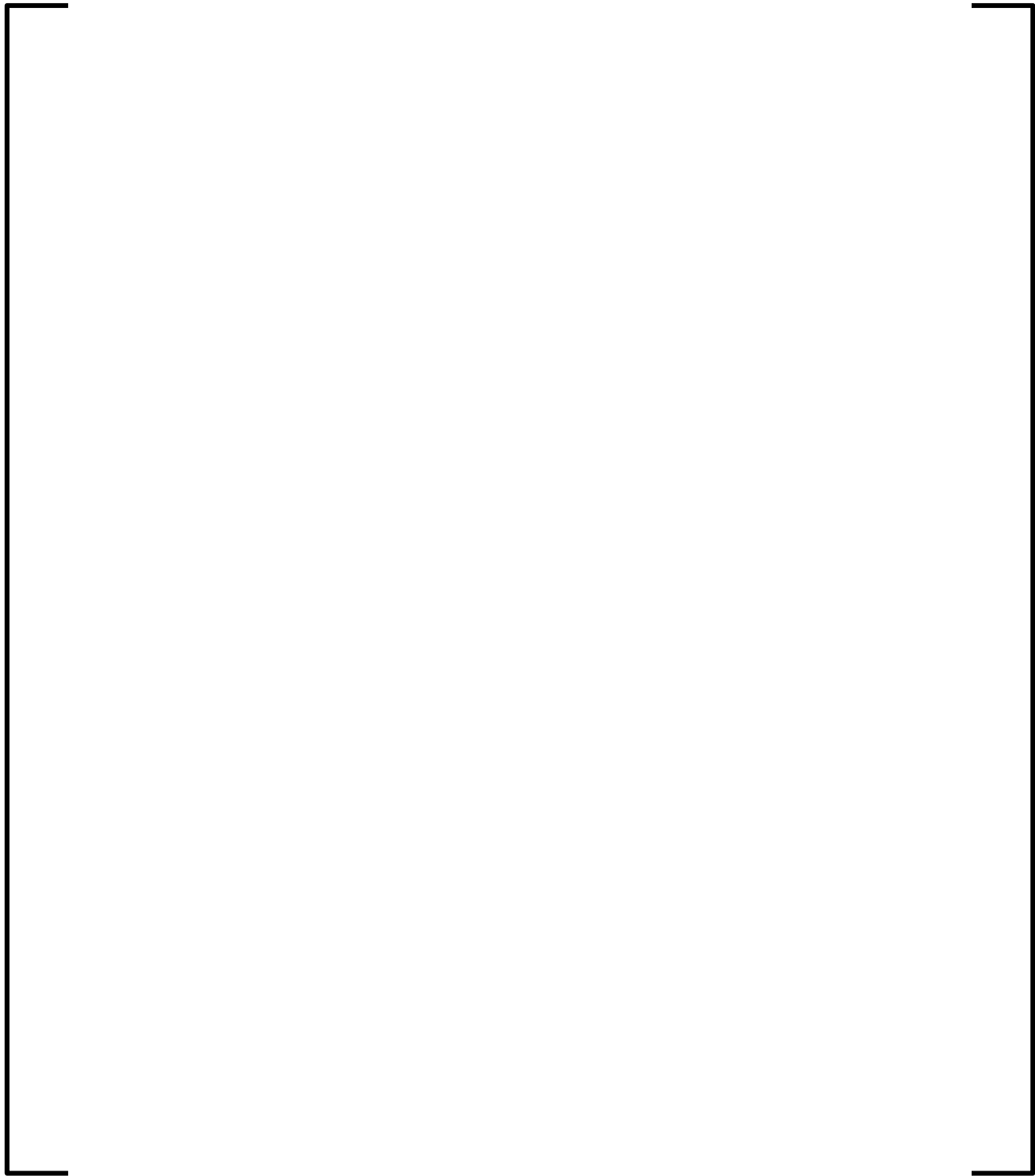
Figure 6-52—HDR Test T31.1 Multi-Volume GOTHIC Model
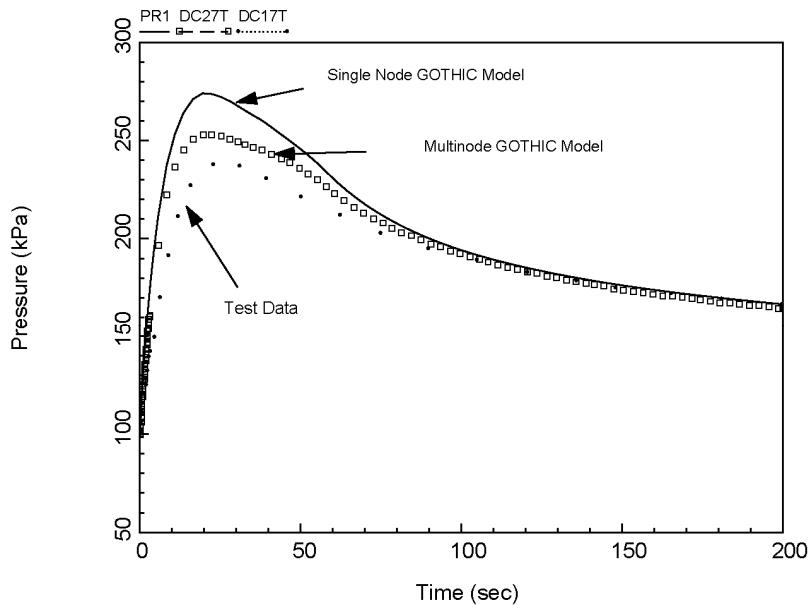
Figure 6-53—HDR Test T31.1 Containment Pressure
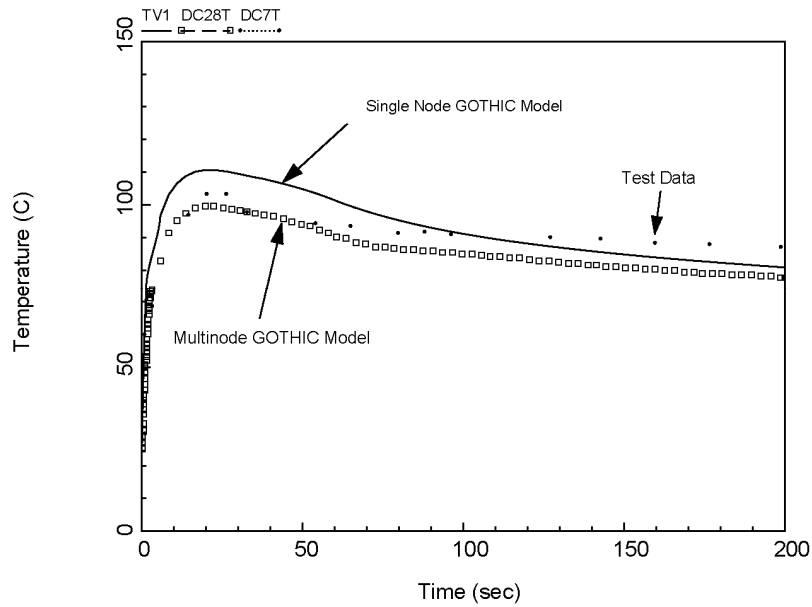
Figure 6-54—HDR Test T31.1 Containment Temperature

6.2.1.4   HDR Test T31.5

HDR test T31.5 was a long-term LBLOCA steam-water blowdown. CSNI-OECD designated test T31.5 as International Standard Problem 23 (References 67 and 68). The experiment was designed to emulate the mass and energy release into a containment without sprays or fan coolers. As such, the main interest was the thermal loads on structures during a large-break blowdown and the long-term temperature and pressure response. The initial condition was a pressure of 11 MPa and a temperature to 390°C, with a coolant level of 7.8 m in the pressure vessel. Blowdown lasted about 55 s and the benchmark calculation was terminated around 1200 s. The experiment continued beyond this time to track a secondary release of a hydrogen simulant; however this portion of the test is outside the scope of the benchmark.

Figure 6-55 shows the HDR test T31.5 GOTHIC multi-volume model. Figure 6-56 compares the calculated containment pressure responses for the single-volume and multi-volume GOTHIC model with the HDR test data. The single-volume GOTHIC model produces a peak pressure higher than the peak containment pressure produced by the multi-volume model, and both are higher than the measured peak pressure. After the peak, both models calculate pressures that compare well with the test data.

Figure 6-57 compares the calculated containment temperature responses with the HDR test data. The figure shows that the single-volume GOTHIC model calculates a higher peak containment temperature than the multi-volume model. However, both fall halfway between the test data for upper and lower containment dome peak temperatures. In the long term, the containment temperatures calculated by the single-volume GOTHIC model are lower than both the multi-volume and test data temperatures.
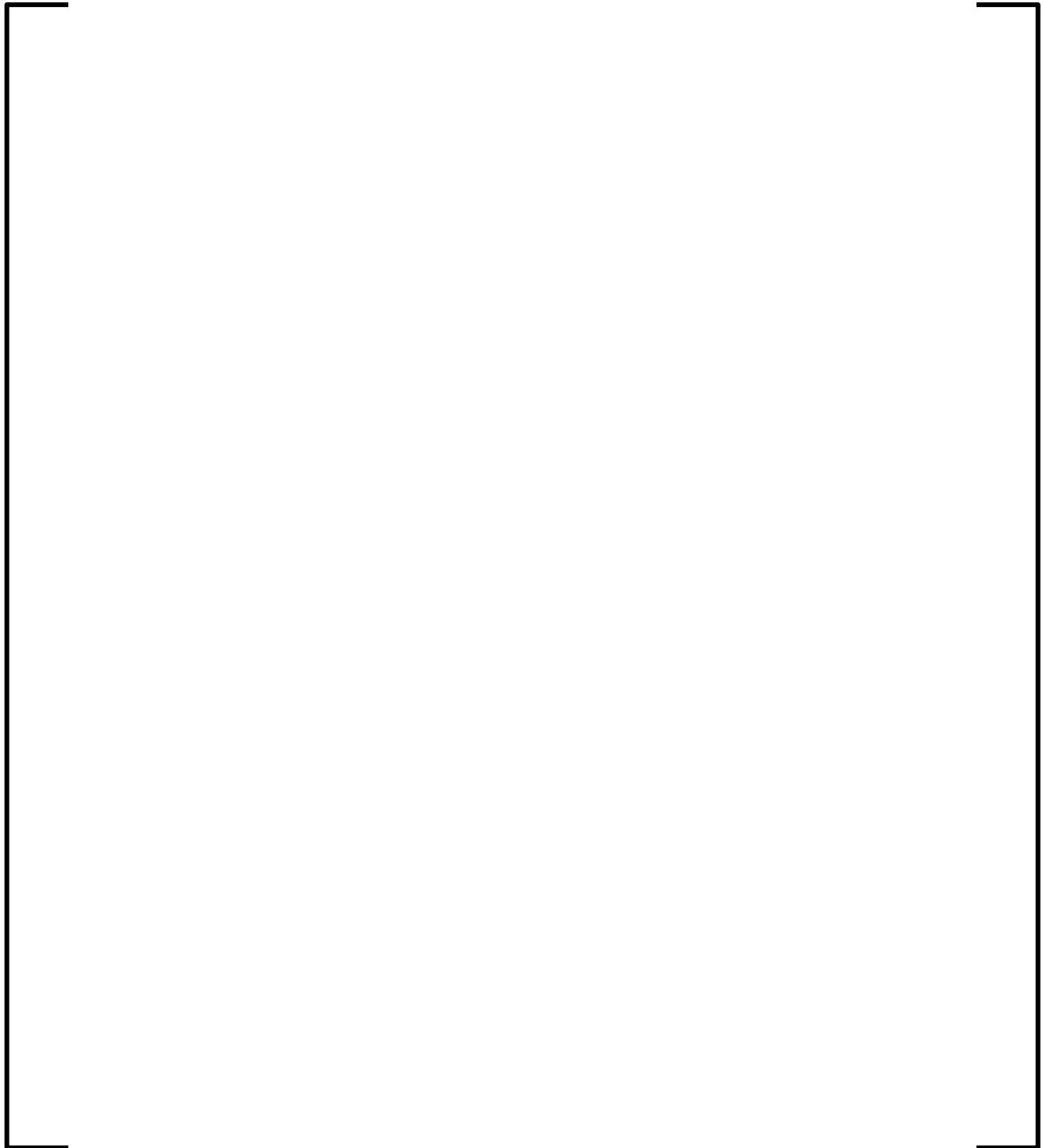
Figure 6-55—HDR Test T31.5 Multi-Volume GOTHIC Model
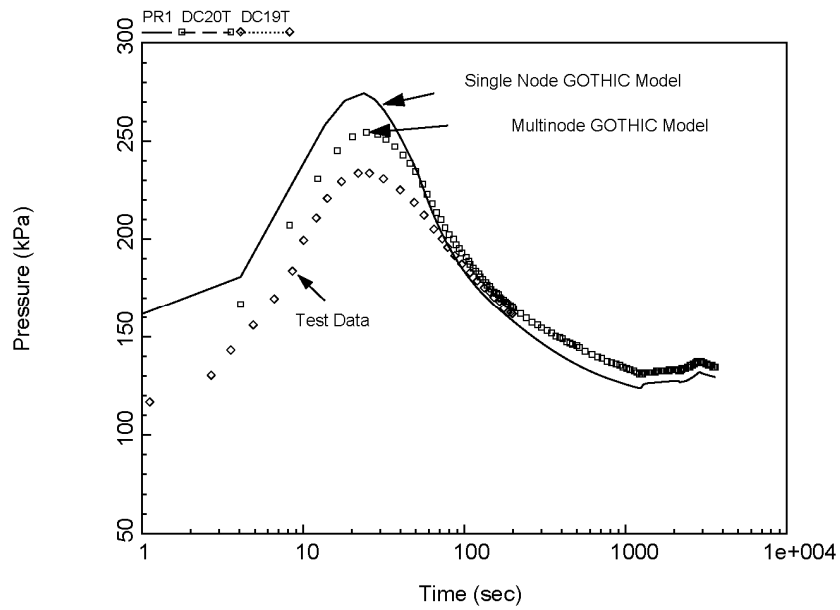
Figure 6-56—HDR Test T31.5 Containment Pressure
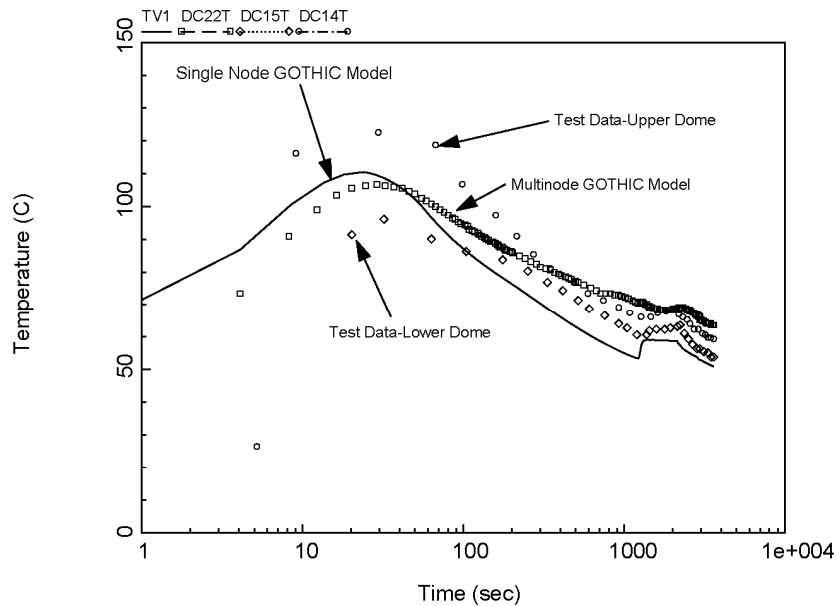
Figure 6-57—HDR Test T31.5 Containment Temperature

6.2.1.5   HDR Test E11.2

HDR test E11.2 (Reference 69 and 70) simulates an SBLOCA in an interior containment room in which steam was released at various injection points. CSNI-OECD designated test E11.2 as International Standard Problem 29. Cooldown was enhanced in test E11.2 through spray actuation on the outer surface of the steel containment shell. The main focus of the test was containment internal natural convection flows, heat absorption by structures, and gas distribution (with an emphasis on hydrogen). The rising steam, in combination with condensation on the containment heat structures, causes natural circulation within the containment.

Figure 6-58 shows the GOTHIC multi-volume model for HDR test E11.2. Figure 6-59 and Figure 6-60, respectively, compare the calculated containment pressure response for the single-volume and multi-volume GOTHIC models with the measured test data. The multi-volume model calculates a peak pressure greater than the measured peak, while the peak pressure calculated by the single-volume model compares well with the test data.

Figure 6-61 and Figure 6-62, respectively, compare the containment temperatures calculated with the multi-volume and the single-volume GOTHIC models with the test data. The multi-volume model slightly under-predicted the containment temperature. As expected, the single-volume model calculates an overall containment temperature average and does not capture the measured temperature stratification.
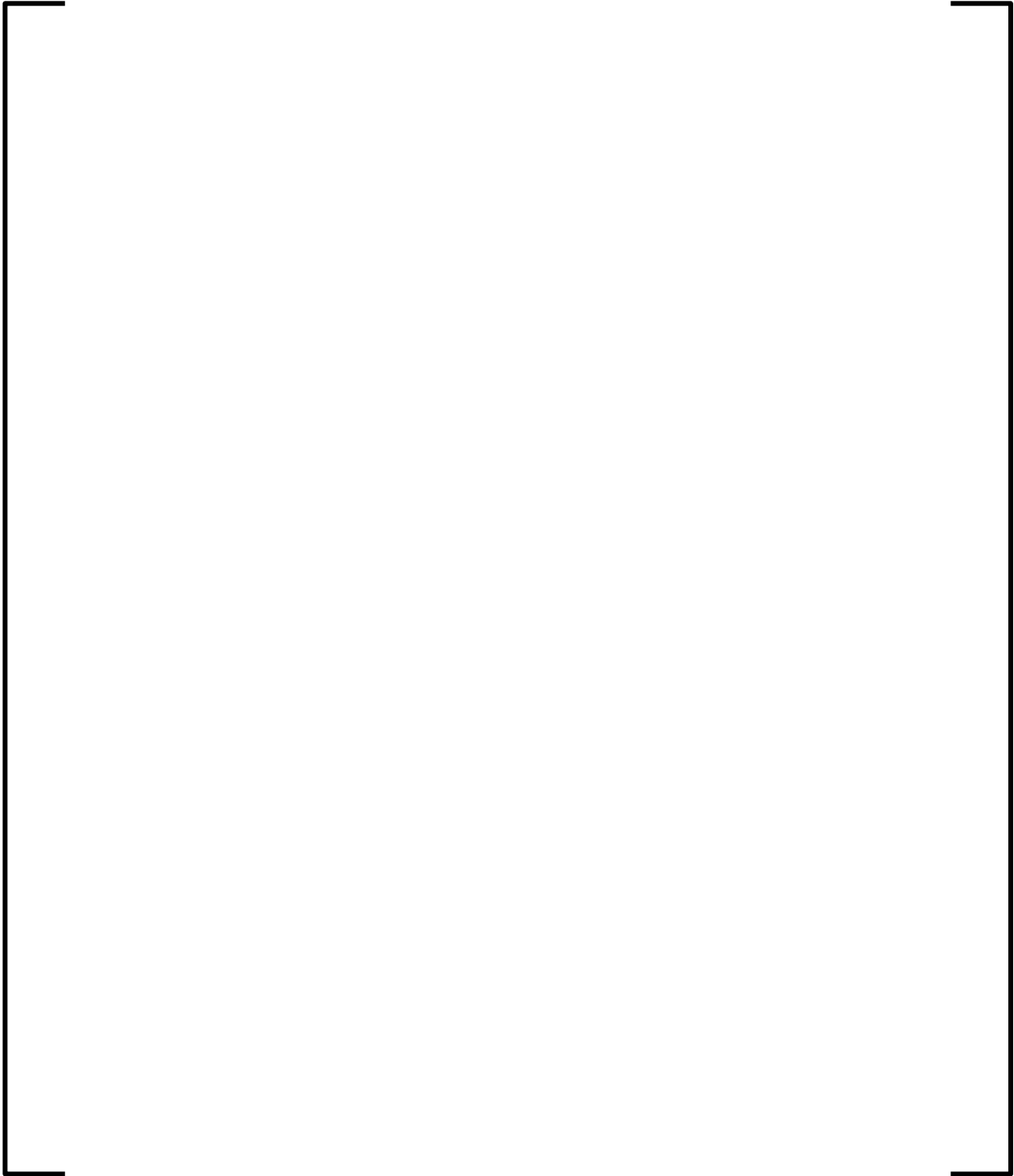
Figure 6-58—HDR Test E11.2 Multi-Volume GOTHIC Model
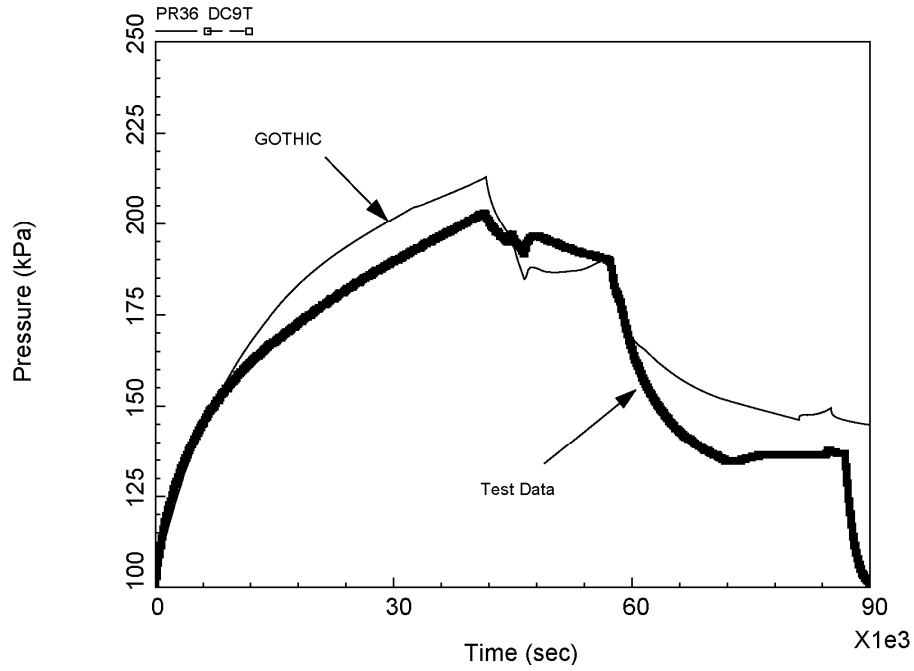
Figure 6-59—HDR Test E11.2 Multi-Volume Inner Containment Room Pressure
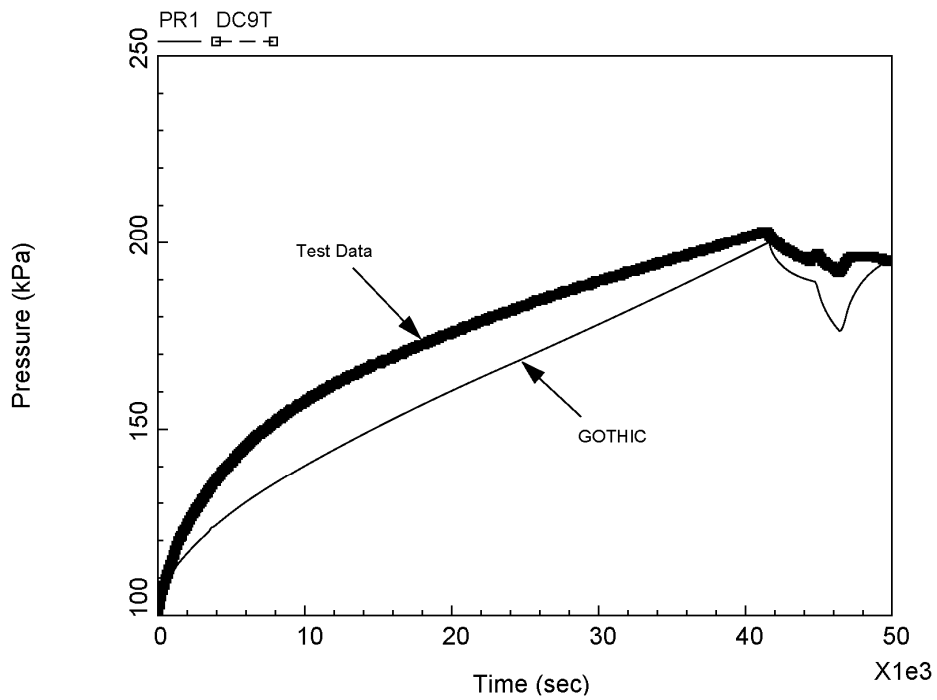
Figure 6-60—HDR Test E11.2 Single-Volume Containment Pressure
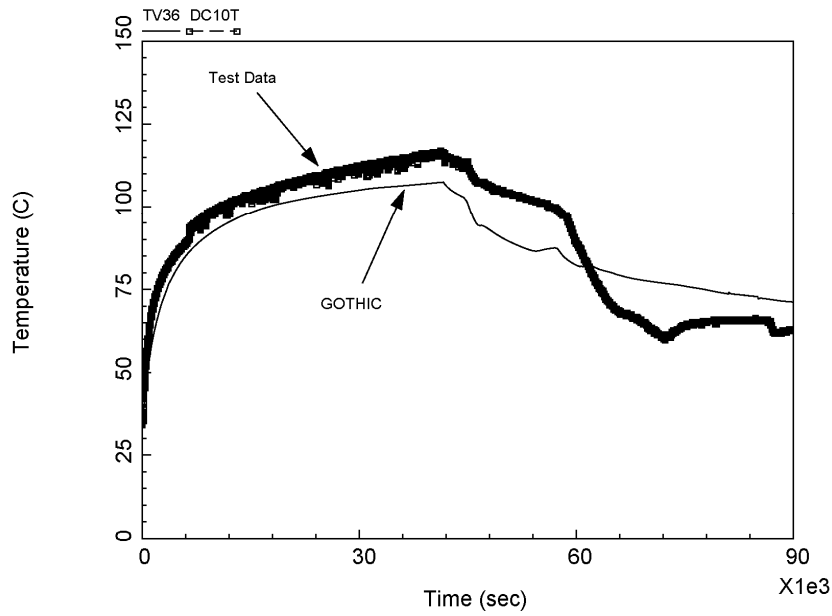
Figure 6-61—HDR Test E11.2 Multi-Volume Inner Containment Room Temperature
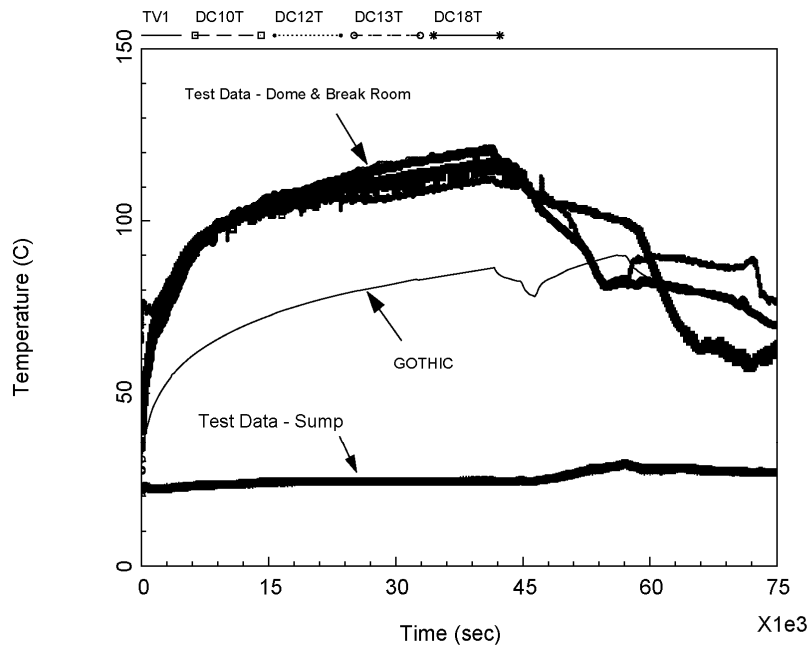
Figure 6-62—HDR Test E11.2 Single-volume Containment Temperature

6.2.1.6   HDR Test E11.4

HDR test E11.4 (References 69 and 70) simulates an SBLOCA in an interior containment room where the containment temperature distribution is a function of the buoyancy-driven flow of the steam released at the various steam injection points. The rising steam, in combination with the steam condensation on the containment heat structures, produces natural circulation within the containment. Figure 6-63 shows the HDR test E11.4 GOTHIC multi-volume model.

Figure 6-64 and Figure 6-65, respectively, compare the containment pressure responses for the multi-volume and single-volume GOTHIC models with the test data. Figure 6-66 and Figure 6-67, respectively, compare the containment temperature responses for the multi-volume and single-volume GOTHIC models with the test data.

Both the multi-volume and single-volume models provided conservative pressure and temperature predictions. This suggests the break energy input used in the GOTHIC models may be significantly higher than the actual test energy. In fact, other containment analysis codes produce similar conservative results for this test.
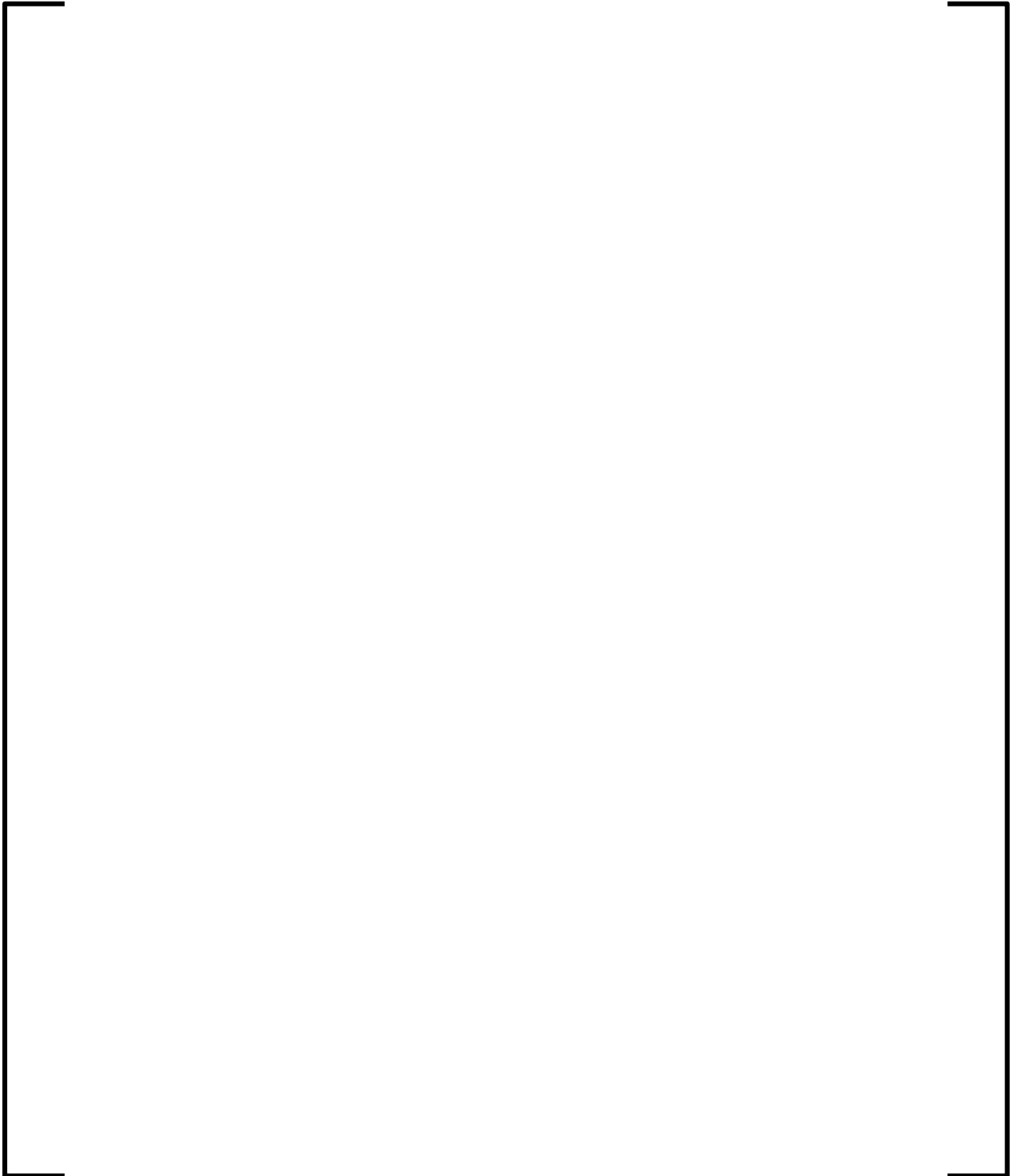
Figure 6-63—HDR Test E11.4 Multi-Volume GOTHIC Model
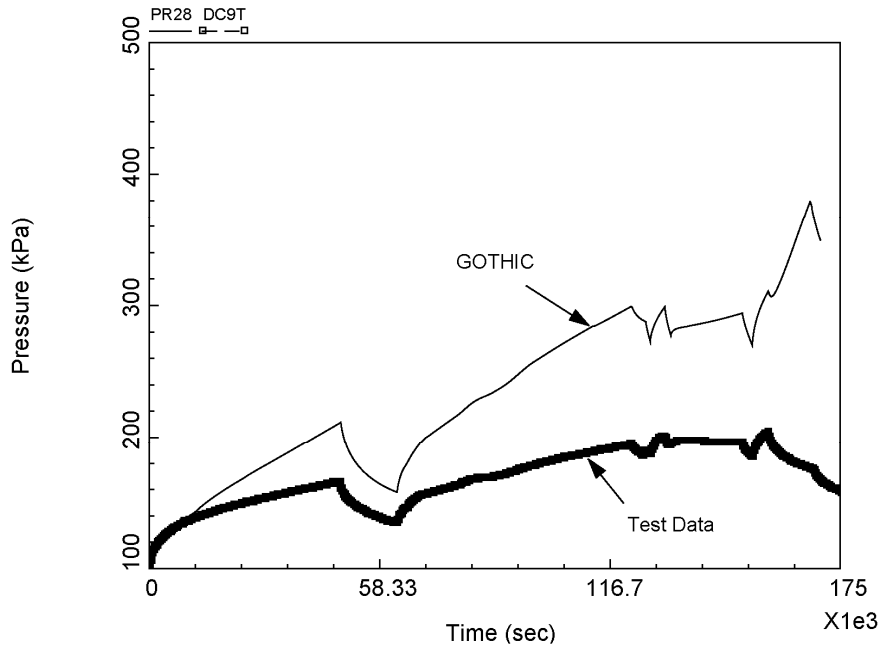
Figure 6-64—HDR Test E11.4 Multi-Volume Interior Containment Room Pressure
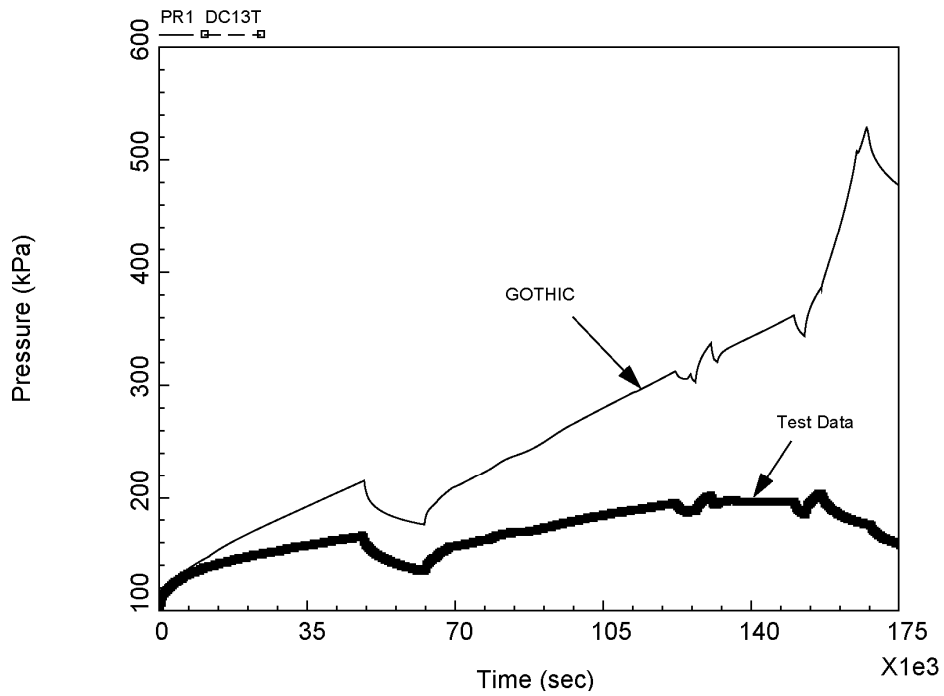
Figure 6-65—HDR Test E11.4 Single-Volume Interior Containment Room Pressure
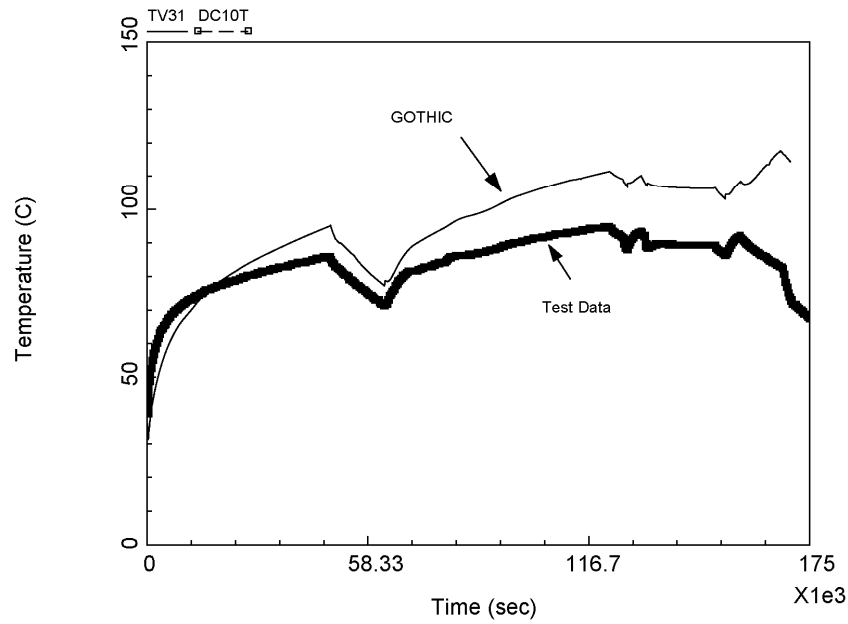
Figure 6-66—HDR Test E11.4 Multi-Volume Interior Containment Room Temperature
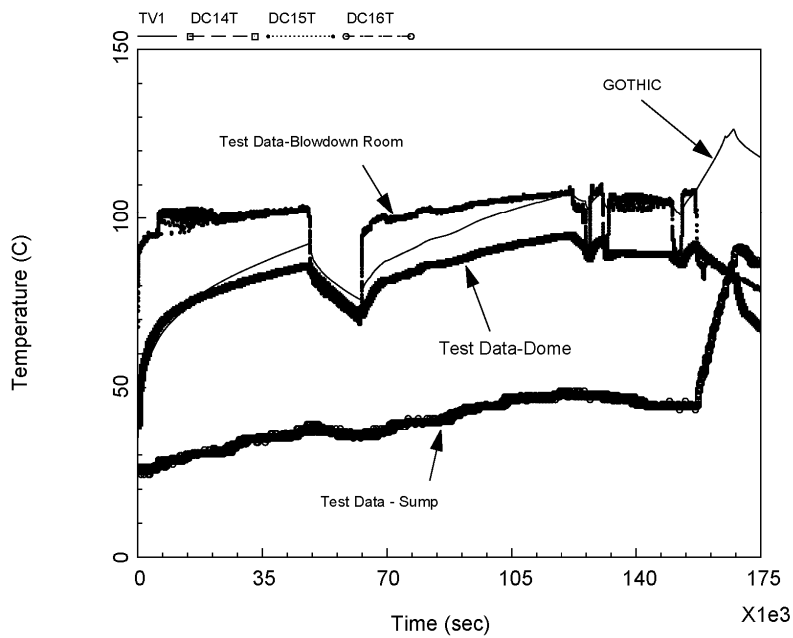
Figure 6-67—HDR Test E11.4 Single-Volume Interior Containment Room Temperature

6.2.2   BFMC Tests

The Battelle-Frankfurt Model Containment (BFMC) was constructed to study the thermal-hydraulic response of a containment system during accident conditions and to generate test data for thermal hydraulic code development and assessment. The BFMC is a multi-room facility in cylindrical geometry, having an outside diameter of 12 m and a height of 12.5 m. The structure is made of steel-reinforced concrete and can withstand pressures to 6 atm. The total volume is about 600 m³, although volume and surface area can be altered by using concrete inserts to change the room configuration and steel plates that block or restrict the openings between rooms.

This flexibility permits a test to be run in a single room or several rooms, and with a variety of geometries and flow paths. Steam is supplied from a pressure vessel in an adjacent building. The pressure vessel can operate up to 140 atm and 300°C and the total volume of the pressure vessel and supply lines is 7 m³. A recirculation system is available to keep the fluid in the supply lines near the condition of the fluid in the vessel. The length of the supply line piping is about 25 m and the pipe diameters are 15 and 20 cm.

The BFMC is easy to model compared to large-scale tests at unfinished or decommissioned reactors, where the rooms, passageways, equipment, and piping make the modeling much more difficult and less certain. For example, in the HDR experiments it is necessary to estimate the loss coefficient for flow through a spiral staircase that connects the upper dome to a room below. In contrast, the BFMC is essentially free of such complex internal fixtures; the rooms and openings between rooms are clearly defined.

The general configuration of the containment is shown in Figure 6-68. The internal room is an open cylinder having discrete diameters over different axial sections. The resulting ledges support inserts used to define separate rooms within this region. An annular region surrounding the inner cylindrical room is divided by a floor about midway up the cylinder. This floor and three radial vertical walls in the annulus form boundaries

that define five distinct rooms in this region. The enclosing walls of the containment form a continuous open annular space outside of that shown in the figure. This outer annular space opens to a domed region that surrounds the top of the containment. Openings between rooms are sharply cut circles, rectangles, trapezoids, and annular segments. Concrete inserts can be placed in the central region of the containment to create additional compartments. Steel plates can be added to block both sides of an opening so that the volume inside the blocked passage within the opening does not participate in the test.

The BFMC and U.S. EPR containment buildings both consist of a cylindrical configuration with multiple volumes, internal flow patterns, and no containment spray. The BFMC has a high surface area-to-volume ratio. The U.S. EPR containment also has a high surface area-to-volume ratio because of its substantial wall, grating, and equipment surface area. Both the BFMC and U.S. EPR are dry, non-suppression pool-type containments. The U.S. EPR has a pool (the IRWST) at the bottom of the central containment region, as does the BFMC containment.

AREVA NP has performed benchmark calculations against the BFMC test data with both single-volume and multi-volume GOTHIC models. The results are presented in the following sections.

6.2.2.1   BFMC Test 6

BFMC Test 6 (Reference 71) consists of hydrogen injection into a thermally stratified room to evaluate dispersion due to natural effects. The U.S. EPR does not have a safety-related spray system or containment cooling system, but relies on natural convection and diffusion processes for containment cooling. Test 6 evaluates these convection and diffusion phenomena.

The BFMC Test 6 GOTHIC model is shown in Figure 6-69. In this case, the multi-volume model is actually a single-volume with a subdivided volume, and the single-volume model is simply a single-volume without subdivision.

AREVA NP Inc.   ANP-10299NP
Applicability of AREVA NP Containment Response Evaluation Methodology to the   Revision 2
U.S. EPR™ for Large Break LOCA Analysis
Technical Report   Page 6-86

The available Test 6 data are limited to hydrogen pressure ratios and volume fractions. The benchmark for the containment hydrogen pressure ratio in Room 1 of the single-volume GOTHIC model and the multi-volume GOTHIC model are shown in Figure 6-70, along with the BFMC test data. The multi-volume GOTHIC model provides good agreement with the test data. The single-volume GOTHIC model provides very limited information and, as expected, is not applicable if combustible gas concentration is a concern.
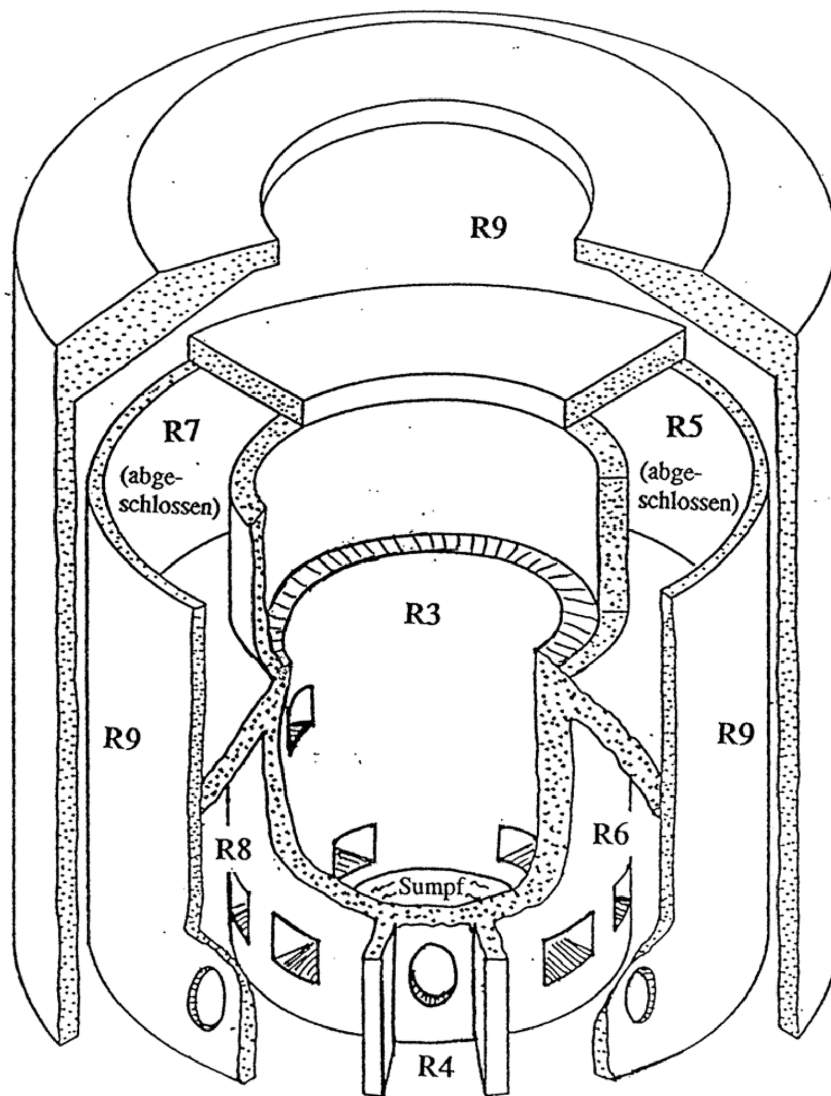
Figure 6-68—BFMC Configuration Cutaway

Figure 6-69—BFMC Test 6 Subdivided Volume GOTHIC Model
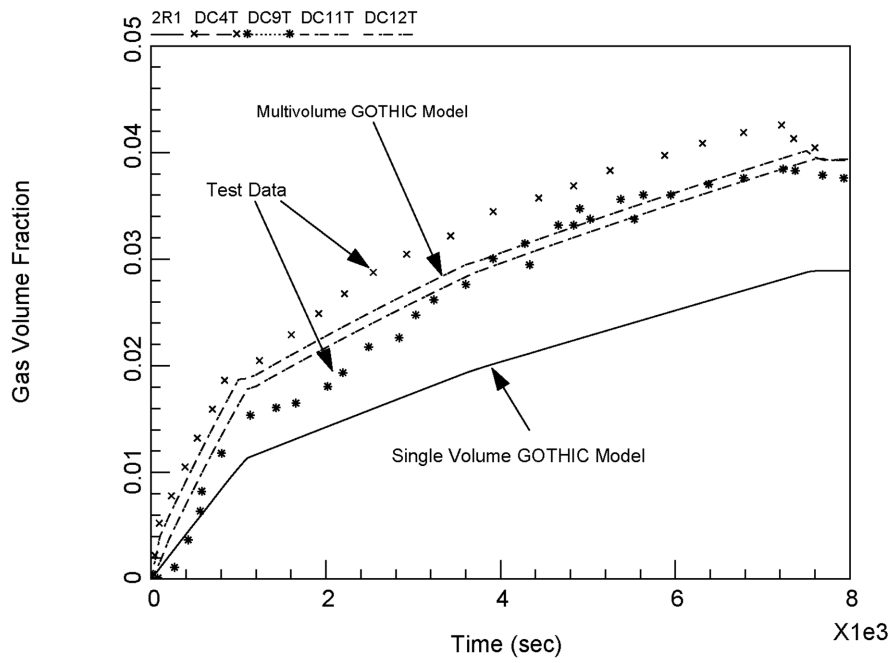
Figure 6-70—BFMC Test 6 Pressure Ratio

6.2.2.2   BFMC Test 12

BFMC Test 12 (Reference 71) involved hydrogen injection into a room connected to several other rooms, all of them isothermal. The hydrogen disperses into the other rooms via natural convection and diffusion. Test 12 is applicable to the U.S. EPR because it did not have a spray system or containment cooling system. Like the U.S. EPR, it relied on natural convection and diffusion processes for containment cooling.

The BFMC Test 12 GOTHIC multi-volume model and the subdivided volume in the model are shown in Figure 6-71 and Figure 6-72, respectively.   (Because the single-volume model for this test is simple, it is not presented in a figure; this is the case for all the BFMC tests that follow.)

The available Test 12 data are limited to hydrogen pressure ratios and volume fractions. The containment hydrogen pressure ratio benchmark calculations for the single-volume GOTHIC model and the multi-volume GOTHIC model are shown in Figure 6-73, along with the BFMC test data. Both the multi-volume and single-volume GOTHIC models produced results that agreed well with the test data over the entire benchmark.

Figure 6-71—BFMC Test 12 Multi-Volume GOTHIC Model

Figure 6-72—BFMC Test 12 Subdivided Volume
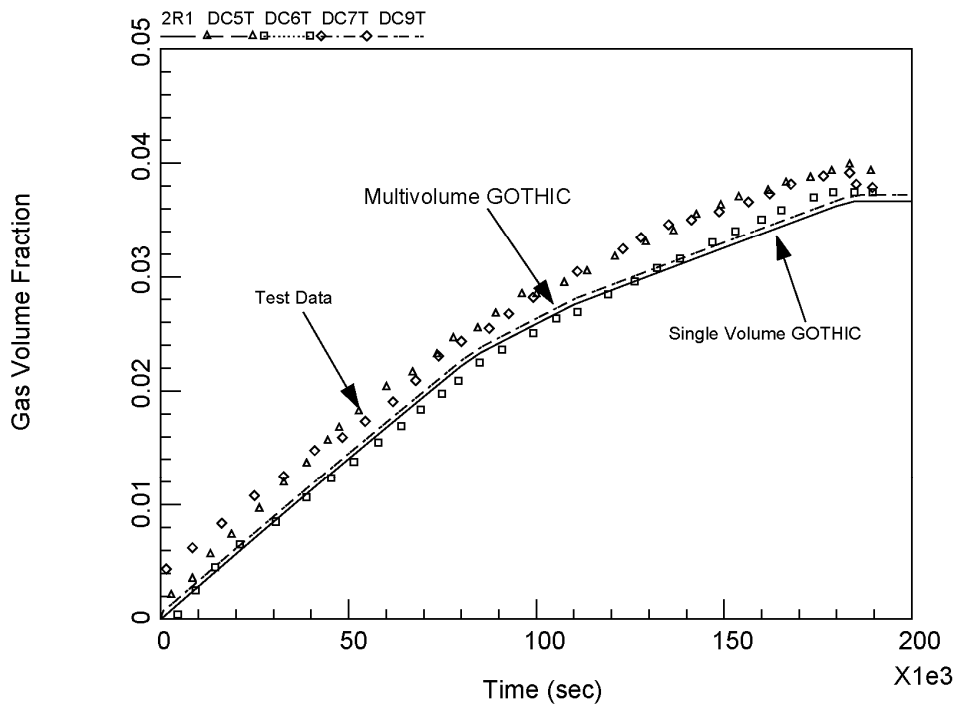
Figure 6-73—BFMC Test 12 Pressure Ratio

6.2.2.3   *BFMC Test c13*

BFMC Test c13 (Reference 72) was a steam and water blowdown into the compartmentalized BFMC test building, which is analogous to a postulated LOCA in a compartmentalized U.S. EPR containment. Water in the pressure vessel was initially at a pressure of 140 bar and a temperature of 295°C. Initial containment pressure was 1 bar. For test c13, initial temperatures ranged between 10°C – 50°C. The BFMC Test c13 GOTHIC multi-volume model is shown in Figure 6-74.

Figure 6-75 shows the benchmark calculations of containment pressure for the single-volume and multi-volume GOTHIC models, along with the BFMC test data. The figure demonstrates that after the initial portion of the event, the single-volume GOTHIC model produces pressures greater than the test data and greater than the calculated pressures produced by the multi-volume GOTHIC model.

The containment temperature benchmark calculation for the single-volume and multi-volume GOTHIC models are shown in Figure 6-76, along with the BFMC test data. For BFMC Test c13, the single-volume GOTHIC model calculated temperatures lower than both the test data and the multi-volume GOTHIC model.
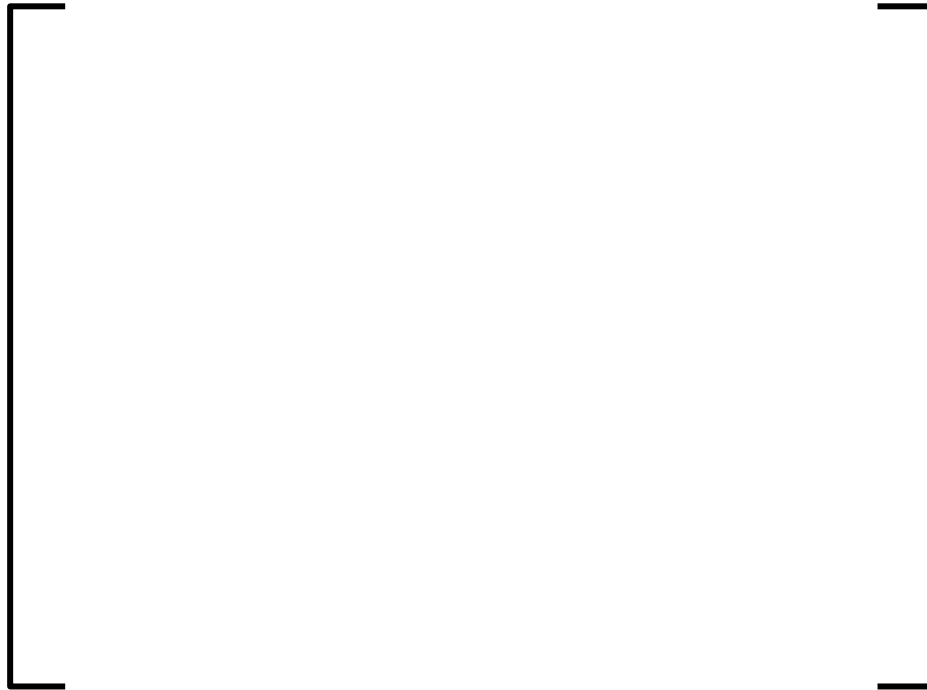
Figure 6-74—BFMC Test c13 Multi-Volume GOTHIC Model
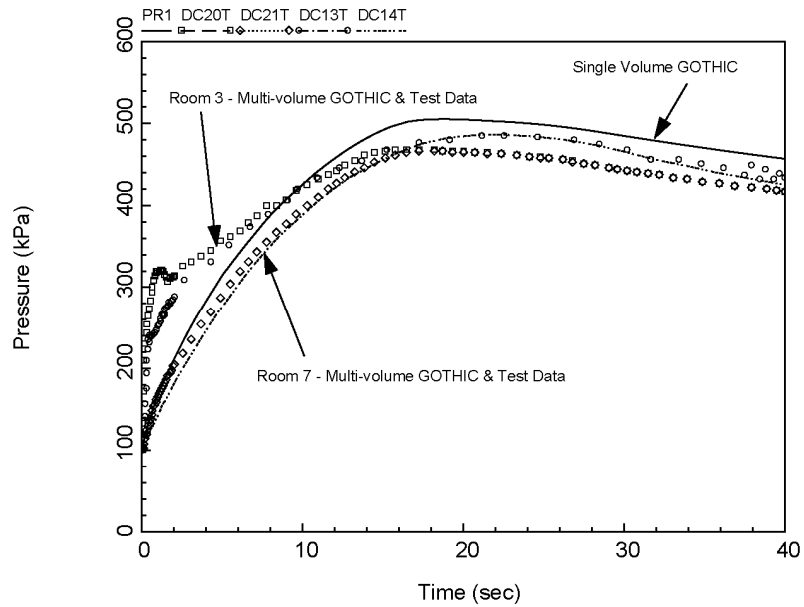
Figure 6-75—BFMC Test c13 Pressure
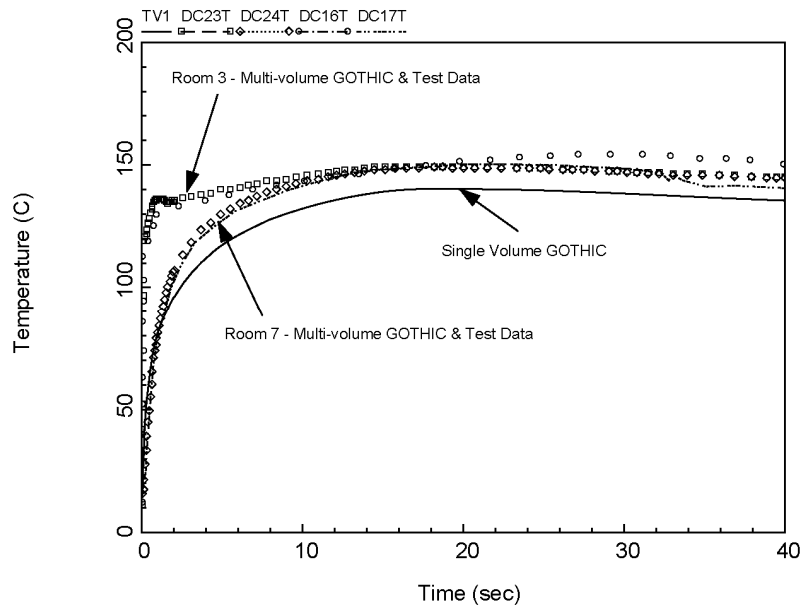
Figure 6-76—BFMC Test c13 Temperature

6.2.2.4   BFMC Test c15

BFMC Test c15 (Reference 73) was a steam and water blowdown into the compartmentalized BFMC test building Tests c13 and c15 are very similar. For test c15, the initial temperatures ranged from 20°C – 68°C. The BFMC Test c15 GOTHIC multi-volume model is shown in Figure 6-77.

The containment pressure benchmark calculations for the single-volume and multi-volume GOTHIC models are shown in Figure 6-78, along with the BFMC test data. The figure shows that after the initial portion of the event, the single-volume GOTHIC model calculates pressures greater than both the test data and the multi-volume GOTHIC model.

Figure 6-79 shows the containment temperature benchmark calculations for the single-volume GOTHIC model, the multi-volume GOTHIC model, and the Test c15 data. The figure shows that the single-volume GOTHIC model produced temperatures lower than both the test data and the multi-volume GOTHIC model.

Figure 6-77—BFMC Test c15 Multi-Volume GOTHIC Model
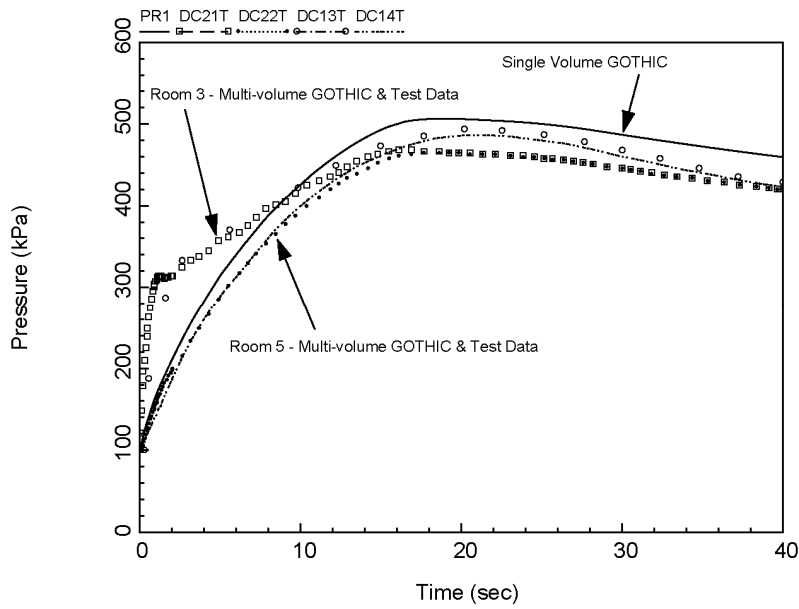
Figure 6-78—BFMC Test c15 Pressure
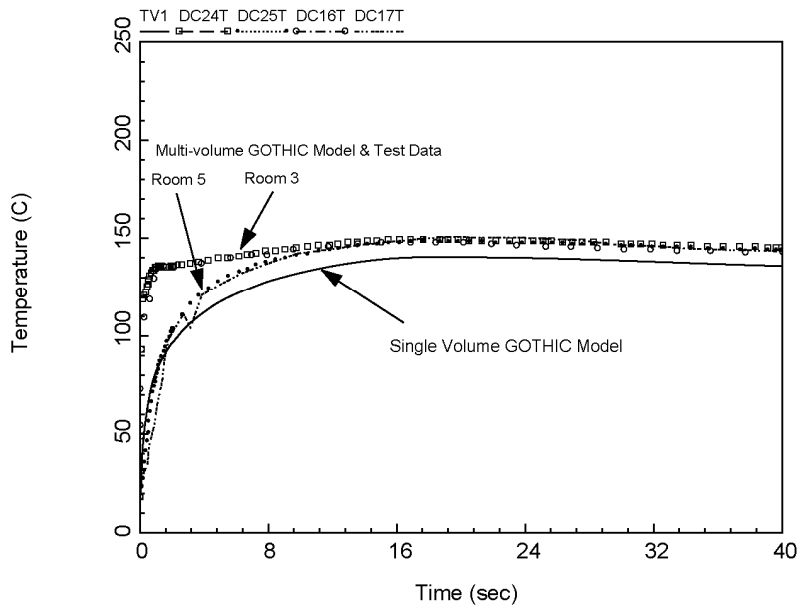
Figure 6-79—BFMC Test c15 Temperature

6.2.2.5   BFMC Test d16

BFMC Test d16 (Reference 74) was a hot water injection over 50 seconds into a single room. As the water flashes, the resulting steam distributes via openings into the other five rooms used in this test. The test simulates a postulated LOCA blowdown of short duration, coupled with natural circulation of steam throughout a U.S. EPR containment. The multi-volume GOTHIC model for BFMC Test d16 is shown in Figure 6-80.

The containment pressure benchmark calculations for the single-volume and multi-volume GOTHIC models are shown in Figure 6-81, along with the BFMC test data. The figure shows that after the initial portion of the event, the single-volume GOTHIC model calculates pressures greater than both the test data and greater than the multi-volume GOTHIC model.

The containment temperature benchmark calculations for the single-volume and the multi-volume GOTHIC models are shown in Figure 6-82, along with the BFMC test data. The figure shows that both the single-volume and multi-volume GOTHIC models produced temperatures within the test data span for most of this short-term event.

Figure 6-80—BFMC Test d16 Multi-Volume GOTHIC Model
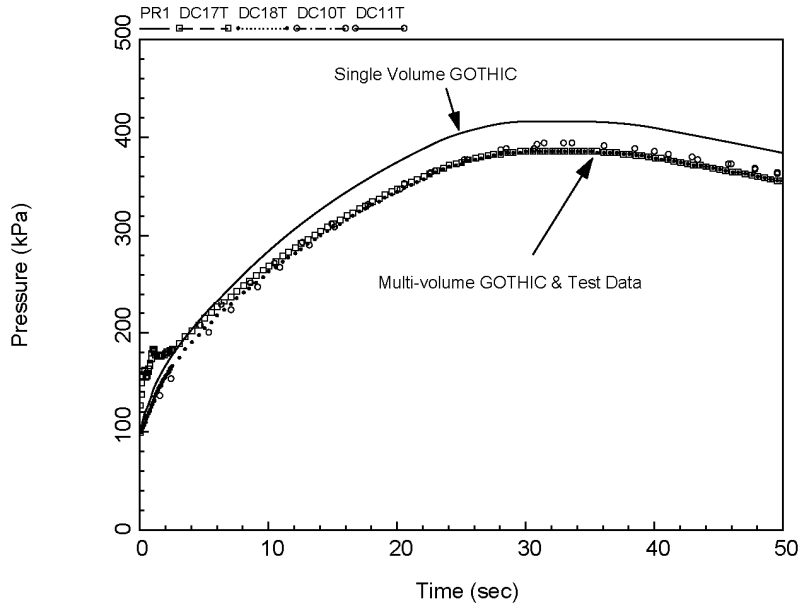
Figure 6-81—BFMC Test d16 Pressure
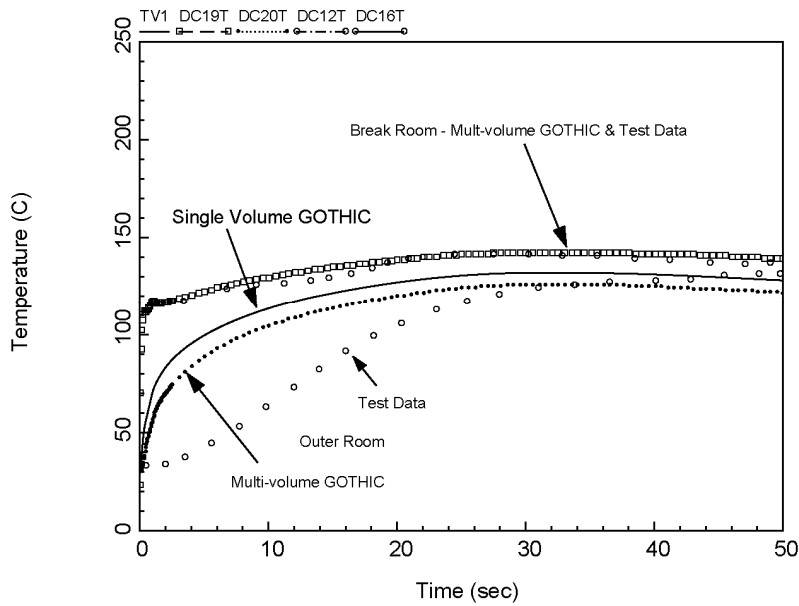
Figure 6-82—BFMC Test d16 Temperature

6.2.2.6   BFMC Biblis Test RX4

The BFMC Biblis Rx series of tests (Reference 75) examined natural circulation and hydrogen distribution produced by a heated sump pool. For Test Rx4, heated vapor rose from the pool region into the dome area of Region 9 (shown in Figure 6-68). The rising vapor was than cooled and condensed via the physical structures in the dome region, causing the flow of cooler vapor into the annular portion of Region 9. The cooler flow then passed through the vent openings into Regions 6 and 8 and then through the inner vent openings back into the vapor space above the sump pool.

Figure 6-83 shows the multi-volume GOTHIC model for the BFMC Biblis Test Rx4. Figures Figure 6-84 through Figure 6-90 compare the multi-volume model to the test data. Figure 6-84, showing the sump liquid temperature, demonstrates that the sump temperature control system in the GOTHIC model reproduces the test sump pool temperatures exactly. Figure 6-85 through Figure 6-90 show the vapor temperature at various elevations. They show that the GOTHIC temperature predictions are generally equal to or slightly higher than the test data.

The figures of vent flow velocity, Figure 6-91 through Figure 6-93, show that the GOTHIC model prediction for vent U49A matches the test results. For vents U69 and U89, the GOTHIC prediction is slightly lower than the test data at low flow rates, but matches the data at higher flow rates.

The GOTHIC predictions for humidity, Figure 6-94 through Figure 6-96, also compare well with the test data. For the dome and annulus regions, the GOTHIC predictions are very close to the test data. For Region 1–3, the GOTHIC prediction is also close to the test data. Note that the test data show a long-term humidity greater than 100%. Figure 6-97 shows that the GOTHIC containment pressure prediction falls in the lower range of the test data.

Figure 6-98 through Figure 6-101 provide the GOTHIC single-volume model results for Test Rx4. The single-volume GOTHIC model significantly over-predicted the

containment vapor temperatures and humidity, and the containment pressure prediction was higher than the multi-volume GOTHIC model results.
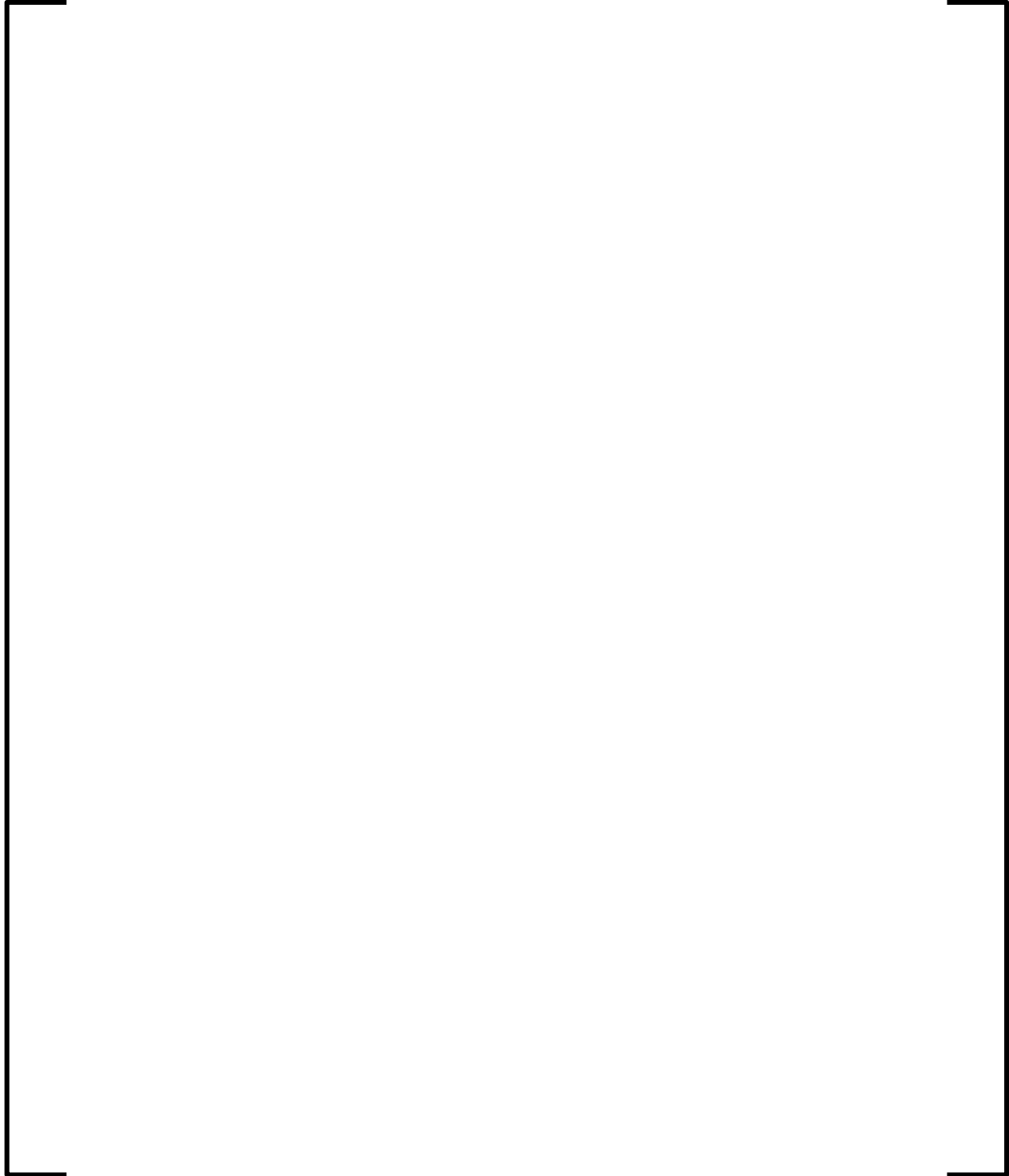
Figure 6-83—BFMC Biblis Test Rx4 Multi-Volume GOTHIC Model

AREVA NP Inc.

ANP-10299NP

Applicability of AREVA NP Containment Response Evaluation Methodology to the

Revision 2

U.S. EPR™ for Large Break LOCA Analysis

Technical Report

Page 6-99

Figure 6-84—BFMC Biblis Test Rx4 Multi-Volume Sump Pool Temperature

Figure 6-85—BFMC Biblis Test Rx4 Multi-Volume Sump Vapor Temperature

Figure 6-86—BFMC Biblis Test Rx4 Multi-Volume Middle Region 1-3 Temperature

Figure 6-87—BFMC Biblis Test Rx4 Multi-Volume Upper Region 1-3 Vapor

Temperature

AREVA NP Inc.
Applicability of AREVA NP Containment Response Evaluation Methodology to the
U.S. EPR™ for Large Break LOCA Analysis
Technical Report

ANP-10299NP
Revision 2

Page 6-101

Figure 6-88—BFMC Biblis Test Rx4 Multi-Volume Dome Vapor Temperature

Figure 6-89—BFMC Biblis Test Rx4 Multi-Volume Upper Annulus Vapor

Temperature

AREVA NP Inc.
ANP-10299NP
Applicability of AREVA NP Containment Response Evaluation Methodology to the
Revision 2
U.S. EPR™ for Large Break LOCA Analysis
Technical Report
Page 6-102

Figure 6-90—BFMC Biblis Test Rx4 Multi-Volume Lower Annulus Vapor Temperature

Figure 6-91—BFMC Biblis Test Rx4 Multi-Volume Vent U49A Flow Velocity

AREVA NP Inc.

Applicability of AREVA NP Containment Response Evaluation Methodology to the
U.S. EPR™ for Large Break LOCA Analysis
Technical Report

ANP-10299NP
Revision 2

Page 6-103

Figure 6-92—BFMC Biblis Test Rx4 Multi-Volume Vent U69 Flow Velocity

Figure 6-93—BFMC Biblis Test Rx4 Multi-Volume Vent U89 Flow Velocity

AREVA NP Inc.

ANP-10299NP

Applicability of AREVA NP Containment Response Evaluation Methodology to the

Revision 2

U.S. EPR™ for Large Break LOCA Analysis

Technical Report

Page 6-104

Figure 6-94—BFMC Biblis Test Rx4 Multi-Volume Middle Region 1-3 Humidity

Figure 6-95—BFMC Biblis Test Rx4 Multi-Volume Dome Humidity

Figure 6-96—BFMC Biblis Test Rx4 Multi-Volume Annulus Humidity

Figure 6-97—BFMC Biblis Test Rx4 Multi-Volume Containment Pressure

Figure 6-98—BFMC Biblis Test Rx4 Single-Volume Sump Pool Temperature

Figure 6-99—BFMC Biblis Test Rx4 Single-Volume Temperatures

Figure 6-100—BFMC Biblis Test Rx4 Single-Volume Humidity

Figure 6-101—BFMC Biblis Test Rx4 Single-Volume Pressure

6.2.2.7   BFMC Biblis Test Rx2

Like Test Rx4, Test Rx2 was also a test of natural circulation and hydrogen distribution produced by a heated sump pool. For Test Rx2, heated vapor rose from the pool region into the dome area of Region 9 (shown in Figure 6-68). The rising vapor was cooled by the structures in the dome region, causing cooler vapor to flow into the annular portion of Region 9. The cooler flow then passed through the vent openings into Regions 6 and 8 and then through the inner vent openings back into the vapor space above the sump pool.

Figure 6-102 shows the GOTHIC multi-volume model for benchmarking BFMC Biblis Rx2.   Figure 6-103 through Figure 6-109 compare the GOTHIC multi-volume model results to the test data. Figure 6-103, showing the sump liquid temperature, demonstrates that the sump temperature control system in the GOTHIC model reproduced the test sump pool temperatures exactly. Figure 6-104 through Figure 6-109 show the vapor temperature at various elevations. They show that the GOTHIC predictions are generally equal to or slightly higher than the test data. In some regions, the GOTHIC temperature predictions are slightly lower than the test data during the initial portion of the test.

The GOTHIC predictions for vent flow velocity, Figure 6-110 through Figure 6-112, are slightly higher than or equal to the test data. During Test Rx2, the vent velocity meters required a minimum critical or "start-up" velocity before flow was measured. As a result, flow data were not recorded for the vents during the early portions of the test.

Figure 6-113 through Figure 6-115 demonstrate that the GOTHIC model slightly under-predicts the humidity early in the test, and matches or slightly exceeds the test data for the later portions of the test.

Figure 6-116 shows that the Test Rx2 containment pressure test data exhibits a significant step-change at approximately 3500 seconds. This change seems to indicate a sudden change in the amount of seal leakage around the containment cap, i.e., a

partial seal failure. This phenomenon is not discussed in any of the BFMC Biblis test documentation, so no attempt was made to duplicate this phenomenon in the GOTHIC benchmark calculations.

Figure 6-117 through Figure 6-120 provide the single-volume GOTHIC model results for Test Rx2. The single-volume GOTHIC model significantly over-predicts the containment vapor temperatures and humidity. The single-volume containment pressure prediction was higher than that obtained with the multi-volume GOTHIC model.
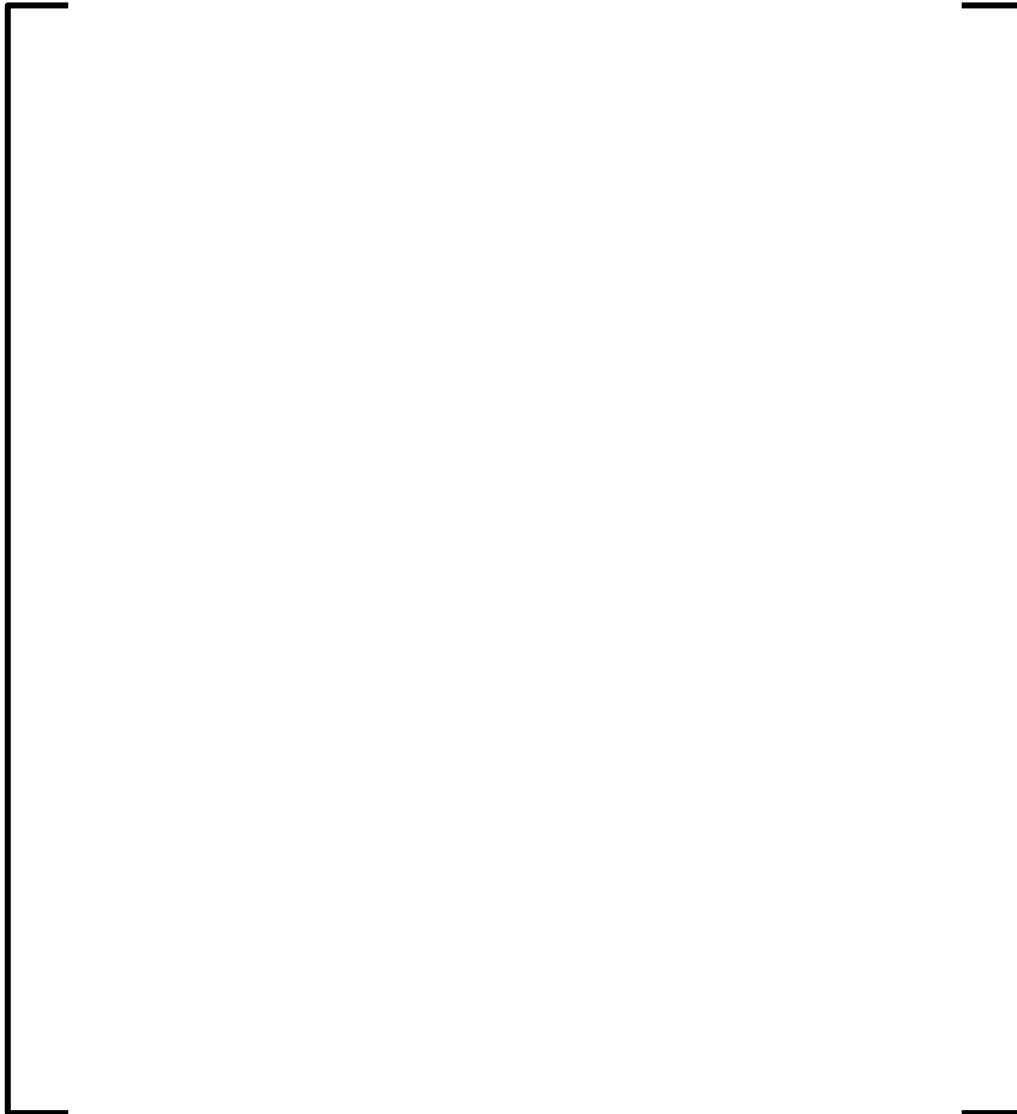
Figure 6-102—BFMC Biblis Test Rx2 Multi-Volume GOTHIC Model

Figure 6-103—BFMC Biblis Test Rx2 Multi-Volume Sump Pool Temperature

Figure 6-104—BFMC Biblis Test Rx2 Multi-Volume Sump Vapor Temperature

Figure 6-105—BFMC Biblis Test Rx2 Multi-Volume Middle Region 1-3 Vapor Temperature

Figure 6-106—BFMC Biblis Test Rx2 Multi-Volume Upper Region 1-3 Vapor Temperature

Figure 6-107—BFMC Biblis Test Rx2 Multi-Volume Dome Vapor Temperature

Figure 6-108—BFMC Biblis Test Rx2 Multi-Volume Upper Annulus Vapor Temperature

Figure 6-109—BFMC Biblis Test Rx2 Multi-Volume Lower Annulus Vapor Temperature

Figure 6-110—BFMC Biblis Test Rx2 Multi-Volume Vent U49A Flow Velocity

Figure 6-111—BFMC Biblis Test Rx2 Multi-Volume Vent U69 Flow Velocity

Figure 6-112—BFMC Biblis Test Rx2 Multi-Volume Vent U89 Flow Velocity

Figure 6-113—BFMC Biblis Test Rx2 Multi-Volume Middle Region 1-3 Humidity

Figure 6-114—BFMC Biblis Test Rx2 Multi-Volume Dome Humidity

AREVA NP Inc.

ANP-10299NP

Applicability of AREVA NP Containment Response Evaluation Methodology to the

Revision 2

U.S. EPR™ for Large Break LOCA Analysis

Technical Report

Page 6-116

Figure 6-115—BFMC Biblis Test Rx2 Multi-Volume Annulus Humidity

Figure 6-116—BFMC Biblis Test Rx2 Multi-Volume Containment Pressure

Figure 6-117—BFMC Biblis Test Rx2 Single-Volume Sump Pool Temperature

Figure 6-118—BFMC Biblis Test Rx2 Single-Volume Temperature

Figure 6-119—BFMC Biblis Test Rx2 Single-Volume Humidity
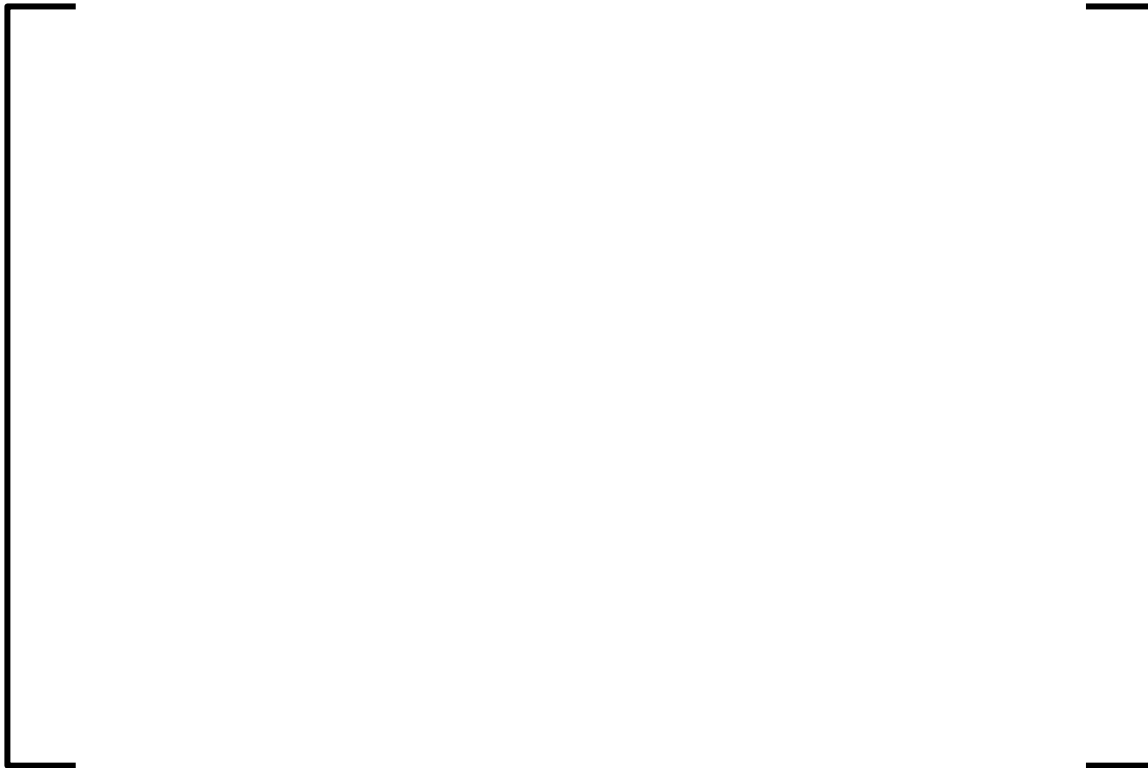
Figure 6-120—BFMC—Biblis Test Rx2 Single-Volume Containment Pressure

6.2.2.8   BFMC Test 20

BFMC Test 20 (Reference 99) involved hydrogen injection into a room that is connected to several other rooms. Substantial vertical stratification existed throughout the experimental facility. The hydrogen dispersed into the other rooms via natural convection and diffusion. Test 20 is applicable to the U.S. EPR because it did not have a spray system or containment forced ventilation system. Like the U.S. EPR, Test 20 relied on natural convection and diffusion processes for containment cooling.

The BFMC Test 20 GOTHIC model is based on the Test 12 model and differs from it only with its extensive use of subdivision, which is necessary to calculate the very non-uniform hydrogen concentrations caused by non-symmetric, stratified temperatures. In the GOTHIC model for Test 20, volumes are subdivided so that volume aspect ratios and lengths between openings are more appropriately defined than possible with a lumped parameter model. Figure 6-121 shows this volume subdivision. On the left of the figure, an elevation view of the subdivided volumes showing the annular rooms unfolded from the interior. Openings from the interior to circumferential regions in the annular rooms are modeled by appropriately defined junctions, which are shown schematically. The plan view on the right of Figure 6-121 provides an additional perspective for evaluating how the cylindrical geometry is modeled with a rectangular grid.

The available Test 20 data are limited to hydrogen pressure ratios and volume fractions. Figure 6-122 through Figure 6-124 compare GOTHIC predictions to measured hydrogen concentration for BFMC Test 20. Excluding results for R6, the room into which hydrogen is injected, the GOTHIC model reasonably predicts hydrogen concentrations.

Figure 6-121—Computational Grid and Junctions for BFMC Test 20 GOTHIC Model
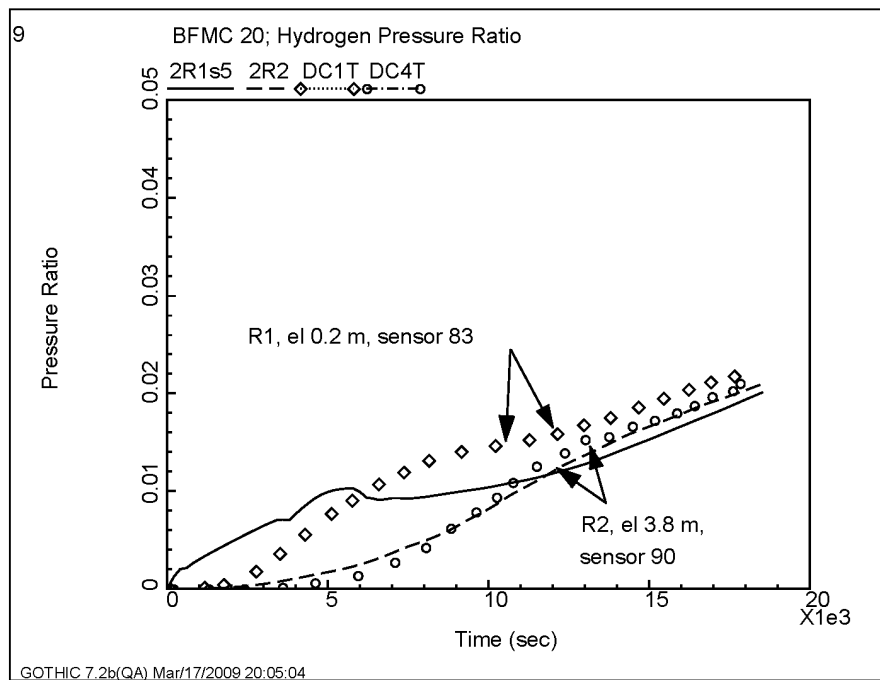
Figure 6-122—Hydrogen Concentration in Rooms R1 and R2 during BFMC Test 20
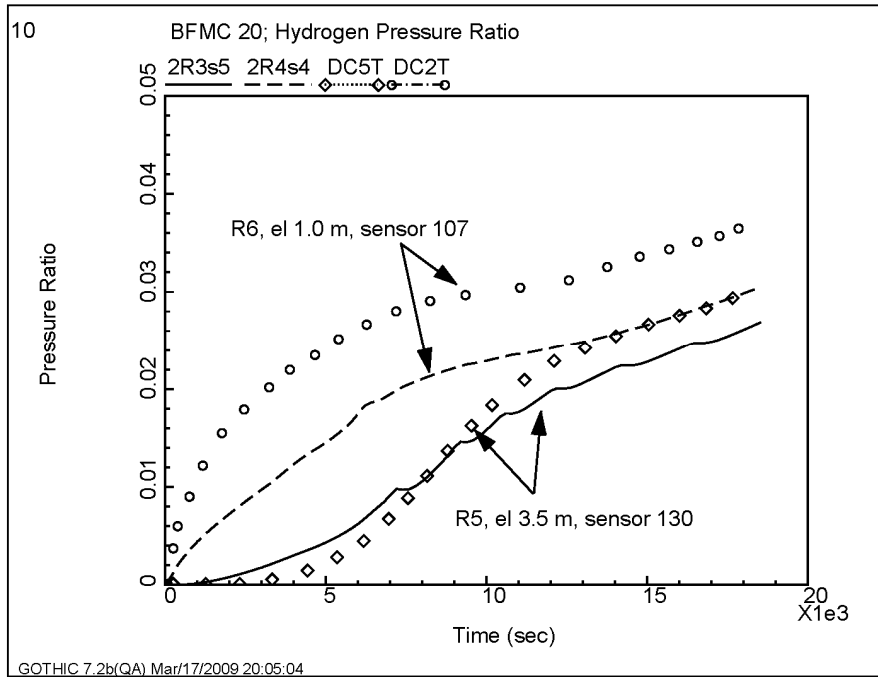
Figure 6-123—Hydrogen Concentration in Rooms R5 and R6 during BFMC Test 20
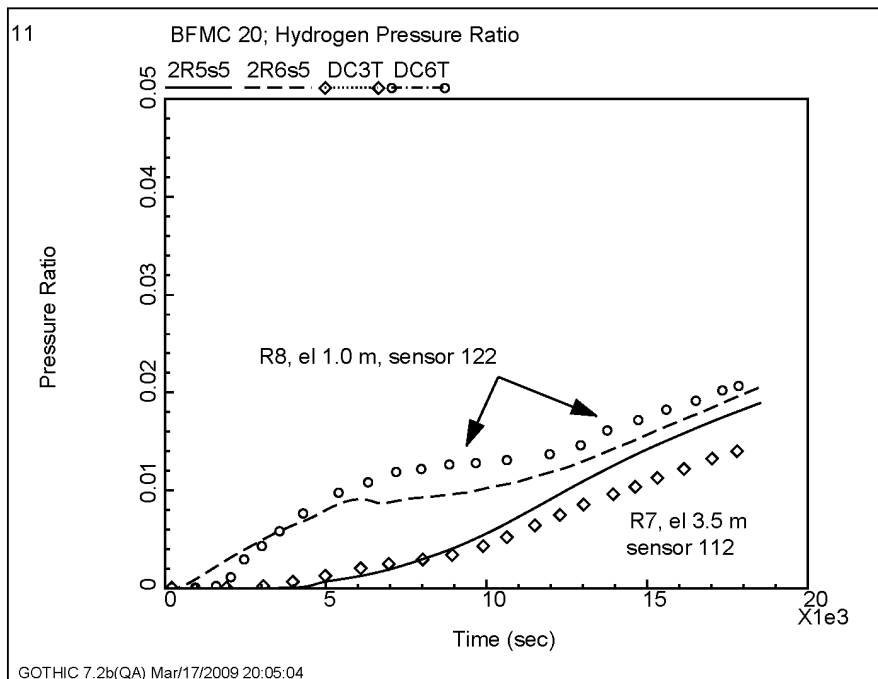
Figure 6-124—Hydrogen Concentration in Rooms R7 and R8 during BFMC Test 20

6.2.3   NUPEC Tests

The Nuclear Power Engineering Corporation (NUPEC) facility is a 1/4-scale model of a PWR dry containment. The facility's containment vessel is comprised of various compartments, structures, hydraulic connections, a spray system, and a diffuser for steam-gas injection.

The containment vessel is an insulated, steel cylinder with a spherical head as shown in Figure 6-125. The inside diameter of the containment vessel is 10.8 m. The overall height, including the drain tank, is almost 20 m. The free volume is approximately 1300 m^3, and does not include the drain tank (which is full of water).

Above the drain tank, the containment is divided into three floors and partitioned into several compartments to simulate a PWR containment, as shown in Figure 6-126, which also displays many of the openings between compartments. The compartment numbers correspond to those used in Reference 100 to summarize information about the facility. On the first and second levels the internal walls extend the full height, from floor to ceiling. On the third floor, compartments simulate the steam generator chimneys and the pressurizer.

Except for the lower section of the pressurizer (compartment 16 in Figure 6-126), the compartments have good hydraulic communication. That is, each compartment has several openings to adjacent compartments. The test report (Reference 100) describes 66 flow paths that allow fluid flow between compartments. The lower section of the pressurizer is a dead-end compartment, having only a single opening to compartment 22.

As described in Reference 31, the GOTHIC model of this facility consists of three subdivided control volumes, including the dome and several lumped parameter control volumes. Condensation heat transfer on the modeled conductors was calculated using the DLM-FM option. The results of benchmark calculations performed against NUPEC test data are presented in the following sections.
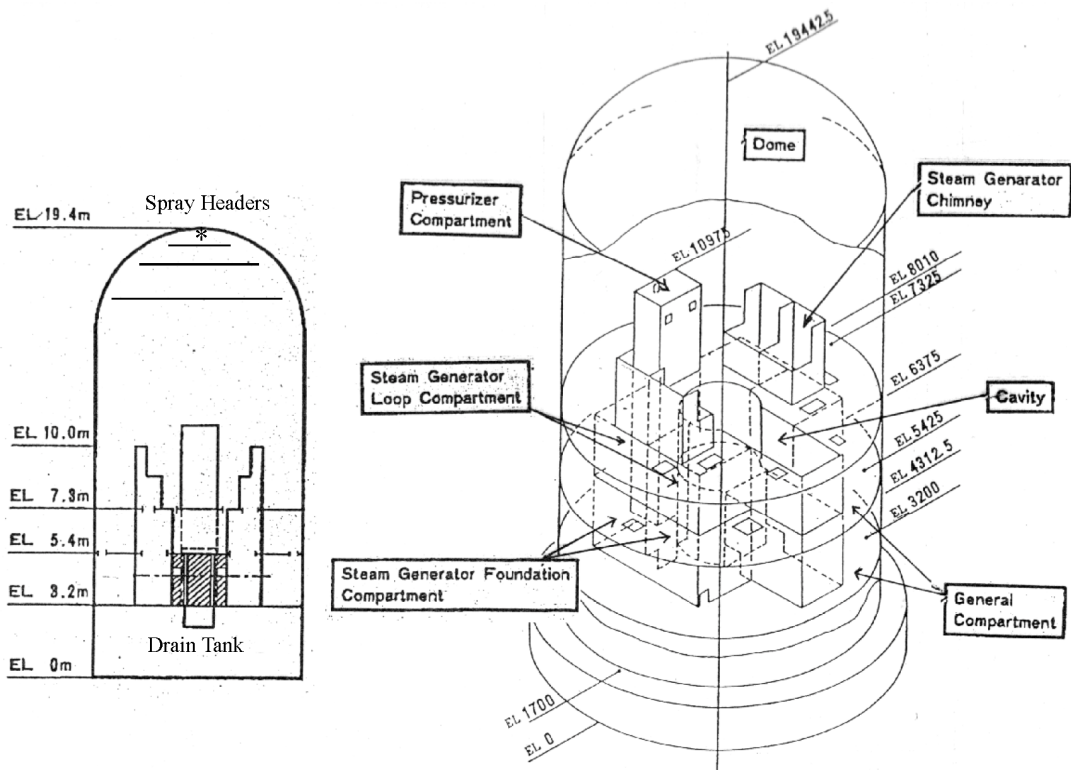
Figure 6-125—NUPEC Containment Vessel Configuration

AREVA NP Inc.   ANP-10299NP
Applicability of AREVA NP Containment Response Evaluation Methodology to the   Revision 2
U.S. EPR™ for Large Break LOCA Analysis
Technical Report   Page 6-124
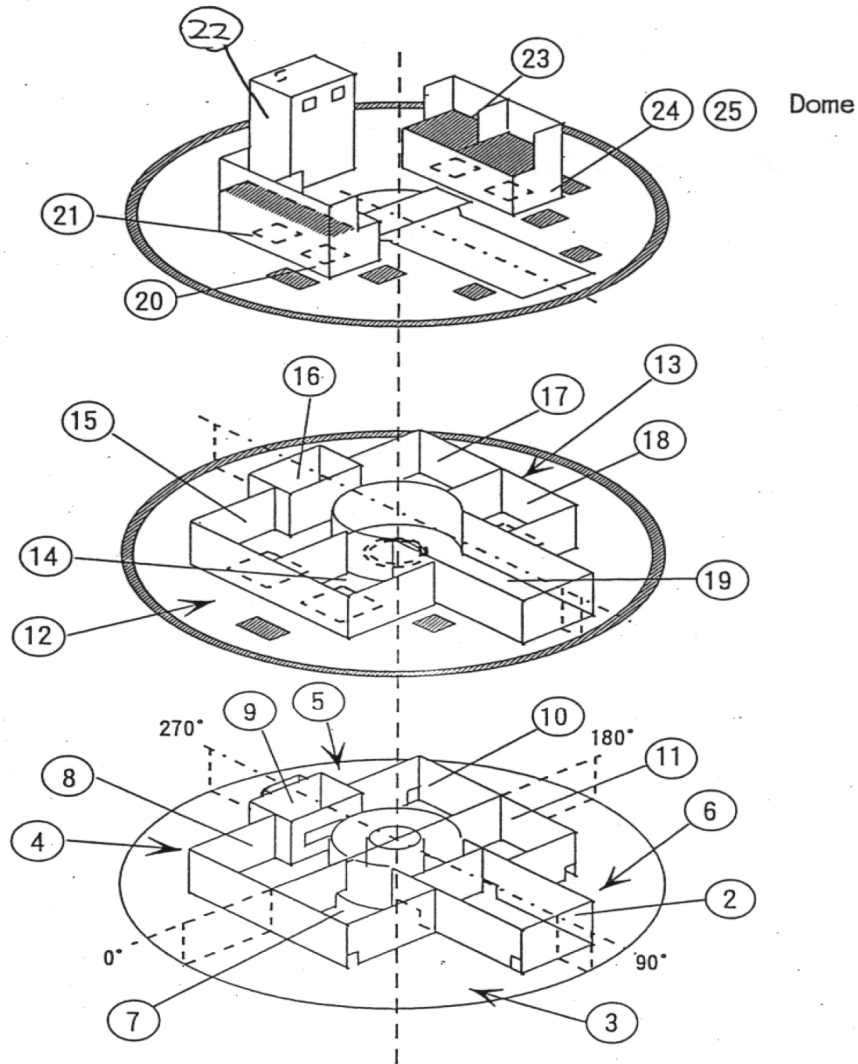
Figure 6-126—NUPEC Containment Compartments and Openings

6.2.3.1   NUPEC TEST M-4-3

NUPEC Test M-4-3 consisted of a steam-helium release into a containment vessel that was not pre-heated. During the test the spray system was not activated. The steam and helium injection rates were constant during the initial 30 minutes of the test, after which the injection was terminated.

Calculated pressure is compared to data for test M-4-3 in Figure 6-127.   The figure indicates that the amount of gas and steam injected and the amount of condensation were consistent with the data.

Measured and calculated temperatures for test M-4-3 are compared in Figure 6-128. Available temperature profiles for compartments 8, 15, and 21, which were presented on a single graph, did not clearly define which curve applied to which compartment. Therefore, the data are represented in Figure 6-128 as plume data. Although the curve representing the GOTHIC prediction of temperature in the injection compartment exceeds the data, other cells could be found in the subdivided mesh that would bound the data. This is shown in Figure 6-129, where the vectors along the boundaries indicate the influx of the vapor mixture from cooler adjacent compartments, and the temperature contours indicate the steep gradients that exist around the plume. The sensor location is significant where the gradients are on the order of 20°C/m. Despite the lack of a definitive specification of the sensor location, this comparison demonstrates reasonable agreement with the data.

Measured and calculated helium concentration in the injection compartment and in the dome for test M-4-3 are compared in Figure 6-130. Available concentration profiles for compartments 8, 15, and 21, which were presented on a single graph, did not clearly define the sensor locations or which curve applied to which compartment. Therefore, the data are represented in Figure 6-130 as plume data.
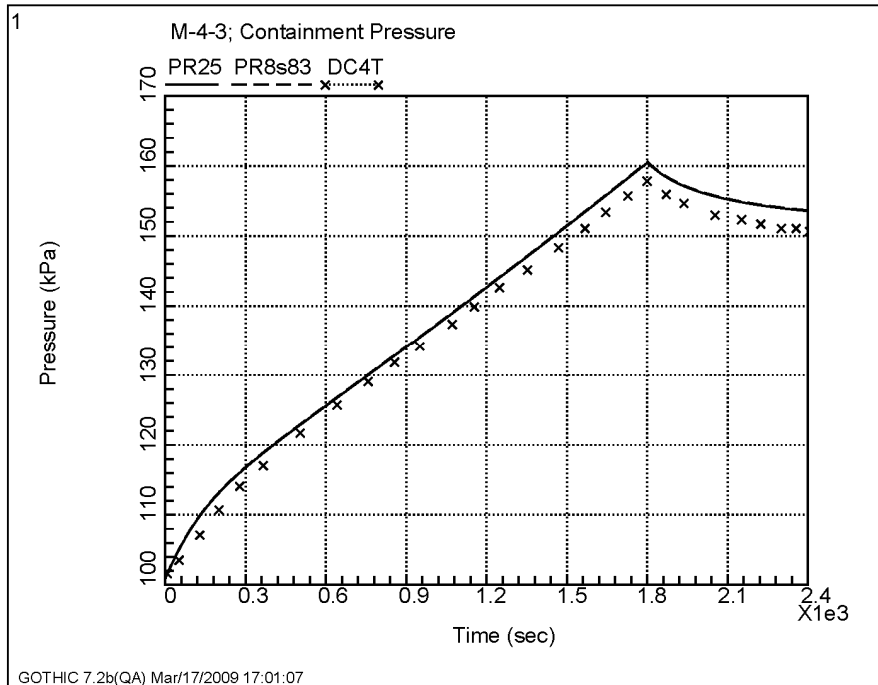
Figure 6-127—Containment Pressure during NUPEC Test M-4-3
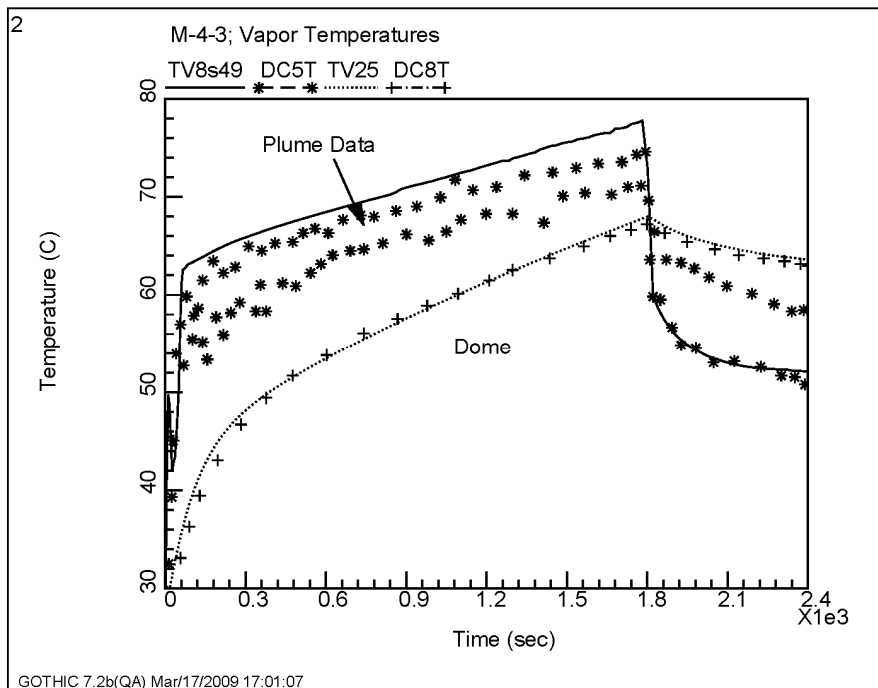
Figure 6-128—Injection Compartment and Dome Vapor Temperatures during

NUPEC Test M-4-3

Scaling Velocity (m/s) = 1
Scaling Power = 1
Time (s) = 901
/ Volume : Cells : Vmax (m/s) /
 / 8 : x(1-5) y(1-7) z(2-2) : 1.07964 /

Minimum = 46 (C)
Maximum = 80 (C)
Time = 901.031 seconds
/ Volume : Cells /
 / 8 : x(1-5) y(1-7) z(2-2)/
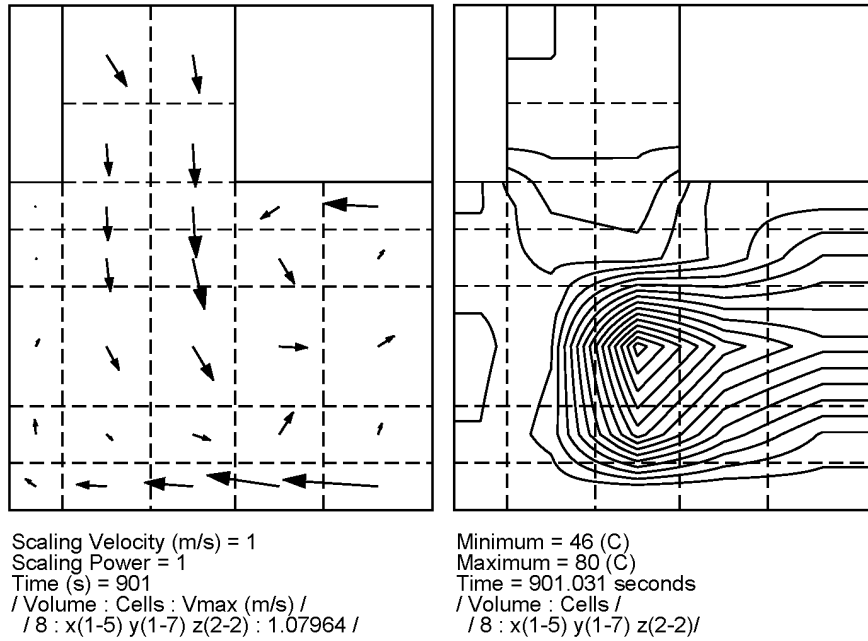
Figure 6-129—Flow Pattern and Temperature Contours in the Injection Compartment during NUPEC Test M-4-3
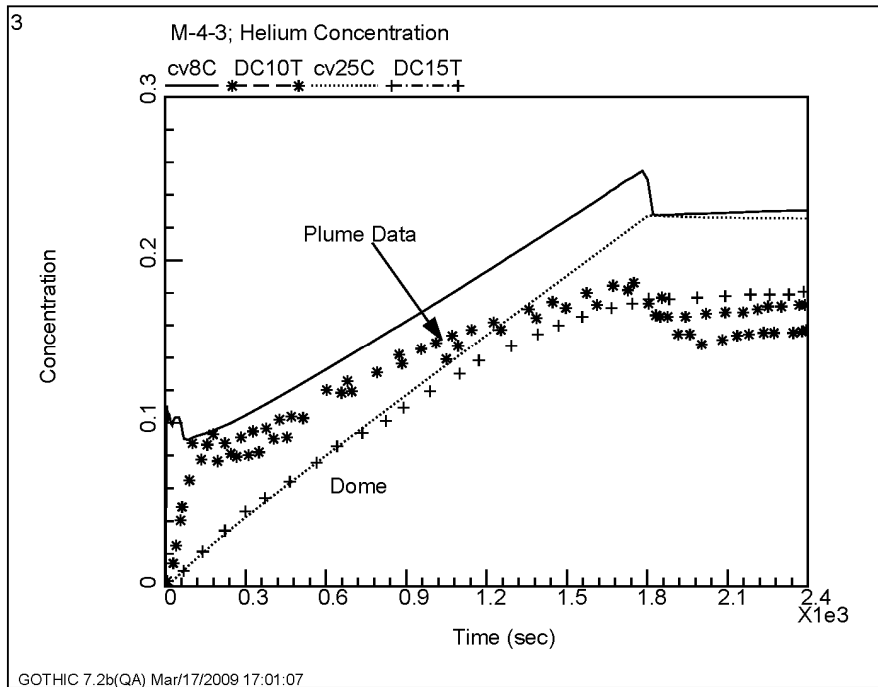
Figure 6-130—Injection Compartment and Dome Helium Concentration during NUPEC Test M-4-3

AREVA NP Inc.
Applicability of AREVA NP Containment Response Evaluation Methodology to the
U.S. EPR™ for Large Break LOCA Analysis
Technical Report

ANP-10299NP
Revision 2

Page 6-128

6.2.3.2 NUPEC TEST M-8-1

NUPEC Test M-8-1 is identical to test M-4-3, with the exception of the location of the steam-helium release.

Calculated pressure is compared to data for test M-8-1 in Figure 6-131. The figure indicates that the amount of gas and steam injected and the amount of condensation were consistent with the data.

Measured and calculated temperatures and helium concentrations for test M-8-1 are compared in Figure 6-132 and Figure 6-133, respectively. Available temperature profiles for compartments 8, 15, and 21, which were presented on a single graph, did not clearly define the sensor locations or which curve applied to which compartment. Therefore, the data are represented in Figure 6-132 as plume data. Likewise, the helium concentration data in Figure 6-133 is also presented as plume data. In general, the GOTHIC model demonstrates the ability to model mixing behavior while producing conservative temperature and pressure results.
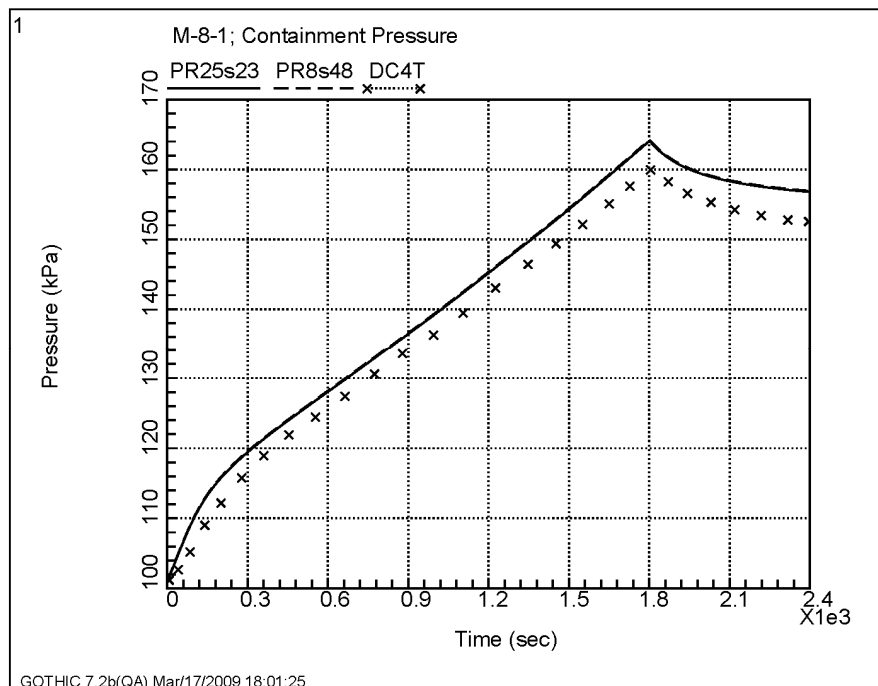
Figure 6-131—Containment Pressure during NUPEC Test M-8-1
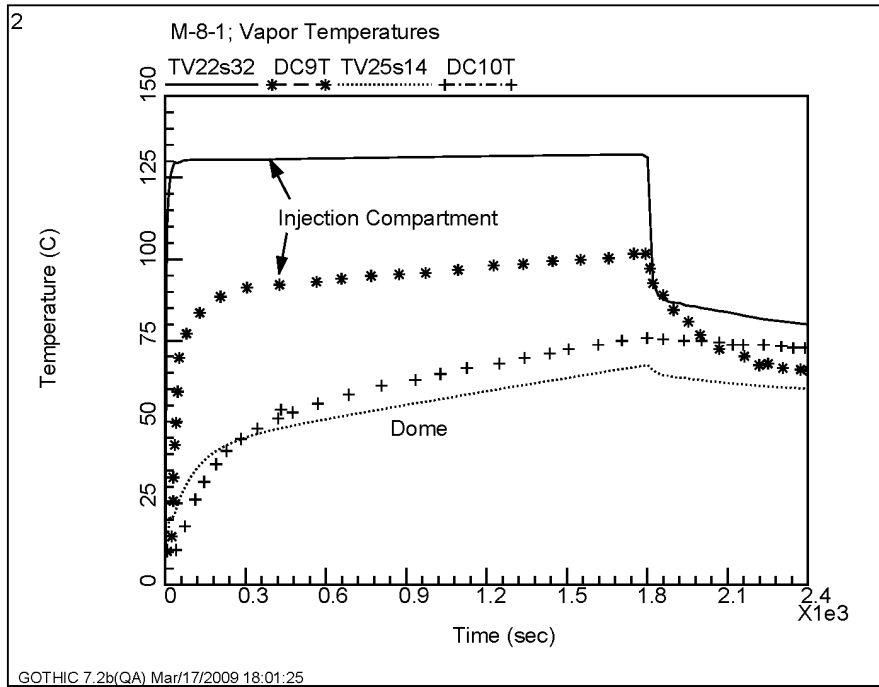
Figure 6-132—Injection Compartment and Dome Vapor Temperatures during NUPEC Test M-8-1
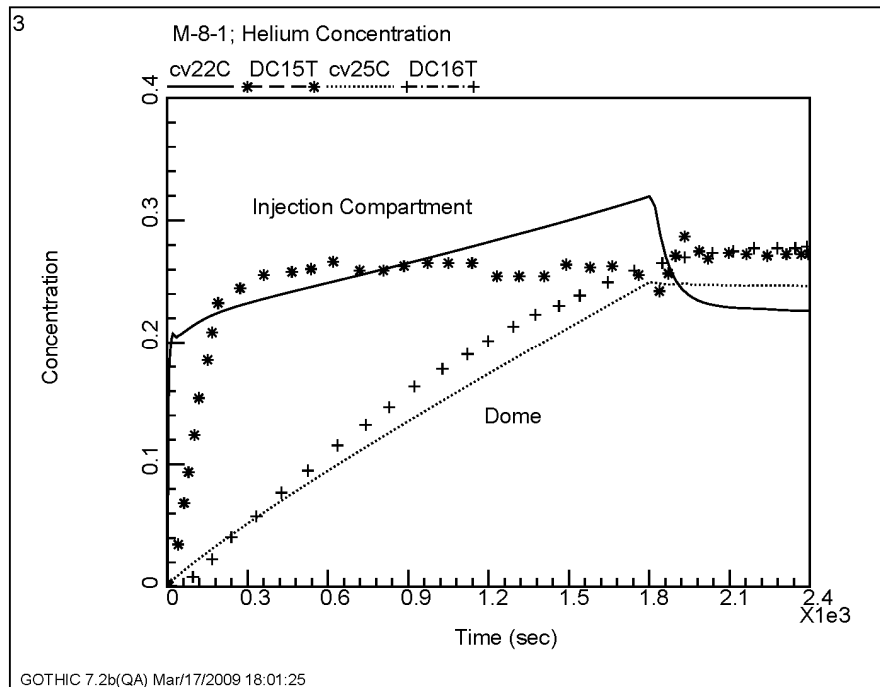
Figure 6-133—Injection Compartment and Dome Helium Concentration during NUPEC Test M-8-1

6.2.3.3   *NUPEC TEST M-2-2*

Test M-2-2 consisted of the injection of helium into an isothermal containment vessel with no steam injection or spray.

Calculated pressure is compared to data for test M-2-2 in Figure 6-134.   The figure indicates that the amount of gas injected was consistent with the data.

Measured and calculated helium concentrations for test M-2-2 are compared in Figure 6-135. Available helium concentration profiles for compartments 8, 15, and 21, which were presented on a single graph, did not clearly define the sensor locations or which curve applied to which compartment. Therefore, the data are represented in Figure 6-135 as plume data. In general, the GOTHIC model demonstrates the ability to model mixing behavior while producing reasonable pressure results.
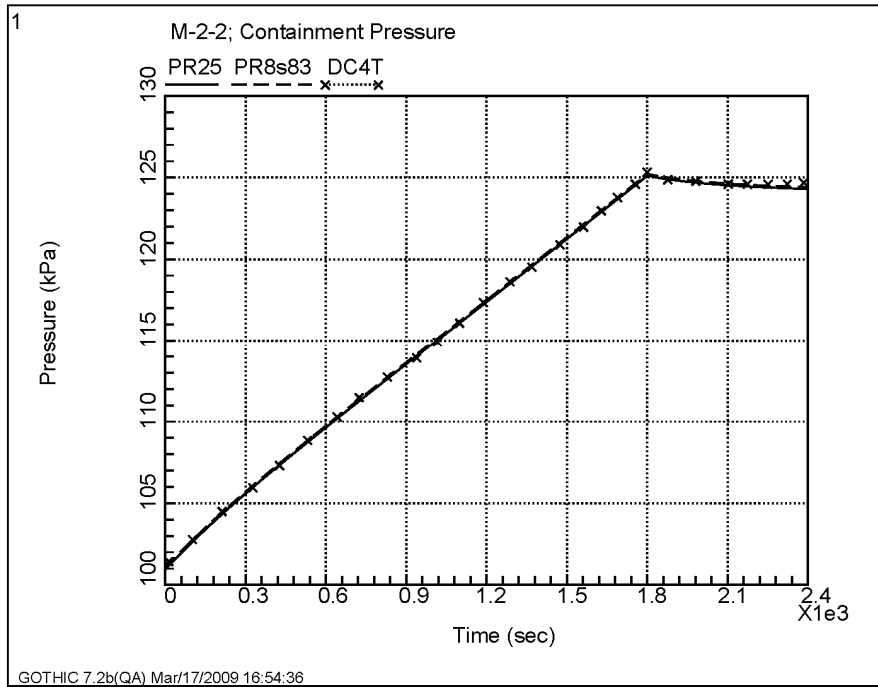
Figure 6-134—Containment Pressure during NUPEC Test M-2-2
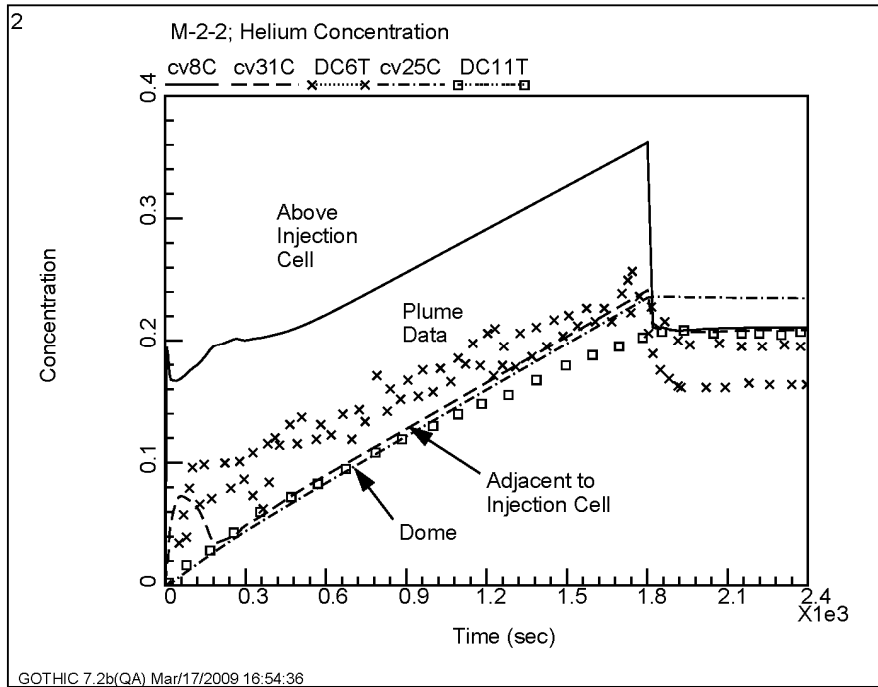
Figure 6-135—Injection Compartment and Dome Helium Concentration during

NUPEC Test M-2-2

6.2.4   CVTR Testing

The Carolinas Virginia Tube Reactor (CVTR) (Reference 31) containment, shown in Figure 6-136, is a reinforced concrete structure which includes a free volume of 227,000 ft^3. The vessel is cylindrical with a flat base and a hemispherical dome. The concrete walls are 2 ft thick and are lined with 1/4 in thick steel plates. A 3/8 in thick air gap separates the steel liner from the concrete. The dome is composed of 1/2 in steel plate covered by 20-1/2 in of concrete, and the basement floor is concrete. The containment is physically divided by floors and equipment into three distinct regions, which are indicated on Figure 6-136 as the operating, intermediate, and basement regions. The volume of the operating region is about 141,000 ft^3 while the combined volume of the regions below the operating floor is about 86,000 ft^3.

Steam for the blowdown experiments is supplied from a coal-fired generating station located near the containment. Steam is delivered through a 10 in diameter pipe that enters the containment building in a horizontal orientation. The steam line passes through a 90°elbow to enter a vertical 10 ft-long pipe section containing approximately 126 1-inch diameter holes cut along the side of the pipe and distributed both axially and circumferentially. This pipe section acts as a diffuser to break up the steam jet to avoid impingement loads on the containment.

Two heat plugs were installed in the containment wall. Heat plug 1 is located at elevation 329.2 ft, which is just above the floor of the upper containment. Heat plug 2 is located at elevation 348.3 ft, which is just above the top of the diffuser. The heat plugs were constructed by removing a 10 in diameter plate from the steel liner that is part of the containment wall. Then, a 1 in diameter concentric hole was drilled through the concrete wall. At each location, these pieces were replaced by a heat plug assembly, which is a steel plate and concrete plug mounted with thermocouples designed to be thermally identical to the original wall.

AREVA NP Inc.
Applicability of AREVA NP Containment Response Evaluation Methodology to the
U.S. EPR™ for Large Break LOCA Analysis
Technical Report

ANP-10299NP
Revision 2

Page 6-133
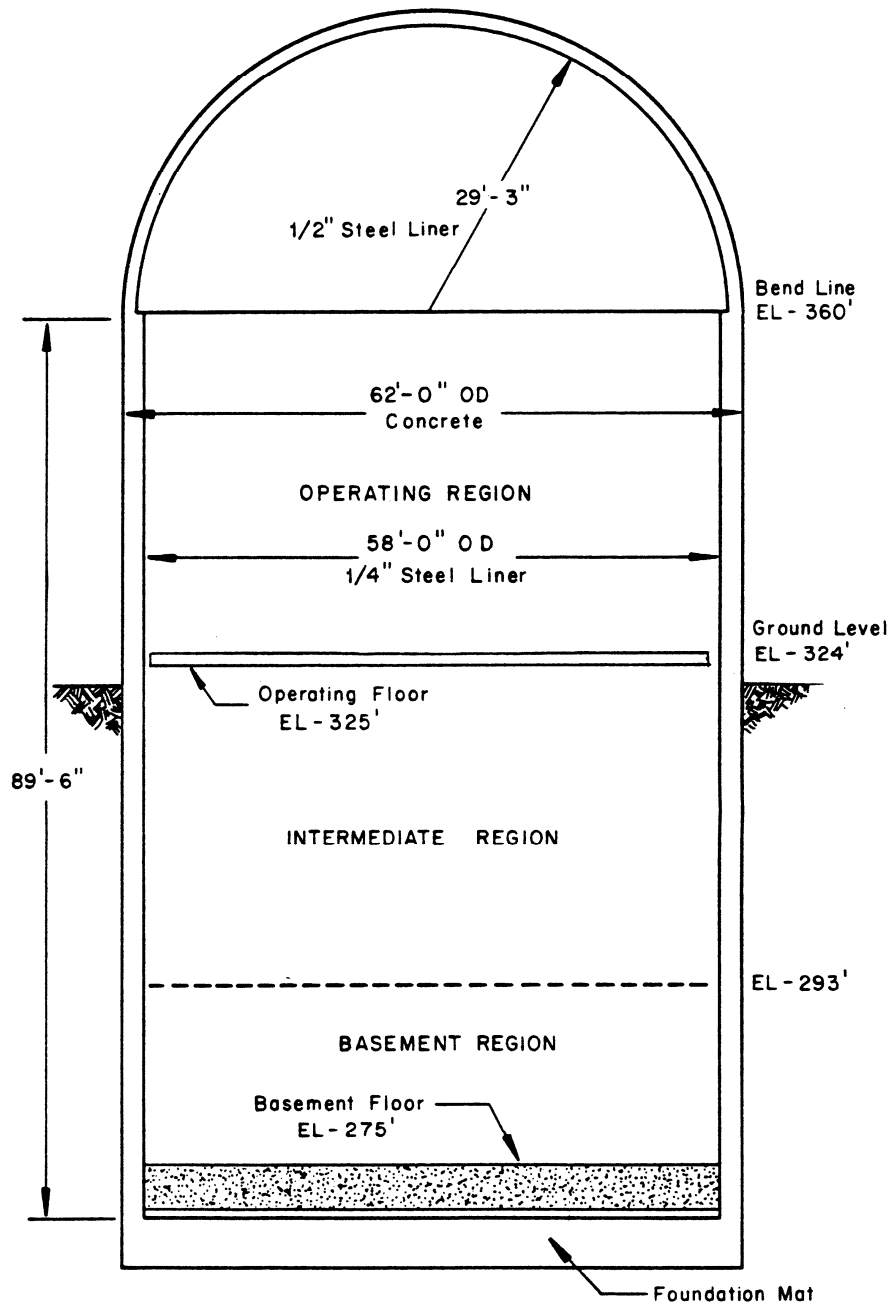
Figure 6-136—CVTR Containment Structure

A 3D GOTHIC model built to simulate the CVTR is shown in Figure 6-137 and Figure 6-138. The 3D model is based on subdivision of the entire containment modeled as a single volume with a uniform 7x7 plan grid and 18 axial levels. The cylindrical shell, the dome, the operating floor, and the two stairway openings in the operating floor are all

defined using the GOTHIC blockage operators. Thermal conductors representing the outer wall, the operating floor, and the dome are attached to the blockages that define these structures. Condensation heat transfer was calculated using the DLM-FM option.

The steam injection system is modeled uniquely because of its diffuser design. The break diffuser, described above, causes the break flow to expand horizontally in all directions, which minimizes the jet effect that would induce mixing throughout the containment. To avoid a jet effect, the 3D model includes eight flow boundary conditions with each boundary condition supplying 1/8 of the total flow while modeling the actual velocity at the outlet of the diffuser. A flow path is used to connect each boundary condition to one of the four faces of the cell at x=3 and y=4 at axial levels 11 and 12. Flow is directed toward the containment wall. The modeled velocity from these eight flow paths is defined to be the same as that from the diffuser.
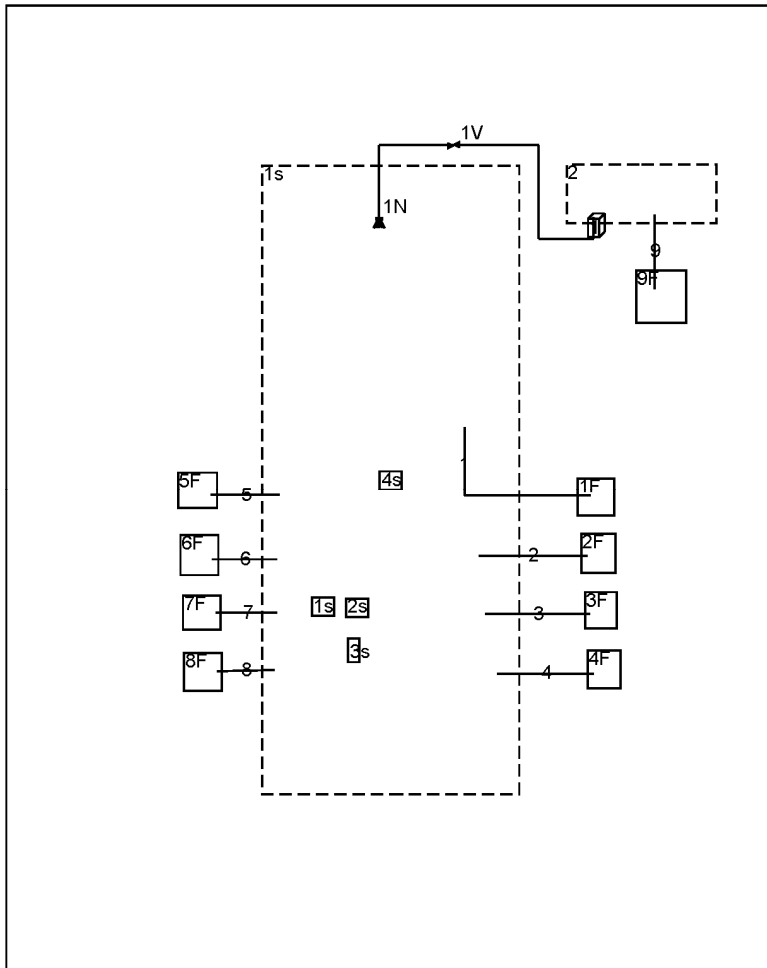
Figure 6-137—GOTHIC 3D Model for CVTR

AREVA NP Inc.   ANP-10299NP
Applicability of AREVA NP Containment Response Evaluation Methodology to the   Revision 2
U.S. EPR™ for Large Break LOCA Analysis
Technical Report   Page 6-136
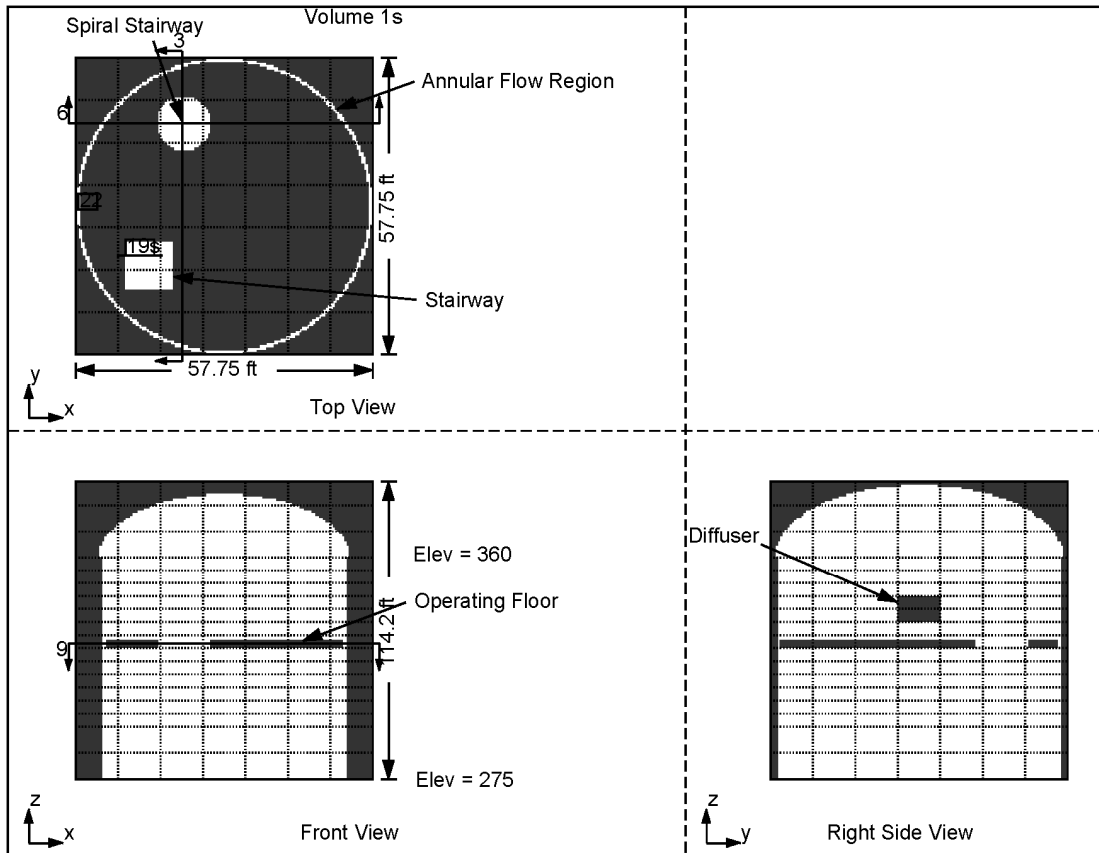
Figure 6-138—GOTHIC 3D Subvolume Diagram for CVTR

6.2.4.1   CVTR Test 3

CVTR Test 3 consisted of a steam release into a containment vessel. Although the vessel was equipped with a spray system, it was not activated. A 3D model was implemented so that steam and thermal stratification, as well as velocity effects, could be computed.

Figure 6-139 and Figure 6-140 show conductor surface temperatures predicted by GOTHIC compared to the data. The predicted surface temperatures for the two conductors in the lower volumes show excellent agreement at the lower measurement point, but tend to over-predict the measurement at the higher point. The upper location shows the same general trends for both the calculated and measured temperatures, but has the characteristic difference caused by comparing imbedded measured

temperatures to calculated surface temperatures. The shape of the calculated and measured temperatures near the bottom of the containment compare well, indicating that about the right amount of steam made its way to the bottom of the lower containment in the calculation.

As shown in Figure 6-141, the peak pressure predicted by the 3D model is very close to the measured value. Later in the transient, the 3D model results are closer to the measured pressure. Local temperatures in the lower containment are over-predicted, as shown in Figure 6-142, but there is good agreement in the upper containment, as shown in Figure 6-143.

The heat plug data comparison shows an under-prediction of wall heat transfer data by the GOTHIC model in Figure 6-144. The locations of the heat plugs are well defined in Reference 101, but neither the elevation nor the planar location of the steam diffuser is defined. The proximity of the heat plugs to the diffuser has an effect on the calculated and reported heat transfer coefficients, as shown in Figure 6-145. Figure 6-145 shows a comparison of the reported HTC and the calculated wall HTC at a location that is close to the heat plug locations. The location is one level below the heat plugs and in the same quadrant, but not in the same circumferential location as the heat plugs. This calculation shows better agreement with the lower heat plug data, but the comparison is about the same as that reported previously for the upper heat plug.
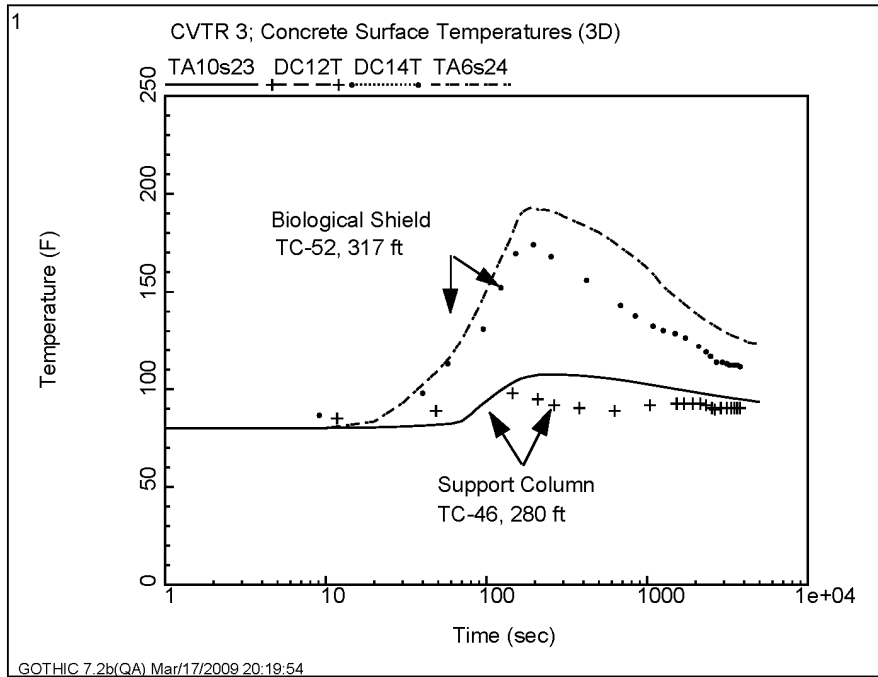
Figure 6-139—Concrete Surface Temperatures in Lower Containment for CVTR Test 3
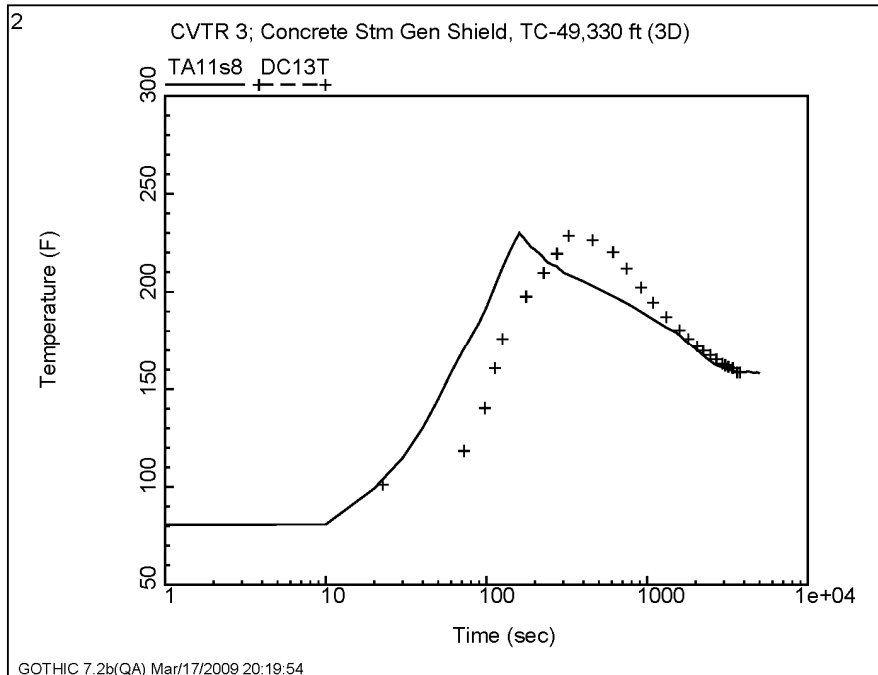
Figure 6-140—Concrete Surface Temperatures in Upper Containment for CVTR Test 3
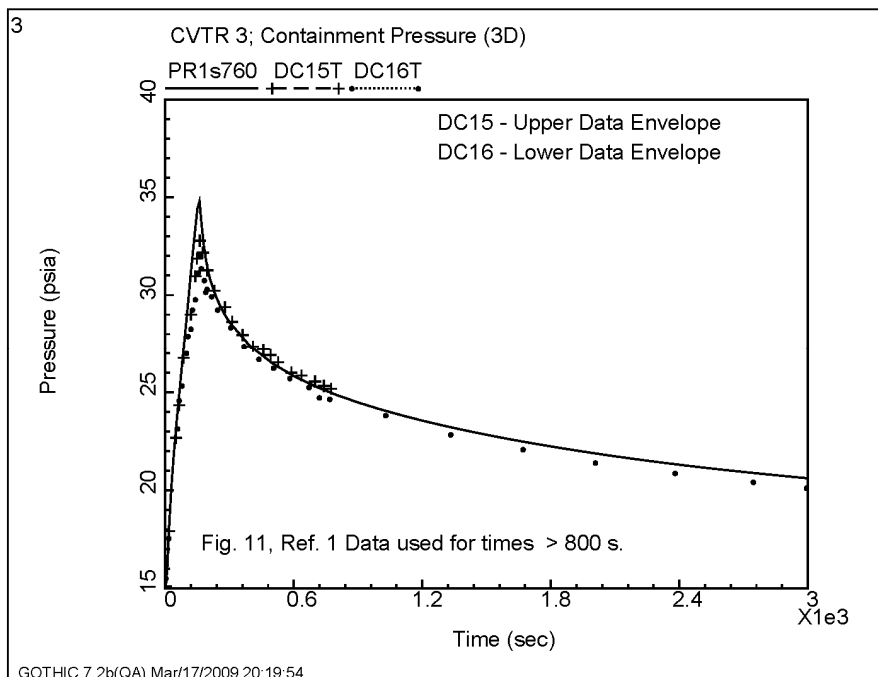
Figure 6-141—Containment Pressure for CVTR Test 3
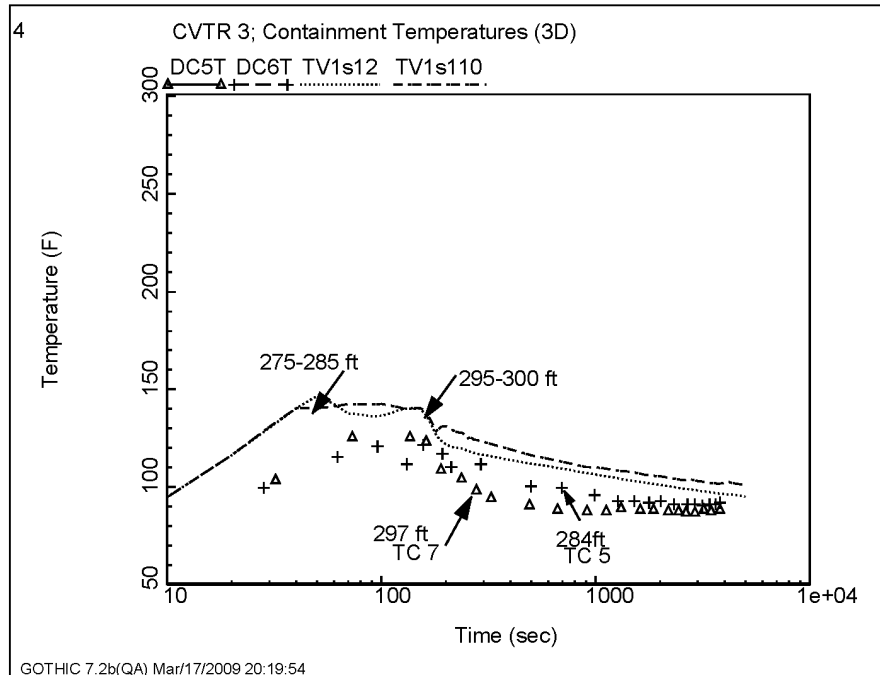
Figure 6-142—Containment Temperatures for CVTR Test 3
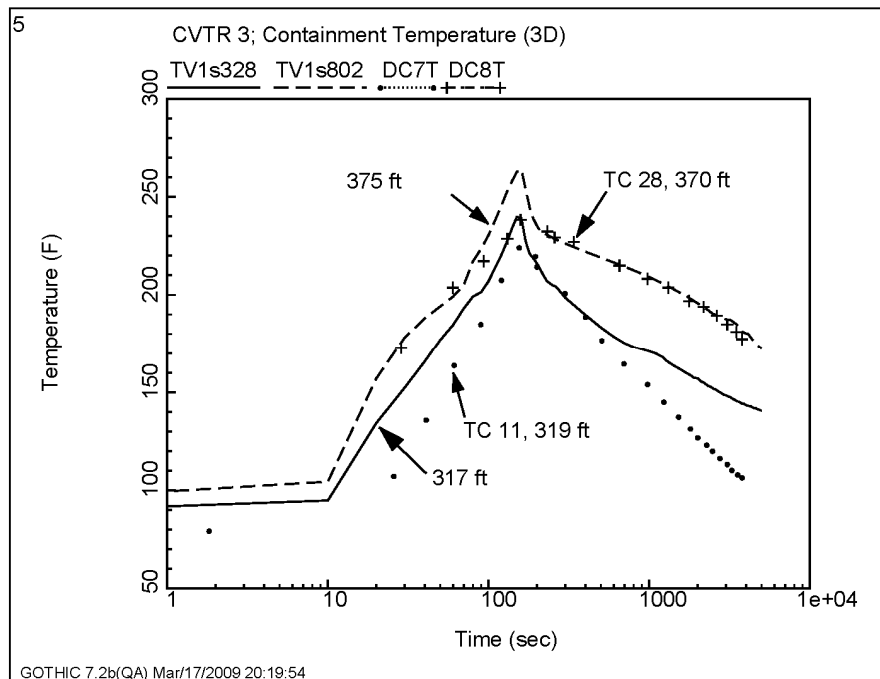
Figure 6-143—Containment Temperatures for CVTR Test

AREVA NP Inc.
Applicability of AREVA NP Containment Response Evaluation Methodology to the
U.S. EPR™ for Large Break LOCA Analysis
Technical Report

ANP-10299NP
Revision 2

Page 6-141
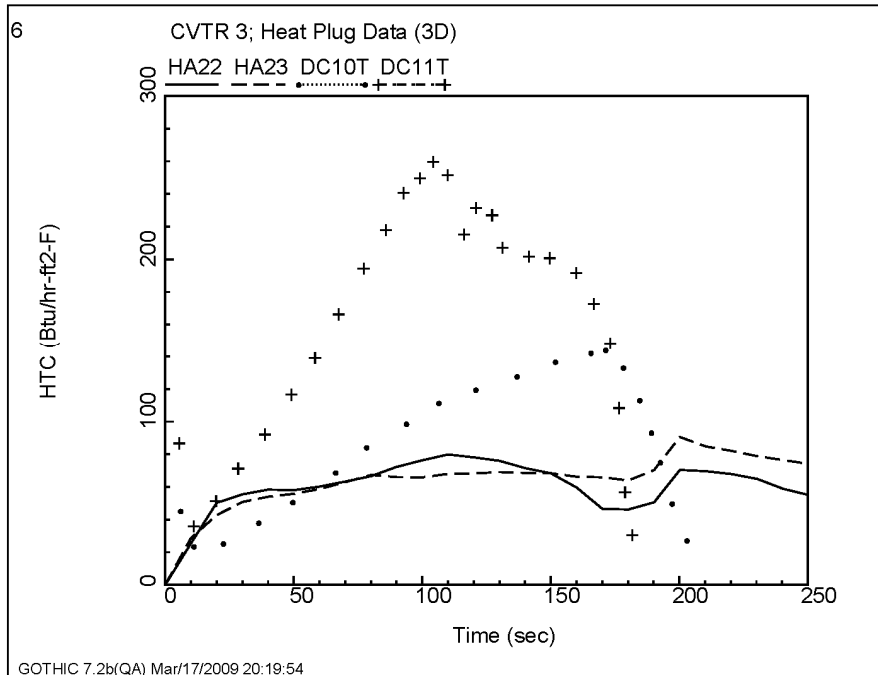
Figure 6-144—Heat Transfer Coefficients for CVTR Test 3
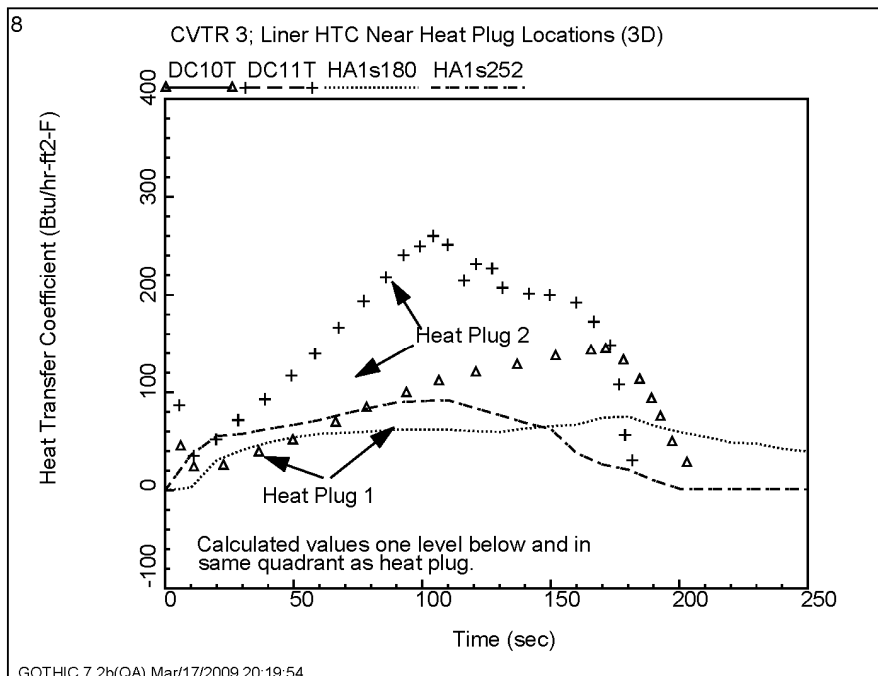
Figure 6-145—Wall Heat Transfer Coefficients for CVTR Test 3 Near Heat Plug Location

6.2.5   ISP-47 Testing

The main objective of the International Standard Problem number 47 (ISP-47) was to assess the capability of CFD and lumped parameter codes to predict containment thermal-hydraulics, including steam condensation in the presence of noncondensing gases, containment pressure, local temperature, and gas concentrations. The ISP consists of tests at several different facilities that cover a range of scale and geometric complexity. The TOSQAN tests (Reference 102), conducted by IRSN, examine condensation in a 7 m^3 vessel with axisymmetric flow.   TOSQAN was an open test with experimental results available to the ISP participant before the final calculations were submitted. The MISTRA test (Reference 102), conducted by CEA, was similar to the TOSQAN tests but was in a larger (100 m^3) vessel and was a blind test.

6.2.5.1   TOSQAN

6.2.5.1.1   Facility Description

The TOSQAN enclosure, shown in Figure 6-146, is a stainless steel cylindrical chamber with a total internal volume of 7.0 m^3. The entire vessel wall is thermostatically controlled by circulating oil inside the various wall sections. The top and bottom (including sump) "hot" zones are maintained at a common temperature that is above the saturation temperature to avoid condensation. The middle "cold" zone is maintained at a lower temperature that promotes condensation.

The 50 mm OD (41 mm ID) injection tube enters the side in the vessel with a 90° bend to direct the flow vertically upwards along the vessel centerline. The tube is straight cut at the end with no nozzle or diffuser. All steam, air, and helium enter through this tube.

The condensed water is collected at the bottom of the condensing area and flows to a small heated vessel connected to the TOSQAN vessel. The exhaust pipes at the top and the bottom of the vessel are closed during the tests.

AREVA NP Inc.
Applicability of AREVA NP Containment Response Evaluation Methodology to the
U.S. EPR™ for Large Break LOCA Analysis
Technical Report

ANP-10299NP
Revision 2

Page 6-143
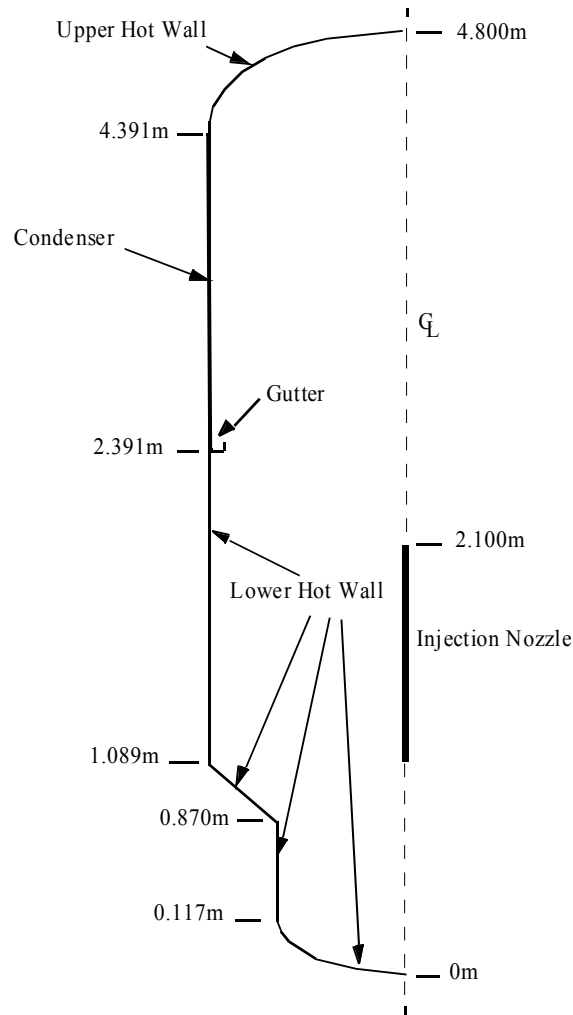
Figure 6-146—TOSQAN Test Vessel

6.2.5.1.2   *Test Description*

The TOSQAN ISP test is composed of a succession of different steady-states obtained by varying the injection conditions in the test vessel. The main stages of concern for the measurements are the four steady-states: three steady-states of air-steam mixture at two different pressure levels, and one steady-state of air-steam-helium mixture. Each steady-state is reached naturally by keeping a constant steam injection flow rate; the total pressure increases together with the condensation mass flow rate until the latter reaches the injection mass flow rate value.

6.2.5.1.3   GOTHIC Model

The overall model for TOSQAN is shown in Figure 6-147. Volume 1s represents the vessel, volume 2 is a mixing volume for the injected steam and gases, and volume 3 is a condensate collection tank. Boundary conditions 1F, 2F, and 3F are used to inject the steam, air, and helium, while boundary condition 4F is used to periodically drain water from the condensate collection tank. Flow path 6 is the drain line from the bottom of the condenser, and is used to maintain the pressure in the condensate tank consistent with the vessel pressure. The drain line discharges to the tank below the water level so that a loop seal is formed.
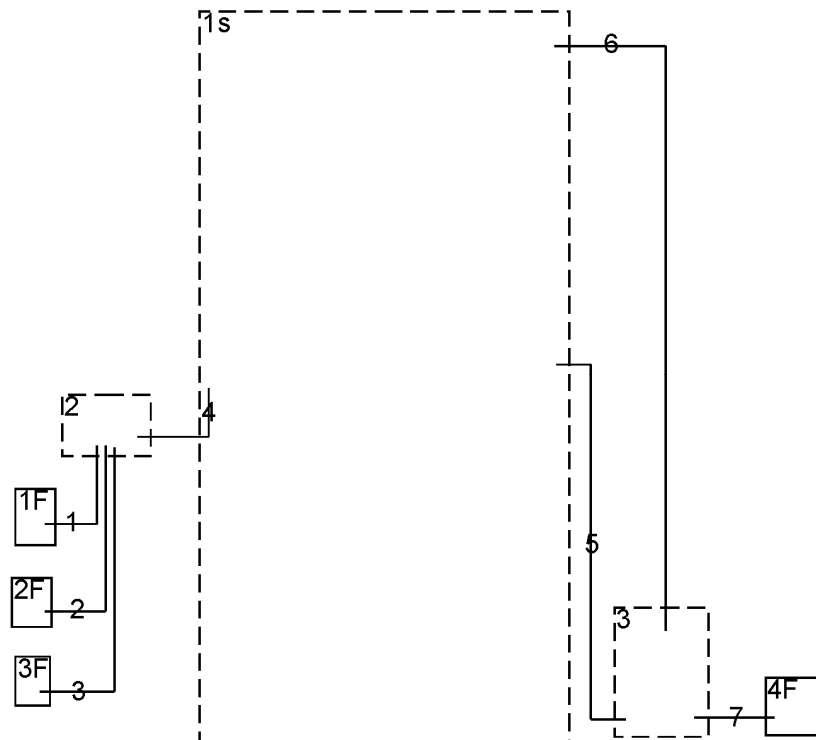
Figure 6-147—GOTHIC TOSQAN Model

Figure 6-148 shows the subdivided volume mesh for the vessel. A two-dimensional mesh is used to model one 15° sector of the facility. Wedge, cylinder, cone, and spherical blockages are used to model the boundaries of the modeled region. The region occupied by the vertical portion of the injection nozzle is blocked out. The heat

AREVA NP Inc.

ANP-10299NP

Applicability of AREVA NP Containment Response Evaluation Methodology to the

Revision 2

U.S. EPR™ for Large Break LOCA Analysis

Technical Report

Page 6-145

loss from the flow through the piping and nozzle to the surrounding containment atmosphere was not modeled.
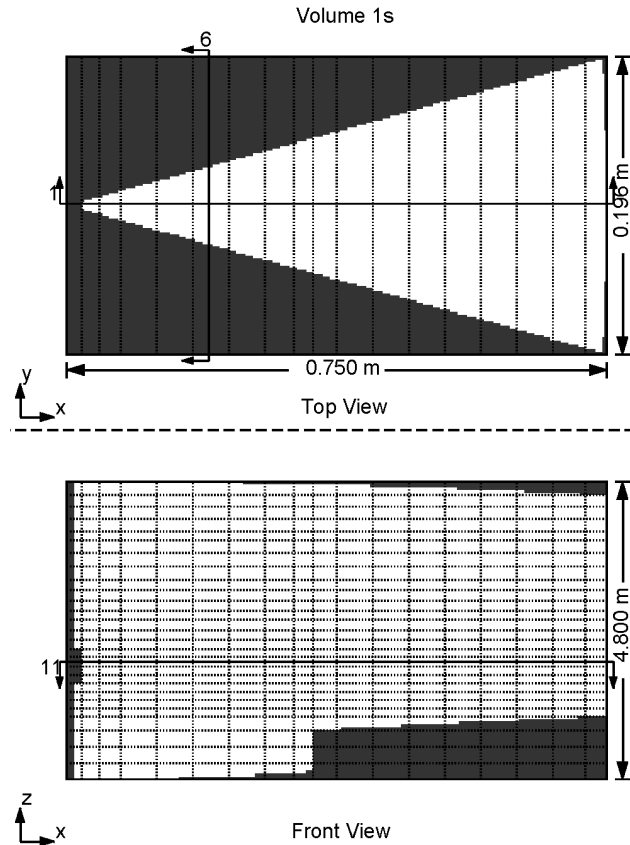
Figure 6-148—Subdivided Volume Mesh for TOSQAN

The wall condensers are modeled using spanned conductors that are in contact with the adjacent cells. The condenser conductors are thin steel with a specified time dependent back face temperature to match the prescribed test conditions. The DLM-FM heat transfer option was used for the condenser surfaces in contact with the fluid.

6.2.5.1.4   Results

For the GOTHIC ISP submittal for TOSQAN, the four steady-state conditions were achieved as part of a long transient that included the air and helium injections as prescribed. The steady conditions were held long enough to ensure that the calculated results were constant. As expected, the results for steady-states 2 and 4 were identical.

To reduce the run time requirements for this Qualification Report, two separate runs were made for steady-states 1 and 4. The transient to steady-state 1 started with the specified initial conditions and the steady-state 1 steam injection rate. The total air for the steady-state 1 conditions was injected at a constant rate over 600 seconds. For the first 100 seconds, the steam/air injection temperature was increased to speed the approach to steady conditions. The transient was run until steady conditions were achieved. The transient to steady-state 4 started with the specified initial conditions and the steady-state 4 steam injection rate. The total air and helium for the steady-state 4 conditions was injected at a constant rate over 600 seconds. The transient was run until steady conditions were achieved.

Measured results in the figures below are from References 103 and 104. Figure 6-149 and Figure 6-150 show the GOTHIC-predicted vessel pressure for the transients to steady-states 1 and 4 and the measured pressure at steady-states 1 and 4. Figure 6-151 through Figure 6-153 show the predicted and measured steam and helium concentrations at two locations in the vessel. The selected locations for the concentrations are at a radius of 0.375 m and elevations of 1.90 and 3.93 m from the bottom of the vessel. Figure 6-154 and Figure 6-155 show the predicted and measured vapor temperature measurements at a radius of 0.4 m and elevations of 1.47 and 3.93 m.

The predicted pressures are in good agreement with the data, with a slight over-prediction at steady-state 4. The steady-state variations in steam and helium concentration away from the injection plume were small, as indicated by the measurements and the GOTHIC results. The measurements indicate less temperature variation than predicted by GOTHIC. Possible thermal radiation effects on the thermocouples from the hot and cold walls may influence the measured temperatures.
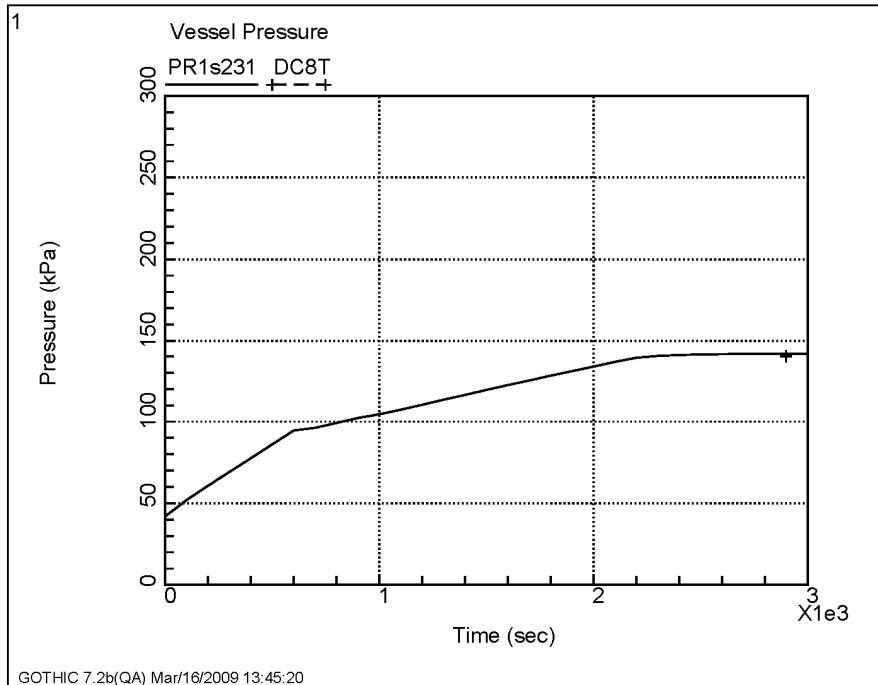
Figure 6-149—TOSQAN Pressure to Steady State 1
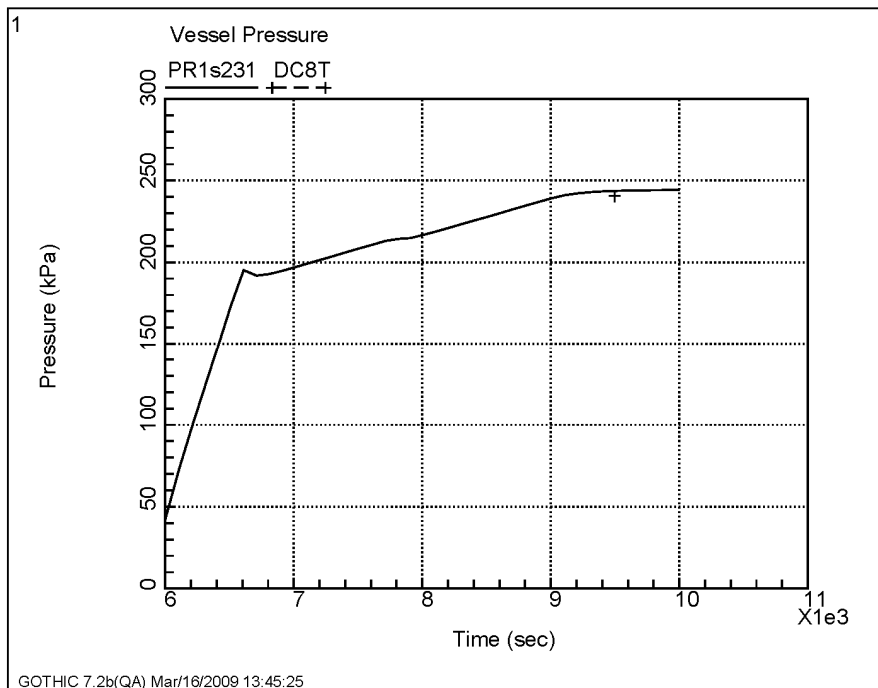
Figure 6-150—TOSQAN Pressure to Steady State 4
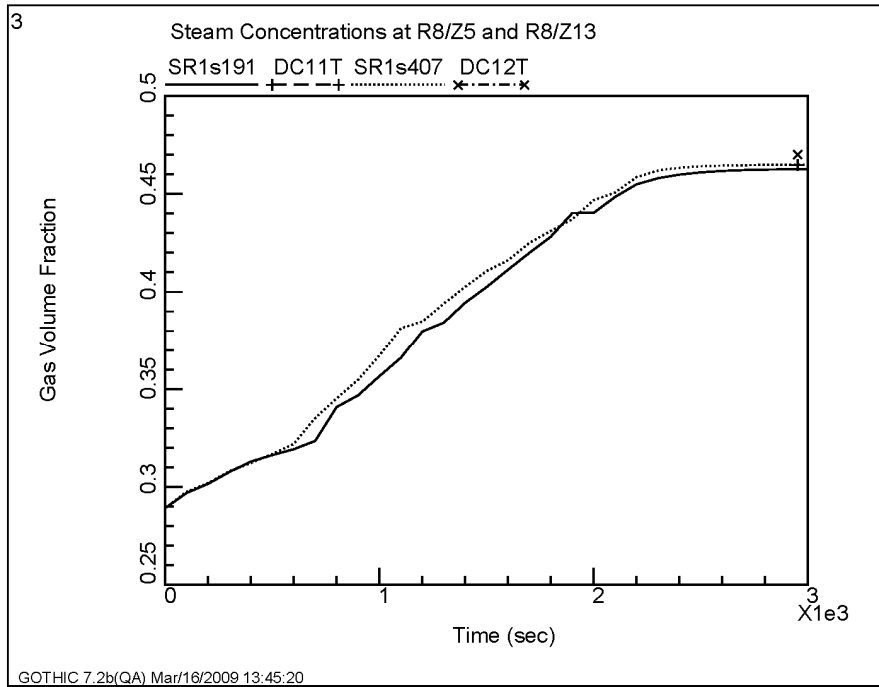
Figure 6-151—TOSQAN Steam Concentrations to Steady State 1
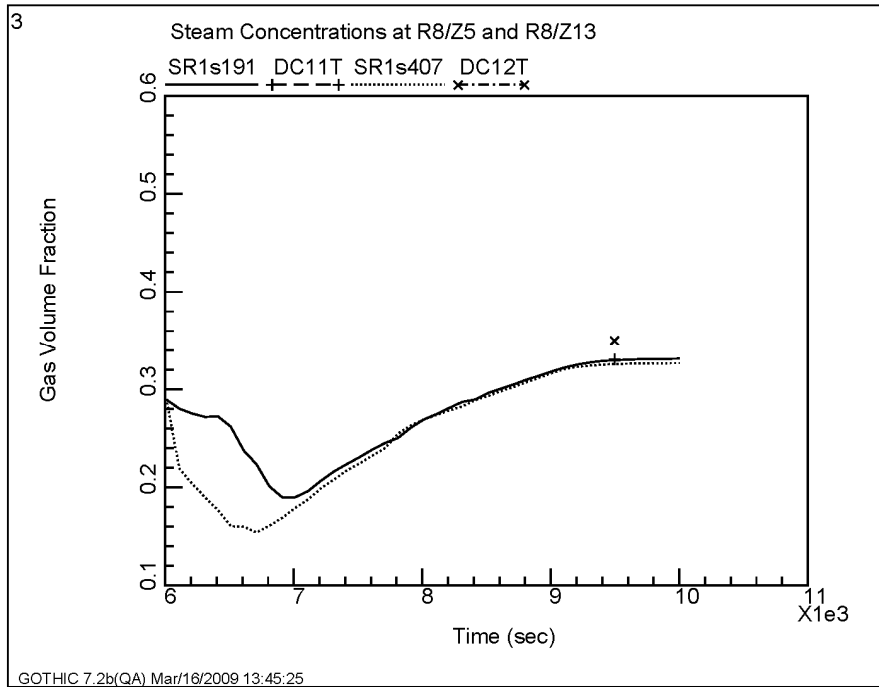
Figure 6-152—TOSQAN Steam Concentrations to Steady State 4
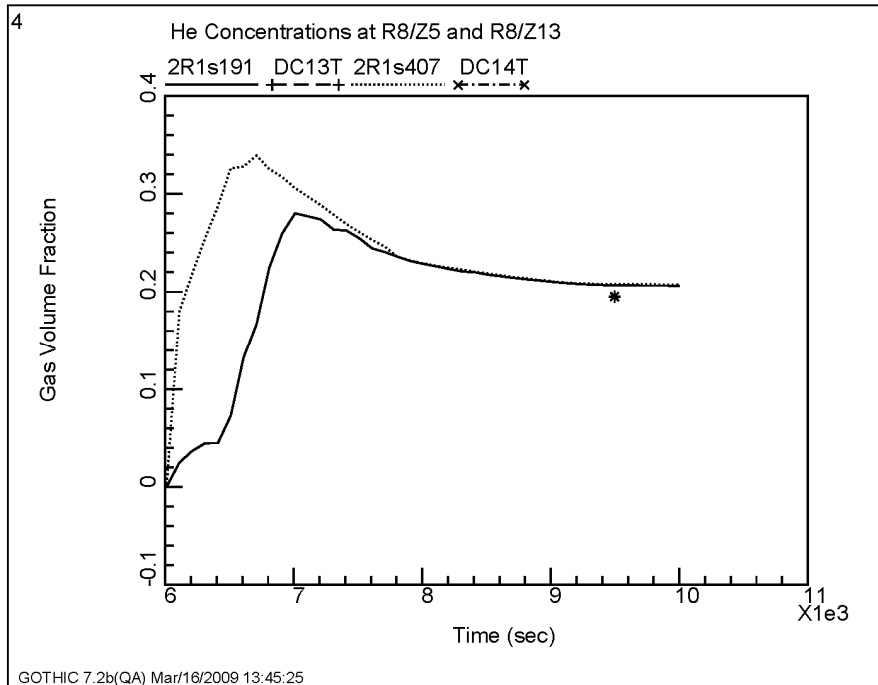
Figure 6-153—TOSQAN Helium Concentrations to Steady State 4
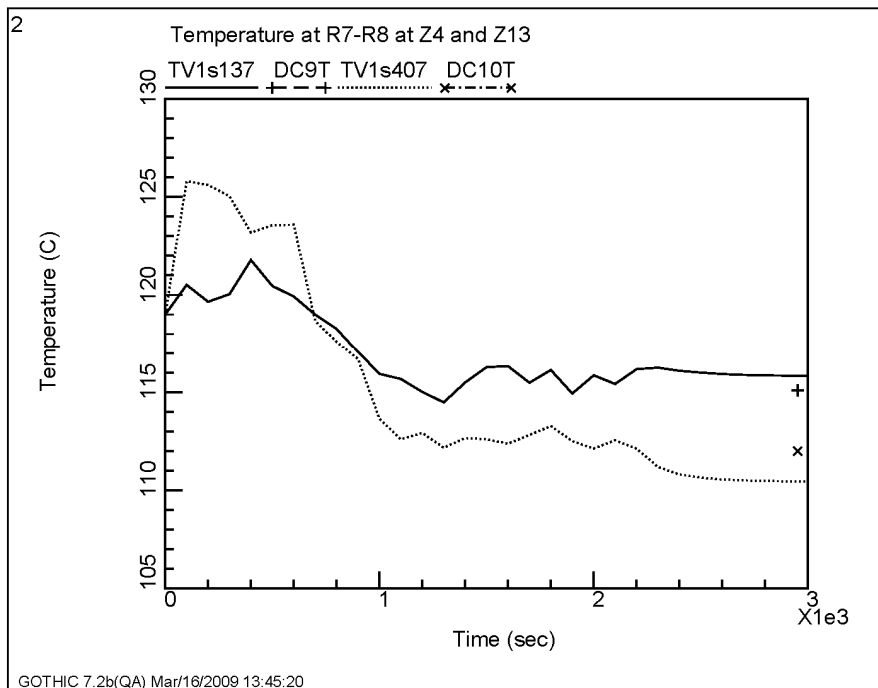
Figure 6-154—TOSQAN Temperatures to Steady State 1
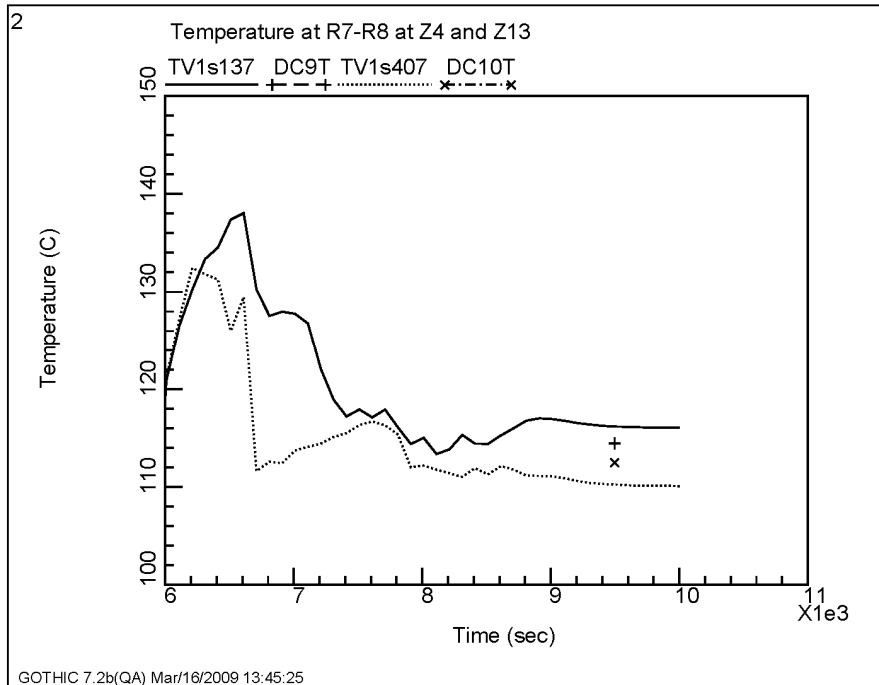
Figure 6-155—TOSQAN Temperatures to Steady State 4

6.2.5.2   MSTRA

6.2.5.2.1   Facility Description

The MISTRA test facility (Reference 102) was constructed to validate multidimensional containment thermal-hydraulic analyses. The vessel is representative of a PWR containment at a 0.1 linear scale. Three condensers are situated adjacent to the vessel wall as shown in Figure 6-156.
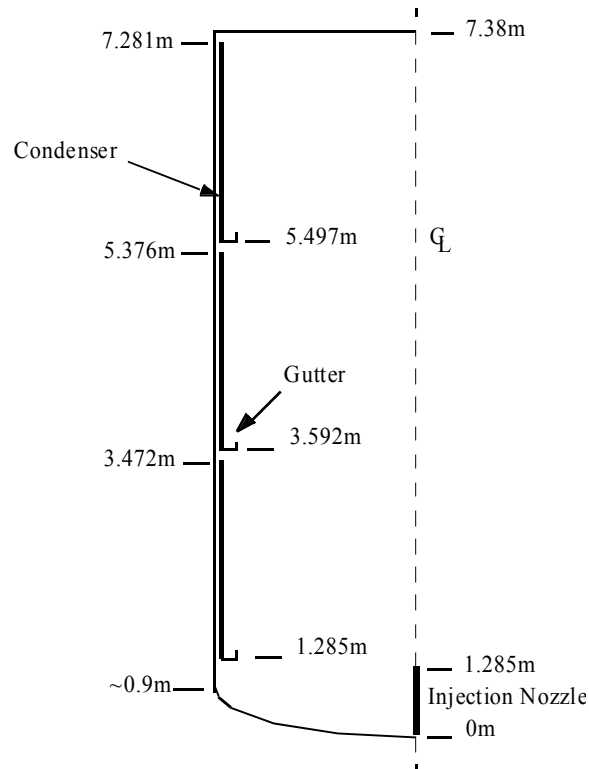
Figure 6-156—MISTRA Vessel

The stainless steel vessel volume is 99.5 m^3 with an internal diameter of 4.25 m and a height of 7.38 m. The outside surface of the vessel is insulated. Water is circulated through pipes at the backside of the condensers to maintain a near constant and uniform temperature on the condensing surface. The backsides of the condenser are insulated from the containment atmosphere. Condensate is collected at the bottom of each condenser and removed from the vessel, as is condensate that accumulates at the bottom of the vessel.

Steam and/or noncondensing gases are injected through the nozzle at the bottom of the vessel. The diameter of the nozzle at the outlet is 200 mm.

6.2.5.2.2   Test Description

The test is a simplified accidental sequence simulating steam and hydrogen release in the containment during five successive phases. The first two phases were used to bring

the vessel and condenser temperature up to typical post-LOCA conditions and were not considered part of the ISP. Phase 3 established steady-conditions with a constant steam injection. Phase 4 covered a transient, during which helium was injected into the vessel along with the steam, and phase 5 established new steady conditions with constant steam injection following the helium injection.

Two measurements were available for the injection temperature for steam and helium. One was measured inside the injection tube at some unspecified location outside of the vessel. The second was measured in the diffusion cone at the exit of the injection tube inside the vessel. The injection tube was insulated outside of the vessel but not inside the vessel. The first is less than the second because of heat losses due to either the ambient outside of the vessel or to the atmosphere inside the vessel.

6.2.5.2.3   *GOTHIC Model*

The overall GOTHIC model for the MISTRA vessel is shown in Figure 6-157. Volume 1s represents the region inside of the condensers. Volume 3s represents the annular region between the condensers and the containment wall, extending to the top and bottom of the containment. Volume 2 is used to distribute the flow across the computational cells representing the nozzle. Volumes 4 through 8 are used to collect the condensate from the condensers and the bottom of the containment.
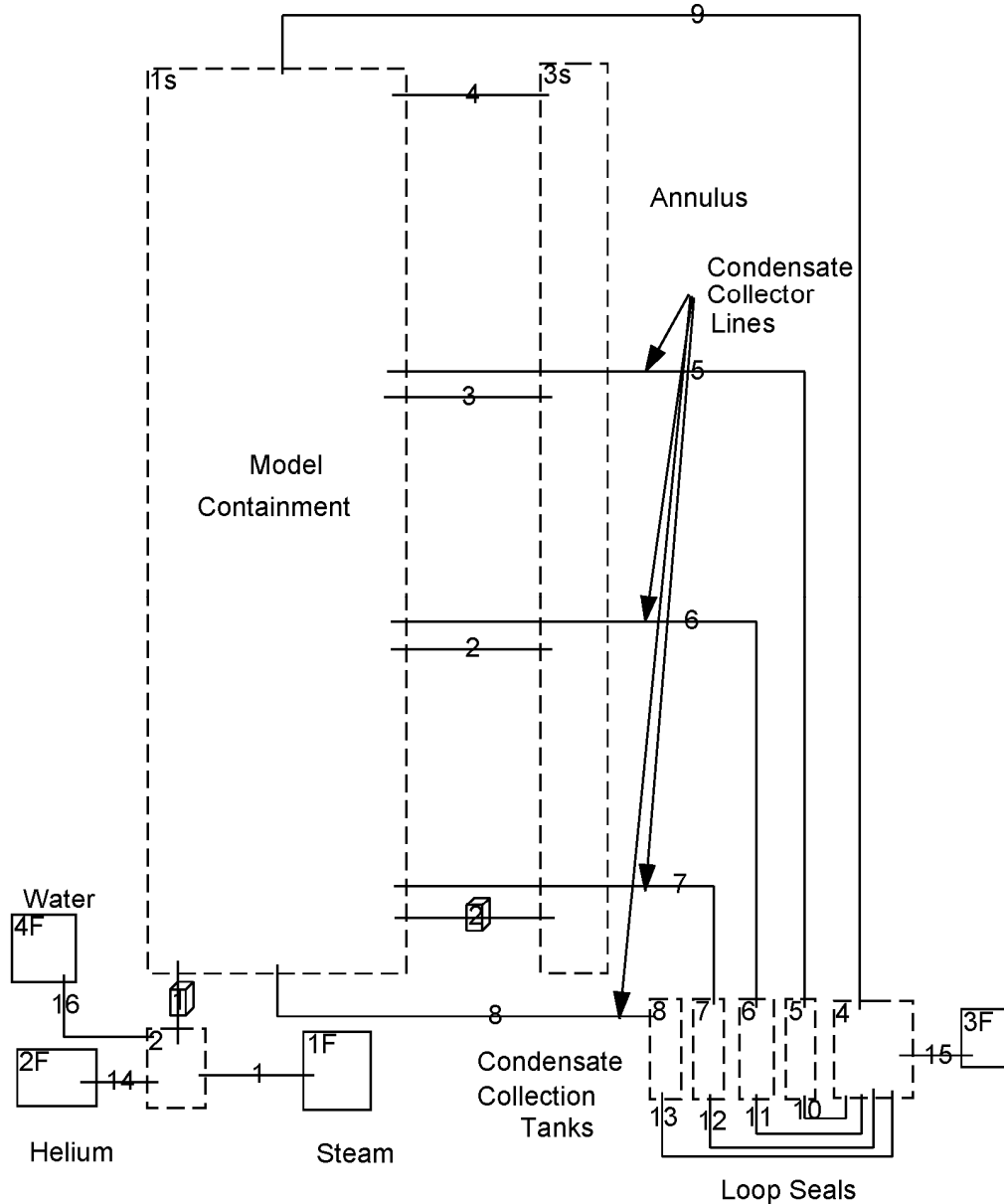
Figure 6-157—GOTHIC System Model for MISTRA

The volume internal to the condensers and the annulus are connected by flow paths 2, 3, and 4 and 3D connector 2. The flow paths represent the open space between the condensers and between the upper condenser and the ceiling. The 3D connector represents the connection between the two regions below the lower condenser.

The condensate collector volumes and associated flow paths form a loop seal; all of these volumes are partially filled with water. The drain lines enter the air space in collector volumes 5, 6, 7, and 8. These volumes are connected at the bottom to the common collector volume 4. The air space in volume 4 for is connected to the containment via flow path 9 to equilibrate the pressure.

The steam is injected via boundary condition 1F through distributor volume 2 and 3D connector 1. The helium is injected via boundary condition 2F. Boundary condition 4F is used for water injection during the helium injection because some data suggest that condensate may have been injected with the helium.

Figure 6-158 and Figure 6-159 show the subdivided volume noding for the region internal to the condensers and the annulus, respectively. A two-dimensional mesh is used to model a 15° sector of the facility. This corresponds to one of the 24 condenser plates. Wedge and spherical (assumed) blockages are used to model the boundaries of the modeled region. The injection nozzle is modeled by blocking the x-direction flow at 0.1 m for the first 1.3 m in the z-direction. The heat loss from the flow through the piping and nozzle to the surrounding containment atmosphere is modeled by using a conductor that coincides with the blocked plane. Heat loss from the injector piping to the room atmosphere was assumed negligible because that portion of the pipes was insulated. The conductor parameters were adjusted so that the calculated temperature drop from the vessel penetration to the nozzle exit matched (approximately) the measured temperature drop.
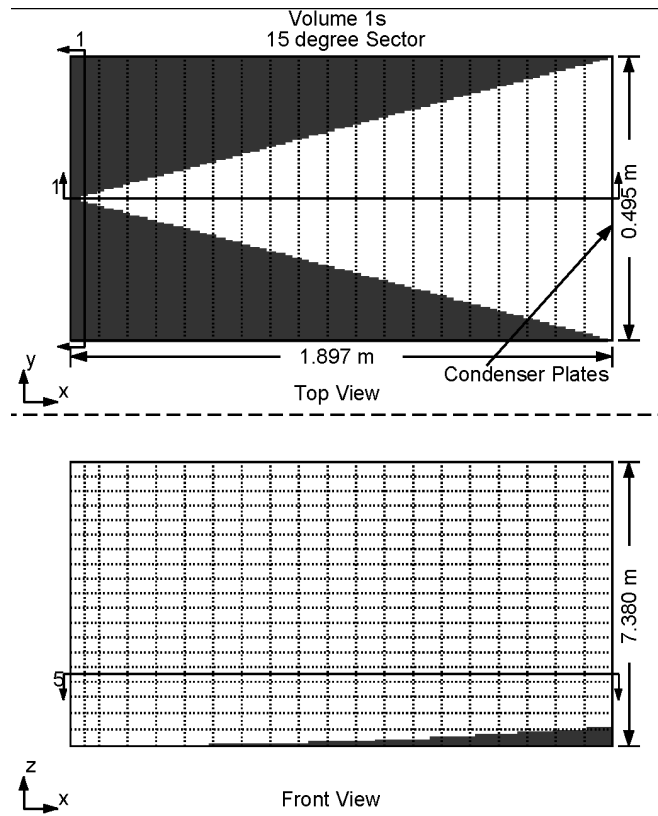
Figure 6-158—MISTRA Subdivided Volume Noding for Region Inside Condensers

AREVA NP Inc.
ANP-10299NP
Applicability of AREVA NP Containment Response Evaluation Methodology to the
Revision 2
U.S. EPR™ for Large Break LOCA Analysis
Technical Report
Page 6-156
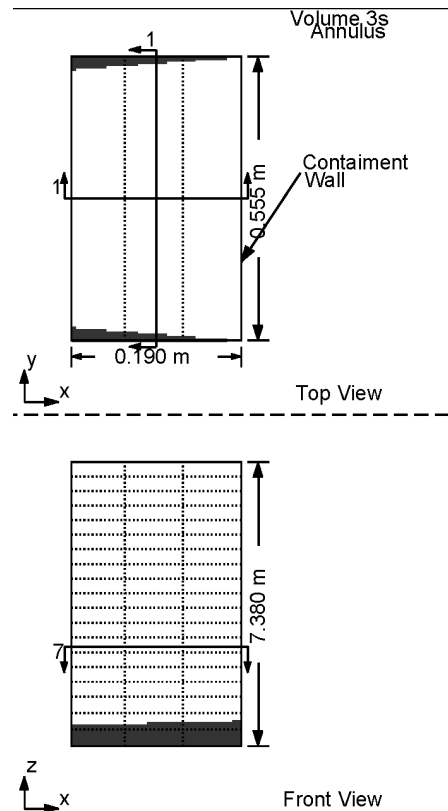
Figure 6-159—MISTRA Subdivided Volume Noding for Annulus Region

The condensers are modeled using three spanned conductors that are in contact with the adjacent cells. The condenser conductors are thin steel plates with a specified back face temperature of 115°C. The DLM-FM heat transfer option is used for the condenser surfaces in contact with the fluid. The containment cylindrical wall is modeled using a 15-mm steel conductor spanned across the adjacent cells. The bottom is modeled with a 25-mm steel conductor assigned to the spherical blockage. Although a conductor was included for the vessel head, it was isolated from the containment atmosphere to avoid condensation on the ceiling. Information from CEA (Atomic Energy Commission) indicated that condensation is not expected on the ceiling. The DLM-FM heat transfer option is used for the interior surface of the cylindrical wall and bottom cap. For the exterior surfaces, it is assumed that there is convection to the room atmosphere at 20°C with a convective heat transfer coefficient of 4.2 W/m²-K. The value of the heat transfer coefficient was selected to give (approximately) the reported condensation rate on these

AREVA NP Inc.   ANP-10299NP
Applicability of AREVA NP Containment Response Evaluation Methodology to the   Revision 2
U.S. EPR™ for Large Break LOCA Analysis
Technical Report   Page 6-157

surfaces. The overall heat transfer coefficient, including the effects of the insulation on the outer surface, should be around 0.2 W/m^2-K. The larger value used in the analysis may account for the heat loss through the top of the vessel and non-uniform insulation coverage.

The containment atmosphere was initialized at 140°C, 5.0 bars, and 100% humidity, which allows for 1 bar of air at 20°C and 50% humidity in the vessel prior to the heatup phase. To accelerate the attainment of steady conditions, the heat capacity of the containment steel was reduced by a factor of 100. Therefore, the predicted transient to the steady conditions from the initial conditions is not representative of any actual transient.

6.2.5.2.4   *Results*

The results from the MISTRA test are described in Reference 105. The pressure response during the helium injection is shown in Figure 6-160. The measured pressures are indicated by the symbols and the calculated pressures are indicated by the lines. The period just before the start of the helium injection corresponds to steady-state 1 and steady-state 2 conditions that are reached at the end of the simulation. The last measured pressure indicator was recorded several hours after the time indicated in the graph. The pressure slowly declined during this period while the injection conditions were maintained constant. The GOTHIC results indicate that the steady pressure is approached from below. GOTHIC predicts higher pressures at both steady-states with the discrepancy larger for the second steady-state after the helium was injected. Possible causes for the difference are a low estimate of the condensation rate by the DLM-FM heat transfer option, unaccounted-for heat loss from the steam line before entering the vessel, and leakage of air and helium from the vessel during the test (possibly indicated by the pressure decline in steady-state 2). The shape of the pressurization during the helium injection is well matched.
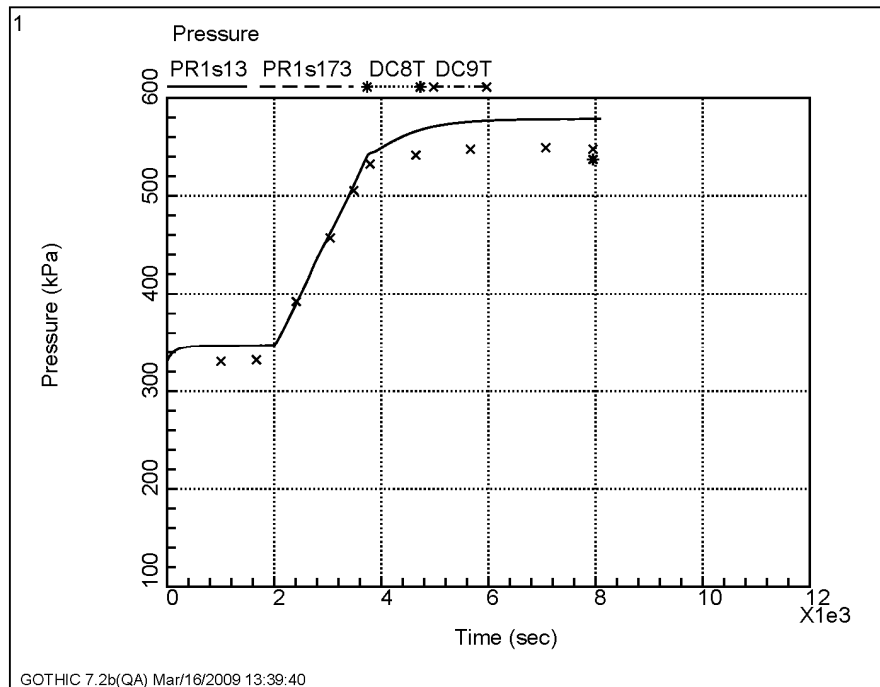
Figure 6-160—MISTRA Vessel Pressure

The steady-state 1 temperature profiles at instrumented radial locations are shown in Figure 6-161 through Figure 6-163. The points with error bars represent the measured data and the solid line represents the GOTHIC results. GOTHIC matches that data throughout the vessel fairly closely with the largest deviation at the bottom of the vessel. The experimental heat loss from the vessel was significant and was not well characterized in terms of where it occurred. The GOTHIC model assumes a uniform ambient temperature and heat transfer coefficient. Local variations in the heat loss could account for some of the minor deviations between the measured and calculated results.

AREVA NP Inc.

Applicability of AREVA NP Containment Response Evaluation Methodology to the
U.S. EPR™ for Large Break LOCA Analysis

Technical Report

ANP-10299NP

Revision 2

Page 6-159
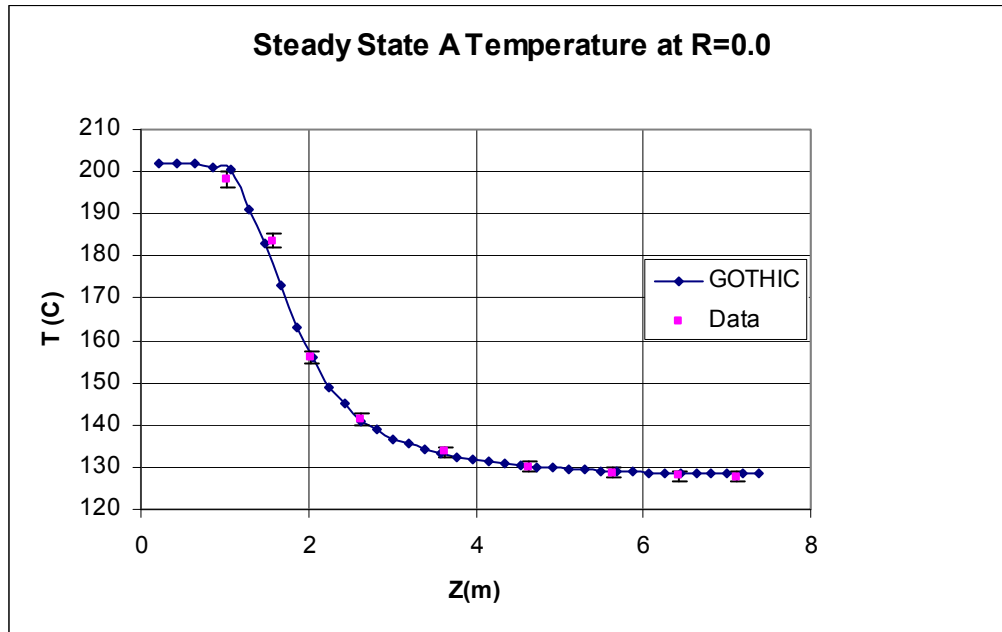
Figure 6-161—MISTRA Temperature Profile at r=0
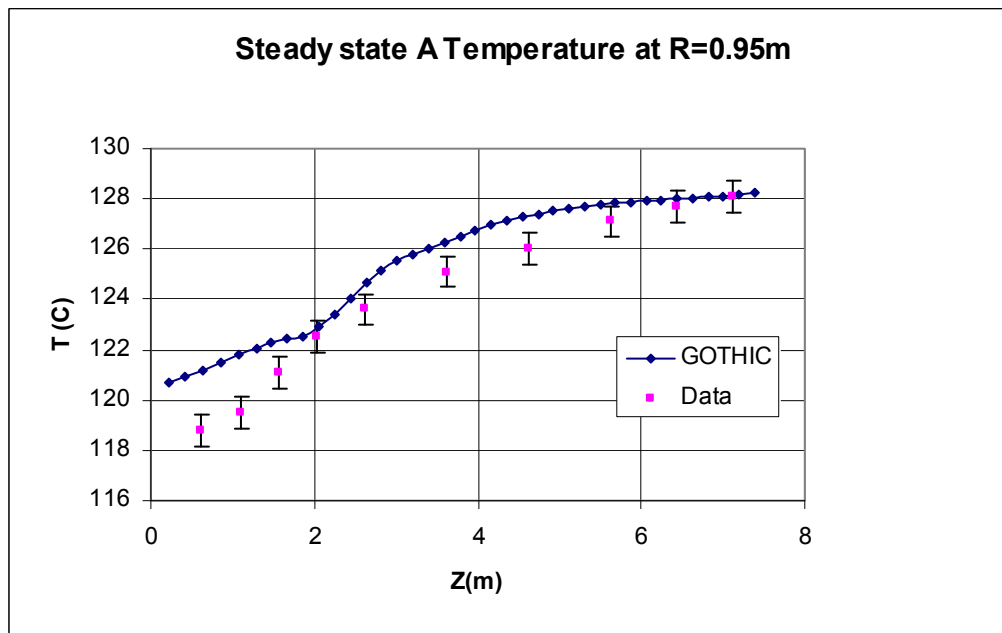
Figure 6-162—MISTRA Temperature Profile at r=0.95 m
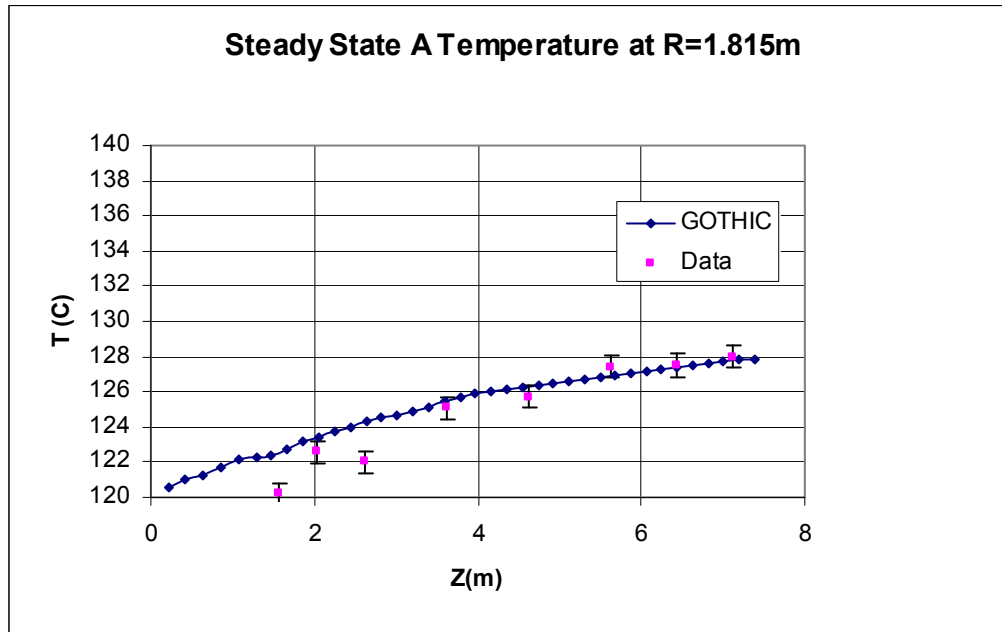
Figure 6-163—MISTRA Temperature Profile at r=1.8 m

Figure 6-164 and Figure 6-165 show the temperature transient during the helium injection period. The temperature dip due to the colder helium and the water coming in with the helium is well predicted. The predicted temperatures after the helium injection are higher than the measured temperatures, which is directly related to the higher pressures predicted for steady-state 2.
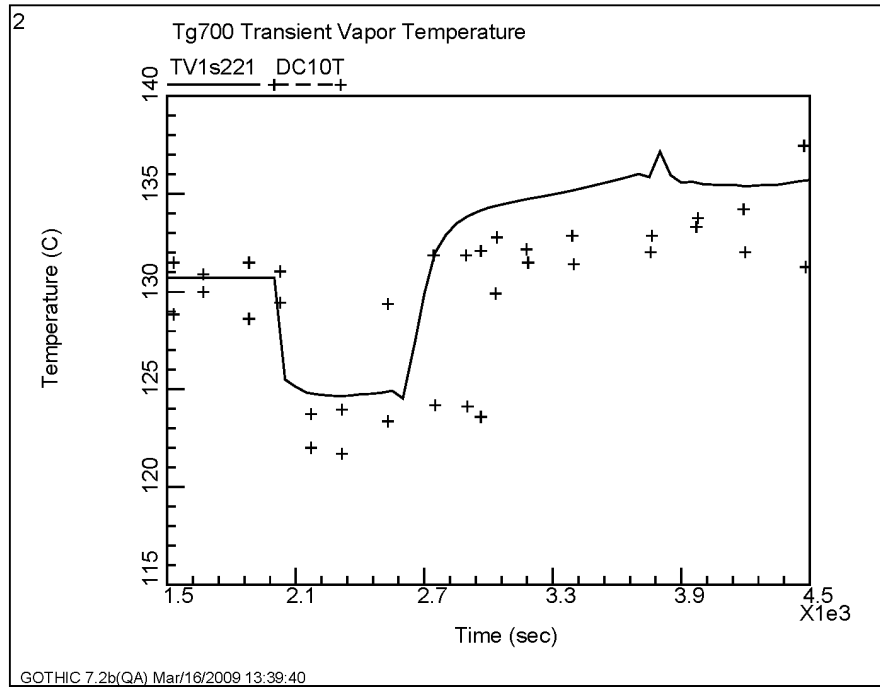
Figure 6-164—MISTRA Temperature Transient at R=0 and Elevation = 4.5 m
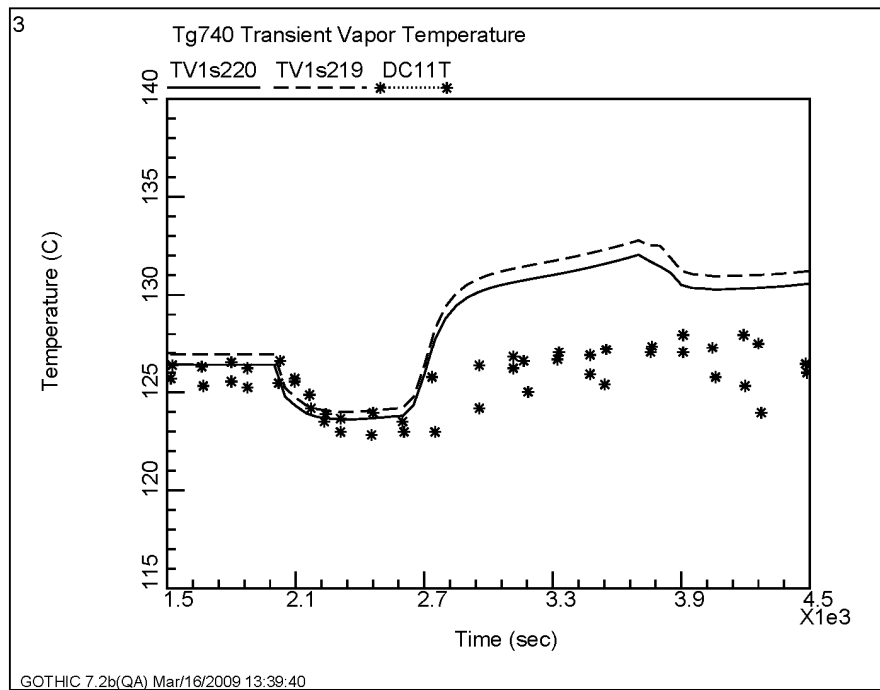
Figure 6-165—MISTRA Temperature Transient at R=1.8 m and Elevation = 4.5 m

6.2.6   Conclusions from Integral Tests Assessments

Different test conditions existed for the various code assessment exercises. Most of the tests were explicitly designed to study LBLOCA phenomena; these included HDR V21.1, T31.1, T31.5, and V44 and BFMC d16. The longest LBLOCA test assessment was about 2 hours. Other tests, such as E11.2 and E11.4, were SBLOCA tests and the test periods for those are much longer. The BFMC Biblis tests emphasized the study of atmospheric mixing, so pressure was not the primary figure-of-merit. Like the SBLOCA tests, the Biblis tests were also much longer. NUPEC tests M-4-3 and M-8-1 evaluated gas-steam distribution, and test M-2-2 was a separate effects test that evaluated only gas distribution. CVTR test 3 was a DBA steam blowdown test. The TOSQAN and MISTRA tests were designed to assess the capability of CFD and lumped parameter codes to predict containment thermal-hydraulics, including steam condensation in the presence of noncondensing gases, containment pressure, local temperature, and gas concentrations.

The GOTHIC assessments of LBLOCAs build on the code's extensive assessment database (Reference 31) by evaluating steam condensation and heat conduction phenomena that are not influenced by the effects of containment sprays. These assessments are directly applicable to the U.S. EPR following an LBLOCA. Most of these tests involved a simulated RCS or steam line break inside the containment. This produces a rapid pressurization followed by a slower cooldown as heat is removed by the passive heat sinks. Many of the assessments used both single- and multi-volume models, and several used subdivided-volume models. In all the assessments the multi-volume model shows excellent agreement with test data. The single-volume model also shows good agreement, however not as precise as those of the multi-volume GOTHIC model. The best agreement with test data was generally achieved by models employing a combination of multi-volume and subdivided modeling or only subdivided modeling.

For global pressure response, the reasons for the differences between the three models arise from how the models treat two principal phenomena: heat conduction and

convection/condensation. For all three nodalization schemes, the heat conduction models are the same. However, the heat conductors in the multi-volume and subdivided models are distributed among the various control volumes and cells. For predicting global response variables, the temperature variations in the multi-volume model are compensating; hence, the only real simulation difference between the models is related to the calculation of the heat removal rates (convection/condensation) from the air/steam space.

With the single-volume nodalization, no flow field is calculated and, thus, forced convection is inherently neglected. Both nodalization schemes adopt similar free convection and steam condensation models that are strictly based on control volume properties. By modeling the flow of the steam/air mixture in the containment, heat transfer by forced convection can be predicted. This results in higher bulk condensation in the air/steam space that is not otherwise predicted in the single-volume model. The multi-volume and subdivided models benefit from this additional heat transfer during the short term with lower containment pressures. For the extended event, forced and free convection diminish as the buoyancy-driven air/steam flow rates reduce as temperatures trend toward equilibrium. In general, the heat absorption process is conduction-limited and the containment depressurization rates are very similar in the two models. The relatively small difference is related to the difference in steam concentrations. With the multi-volume and subdivided models, the enhanced short-term bulk steam condensation leads to lower late-term steam concentrations; thus, lower rates of condensation and slightly lower depressurization rates than with the single-volume model.

The SBLOCA tests illustrate GOTHIC's performance in the long-term. The slower event progression of the SBLOCA tests leads to less fully-developed conditions for heat transfer. As such, the single-volume models exhibit large error when compared to representative measurements (i.e., measurements were not averaged to estimate equivalent global results). In contrast, the multi-volume and subdivided models produce much better agreement with the data.

A few general conclusions can be drawn from these integral test assessments. When used with a multi-volume or subdivided model, GOTHIC provides a reliable simulation of both global and local containment thermal-hydraulic phenomena. Code-to-data comparisons improve when the containment atmosphere is well-mixed, such as during an LBLOCA. The single-volume model performed well in the LBLOCA exercises, fair in the BFMC atmospheric mixing exercises, and poorly in the SBLOCA studies.

6.3 *GASFLOW Analysis of Containment Mixing*

AREVA NP performed a GASFLOW analysis to assess the atmospheric mixing phenomena in the U.S. EPR containment. Good atmospheric mixing in the U.S. EPR containment is implicitly assumed in the single-volume GOTHIC calculations performed for a design-basis LBLOCA. The GASFLOW model represents the U.S. EPR and includes all relevant systems and structures for a LOCA simulation. The CONVECT system—which separates the non-accessible areas (equipment rooms, pipe break location, etc.) from accessible areas (annular rooms, dome, operation area, etc.) during normal operation—is also simulated. That system uses rupture and convection foils atop the steam generator cavities and mixing dampers located between in the air space above the IRWST and the lower area of the accessible space region. During an accident involving a breach of the RCS, these foils and dampers open, effectively converting the two-room containment into a one-room containment.

The GASFLOW simulation is a best-estimate calculation, meaning that not only were best-estimate phenomenological models were used and the physical behavior of all systems was realistically modeled. This includes access doors between compartments and rooms. While many of these doors are safety-related to prevent compartment over-pressurization, they are usually not considered when evaluating the containment atmosphere response. While the CONVECT system components open to create a particular circulation path, doors between the accessible and inaccessible containment regions can also open due to the pressure differential during an LBLOCA. Opening these pathways improves containment atmosphere mixing and limits the pressure

AREVA NP Inc.

Applicability of AREVA NP Containment Response Evaluation Methodology to the
U.S. EPR™ for Large Break LOCA Analysis
Technical Report

ANP-10299NP
Revision 2

Page 6-165

differences across the internal walls. Opening of these doorways is modeled in the GASFLOW analysis.

6.3.1   The GASFLOW Code

GASFLOW (Reference 76) is a 3D finite-volume computer code that solves the time-dependent, compressible Navier-Stokes equations for multiple gas species. GASFLOW was originally developed at the Los Alamos National Laboratory (LANL), with funding from the NRC and the U.S. DOE. Since 1994, the research center Forschungszentrum Karlsruhe (FZK) in Germany and LANL, through a co-operative agreement, have jointly developed and applied the GASFLOW code.

GASFLOW supports meshes in both 3D Cartesian or cylindrical coordinates. It uses a staggered mesh, where the scalar quantities are evaluated at the midpoints of the fluid cells and the vector quantities at the midpoints of the cell surfaces. It applies a linearized Lagrangian-Eulerian integration scheme to provide an implicit solution for pressure. Turbulent transport processes are evaluated using an algebraic or a k-ε turbulence model. The turbulent transport parameters are used to simulate the combined diffusion effect from turbulence and the molecular diffusion from concentration gradients. The solution has no restrictions on compressibility. The fluid-dynamics algorithm can model both natural- and forced-flow phenomena, including the effect of containment sprays. In addition, a chemical kinetics model is available for simulating the diffusion and propagation of flames resulting from the combustion of liquids or gases.

The flow processes are solved in a 3D grid, which includes obstacles (no flow volumes) and walls (surfaces that divide two adjacent layers of fluid flow and prevent cross flow). Obstacles and walls are used to build the representative geometry model within which the flow is simulated. Heat transfer to obstacles and walls can be simulated by applying 1D heat conduction. In addition, volumetric heat sinks can be defined to account for details of internal structures that cannot be resolved by the fluid mesh.

AREVA NP Inc.

Applicability of AREVA NP Containment Response Evaluation Methodology to the
U.S. EPR™ for Large Break LOCA Analysis
Technical Report

ANP-10299NP
Revision 2

Page 6-166

The GASFLOW code can also be used to study steam–hydrogen distribution and combustion in complex containment geometries where the steam–hydrogen sources arise from core melt accidents. The code has been validated for hydrogen and steam transport, including validation from the HDR and the BFMC test programs. The code has also been used to analyze complex containment geometries.

6.3.2 GASFLOW Model of the U.S. EPR

GASFLOW applications require delineation of the containment to accurately predict the local atmospheric gas concentrations, especially when the steam and air concentrations are non-uniform (e.g., during the release period). For the U.S. EPR containment, the GASFLOW model consists of:

- 29 radial meshes with spacing of 0.35 – 1.3 m

- 82 axial meshes with spacing of 0.55 – 1 m

- 120 azimuthal meshes (3°).

The major components explicitly modeled are the:

- Walls (passive heat sinks)

- The steel liner (passive heat sink)

- The CONVECT system (i.e., rupture foils, convection foils, and mixing dampers)

- Access doors (non-safety-related "failure" junctions)

- Primary circuit, including main coolant lines and SGs, accumulators, pressurizer, pressurizer relief tank, and outlet pipes from the pressurizer relief tank (passive heat sinks)

- Main steam piping (passive heat sinks)

- Ventilation ducts (i.e., ventilation of the reactor cavity)

- Core melt stabilization system (spreading area)

- Polar cranes (passive heat sinks)

- Refueling machine (passive heat sinks)

- Walking grids and stairs and their supports (passive heat sinks).

The GASFLOW model does not explicitly model the IRWST pool. Rather, the IRWST is assumed to behave like a passive heat sink. This assumption is acceptable for the event simulations up to a few hours, during which the temperature in the air-space above the pool is warmed by the flow of condensate draining from all locations in the containment. Pool cooling by the LHSI heat exchanger will eventually mitigate this temperature response.

Figure 6-166 illustrates the containment geometry nodalization for the GASFLOW model of the U.S. EPR. Figure 6-167 shows the nodalization of the primary circuit. The green shading in this figure indicates "failure" junctions, and includes the CONVECT system (i.e., rupture/convection foils and mixing dampers) for transforming the U.S. EPR containment from a two-room to a one-room configuration. It also includes the doors separating rooms and interconnecting the inaccessible equipment rooms and accessible areas. Figure 6-168 presents the planer representation of the GASFLOW model. Key containment components are identified; these include the reactor, steam generators, pump room, break location, the accessible space and dome areas, and the core melt stabilization system (CMSS). The CMSS area does not have a direct flow path from the lower accessible space area or the IRWST. This figure illustrates the distributed behavior of steam concentration and temperature predicted by GASFLOW. In this view, flow through the dampers is either into or out of the graphic.
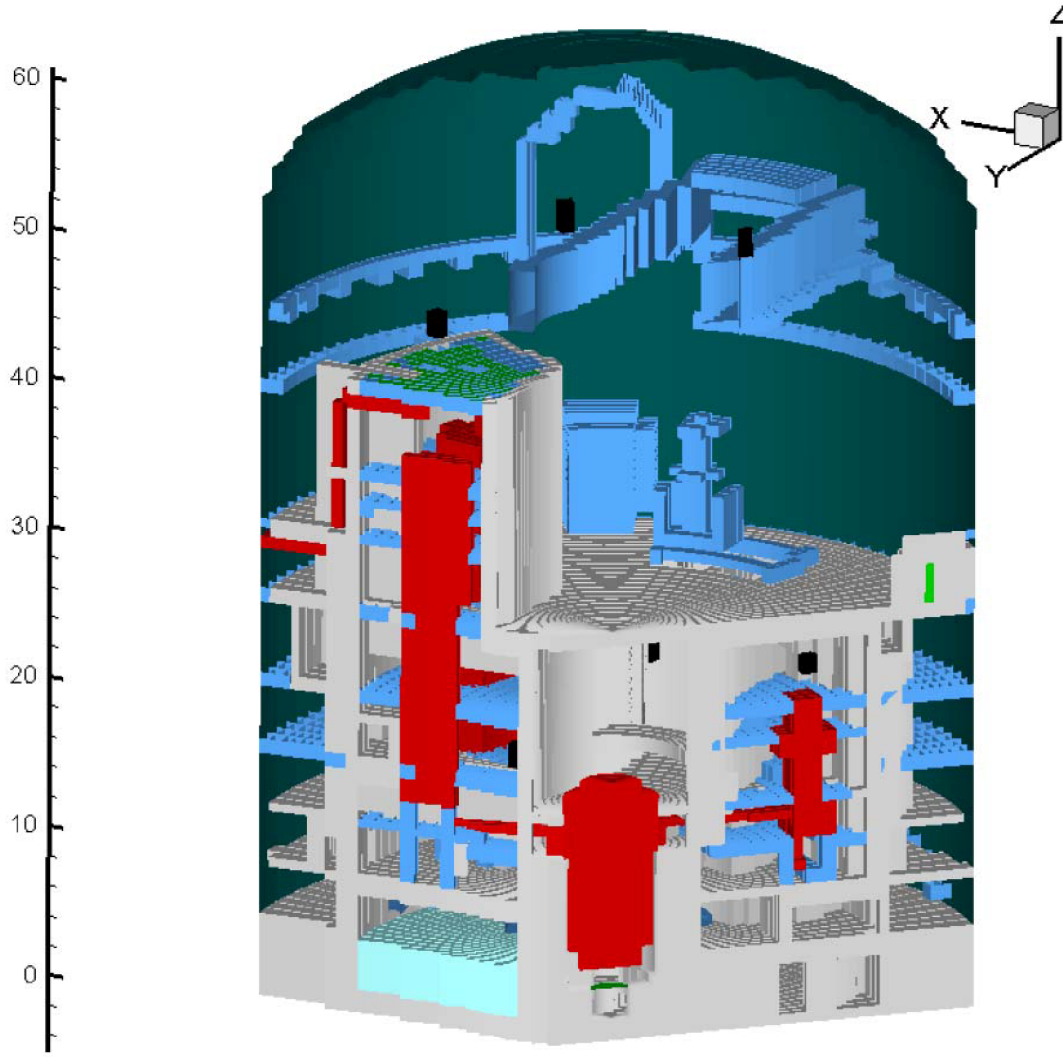
Figure 6-166–GASFLOW Delineation of the U.S. EPR Containment

AREVA NP Inc.   ANP-10299NP
Applicability of AREVA NP Containment Response Evaluation Methodology to the   Revision 2
U.S. EPR™ for Large Break LOCA Analysis
Technical Report   Page 6-169
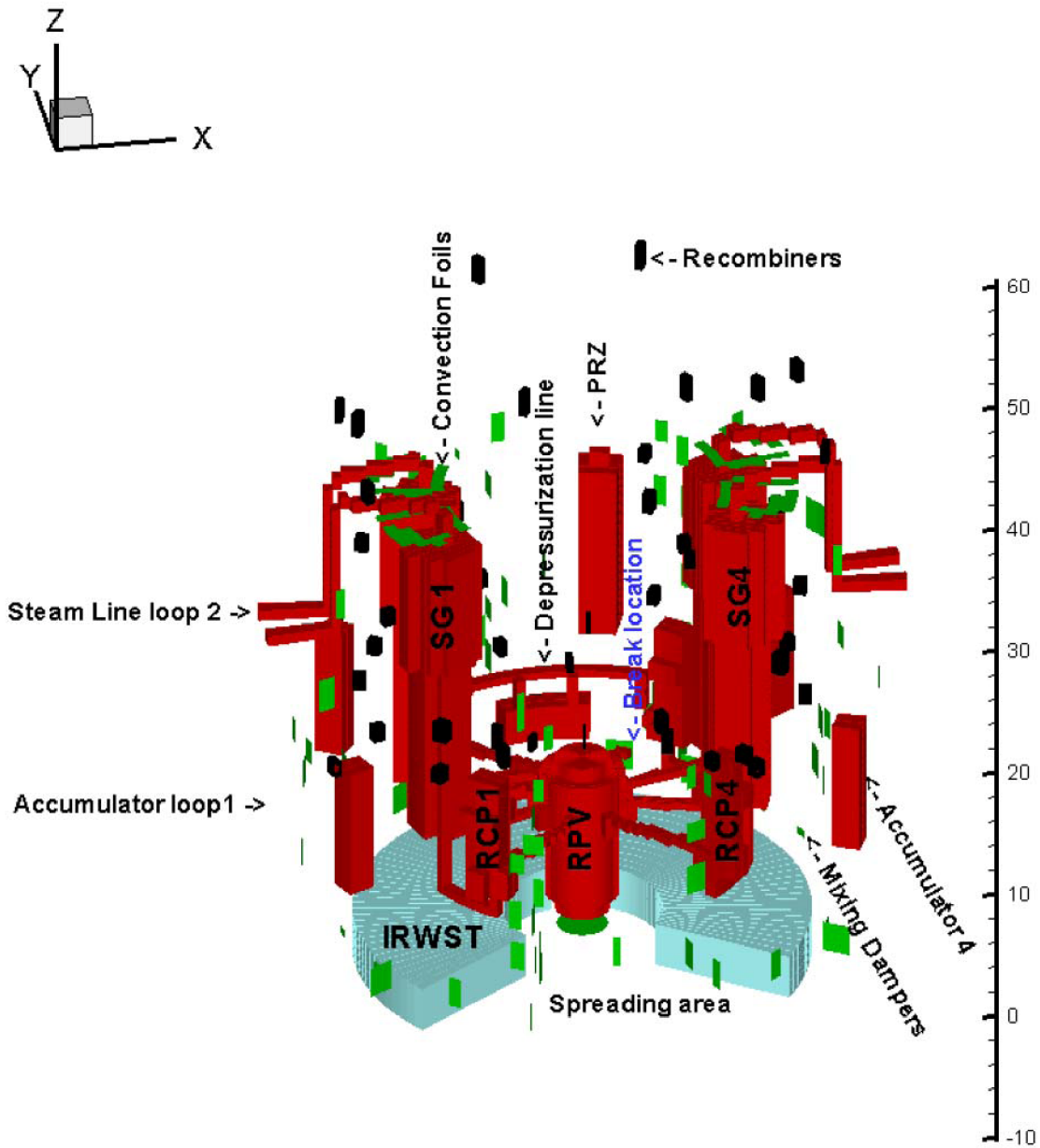
Figure 6-167–Simulated Primary Circuit
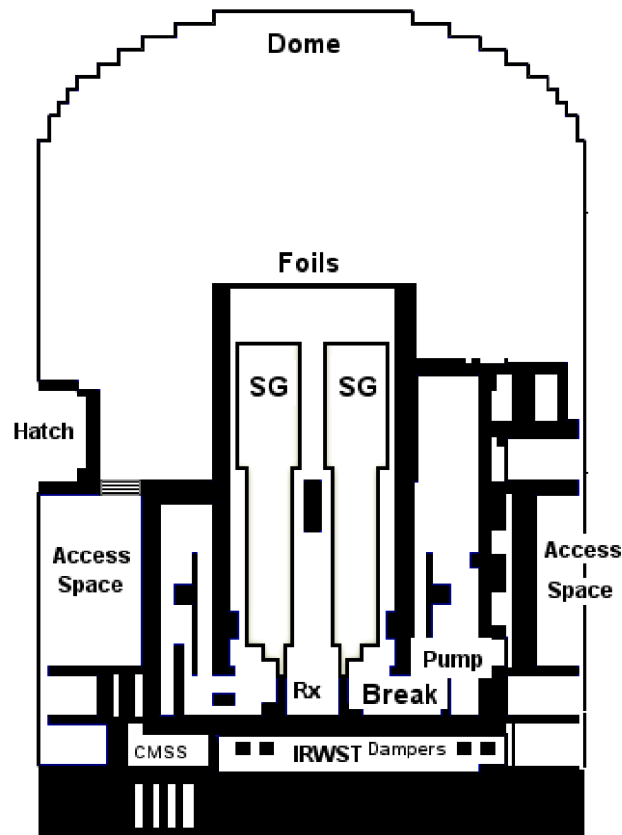
Figure 6-168–Planar Representation of the Containment

At the start of the GASFLOW calculation, all mixing dampers, rupture and convection foils, and doors are closed. At the initiation of the break event, the GASFLOW calculation uses the following initial values for the atmospheric conditions:

- Air atmosphere at 1 bar

- Temperature of the atmosphere:

    - Accessible area 30°C

    - Equipment rooms 40°C

The break location is assumed to be in the lower part of the pump room of loop 3; Figure 6-167 shows the area around the break location. Two jets are modeled to simulate the liquid and steam release rates. Nitrogen release from the accumulator nitrogen discharge is not simulated.

The applied mass and energy releases for the GASFLOW analysis were determined by a RELAP5 simulation of a cold leg pump suction break. Figure 6-169 shows the released masses of the steam and liquid water and the corresponding mass flow rates from the reactor pressure vessel side and the steam generator side, respectively.
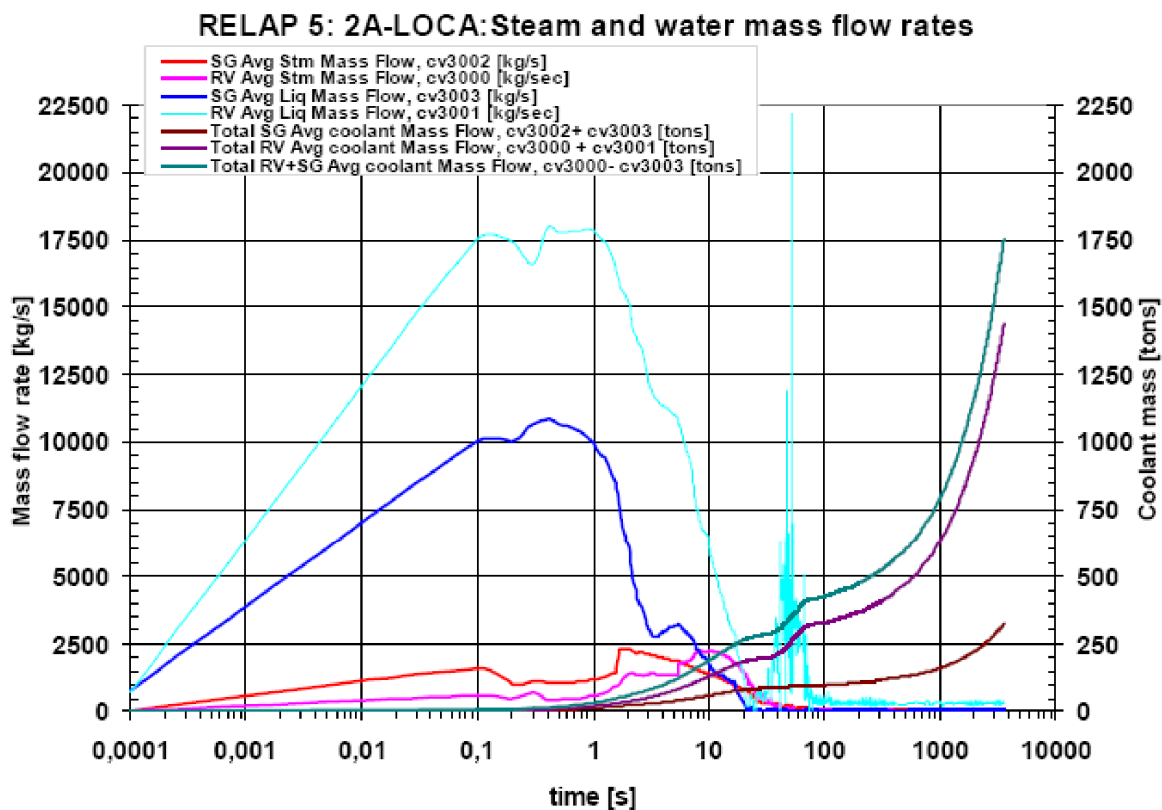
Figure 6-169—Coolant Mass Releases into the Containment

6.3.3   GASFLOW Results

The GASFLOW calculation covered the first hour following the LBLOCA initiation. Characteristic of an LBLOCA, the RCS inventory is released into the containment as a

high-energy, two-phase mixture, and the GASFLOW simulation immediately reflects the rapidly changing containment conditions. The coolant escapes from the primary system at high velocities and is considerably superheated at containment conditions. During the early blowdown phase of the LOCA, increasing amounts of steam in the containment cause a corresponding increase in containment pressure and temperature.

During normal operation, the equipment rooms surrounding the RCS are isolated from the rest of the containment. However, soon after a postulated LBLOCA, communication is established between these equipment rooms, thereby exposing the full containment volume to the two-phase effluent leaving the RCS.

The CONVECT system (see Section 2.2) transforms the containment into a single convective volume. The CONVECT system consists of rupture and convection foils in the pressure equalizing ceiling (PEC) above the equipment rooms and eight dampers at the bottom of the containment towards the air space of the IRWST. The LBLOCA-induced pressure wave and temperature increase opens a sufficiently large fraction of the PEC and the mixing dampers around the air space of the IRWST, and the GASFLOW model mechanistically simulates the opening of these flow paths.

6.3.3.1   *Steam Distribution and Convection Flows: 0 – 100 s*

In the U.S. EPR the principal containment pressure mitigating system is natural convection and condensation heat transfer to the colder containment walls. In this analysis, transformation to a single convective volume by opening the rupture foils, convection foils, and dampers exposes all containment steel and concrete surfaces to the highly concentrated steam environment created by the LBLOCA. The early phase of the LBLOCA is characterized by the release of the high-energy effluent from the plant's RCS, which pressurizes the containment. Eventually, the containment pressure equalizes with the primary system and flow through the break decreases to an equilibrium value, primarily the injected ECC water removing decay heat and some stored heat. The containment pressure begins to decrease in response to the heat transfer to the containment's passive heat sinks.

Water vapor condenses on the containment heat sinks located throughout the containment building. The condensation induces circulation zones that promote a mixed atmosphere inside the building during and after blowdown. The saturated water collects on heat sinks throughout the containment and drains along the intermediate floors, grates, stairwells, and walls to the heavy floor supporting the RCS, or to the lower accessible space areas of the containment building, before draining into the IRWST. (The water drains through holes located at the base of the lower floor in the accessible areas and in the heavy floor, first overflowing a threshold that surrounds these drain holes.)

Figure 6-170 and Figure 6-171 show the GASFLOW results for volumetric flow rates through the pressure equalization ceiling rupture foils, convection foils, and mixing dampers, respectively, for the short term phase (i.e., 0 – 100 s). The flows presented represent flow averages over particular containment regions. For example, "loop 1" flow rates are the average flow rates at the rupture/convection foils or mixing dampers associated with loop 1. "Loop 1 and 2" are the average flow rates at the rupture/convection foils or mixing dampers associated with both loop 1 and 2. "Total RF+CF" or "Total MD" is the sum of all flow across the failed rupture/convection foils and all mixing dampers, respectively.

The coolant release rates are very high at the start of the LOCA event. This produces a pressure wave with sufficient strength to open the majority of the rupture/convection foils. The dynamics of the volumetric flow rates through the rupture foils is basically the same as through the convection foils. The difference is that at 4.7 s (the time when the remaining, unopened convection foils reach the temperature required for them to open) the volumetric flow rates through the rupture foils decrease due to the opening of the remaining convection foils and the increase in the free cross-sectional area for gas flow.

An assumed five seconds delay time was modeled to address the

AREVA NP Inc.
Applicability of AREVA NP Containment Response Evaluation Methodology to the
U.S. EPR™ for Large Break LOCA Analysis
Technical Report

ANP-10299NP
Revision 2

Page 6-174

time required for the mechanical operation of the mixing dampers. The initial pressure wave is also strong enough to open many doors between rooms, particularly those located near the break, further increasing the venting area.

The flow direction through the pressure equalization ceiling is from the equipment rooms to the containment dome. Similarly, the flow direction through the mixing dampers is from the equipment rooms, via the IRWST air volume, to the lower part of the annular areas. In both cases the flow is asymmetric, and depends on the proximity of the damper or foil to the break (located in loop 3). As expected, flows from the equipment rooms containing loops 3 and 4 are much higher than the flows from the equipment rooms containing loops 1 and 2. Because of the much larger flow area appearing in the pressure equalization ceiling, the majority of the break effluent flows upward through this area.
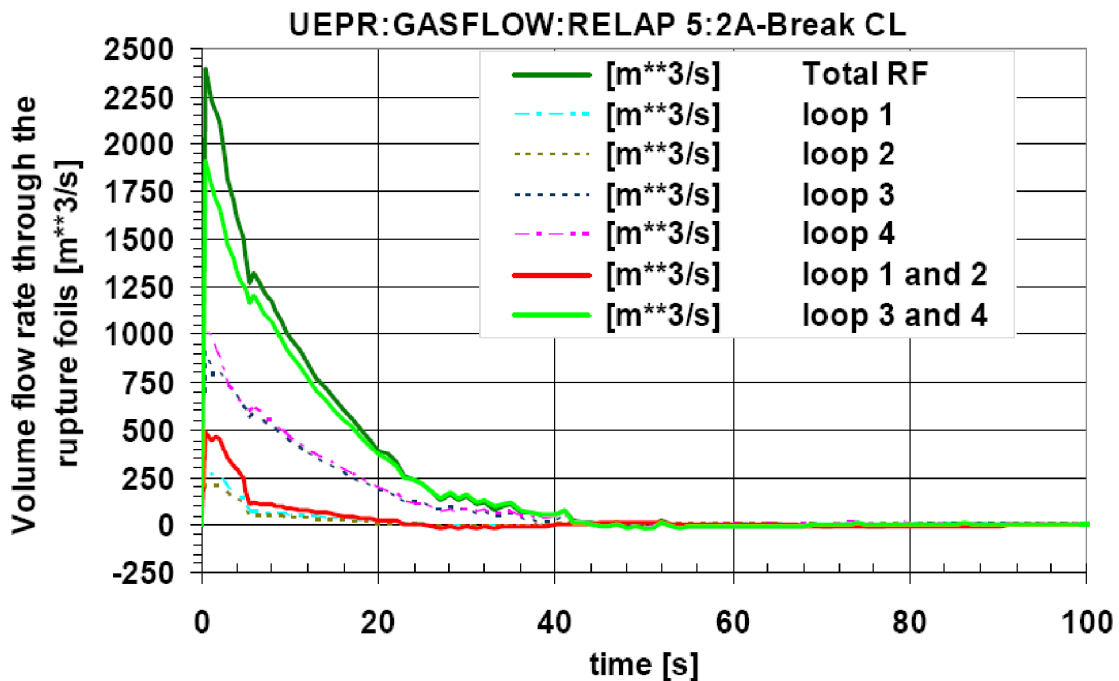
Figure 6-170—Short-Term Volume Flow Rates Through the PEC

AREVA NP Inc.

Applicability of AREVA NP Containment Response Evaluation Methodology to the
U.S. EPR™ for Large Break LOCA Analysis
Technical Report

ANP-10299NP
Revision 2

Page 6-175
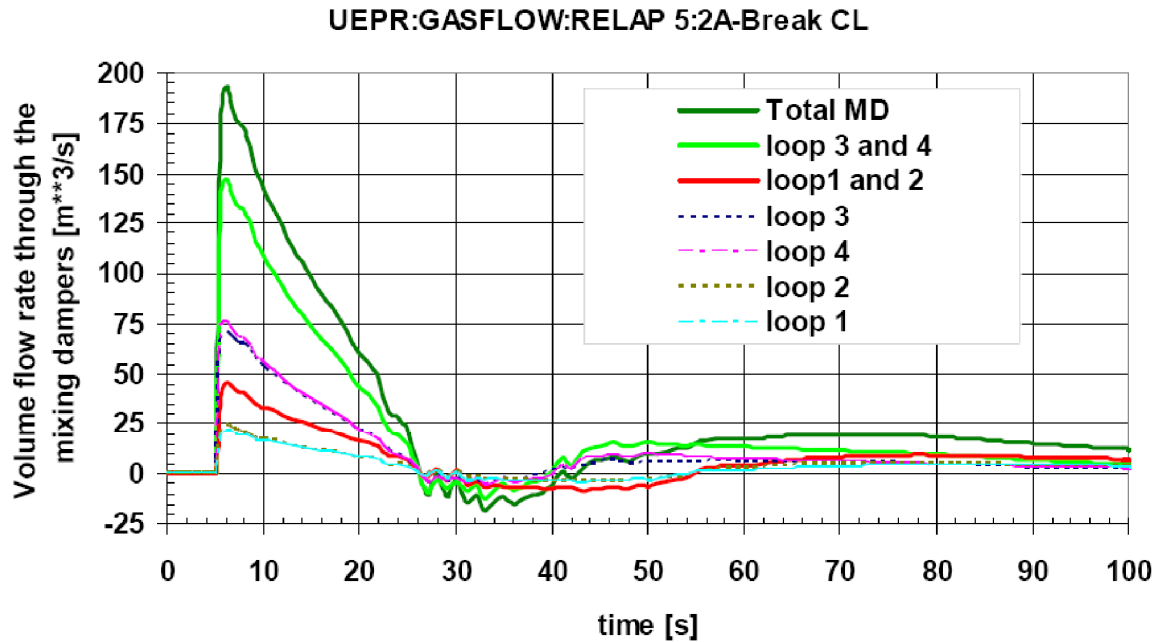
Figure 6-171—Short-Term Volume Flow Rates Through the Mixing Dampers

Figure 6-172 shows the steam and temperature distributions in the containment at one, 10, and 30 s, respectively. The areas of bright red indicate high steam concentration or temperature, and areas of bright blue indicate low steam concentration or temperature. The progression of the steam and temperature distribution reinforces the observations from Figure 6-170 and Figure 6-171. Specifically, the propagation of the high-energy break effluent originating in a lower equipment room and moving to the broader containment via the principal CONVECT system components (i.e., rupture/convection foils and mixing dampers). Flow through the pressure equalization ceiling appears as two jets delivering steam directly towards the uppermost part of the dome, and from there disbursing in all directions. By 30 s all areas of the containment have experienced the consequences of the LBLOCA. Figure 6-172 also shows that during the event's early phase, the highest gas temperatures occur in the non-accessible area. This high-temperature steam propagates to the dome and the lower part of annular area (the level of the mixing dampers) while the lowest gas temperature occurs in the annular area at the level of the break location.
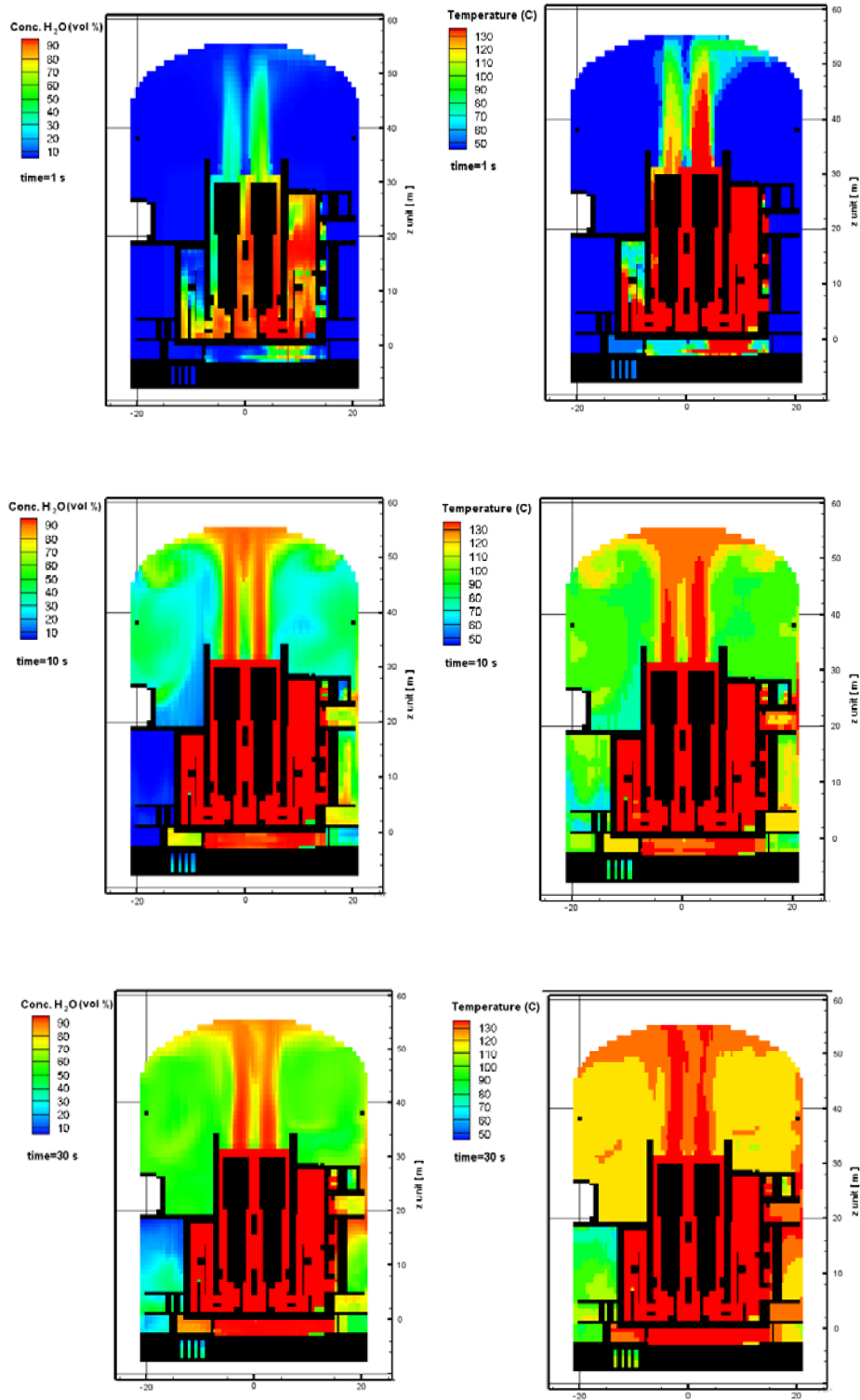
Figure 6-172—GASFLOW Steam and Temperature Distributions (0 – 30 s)

6.3.3.2   Steam Distribution and Convection Flows: 100 – 3600 s

Figure 6-173 and Figure 6-174 present the GASFLOW results for volume flow rates through the pressure equalization ceiling and mixing dampers, respectively, from 100 s to the end of the calculation at 3600 s. By this time the mass and energy release for the reactor coolant system is significantly less than it was during the early phase of the LOCA event. For the majority of this simulation, the flow direction continues to be from the equipment rooms and the IRWST towards the accessible space, indicating that the accessible space remains at a slightly lower pressure than the equipment rooms much longer than just through the early blowdown phase. This is a consequence of continuing condensation on the relatively cooler steel and concrete surfaces in this area.

Unlike the early phase of the LBLOCA, the flowrates through the PEC and the mixing dampers do not provide a complete view of atmospheric mixing. At these lower flow rates several secondary circulation paths appear and become important. These result from asymmetries produced by the LOCA, which are modeled in the simulation both as initial conditions and from the asymmetric opening of "failure" junctions (i.e., foils and doors). From about 200 – 500 s, a circulation path is established in which effluent passes through the PEC above loops 1 and 2 and drafts down and back through the mixing dampers associated with those two loops. Meanwhile, the average flow through the PEC above the break (i.e., loops 3 and 4) essentially stagnates. There is some steam flow from the equipment room surrounding the break into the air space above the IRWST, which then passes through the mixing dampers associated with loops 3 and 4. This unusual "reverse" circulation pattern is offset by a flow circulation pathway from the equipment room housing loop 3 to the accessible space. This pathway is created by the opening of several doors because of the initial pressure wave. This circulation path can be inferred from the steam and temperature distribution presented in Figure 6-175. Other circulations pathways created by the LOCA-induced opening of doorways are also present.

Beyond 1000 s the dominant flow is from the air space above the IRWST to the accessible space. This may be, in part, an artifact of the simplified modeling of the IRWST as an un-cooled passive heat sink. Condensate draining from all locations in the containment into the IRWST causes warmer liquid to stratify on top of the cooler initial pool inventory. Therefore, for the time period simulated, the IRWST space is relatively warmer than neighboring regions. Cooling of the IRWST pool by the LHSI heat exchangers takes time and might be more evident in the long-term.

The overall flow through the rupture- and convection-foils is very small. A secondary circulation is apparent at this elevation between the loops 1 and 2 and loops 3 and 4 equipment rooms. The flow dynamic at the pressure equalization ceiling is influenced by secondary circulation pathways created by the opening of access doorways. As shown in Figure 6-175, the steam and temperature distribution becomes more homogenous with time, indicating ongoing atmospheric mixing. Such secondary circulation pathways support the local atmospheric mixing and the role of the CONVECT system to guarantee a minimum open area between the accessible space region and the inaccessible equipment rooms required to provide sufficient atmospheric mixing.
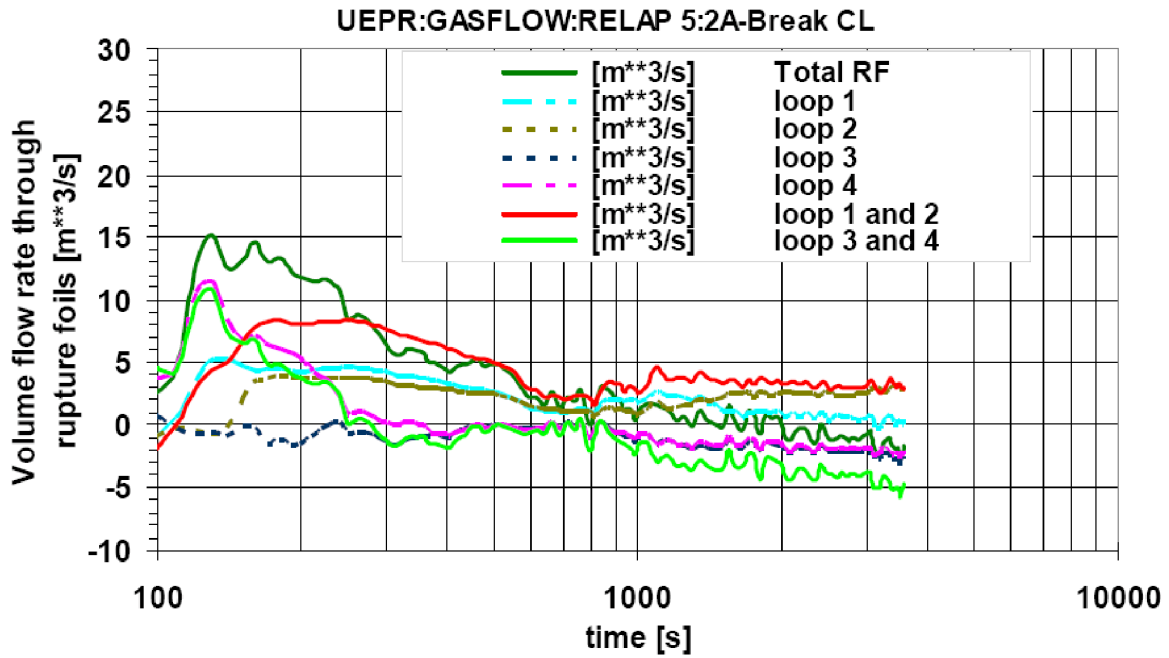
Figure 6-173—Long-Term Volume Flow Rates Through the PEC
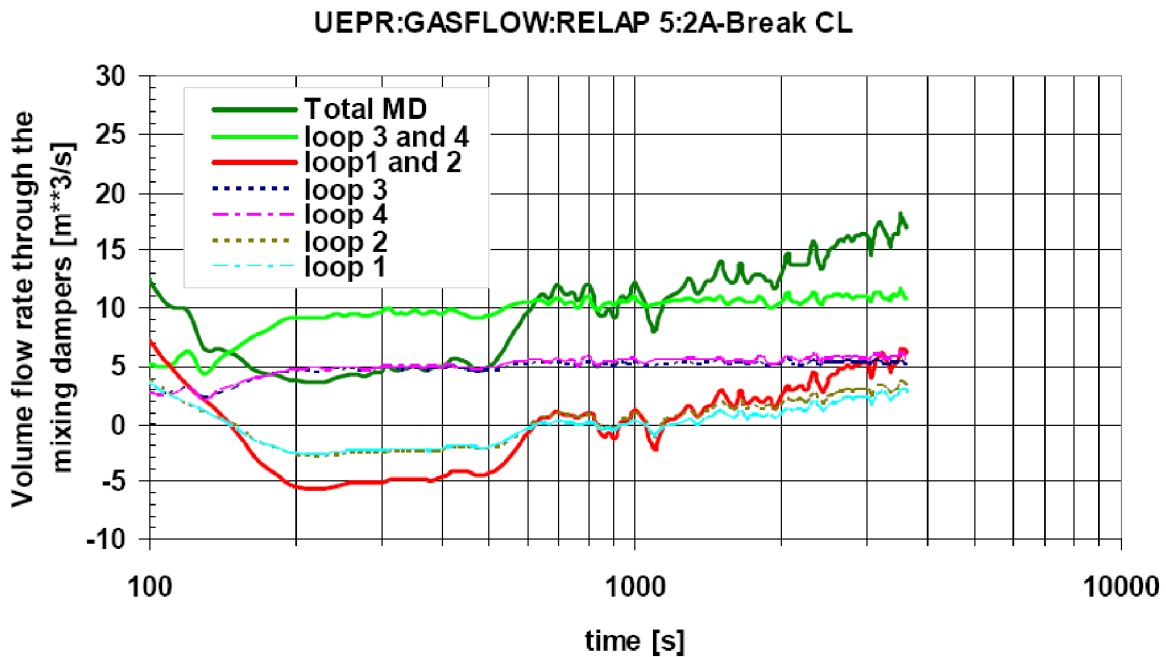
Figure 6-174—Long-Term Volume Flow Rates Through the Mixing Dampers
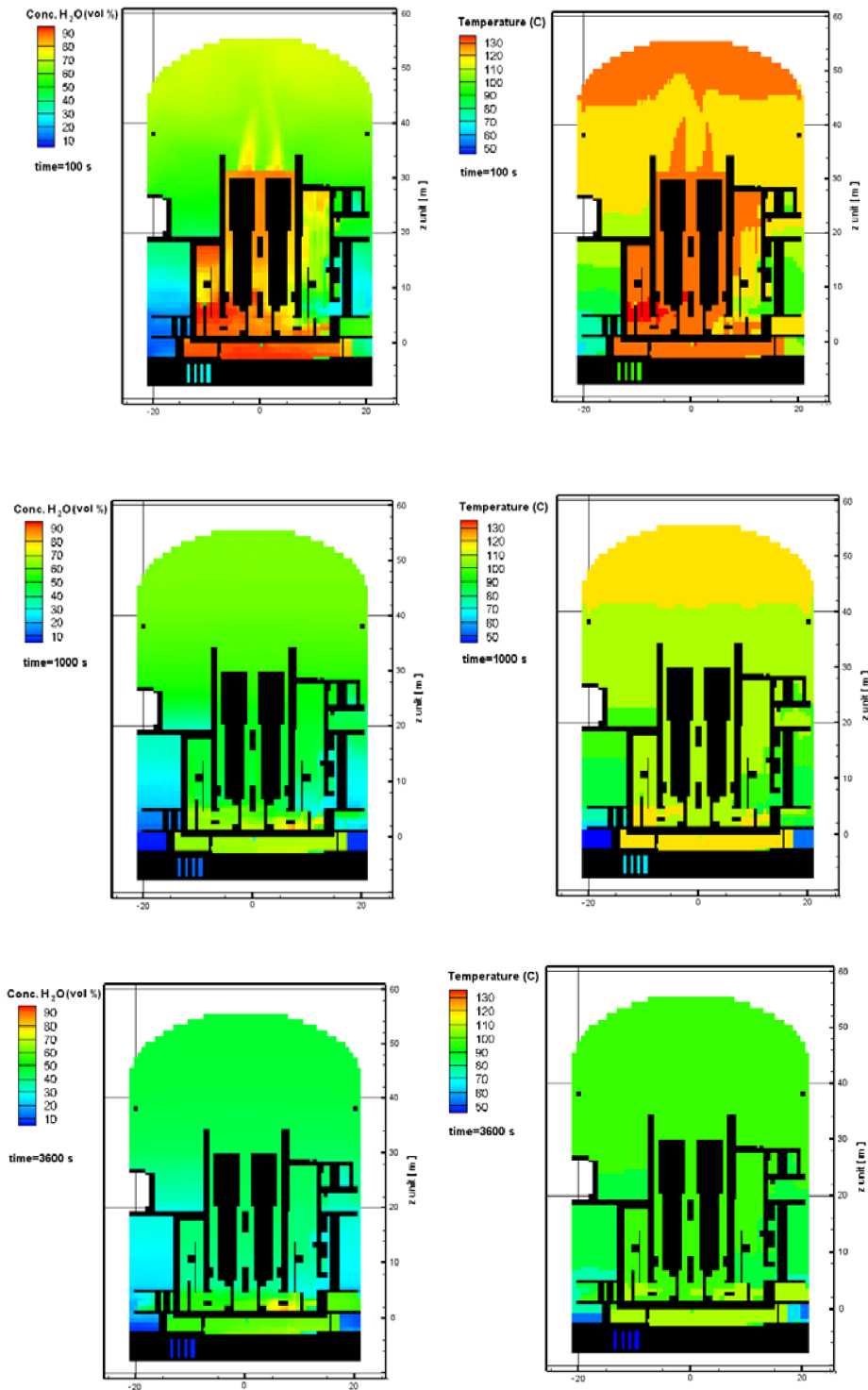
Figure 6-175—GASFLOW Steam and Temperature Distributions (100 – 3600 s)

6.3.3.3   Global Pressure, Temperature, and Steam Concentration

Figure 6-176 shows the GASFLOW prediction the containment pressure response. The mixing dampers open and a portion of the rupture foils and convection foils open immediately after initiation of the event.

The maximum containment pressure is about 3.2 bar (47 psia) and it occurs 43 s after event initiation. By the end of the calculation at one hour, containment pressure has decreased to about 1.95 bar (28 psia).
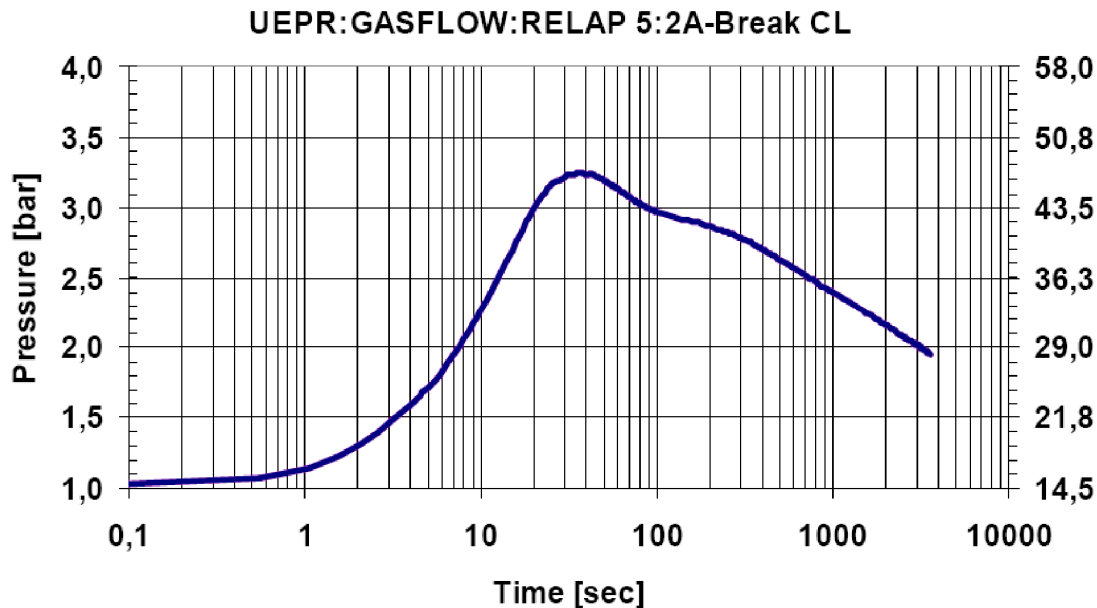
Figure 6-176—GASFLOW Prediction of Containment Pressure

Figure 6-177 shows the GASFLOW prediction of the average atmosphere temperature in the containment. The maximum average gas temperature is about 138°C (280°F) and occurs within two seconds of break opening. It reduces to about 93°C (200°F) by the end of the calculation at one hour.

UEPR:GASFLOW:RELAP 5:2A-Break CL
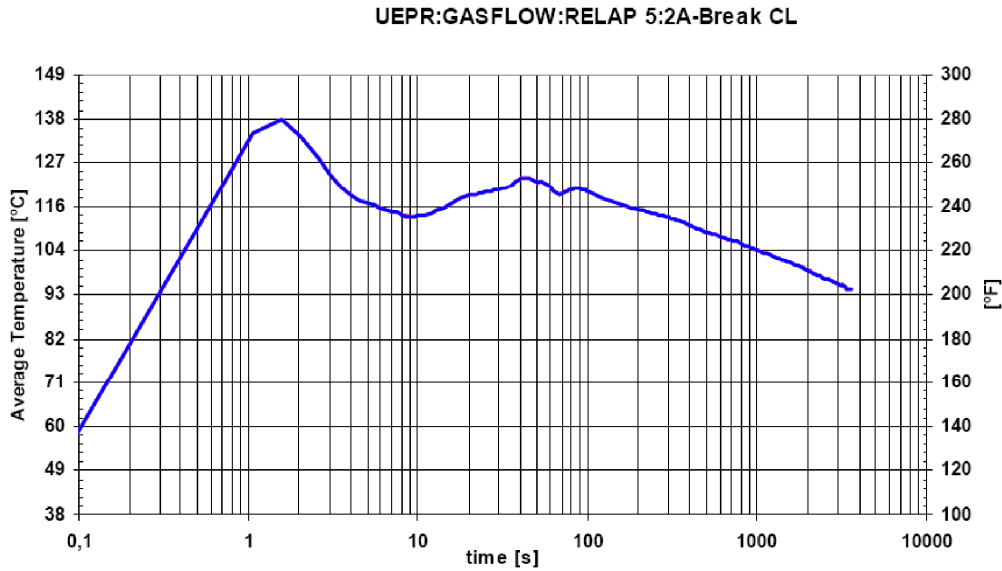
Figure 6-177—GASFLOW Prediction of Average Containment Temperature

Figure 6-178 shows the average steam volume concentration in the containment. The maximum average steam volume concentration of about 61 volume percent occurs 36 s after the break opening. It decreases to about 40 volume percent by the end of the calculation atone hour.

UEPR:GASFLOW:RELAP 5:2A-Break CL
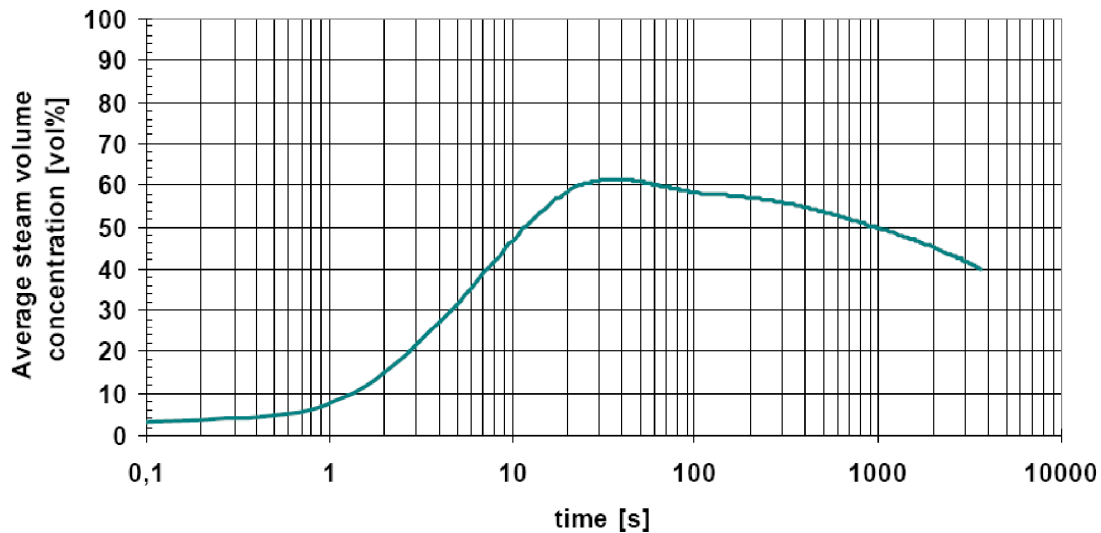
Figure 6-178—GASFLOW Prediction of Average Containment Steam Concentration

6.3.4   Conclusions

A best-estimate LOCA containment pressure response calculation was performed for the U.S. EPR using the 3D containment analysis code GASFLOW. The mass and energy release used for the GASFLOW analysis was calculated with RELAP5, applying conservatisms consistent with the NRC's Standard Review Plan. The analysis demonstrates that:

- All mixing dampers open within five second of break initiation

- Convection flows are established through all SG compartments

- The primary direction flow for most of the simulation was from the break location to the dome via foils, and to the lower part of the annular area via the IRWST

- Secondary circulation developed via access doorways

- Strong stratification of the steam occurred locally during the blow down phase

AREVA NP Inc.

ANP-10299NP

Applicability of AREVA NP Containment Response Evaluation Methodology to the

Revision 2

U.S. EPR™ for Large Break LOCA Analysis

Technical Report

Page 6-184

- After 10 minutes, moderate stratification of the steam develops in almost the entire containment

- There is sufficient steam for condensation on the surface of the structures at any time during the break event

- Highest gas temperature occurs in the non-accessible areas

- Low gas temperature differences predominate in the containment in the long term.

- Steam is distributed well throughout the entire containment

- Containment pressure remains below the design pressure.

6.4   Scalability of Data (EMDAP 19)

All integral tests and some of the separate-effects tests are scaled. These tests are scaled to preserve certain features of the full-scale phenomena. For this reason, tests with different scaling are used to address different phases of an LBLOCA. If a test is considered appropriately scaled for the phenomena of interest, then code assessment conclusions are considered applicable to the full-scale nuclear power plant.

The test facilities supporting the PIRT span a scaling range of 1:1500 to 1:1. In addition, some specific tests were performed as a counterpart to tests performed in other facilities. Where data were available, these tests were included in the assessment matrix.

The principal purpose of the assessment base for AREVA NP's containment response evaluation methodology is to asses the ability of RELAP5-BW and GOTHIC to predict the important phenomena in the U.S. EPR design. As previously discussed, both of these codes have been individually assessed to support their application to LBLOCA analysis (References 19 and 20, respectively). Both RELAP5-BW and GOTHIC were used to simulate a large variety of tests. These tests are a significant portion of the basis for the containment analysis evaluation methodology. In general, the credibility of

the analysis codes and the evaluation methodology is enhanced with every additional validation exercise. Collectively, the common trend of good or conservative agreement over this large assessment knowledge base addresses the closure and scalability of models, and thus covers the domain of nuclear power plant operational and accident conditions.

7.0   UNCERTAINTY ANALYSIS

Application of the NRC's Standard Review Plan (SRP) for containment analysis of an LBLOCA imposes several conservatisms on the more important containment thermal-hydraulic phenomena that occur during an LBLOCA. Performing an uncertainty analysis quantifies the overall conservatism in this very conservative approach. The general analytical methodology for preparing the U.S. EPR containment response uncertainty analysis is Code Scaling, Applicability and Uncertainty (CSAU) (Reference 16). Parameters considered in an uncertainty analysis are defined by a range of values that bounds the expected value of the parameter. This range should bound sources of uncertainty such as inherent drift, measurement error, incompleteness, and model error. The set of sensitivity parameters and the quantification of their uncertainty ranges comprise the uncertainty domain.

The baseline for the uncertainty analysis is a GOTHIC model that reflects a reference plant state. The reference plant state describes a plant at nominal operating conditions responding in a best-estimate manner. To reduce the scope of the uncertainty analysis, some parameters are treated deterministically through conservative biasing. This baseline GOTHIC model uses a combination of realistic and conservatively biased parameters to describe the containment geometry, initial and boundary conditions, and the sequence of events.

The event assessed in the uncertainty analysis is a double-ended guillotine break occurring in the cross-over leg between the SG and the RCP. One train of the ECCS is assumed to be out of service for maintenance. Three ECCS trains of pumped injection and four accumulators are available to mitigate the event. Three LHSI heat exchangers are available for cooling the IRWST inventory. At 90 minutes into the event, the operators realign the LHSI from their respective cold legs to their hot legs. Offsite power is assumed to be available during the entire event.

7.1 Quantify Phenomenological Uncertainties (EMDAP Step 9)

For an uncertainty analysis, the quantification of phenomenological uncertainties involves identifying the important code input parameters and determining their domain of state. This begins with identifying the important containment phenomena through a process such as the PIRT presented in Section 3.0. For the U.S. EPR containment response uncertainty analysis, the quantification of phenomenological uncertainty also considered two other sources: the GOTHIC user-specified modeling options (as described in Section 8.3.1.2) and the complete containment response uncertainty analysis and importance study presented in Reference 78. A review of these sources provides more completeness from an independently-performed assessment and quantification of important containment modeling parameters. The study in Reference 78 was performed by the Gesellschaft fur Anlagen- und Reaktorsicherheit (GRS) in Garching, Germany, using data from the HDR T31.5 Test (Reference 67). Reference 78 provides a useful model for performing the U.S. EPR containment response uncertainty analysis.

7.1.1 U.S. EPR Containment Response PIRT

The U.S. EPR containment response PIRT presented in Section 3.4 identifies the following important phenomena for containment pressure response (includes relative ranking):

- Convective Heat Transfer (with condensation/evaporation) – High

- Structure conduction – High

- Pool (IRWST) free convection (condensation/evaporation) – High

- Expansion/compression of multi-component gases – Medium

- Blowdown/Spray (includes entrained liquid droplets exiting RCS) – Medium

- Intercompartment transport by buoyancy – Medium

- Local buoyancy/stratification – Low/Medium

- Liquid advection (transport only) – Low/Medium.

Based on this PIRT result, Table 7-1 lists the GOTHIC code model parameters requiring assessment to describe important phenomena.

Table 7-1—Relevant Model Parameters for Containment Pressure Response

Phenomena	Model Parameters
Free convection (condensation/evaporation)	Convection and condensation heat transfer coefficients
Structure conduction	Material properties (specific heat, thermal conductivity, material density, gap thickness, structure surface area), temperature initial condition
Pool (IRWST) free convection (condensation/evaporation)	Convection and condensation heat transfer coefficients; pool surface area; heat exchanger process model parameters
Expansion/compression of multi-component gases	Containment initial conditions: volume, pressure, temperature, and humidity; mist auto-conversion threshold (maximum mist density); accumulator nitrogen mass
Blowdown/Spray	Droplet size and containment initial conditions
Intra- and Inter-compartment buoyancy/stratification	Flow resistances, containment internal geometry, break location (total structural surface area in contact with well-mixed atmosphere)
Liquid advection	Water entrainment, revaporization fraction

7.1.2   Containment Analysis Evaluation Methodology Considerations

AREVA NP's containment analysis evaluation methodology (see Section 8.0) identifies several run options and boundary conditions that define how GOTHIC is used to perform design basis containment analysis in accordance with the NRC's SRP. Table 7-2 identifies the NRC SRP guidelines, code options, and boundary conditions that are addressed in the uncertainty analysis. The default parameters in the original methodology are retained unless identified as an important uncertainty parameter for containment analysis.

Table 7-2—Treatment of Important GOTHIC Run Options and Boundary Conditions

GOTHIC Option	SRP Methodology Default	Uncertainty Analysis
Blowdown droplet size	100 microns	Explicitly treated, see Section 7.1.4.5
Phase separation	BE estimate of flashing of M&E blowdown to the saturation temperature at the containment steam partial pressure	Use methodology default
Revaporization fraction	LBLOCA: GOTHIC interface heat and mass transfer models	Use methodology default
Spray droplet size	Use spray droplet size from spray nozzle vendor specification.	N/A for U.S. EPR
Wall condensation heat transfer	For LOCA, Tagami / Uchida or MDLM (with NRC restrictions) wall condensation heat transfer models	Explicitly treated, see Section 7.1.4.1.2
Fog model	FOG model OFF (MIST model activated)	Use methodology default
Maximum mist density	Default input ($1 g/m^3$)	Explicitly treated, see Section 7.1.4.4.5
Drop diameter from mist	Default input (200 microns)	Use methodology default
Minimum heat transfer coefficient	0.0	Use methodology default
Reference pressure	IGNORE	Use methodology default
Forced entrainment drop diameter	N/A (arbitrarily set to default input)	Use methodology default
Vapor phase head correction	INCLUDE	Use methodology default
Kinetic Energy	IGNORE	Use methodology default
Vapor, Liquid, and Drop phases	INCLUDE	Use methodology default
Force equilibrium	IGNORE	Use methodology default
Drop-liquid conversion.	INCLUDE	Use methodology default

AREVA NP Inc.

ANP-10299NP

Applicability of AREVA NP Containment Response Evaluation Methodology to the

Revision 2

U.S. EPR™ for Large Break LOCA Analysis

Technical Report

Page 7-5

7.1.3 Previous Work: GRS Uncertainty Analysis for HDR T31.5

An uncertainty analysis performed by the GRS (Reference 78) produced a useful method for performing the containment response uncertainty analysis for the U.S. EPR. The GRS approach is similar to AREVA NP's other best-estimate-plus-uncertainty methodologies for LBLOCA (Reference 79) and severe accidents (Reference 80). As for any uncertainty analysis, the GRS study identifies a set of model parameters and associated uncertainty ranges.

In the GRS analysis, the COCOSYS code (Reference 81) was used to model HDR Test T31.5 (Reference 67). The experiment T31.5 lasted 20 hours; however, only the first 20 minutes of the experiment reflected conditions typical of a design-basis LBLOCA. Seventy-nine containment model parameters or parameter groups were characterized and utilized in the GRS's Software System for Uncertainty and Sensitivity Analyses (SUSA) methodology for evaluating phenomenological importance through code simulations (Reference 82). Of interest to the U.S. EPR uncertainty assessment task are the particular modeling parameters considered in the GRS study and the corresponding uncertainty ranges and distributions. These were based on engineering judgment. Table 7-3 presents the uncertainty ranges employed by the GRS for the high rank phenomena identified in Section 7.1.1. The GRS also quantified and incorporated the uncertainty in compartment geometry, junction flow resistance, liquid mass, diffusion constants, and water entrainment. These parameters were sampled within a band of either +/- 10% or +/- 20%.

Table 7-3—Summary Description of GRS Uncertainty Analysis Parameters

Description	Uncertainty Ranges
Free Convection and Condensation Heat Transfer	+/- 50%
Forced Convection Heat Transfer	+/- 100%
Material Properties – Steel	+/- 10%
Material Properties – Concrete	+/- 30%
Structure Geometry – Surface Area	+/- 30% (max)
Structure Geometry – Material Thickness	+/- 30%

Using the SUSA software, values for these parameters were chosen randomly according to the specified probability distributions, COCOSYS code inputs were created to perform 200 calculations. The GRS analysis showed the effect individual parameters have on the total uncertainty of the principal figures-of-merit (i.e., containment pressure among others considered).

The GRS performed three analyses, each of which evaluated 200 random samples. Triangular distributions were applied to the data in one set. Uniform distributions were applied to the other two. The triangular distribution produced a concentration of results around the reference values. In the second set, the ranges and distributions of the model parameters were only specified in one direction, from nominal to the smaller limit. In the third set, the ranges of distribution of the model parameters were specified uniform to over the defined range. While model parameter uncertainty ranges were quantified using engineering judgment, The GRS believed they were varied within physically meaningful boundaries. All calculations were executed without error and without interruption over the entire calculated time span.

The application of the SUSA methodology identified the following important model parameters:

1. Influencing the short-term response (i.e., through the blowdown peak):

- Free convection

- Forced convection

- Condensation.

2. Influencing the long-term response:

- Thickness of the liner

- Surface area of the liner

- Heat capacity of the concrete structures.

AREVA NP Inc.

Applicability of AREVA NP Containment Response Evaluation Methodology to the
U.S. EPR™ for Large Break LOCA Analysis
Technical Report

ANP-10299NP
Revision 2

Page 7-7

A measure of the appropriateness of the set of uncertainty parameters and ranges is that the resulting pressure response range is nearly equivalent to the range of pressure response results reported by ISP-23 participants. Specifically, Reference 83 reported that for the medium-term (50 seconds) and long-term (1,200 seconds) analysis, the majority of the containment pressure predictions ranged between 87% – 110% and 90% – 137% relative to test data, respectively. Ignoring the apparent bias to over-predict the pressure response, an appropriate uncertainty range based on the ISP results is +/- 10%. In the GRS study, 200 calculations sampling 79 model parameters were performed using the COCOSYS code. Figure 7-1 presents the results of the uncertainty analysis by identifying the 95% coverage/95% confidence estimate of the combined influence of all considered uncertainties on the calculated pressure.

◇ Experiment CP409
● Reference calculation
■ Lower limit
▲ Upper limit
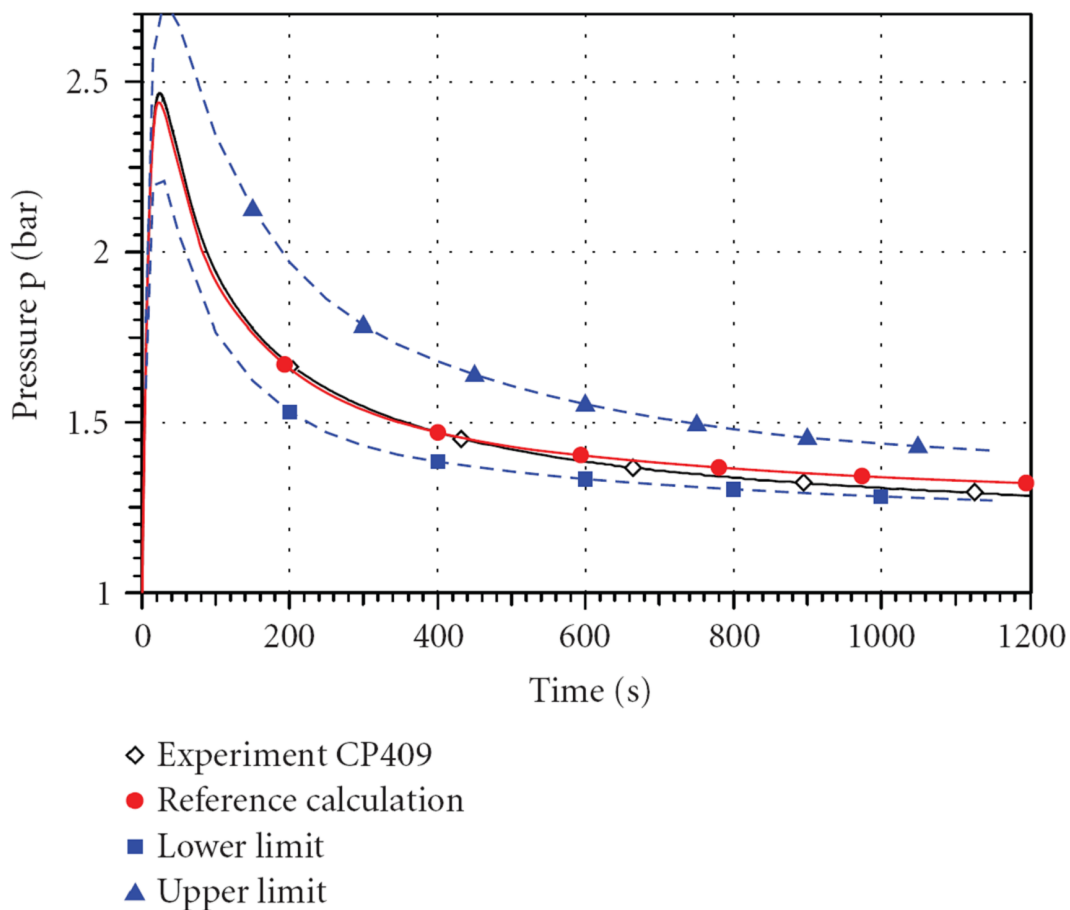
Figure 7-1—HDR Test T31.5 Containment Pressure Response

Given the similarity between the total containment pressure uncertainty range predicted by ISP 23 participants and that from the GRS study, it follows that the set of containment model parameters evaluated as being important, and their associated uncertainty ranges, are sufficiently characterized for the expected uncertainty range. Because no new phenomena are introduced beyond the 1200 s timeframe, this conclusion extends indefinitely.

7.1.4   Assessment of Uncertainty Ranges

This section characterizes the uncertainty ranges of important GOTHIC model parameters identified in Section 7.1.1. Unless otherwise stated, the probability distributions for the derived uncertainty ranges are chosen subjectively to be uniform unless otherwise stated. Uniform distributions are generally regarded to be conservative because the more limiting values of model parameters tend to appear near the extremes of the uncertainty range. Uniform distributions increase the likelihood of sampling close to the extremes.

The model parameters are assessed using the single-node GOTHIC model. The conclusions from this analysis are applicable to the multi-node model because the major model parameters are either modeled explicitly or biased in a conservative manner.

7.1.4.1   Convective Heat Transfer

The phenomena associated with convective heat transfer considered for the uncertainty analysis are free and forced convection and structure wall condensation.

7.1.4.1.1   Free and Forced Convection

Without explicit modeling of fluid flow in the single-volume GOTHIC model, forced convection is inherently neglected. The general correlation for free convection on a vertical plate (Reference 77) is applied. These assumptions are considered conservative biases (i.e., cause higher pressure) in the follow-on uncertainty analysis.

AREVA NP Inc.
Applicability of AREVA NP Containment Response Evaluation Methodology to the
U.S. EPR™ for Large Break LOCA Analysis
Technical Report

ANP-10299NP
Revision 2

Page 7-9

7.1.4.1.2   Structure Wall Condensation

AREVA NP's containment response methodology uses the Uchida correlation. In Reference 31, the implementation of the Uchida model in the GOTHIC code was assessed as illustrated in Figure 7-2. Reference 31 does not identify an uncertainty range other than the +/- 20% bounds. Using the bounds as a reference, the uncertainty range is approximately +/- 50%, consistent with the uncertainty range used in the GRS analysis.
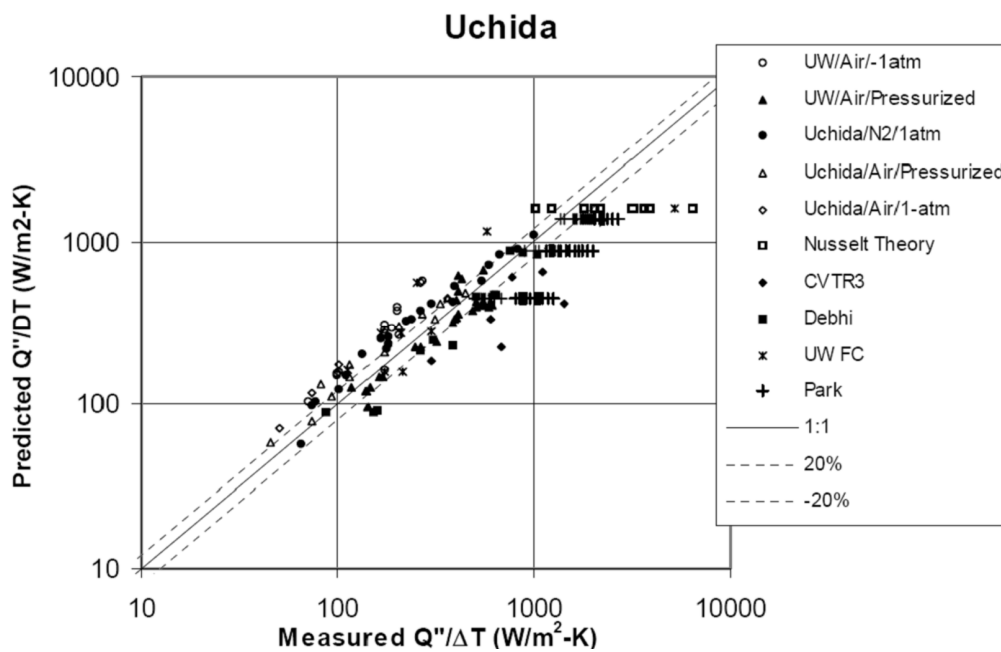
Figure 7-2—Uchida Assessment Results

7.1.4.2   Structure Material Properties

The structure material properties considered for the uncertainty analysis are the intrinsic material properties (i.e., heat capacity, heat conductance, and material density) and liner/concrete gap conductance.

AREVA NP Inc.
ANP-10299NP
Applicability of AREVA NP Containment Response Evaluation Methodology to the
Revision 2
U.S. EPR™ for Large Break LOCA Analysis
Technical Report
Page 7-10

7.1.4.2.1   Intrinsic

Table 7-4 shows the specific material property values used in the U.S. EPR FSAR analysis. Material property uncertainty is small; however, variations in manufacturing can introduce differences. The GRS study shows that material properties have a strong effect on containment pressure response. Given the good agreement between the total uncertainty range evaluated by the GRS and the expected calculated uncertainty range evaluated in ISP 23, the uncertainty ranges for the intrinsic material properties are adopted from the GRS analysis as shown in Table 7-5.

Table 7-4—Nominal Material Properties for Steel and Concrete

Material	Heat Capacity, C_p		Thermal Conductivity, K		Density, ρ	
	BTU/lbm-°F	J/kg-K	BTU/ft-hr-°F	W/m-K	lbm/ft^3	kg/m^3
Stainless Steel (liner)	0.11942	500	9.249	16	490	7850
Carbon Steel (other)	0.11942	500	26.012	45	490	7850
Concrete	0.22928	960	1.012	1.75	150	2400

Table 7-5—Uncertainty ranges for steel and concrete

Parameter	Uncertainty Range for Steel	Uncertainty Range for Concrete
Heat capacity	10%	30%
Heat conductance	10%	30%
Material density	10%	20%

7.1.4.2.2   Liner/Concrete Gap Properties and Thickness

Table 7-6 shows the specific material property values for the liner/concrete air gap used in the U.S. EPR FSAR analysis. The U.S. EPR FSAR analysis used a conservative value of 3 mm for the air gap thickness over 100% of the liner surface. A best-estimate value of the air gap thickness of 3 mm is 7.5% of the liner surface. This reflects the fact that the reactor building concrete is poured with the liner already in place. For the

simplified GOTHIC model, an effective best-estimate value is 0.225 mm, the product of 3mm and 7.5%. The best-estimate and analysis values for the liner gap thickness present endpoints for a conservative and, therefore, appropriate uncertainty range.

Table 7-6—Nominal Liner/Concrete Air Gap Properties

Material	Heat Capacity, Cp		Thermal Conductivity, K		Density, ρ	
	BTU/lbm-°F	J/kg-K	BTU/ft-hr-°F	W/m-K	lbm/ft^3	kg/m^3
Air gap	0.23979	1004	0.0162	0.028	0.0738	1.182

7.1.4.3   Pool Free Convection

The phenomena associated with the pool (IRWST) free convection considered for the uncertainty analysis are the IRWST condensation/evaporation and the LHSI heat exchanger performance.

7.1.4.3.1   IRWST Condensation/Evaporation

Considering the single volume nodalization applied in GOTHIC uncertainty studies and the thermally non-homogeneous conditions anticipated during the LBLOCA event, justification of the quantification of the interfacial heat transfer uncertainty is difficult. The uncertainty range is conservatively bounded by assuming that there is no heat transfer across the pool surface by setting the interface surface area to zero.

7.1.4.3.2   LHSI Heat Exchanger Process Model

A best-estimate model has been developed for the GOTHIC model, and its principal impact on containment response is the temperature of the safety injection coolant. As such, the statistical treatment of the IRWST temperature is sufficient to address this uncertainty (see Section 7.1.4.5.2).

7.1.4.4   Expansion / Compression of Gases

The phenomena associated with the expansion and compression of gases considered for the uncertainty analysis are the containment initial conditions (i.e., volume, pressure,

temperature, and humidity), mist auto-conversion threshold (maximum mist density) and accumulator nitrogen mass.

7.1.4.4.1   Initial Containment Volumes

In AREVA NP's containment safety analysis methodology (see Section 8.0), the specified containment net free-volume is conservatively minimized to maximize the predicted pressure. In addition, the initial IRWST pool volume influences the calculated pool temperature (see Section 7.1.4.5.2), and its value is also conservatively minimized. Because of the expected importance of these design parameters, both are considered in this uncertainty analysis. The minimum and nominal estimates for the containment free volume are 2,754,237 ft^3 and 2,810,148 ft^3, respectively. Similarly, the IRWST pool volume is allowed to vary from a minimum of 50,996 ft^3 to a nominal 68,397 ft^3.

7.1.4.4.2   Initial Containment Pressure

The allowable containment pressure range is set to be consistent with the U.S. EPR Technical Specifications (Reference 2, Chapter 16, Section 3.6.4), which state that the "Containment pressure shall be ≥ -0.2 psig and ≤ 1.2 psig."

7.1.4.4.3   Initial Containment Temperature

For a given pressure, minimizing the initial containment temperature provides a greater mass of non-condensable air in the containment but a lower initial heat sink conductor temperature. Conversely, maximizing the initial containment temperature maximizes the temperature of the heat conductor surfaces, making them less effective heat sinks, but reduces the initial mass of non-condensable air.

A larger mass of non-condensable air increases the containment pressure response because of an increase in the partial pressure from non-condensables and a reduction in the condensation heat transfer for conductor surfaces exposed to steam as a result of the decrease in the steam/air mass ratio. These penalizing effects are partially offset,

however, by an increase in the conductor heat removal capacity due to the lower initial temperature. The converse is true when the initial containment temperature is high.

The minimum containment temperature is assumed to be the Technical Specification value for the minimum IRWST temperature of 59°F (Reference 2, Chapter 16, Section 3.5.2). The maximum temperature in the accessible area is 86°F, the analysis value in the U.S. EPR FSAR calculations. The Technical Specification maximum temperature in the equipment room is 131°F (Reference 2, Chapter 16, Section 3.6.2). For sampling purposes, there are three parameters to consider: the structure temperature in the accessible area, the structure temperature in the inaccessible area, and the gas temperature. The three values are assumed to be in the uncertainty analysis.

7.1.4.4.4   Initial Containment Humidity

Containment humidity in the U.S. EPR is maintained at or below 70% relative humidity. The radiological filter air heaters (a non-safety system) are designed to limit the relative humidity to a maximum of 70% to maintain the capability of the carbon absorbers for the removal of radioiodine from the containment building atmosphere. A low humidity is conservative for the containment maximum pressure analyses because it produces a greater initial volume of air.

7.1.4.4.5   Maximum Mist Density

The mist phase considers formation of mist, mist vaporization and depletion of excess mist. RCS break discharge effluent is the dominant contributor to the mist phase. Pressure and temperature variations impact the mass balance. When the macroscopic mist density exceeds a specified limit, the excess mist calculated by the lump parameter model is removed by deposition to the liquid phase. Reference 84 describes this auto-conversion process of converting mist to droplets. While GOTHIC recommends a value of 1 g/m^3, Reference 84 identifies 0.5 – 1.0 g/m^3 as a realistic range for this parameter based on experimental observations.

7.1.4.4.6   Accumulator Nitrogen Mass

Accumulator nitrogen mass is a part of the overall RCS mass and energy release. As discussed in Section 7.1.4.9, mass and energy releases are not treated statistically. Instead, a best-estimate treatment of mass and energy is used, which includes a best-estimate treatment of accumulator nitrogen mass.

7.1.4.5   Blowdown/Spray Phenomena

The U.S. EPR design does not credit a containment spray system in the containment design basis analysis. While the related uncertainties are not relevant, those associated with a spray can be present in the early phase of a LOCA phase when liquid discharges from the RCS.

7.1.4.5.1   Droplet Size

AREVA NP's containment response methodology uses a droplet average diameter of 100 microns. The uncertainty range is drawn from the work of Park & Lee (Reference 85), where droplet size in partially flashing jets ranged from 90 – 200 microns with a mean drop diameter ranging from 90 – 120 microns.

7.1.4.5.2   Temperature Initial Condition

Technical Specifications for IRWST temperature (Reference 2, Chapter 16, Section 3.5.4.1) state that IRWST temperature is between 59°F and 122°F. This parameter is strongly correlated with the containment temperature discussed in Section 7.1.4.4.3.

7.1.4.6   Local Buoyancy / Stratification

This phenomena class relates to local gas behavior at a scale much smaller than typically considered with a lump parameter model. This uncertainty is the result of inefficiencies in atmospheric mixing. The AREVA NP containment analysis evaluation methodology conservatively treats the heat transfer to the structure as described in Section 8.2.3. With regard to condensation heat transfer, significant flow resistances

may cause regional differences in the steam concentration. Because condensation heat transfer is a function of steam concentration, there is a compensating effect for inefficient atmospheric mixing. The uncertainty treatment on structure surface area (Section 7.1.4.7.1) addresses the sensitivity of condensation heat transfer to such atmospheric mixing inefficiencies.

7.1.4.7   Containment Internal Geometry

The phenomena associated with the containment internal geometry considered for the uncertainty analysis are associated with atmospheric mixing inefficiencies resulting from containment structure. By assuming a single-volume to represent the containment, the treatment of atmospheric mixing efficiencies can be addressed only using structure surface area. Atmospheric mixing efficiency has been shown to be a function of break elevation with degraded mixing efficiency corresponding to higher elevations. RCS piping in the U.S. EPR is located low in the containment.

7.1.4.7.1   Structure Surface Area

The uncertainty ranges for structure surface area was addressed in the GRS analysis (Reference 78). The GRS approach to surface area sampling cannot be applied to the single-volume GOTHIC model because the COCOSYS model used in the GRS study is subdivided into approximately 50 volumes. In the GRS method, about one-third of the individual volume dimensions were sampled while the overall area and volume were preserved. In addition, the surface area of selected structures was sampled over a range of ±30%.

An alternative uncertainty treatment for surface area is applied in this uncertainty analysis. The total surface area of passive heat sinks is sampled from a best-estimate analysis value to a conservative minimum value. With the single-volume GOTHIC model, the dominant heat transfer mechanism is condensation. Since condensation is a strong function of steam concentration, heat transfer by condensation has a compensating response to atmospheric mixing inefficiencies. As such, the impact of

possible mixing inefficiencies is partially mitigated by this coupled dependency.
Nonetheless, as a conservative treatment of this uncertainty, a -5% lower bound is
assumed to address the impact of mixing inefficiencies and fluid transport lag.

7.1.4.7.2   Break Location

It is not possible to evaluate the sensitivity of break location on containment pressure
response using the single-volume GOTHIC model. The important question with regard
to break location is whether there is sufficient mixing in the containment to provide a
sufficiently uniform steam concentration throughout the containment. The U.S. EPR
RCS is located very low in the containment. Several tests, including HDR and BFMC,
have shown that the lower injection location, the better the atmospheric mixing.
Therefore, good atmospheric mixing will occur and the break location is unimportant for
the U.S. EPR configuration.

7.1.4.8   Liquid Advection

The term liquid advection is used to capture the phenomena associated with the
transport of condensate from structure surfaces. In the U.S. EPR, condensate will
agglomerate on the structure surfaces and drain by gravity into the IRWST. The two
principal liquid advection phenomena are droplet entrainment and condensate re-
vaporization.

7.1.4.8.1   Water Entrainment

With the single-volume GOTHIC model, liquid flowing in films along containment
structures or falling from RCS piping are placed directly into the IRWST. Heat transfer
to the heavy floor and liquid spilling across it are not simulated in the single-volume
GOTHIC model. This approach is conservative.

7.1.4.8.2   Condensate Revaporization

Condensate revaporization may occur when the steam is superheated. This is not expected following a LBLOCA. Therefore, no condensate re-vaporization is assumed.

7.1.4.9   Mass and Energy Release

Mass and energy release are initially provided by a RELAP5 calculation. This calculation extends through the end of reflood and, depending on the postulated break location, to the manual realignment of LHSI from cold leg locations to hot leg locations at 60 minutes[*].⎡

⎦Beyond the RELAP5 simulation, mass and energy releases are assumed to be steam generated by decay heat, steam generator heat transfer, and residual structural sensible heat release. Treatment for long-term mass and energy releases is described in Section 8.2.3.

Due to the time-intensive nature of the RELAP5 simulations, it is impractical to explicitly treat mass and energy release uncertainties through the end of the RELAP5 simulation. Rather, a nominal model is used. An analytical approach is applied for the remainder of the analysis after termination of the RELAP5 calculation. This is described in Section 7.2.2.

---

[*] The US EPR has implemented earlier manual realignment of LHSI from cold leg locations to hot leg locations (60 minutes).

7.1.5   Uncertainty Treatment Summary

Table 7-7 summarizes the treatment of uncertainties for the GOTHIC-based analysis.

Table 7-7—Uncertainty Treatment Summary

Phenomena	Low Bound	High Bound
Convective Heat Transfer		
Free and Forced Convection	N/A in Single-Volume Model	
Condensation (Uchida)	0.5	1.5
Material Properties		
Steel Heat Capacity	0.9	1.1
Steel Heat Conductance	0.9	1.1
Steel Material Density	0.9	1.1
Concrete Heat Capacity	0.7	1.3
Concrete Heat Conductance	0.7	1.3
Concrete Material Density	0.8	1.2
Liner/Concrete Gap Thickness (mm)	0.225	3
Pool Free Convection		
Direct contact condensation (via pool surface area)	Conservatively bounded, pool surface area neglected	
LPSI Heat Exchanger	Best-estimate model	
Expansion/Compressions of Gases		
Initial Containment Vapor Space Volume (ft^3)*	2,754,237 ft^3	2,810,148 ft^3
Initial Containment IRWST Volume (ft^3)*	50,996 ft^3	68,397 ft^3
Initial Containment Pressure (psia)	14.5	15.9
Initial Containment Temperature (gas temperature, °F)†	59	131
Initial Containment Temperature (structure, accessible area, °F)†	59	86
Initial Containment Temperature (structure, inaccessible area, °F)†	59	131
Initial Containment Humidity (%)	0	70
Maximum Mist Density	0.5 g/m^3	1.0 g/m^3
Blowdown/Spray Phenomena		
Droplet Size (microns)	90	120
Temperature Initial Condition (°F)†	59	122

* Containment volumes are explicitly correlated, see description in text. These values reflect a conservative bias relative to the best-estimate nominal values given in Table 7-8

† Temperature values are explicitly correlated, see description in text.

Table 7-7—Uncertainty Treatment Summary		
Phenomena	**Low Bound**	**High Bound**
Local Buoyancy/Stratification		
Flow resistances	N/A in Single-Volume Model	
Containment Internal Geometry	95%	100% (plus basemat)
Liquid Advection		
Water Entrainment	N/A for Single-Volume Model	
Condensate Revaporization	N/A for LBLOCA	

7.2   U.S. EPR GOTHIC Model for Uncertainty Analysis

The GOTHIC model used for the uncertainty analysis is derived from the GOTHIC input
model used for the U.S. EPR FSAR analysis. The latter model uses conservative inputs
and assumptions in accordance with the SRP guidance and is described in Section 8.0
and Section 9.0. The revised GOTHIC model for the uncertainty analysis applies a
combination of realistic and conservative values to describe the containment, initial and
boundary conditions, and event sequence. It is referred to as the relaxed conservatism
model or the RC model.

7.2.1   Relaxed Conservatism Model Description

A single control volume GOTHIC model was used to model the net free volume within
the steel inner containment vessel. This is similar to the model that was used to
perform the LOCA containment pressure response calculations for the FSAR. The
relaxed conservatism model retains the majority of the design inputs and assumptions
from the FSAR model, including the modeling of the passive structural heat sinks. A
single control volume model limits the physical geometry description to the height, area,
and volume of the air/vapor and liquid spaces.

The principal changes to the containment model are the free volume and volume of
IRWST water. These are treated conservatively in the FSAR model (i.e., to maximize

containment pressure). Nominal values are selected in the relaxed conservatism model. Similarly, the conservative values used in the FSAR model for associated initial fluid properties for the air/vapor and pool regions were replaced with nominal design values. Table 7-8 summarizes the important initial and boundary conditions for the relaxed conservatism GOTHIC containment model. These represent either nominal or mean values.

The containment walls—walls and slabs in the accessible and non-accessible areas, steel liners, IRWST walls, and containment basemat floor—are modeled explicitly as passive heat sinks in the relaxed conservatism model. The basemat floor was neglected in the FSAR model. The initial temperatures of the passive heat sinks are determined by the respective room temperatures of the regions where they are located (see Table 7-8).

Although GOTHIC provides flexibility with regard to heat transfer modeling, no changes were made in this regard to AREVA NP's approved GOTHIC-based containment analysis methodology (Reference 14). Specifically, heat transfer to passive heat sinks is limited to direct condensation and natural convection. For a LOCA, the direct condensation heat transfer was approved with use of Tagami-Uchida with an initial heat transfer coefficient value of 2.0 BTU/ft^2-hr-°F. Because there is no strong data to support crediting condensation on the surface of the IRWST, the relaxed conservatism model retains the FSAR model assumption that severely degrades this heat transfer mechanism.

Table 7-8—Key Containment Model Initial and Boundary Conditions

Parameter	Inputs
Containment free volume	2,827,498 ft^3
Initial IRWST water volume	68,397 ft^3
Initial containment pressure	14.7 psia
Initial containment temperature	95°F
Initial containment relative humidity	50%
Initial IRWST temperature	90.5°F

AREVA NP Inc.

ANP-10299NP

Applicability of AREVA NP Containment Response Evaluation Methodology to the
Revision 2
U.S. EPR™ for Large Break LOCA Analysis

Technical Report
Page 7-21

Parameter	Inputs
CCW temperature at inlet of RHR heat exchanger	104°F
3 CCW flow rates	2486.7 lbm/sec
Decay heat	ORIGEN2 for long term Best Estimate decay heat
Initial heat sinks temperature	Containment walls and accessible areas at 72.5 °F, non-accessible areas at 95 °F, and IRWST walls/slabs/basemat 83.75°F.
Core power	4590 MWth

Note: The uncertainty analysis calculation described in Section 7.3 considers several of the parameters in Table 7-8 in the evaluation of total uncertainty. The respective uncertainty ranges are defined in Section 7.1.4.

7.2.2 Short-Term Mass and Energy Release into the Containment

Several conservatisms were applied to obtain the short-term LOCA mass and energy releases used for calculating the containment pressure response presented in the FSAR. The majority of these are removed for the relaxed conservatism model. Rather than altering the RELAP5-BW model used in the FSAR analysis, the calculation of mass and energy releases with relaxed conservatisms was prepared using S-RELAP5. The S-RELAP5 model of the U.S. EPR includes model elements developed for AREVA NP's non-LOCA, small-break LOCA, and realistic large-break LOCA (RLBLOCA) safety analysis (References 79, 86, 87).

This model contains detailed nodalization of the primary and secondary systems. The primary system includes the reactor vessel and the explicit simulation of all four loops, including the cold and hot legs, the pressurizer (with pressurizer relief valves and sprays), the SGs, and the RCPs. In the secondary systems, the S-RELAP5 model includes a complete description of the SGs, the emergency feed water system, the main steam relief valves, the main steam safety valves, and the common header of the steam lines. The ECCS includes models for the accumulator, MHSI, and LHSI and the associated piping connecting these components to the RCS. Sufficient detail is provided to allow S-RELAP5 to predict LHSI flow splits for low-pressure injection flows

when the cross-connect lines are open because a train of LHSI is out of service for preventative maintenance.

The containment is defined separately from the S-RELAP5 input. In AREVA NP's RLBLOCA methodology the containment pressure response is calculated with the ICECON code concurrently with the coupled S-RELAP5 calculation (Reference 88). ICECON is the AREVA NP proprietary version of the CONTEMPT code (Reference 89). The ICECON input description is appended to the S-RELAP5 input file. S-RELAP5 calculates the mass flow and enthalpy release to the containment while the ICECON code calculates the resulting containment pressure and temperature. These values are returned each timestep to S-RELAP5 to update the time-dependent volumes representing the containment in the calculation.

Consistent with AREVA NP's RLBLOCA methodology, nominal or best-estimate values are used for initial conditions, boundary conditions, and setpoints. Table 7-9 summarizes the inputs for the S-RELAP5 relaxed conservatism model and compares them to the RELAP5-BW design certification model. The changes are marked in bold italics font for easy recognition.

The changes having the largest impact on mass and energy releases are the elimination of the preventive maintenance assumption that removes an ECCS train, decay heat, and the break model. The FSAR model assumes the loss of two ECCS trains via the preventive maintenance and single-failure assumptions. In the relaxed conservatism model, only one ECCS train is assumed lost via the single-failure assumption. Decay heat in this model is based on a realistic characterization of decay heat as calculated with the ORIGEN2 code (Reference 90). Blowdown critical flow is modeled using the Homogeneous Equilibrium Model (HEM), the best-estimate leak flow model used in AREVA NP's RLBLOCA methodology. HEM replaces the Moody model used in FSAR mass and energy release calculations. In addition to these more significant model changes, the relaxed conservatism model implements the post-LOCA partial steam generator cooldown feature of the U.S. EPR. On receipt of a safety

injection signal, the safety-related main steam relief train (MSRT) is used to automatically depressurize the secondary side of the steam generators at a rate corresponding to 180°F/hr down to a pressure of approximately 870 psia. The partial cooldown of the steam generators is designed to cool the primary system and, thereby, lower the RCS pressure below the MHSI shutoff head for mitigating small break LOCAs and steam generator tube ruptures. The partial cooldown is performed by a steam dump to the atmosphere via the main steam relief train connected to each SG. It automatically decreases the respective relief valve setpoints. For large break LOCAs, this feature has a minor effect on event progression.

Table 7-9—Comparisons Between RC and FSAR Models

Parameters	RC Model	FSAR Model
RCS		
Core Power (MWt)		
Decay Heat		
RCS Cross-over Leg Temperature (°F)		
RCS Flow Rate per Loop (gpm)		
RCP		
Rated Head (ft)		
Rated Flow (gpm)		
Rated Torque (ft-lb)		
Rated Speed (rpm)		
Rated Density (lb/ft3)		
Moment of Inertia (lb-ft2)		
Pressurizer		
Pressure (psia)		
PZR Liquid Level (span, %)		
Steam Generators		
MFW Temperature (°F)		
MFW Isolation Signal		
MFW Isolation Valve Closing Time (s)		
Tube Plugging (%)		

Table 7-9—Comparisons Between RC and FSAR Models

Parameters	RC Model	FSAR Model
ECCS		
# of Available ECCS Trains		
SIS Actuation Delay Time (s)		
MHSI Flow Rate		
MHSI Source Temperature		
LHSI Flow Rate		
LHSI Source Temperature		
Accumulators		
Injection Location		
Nominal Liquid Volume (ft3)		
Total Volume (ft3)		
Nominal Operating Pressure (psia)		
Nominal Liquid Temperature (°F)		
Containment/Break Model		
Pressure		
Critical Flow Model		
Protection Functions		
Low Pressurizer Pressure (MIN3) (psia)		
Low ΔP across RCP		
Partial Cooldown System		
Cooling Rate (°F/hr)		

7.2.3   Long-Term Mass and Energy Release into the Containment

The long-term RCS mass and energy releases are determined in GOTHIC. The analysis takes into account decay heat and removal of sensible stored heat. This phase begins when the operator realigns the LHSI to the respective hot legs at 90 minutes and terminates 24 hours after the postulated accident.

Implementation of the relaxed conservatism model for long-term mass and energy releases is similar to the FSAR model (see Section 8.0) with the exception that three trains of pumped safety injection are assumed to operate instead of two.   The long-term

mass release is primarily a function of the LHSI flow rate and the core and sensible heat removal rates. The LHSI model considers IRWST recirculation, the LHSI pumps, and associated heat exchangers that draw water from the IRWST. The constituent energy sources remaining at the RELAP5 to GOTHIC transition time are:

- Core decay heat

- Primary system fluid stored energy

    – Primary system passive metal stored energy (including core metal stored energy)

- Secondary system stored energy (fluid + metal)

- Safety injection pump heat addition.

The relaxed conservatism model calculates the release of RCS passive metal stored energy in the same manner as the FSAR model. The energy is released to the containment atmosphere or the liquid region based on the path to the break. This is described in Section 8.2.3.1

7.2.4   GOTHIC Model Nodalization

Figure 7-3 shows the GOTHIC input model nodalization. The large block delineated with a dotted line (Volume 1) represents the containment. The smaller block represents the RCS. The heater components (i.e., trapezoidal icons) shown within the RCS block (Volume 2) represent the five sources of energy discussed in the previous section. Volume 1 utilizes 14 heat sinks to represent the containment structure: steel, concrete, etc. The blocks identified with either an "F" or "C" are flow boundary conditions that respectively simulate the short-term mass and energy releases and safety injection. The short-term mass and energy releases are provided in tables of liquid and steam flow rates generated by RELAP5-BW (FSAR model) or S-RELAP5 (relaxed conservatism model) from the two sides of the double-ended guillotine break. The safety injection model simulates the LHSI system from the IRWST, through the pumps and heat exchangers, and the split that returns a portion of the flow to the IRWST for

cooling while the rest is delivered to the RCS. The MHSI system is modeled similarly but does not interface with the IRWST cooling chain.
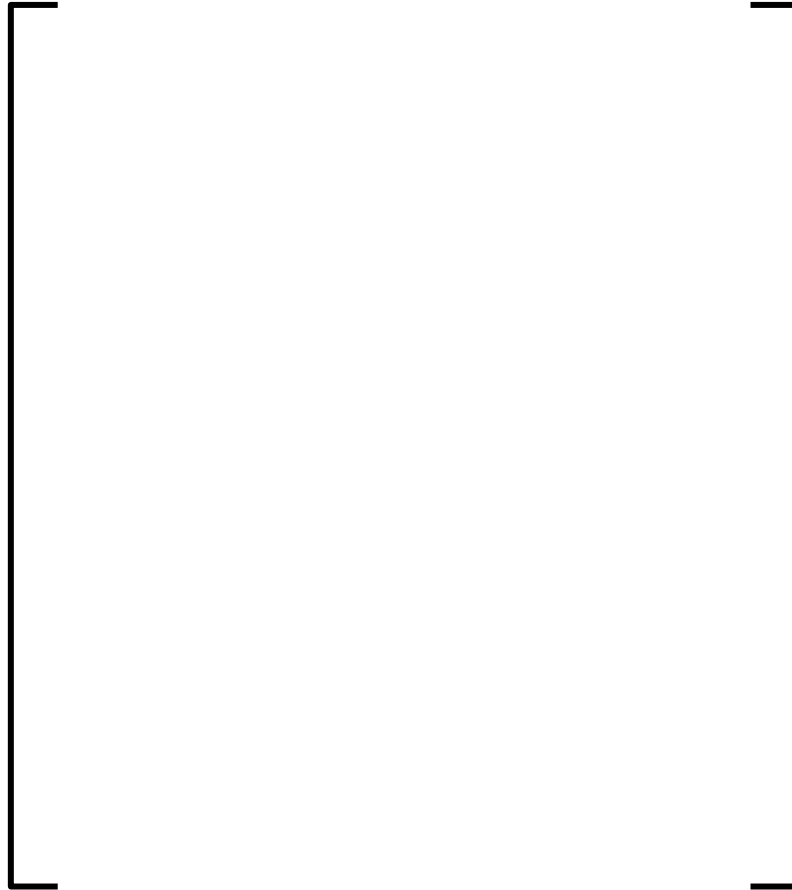
Figure 7-3—GOTHIC Nodalization Diagram

7.3   Propagation of Uncertainties (EMDAP Step 20)

An uncertainty analysis quantifies design sensitivity to a realistic variation in important parameters. The uncertainty analysis presented in this section was performed to quantify the inherent conservatism of the U.S. EPR design basis LOCA containment pressure response and, thereby, the design safety margin. The design basis response is determined using AREVA NP's deterministic containment analysis evaluation methodology described in Section 8.0. The approach used for the uncertainty analysis is patterned after AREVA NP's RLBLOCA (Reference 79) and severe accident evaluation (Reference 80) methodologies. Both include an assessment of

phenomenological importance, identification of dominant contributors influencing key assessment metrics, and the application of nonparametric statistics.

The uncertainty analysis uses the set of parameters and associated ranges described in Section 7.1.4 as inputs to a suite of calculations quantifying the best-estimate margin to acceptance criteria limits and the relative importance of individual contributors. This analysis generates coverage bands for the containment pressure by evaluating a large number of randomly sampled variations in the uncertainty parameter values over their specified uncertainty range.

7.3.1   Statistical Approach

The statistical approach demonstrates a realistic evaluation of the event through the convolution of uncertainties associated with important containment phenomena and processes. It supports the deterministic approach through the demonstration of the inherent margin in the deterministic approach. The contributors (Table 7-7) to total uncertainty in the LBLOCA containment pressure response can be addressed through either parametric or nonparametric methods. The response surface method, a parametric method, was the approach demonstrated in the CSAU sample problem (Reference 16). The objective of parametric methods is to develop a response surface describing the sensitivity of the figure-of-merit (i.e., containment pressure in this example) to the dominant LBLOCA uncertainty contributors. The number of calculations required for that approach is dependent on the number of uncertainty parameters considered. In contrast, a nonparametric approach decouples the association between the number of uncertainty parameters and the number of required calculations. The desired quantification of containment pressure uncertainty is the identification of a specific result that estimates the tolerance limits of the results domain. For this containment pressure uncertainty analysis, this estimate is found by evaluating the one-sided 95/95 coverage/confidence condition.

The minimum number of sampled cases is determined from Wilks' formula for one-sided tolerance limits (Reference 91). Beginning with the probability statement:

AREVA NP Inc.   ANP-10299NP
Applicability of AREVA NP Containment Response Evaluation Methodology to the   Revision 2
U.S. EPR™ for Large Break LOCA Analysis
Technical Report   Page 7-28

$$P[F(x_k) > \beta] = \frac{n!}{(k-1)!(n-k)!} \int_\beta^1 \xi^{k-1}(1-\xi)^{n-k}\,d\xi$$

For the case in which $k = n$, that is, the largest value of all of the samples, this relationship reduces to:

$$\gamma = 1 - \beta^n$$

where β is the coverage, γ is the confidence, and n is the minimum number of sampled calculations. For the 95/95 coverage/confidence condition, $n = 59$. This means in a random sample of 59 calculations, one case, the case with the highest containment pressure at any particular time of interest, will bound the 95/95 coverage/confidence condition for containment pressure. A disadvantage of this method is that there may be significant conservatism in a result bounding the 95/95 condition.

7.3.2   Performance Details of the Uncertainty Analysis

The process of evaluating the uncertainty domain involves the performance of "Monte Carlo"-like simulations using the GOTHIC computer code and the U.S. EPR plant model. For each execution of the GOTHIC code, each of the important uncertainty parameters in Table 7-7 is randomly sampled based on a previously-determined probability distribution.

The common random number generators available on UNIX workstations are sufficient to provide uniformly distributed sample values. A uniform probability distribution function ensures an equal probability of selecting any given value over the range of interest. Using the uniform random number generator producing a random value r between 0 and 1, a sample, z, from a uniform probability distribution function ranging between two points, a and b, is defined as:

$$z = a + (b-a) \cdot r$$

Each execution of GOTHIC can be viewed as the performance of an experiment with the experimental parameters being the important phenomena and plant process parameters and the result being any appropriately represented performance metric (i.e., based on correlation with uncertainty parameters). After 59 calculations are performed, the containment pressure results from each calculation are sorted to identify the highest containment pressure at any particular time of interest. Total uncertainty can be estimated by the difference between the highest containment pressure result and the median containment pressure result.

7.3.3   Calculation

The best-estimate single-node GOTHIC model described in Section 7.2.1 was the base model for calculating the containment response to a cold leg pump suction (CLPS) LOCA. The uncertainty parameters presented in Table 7-7 were all sampled through the creation of 59 GOTHIC input files. Notable features of this model that were not varied as a part of this uncertainty analysis are:

- The short-term best-estimate mass and energy release boundary conditions. These were obtained from the best-estimate S-RELAP5 4-loop system calculation described in Section 7.2.2. The short-term mass and energy calculation extends to 90 minutes, the time of switchover to hot leg injection of LHSI flow.

- The decay heat forcing function.
  This forcing function was calculated by the ORIGEN2 computer code and incorporated into the long-term GOTHIC mass and energy calculation (beyond 90 minutes and up to 24 hours transient time).

- The bounding sensible heat forcing functions.
  These forcing functions were obtained from the original U.S. EPR FSAR calculation for the CLPS LOCA event. These forcing functions represent the

remaining sensible heat in the RCS/SGs and are used in the long-term GOTHIC

mass and energy calculation.

- For conservatism, the IRWST pool condensation is not credited.

In performing the uncertainty analysis, the 59 GOTHIC input files were executed with

the uncertainty parameters randomly sampled. The resulting containment pressure

responses are presented in Figure 7-4.
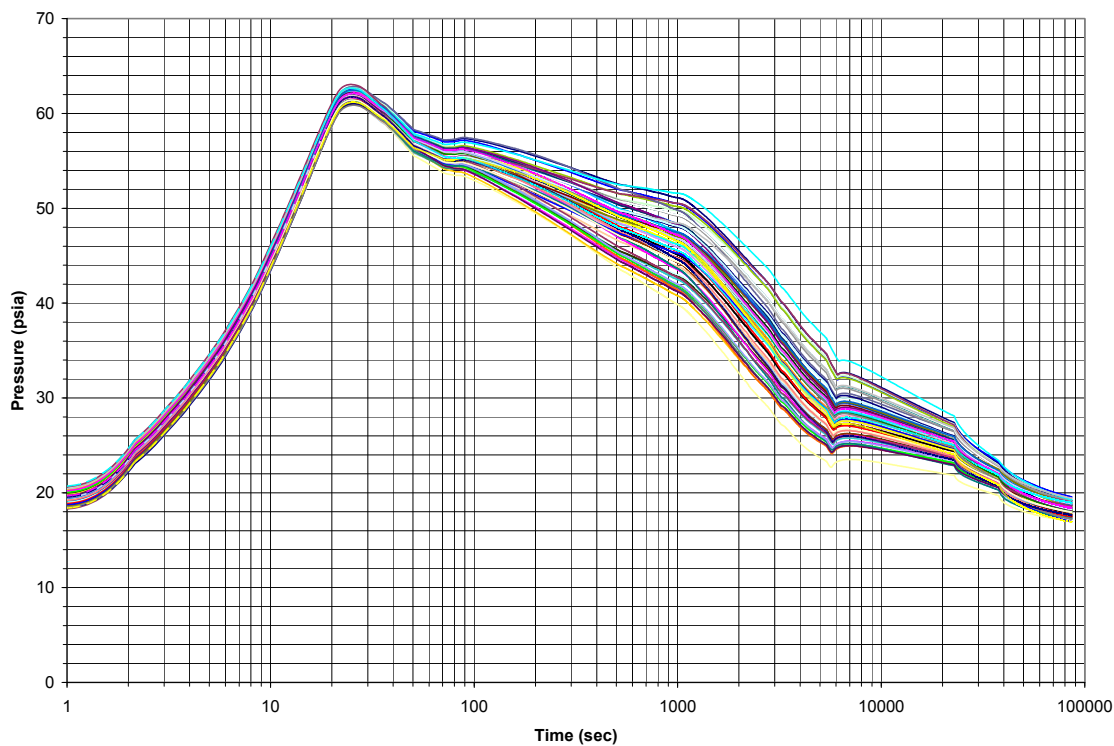
Figure 7-4—Containment Pressure Response to a CLPS LBLOCA

7.3.4   *Quantifying Phenomenological Importance*

The quantification of phenomenological importance demonstrates that the methodology

is self-consistent. For the best-estimate plus uncertainty approach adopted in this

study, this includes the identification of uncertainty contributors, quantification of

AREVA NP Inc.
ANP-10299NP
Applicability of AREVA NP Containment Response Evaluation Methodology to the
Revision 2
U.S. EPR™ for Large Break LOCA Analysis
Technical Report
Page 7-31

uncertainty ranges, applicability of computational models, and consistency of analysis results with expectation (both qualitatively and from the scaling analysis).

7.3.4.1 *Importance Methodology*

An analysis technique has been developed for quantifying the importance of processes and phenomena that affect the principal analysis measures related to regulatory acceptance criteria. This technique was applied as part of the AREVA NP approach. Beginning with open literature reports on containment processes and phenomena occurring during an LBLOCA, this method explicitly extracts the expertise inherent in the specific analysis computer code being applied. Application of non-parametric-based best-estimate plus uncertainty methods generates a surplus of possible uncertainty contributors to be analyzed. The result of this importance analysis is identification of those uncertainty contributors having the greatest influence on key analysis measures. This in turn supports the credibility of the uncertainty analysis, GOTHIC applicability, and even the containment safety analysis evaluation methodology through the validation of the engineering judgments that guide methodology development. In addition, it provides insight into the processes and phenomena that affect key analysis measures and, thus, limits the unnecessary characterization of uncertainty contributors of low importance.

Given a best-estimate predictor model, such that

$$x_o = fct(x_1, x_2, x_3, ..., x_n)$$,

total variance in a particular dependent variable, x_o, is a statistical measure relating the combined variance of several independent uncertainty contributors x_i. From the definition of statistical variance, the total variance in the particular dependent variable, $Var[x_o]$, is expressed as

$$Var[x_o] = \sum_{i=1}^{n} Var[x_i]$$

The task of quantifying the uncertainty contribution of specific code parameters requires a decomposition of the total variance measure. This is accomplished through the evaluation of a multiple-regression model. A multiple-regression model extends the application of curve-fitting to multiple variables. The main assumption is that a linear relationship exists between a dependent variable, x_o, and two or more independent variables, x_i, such that

$$x_o = \eta + fct(x_1) + fct(x_2) + ... + fct(x_n)$$

A direct solution for the regression coefficients in the multiple-regression model can be evaluated by applying least-squares techniques; however, for this application, successive evaluation of the model is performed because the limited data sizes provide only limited information useful for resolving of the model. In addition, the successive evaluation approach allows for choices among possible estimator functions derived from the least-squares technique.

The initial tasks for this approach include defining a measure that identifies the importance of sampled model parameters and defining a measure that identifies when the usefulness of the data for resolving the model is exhausted. For the first measure, several rank and correlation expressions from sensitivity analysis are available, such as the Standardized Rank Regression Coefficient, Rank Correlation Coefficients, and Correlation Ratios. The "Rank" methods replace the data with the corresponding ranks. This transformation inherently removes information from the data and is, therefore, not the optimal choice.

In contrast, the sample correlation coefficient retains that information. In this application, the correlation of interest is between the sampled model parameters and the analysis measure results. With relatively small sample sizes, sample sets of uncorrelated parameters will have non-zero correlation. The multiple regression exercise objective is to identify a sample correlation threshold where there is high confidence that the correlation is not simply coincidence. A test must be defined to identify the threshold below which no more information about the model can be

resolved. This test is derived from knowledge of the correlation coefficient sampling distribution. For this problem in which specific model parameters have been independently sampled, the sampling distribution corresponds to the Student's t-distribution and the desired "threshold of correlation" is evaluated from the t-test (Reference 92).

The initial important model parameter (considered in the sampling) is identified by the largest correlation between the sampled model parameters and the dependent analysis measure, assuming there is at least one above the threshold of correlation. A function retaining information on the figure-of-merit without the contribution of the initial important model parameter is estimated from the error between the output variable of interest and the curve-fit estimate derived for the first individual uncertainty contributor against the output variable of interest. Further resolution of the independent sampled model parameters continues following the same procedure with the dependent variable transformed by the functional estimates of the previously evaluated important model parameters.

This evaluation continues until no result within the set of correlations between the specific uncertainty contributors and the analysis measure exceeds the threshold of correlation. At this point, the remaining variance can not be further decomposed without significant and immeasurable degradation in the precision of the results.

The principal results from the importance analysis include three statistical measures: the correlation coefficient, the standard deviation of the figure-of-merit relative to the variation in a particular uncertainty contributor, and the estimate of the standard deviation of the figure-of-merit considering only the identified important uncertainty parameters. The sign of the correlation coefficient indicates how the particular parameter affects the result. A positive sign means that a positive change in a given uncertainty contributor causes a positive change in the figure-of-merit. A negative sign means that a positive change in a given uncertainty contributor causes a negative

change in the figure-of-merit. The magnitude of the correlation coefficient is only meaningful for identifying the important parameters in the process previously described.

The standard deviation in the figure-of-merit, relative to the variation in a particular uncertainty contributor, quantifies the importance of that uncertainty parameter in the evaluation of the figure-of-merit. The higher this value, the greater its impact on the figure-of-merit.

To measure how well this procedure captures the most important uncertainty contributors, the standard deviation of the figure-of-merit is estimated in each analysis using the convolution of the calculated uncertainties (i.e., the square root of the sum of the squares of the standard deviations, i.e., the variances); that is,

$$\sigma|_{est} = sqrt\left(\sum_{i=1}^{m} \sigma_i^2|_{est} \right)$$

where m is the number of important uncertainty contributors identified in the analysis, σ_{est} is the estimate of the standard deviation of the figure-of-merit considering the complete uncertainty domain, and σ_i represents the set of standard deviations on the figure-of-merit relative to the variation in the important uncertainty contributors. The ratio of this estimate to the true standard deviation of the figure-of-merit (i.e., calculated directly from the raw results for the figure-of-merit) represents the measure of the completeness of the importance study.

7.3.4.2   *Evaluation of Containment Phenomena Importance*

The analysis to quantify the importance of the individual uncertainty parameters on the output metric of interest (i.e., pressure response) was performed following the procedure explained in Section 7.3.4.1. To fully characterize the containment pressure response, the uncertainty importance analysis is evaluated at several transient times up to the post-LOCA time of 24 hours (calculation end time). The transient times selected are the time of the blowdown peak (~25 seconds), 100 seconds, 10 minutes, 20

AREVA NP Inc.   ANP-10299NP
Applicability of AREVA NP Containment Response Evaluation Methodology to the   Revision 2
U.S. EPR™ for Large Break LOCA Analysis
Technical Report   Page 7-35

minutes, 1 hour, 1.5 hours, 2 hours, 3 hours, 6 hours, 9 hours, 12 hours, 18 hours, and 24 hours.

Table 7-13 and Table 7-14 provide a qualitative summary of the important uncertainty contributors at each of these times. Quantitative results at the time of peak pressure, at 10 minutes into the event, and at 24 hours into the event are presented in the following subsections.

7.3.4.2.1 *Importance Results at Time of Peak Pressure*

Table 7-10 provides the results of the uncertainty importance analysis at the time of the blowdown peak in containment pressure. For this particular CLPS LOCA transient, the peak pressure occurred at approximately 25 seconds. As shown in Table 7-10, eight model parameters have discernable impact on the short-term peak containment pressure. Over the uncertainty domain considered, the mean peak containment pressure is 61.90 psia with a standard deviation of 0.605 psi. The dominant contributor to this uncertainty is the initial containment pressure. The list of important contributors to containment pressure uncertainty, in decreasing order of importance, is as follows:

1. Initial containment pressure; positively correlated

2. Initial containment volume; negatively correlated

3. Initial IRWST liquid volume; positively correlated

4. Initial temperatures (containment atmosphere, IRWST and structures); negatively correlated

5. Concrete thermal conductivity; negatively correlated

6. Surface of medium steel; negatively correlated

7. Initial relative humidity; negatively correlated

8. Concrete specific heat; negatively correlated.

Because the short-term peak is a strong function of the initial RCS fluid energy, which is held constant in all sample calculations, the dominant contributors are other initial conditions parameters. Specifically, initial containment pressure and volume (free volume plus IRWST liquid volume) are the most dominant initial conditions. The initial temperature parameter has less effect and is negatively correlated with containment pressure. Containment temperature has two compensating effects on containment pressure: heat transfer to structure and mass of non-condensables. At 25 seconds, heat transfer to the structures is not as significant as the effect of the mass of non-condensables. Following containment initial conditions, material properties and structural surface area are evaluated as being important.

The estimate of the standard deviation of the containment pressure, derived solely from the contributions of important parameters, is calculated to be 0.600 psi, representing 99% of the true standard deviation (i.e., 0.605 psi). Therefore, the peak containment pressure is well characterized by these eight uncertainty contributors

Table 7-10—Importance Results at Blowdown Containment Peak Pressure

Uncertainty Contributor	Correlation Coefficient	Standard Deviation of Contributor
Blowdown Peak Containment Pressure (η = 61.90 psia)	N/A	0.605
Initial Containment Pressure	0.887	0.537
Initial Containment Volume	-0.856	0.229
Initial IRWST Liquid Volume	0.606	0.098
Initial Temperatures (containment atmosphere, IRWST and structures)	-0.626	0.081
Concrete Thermal Conductivity	-0.368	0.037
Surface of Medium Steel	-0.340	0.031
Initial Relative Humidity	-0.354	0.031
Concrete Specific Heat	-0.260	0.021
Convolution of Important Contributors: $\sigma\big|_{est} = sqrt(\sum_{i=1}^{m} Var[x_i])$		0.600

Uncertainty Contributor	Correlation Coefficient	Standard Deviation of Contributor
Ratio of Estimate to Actual		0.99

7.3.4.2.2 Uncertainty Importance Analysis Results at 10 Minutes

Table 7-11 provides the results of the uncertainty importance analysis at 10 minutes following the start of the LBLOCA event. As shown in Table 7-11, ten model parameters have a discernable impact on the containment pressure at 10 minutes. Over the uncertainty domain considered, the mean peak containment pressure is 47.89 psia with a standard deviation of 2.393 psi. The most dominant contributor to this uncertainty is the initial containment temperature. The list of important contributors to containment pressure uncertainty, in decreasing order of importance, is as follows:

1. Initial temperatures (containment atmosphere, IRWST and structures); positively correlated

2. Concrete thermal conductivity; negatively correlated

3. Initial containment pressure; positively correlated

4. Uchida model multiplier; negatively correlated

5. Concrete specific heat; negatively correlated

6. Concrete density; negatively correlated

7. Liner/concrete air gap; positively correlated

8. Steel specific heat; negatively correlated

9. Steel density; negatively correlated

10. Surface of IRWST ceiling/heavy; negatively correlated.

In contrast to the blowdown peak, heat transfer to the containment structure has been ongoing for a sufficient amount of time such that air/steam temperature is a greater

AREVA NP Inc.

Applicability of AREVA NP Containment Response Evaluation Methodology to the
U.S. EPR™ for Large Break LOCA Analysis
Technical Report

ANP-10299NP
Revision 2

Page 7-38

factor than the initial differences in non-condensable mass. This ongoing heat transfer is by steam condensation, which is modeled in GOTHIC with the Uchida correlation. With the close coupling between heat transfer and temperature, it follows that the uncertainty in the Uchida correlation is as important as initial containment temperature. Following the parameters influencing steam condensation (Uchida and concrete thermal conductivity), the containment structure material properties that affect stored energy (e.g., concrete specific heat and density) have the next strongest impact on containment pressure. Thermal conductivity is a dynamic property because it is rate–dependent, where specific heat and density are static properties.

The estimate of the standard deviation of the containment pressure, derived solely from the contributions of important parameters, is calculated to be 2.334 psi, representing 98% of the true standard deviation (i.e., 2.393 psi). Therefore, the peak containment pressure is well characterized by these ten uncertainty contributors.

Table 7-11—Importance Results for Containment Pressure at 10 min

Uncertainty Contributor	Correlation Coefficient	Standard Deviation of Contributor
10 min Containment Pressure (η = 47.89 psia)	N/A	2.393
Initial Temperatures (containment atmosphere, IRWST and structures)	0.695	1.662
Concrete Thermal Conductivity	-0.464	0.798
Initial Containment Pressure	0.463	0.707
Uchida Model Multiplier	-0.469	0.634
Concrete Specific Heat	-0.475	0.567
Concrete Density	-0.436	0.458
Liner/Concrete Air Gap	0.502	0.475
Steel Specific Heat	-0.492	0.403
Steel Density	-0.625	0.446
Surface of IRWST Ceiling/Heavy Floor	-0.296	0.165
Convolution of Important Contributors($\sigma\big|_{est} = sqrt(\sum_{i=1}^{m} Var[x_i])$)		2.334

AREVA NP Inc.

ANP-10299NP

Applicability of AREVA NP Containment Response Evaluation Methodology to the
U.S. EPR™ for Large Break LOCA Analysis

Revision 2

Technical Report

Page 7-39

Uncertainty Contributor	Correlation Coefficient	Standard Deviation of Contributor
Ratio of Estimate to Actual		0.98

7.3.4.2.3   Trends from 10 Minutes to 24 Hours

Table 7-13 and Table 7-14 show that the initial containment temperature remains the dominant contributor to containment pressure through 9 hours into the event, while steam condensation, as predicted by the Uchida correlation, slowly diminishes in importance. This is a result of conduction limited surfaces, as illustrated by the importance of material properties during this time. The large mass of low thermal conductivity concrete becomes the principal heat sink as the steel temperature equalizes with the containment temperature as a result of its low mass and high thermal conductivity.

There is reemergence of initial containment pressure as being important around 9 hours, and later a decrease in the importance of initial containment temperature. Both of these behaviors follow from the quenching of steam in the core that occurs after the partial safety injection switchover from cold leg locations to hot leg locations.

Table 7-12 provides the results of the uncertainty importance analysis at 24 hours following the start of the LBLOCA event. As shown in Table 7-12, five model parameters have a discernable impact on the containment pressure at 24 hours. Over the uncertainty domain considered, the mean peak containment pressure is 18.18 psia with a standard deviation of the containment pressure of 0.630 psi. The most dominant contributor to this uncertainty is the initial containment pressure. The list of important contributors to containment pressure uncertainty, in decreasing order of importance, is as follows:

1. Initial containment pressure; positively correlated

2. Concrete specific heat; negatively correlated

3. Initial relative humidity; negatively correlated

4. Concrete density; negatively correlated

5. Concrete thermal conductivity; negatively correlated

The initial conditions are important because the transient is practically terminated by 24 hours and the system is attempting to return to its original state. The physical properties of concrete are important because concrete is the ultimate heat sink.

The estimate of the standard deviation of the containment pressure, derived solely from the contributions of important parameters, is calculated to be 0.613 psi, representing 97% of the true standard deviation (i.e., 0.630 psi). Therefore, the peak containment pressure is well characterized by these five uncertainty contributors.

Table 7-12—Importance Results for 24 HR Containment Pressure

Uncertainty Contributor	Correlation Coefficient	Standard Deviation of Contributor
24 HR Containment Pressure (η = 18.18 psia)	N/A	0.630
Initial Containment Pressure	0.697	0.439
Concrete Specific Heat	-0.629	0.284
Initial Relative Humidity	-0.661	0.232
Concrete Density	-0.764	0.201
Concrete Thermal Conductivity	-0.531	0.090
Convolution of Important Contributors($\sigma\big|_{est} = sqrt(\sum_{i=1}^{m} Var[x_i])$		0.613
Ratio of Estimate to Actual		0.97

7.3.5   *Uncertainty Importance Analysis Results Summary*

The uncertainty analysis confirmed the expert assessment given in the Section 3.4.2 for the containment PIRT. Specifically, structure conduction and condensation have been shown to be the dominant phenomena influencing the containment pressure response. By applying consistent containment mass and energy release information, the impact of

containment thermal-hydraulic phenomena on containment pressure is highlighted. The impact of containment mass and energy uncertainties are addressed in AREVA NP's containment response evaluation methodology by implementing the conservatisms required by the SRP. Section 9.5 provides an assessment of the impact of containment mass and energy on the containment pressure and on the overall retained margin of AREVA NP's containment response evaluation methodology. The principal observations from the uncertainty and importance analysis are as follows (see Table 7-13 and Table 7-14, input parameters color-coded to track their influences during transient progression):

1. In general, the dominant phenomena are those associated with concrete physical properties and initial conditions. The importance of concrete physical properties was essentially constant with time. The importance of initial conditions was essentially constant with time (from 20 minutes to 6 hours transient time), then increased afterwards. By 18 hours transient time, the dynamic phenomena are completely displaced by concrete physical properties and initial conditions. The dynamic phenomena post-blowdown are significant in the interval extending to 1.5 hours, as shown by the importance of the Uchida condensation parameter.

2. Blowdown peak pressure is strongly influenced by phenomena associated with initial conditions and heat sinks. With the timing of the peak so close to the initiating event (~25 seconds after LOCA), initial conditions (containment pressure, free volume plus IRWST volume and initial atmosphere temperature) play an important role. Initial atmosphere temperature is important based on the negative correlative effect to output pressure where the mass of non-condensables is controlling. This was followed in importance by the heat sink properties (concrete and steel). As the containment is subjected to the blowdown mass and energy releases, the initial conditions (pressure, temperature, free volume) and heat sinks tend to determine the magnitude of the peak pressure resulting from the mass and energy releases.

AREVA NP Inc.

ANP-10299NP

Applicability of AREVA NP Containment Response Evaluation Methodology to the

Revision 2

U.S. EPR™ for Large Break LOCA Analysis

Technical Report

Page 7-42

For the 100 second and 10 minute transient times, the effect of the initial containment state is significant. The influence of initial conditions is much more significant at 100 seconds than at 10 minutes, as can be seen in Table 7-13.

3. The initial temperature parameter is positively correlated with output pressure from 100 seconds to 18 hours transient time. It has no importance at 24 hours transient time.

   The positive correlation demonstrates the importance of initial heat sink temperature in relation to output pressure. Higher heat sink temperature results in lower heat absorption by the heat sinks and, thereby, higher pressure. Conversely, lower heat sink temperature causes higher heat absorption by the heat sinks and, therefore, lower pressure. The positive correlative effect of initial heat sink temperature exhibits a sustained strong influence from 100 seconds to 9 hours and it decreases in importance afterwards.

4. The effect of hot leg injection of SI (after 1.5 hours) in suppressing steaming can be seen in the eventual return of initial conditions as the most important parameters.

AREVA NP Inc.
Applicability of AREVA NP Containment Response Evaluation Methodology to the
U.S. EPR™ for Large Break LOCA Analysis
Technical Report

ANP-10299NP
Revision 2

Page 7-43

Table 7-13—Effect of Important Input Parameters on Containment Pressure Responses, Pre-Hot-Leg Injection

Sampled Parameters (decreasing order of importance)	Time Into Transient					
	Blowdown Peak	100 Sec	10 Min	20 Min	1 Hr	1.5 Hr
	1. Initial Containment Pressure — Positive Correlation	1. Initial Temperatures[1] — Positive Correlation	1. Initial Temperatures[1] — Positive Correlation	1. Initial Temperatures[1] — Positive Correlation	1. Initial Temperatures[1] — Positive Correlation	1. Initial Temperatures[1] — Positive Correlation
	2. Initial Containment Volume — Negative Correlation	2. Initial Containment Pressure — Positive Correlation	2. Concrete Thermal Conductivity — Negative Correlation	2. Concrete Thermal Conductivity — Negative Correlation	2. Concrete Thermal Conductivity — Negative Correlation	2. Concrete Specific Heat — Negative Correlation
	3. Initial IRWST Liquid Volume — Positive Correlation	3. Uchida Model Multiplier — Negative Correlation	3. Initial Containment Pressure — Positive Correlation	3. Concrete Specific Heat — Negative Correlation	3. Concrete Specific Heat — Negative Correlation	3. Concrete Thermal Conductivity — Negative Correlation
	4. Initial Temperatures[1] — Negative Correlation	4. Steel Specific Heat — Negative Correlation	4. Uchida Model Multiplier — Negative Correlation	4. Concrete Density — Negative Correlation	4. Concrete Density — Negative Correlation	4. Concrete Density — Negative Correlation
	5. Concrete Thermal Conductivity — Negative Correlation	5. Steel Density — Negative Correlation	5. Concrete Specific Heat — Negative Correlation	5. Liner/Concrete Air Gap — Positive Correlation	5. Liner/Concrete Air Gap — Positive Correlation	5. Liner/Concrete Air Gap — Positive Correlation
	6. Surface of Medium Steel — Negative Correlation	6. Concrete Thermal Conductivity — Negative Correlation	6. Concrete Density — Negative Correlation	6. Initial Containment Pressure — Positive Correlation	6. Initial Containment Pressure — Positive Correlation	6. Initial Containment Pressure — Positive Correlation
	7. Initial Relative Humidity — Negative Correlation	7. Concrete Specific Heat — Negative Correlation	7. Liner/Concrete Air Gap — Positive Correlation	7. Uchida Model Multiplier — Negative Correlation	7. Uchida Model Multiplier — Negative Correlation	7. Initial Relative Humidity — Negative Correlation
	8. Concrete Specific Heat — Negative Correlation	8. Initial Containment Volume — Negative Correlation	8. Steel Specific Heat — Negative Correlation	8. Steel Specific Heat — Negative Correlation	8. Steel Specific Heat — Negative Correlation	8. Uchida Model Multiplier — borderline importance — Negative Correlation
		9. Concrete Density — Negative Correlation	9. Steel Density — Negative Correlation	9. Steel Density — Negative Correlation	9. Steel Density — Negative Correlation	
		10. Liner/Concrete Air Gap — Positive Correlation	10. Surface of IRWST Ceiling/Heavy Floor — Negative Correlation	10. Surface of IRWST Ceiling/Heavy Floor — Negative Correlation		
		11. Surface of Medium Steel — Negative Correlation				
		12. Initial Relative Humidity — Negative Correlation				
		13. Initial IRWST Liquid Volume — Positive Correlation				
		14. Surface of Containment Wall — Negative Correlation				

Notes for Tables 7-13 and 7-14:

Sampled parameters are color-coded to track their influence during transient progression. Different colors are assigned based on common phenomenological importance. The following groupings are defined for color assignments:

a) Initial conditions and concrete physical properties

b) Surface area of heat sinks

c) Uchida model multiplier

d) Steel physical properties

e) Liner/concrete air gap

The color coding is allowed to change for key parameters as the transient progresses to highlight increased or reduced importance and/or correlative sign change

[1] **Containment atmosphere, IRWST, and structures**

AREVA NP Inc.
Applicability of AREVA NP Containment Response Evaluation Methodology to the
U.S. EPR™ for Large Break LOCA Analysis
Technical Report

ANP-10299NP
Revision 2
Page 7-44

Table 7-14—Effect of Important Input Parameters on Containment Pressure Responses, Post-Hot-Leg Injection

Sampled Parameters (decreasing order of importance)	Time Into Transient						
	2 Hr	3 Hr	6 Hr	9 Hr	12 Hr	18 Hr	24 Hr
	1. Initial Temperatures[1] — Positive Correlation	1. Initial Temperatures[1] — Positive Correlation	1. Initial Temperatures[1] — Positive Correlation	1. Initial Temperatures[1] — Positive Correlation	1. Concrete Specific Heat — Negative Correlation	1. Initial Containment Pressure — Positive Correlation	1. Initial Containment Pressure — Positive Correlation
	2. Concrete Specific Heat — Negative Correlation	2. Concrete Specific Heat — Negative Correlation	2. Concrete Specific Heat — Negative Correlation	2. Concrete Specific Heat — Negative Correlation	2. Concrete Density — Negative Correlation	2. Concrete Specific Heat — Negative Correlation	2. Concrete Specific Heat — Negative Correlation
	3. Concrete Thermal Conductivity — Negative Correlation	3. Concrete Thermal Conductivity — Negative Correlation	3. Concrete Thermal Conductivity — Negative Correlation	3. Concrete Thermal Conductivity — Negative Correlation	3. Concrete Thermal Conductivity — Negative Correlation	3. Initial Relative Humidity — Negative Correlation	3. Initial Relative Humidity — Negative Correlation
	4. Concrete Density — Negative Correlation	4. Concrete Density — Negative Correlation	4. Concrete Density — Negative Correlation	4. Concrete Density — Negative Correlation	4. Initial Temperatures[1] — Positive Correlation	4. Concrete Density — Negative Correlation	4. Concrete Density — Negative Correlation
	5. Liner/Concrete Air Gap — Positive Correlation	5. Liner/Concrete Air Gap — Positive Correlation	5. Liner/Concrete Air Gap — Positive Correlation	5. Initial Containment Pressure — Positive Correlation	5. Initial Containment Pressure — Positive Correlation	5. Concrete Thermal Conductivity — Negative Correlation	5. Concrete Thermal Conductivity — Negative Correlation
	6. Initial Containment Pressure — Positive Correlation	6. Initial Containment Pressure — Positive Correlation	6. Initial Containment Pressure — Positive Correlation	6. Liner/Concrete Air Gap — Positive Correlation	6. Initial Relative Humidity — Negative Correlation	6. Initial Temperatures[1] — Positive Correlation	
	7. Initial Relative Humidity — Negative Correlation	7. Initial Relative Humidity — Negative Correlation	7. Initial Relative Humidity — Negative Correlation	7. Initial Relative Humidity — Negative Correlation	7. Liner/Concrete Air Gap — Positive Correlation		
				8. Surface of Horizontal Concrete to Accessible Space — Negative Correlation	8. Blowdown Droplet Size — Negative Correlation		
					9. Surface of Horizontal Concrete to Accessible Space — Negative Correlation		

[1] Containment atmosphere, IRWST, and structures

8.0   ANALYSIS METHODS AND REGULATORY COMPLIANCE SUMMARY

The containment analysis evaluation methodology employed during U.S. EPR design
engineering is an adaptation of the methodology AREVA developed for conventional
Westinghouse, Combustion Engineering, and B&W PWRs (Reference14). This
methodology incorporates the guidelines presented in the NRC's Standard Review Plan
(Reference 8) and ANSI/ANS-56.4 (Reference 11) for maximizing coolant mass and
energy releases. The technical basis for this methodology is built upon a broad
foundation of thermal-hydraulic research and development programs and associated
code development activities for RELAP5-BW and GOTHIC and their predecessor code
versions.

Sections 8.1 - 8.3 describe AREVA NP's general approach to performing containment
analysis. This general discussion acknowledges that several parametric studies are
performed to identify the appropriate modeling prior to finalizing the models and event
scenarios. These sections address short-term containment mass and energy release
rates using RELAP5-BW, the long-term containment mass and energy release rates
using GOTHIC, and the prediction of containment pressure and temperature using
GOTHIC. Section 8.4 summarizes SRP compliance for the U.S. EPR-specific
calculations. The sample problem given in Section 9.0 has been prepared consistent
with the statements presented in Section 8.4.

8.1   Short-Term Mass and Energy Release for a LOCA

The short-term mass and energy release rates immediately following the postulated
rupture of the RCS piping is determined using the RELAP5-BW thermal-hydraulic
analysis code (Reference19). The RELAP5-BW code was originally developed for the
PWR design basis analysis of a hypothetical LBLOCA in compliance with the 10 CFR
50.46 and 10 CFR 50 Appendix K. Because the objective of Appendix K methods is to
bound phenomenological uncertainties in a manner that maximizes cladding
temperature, the inherent assumptions in these methods do not necessarily produce

AREVA NP Inc.

ANP-10299NP

Applicability of AREVA NP Containment Response Evaluation Methodology to the
U.S. EPR™ for Large Break LOCA Analysis

Revision 2

Technical Report

Page 8-2

conservative mass and energy release rates for performing containment integrity analyses.

The Appendix K models described in Reference 25 were used as a starting point, but they were adjusted to conservatively determine mass and energy release rates for containment analyses. The RELAP5-BW code is used exclusively to calculate short-term LOCA mass and energy release rates. The RELAP5-BW code package includes reflood heat transfer models as benchmarked in the BEACH Topical Report (Reference 26). The BEACH heat transfer models are incorporated in the RELAP5-BW code as approved in Reference 19. The mass and energy calculation does not utilize the REFLOD3B code (Reference 93).

The initial and boundary conditions for the mass and energy release calculations are chosen to maximize the stored energy in the primary and secondary coolant systems and to maximize the removal of this energy to containment. The sources of energy in the these analyses include: reactor power; decay heat; stored energy in the core; stored energy in the RCS metal, including the reactor vessel (RV) and RV internals; metal-water reaction energy; and stored energy in the secondary system, including SG tubing and secondary water. Maximizing the heat removal rate from these sources adds the most mass and energy to the containment in the shortest amount of time, thereby providing a conservative containment analysis. The treatment of principal short-term mass and energy release uncertainties is described in the following sections. For items not discussed, the approach used in the approved LOCA methods is used.

8.1.1   Sources of Energy

The sources of stored and generated energy in the analyses include: primary system fluid stored energy; reactor power; decay heat; stored energy in the core; stored energy in the RCS metal, including the RV and RV internals; metal-water reaction energy; and stored energy in the secondary system, including SG tubing and secondary water.

The primary system fluid stored energy is a function of the reactor power, RCS pressure, fluid flow, and heat removal from the RCS through the steam generators. The short-term containment pressure peak is primarily the result of mixing all the primary coolant with the containment atmosphere. The initial mass of water in the reactor coolant system is determined by the reactor coolant system volume calculated for the temperature and pressure conditions existing at full power, taking into account calorimetric uncertainty (i.e., hot, full power conditions).

Immediately after the initiating event, reactor power is calculated as a function of the negative reactivity caused by higher fuel temperatures and the generation of coolant voids (i.e., bubbles, slugs, etc.). The fuel-temperature coefficient and the void-moderator coefficient are modeled during blowdown. [

]A conservative initial stored energy in the core is obtained by utilizing a conservatively high initial fuel temperature. The RCS metal and secondary-side SG metal are modeled to reflect their size, location and composition. The system code includes a best-estimate model of the heat transfer across the SG tubes.

8.1.2   Break Flow Calculations

The short-term break flow is calculated using the Moody critical flow model, which conservatively over-predicts the discharge rate in comparison to experimental data. This model is approved for use in ECCS analyses (References 19 and 25). Since the thermal energy equations in RELAP5-BW are expressed in terms of phasic internal energies, a kinetic energy term is explicitly added to the energy release model in GOTHIC to capture the total energy contribution to the containment. This kinetic energy term is evaluated from the original RELAP5-BW calculation.

During certain conditions following a LOCA, the condensing of steam due to the injection of the relatively cold ECCS fluid causes a reduction of the RCS pressure below the containment pressure. Once the RCS pressure drops below the containment pressure, the potential exists for the inflow of air from the containment. This is not permitted (via an artificially large reverse form loss at the break).

8.1.3   Length of Refill Period

After the blowdown phase, the reactor vessel lower plenum is refilled by the ECCS. For LOCA mass and energy release rate calculations, a conservative refill period is one that is minimized to advance the heat transfer from the fuel elements to the fluid in the core.
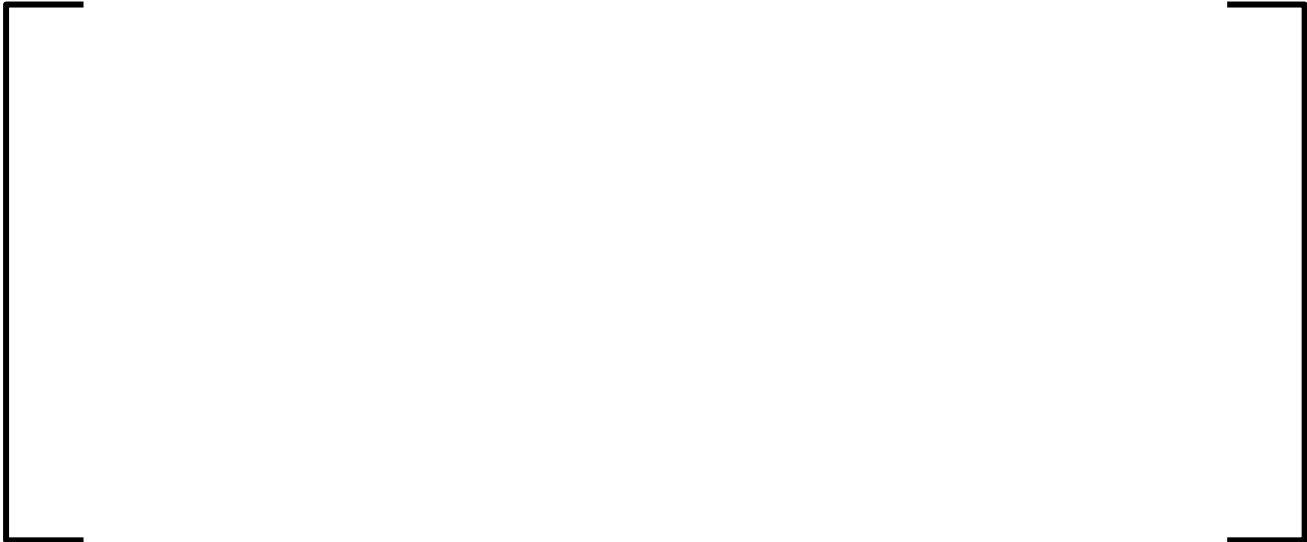
8.1.4   Emergency Core Cooling System Injection

The ECCS for the U.S. EPR includes four MHSI trains, four LHSI trains, and four passive accumulators, all of which inject into the cold legs. The LHSI trains for loops 1 and 2 and separately, 3 and 4 are cross-connected whenever one train of LHSI is removed from service for preventive maintenance. After 60 minutes, the operator realigns to operating LHSI to inject into the bottoms of respective hot legs.

To obtain maximum ECCS flow, best estimate pump performance data is used and all four ECCS trains are assumed to be available. To obtain minimum ECCS flow, only 2 out of the 4 trains are assumed to be available. One train is assumed to be out of

service for maintenance and another train is assumed to fail. In this case, degraded pump performance data is used to minimize ECCS flow rates for each train. Depending on the location of the break (hot leg or cold leg) and which loops the ECCS injects to, the amount of ECCS reaching the reactor vessel could vary. The cross-connect flow between loops is modeled conservatively to maximize mass and energy release to the containment.

The ECCS injection delay times correspond to the availability of offsite power.

8.1.5   ECCS Source Water Temperature

The Technical Specification maximum liquid temperature is assumed for the ECCS (MHSI and LHSI) liquid for performing the short-term mass and energy release analysis. Using the maximum liquid temperature minimizes the liquid subcooling, thus maximizes the steaming potential.

8.1.6   Reactor Coolant Pump Operation

The availability of offsite power determines the RCP operation. If offsite power is lost, the pumps coast down coincident with LOOP. If offsite power is available, the pumps continue to run until they are tripped automatically on a coincident safety injection (SI) signal and low pressure differential across the pumps. For a LBLOCA, this occurs very soon after initiation of the event.

In cases where the RCPs continue to run until tripped, a two-phase degradation curve is applied. The RCP anti-rotation devices are not safety grade equipment and are not credited in the analysis.

8.1.7   Main Feedwater

The main feedwater system in the U.S. EPR continues to feed the steam generators until receipt of an isolation signal or there is a loss of offsite power. Because additional mass increases the stored energy on the secondary side, main feedwater system

delivery is maximized. In cases without LOOP, the main feedwater system is isolated conservatively.

8.1.8   Emergency Feedwater System

Emergency feedwater (EFW) is significantly colder than the fluid in the RCS and SG secondary side. Therefore, the introduction of EFW decreases the temperature difference across the tubes and, therefore, secondary-to-primary heat transfer. Because of this, actuation of the emergency feedwater (EFW) system is either delayed conservatively or not credited. This modeling approach maximizes the secondary side fluid energy available for transfer to the primary system.

8.1.9   Accumulator Cover Gas Injection

The injection of the accumulator cover gas into the RCS is considered explicitly, including both the dissolved gas in the accumulator liquid and the direct gas injection after the liquid in the accumulators is discharged. The addition of the accumulator cover gas affects the partial pressure of the containment atmosphere, effectively raising the total pressure. The mass of the accumulator cover gas being discharged into the containment building is set conservatively equal to the total available in the accumulators.

8.1.10   SG Tube Plugging

In order to maximize primary inventory and enhance inverse heat after blowdown when inverse heat transfer from the SG secondary side to the primary side is possible, no SG tube plugging is assumed.

8.1.11   Steam Generator Tube Heat Transfer

RELAP5-BW is used to calculate the heat transfer from the SG secondary side to the primary side. Heat transfer to the primary side is conservatively maximized to allow quick energy dissipation to the containment. The Becker CHF option is used on both

boundaries of the SG tube heat structures. Using the Becker option expedites heat transfer from the SG secondary side to the primary side as discussed in Section 6.1.3.

8.1.12 Turbine Trip and Turbine Stop Valves

A turbine trip is modeled to occur coincident with break opening. A conservative delay time and a conservative valve stroke time are assumed. Minimizing the turbine trip delay time quickly isolates the secondary side, thereby maximizing the stored energy in the secondary system.

8.1.13 Main Steam Safety Valves

The U.S. EPR has two MSSVs per SG. The MSSV opens when the secondary pressure reaches the valve setpoints and allows relief to the secondary system. For LOCA mass and energy release analysis, it is conservative to assume all the MSSVs remain closed to keep the energy in the secondary side where it can be transferred to the primary system.

8.1.14 Partial Cooldown Mechanism

The programmed partial cooldown of the steam generators on receipt of an SI signal is a feature of the U.S. EPR. The partial cooldown is accomplished by lowering the MSRT pressure control setpoints of the four SGs at a rate corresponding to 180°F/h. Initiation of safety injection is conservatively delayed to the partial cooldown activation.

8.1.15 Containment Backpressure

The containment backpressure is modeled in the RELAP5-BW system calculations to provide a conservative calculation of a mass and energy release rate. A time-dependent backpressure is specified that is refined through iterative calculations of mass and energy release and containment pressure response. In this way, the containment pressure is consistent with the mass and energy release rate for each break size and location.

8.1.16 Transition Time between RELAP5 and GOTHIC

The short-term mass and energy releases calculated with RELAP5-BW code are input as boundary conditions to the GOTHIC containment pressure response calculation. A simplified analytical model is incorporated into the GOTHIC code to calculate the long-term mass and energy releases.
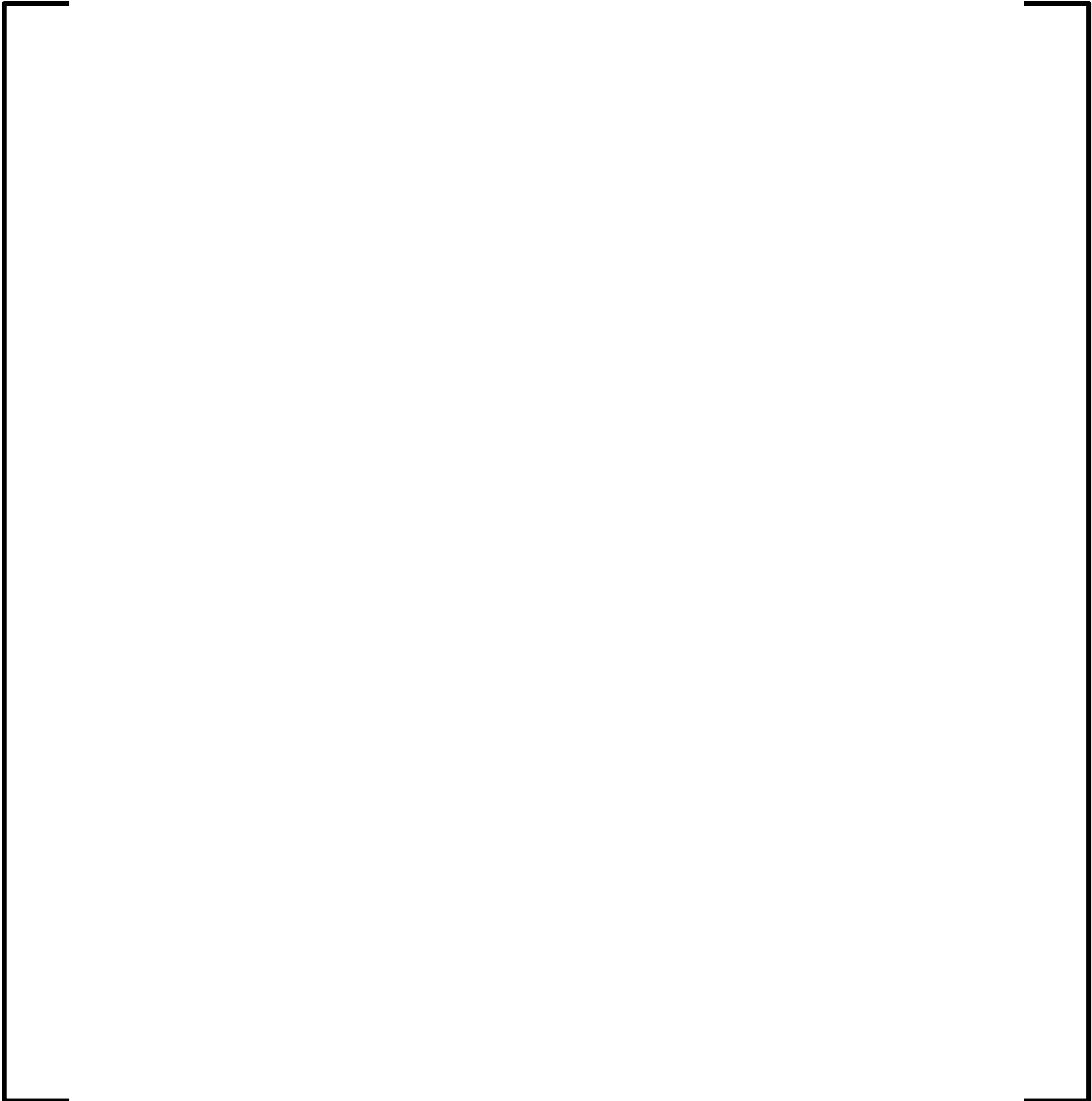
8.2   Long-Term Mass and Energy Release for LOCA

Once the core is quenched, the LBLOCA proceeds into the long-term cooling phase of the analysis (post-reflood and decay heat phases). The reactor vessel coolant is in a quasi-steady-state condition, characterized by the vessel level recovered to the RCS loop nozzle elevations and the ECCS injection maintaining the core covered so that core decay heat and sensible heat are being removed. The long-term mass and energy releases are modeled in GOTHIC by adding a node to representing decay heat and sensible heat.

On the containment side, GOTHIC models are provided for the IRWST recirculation, the emergency core cooling function of the ECCS (SIS/RHR pumps and RHR heat exchangers), and containment heat removal by steam condensation/convection on the containment passive heat sinks.

The long-term sources of energy are:

- Core decay heat

- Primary system fluid stored energy

- Primary system passive metal stored energy (including core metal stored energy)

- Secondary system stored energy (fluid + metal)

- Safety injection pump heat addition

The treatment of each of these sources in the long-term GOTHIC model is described in the following sections.

8.2.1 Core Decay Heat

[

]

8.2.2 Primary Fluid Stored Energy

The stored energy component is included in the initial conditions specified for the vessel in the long-term GOTHIC containment model. These initial conditions are taken from the RELAP5-BW calculation at the transition time to GOTHIC. They represent the liquid volume fraction in the RCS (vessel + loop piping) and the averaged quantities of RCS liquid and vapor temperatures and RCS pressure.

8.2.3 Sensible Heat

The modeling of sensible heat sources in the GOTHIC model considers the principal sources from the primary system passive metal stored energy, the secondary-side fluid, and safety injection pump heat.

8.2.3.1 Primary System Passive Metal Stored Energy

The release of the RCS passive metal stored energy remaining at the transition time to containment atmosphere or liquid region is modeled based on the path to the break. Specifically, sensible energy in the steam path to the break is modeled as a heater component in the vessel node. This increases the steaming rate at the break. This heater primarily accounts for the stored energy from the metals above the RV nozzles including the upper plenum, upper head, broken loop hot leg and the broken loop steam

8.2.3.2   *Secondary Stored Energy*

AREVA NP Inc.

Applicability of AREVA NP Containment Response Evaluation Methodology to the
U.S. EPR™ for Large Break LOCA Analysis
Technical Report

ANP-10299NP
Revision 2

Page 8-12
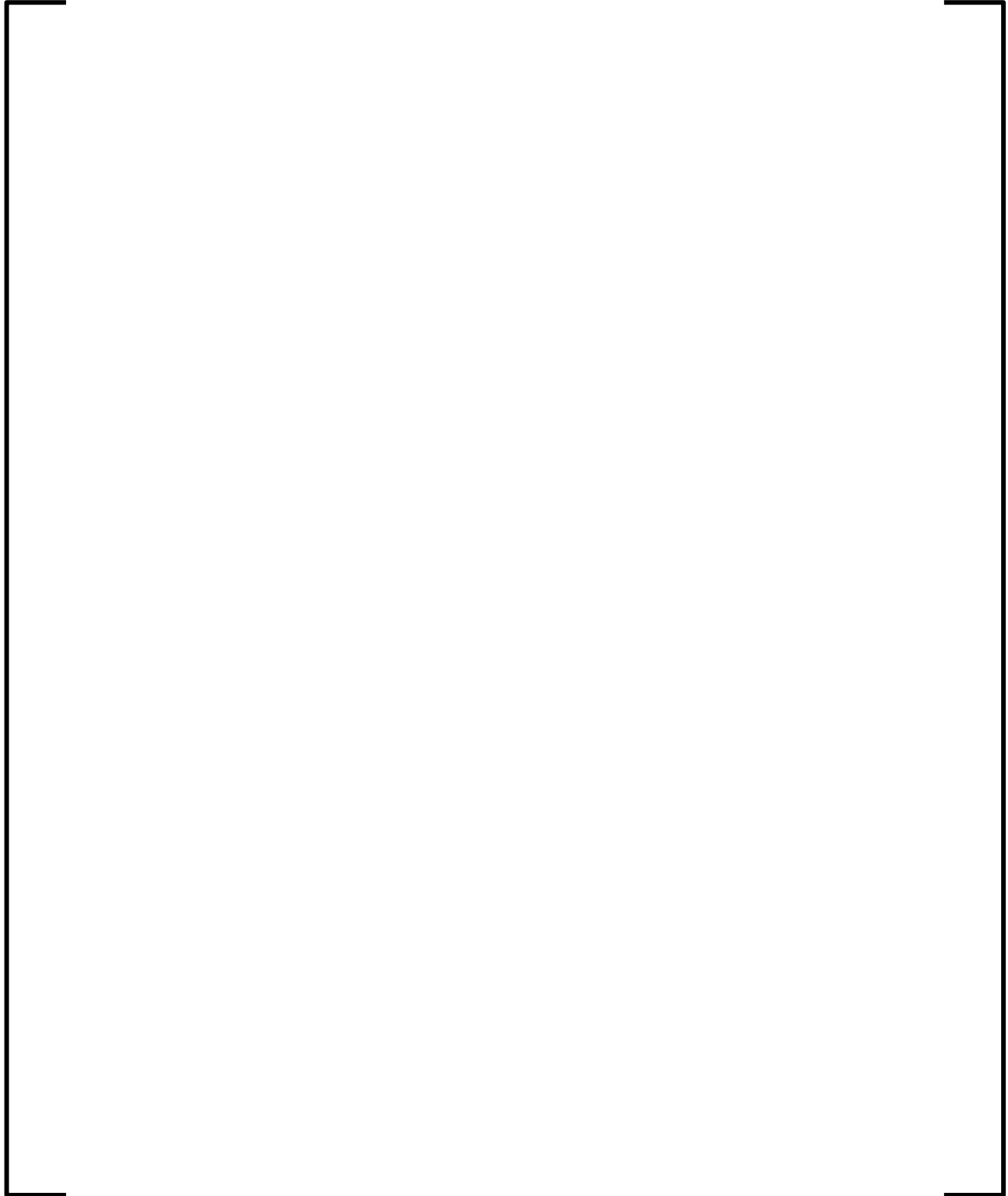
8.2.3.3 Safety Injection Pump Heat Addition

The ECCS pump also adds energy to the containment. This additional energy is included as a heater component placed in the IRWST. The time history of the power input reflects ECCS pump start times and the total number of pumps in operation.

8.2.3.4 Summary of Sensible Heat Treatment

The following table summarizes the description and treatment of each of these sensible heat sources in the long-term GOTHIC model.

Table 8-1—Summary of Sensible Heat Calculation and Modeling

Sensible Heat Components	Method of Sensible Heat Dissipation	GOTHIC Model
Primary Side Sensible Heat (RCS Metal)		
Intact Loops and Broken Loop Cold Legs		
Reactor Vessel (below the nozzles)		
Reactor Vessel (above the nozzles) and the Broken Loop Hot Leg		
Pressurizer		
Secondary Side Sensible Heat (SGs)		
Broken Loop SG		
Intact Loop SG		
ECCS Pumps		
Safety injection pump heat addition		

8.3   GOTHIC Containment Model

A multi-node GOTHIC model with a three-dimensional, subdivided mesh in the containment dome is used to predict the natural circulation patterns and any potential thermal stratification. A simplified nodalization scheme is included as Figure 9-7.

The containment net-free volume is conservatively minimized to maximize the predicted pressures. The heat transfer between the IRWST liquid and vapor is conservatively removed by setting the liquid-to-vapor interfacial area to an arbitrarily small value.

Section 8.3.1 describes the GOTHIC modeling options selected for performing containment analysis. Section 8.3.2 presents instructions for the long-term mass and energy release calculation before and after hot leg injection.

8.3.1   GOTHIC Model Description

The GOTHIC computer code allows the user the flexibility of specifying different modeling options. Unless specifically noted in this section, the user specified GOTHIC options described in Section 4.0 of Reference 14 are applied to the calculation of LOCA containment pressure response for the U.S. EPR.

8.3.1.1   Mass and Energy Release Boundary Conditions

The mass and energy releases calculated by RELAP5-BW are implemented in GOTHIC through four individual phasic boundary conditions. These four boundary conditions respectively represent the steam and liquid streams discharged from reactor vessel and SG sides of the break. Using phasic boundary conditions instead of combined boundary conditions enables subcooled liquid to be discharged to the containment when steam is present, thereby allowing more energy to be carried out to the containment by the steam phase.

The ANSI/ANS 56.4 guidelines (Reference 11) describe an acceptable model for the phase separation to be used in pressure and temperature transient analyses in PWRs. This phase separation model is implemented in GOTHIC by flashing the blowdown

effluent directly to the vapor region of the containment to the saturation temperature at the containment total pressure. During blowdown and up to the first pressure peak, the droplet model specified in Section 4.1 of Reference 14 is activated. Following blowdown, the droplet model is deactivated; that is, mass from the RCS appearing in the containment is modeled as only liquid or vapor.

8.3.1.2   User-Specified Modeling Options

The GOTHIC computer code allows the user the flexibility of specifying different modeling options. The user specified GOTHIC options are:

- Phase separation assumption and droplet size for the blowdown mass and energy release.

- Spray droplet size.

- Revaporization fraction.

- Wall condensation heat transfer.

- Fog model.

- Maximum mist density.

- Drop diameter from mist.

- Minimum heat transfer coefficient.

- Reference pressure.

- Forced entrainment drop diameter.

- Vapor phase head correction.

- Kinetic energy.

- Vapor phase.

- Liquid phase.

- Drop phase.

- Force equilibrium.

- Drop-liquid conversion.

The AREVA method bases selection of options on one or more of the following: supporting experimental data, code vendor recommendations (Reference 20), regulatory guidelines, or industry consensus. A summary of the selected options is provided in Table 8-2. These modeling options are applied in the sample calculation presented in Section 9.0 of this report.

Table 8-2—Summary of Selected GOTHIC User Options for LOCA Analyses

GOTHIC User Option	Selection
Blowdown Droplet Size	100 microns
Phase Separation during Blowdown	Flashing of M&E blowdown to the saturation temperature at the containment total pressure
Revaporization Fraction	GOTHIC condensate revaporization model (default input)
Spray Droplet Size	N/A
Wall Condensation Heat Transfer	Diffusion Layer Model (DLM or DLM-FM) with radiation heat transfer
FOG/MIST Model	FOG model OFF (MIST model activated)
Maximum Mist Density	Default input (1 g/m^3)
Mist Droplet Diameter	Default input (200 microns)
Reference Pressure	IGNORE
Forced Entrainment Droplet Diameter	N/A (set to default input)
Vapor Phase Head Correction	INCLUDE
Kinetic Energy	IGNORE

GOTHIC User Option	Selection
Vapor Liquid and Drop Phases	INCLUDE
Force Equilibrium	IGNORE
Drop-Liquid Conversion	INCLUDE
Minimum Heat Transfer Coefficient	0 Btu/hr-ft^2-$^\circ$F

8.3.1.3   Vessel Node Initial Conditions

The vessel node is initialized to maintain continuity from the RELAP5-BW calculation and to avoid nonphysical behavior. The initial pressure of the vessel node is set equal to the containment total pressure at the time of transition. The liquid temperature is set to the saturation temperature so that there is no steam condensation. The vapor temperature is set to the average vapor temperature of the RCS based on the RELAP5-BW calculation at the transition time. The vessel node initial liquid volume fraction is set to the average liquid volume fraction of the RCS based on the RELAP5-BW calculation at the transition time.

The break elevation is set equal to the collapsed liquid level elevation in the vessel. The break area is set consistent with the break area in the RELAP5-BW calculations, and the height of the break path is set to an arbitrary value of 3 feet to avoid possible flow oscillations at the break. These break modeling assumptions have no effect on the intended application because the long-term GOTHIC models ignore the kinetic energy transport terms. This is a reasonable assumption considering the low mass and energy release rates associated with the long-term phase. As described in Section 8.1.2, the short-term GOTHIC model kinetic energy transport terms are included in the stagnation enthalpy of the break effluent.

8.3.1.4   ECCS Injection Flow Rates

For the minimum ECCS scenarios, degraded LHSI and MHSI flow rates will be used in the calculation of both short-term and long-term mass and energy releases. However, for maximum ECCS scenarios, the best-estimate LHSI and MHSI flow rates will be used

in the calculation of both short-term and long-term mass and energy releases. The assumed cold leg pressure lookup value used to determine ECCS volume flow rates is chosen conservatively.

8.3.1.5   *Hot Leg Injection*

As a long-term cooling and boron management strategy, LHSI is sometimes realigned by the operators to inject into the hot legs. With this realignment, a fraction of the LHSI continues to be delivered to the cold leg and to the IRWST (i.e., as part of the recirculation process for cooling the IRWST).   The MHSI pumps continue injection into the cold legs only.

In the long-term GOTHIC model, the ECCS flow to the vessel is modeled to obtain a conservative steam release to containment, based on the following methods:

The detailed long-term mass and energy release calculation is discussed in Section 8.3.2.

8.3.1.6   Pool Condensation

The IRWST pool in the U.S. EPR is designed to be cooled and mixed by recirculating water through the heat exchanger of the RHR system. The GOTHIC model calculates heat and mass transfer on the liquid pool surface based on the vapor and liquid bulk temperature with interface temperature solved internally by GOTHIC. In reality, the steam condensation on the water layer is reduced by a condensate layer formed on the top of the sump. Though the latest version of GOTHIC is capable of modeling water stratification in the IRWST, to avoid uncertainties associated with pool surface condensation, AREVA NP conservatively assumes there is no heat transfer between the containment vapor and IRWST liquid regions.

8.3.2   Long-term Mass and Energy Release Calculation

In the long-term phase, the vessel thermal-hydraulics are assumed to be at a quasi-steady-state condition so that the phenomena to be modeled are: a nearly constant coolant level in the vessel, steam production in the core, and the transfer of heat from the remaining heat sources in the primary and secondary systems (sensible heat). The LOCA mass and energy releases associated with the long-term phase are modeled in GOTHIC by adding a node to represent the RCS and including heat sources to represent decay heat and sensible heat.

8.3.2.1   Long-Term Model Configuration before ECCS realignment

Prior to ECCS realignment of the LHSI, all ECCS injects to the cold legs. The ECCS flow rate to the vessel node is set to match the boil-off rate in the vessel node. The remainder of the ECCS will be bypassed and directed to the sump with no heat added. The ECCS water to the vessel node is raised to saturation by decay heat and metal stored energy with excess energy going to boiling. The GOTHIC long-term model for the calculation of mass and energy release prior to the ECCS realignment is shown in Figure 8-1.

Figure 8-1—GOTHIC Long-Term Model prior to LHSI Realignment

AREVA NP Inc.

Applicability of AREVA NP Containment Response Evaluation Methodology to the
U.S. EPR™ for Large Break LOCA Analysis
Technical Report

ANP-10299NP
Revision 2

Page 8-22

8.3.2.2   Long-Term Model Configuration following ECCS Realignment

Following the alignment of the LHSI to the hot legs, the RCS evolves from a simple boiling bot to a slightly more complex but self-contained circulation loop. In the GOTHIC model, the RCS is still modeled as a single volume node. However, to model the mixing effects in the vessel, the hot leg injection must be split into two paths: the vessel injection path and the vessel bypass path directly to the IRWST. The basis for the flow split is described in Figure 8-2.

The natural circulation flow patterns in the reactor vessel during hot leg injection are driven by core decay heat and the influx of cold ECCS water from the hot legs. The result is vigorous mixing in the core and plena that suppresses net steaming from the reactor vessel. Core heat is carried away with the flow of warmed ECCS water to the cold leg break. Figure 8-3 shows the overall mass and energy balance on the reactor vessel.

Figure 8-2—Flow Patterns in the Reactor Vessel during Hot Leg Injection

Figure 8-3—Reactor Vessel Mass and Energy Balance during Hot Leg Injection
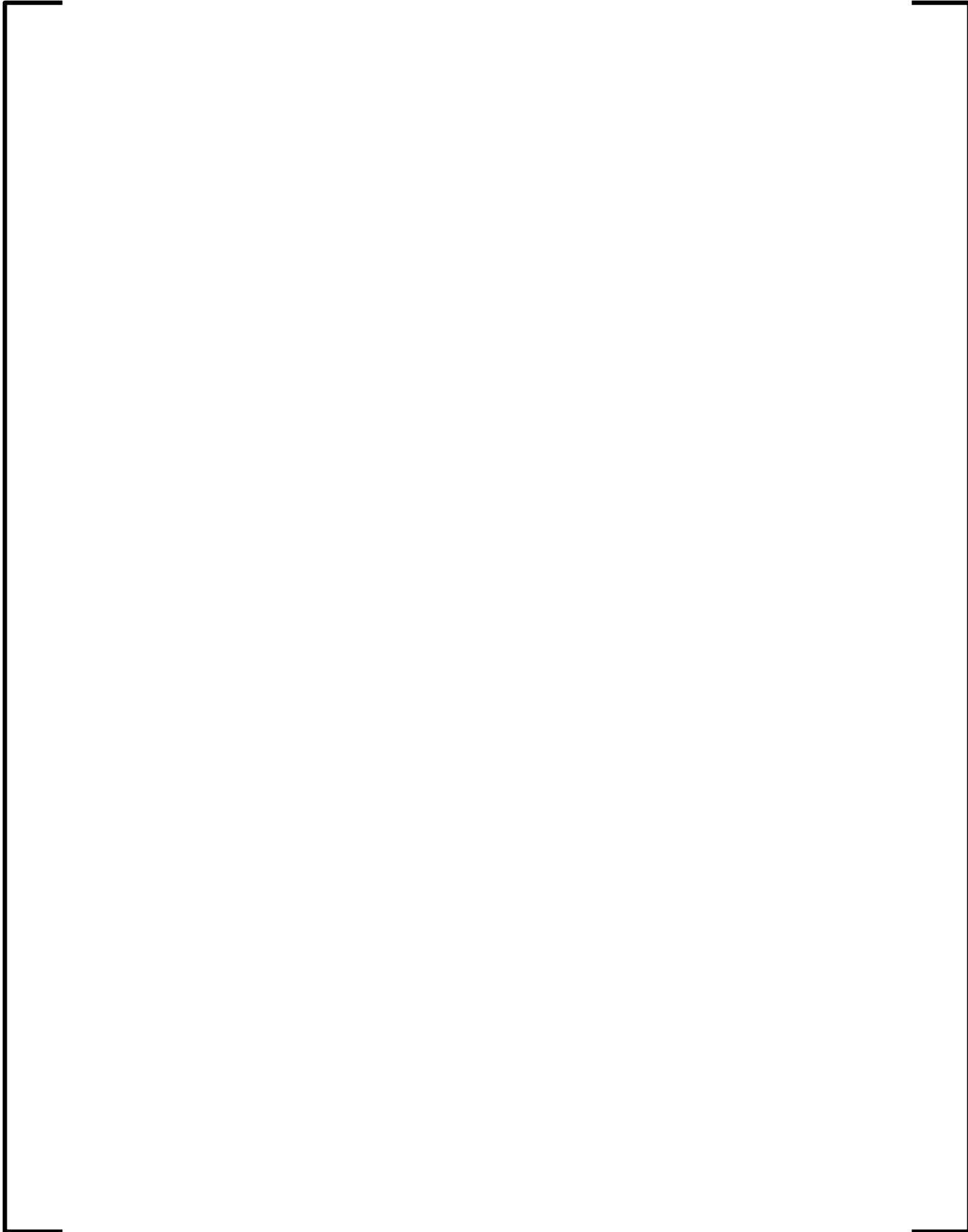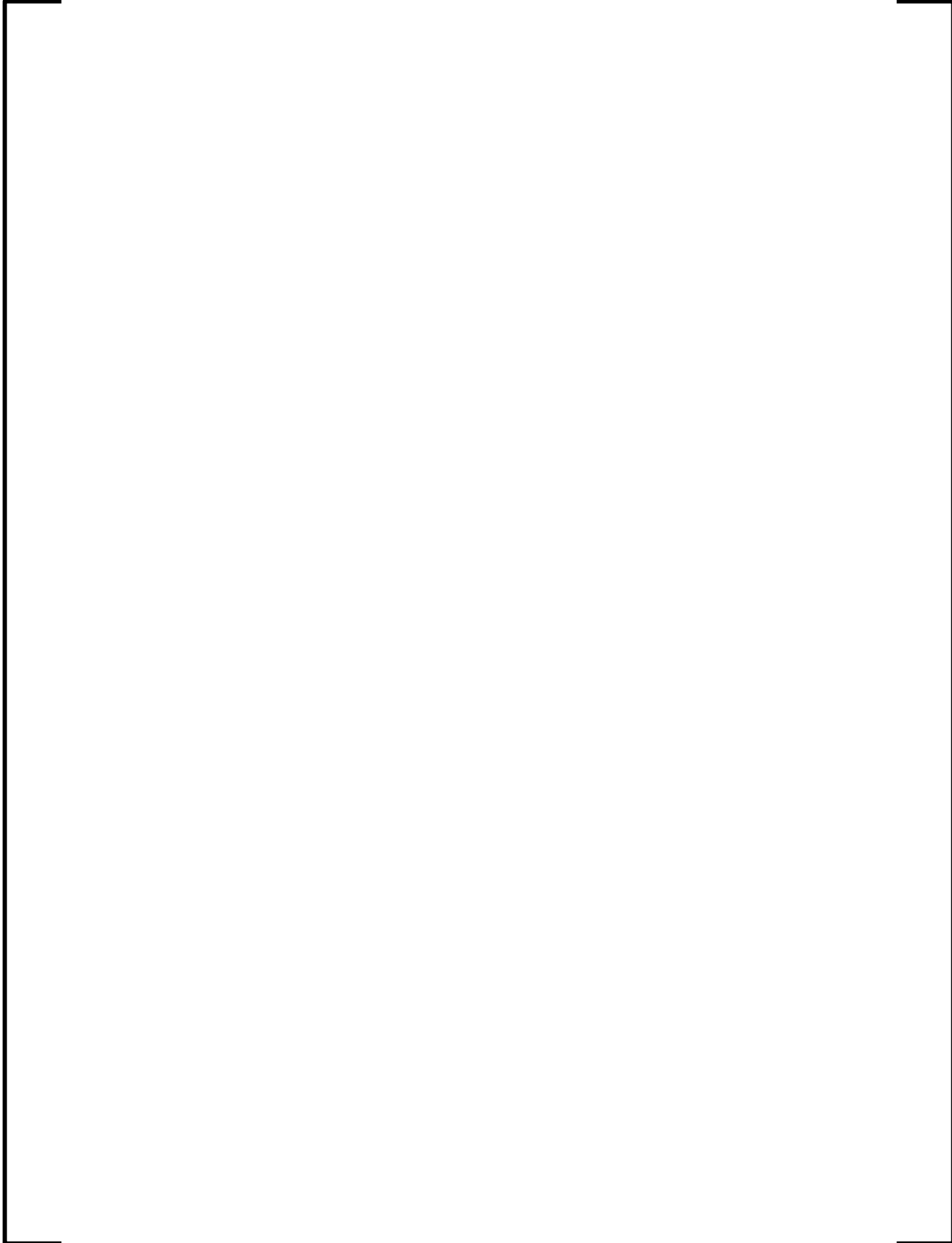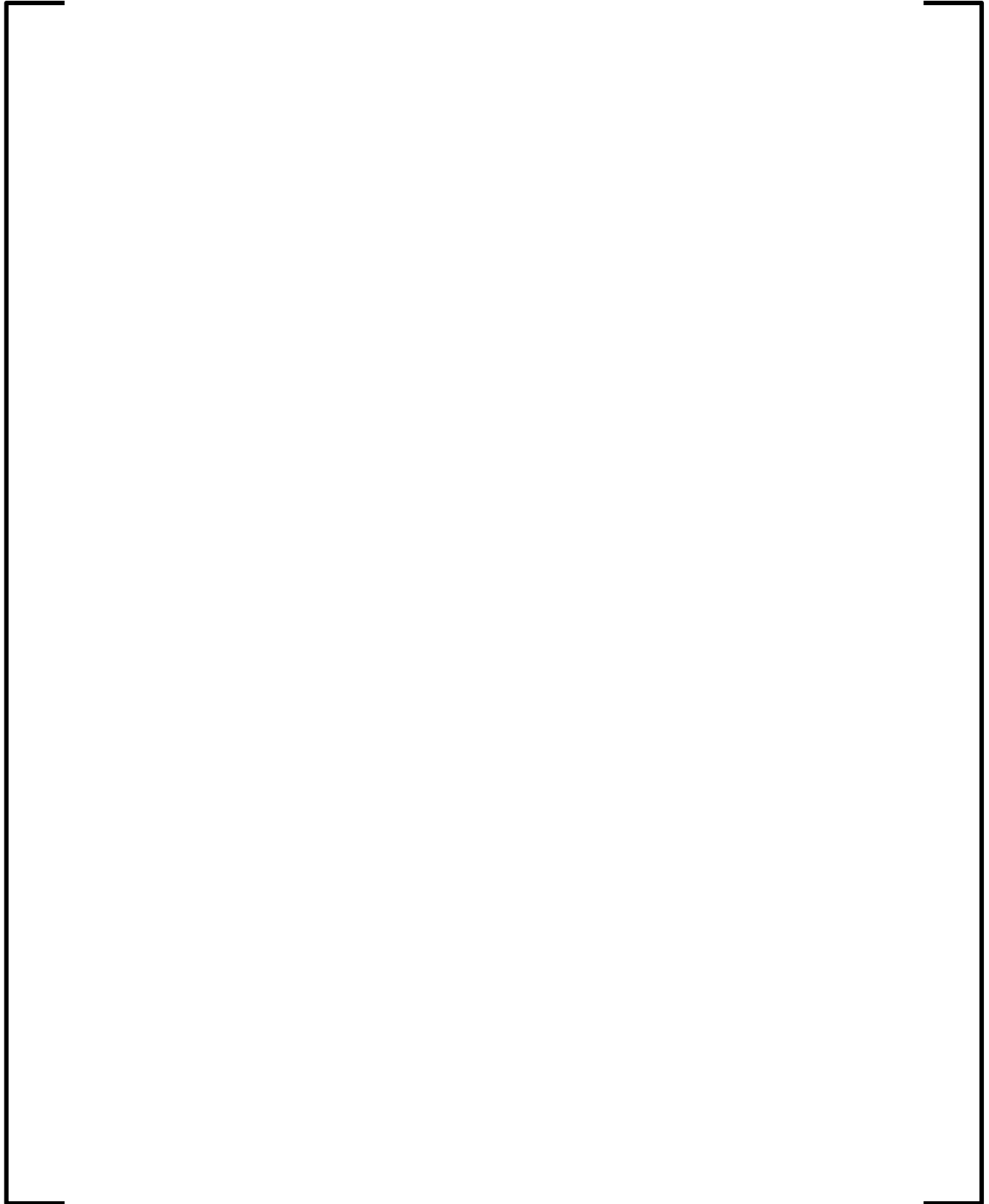
Figure 8-4—GOTHIC Long-Term Model after Actuation of HL Injection

8.4 Regulatory Compliance Matrix

This section compares the AREVA NP containment response evaluation methodology as applied to the U.S. EPR to NUREG-0800 and ANSI/ANS-56.4 guidelines:

AREVA NP Inc.

Applicability of AREVA NP Containment Response Evaluation Methodology to the
U.S. EPR™ for Large Break LOCA Analysis
Technical Report

ANP-10299NP
Revision 2

Page 8-30

SRP 6.2.1.1.A PWR Dry Containments, Acceptance Criteria		AREVA Methodology
6.1.a	GDC 16 and 50- The peak calculated containment pressure following a loss-of coolant accident, or a steam or feedwater line break, should be less than the containment design pressure	
6.1.b	GDC 38 – The containment pressure should be reduced to less than 50% of peak calculated pressure for the design basis loss of coolant accident with 24 hours after the postulated accident	
6.1.c	GDC 38 – The containment pressure for sub-atmospheric containments should be reduced to below atmospheric pressure within one hour after the postulated accident, and the sub-atmospheric condition maintained for at least 30 days.	
6.1.d	GDC 38 and 50 – For containment response to the loss-of–coolant accident, the analysis should be based on the assumption of loss of off-site power and the most severe single failure in the emergency power system (e.g., a diesel generator failure) the containment heat removal systems (e.g., a fan, pump, or valve failure), or the core cooling systems (e.g., a pump or valve failure). The selection made should result in the highest calculated containment pressure.	

SRP 6.2.1.1.A PWR Dry Containments, Acceptance Criteria	AREVA Methodology
6.1.e	GDC 38 and 50 – For containment response to secondary system pipe ruptures, the analysis should be based on the most severe single failure in the containment heat removal systems (e.g., a fan, pump, or valve failure. The analysis should also be based on a spectrum of pipe break sizes and reactor power levels. The accident conditions selected should result in the highest calculated containment pressure or temperature depending on the purpose of the analysis.	

AREVA NP Inc.

Applicability of AREVA NP Containment Response Evaluation Methodology to the
U.S. EPR™ for Large Break LOCA Analysis
Technical Report

ANP-10299NP
Revision 2

Page 8-32

SRP 6.2.1.3 M&E for LOCA Sources of Energy (II.B.1) (10 CFR Part 50 Appendix K, I.A)	AREVA Methodology
1	Reactor Power – The reactor should be assumed to have operated continuously at least 1.02 times the licensed power level; however, a lower core power level – no less than licensed power – could be justified.	
2	Stored Energy in the Core – The steady-state temperature distribution and stored energy in the fuel shall be calculated for the burn-up that yields the highest calculated stored energy.	
3	Fission Heat - Fission heat shall be calculated using reactivity and reactor kinetics. Shutdown reactivity resulting from temperatures and voids shall be given their minimum plausible values, including allowance for uncertainties.	
4	Decay of Actinides – The heat from the radioactive decay of actinides, including neptunium and plutonium generated during operation, as well as isotopes of uranium, shall be calculated in accordance with fuel cycle calculations and known radioactive properties.	
5	Fission Product Decay – The heat generation rates from radioactive decay of fission products shall be assumed to be equal to 1.2 times the values for infinite operating time in the 1971 ANS Standard. The fraction of the locally generated gamma energy that is deposited in the fuel (including the cladding) may be different from 1.0; the value used shall be justified by a suitable calculation.	
6	Metal – Water Reaction Rate – The rate of energy release, hydrogen generation, and cladding oxidation from the metal/water reaction shall be calculated using the Baker-Just equation. The reaction shall be assumed not to be steam limited.	
7	Stored Energy in the Reactor Coolant system metal – Heat transfer from piping, vessel walls, and non-fuel internal hardware shall be taken into account.	
8	Stored Energy in the Secondary System – Heat transfer between the primary and secondary systems in the SG shall be taken into account.	
9	Fuel Clad Swelling and Rupture – The prediction of fuel clad swelling and rupture should not be considered.	

SRP 6.2.1.3 M&E for LOCA Break Size and Location (II.B.2)		AREVA Methodology
1	Containment design basis calculations should be performed for a spectrum of possible pipe breaks sizes and locations to assure that the worst case has been identified.	

SRP 6.2.1.3 M&E for LOCA Blowdown Calculations (II.B.3.b)		AREVA Methodology
1	The initial mass of water in the reactor coolant system should be based on the reactor coolant system volume calculated for the temperature and pressure conditions existing at 102% of full power.	
2	Mass release rates should be calculated using a model that has been demonstrated to be conservative by comparison to experimental data.	
3	Calculations of heat transfer from surfaces exposed to the primary coolant should be based on nucleate boiling heat transfer. For surfaces exposed to steam, heat transfer calculations should be based on forced convection.	
4	Calculations of heat transfer from the secondary coolant to the SG tubes for PWRs should be based on natural convection heat transfer for tube surfaces immersed in water and condensing heat transfer for the tube surfaces exposed to steam.	

AREVA NP Inc.

ANP-10299NP

Applicability of AREVA NP Containment Response Evaluation Methodology to the

Revision 2

U.S. EPR™ for Large Break LOCA Analysis

Technical Report

Page 8-34

	SRP 6.2.1.3 M&E for LOCAPWR Core Reflood Calculations (II.B.3.c)	AREVA Methodology
1	Following initial blowdown of the RCS, the water remaining in the RV should be assumed to be saturated.	
2	Justification should be provided for the refill period. An acceptable approach is to assume a water level at the bottom of the active core at the EOB so there is no refill time.	
3	Calculations of the core flooding rate should be based on the ECCS operating condition that maximizes the containment pressure either during the core reflood phase or the post-reflood phase.	
4	Calculations of liquid entrainment should be based on PWR FLECHT experiments.	
5	Liquid entrainment should be assumed to continue until the water level in the core is 2ft from the top of the core.	
6	The assumption of steam quenching should be justified by comparison with applicable experimental data. Liquid entrainment calculations should consider the effect on the carryout rate fraction of the increase core inlet water temperature caused by steam quenching assumed to occur from mixing with the ECCS water.	
7	For Cold Leg Breaks only. Steam leaving the steam generators should be assumed to be superheated to the temperature of the secondary coolant.	

AREVA NP Inc.

ANP-10299NP

Applicability of AREVA NP Containment Response Evaluation Methodology to the

Revision 2

U.S. EPR™ for Large Break LOCA Analysis

Technical Report

Page 8-35

SRP 6.2.1.3 M&E for LOCA PWR Post-Reflood Calculations (II.B.3.d)		AREVA Methodology
1	All remaining stored energy in the primary and secondary systems should be removed during the post-reflood phase.	
2	Steam quenching should be justified by comparison with applicable experimental data.	
3	The results of post-reflood analytical models should be compared to applicable experimental data.	.

SRP 6.2.1.3 M&E for LOCA PWR Decay Heat Phase Calculations (II.B.3.e)		AREVA Methodology
1	The dissipation of the core decay heat should be considered during this phase of the accident. The fission product decay energy model is acceptable if it is equal to or more conservative than the decay energy model given in Branch Technical Position ASB 9-2 in SRP §9.2.5.	
2	Steam from decay heat boiling in the core should be assumed to flow to the containment by the path which produces the minimum amount of mixing with ECCS injection water.	

SRP 6.2.1.4, M&E for Secondary System Pipe Ruptures, II.1, Sources of Energy	AREVA Methodology
1	The stored energy in the affected SG metal, including the vessel tubing, feedwater line, and steam line.	
2	The stored energy in the water contained within the affected SG.	
3	The stored energy in the feedwater transferred to the affected SG prior to closure of the isolation valve in the FW line.	
4	The stored energy in the steam from the unaffected SG(s) prior to closure of the isolation valves in the SG crossover lines.	
5	The energy transferred from the primary coolant to the water in the affected SG during blowdown.	
6	The SLB should be analyzed for a spectrum of pipe sizes and various plant conditions from hot standby to 102% of full power. Only the 102% power condition need be analyzed provided the applicant can demonstrate that the feedwater flows and fluid inventory are greatest at full power.	

SRP 6.2.1.4 M&E for Secondary System Pipe Ruptures, II.2, M&E Release Rate Calculations	AREVA Methodology
1	Mass release rates should be calculated using the Moody model for saturated conditions, or a model that is demonstrated to be equally conservative.	
2	Calculations of heat transfer to the water in the affected SG should be based on nucleate boiling heat transfer.	
3	Calculations of mass release should consider the water in the affected SG and FW line, the FW transferred to the affected SG prior to the closure of the isolation valves in the FW lines, the steam in the affected SG, and the steam coming from the unaffected SG(s) as the secondary system is being depressurized prior to the closure of the isolation valves in the SG crossover lines.	

AREVA NP Inc.   ANP-10299NP

Applicability of AREVA NP Containment Response Evaluation Methodology to the   Revision 2
U.S. EPR™ for Large Break LOCA Analysis

Technical Report   Page 8-37

SRP 6.2.1.4 M&E for Secondary System Pipe Ruptures, II.2, M&E Release Rate Calculations	AREVA Methodology
4 If liquid entrainment is assumed in the SLB, experimental data should support the predictions of the liquid entrainment model.	
5 The effect on the entrained liquid of steam separators located upstream from the break should be taken into account.	
6 A spectrum of SLB should be analyzed, beginning with the double-ended break and decreasing in area until no entrainment is calculated to occur, to allow section of the maximum release case.	
7 If no liquid entrainment is assumed, a spectrum of the SLBs should be analyzed beginning with the double-ended break and decreasing in area until it has been demonstrated that the maximum release rate has been considered.	
8 A single active failure in the steam or feedwater line isolation provisions or feedwater pump, such that the containment peak pressure and temperature are maximized, should be assume to occur in steam and feedwater line break analyses. For the assumed failure of a safety grade steam or feedwater line isolation valve, operation of non-safety grade equipment may be relied upon as a backup to the safety grade equipment.	
9 Operator action to terminate auxiliary feedwater flow will be reviewed by ASB (i.e., must be justified).	

Conformance to ANSI-ANS-56.4-1983:

ANSI-ANS-564.4-1983	AREVA Methodology
4.2.1 Postulated Accidents	
4.2.2 Duration of Analyses	
4.2.3 Dry Primary Containment Analysis Model	
4.2.3.1 Thermodynamic State Conditions	

ANSI-ANS-564.4-1983	AREVA Methodology
4.2.3.1.2 Dry Primary Containment Sump Region	
4.2.3.2 Mass and Energy Transfer Mechanism	
4.2.3.2.2 Energy Source Terms	
4.2.3.2.3 Structural Heat Transfer	
4.2.3.2.4 Dry Primary Containment Spray	
4.2.3.2.5 Containment Heat Removal Systems	
4.2.3.2.6 Atmosphere-Sump Interface	

ANSI-ANS-564.4-1983	AREVA Methodology
4.2.3.3 Modeling Consideration	
4.2.4.1 Net Free Volume	
4.2.4.2 Heat Sinks	
4.2.4.3 Primary Containment Pressure	
4.2.4.4 Primary Containment Atmosphere Temperature.	
4.2.2.5 Primary Containment Dewpoint (Humidity)	
4.2.5 Single Failure Criteria	

AREVA NP Inc.   ANP-10299NP
Applicability of AREVA NP Containment Response Evaluation Methodology to the   Revision 2
U.S. EPR™ for Large Break LOCA Analysis
Technical Report   Page 9-1

9.0   SAMPLE PROBLEM

This section describes the application of the LOCA containment pressure response methodology described in Section 8.0 to the analysis of a sample problem for the U.S. EPR, a double-ended guillotine break in the cold leg pump suction (CLPS) piping. As conservatively analyzed, it is the limiting containment pressure response scenario for the U.S. EPR.

9.1   Event Description

It is assumed that the reactor is at full power prior to the postulated LOCA event. The double-ended guillotine break in the cold leg pump suction piping is assumed to open instantaneously, releasing mass and energy into the containment. This break causes the rapid depressurization of the reactor coolant system. When the RCS pressure falls below the accumulator pressure, cold ECCS water from the accumulators is discharged into the RCS. Offsite power is assumed to be available during the entire event. It is assumed that one train of pumped ECCS is unavailable because of a single failure, and one train of pumped ECCS is out of service for preventative maintenance. Therefore, two trains of pumped ECCS and four accumulators are available to provide coolant to the core and remove heat from the reactor vessel. At 60 minutes into the event, the operator realigns the operating LHSI trains from injecting solely into the cold legs to the hot leg injection mode in which most of the LHSI water is injected into respective hot legs. The hot leg injection suppresses net steaming in the reactor vessel, resulting in less steam release into the containment. The event was analyzed for a 24-hour time.

Table 9-1 summarizes major initial conditions for the containment pressure response analysis of the DEGB CLPS LOCA scenario.

Table 9-1—Summary of Major Initial Conditions

Parameter	Value
RCS Conditions	
Core Power	4612 MWt
Core Inlet Temperature	565.5°F
Total RCS Flow Rate	51194 lbm/s
Pressurizer	
Pressure (psia)	2286 psia
PZR Liquid Level	59.7%
MFW & SG	
Temperature	446°F
Flow / SG	1445 lbm/s
Pressure	1121 psia
Tube Plugging	0%
Containment	
Pressure	15.96 psia
Temperature	86°F
IRWST Liquid Temperature	122°F
Relative Humidity	0%

9.2   Sample Problem Calculation

The short-term portion of the transient refers to the period in which RELAP5-BW is used to calculate the mass and energy release. Applying AREVA NP's containment response evaluation methodology, the transition time for the CLPS break case is 1,200 seconds.

Figure 9-1, Figure 9-2, Figure 9-3, Figure 9-4, and Figure 9-5 show the respective nodalization diagrams for the US EPR, broken loop steam generator (BL SG), intact loop steam generator (IL SG), RPV, and ECCS systems used for the RELAP5-BW input models.

Figure 9-1—U.S. EPR RELAP5-B&W Nodalization Diagram
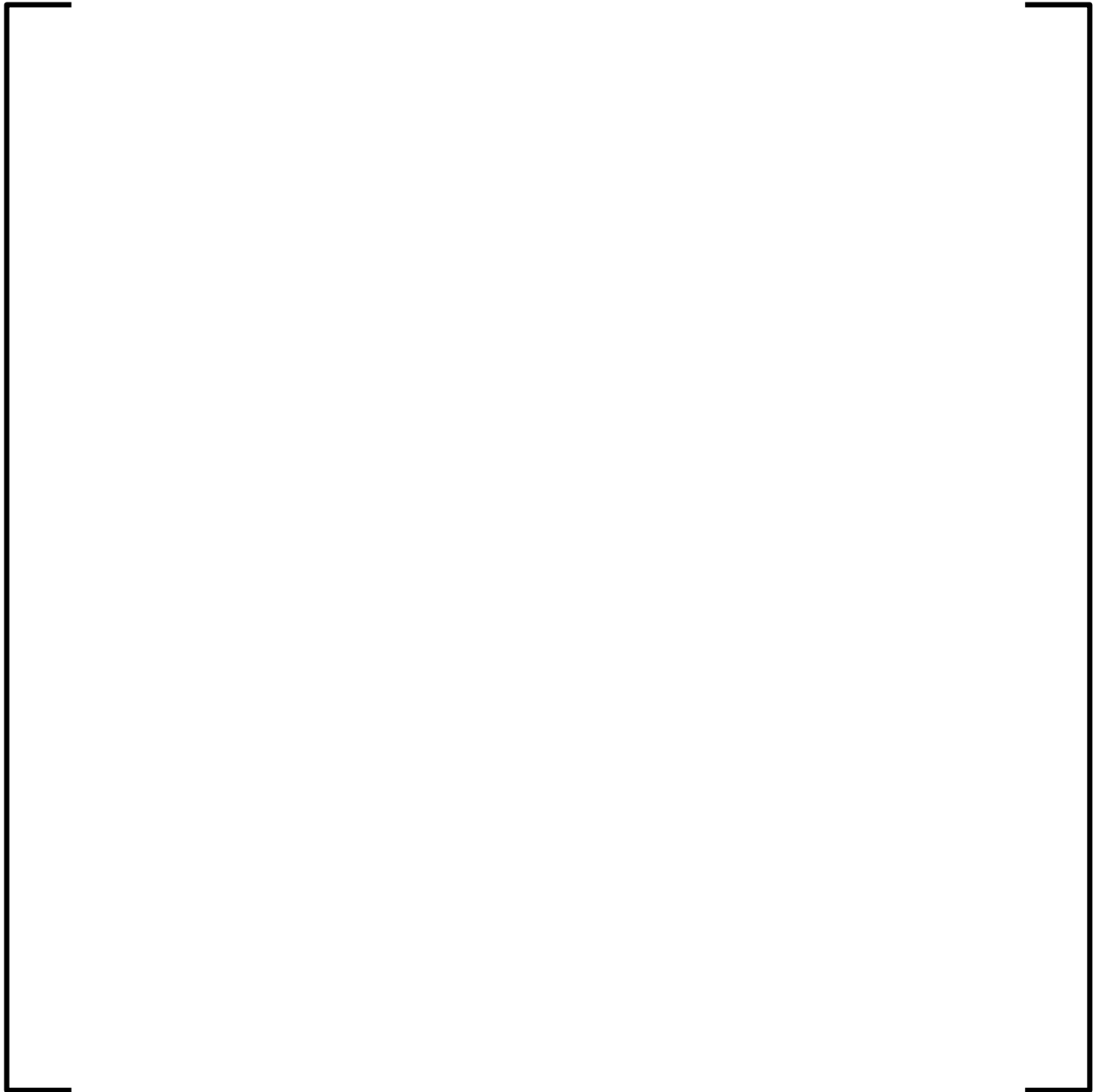
Figure 9-2—U.S. EPR Single Loop SG Nodalization Diagram using RELAP5-B&W
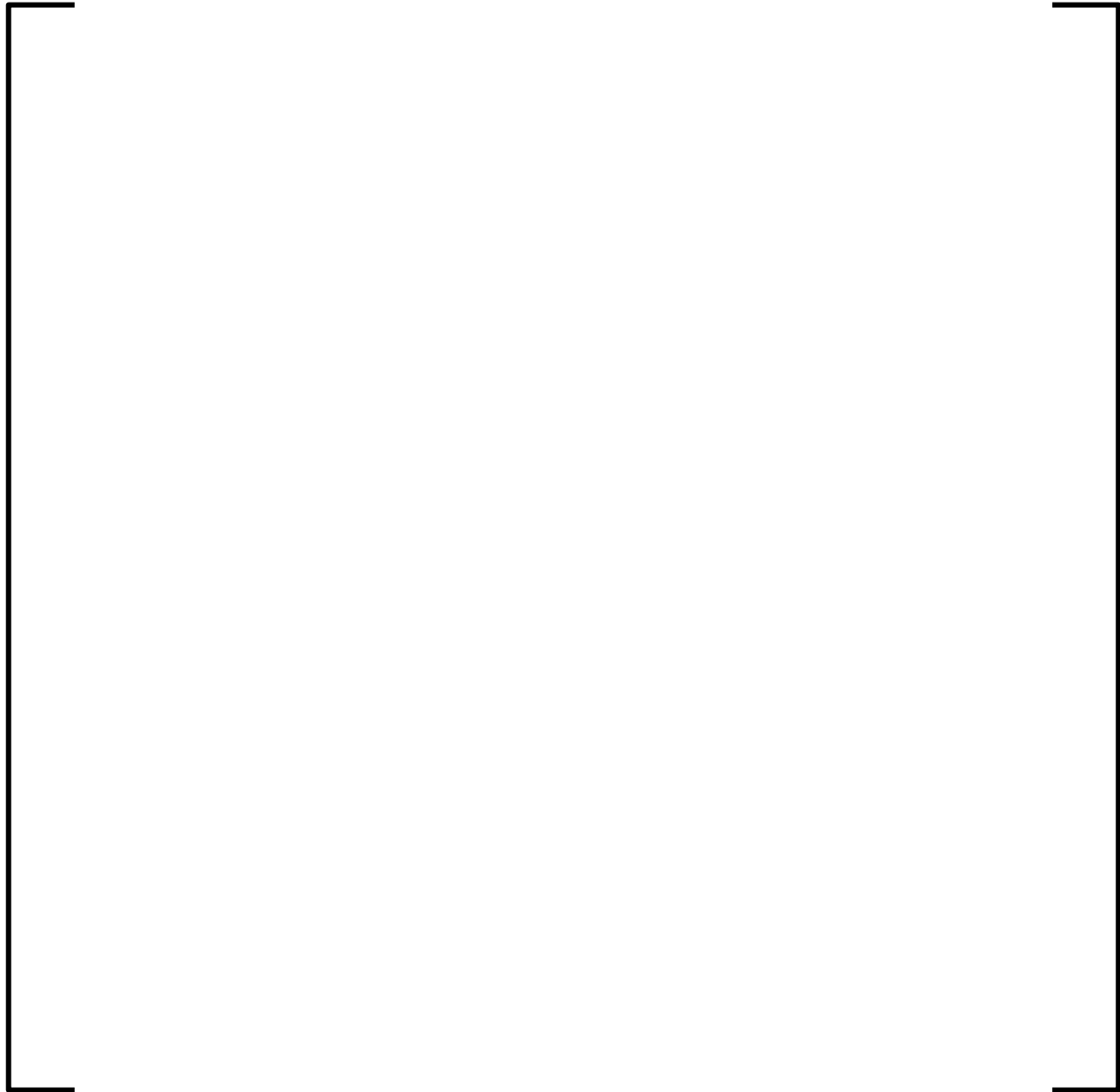
Figure 9-3—U.S. EPR Triple Loop SG Nodalization Diagram using RELAP5-B&W
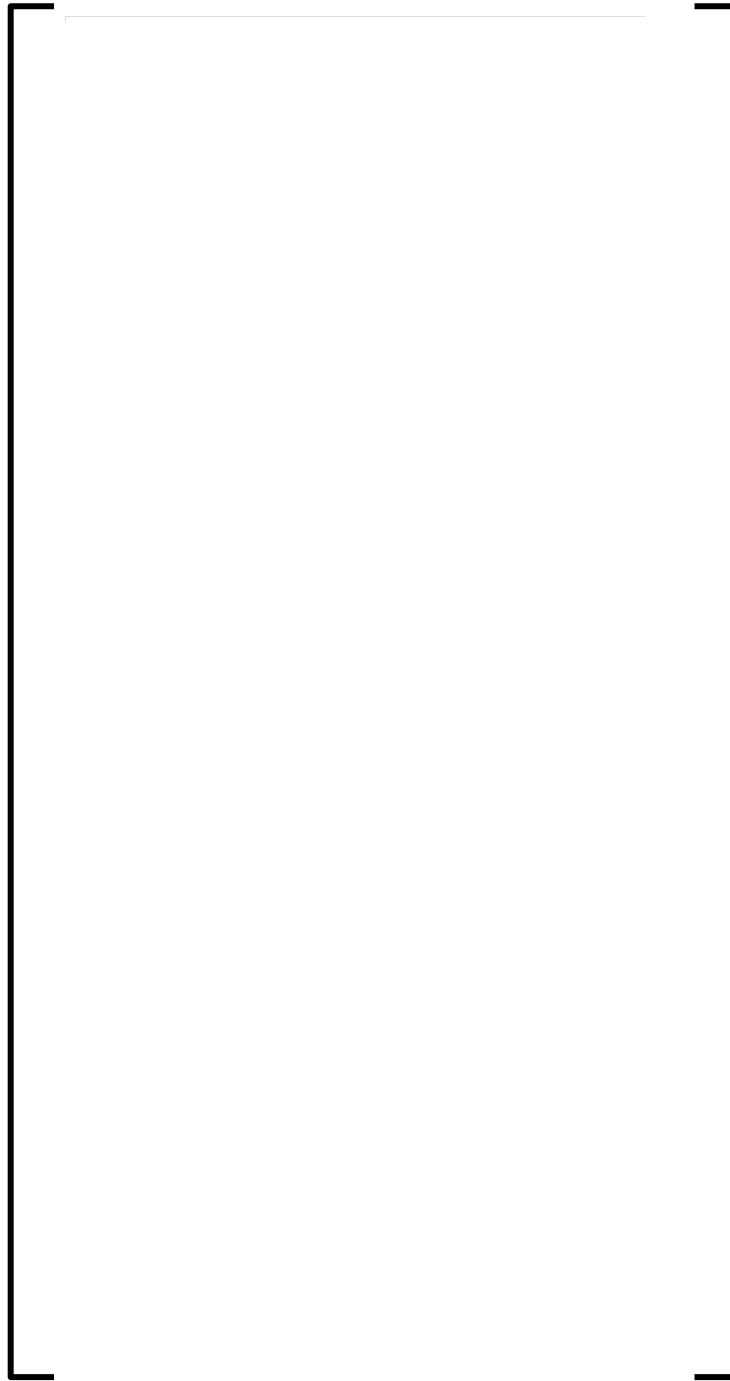
Figure 9-4—U.S. EPR RPV Nodalization Diagram using RELAP5-B&W

AREVA NP Inc.   ANP-10299NP

Applicability of AREVA NP Containment Response Evaluation Methodology to the   Revision 2
U.S. EPR™ for Large Break LOCA Analysis
Technical Report   Page 9-7
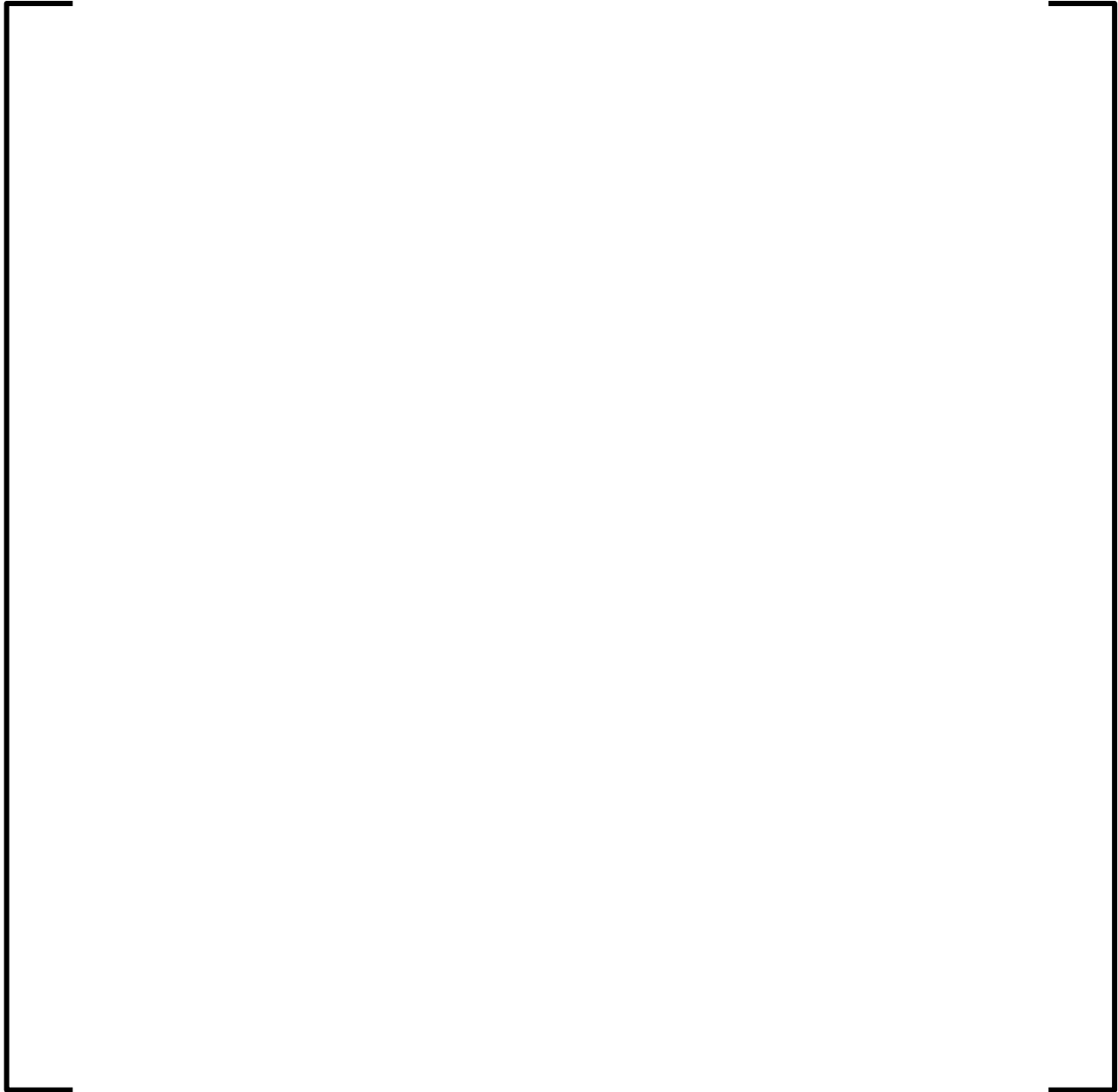
Figure 9-5—ECCS Nodalization Diagram

AREVA NP Inc.
Applicability of AREVA NP Containment Response Evaluation Methodology to the
U.S. EPR™ for Large Break LOCA Analysis
Technical Report

ANP-10299NP
Revision 2

Page 9-8

Figure 9-6 shows the RELAP5-BW break nodalization for CLPS breaks.

$$\left[\right]$$

Figure 9-6—Cold Leg Pump Suction Break Nodalization diagram

Once the core is quenched, the LBLOCA proceeds into the long-term cooling phase of the analysis (post-reflood and decay heat phases). At the start of the long-term phase of LBLOCA, the core is quenched, the vessel level has recovered to the RCS loop nozzle elevations, and the ECCS injection maintains the core covered for removal of sensible heat and core decay heat.

Thermal hydraulics conditions in the vessel are quasi-steady state during the long-term cooling phase. The phenomena modeled are:

- Nearly constant coolant level in the vessel

- Steam production in the core

- The transfer of heat from the remaining heat sources in the primary and secondary systems (sensible heat).

AREVA NP Inc.

ANP-10299NP

Applicability of AREVA NP Containment Response Evaluation Methodology to the
U.S. EPR™ for Large Break LOCA Analysis

Revision 2

Technical Report

Page 9-9

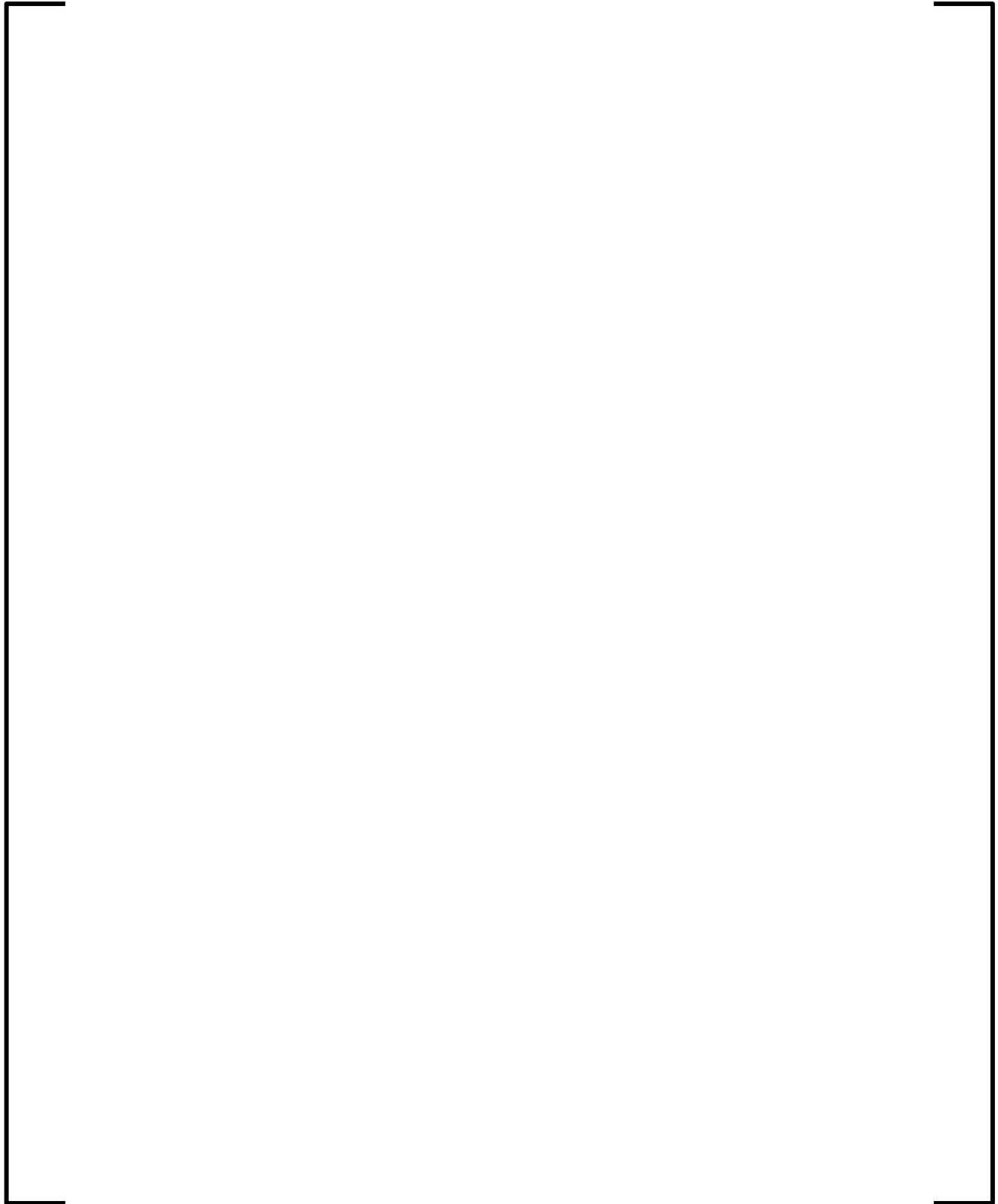The long-term phase is modeled using GOTHIC to represent the RCS and containment, including heat sources to represent decay heat and sensible heat. The GOTHIC model calculates the long-term mass and energy releases from the RCS to the containment. The GOTHIC method calculates mass and energy releases from the time of core quench (end time of the short-term mass and energy releases) until termination of the simulation (at least 24 hours after the postulated accident).

The GOTHIC containment model accounts for IRWST recirculation, the emergency core cooling function of the ECCS (SIS/RHR pumps and RHR heat exchangers) during IRWST recirculation of the ECCS fluid, and containment heat removal by steam condensation/convection on the containment passive heat sinks.

The constituent energy sources (sensible heat) remaining at the transition time are:

- Core decay heat

- Primary system fluid stored energy

    – Primary system passive metal stored energy (including core metal stored energy)

- Secondary system stored energy (fluid + metal)

- Safety injection pump heat addition.

- The RCS passive metal stored energy remaining at the transition time is modeled as described in Section 8.

The flow of ECC water removes the sensible heat from structures in its path before discharge to containment through the break. After the assumed RELAP5-BW-to-GOTHIC transition time of 1200 seconds for the CLPS break, the rate of sensible heat removal is maintained at the preceding average rate until all RCS stored heat is removed.

The liquid entrained in the steam and froth carried into the broken loop SG vaporizes, which contributes to steam release at the break. In the GOTHIC model, the sensible heat from the broken SG and the RCS metal in the steam path (including the upper plenum, upper head, and broken loop HL) are combined. The rate of energy transfer is calculated (carry out rate fraction) assuming that 5% of the ECCS flow (two trains) is distributed equally to the four SGs as described in Section 8.2.3.

A multi-node subdivided control volume is used to model the net–free volume within the steel inner containment vessel. A single node model assumes perfect mixing in the containment volume. A multi-node subdivided GOTHIC model was used in order to predict the natural circulation flow patterns and potential thermal stratification in the containment.

Natural circulation is a multi-dimensional phenomenon where heated equipment or effluent lowers the density of fluid in one region, causing upward flow that displaces fluid above and forcing some downward in other areas. Condensation on cooler equipment and walls raises the fluid density, driving the circulation flow further. The specified containment net–free volume is conservatively minimized to maximize predicted pressures. The subdivided control volume was applied only to the dome region of the containment. The heat transfer between the liquid and the vapor is neglected by setting the liquid-to-vapor interfacial area to a conservatively small value. Figure 9-7 shows the multi-node subdivided volume GOTHIC input model diagram.

Figure 9-7—GOTHIC Nodalization Diagram for CLPS

9.3   Containment Pressure and Temperature Response

The CLPS break scenario was evaluated for both short-term and long-term containment pressure response. RELAP5-BW was used to obtain the short-term mass and energy release to 1,200 seconds as input to the GOTHIC containment pressure response calculation.

AREVA NP evaluated a range of potential single failures to determine which one was most penalizing. This established that the single failure of one pumped ECCS train in conjunction with another train of pumped ECCS being unavailable because of preventive maintenance provides the most limiting scenario for containment pressure response. Under these circumstances, only two trains of pumped ECCS are available to mitigate the postulated LOCA. The assessment also evaluated the effect of the

location of these operating ECCS trains on containment pressure response for this scenario and concluded the most penalizing condition was for them to be in intact loops.

Figure 9-8 shows the containment pressure response for a 24-hour time period for the limiting peak pressure case. A blowdown peak of 64.2 psia occurs around 28 seconds into the transient, which is below the containment pressure acceptance criteria of 76.7 psia. A post-reflood peak of 66.72 psia occurs at 60 minutes into the transient when hot leg injection of LHSI is initiated to suppress steaming from the core. Containment pressure then steadily decreases, reaching 32 psia by the end of the analysis at 24 hours.

Figure 9.9 shows the containment vapor temperature in the containment control volume in which the postulated break occurs. It reached its peak value of $308°F$ for the limiting peak pressure case. This peak temperature is the short-term peak that occurs early in the transient. Upon further flow mixing in the containment, the temperature profiles at different locations in the containment merge and no thermal stratification was observed for the long-term response.

Figure 9-10 shows the containment liquid (IRWST) temperature. The liquid temperature continues to increase until about 3 hours into the event when the heat removal capacity of the LHSI heat exchangers exceeds the heat addition to the pool by the liquid break flow.

Figure 9-11 shows the containment dome vapor temperatures at 5 vertical elevations. These temperatures correspond to center node in 5 horizontal layers in the subdivided dome region. (The dome region was divided into 19 vertical nodes and in each horizontal plane there were 5x5 nodes.) As seen from the long-term response, there is no thermal stratification in the dome region and all temperature profiles gradually merge. At the start of the transient, as expected, there is some temperature gradient in the vertical direction. As time progresses and mixing occurs in the containment, the temperatures at different elevations converge.
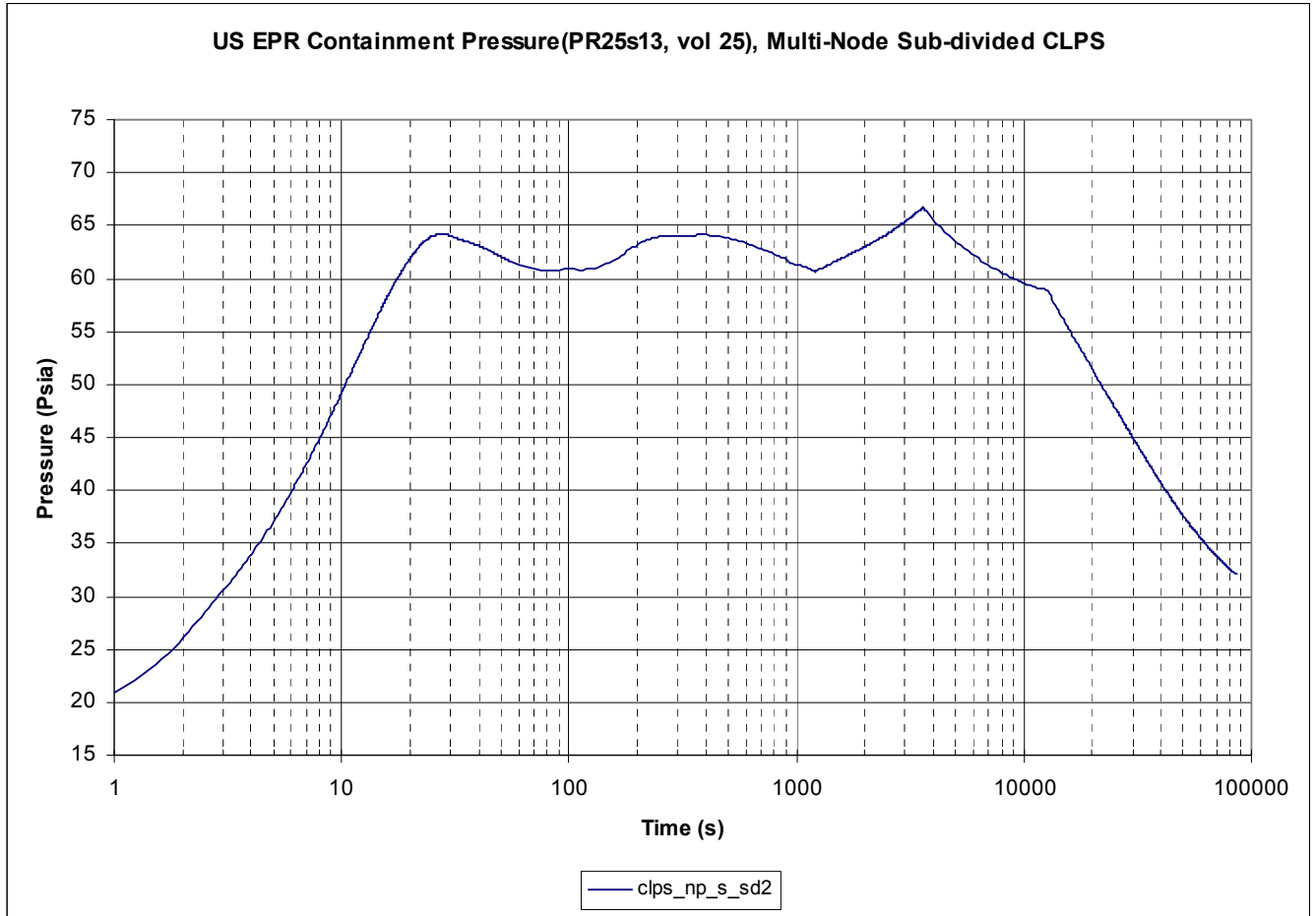
Figure 9-8—Containment Pressure Response
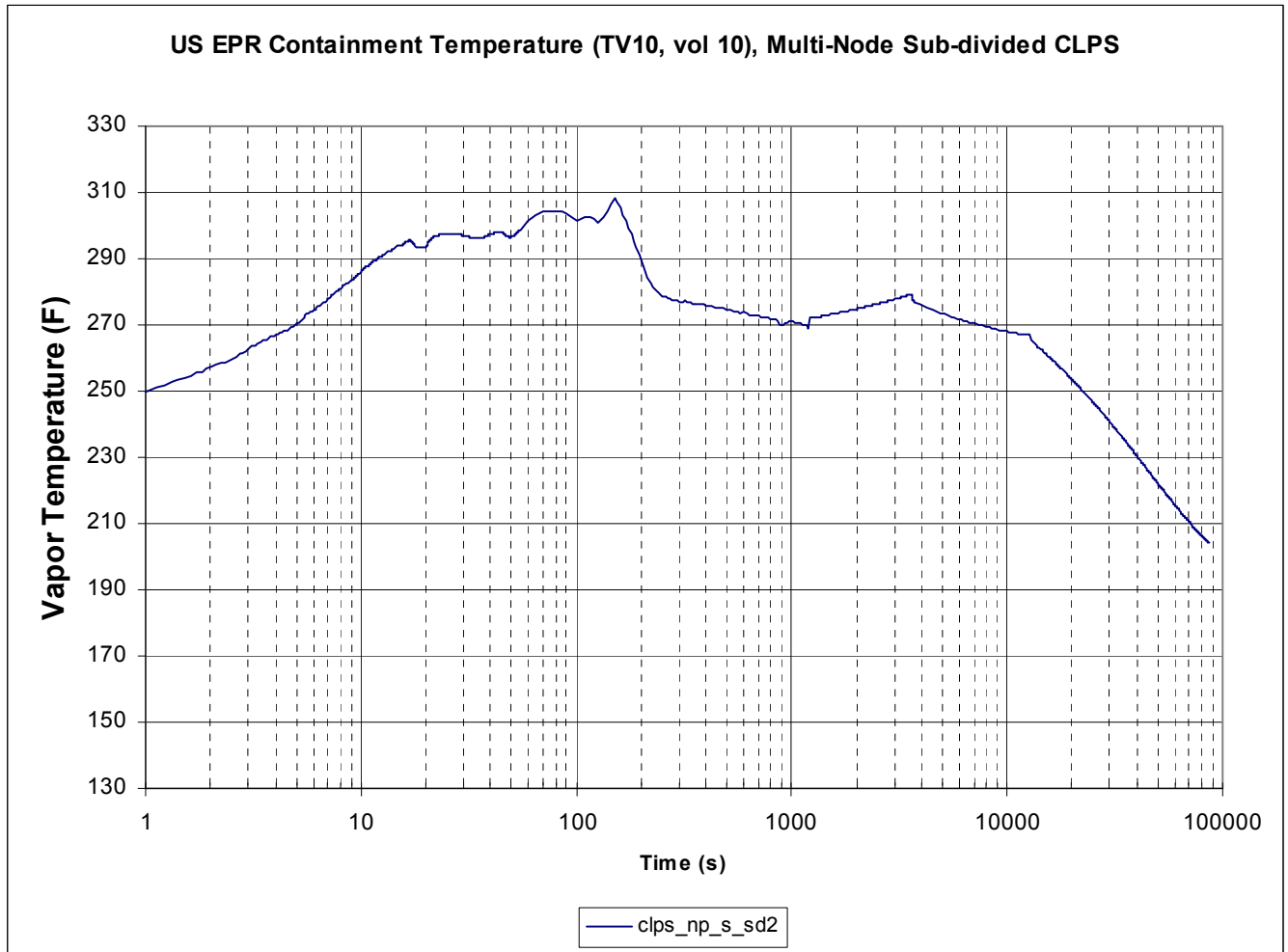
Figure 9-9—Containment Temperature Response

US EPR Containment Liquid Temperature (TL2, vol 2), Multi-Node Sub-divided CLPS
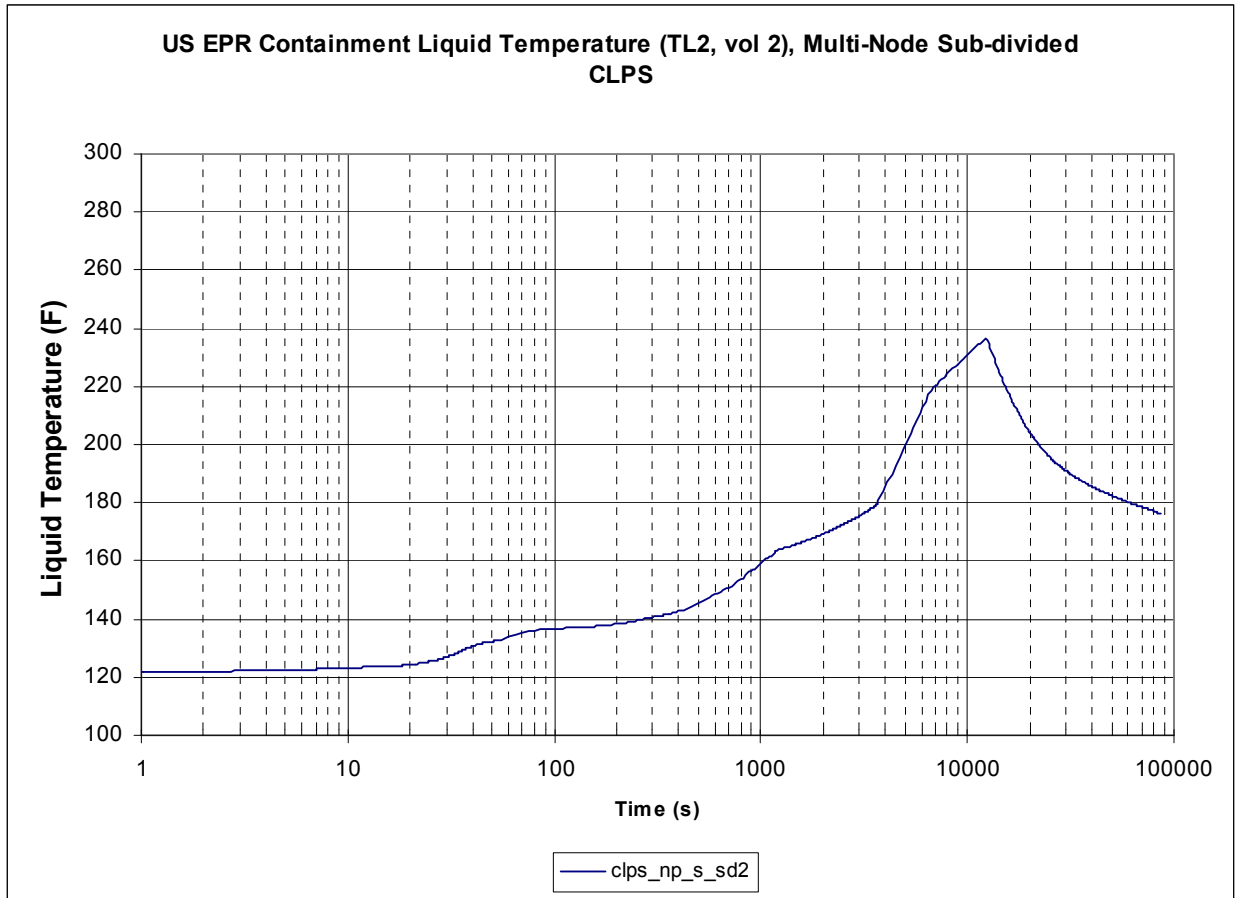
Figure 9-10—Containment Liquid Temperature Response
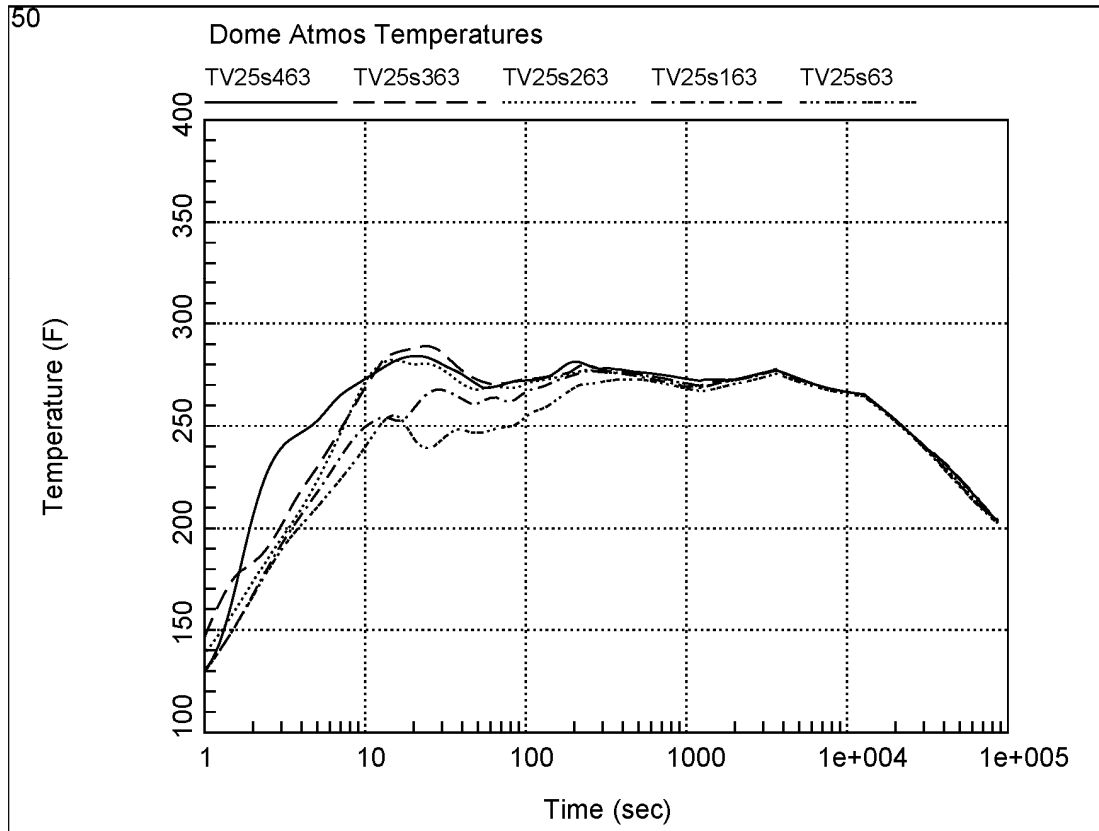
Figure 9-11— Containment Dome Temperature Response

Steam flow into the containment is the driving force in increasing the containment pressure. Figure 9-12 shows the respective short-term steam flows from the reactor vessel (FV106) side of the break and from the SG (FV108) side of the break. At the start of the event, the steam flows from both sides of the break are very high. They decrease as the RCS loses inventory and depressurizes. Figure 9-13 shows the long-term (1,200 seconds to 24 hours) steam flow from the RCS into the containment. After transition to the long-term GOTHIC model, the steam flow to the containment is higher than that predicted by RELAP5 B&W at the transition time because of the conservative methodology that AREVA NP implements, i.e., the total ECCS to the vessel matches the steam that is produced. As the decay heat decreases, the steam flow to the containment also decreases.

Prior to the hot leg injection, the water level in the vessel node is below the break elevation so that only steam is discharged to the containment. After hot leg injection, as a consequence of excess ECCS to the vessel, the steam flow to the containment suddenly drops. Part of the core decay heat and sensible energy is used to heat up the excess water in the core.

After the water level in the vessel node reaches the break elevation, excess water is discharged to the containment and steam flow reaches to quasi steady-state condition. About 12,000s into the transient when the sensible heat in RCS is dissipated, steam flow to the containment drops further, and from this time on, only decay heat is available to contribute to steam production.
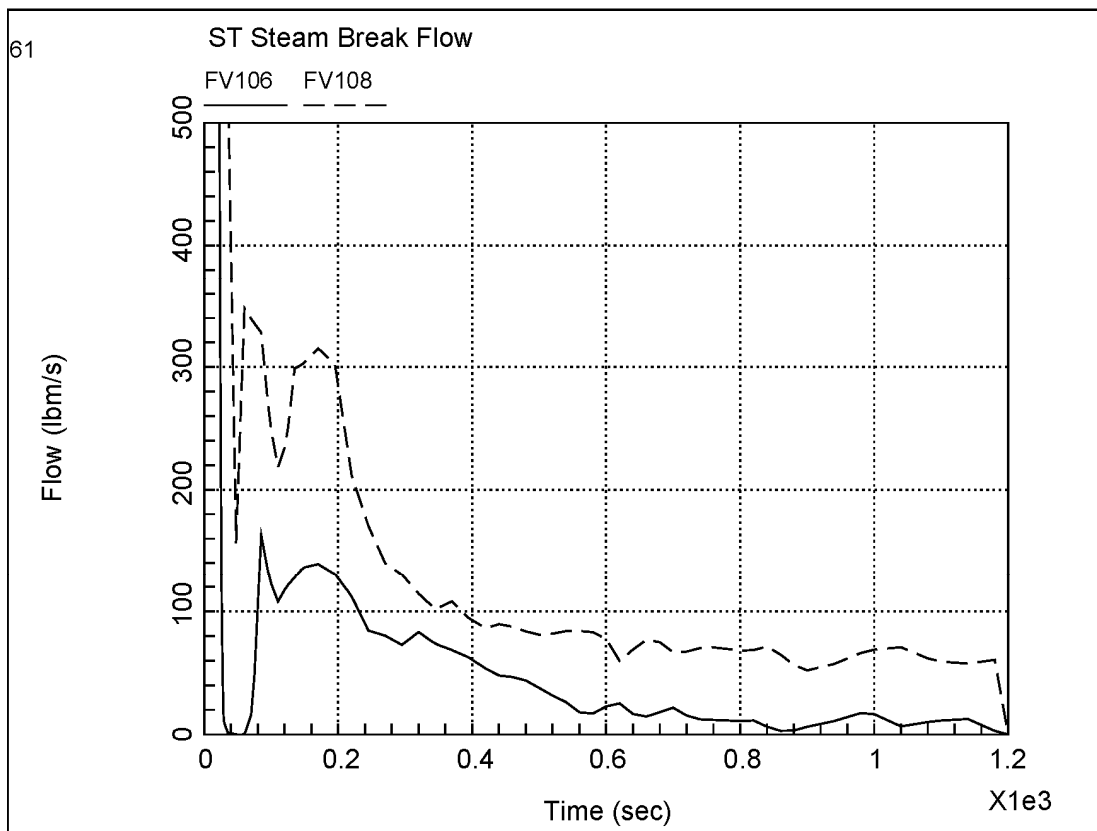
Figure 9-12—Short-Term Steam Flow from RPV (FV106) and SG (FV108) Sides of the Break
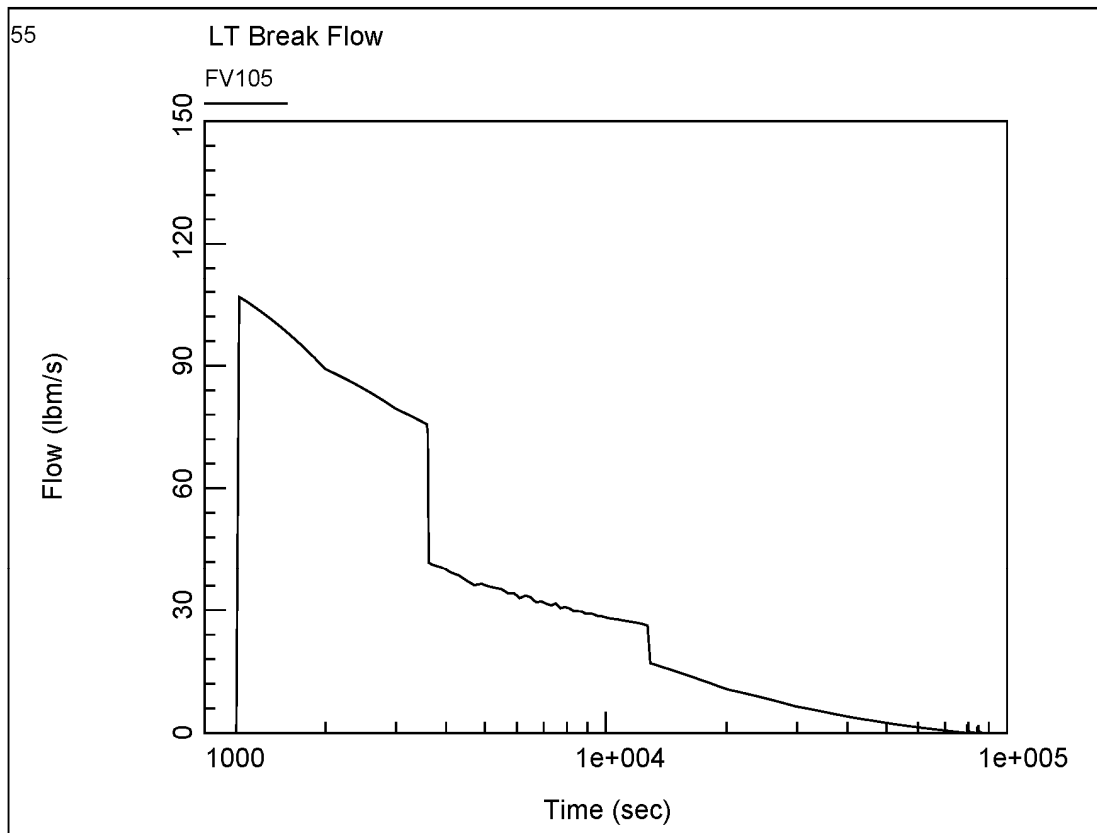
Figure 9-13—Long-Term Steam Flow into the Containment (FV105)

9.4   Summary of the CLPS Break Results

The containment response to a postulated CLPS LOCA was analyzed for the U.S. EPR.
The RELAP5-BW computer code was used to obtain the short-term mass and energy
release.

A multi-node subdivided control volume GOTHIC model was used to calculate the
containment response for pressure and temperature and to evaluate containment
mixing following postulated LOCA events. The containment peak pressure was 66.72
psia and containment peak temperature was 308°F. Both of these values are below the
acceptance criteria values of 76.7 psia and 338°F for the U.S. EPR. The containment

peak pressure was reduced to 40.71 psia, less than half its peak value in less than 11 hours into the transient. By 24 hours, containment pressure had dropped to 32 psia.

9.5 Assessment of Retained Margin in Pressure Response

Figure 9-14 presents the containment pressure result from AREVA NP's containment response evaluation methodology with the best-estimate plus uncertainty result given in Figure 7-4. Given that the uncertainty analysis explicitly addressed containment phenomena uncertainty, the large margin observed in Figure 9-14 is the result of AREVA NP's implementation of the containment mass and energy release conservatism specified the SRP. Consistent with the containment mass and energy release PIRT in Section 3.4, the changes having the largest impact on mass and energy releases are:

- Preventative maintenance assumption, i.e., eliminating two ECCS trains rather just the one ECCS train lost with the single-failure assumption

- Accelerated removal of sensible heat from the RCS and steam generators

- Conservative decay heat model (1.2 times the 1971 ANS Standard for infinite operating time; Multiplier reduced to 1.1 after 1000 seconds)

- Conservative Moody critical flow model.

The affect of these conservatisms appear at different periods in the simulation and hence can be distinguished in Figure 9-14. During the blowdown phase (~30 s), the faster rise in containment pressure is evidence of the critical flow model assumption. The decay heat model and the additional lost ECCS train act to slow the cooling process and are reflected in the elevated pressure following the peak. After the transition from RELAP5-BW to GOTHIC, the abrupt increase in containment pressure reflects the accelerated removal of sensible energy from the RCS and steam generators.

AREVA NP Inc.
Applicability of AREVA NP Containment Response Evaluation Methodology to the
U.S. EPR™ for Large Break LOCA Analysis
Technical Report

ANP-10299NP
Revision 2

Page 9-20

Collectively, these analyses fully characterize the uncertainties inherent in the containment response to an LBLOCA and the treatment of these uncertainties in AREVA NP's containment response evaluation methodology. This characterization validates the methodology and demonstrates that the regulatory criteria specified in GDC 16, 38 and 50 are satisfied.

Design Basis Envelope to the Coverage Bands for the US EPR CLPS LOCA Containment Pressure Response
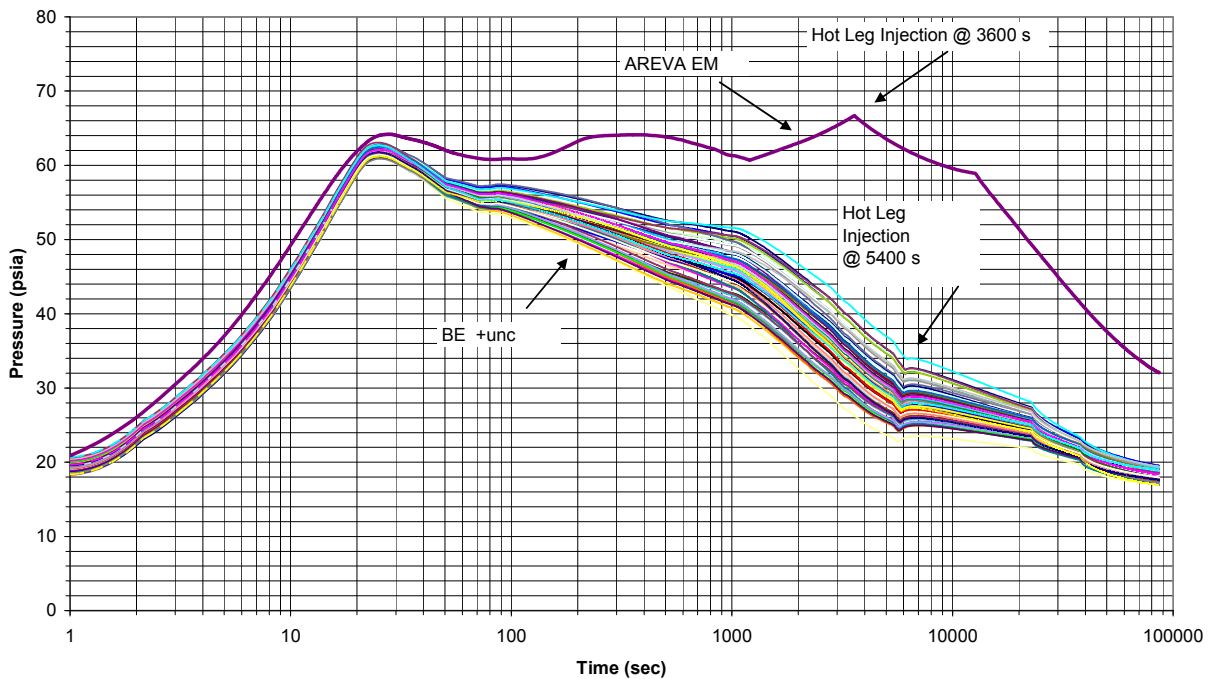
Figure 9-14—Assessment of Retained Margin in Containment Pressure Calculation

10.0   REFERENCES

1.   U.S. Federal Register Notice, "Regulation of Advanced Nuclear Power Plants; Statement of Policy," 51 FR 24643, July 8, 1986, as revised in Federal Register 59 FR 35461, July 12, 1994, and as revised in Federal Register 73 FR 60612, October 14, 2008.

2.   AREVA NP Inc. Document, "U.S. EPR Final Safety Analysis Report," Rev. 0, Chapter 6: Engineered Safety Features, ADAMS Accession # ML073531519 –44, December 2007.

3.   U. S. Nuclear Regulatory Commission, "Standard Review Plan," NUREG-0800, most recent revision.

4.   U.S. Nuclear Regulatory Commission, "Combined License Application for Nuclear Power Plants," Regulatory Guide 1.206, June 2007.

5.   U.S. Federal Register Notice, "Nuclear Power Plant Standardization," Federal Register, Federal Register 51 FR 28044, August 4, 1986.

6.   U.S. Nuclear Regulatory Commission, "Safety Goals for the Operations of Nuclear Power Plants," Federal Register, Vol. 51, No. 149, pp. 28044-28049, August 4, 1986.

7.   U. S. Code of Federal Regulations, most recent revision, Title 10, Part 50.

8.   U. S. Nuclear Regulatory Commission, "Standard Review Plan," NUREG-75/087, July 1975.

9.   U. S. Nuclear Regulatory Commission, "Interim Staff Position on Environmental Qualification of Safety-Related Electrical Equipment," NUREG-0588, July 1981.

10. Electric Power Research Institute (EPRI), "Advanced Light Water Reactor Utility Requirements Document," EPRI NP-6780-L, Vol. 2 (ALWR Evolutionary Plant), Palo Alto, Calif., 1992.

11. "American National Standard for Pressure and Temperature Transient Analysis for Light Water Reactor Containments," ANSI/ANS 56.4, 1988.

12. U. S. Nuclear Regulatory Commission, "A Prioritization of Generic Safety Issues," NUREG-0933, September 2007.

13. U. S. Nuclear Regulatory Commission, "Transient and Accident Analysis Methods," Regulatory Guide 1.203, December 2005.

AREVA NP Inc.   ANP-10299NP
Applicability of AREVA NP Containment Response Evaluation Methodology to the   Revision 2
U.S. EPR™ for Large Break LOCA Analysis
Technical Report   Page 10-2

14. AREVA NP Inc. Document Topical Report BAW-10252PA, "Analysis of Containment Response to Postulated Pipe Ruptures Using GOTHIC," September 2005.

15. P. F. Peterson, "Scaling and Analysis of Mixing in Large Stratified Volumes," Int. J. Heat Mass Transfer, 37 (suppl. 1), 97-106, 1994.

16. Technical Program Group, "Quantifying Reactor Safety Margins, Application of Code Scaling, Applicability, and Uncertainty Evaluation Methodology to a Large Break, Loss-of-Coolant Accident," NUREG/CR-5249, December 1989.

17. R. P. Ofstun, L. C. Smith, "PIRT for Large Break LOCA Mass and Energy Release Calculations," BE 2004 Meeting, Washington, D.C., 2004.

18. OECD/NEA Group of Experts, "SOAR on Containment Thermal-Hydraulics and Hydrogen Distribution," NEA/CSNI(1999)(16), 1999.

19. AREVA NP Inc. Document Topical Report BAW-10164PA, Rev. 4, "RELAP5/MOD2-B&W – An Advanced Computer Program for Light-Water Reactor LOCA and Non-LOCA Transient Analysis," ADAMS Accession # ML030220290, November 2002.

20. Numerical Applications, Inc., "GOTHIC Containment Analysis Package Users Manual, Version 7.2b(QA)," NAI-8907-02, Revision 18, March 2009.

21. V. H. Ransom, et al., RELAPS/MOD2 Code Manual, NUREG/CR-4312, EGG-2396, August 1985.

22. RELAP5/MOD3 Code Manual, Idaho National Engineering Laboratory, NUREG/CR-5535, INEL-95/0174, 7 Volumes, August 1995.

23. D. R. Liles, et al., TRAC-PF1/MOD1: An Advanced Best Estimate Computer Program for PWR Thermal-Hydraulic Analysis, NUREG/CR-3858, July 1986.

24. AREVA NP Inc. Document EMF-2100(P), "S-RELAP5: Models and Correlation Code Manual," see letter, J. F. Mallay (FRA-ANP) to Document Control Desk (NRC), "Request for Review of EMF-2103(P) Revision 0, Realistic Large Break LOCA Methodology for Pressurized Water Reactors," August 2001.

25. AREVA NP Inc. Document Topical Report BAW-10168PA, Rev. 4, "BWNT Loss-of-Coolant Accident Evaluation Model for Recirculating Steam Generator Plants," July 2000.

26. AREVA NP Inc. Document Topical Report BAW-10166PA, Rev. 5, "BEACH – Best Estimate Analysis Core Heat Transfer, A Computer Program for Reflood Heat Transfer during LOCA," December 2001.

27. R. R. Schultz, International Code Assessment and Applications Program: Summary of Code Assessment Studies Concerning RELAP5/MOD2, RELAP5/MOD3, and TRA C-B, Idaho National Engineering Laboratory, NUREG/IA-0 128, EGG-EAST-8719, December 1993.

28. V. H. Ransom, et. al., "RELAP5/MOD2 Code Manual, Volume 3: Developmental Assessment Problems," EGG-TFM-7952, December 1987.

29. AREVA NP Inc. Document EMF-2102(P), Revision 0, S-RELAP5: Code Verification and Validation, August 2001.

30. U. S. Nuclear Regulatory Commission, "Compendium of ECCS Research for Realistic LOCA Analysis", NUREG-1230, Appendix A, 1989.

31. Numerical Applications, Inc., "GOTHIC Containment Analysis Package Qualification Report, Version 7.2b(QA)," NAI-8907-09, Revision 10, March 2009.

32. H. Karwat, OECD/CSNI International Standard Problem No. 23, "Rupture of a Large Diameter Pipe in the HDR-Containment," OECD/CSNI Report No. 160, December 1989.

33. H. Karwat, "Distribution of Hydrogen within the HDR-Containment Under Severe Accident Conditions, Final Comparison Report," OECD International Standard Problem OECD/CSNI-ISP29, NEA/CSNI 1R193/4, February 1993.

34. "Final Comparison Report on ISP-35: NUPEC Hydrogen Mixing and Distribution Test (Test M-7-1)," NEA/CSNI/R(94)29, December 1994.

35. M. Firnhaber, "VANAM M3 – A Multi Compartment Aerosol Depletion Test with Hygroscopic Aerosol Material," OECD/CSNI International Standard Problem ISP37, NEA/CSNI/R (96)26, 1996.

36. H. J. Allelein, et. al., "International Standard Problem ISP-47 on Containment Thermal-Hydraulics," NEA/CSNI-(2007)10, September 2007.

37. AREVA NP Inc. Document Topical Report BAW-10162P-A, "TAC03, Fuel Rod Thermal Analysis Computer Code," Rev 0, November 1989.

38. "American Nuclear Society Proposed Standard ANS 5.1, Decay Energy Release Rates Following Shutdown of Uranium-Fueled Thermal Reactors," October 1971, revised October 1973.

39. "American National Standard for Decay Heat Power in Light Water Reactors," ANSI/ANS-5.1. 1979.

40. A. G. Croff, ORIGEN2 -Revised and Updated Version of the Oak Ridge Isotope Generation and Depletion Code, Oak Ridge National Laboratory, ORNL-5621, July 1980.

41. J. F. Wilson, et al., "Velocity of Rising Steam in a Bubbling Two-Phase Mixture," ANS Trans. Vol. 5, pp. 151-152, 1962.

42. H. C. Unal, "Maximum Bubble Diameter, Maximum Bubble-Growth Time and Bubble-Growth Rate During the Subcooled Nucleate Flow Boiling of Water up to 17.7 MN/m^2," International Journal of Heat and Mass Transfer, Volume 19, pp. 643-649, 1976.

43. T. G. Theofanous, "Modeling of Basic Condensation Processes," The Water Reactor Safety Research Workshop on Condensation, Silver Springs, MD, May 24-25, 1979.

44. Numerical Applications, Inc., "GOTHIC Containment Analysis Package Technical Manual, Version 7.2b(QA)," NAI-8907-06, Revision 17, March 2009.

45. H. S. Crapo, et al, "Experimental Data Report for Semiscale Mod-1 Tests S-04-5 and S-04-6' (Baseline ECC Tests)," TREE-NUREG-1045, January 1977.

46. J. F. Wilson, et al., "The velocity of Rising Steam in Bubbling Two-Phase Mixture," ANS Trans. Vol. 5, pp. 151-152, 1962.

47. "PWR FLECHT-SEASET Unblocked Bundle, Forced And Gravity Reflood Task Data Report," Volume 1 and Volume 2, NUREG/CR-1532, EPRI NP-1459, WCAP-9699, June 1980.

48. R.C. Howard, et. al., "PWR FLECHT SEASET Steam Generator Separate Effects Test Data Report," NUREG/CR-1366, NRC/EPRI/Westinghouse Report No. 4, Westinghouse Electric Co., January 1980.

49. L. Biasi et. al., "Studies on Burnout Part 3 - A New Correlation for Round Ducts and Uniform Heating and Its Comparison with World Data," Energia Nucleare, Volume 14, pp. 530-536, 1967.

50. P. Griffith, J. F. Pearson, and R. J. Lepkowski, "Critical Heat Flux During a Loss-of Coolant Accident," Nuclear Safety Volume 18, pp. 298-309, 1977.

51. Becker, K. M., et al., "Burnout Data for Flow of Boiling Water in Vertical Round Ducts, Annuli and Rod Clusters," AE-177 (1965).

52. P. S. Damerell and J. W. Simons, "2D/3D Program Work Summary Report," NUREG/IA-0126, GRS-100, MPR-1345, June 1993.

53. JAERI Memo, "Evaluation Report on SCTF CORE-III test S3-SH1 {Effect of Hot Leg Injection on Core Thermal-Hydraulics for PWRs with a Combined Injection Type ECCS," 88-125, July 1988.

54. F. Mayinger, H. G. Sonnenburg, R. Zipper, J. Liebert, H. P. Gaul, R. Hertlein: Erkenntnisse aus dem UPTF-TRAM-Versuchsvorhaben; Gemeinsamer Bericht von GRS, SIEMENS und TU München ; GRS-A-2679, January 1999.

55. JAERI Memo, "Data Report on Large Scale Reflood Test-128 – CCTF CORE-II Test C2-19 (Run 79)," 63-081, March 1988.

56. JAERI Memo, "Evaluation Report on CCTF CORE-II Reflood Test C2-19 (Run 79)," 62-334, September 1987.

57. R. Sangras, Z. Dai, G. M. Faeth, "Buoyant Turbulent Jets and Flames: I. Adiabatic Wall Plumes," National Institute of Standards and Technology Laboratory for Building and Fire Research, Washington, D.C., October 1999.

58. Cunningham, J. P., and H. C. Yee, "Experiments and Void Correlation for PWR Small-Break LOCR Conditions," ANS Transactions (1973) pp 369-370.

59. STAR-CD V4, Computational Dynamics, London, UK, 2006.

60. M. Schall, "Design Report for the HDR Containment Experiments V21.1 to V21.3 and V42 to V44 with Specifications for the Pre-Test Computations," Report No. 3.280/82, January, 1982.

61. M. Schall and L. Valencia, "Data Compilation of the HDR Containment for Input Data Processing for Pre-Test Calculations," PHDR Technical Report No. 3.143/79, Karlesruhe, FRG, January, 1982.

62. T. Kanzleiter, and L. Valencia, "Blowdown-Experiments in a Reactor Containment, Quick Look Report, Test Group CONW and COND, Experiments V21.1, V21.3, V45," (in German), PHDR Technical Report 49-84, Karlesruhe, FRG,May 1984.

63. PHDR Technical Report No. 72-87, Test V21.1, September, 1987.

64. L. Valencia and T. Kanzleiter, "Blowdown-Experiments in a Reactor Containment, Quick Look Report, Test Group COND, Experiments V42, V43, V44," (in German), PHDR Technical Report 38-83, Karlesruhe, FRG, May 1983.

65. M. Firnhaber, "International Standard Problem ISP 16, Rupture of a Steam Line Within the HDR-Containment Leading to an Early Two-Phase-Flow," CSNI Report No.112, Karlesruhe, FRG, June 1985.

66. L. Valencia, "Blowdown Investigations Concerning Reactor Containment Pressurization-Steamline Break, Quick Look Report, Test Group CON, Experiments T31.1-3," (in German), PHDR Technical Report 57-84, Karlesruhe, FRG, June 1985.

67. H. Wenzel et al., Versuchsprotokoll: Blowdown and Wasserstoffverteilungs-Versuchsgruppe CON Versuch T31.5 [Test protocol: Blowdown and hydrogen distribution test series CON test T31.5], PHDR Working Reports 3.520/88 and 3.524/88, Karlesruhe, FRG, February, 1988.

68. H. Karwat, "International Standard Problem ISP 23: Rupture of a Large-Diameter Pipe within the HDR Containment," CSNI Report No. 160, December 1989.

69. T. Cron, D. Schrammel, "Investigations on Hydrogen Distribution in a Reactor Containment, Quick Look Report, Test Group E11, Experiments E11.0-6," (in German), PHDR Technical Report 111-92, Karlesruhe, FRG, March 1993.

70. H. Holzbauer, L. Wolf, and T. Cron, "Evaluation of Experimental and Analytical Results of the HDR-Hydrogen Distribution Experiments, Final Evaluation Report, Test Group E11, Experiments E11.0-6," (in German), PHDR Technical Report 117-94, Karlesruhe, FRG, February 1994.

71. Battelle-Frankfurt Institute Report BF-RS 50-32-D1, Investigation of the Phenomena Occurring within a Multi-Compartment Containment after Rupture of the Primary Cooling Circuit in Water-Cooled Reactors, March, 1977 (German).

72. Battelle-Frankfurt Institute Report BF-RS 50-32-C13-1, Investigation of the Phenomena Occurring within a Multi-Compartment Containment after Rupture of the Primary Cooling Circuit in Water-Cooled Reactors, July, 1976, (German).

73. Battelle-Frankfurt Institute Report BF-RS 50-32-C15-1, Investigation of the Phenomena Occurring within a Multi-Compartment Containment after Rupture of the Primary Cooling Circuit in Water-Cooled Reactors, July, 1976, (German).

74. Battelle-Frankfurt Institute Report BF-RS 50-21-1, Die Containment-Versuchsanlage (C-und D-Versuche), March, 1978, (German with English summary).

75. Battelle-Frankfurt Institute Report V 68270.1, Naturkonvektionsströmungen und Wasserstoffverteilungen im Containment bei erhöhten Sumpfwassertemperaturen ("Natural Convection Flows and Hydrogen Distribution in Containment with a Raised Sump Temperature"), October 1994.

76. Travis J. R. et al., "GASFLOW: A Computational Fluid Dynamic Code; Gases, Aerosols, and Combustion, Vol. 1: Theory and Computational Models, Vol. 2: User's Manual, Vol. 3: Assessment Manual", LA-13357-M, FZK-5994, October 1998.

77. McAdams, W.H., Heat Transmission, Third Edition, McGraw-Hill, New York, 1954.

78. H. Bartalszky, H. Glaeser, and B. Krzykacz-Hausmann, "Prediction Capability of Computer Code Calculations for Cooling System and Containment," Reactor Safety Research-Project Number RS 1142, July 2005 (in German).

79. AREVA NP Inc. Document Topical Report EMF-2103 (NP)(A), "Realistic Large Break LOCA Methodology for Pressurized Water Reactors", ADAMS Accession #, ML032691424, April 2003.

80. AREVA NP Inc. Document Topical Report ANP-10268(PA), Revision 0, "U.S. EPR Severe Accident Evaluation," Nov. 2007.

81. Klein-Heßling, W., et al., "COCOSYS Short Description," Gesellschaft für Anlagen- und Reaktorsicherheit (GRS) mbH, May 2008 (in German).

82. Glaeser, H., "GRS Method for Uncertainty and Sensitivity Evaluation of Code Results and Applications," Science and Technology of Nuclear Installations, Article ID 798901, 2008.

83. Karwat, H., "Rupture of a Large-Diameter Pipe within the HDR-Containment," International Standard Problem ISP-23, CSNI-Report 160, December 1989.

84. Kessler, E., "On the continuity and distribution of water substance in atmospheric circulations," Atmospheric Research, Vol. 38, Issue 1-4, pp. 109-145, Sept 1993.

85. Park, B. S., and Lee, S. Y., "An Experimental Investigation of the Flash Atomization Mechanism", Atomization and Sprays, Vol. 4, pp. 159-179, 1994.

86. AREVA NP Inc. Document Topical Report EMF-2328 (NP)(A), "PWR Small Break LOCA Evaluation Model, S-RELAP5 Based," ADAMS Accession # ML003675736, March 2001.

87. AREVA NP Inc. Document Topical Report EMF-2310 (NP), "SRP Chapter 15 Non-LOCA Methodology for Pressurized Water Reactors," ADAMS Accession #ML032460863, May 2003.

88. EMF-CC-039(P) Revision 2, "ICECON Code User's Manual: A Computer Program Used to Calculate Containment Back Pressure for LOCA Analysis (Including Ice Condenser Plants)," March 1999.

89. EMF-CC-039(P) Revision 2 Supplement 1, "ICECON Code User's Manual: A Computer Program Used to Calculate Containment Back Pressure for LOCA Analysis (Including Ice Condenser Plants)," December 1999.

90. A. G. Croff, "ORIGEN2 -Revised and Updated Version of the Oak Ridge Isotope Generation and Depletion Code," Oak Ridge National Laboratory, ORNL-5621, July 1980.

91. S. S. Wilks, "Determination of Sample Sizes for Setting Tolerance Limits," Ann. Math. Stat., Vol. 12, pp. 91-96, 1941.

92. W. J. Conover, "Practical Nonparametric Statistics," 3rd Edition, Wiley and Sons, 1999.

93. AREVA NP Inc. Document Topical Report BAW-10171PA, Rev. 3, "REFLOD3 – Model for Multiode Code Reflooding Analysis," December 1995.

94. Tagami, T., Interim Report on Safety Assessments and Facilities Establishment Project in Japan for Period Ending June 1965 (No. 1), unpublished work, 1965.

95. Uchida, H., A. Oyama and Y. Togo, Evaluation of Post-Incident Cooling Systems of Light Water Power Reactors, U. of Tokyo, International Conference on Peaceful Uses of Atomic Energy, New York, 1965.

96. AREVA NP Inc. Document Topical Report, BAW-10192P-A, Rev. 0 "BWNT Loss-of-Coolant Accident Evaluation Model for Once-Through Steam Generator Plants," June 1998.

97. AREVA NP Inc. Document Topical Report, BAW-10193P-A, Rev. 0 "RELAP5/MOD2-B&W For Safety Analysis of B&W-Designed Pressurized Water Reactors," January 2000.

98. R. Brown and J. L. York, "Sprays Formed by Flashing Liquid Jets," AICHE J., Vol. 8, No. 2, May 1962.

99. Langer, G., et al., Experimental Investigation of the Hydrogen Distribution in a Model Containment (Preliminary Experiments II), BF-R-64.036-3, Battelle-Institut e.V., 6000 Frankfurt am Main 90, Am Romerhof 35, Postfach 900160, March, 1977, (German with English summary).

100. NUPEC, Final Comparison Report on ISP-35: NUPEC Hydrogen Mixing and Distribution Test (Test M-7-1), CSNI Report NEA/CSNI/R(94)29, December, 1994.

101. Schmitt, R.C., et al., Simulated Design Basis Accident Tests of the Carolinas Virginia Tube Reactor Containment Final Report, IN-1403, Idaho Nuclear Corporation, Idaho Falls, ID, 1970.

102. Specification of International Standard Problem on Containment Thermal-Hydraulics, ISP 47, Step 1: TOSQAN - MISTRA, Revision 1, July 2002.

103. ISP 47 International Standard Problem on Containment Thermal-Hydraulics, ISP 47, Step 1: TOSQAN - MISTRA, Phase A: Air - Steam Mixtures, TOSQAN Experimental Results of the Air-Steam Phase, Revision 0, October 30, 2002.

104. ISP 47 International Standard Problem on Containment Thermal-Hydraulics, ISP 47, Step 1: TOSQAN - MISTRA, Phase B: Air - Helium - Steam Mixtures, TOSQAN Experimental Results of the Air Helium Steam Phase, Revision 0, October 17, 2003.

105. ISP 47 - Phase B - MISTRA Experimental Results, August, 2003.

106. P.F. Peterson, VE Schrock and T Kageyama, Diffusion Layer Theory for Turbulent Vapor Condensation with Noncondensable Gases, ASME Journal of Heat Transfer, Vol. 115, pp 998-1003, 1993.

107. P.F. Peterson, Theoretical Basis for the Uchida Correlation for Condensation in Reactor Containments, Nuclear Engineering and Design, 162, pp 301-306, 1996.

108. M.L. Corradini, Turbulent Condensation on a Cold Wall in the Presence of a Noncondensable Gas, Nuclear Technology, Vol. 64, February 1984.

109. M.H. Anderson, Steam Condensation on Cold Walls of Advanced PWR Containments, Ph.D. Dissertation, University of Wisconsin, Madison, 1998.

110. I. Huhtiniemi, A Pernsteiner and ML Corradini, Condensation in the Presence of a Noncondensable Gas: Experimental Investigation, Dept. of Nuclear Engineering and Engineering Physics, University of Wisconsin, Madison, Wisconsin, April 1991.

111. A.A. Dehbi, The Effects of Noncondensable Gases on Steam Condensation Under Turbulent Natural Convection Conditions, Ph.D. Thesis, Department of Nuclear Engineering, MIT, 1991.

112. McAdam, W.H., Heat Transmission, Third Edition, McGraw-Hill, New York, 1954.

113. R.C. Schmitt, GE Bingham and JA Norberg, Simulated Design Basis Accident Tests of the Carolinas Virginia Tube Reactor Containment - Final Report, Idaho Nuclear Corporation, Idaho Falls, Idaho, prepared for the US Atomic Energy Commission, UC-80, December 1970.

114. S.K. Park, MH Kim and KJ Yoo, Condensation of Pure Steam and Steam-Air Mixture with Surface Waves of Condensate Film on a Vertical Wall, International Journal of Multiphase Flow, Vol. 22, No. 5, 1996.

115. M.H. Kim, Data Set for Reference I, personal communication, February, 2004.

116. P.F. Petersen, "Theoretical Basis for the Uchida Correlation for Condensation in Reactor Contaiments", Nuclear Engineering and Design, 162, pp301-306, 1996.

11.0   APPENDIX A – PIRT PANEL QUALIFICATIONS

This appendix provides qualifications of the PIRT panel members. Detailed resumes of

the panel members are available for inspection at AREVA NP offices.

- PIRT Panel Member #1 has 27 years of experience in the nuclear industry and was
  appointed to AREVA NP's College of Experts in 2005. His experience includes
  development of LBLOCA simulation tools and methods for AREVA NP.

- PIRT Panel Member #2 has over 40 years of experience in the nuclear industry and
  has published dozens of NRC-reviewed topical and technical reports on LOCA and
  fuel performance. Member #2 participated in the U.S. NRC High Burnup Fuel
  Design Basis Accident Technical Evaluation PIRT Panel. Member #2 was the
  technical co-lead for the evaluation of best-estimate LOCA licensing techniques.

- PIRT Panel Member #3 has a PhD and over 35 years experience in the nuclear
  industry, primarily as the Principal Technical Investigator at dozens of experimental
  facilities. He is a Professor of Nuclear and Mechanical Engineering at a major
  University. He has published dozens of U.S. NRC-reviewed topical and technical
  reports on LOCA/Non-LOCA transients, containment analyses, and severe
  accidents, and 160 full-paper articles for conferences and journals; he has delivered
  technical presentations to utilities and both foreign and domestic safety authorities.
  He has served as a consultant for the Nuclear Regulatory Commission and has
  helped developed PIRTs to address accident aspects for high burn-up fuel. He
  consulted and served on a panel of experts to develop a PIRT for the LBLOCA for
  the next generation Korean nuclear power plants.

- PIRT Panel Member #4 has 29 years of experience in the nuclear industry and has
  published several NRC-reviewed topical and technical reports on LBLOCA and
  SBLOCA. He has delivered technical presentations to utilities and American safety
  authorities. He was the technical lead for MIST pre- and post-test analysis
  predictions with RELAP5/MOD2-B&W. He developed and evaluated
  RELAP5/MOD1 and MOD2 SBLOCA input decks for predicting the thermal-hydraulic
  performance of the MIST facility, OTIS facility, and B&W nuclear steam supply
  systems. His other duties included the preparation of the scaling philosophy utilized
  in the MIST facility reactor.

- PIRT Panel Member #5 has a PhD and 20 years of experience in the nuclear
  industry. He has published several U.S. NRC-reviewed topical and technical
  reports on LBLOCA, containment analysis, and severe accidents and approximately
  25 full-paper articles for conferences and journals. He has delivered technical
  presentations to utilities and American safety authorities. He was the primary
  contributor and technical leader for AREVA NP's original Realistic LBLOCA
  evaluation model, a first-of-a-kind, statistically-based PWR safety analysis

methodology. He was appointed to AREVA NP's College of Experts in thermal hydraulics of LBLOCA transients in 2005.

- PIRT Panel Member #6 has twelve years of experience in the Nuclear Industry. He is the technical leader for AREVA NP's U.S. EPR LBLOCA containment analysis methodology. He was the Chapter 15 Technical Lead on multiple Replacement Steam Generator Projects. He has prepared preliminary safety evaluations that were used to determine the analysis scope required to complete the licensing of the steam generator replacement within the guidelines of the 10CFR50.59. His external publications include U.S. NRC-reviewed topical and technical reports on LBLOCA and containment analysis, and he has delivered technical presentations to utilities and American safety authorities.

- PIRT Panel Member #7 has 23 years of experience in the nuclear industry. He has delivered technical presentations to utilities and French, German, and American safety authorities. He developed best-estimate accident analysis methodology for the French N4 reactor design and provided expertise in analyses methods development, computer code modeling, and recommendations for enhancement of the N4 plant.

- PIRT Panel Member #8 has over 38 years of experience in nuclear engineering with expertise in safety analysis, heat transfer, plant support and thermal hydraulic analysis. She has directed and participated in a variety of safety and licensing analyses to support operating boiling and pressurized water reactors. She has expertise in developing and assessing computer codes for LOCA and containment analyses, and has performed numerous code simulations and predictions of experimental tests in facilities such as loss of fluid test (LOFT), thermal-hydraulic test facility (THTF), and numerous separate effect tests.

- PIRT Panel Member #9 has a PhD and eight years of experience in nuclear engineering primarily focused on nuclear reactor thermal-hydraulic models for containment safety analyses.

- PIRT Panel Member #10 has 21 years of experience in the nuclear industry with a focus on the improvement of models, calculation methods, and computing automation procedures to analyze loss of coolant accidents.   He has experience in a wide range of computer codes, including CATHARE 2V2.5 V1.3L, TRAC PF1 MOD2/MOD1, Westinghouse ORIGIN codes with Framatome improvements MEDUSE, PERSEE, ACONDA, BART-F, REFLET (Satan VI, W-Reflood, Locta IV, Bart, and Froth).

12.0   APPENDIX B – U.S. EPR SCALING ANALYSIS

This appendix documents the top-down scaling analysis of the detailed non-dimensional governing equations for the physical processes occurring during U.S. EPR LBLOCAs. The characteristic time ratios or coefficients for the terms in the governing equations are referred to as Pi (∏) coefficients. Top-down scaling analysis results are used to identify which phenomena are important to the system behavior and therefore need to be well-scaled in the test facilities. The equations are also useful for identifying distortions in the test facilities. Significant differences between the values of larger ∏s for the prototype and a test facility indicate distortions in application of the test data to the U.S. EPR plant.

12.1   NOMENCLATURE

Nomenclature	Description	SI Unit
A	Area	m^2
c	Specific heat	J/(kg-K)
C	Participating wall thermal capacitance	J
D	Diameter	m
E	Total energy in the system	J
e	Total energy per unit mass	J/kg
F	Fraction of heat transfer area not involved in condensation	(dimensionless)
G	Volumetric flow rate	m^3/s
g	Acceleration of gravity	m/s^2
h	Specific enthalpy	J/kg
H	Heat transfer coefficient	$W/(m^2\text{-}K)$
k	Thermal conductivity	W/(m-K)
K	Pressure loss coefficient	(dimensionless)
L	Level	m
ℓ	Participating length for thermal capacity or conductivity	m
M	Mass	kg
$\dot{m}$	Mass flow rate	kg/s
p	System pressure	pascal
P	Hydrostatic pressure	pascal
$\dot{q}, Q$	Heat transfer rate	W
R	Ideal gas constant	J/(kg-K)
s	Entropy	J/(kg-°C)
SF	Fraction of heat transfer surface where condensation is occurring	(dimensionless)
t	Time	second

Nomenclature	Description	SI Unit
T	Temperature	°C
T^k	Temperature	K
u	Flow velocity (as associated with kinetic energy)	m/s
U	Overall heat transfer coefficient	$W/(m^2\text{-}K)$
v	Specific volume	$m^3/\,kg$
V	Control volume or component volume	m^3
$\dot{W}$	Rate of work done	W
x	Steam quality, mass fraction in steam/air mixture	(dimensionless)
$z\,,Z$	Elevation difference	m
Greek Letter	**Description**	**SI Unit**
α	Steam void fraction	(dimensionless)
μ	Specific internal energy	J/kg
ρ	Density	$kg/\,m^3$
Γ	Wall condensation mass flow rate	kg/s
$\prod$	Non-dimensional coefficient in dynamic system equations	(dimensionless)

Subscripts	Description
0	Reference state
a	Air
b	Associated with the break
CNT	Containment
$conv$	Convective heat transfer
$core$	Reactor core
f	Saturated liquid
fg	Difference between saturated steam and liquid phase
g	Saturated steam
gap	Air gap between steel liner and concrete wall
gas	Gaseous phase
i	Corresponds to component i
$i,\,j$	Interface or interaction between components i and j
in	Input
$liner$	Steel liner
liq	Liquid phase
out	Output or outside of system
p	Pressure
R	Ratio
sat	Saturated condition
SG	Steam Generator
SI	Safety Injection
w	Wall
wc	Wall Condensation

Acronym	Description
AS	Accessible Space
CLPD	Cold-Leg Pump Discharge
CLPS	Cold-Leg Pump Suction
ER	Equipment Room
IET	Integral Effects Test
HL	Hot-Leg
IRWST	In-containment Refueling Water Storage Tank
LBLOCA	Large-Break Loss-of-Coolant-Accident
LHSI	Low-Head Safety Injection
LHSIHX	Low-Head Safety Injection Heat Exchanger
PIRT	Phenomena Identification and Ranking Table
RCS	Reactor Cooling System
RPV	Reactor Pressure Vessel
SAHRS	Severe Accident Heat Removal System
SET	Special Effects Test
SG	Steam Generator

12.2   ANALYTICAL METHODOLOGY

The objective of the scaling analysis is to identify the processes, variables, and parameters that govern the system's response in non-dimensional space. Having determined these, one can validate the Phenomena Identification and Ranking Table (PIRT) generated by expert opinion, relate prototype behavior to small-scale experiments, identify potential distortions and evaluate the impact of such distortions, and ultimately determine if the available body of data is sufficient to envelope the expected accident phenomena.

The specific methodology applied here was based on the scaling analysis work done in (Reference 12.2), using test data from various test facilities.

The strategy is to apply rigorous analysis, existing data, and first principles to achieve the objective. These are the specific steps:

- Develop a scenario description

- Discretize the scenario in a manageable set of components or elements

- Based on conservation laws and first principles, develop a closed set of governing equations for these elements

- Use the closed set of equations to conduct scaling analysis, as follows:

  - Non-dimensionalize the equations to develop non-dimensional coefficients (∏s)

  - Determine the proper reference parameters according to the time period (accident phase) of interest

  - Choose a reference time (a potentially recurrent step) according to the time scale of interest

  - Evaluate ∏s and establish their rankings per component and complete system. The figure of merit or primary safety criterion defines the metric that determines what process is more or less important.

  - Compare with experimental data to identify and evaluate the impact of scaling distortions on the figure of merit

  - Compare the dominant ∏s and process ranges with the available data and assess data sufficiency

  - Relate the PIRT phenomena with system processes and ∏s to determine if the ranges of data are sufficient and complete.

12.3   ASSUMPTIONS

The main assumption is that the internal behavior in each selected component is uniform enough to be reasonably approximated by the lump parameter approach. The resulting model is not a substitute for a system code calculation; rather it is performed to provide analytical insight into the response of the system as a whole.

It is also assumed that gases (containment air and steam) behave as ideal gases, and they are well mixed enough in each large volume so that the entire volume can be represented with a single set of state variables.

Additionally, it is assumed that each phase of the accident – blowdown, pre-hot leg injection, and post-hot leg injection – can be modeled independently and that the thermodynamic states remain constant throughout each phase.

12.4 U.S. EPR Containment Scaling Models

12.4.1 Step 1: Scenario Description

Figure 12-1 is a schematic of a cold leg LBLOCA scenario showing the processes and components that participate in the transient. The containment response in the LBLOCA scenario can be characterized by three distinct phases:

1. Blowdown phase (0-35 sec)

2. Pre-HL Injection phase (35 sec – 60 min)

3. Post-HL Injection phase (>60 min)

The first phase (Blowdown) is characterized by a large injection of a mixture of super-heated steam and saturated water into the containment ER volume from the RCS break. The Blowdown phase ends when the RCS is completely depressurized and reaches pressure equilibrium with the containment. The high rate of steam injection rapidly increases the pressure in the ER. This ruptures the convection foils and opens the lower mixing dampers separating the ER and AS volumes, while the saturated water from the break and the condensate are channeled down to the IRWST. The ER and AS pressures increase rapidly and reach a maximum at the end of the blowdown phase. Forced convection resulting from the blowdown and condensation on the containment structures are the two most important heat transfer mechanisms.

The second phase (Pre-HL injection) is distinguished by much less atmospheric turbulence in the containment, so that natural convection between the ER and AS volumes and steam condensation on the containment structures are the principal heat transfer processes. During this phase, the ER and AS pressures decreases gradually while the rate of energy removed (due to steam condensing on the walls and conduction heat transfer to the structures and passive sink) surpasses the steam boil-off energy release rate due to decay heat in the core. The reactor core acts like a boiling pot, releasing steam into the containment until the LHSI is switched from cold-leg to hot-leg injection and causes boiling in the core to cease.

The third and final phase (Post-HL Injection) begins when safety injection (SI) is switched from the cold-leg to the hot-leg. The change in safety injection location results in rapid steam condensation in the reactor vessel upper plenum caused by the injection of cold water above the core, and terminates the steam boil-off in the core. The atmospheric turbulence in the containment space also ceases. This phase is characterized by an increased containment depressurization rate. The primary heat transfer mechanisms for this phase are conduction through the containment wall to the passive sink (environment) and convective heat transfer through the LHSI heat exchanger in the IRWST to the environment.

12.4.2   Step 2: Discretization

Normally, there are three types of components or elements to be considered in the analysis:

- Volumes in which fluid enters, can be stored, or leaves. The state of gas volumes is defined by their gas mixture temperature and pressure. The state of liquid volumes (or tanks) is defined by their level or hydrostatic pressure at the lowest exit point and the temperature of the liquid. The reactor vessel can be a special case when it is essentially a two-phase mixture in which collapsed liquid

level and steam quality are directly related, and in this case the system state requires temperature or pressure and quality.

- Masses of structures or components which store and conduct heat. Their state is defined by their temperature, which measures the amount of energy they contain.

- There are also inputs and boundary conditions that are not considered "elements," but which have an indirect dynamic contribution to the system. They are represented as static algebraic relationships, and include components such as the LHSI heat exchangers and pumps.
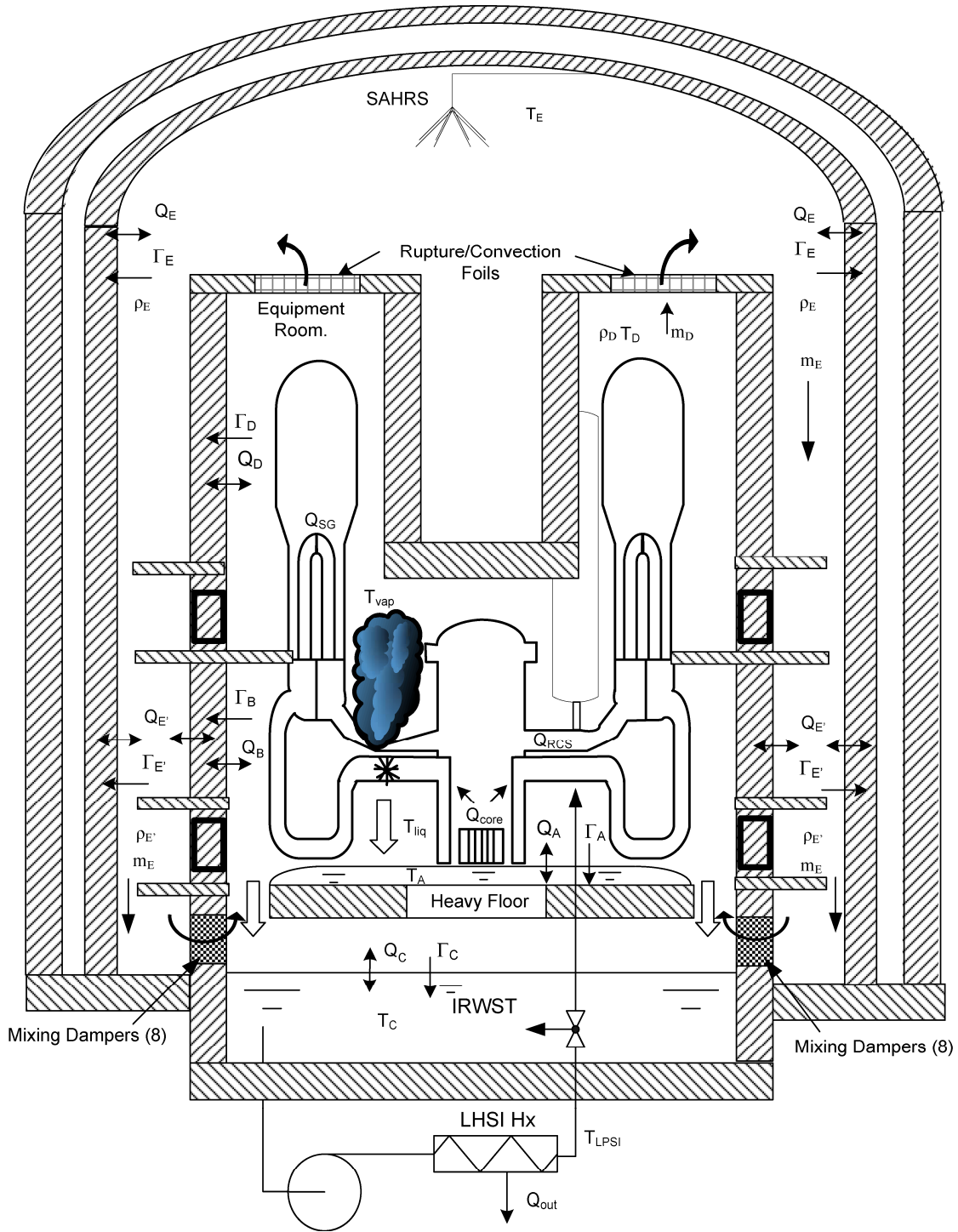
Figure 12-1—Schematic of a LBLOCA Scenario

Following the flow of energy from the reactor core to the passive heat sink (as illustrated in Figure 12-2), the following components are of interest:
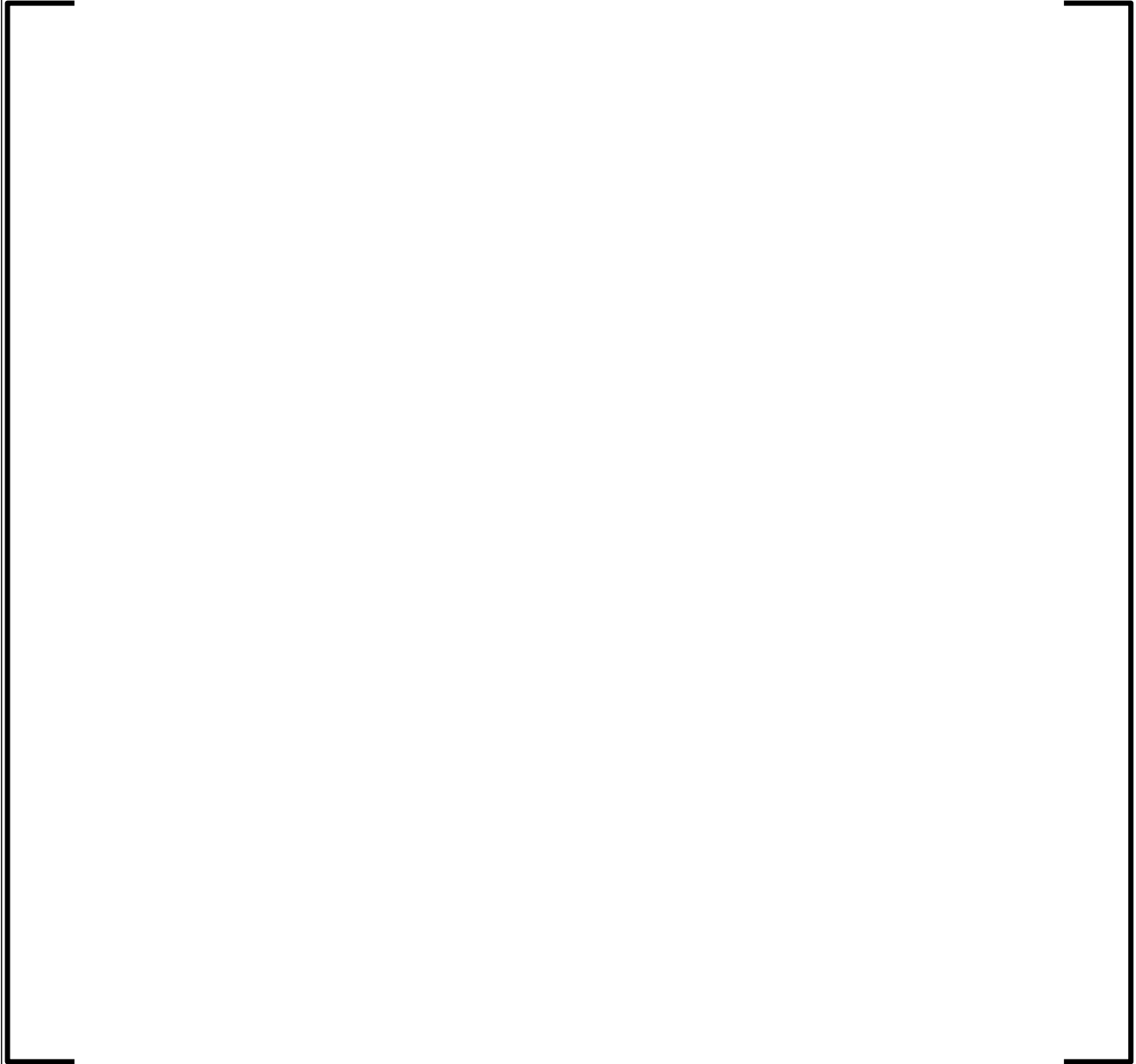
The arrows in Figure 12-2 suggest the interaction between components. This is important because this schematic of the system interactions is used to develop the governing equations.

AREVA NP Inc.

Applicability of AREVA NP Containment Response Evaluation Methodology to the
U.S. EPR™ for Large Break LOCA Analysis

Technical Report

ANP-10299NP
Revision 2

Page 12-10

Figure 12-2—U.S. EPR Containment Scaling Model System Components

12.4.3   Step 3: PIRT Considerations

A panel of experts determined the LBLOCA mass and energy release and containment
pressure PIRTs in order to establish the appropriate modeling treatment for the code
parameters impacting an important phenomenon.

The Organization for Economic Cooperation and Development / Nuclear Energy Agency (OECD/NEA) experts prepared a PIRT that considered an LBLOCA through the "core damage phase of a severe accident," and addressed three figures-of-merit: pressure, local temperature, and steam-air-hydrogen composition (Reference 12.4). Table 12-1 shows the OECD/NEA PIRT, expressing phenomena ranking of L, M, or H (low, medium, or high) for total pressure only, with some modifications reflecting the U.S. EPR design, such as removal of phenomena related to sprays and fan coolers. Furthermore, for the Pre- and Post-HL Injection phases, the gas expansion process has ceased and the system enters into a quasi-steady state, hence, the "multi-component gas compression/ expansion'' phenomenon ranking becomes "L". Moreover, during the Post-HL Injection phase, the "free convection" phenomenon in the condensation process on the structure surface becomes insignificant as compared to the conduction heat transfer process; therefore, its ranking is reduced from "H" to "L." Finally, the free convection phenomenon of the condensation process on the pool surface is not credited for the U.S. EPR plant as being conservative.

The system level codes model those phenomena with "High" ranking (H in Table 12-1) to a degree meriting their phenomenological importance in this calculation.

12.4.4   Step 4: Scaling Considerations

In order to assess the capability of a code model to predict the important phenomena identified in the PIRT, evaluations against special effects test (SET) and integral effects test (IET) data should be performed. Since it is not possible to build and conduct destructive LBLOCA tests on the prototype (U.S. EPR plant), scaling analysis on test facilities must be evaluated in order to properly account for any distortions in the test results with respect to the prototype. Therefore, the selection of tests must be such that the important phenomena in a PWR LBLOCA are captured. In addition, the selection of tests must be scalable to both the LBLOCA phenomena and the U.S. EPR plant.

AREVA NP Inc.
Applicability of AREVA NP Containment Response Evaluation Methodology to the
U.S. EPR™ for Large Break LOCA Analysis
Technical Report

ANP-10299NP
Revision 2

Page 12-12

12.4.5 RCS Scaling Model

Figure 12-3 illustrates the components with which the RCS has direct interaction.

Table 12-1—PIRT for U.S. EPR Containment Pressure Following an LBLOCA

Component	Process	Phenomena	Rank
Atmosphere	Pressurization / Depressurization	Multi-component gas compression/expansion	M
		Aerosol mass and energy exchange	*(N/A)*
		Spray mass and energy exchange	*(N/A)*
		Volume displacement/pool filling or draining	L
		Atmosphere cooling by fan-cooler	*(N/A)*
	Mixing (intracompartment)	Jet-plume gas interaction/entrainment (localized)	L
		Buoyancy/stratification (regional)	L-M
		Buoyancy/wall interaction (regional)	L
		Diffusion (turbulent)	L
		Spray dynamics	*(N/A)*
		Fan dynamics	*(N/A)*
	Transport (intercompartment)	Buoyancy/stratification	M
		Form and friction losses	L
		Aerosol coupling	L
		Liquid water carryover	L
Structure Interior	Heat Transfer	One-dimensional transient conduction	**H**
		Two- or three-dimensional transient conduction	L
	Mass Transfer	Outgassing (concrete)	L
Structure: Surface (solid and film)	Sensible Heat Transfer	Spray/aerosol deposition or impingement	*(N/A)*
		Free convection	L
		Forced/mixed convection	L
		Radiation (structure to atmosphere)	L
		Radiation (structure to structure)	L
		Liquid film resistance	L
		Liquid film advection	L
	Latent Heat and Mass Transfer (condensation/ evaporation)	Free convection	**H**
		Forced/mixed convection	L
	Transport (film flow)	Liquid film advection	L-M
		Interfacial shear (film/gas interaction)	L
Pool: Interior	Mixing	Buoyancy/stratification	L
		Bubble dynamics	L
	Transport	Filling and draining	L
		Displacement (pressure driven)	L
	Heat Transfer	Convection (flooded structures)	L
		Boiling	L
		Steam condensation (bubbles)	L
Pool: Surface	Sensible Heat Transfer	Free convection	L
		Forced/mixed convection	L
		Aerosol/spray deposition	*(N/A)*

Component	Process	Phenomena	Rank
	Latent Heat and Mass Transfer (condensation/ evaporation)	Free convection	**H**
		Forced/mixed convection	L

12.4.5.1 Assumptions

The main assumptions for the RCS component model are:

AREVA NP Inc.

ANP-10299NP

Applicability of AREVA NP Containment Response Evaluation Methodology to the

Revision 2

U.S. EPR™ for Large Break LOCA Analysis

Technical Report

Page 12-14

Figure 12-3—RCS Components and Interactions with Neighboring Components

12.4.5.2   *Generalized RCS Mass and Energy Conservation Equations*

The derivation of the generalized RCS component mass and energy conservation equation is given in Appendix C.

The generalized RCS mass conservation equation is given by:

$$\frac{dM_1}{dt} = \sum \dot{m}_{in} - \sum \dot{m}_{out}$$

(12.1)

where:

$$M_1 = (V\rho)_1 \tag{12.2}$$

The generalized RCS energy conservation equation is given by:

$$\frac{dE_1}{dt} = \left(\sum \dot{W}_{in} - \sum \dot{W}_{out} \right) + \left(\sum \dot{q}_{in} - \sum \dot{q}_{out} \right) + \sum (e\dot{m})_{in} - \sum (e\dot{m})_{out} \tag{12.3}$$

where:

$$E = eM = \text{total energy} \tag{12.4}$$

$$e = \mu + \frac{u^2}{2} + gz = \text{specific energy} \tag{12.5}$$

$$\mu = h - pv = \text{specific internal energy} \tag{12.6}$$

12.4.5.3   RCS Model for Blowdown and Pre-HL Injection Phases

The derivation of the RCS model for the saturated Blowdown phase is given in Appendix A of Reference 12.1 and in Appendix C. The mass conservation equation is given by:

$$\frac{dM_1}{dt} = \dot{m}_{SI} - \dot{m}_b \tag{12.7}$$

For the U.S. EPR RCS, the depressurization rate for the saturated Blowdown phase is given by Eq. (13.28) in Appendix C:

$$\frac{dp_1}{dt} = \frac{1}{M_1 \left(\frac{\partial \mu}{\partial p} \big|_v \right)_1} \left[\dot{m}_{SI} \left\{ h_{SI} - \mu_1 + v_1 \left(\frac{\mu_{fg}}{v_{fg}} \right)_1 \right\} - \dot{m}_b \left\{ h_b - \mu_1 + v_1 \left(\frac{\mu_{fg}}{v_{fg}} \right)_1 \right\} + \dot{q}_{core} - \dot{q}_{SG} - \dot{q}_{w,1,4} \right] \tag{12.8}$$

where:

$$\mu_1 = \mu_{f,1} + x_1 \mu_{fg,1} \tag{12.9}$$

$$v_1 = v_{f,1} + x_1 v_{fg,1} \tag{12.10}$$

$$h_b = h_{f,1} + x_b h_{fg,1} \tag{12.11}$$

$$\rho_1 = \frac{M_1}{V_1} \tag{12.12}$$

$$\alpha_1 = \left(\frac{\rho_f - \rho}{\rho_f - \rho_g} \right)_1 \tag{12.13}$$

$$x_1 = \alpha_1 \left(\frac{\rho_g}{\rho_f} \right)_1 \bigg/ \left(1 + \alpha \left(\frac{\rho_g}{\rho_f} - 1 \right) \right)_1 \tag{12.14}$$

The partial derivative of specific energy with respective to pressure is given by Eq. (C-47) in Reference 12.1:

$$\left(\frac{\partial \mu}{\partial p} \bigg|_v \right)_1 = \left((1-x) \frac{d\mu_f}{dp} + x \frac{d\mu_g}{dp} - \frac{\mu_{fg}}{v_{fg}} \left((1-x) \frac{dv_f}{dp} + x \frac{dv_g}{dp} \right) \right)_1 \tag{12.15}$$

and

$\dot{q}_{core}$ = reactor core power

$\dot{q}_{SG}$ = steam generator heat transfer rate

$\dot{q}_{w,1,4}$ = heat loss to the primary system structure (refer to Section 12.4.5.6)

Where the reactor core power, $\dot{q}_{core}$, and steam generator heat transfer rate, $\dot{q}_{SG}$, are treated as known boundary conditions in this model.

AREVA NP Inc.   ANP-10299NP
Applicability of AREVA NP Containment Response Evaluation Methodology to the   Revision 2
U.S. EPR™ for Large Break LOCA Analysis
Technical Report   Page 12-17

For a test facility with single reactor vessel such as Heissdampfreaktor (HDR), the void fraction of the vessel is defined as Eq. (A-36) in Reference 12.1:

$$\alpha_1 = 1 - \frac{L_1}{L_{1,0}} \tag{12.16}$$

And the quality is defined as Eq. (A-47) in Reference 12.1:

$$x_1 = \frac{1 - L_1^*}{1 + L_1^*\left(\left(\frac{v_g}{v_f}\right)_1 - 1\right)} \tag{12.17}$$

where:

$$L_1^* = \frac{L_{RV}}{L_{RV,0}};$$

L_{RV} = collapsed water level in the reactor pressure vessel

12.4.5.4   *Non-dimensional RCS Scaling Model for Blowdown and Pre-HL Injection Phases*

Normalize the following system parameters by reference values at state = 0:

AREVA NP Inc.

Applicability of AREVA NP Containment Response Evaluation Methodology to the
U.S. EPR™ for Large Break LOCA Analysis
Technical Report

ANP-10299NP
Revision 2

Page 12-18
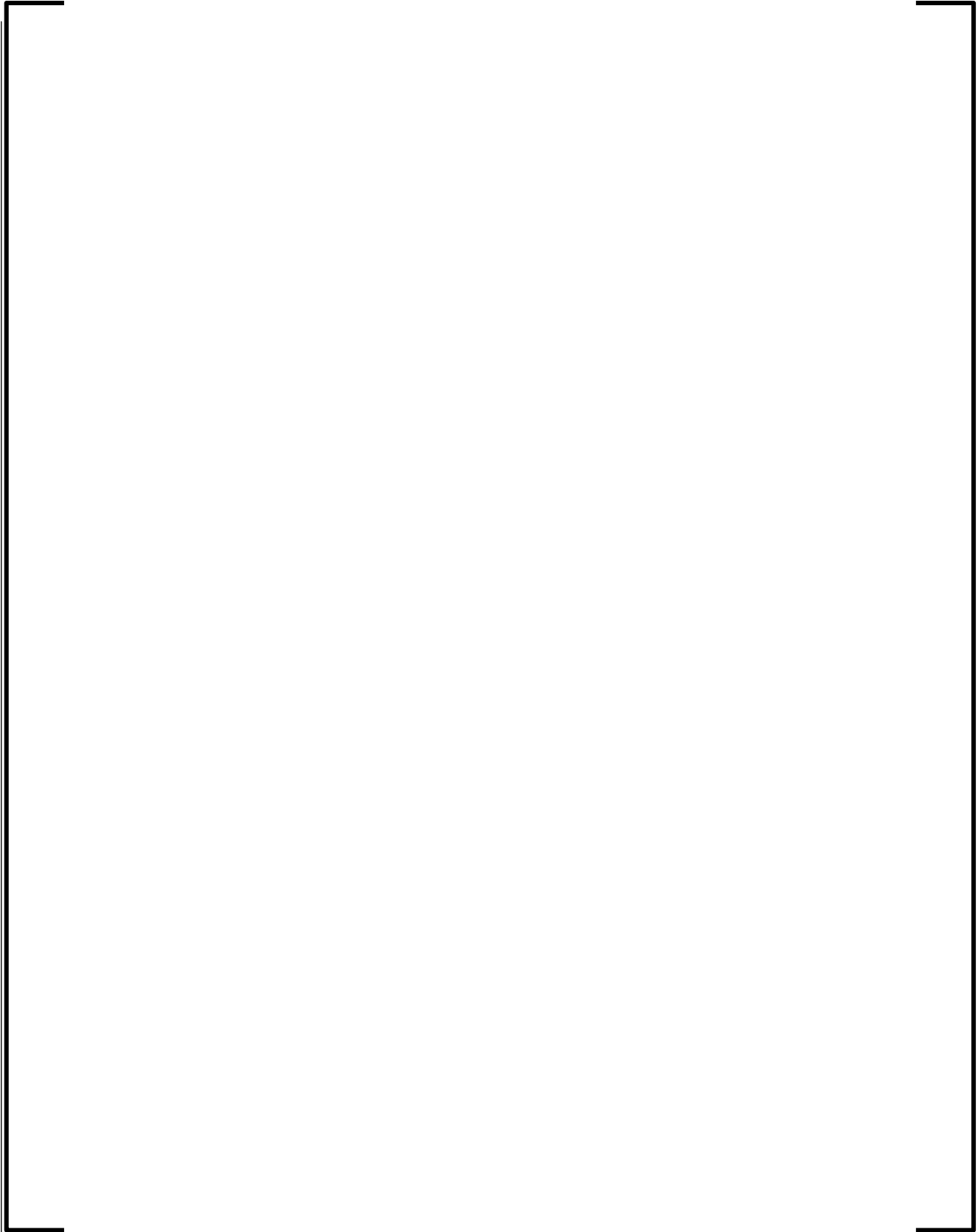
Generally, it is assumed that system parameters $(x_{1,0}y_{1,0})$ are equivalent to $(x_1y_1)_0$.

The non-dimensional form of mass conservation equation, Eq. (12.1), becomes:

$$\left[\right]$$
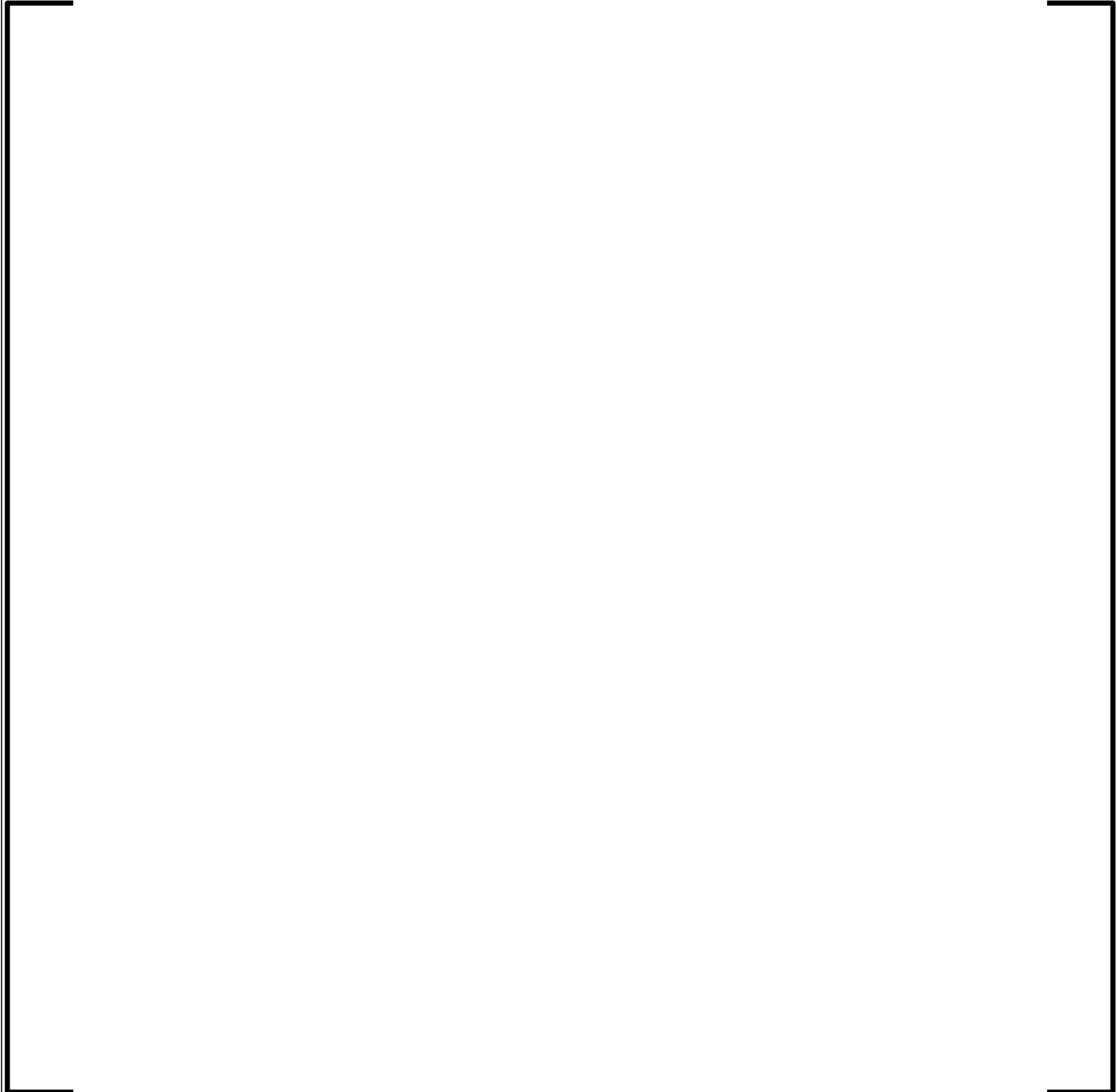
The non-dimensional form of the energy conservation equation, Eq. (12.3), follows the

derivation for Eq. (A-59) given in Appendix A of Reference 12.1, and becomes:

AREVA NP Inc.

Applicability of AREVA NP Containment Response Evaluation Methodology to the
U.S. EPR™ for Large Break LOCA Analysis
Technical Report

ANP-10299NP
Revision 2

Page 12-19

AREVA NP Inc.
Applicability of AREVA NP Containment Response Evaluation Methodology to the
U.S. EPR™ for Large Break LOCA Analysis
Technical Report

ANP-10299NP
Revision 2

Page 12-20

The RCS model Pi groups for the blowdown and pre-hot leg injection phases are summarized in Table 12-2.

Table 12-2—RCS Model Pi Groups for the Blowdown and Pre-HL Injection Phases

Pi Group	Algebraic Expression	Definition
$\Pi_{1,1}$		
$\Pi_{1,2}$		
$\Pi_{1,3}$		
$\Pi_{1,4}$		
$\Pi_{1,5}$		

Pi Group	Algebraic Expression	Definition
$\Pi_{1,6}$		
$\Pi_{1,7}$		
$\Pi_{1,8}$		
$\Pi_{1,9}$		

12.4.5.5 RCS Model for Post-HL Injection Phase

AREVA NP Inc.

Applicability of AREVA NP Containment Response Evaluation Methodology to the
U.S. EPR™ for Large Break LOCA Analysis
Technical Report

ANP-10299NP
Revision 2

Page 12-22
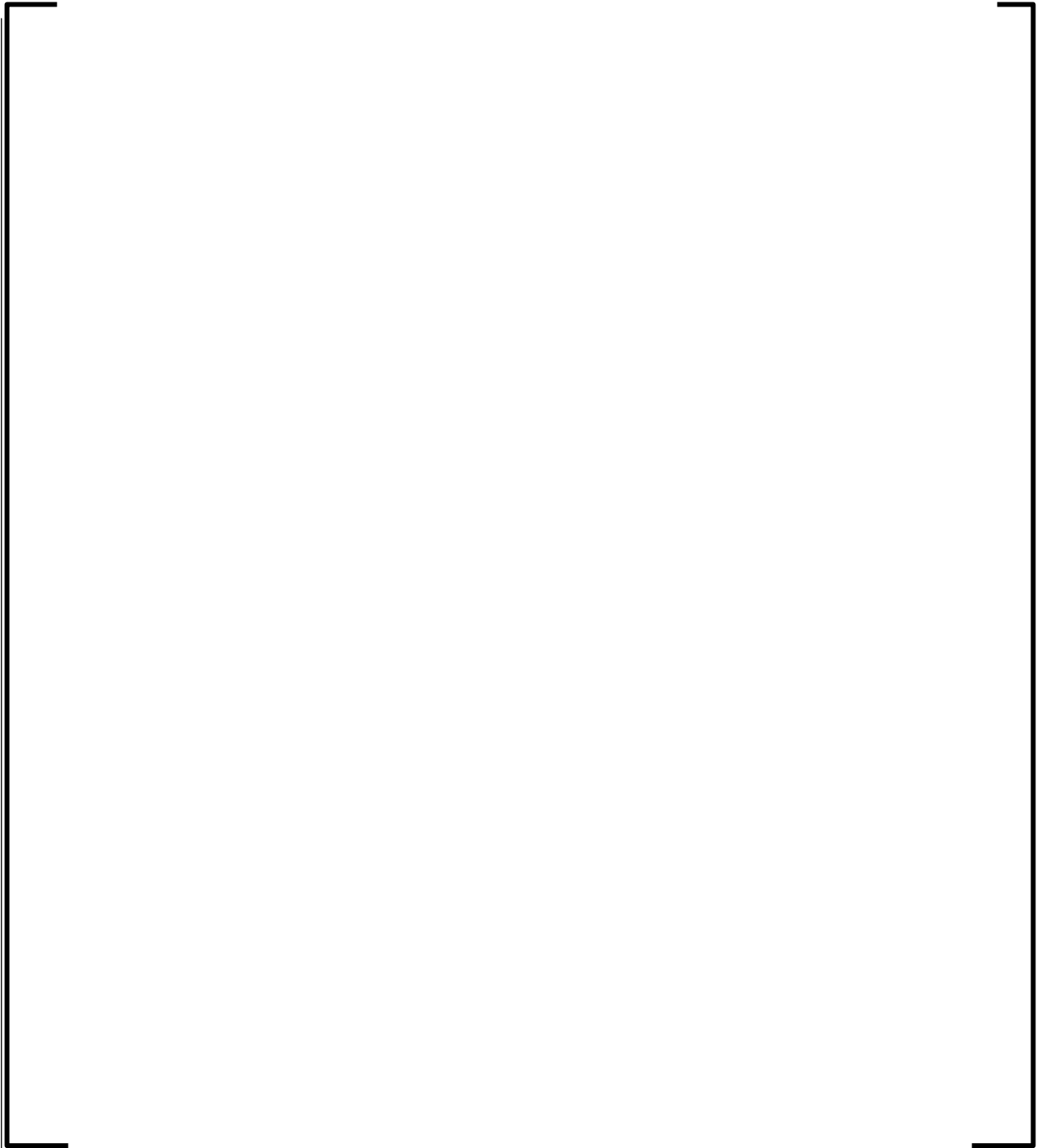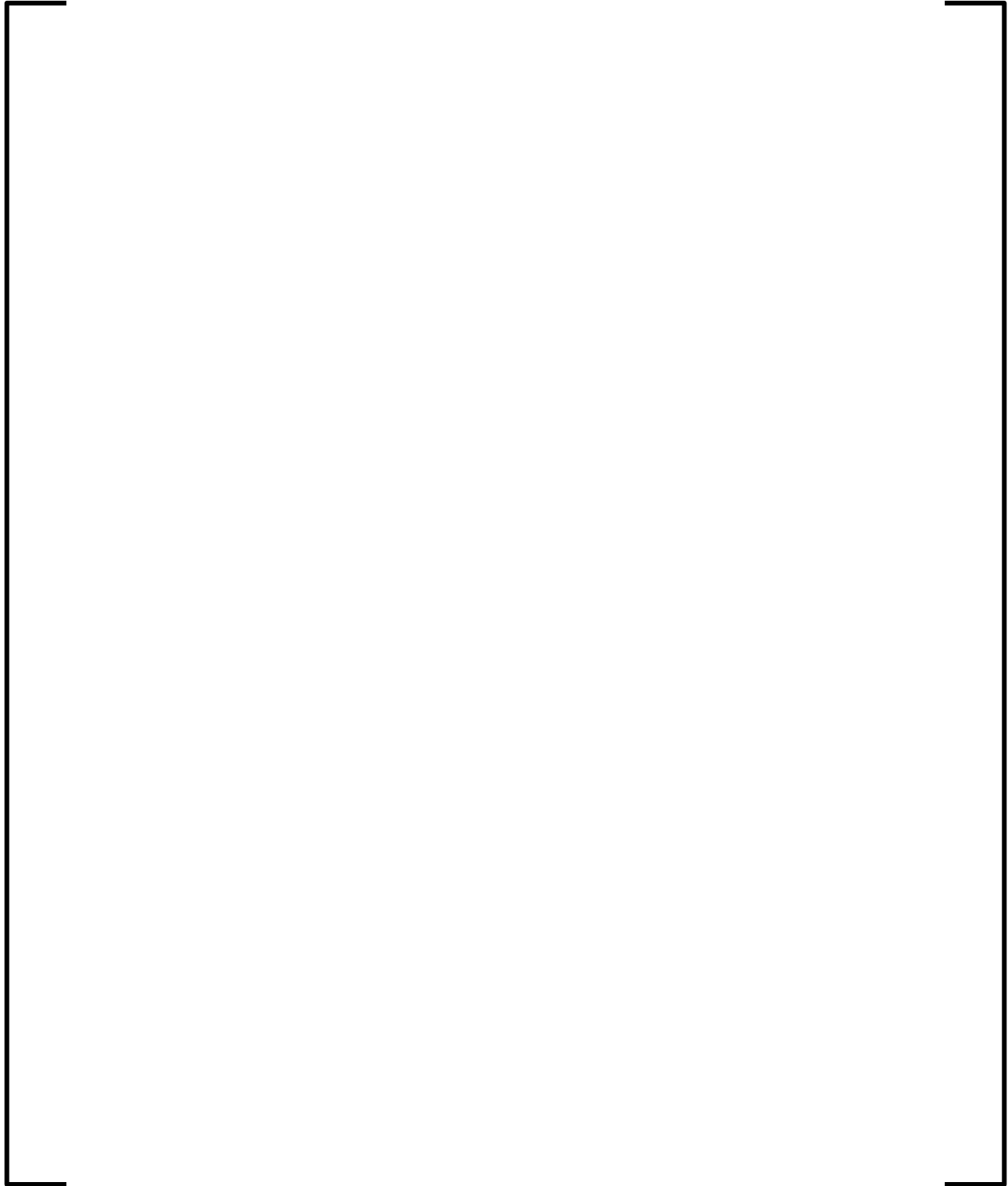
The RCS model Pi groups for the post-hot leg injection phase are summarized in Table 12-3.

Table 12-3—RCS Model Pi Groups for the Post-HL Injection Phase

Pi Group	Algebraic Expression	Definition
$\Pi_{1,11}$		
$\Pi_{1,12}$		
$\Pi_{1,13}$		
$\Pi_{1,14}$		

---

[1] The majority of heat in the steam generators will be transferred by natural circulation inside the intact loops due to loop seals during the post-HL injection phase.

12.4.5.6 Primary System Structure Energy Model
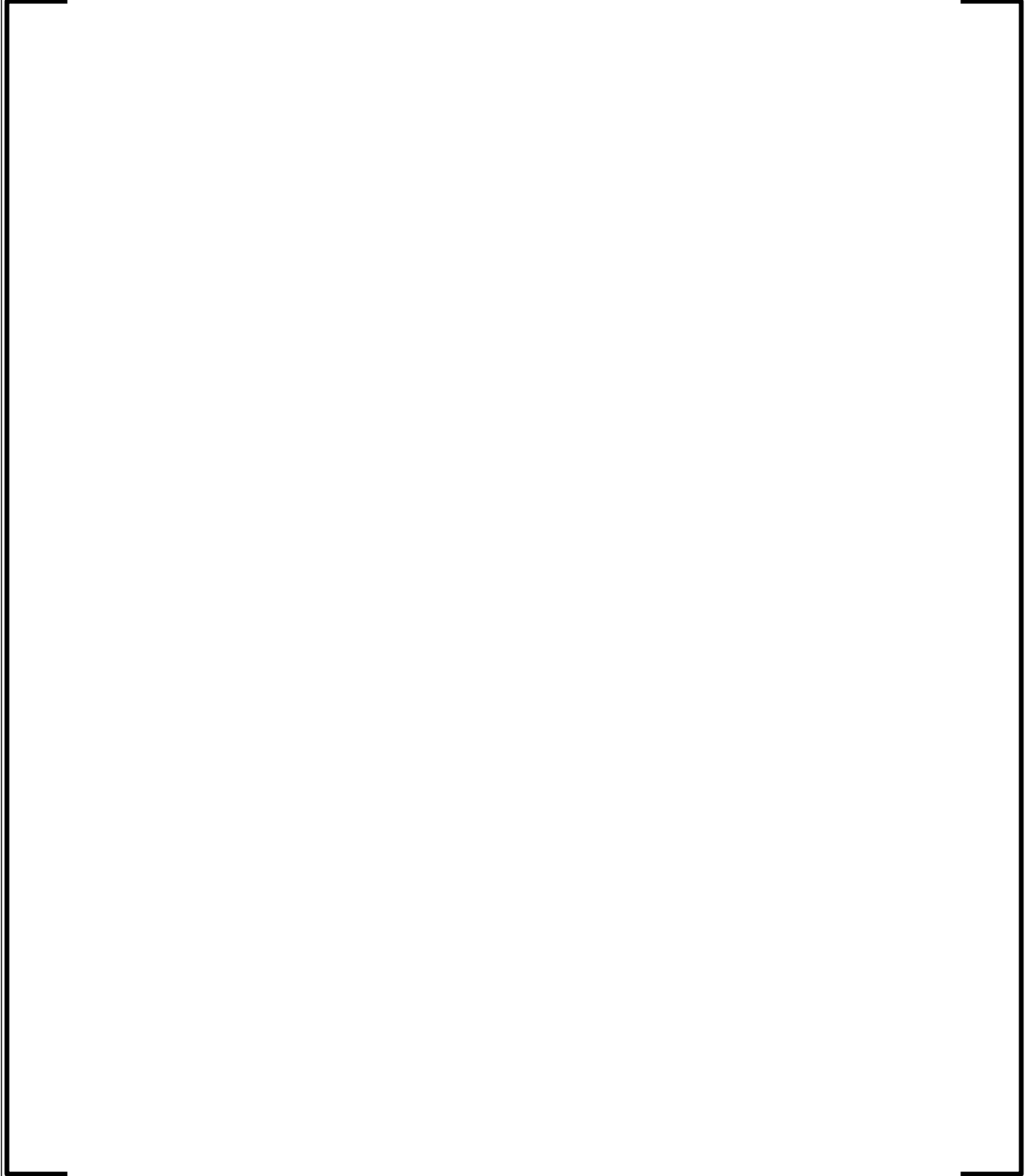
The Pi group for the primary system structure model is presented in Table 12-4.

Table 12-4—Pi Group for the Primary System Structure Model

Pi Group	Algebraic Expression	Definition
$\Pi_{4,1}$		

12.4.6   Equipment Room (ER) Scaling Model

The gas in the ER is a mixture of steam and air; Figure 12-4 depicts the ER control volume and its interactions with neighboring components.

12.4.6.1   Assumptions

The assumptions applied for the Blowdown and Pre-HL Injection phases of the containment scaling model are as follows:
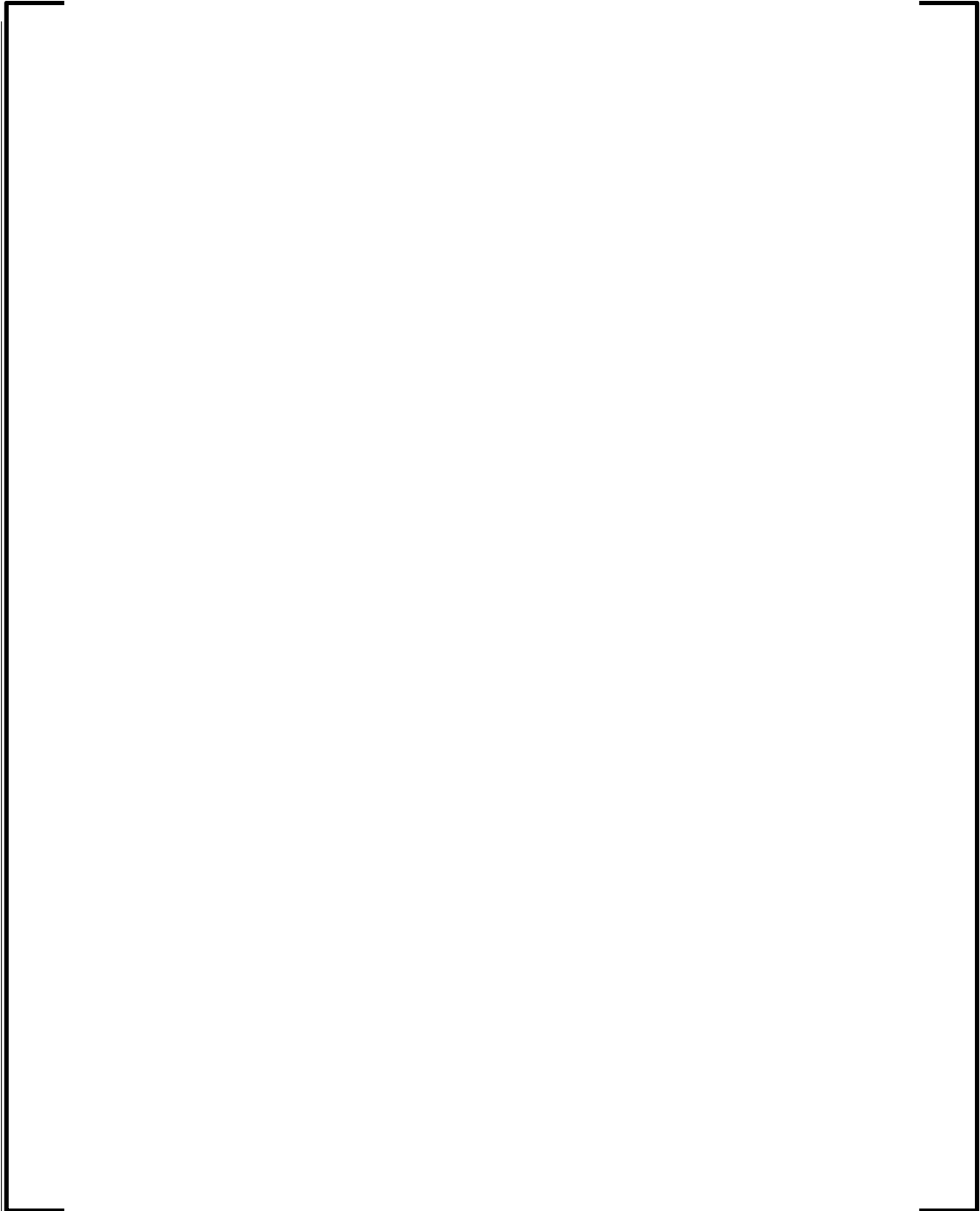
Figure 12-4—ER Control Volume and Interactions with Neighboring Components

AREVA NP Inc.

Applicability of AREVA NP Containment Response Evaluation Methodology to the
U.S. EPR™ for Large Break LOCA Analysis
Technical Report

ANP-10299NP
Revision 2

Page 12-28

12.4.6.2 Equipment Room (ER) Model for Blowdown and Pre-HL Injection Phases

12.4.6.2.1 ER Mass Conservation Equations
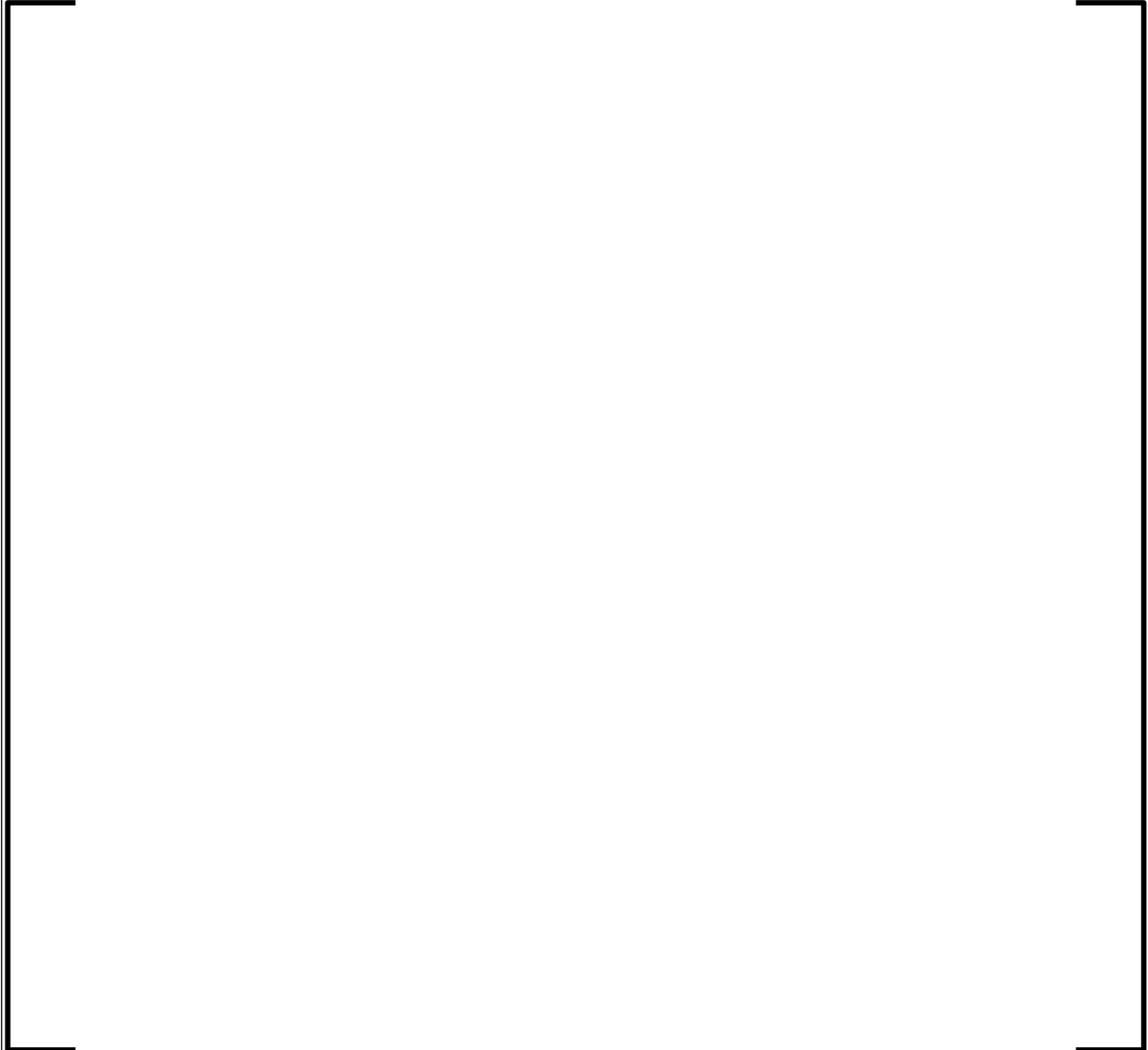
12.4.6.2.2   ER Mixture Energy Conservation Equation

---

[1] The absolute value $\left|\dot{m}_{7,2}\right|$ is necessary due to the sign convention defined in the momentum equations in Section 12.4.6.3.

AREVA NP Inc.

Applicability of AREVA NP Containment Response Evaluation Methodology to the
U.S. EPR™ for Large Break LOCA Analysis
Technical Report

ANP-10299NP
Revision 2

Page 12-32

AREVA NP Inc.

Applicability of AREVA NP Containment Response Evaluation Methodology to the
U.S. EPR™ for Large Break LOCA Analysis
Technical Report

ANP-10299NP
Revision 2

Page 12-35

AREVA NP Inc.

ANP-10299NP

Applicability of AREVA NP Containment Response Evaluation Methodology to the

Revision 2

U.S. EPR™ for Large Break LOCA Analysis

Technical Report

Page 12-36

12.4.6.2.3   Non-Dimensional ER Model for Blowdown and Pre-HL Injection Phases
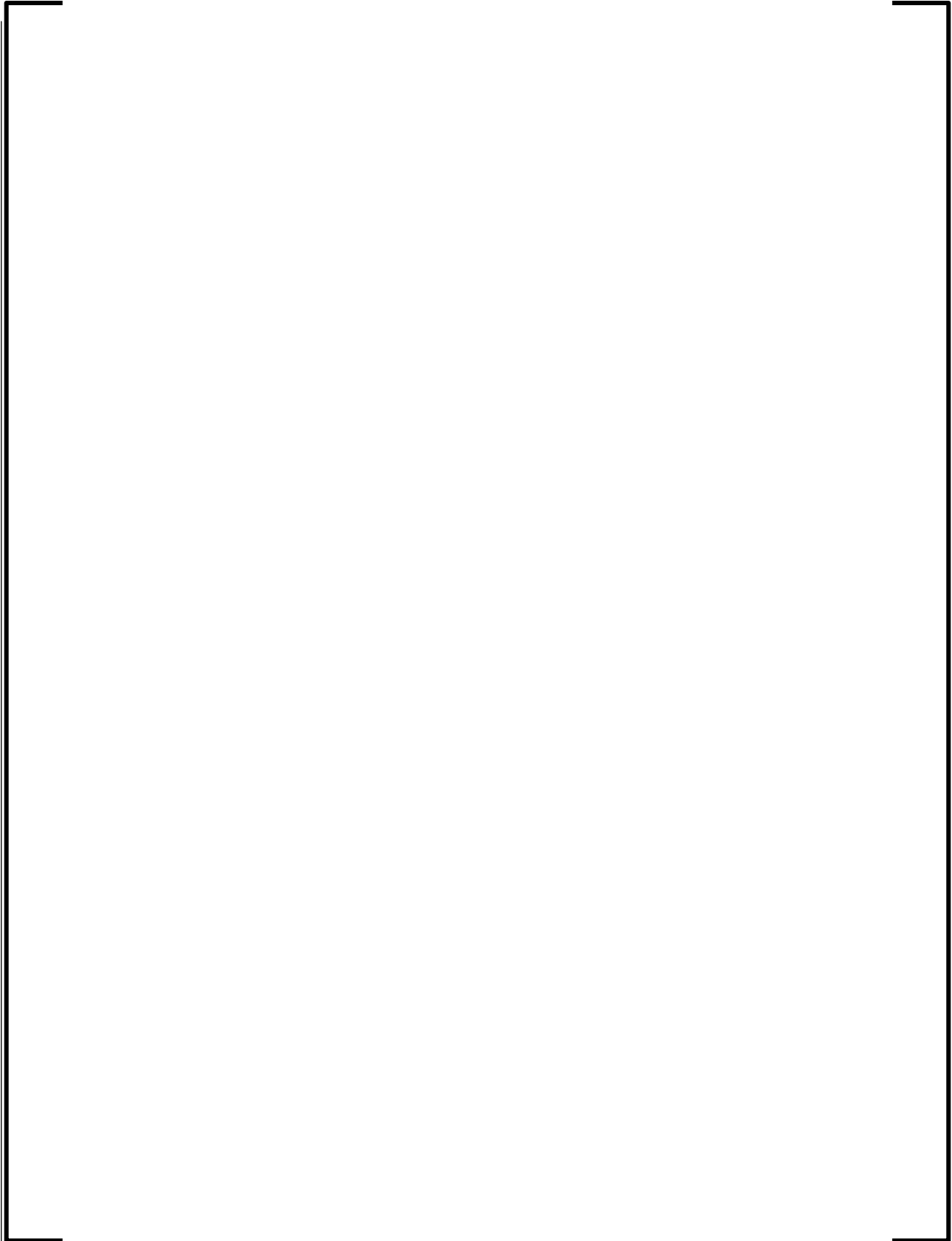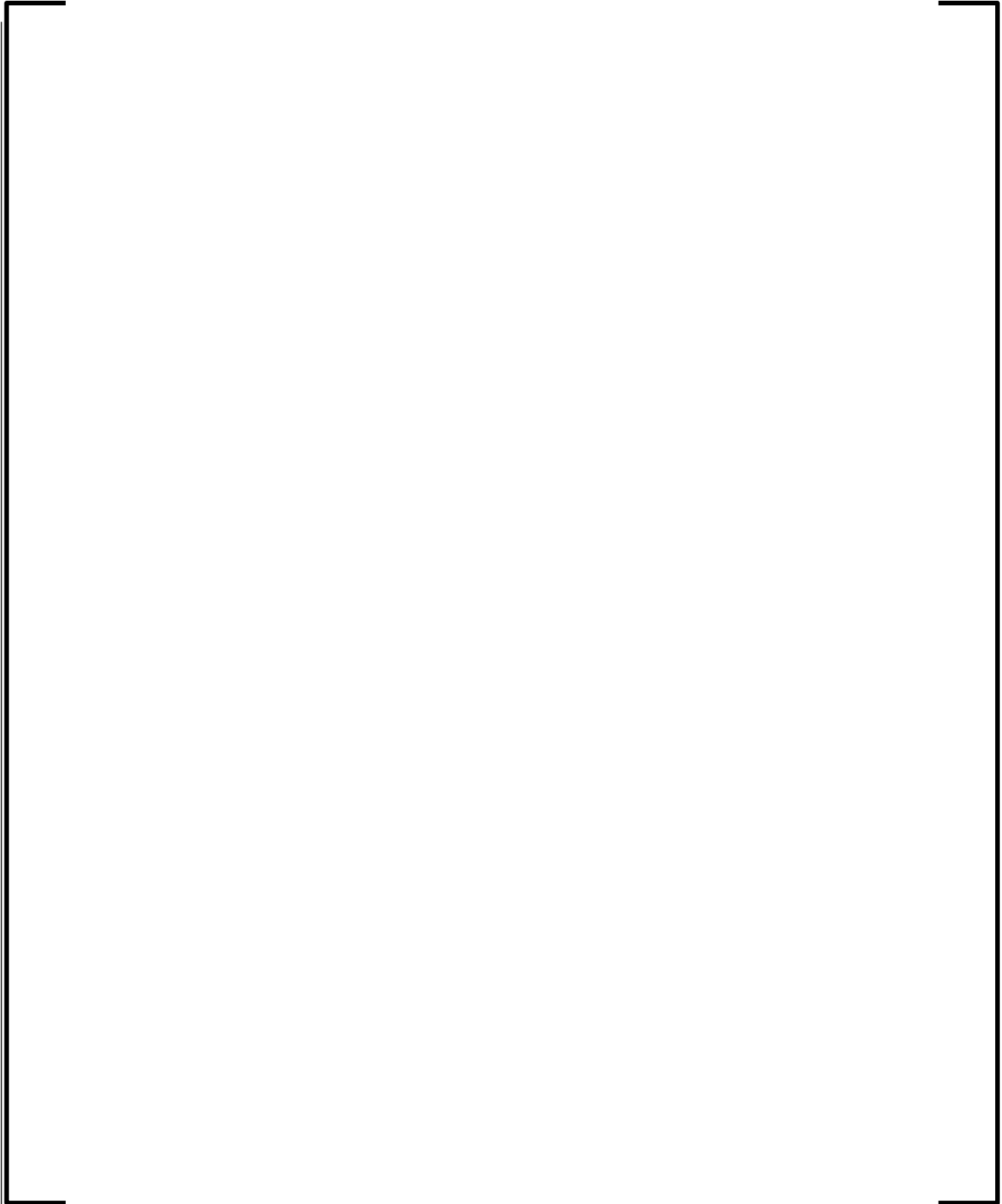
AREVA NP Inc.

Applicability of AREVA NP Containment Response Evaluation Methodology to the
U.S. EPR™ for Large Break LOCA Analysis
Technical Report

ANP-10299NP
Revision 2

Page 12-37

The ER model Pi groups for the blowdown and pre-hot leg injection phases are summarized in Table 12-5.

Table 12-5—ER Model Pi Groups for the Blowdown and Pre-HL Injection Phases

Pi Group	Algebraic Expression	Definition
$\Pi_{2,1}$		
$\Pi_{2,2}$		
$\Pi_{2,3}$		
$\Pi_{2,4}$		
$\Pi_{2,5}$		

AREVA NP Inc.

Applicability of AREVA NP Containment Response Evaluation Methodology to the
U.S. EPR™ for Large Break LOCA Analysis
Technical Report

ANP-10299NP
Revision 2

Page 12-40

Pi Group	Algebraic Expression	Definition
$\Pi_{2,6}$		
$\Pi_{2,7}$		
$\Pi_{2,8}$		
$\Pi_{2,9}$		
$\Pi_{2,10}$		
$\Pi_{2,11}$		
$\Pi_{2,12}$		

AREVA NP Inc.   ANP-10299NP

Applicability of AREVA NP Containment Response Evaluation Methodology to the   Revision 2
U.S. EPR™ for Large Break LOCA Analysis
Technical Report   Page 12-41

Pi Group	Algebraic Expression	Definition
$\Pi_{2,13}$		

12.4.6.3   ER/AS Momentum Model for Blowdown and Pre-HL Injection Phase

AREVA NP Inc.

Applicability of AREVA NP Containment Response Evaluation Methodology to the
U.S. EPR™ for Large Break LOCA Analysis
Technical Report

ANP-10299NP
Revision 2

Page 12-42

AREVA NP Inc.

ANP-10299NP

Applicability of AREVA NP Containment Response Evaluation Methodology to the

Revision 2

U.S. EPR™ for Large Break LOCA Analysis

Technical Report

Page 12-43
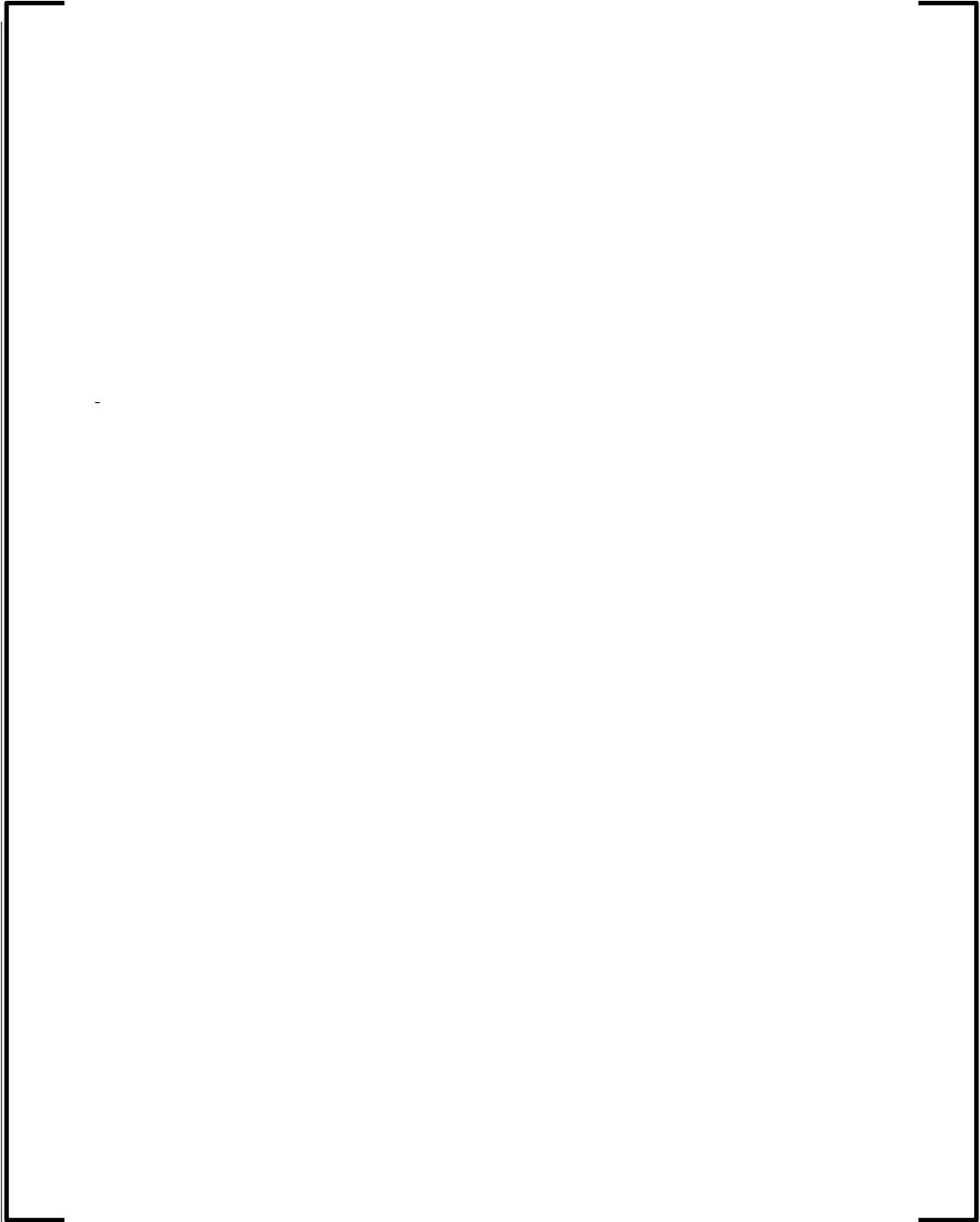
The ER/AS momentum model Pi groups for the blowdown and pre-hot leg injection phases are summarized in Table 12-6.

Table 12-6—ER/AS Momentum Model Pi Groups for the Blowdown and Pre-HL Injection Phases

Pi Group	Algebraic Expression	Definition
$\Pi_{11,1}$		
$\Pi_{11,2}$		
$\Pi_{11,3}$		
$\Pi_{11,4}$		

Pi Group	Algebraic Expression	Definition
$\Pi_{11,5}$		
$\Pi_{11,6}$		

12.4.6.4   ER Structure Heat Transfer Model

AREVA NP Inc.

Applicability of AREVA NP Containment Response Evaluation Methodology to the
U.S. EPR™ for Large Break LOCA Analysis
Technical Report

ANP-10299NP
Revision 2

Page 12-45
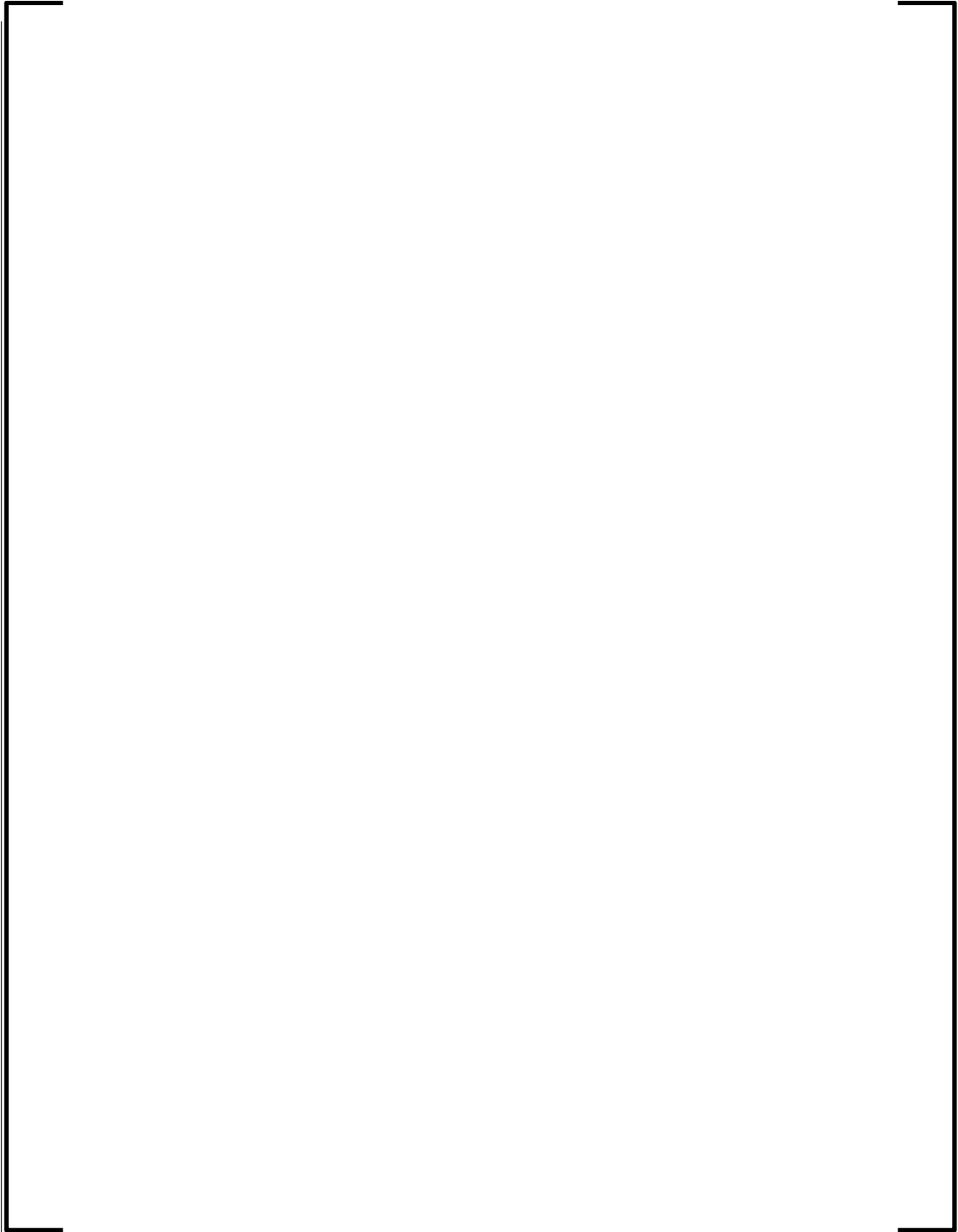
The ER structure model Pi group is presented in Table 12-7.

Table 12-7—Pi Group for ER Structure Model

Pi Group	Algebraic Expression	Definition
$\Pi_{5,1}$		

12.4.7   Accessible Space (AS) Scaling Model

The gas in the AS is also a mixture of steam and air; Figure 12-5 depicts the AS control volume and its interactions with neighboring components.

AREVA NP Inc.

Applicability of AREVA NP Containment Response Evaluation Methodology to the
U.S. EPR™ for Large Break LOCA Analysis
Technical Report

ANP-10299NP
Revision 2

Page 12-47

Figure 12-5—AS Control Volume and Interactions with Neighboring Components

12.4.7.1   AS Model for Blowdown and Pre-HL Injection Phases

12.4.7.1.1   Assumptions

The assumptions applied for the AS scaling model for the Blowdown and Pre-HL
Injection phases are the same as those for the ER model given in Section 12.4.6.1.

12.4.7.2   AS Mass Conservation Equations

AREVA NP Inc.

Applicability of AREVA NP Containment Response Evaluation Methodology to the
U.S. EPR™ for Large Break LOCA Analysis
Technical Report

ANP-10299NP
Revision 2

Page 12-48
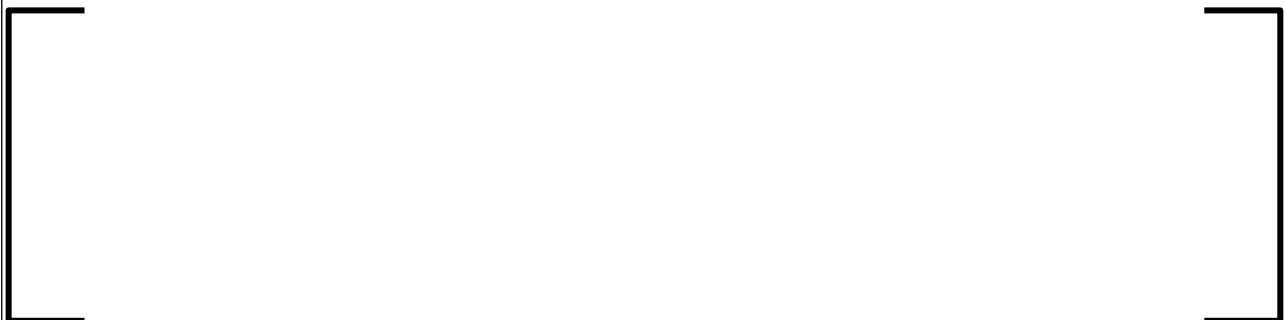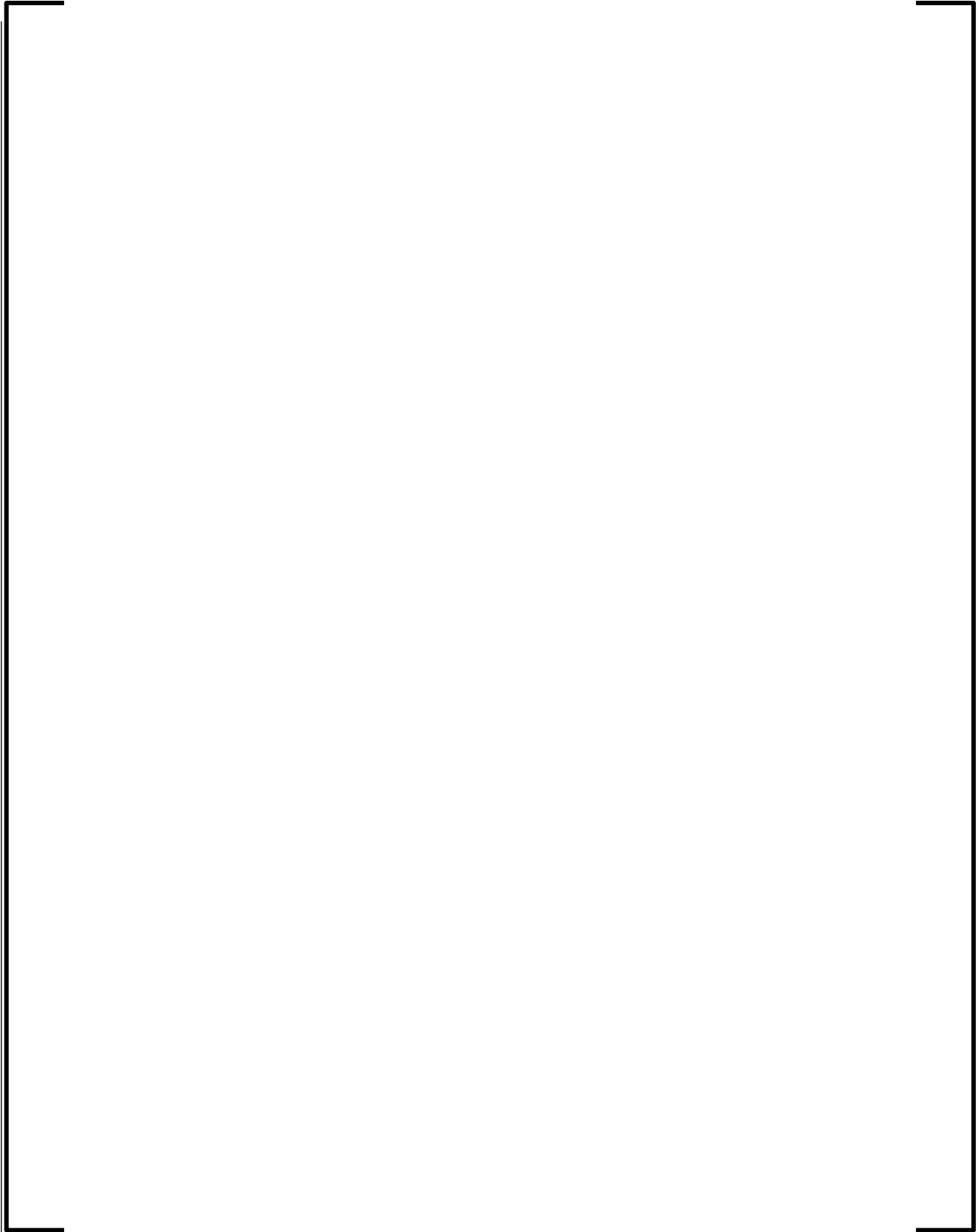
12.4.7.2.1   AS Mixture Energy Conservation Equation

The energy conservation equation of the steam/air mixture is given by:
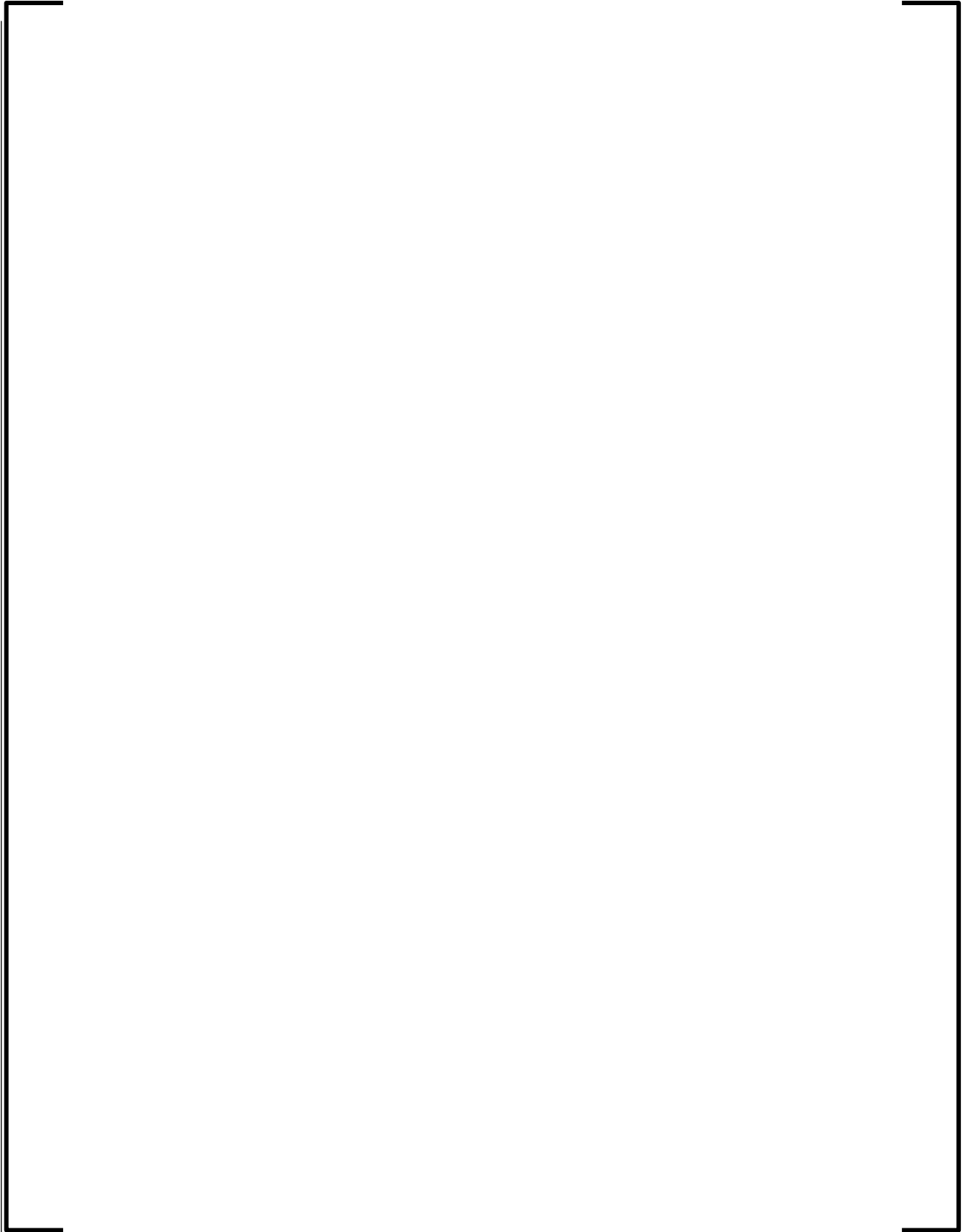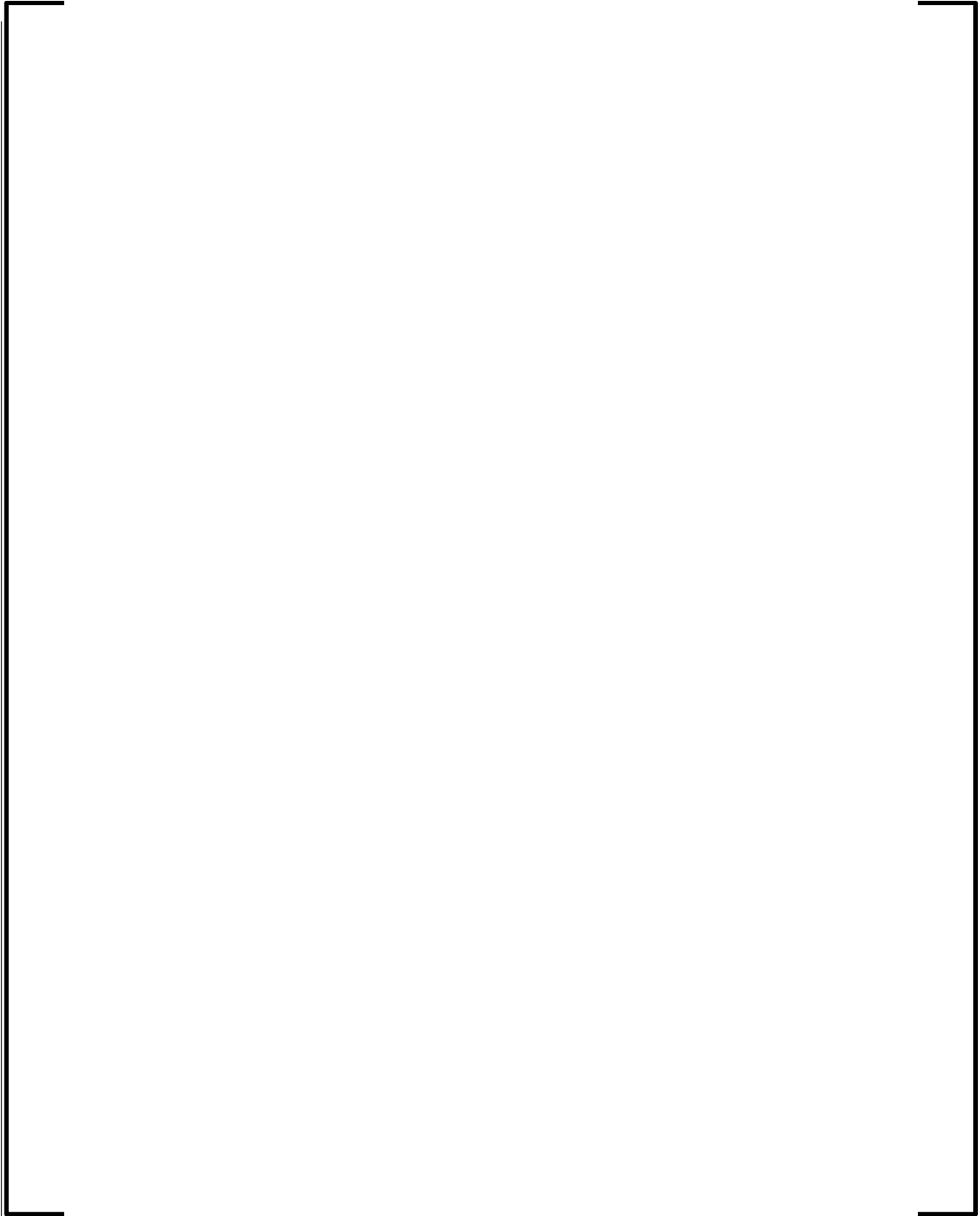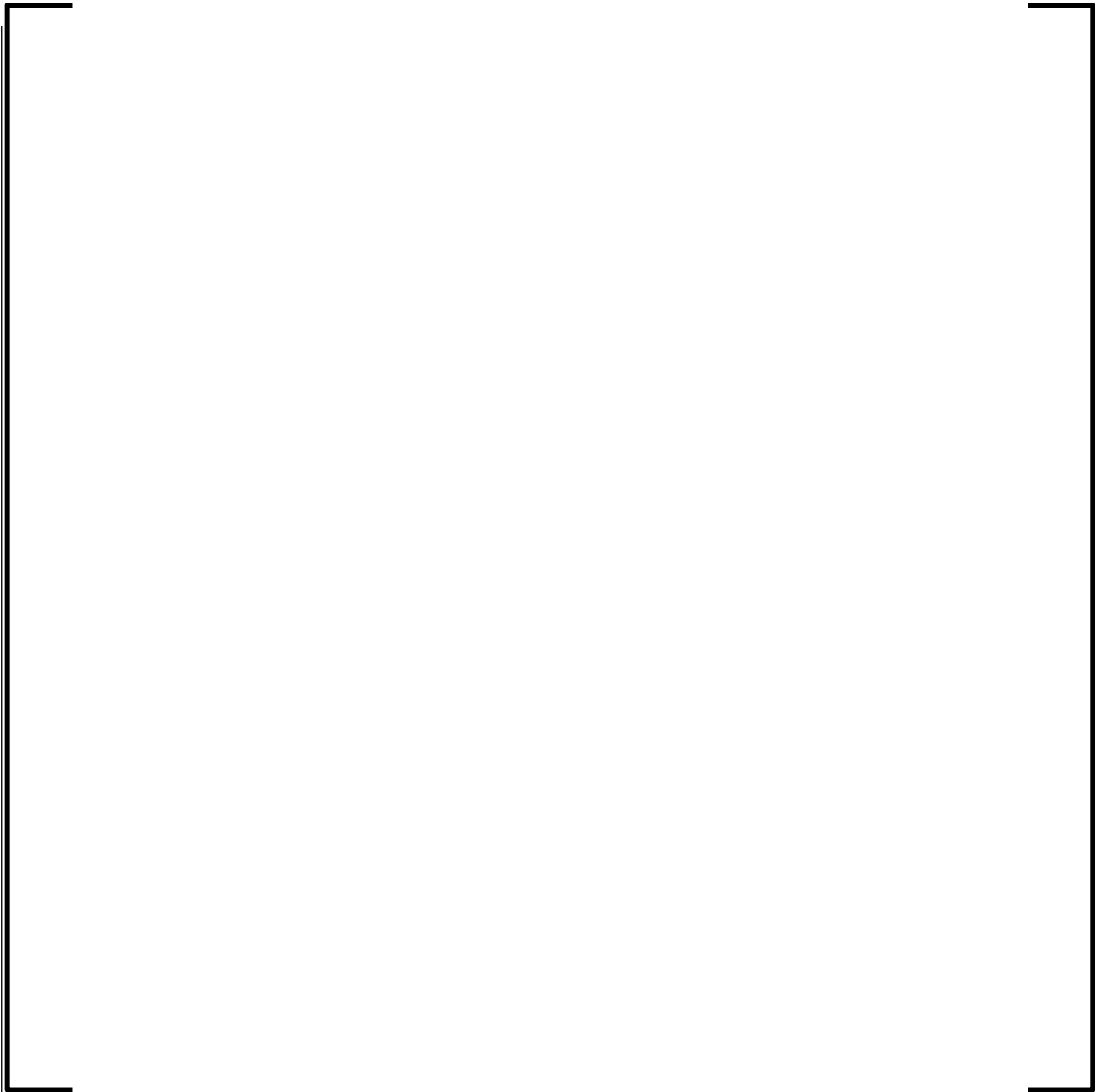
AREVA NP Inc.

Applicability of AREVA NP Containment Response Evaluation Methodology to the
U.S. EPR™ for Large Break LOCA Analysis
Technical Report

ANP-10299NP
Revision 2

Page 12-50

AREVA NP Inc.

ANP-10299NP

Applicability of AREVA NP Containment Response Evaluation Methodology to the

Revision 2

U.S. EPR™ for Large Break LOCA Analysis

Technical Report

Page 12-52

The AS model Pi groups for the blowdown and pre-hot leg injection phases are summarized in Table 12-8.

Table 12-8—AS Model Pi Groups for the Blowdown and Pre-HL Injection Phases

Pi Group	Algebraic Expression	Definition
$\Pi_{7,1}$		
$\Pi_{7,2}$		
$\Pi_{7,3}$		
$\Pi_{7,4}$		
$\Pi_{7,5}$		
$\Pi_{7,6}$		
$\Pi_{7,7}$		
$\Pi_{7,8}$		
$\Pi_{7,9}$		

Pi Group	Algebraic Expression	Definition
$\Pi_{7,10}$		
$\Pi_{7,11}$		
$\Pi_{7,12}$		
$\Pi_{7,13}$		
$\Pi_{7,14}$		

12.4.7.3   AS Internal Structure Heat Transfer Model

AREVA NP Inc.

ANP-10299NP

Applicability of AREVA NP Containment Response Evaluation Methodology to the

Revision 2

U.S. EPR™ for Large Break LOCA Analysis

Technical Report

Page 12-56
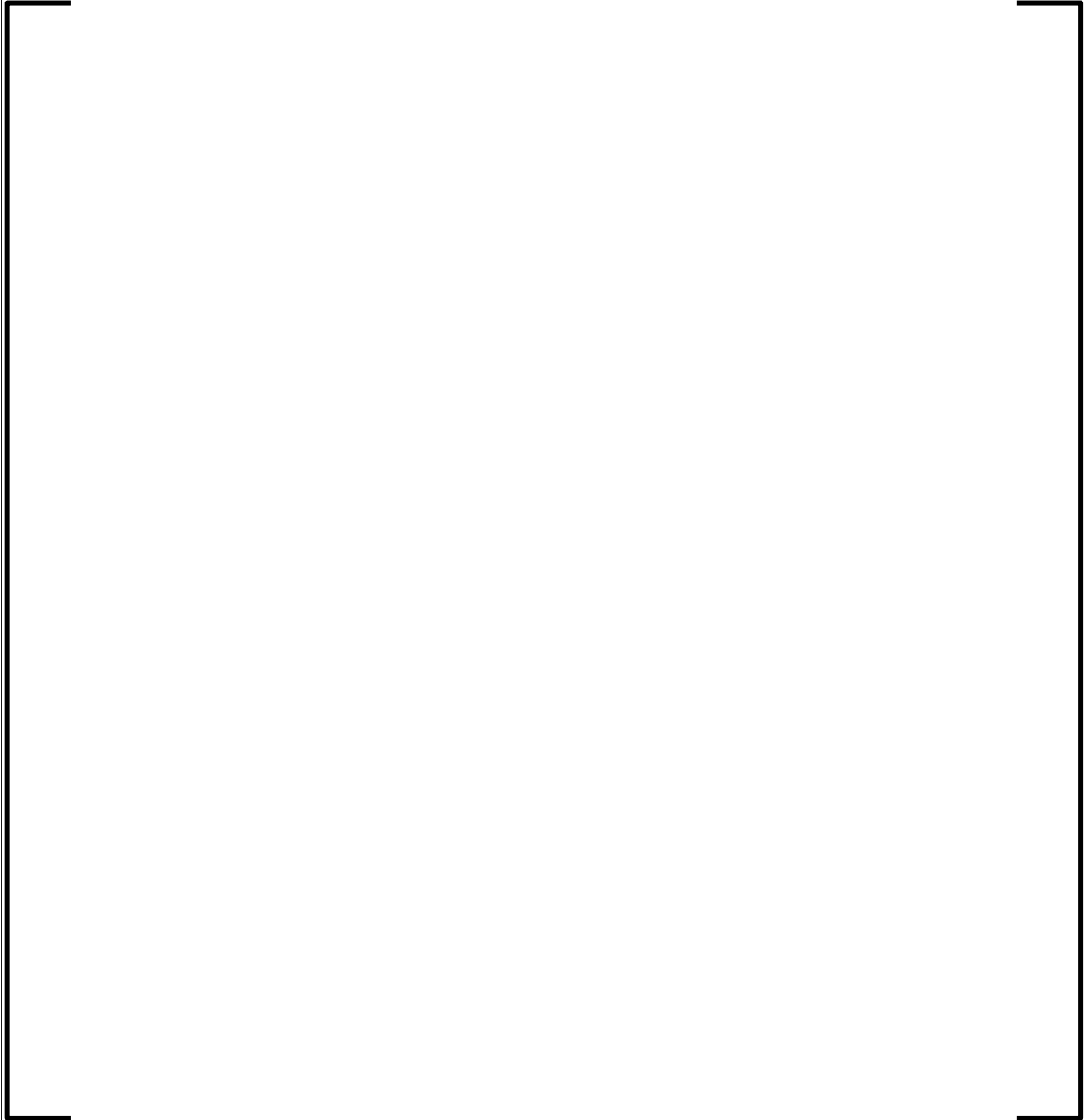
12.4.7.4   AS Containment Wall Heat Transfer Model

The AS containment wall (component #10) heat transfer conduction equation, assuming an adiabatic boundary condition, is given by:

AREVA NP Inc. ANP-10299NP

Applicability of AREVA NP Containment Response Evaluation Methodology to the Revision 2
U.S. EPR™ for Large Break LOCA Analysis
Technical Report Page 12-57
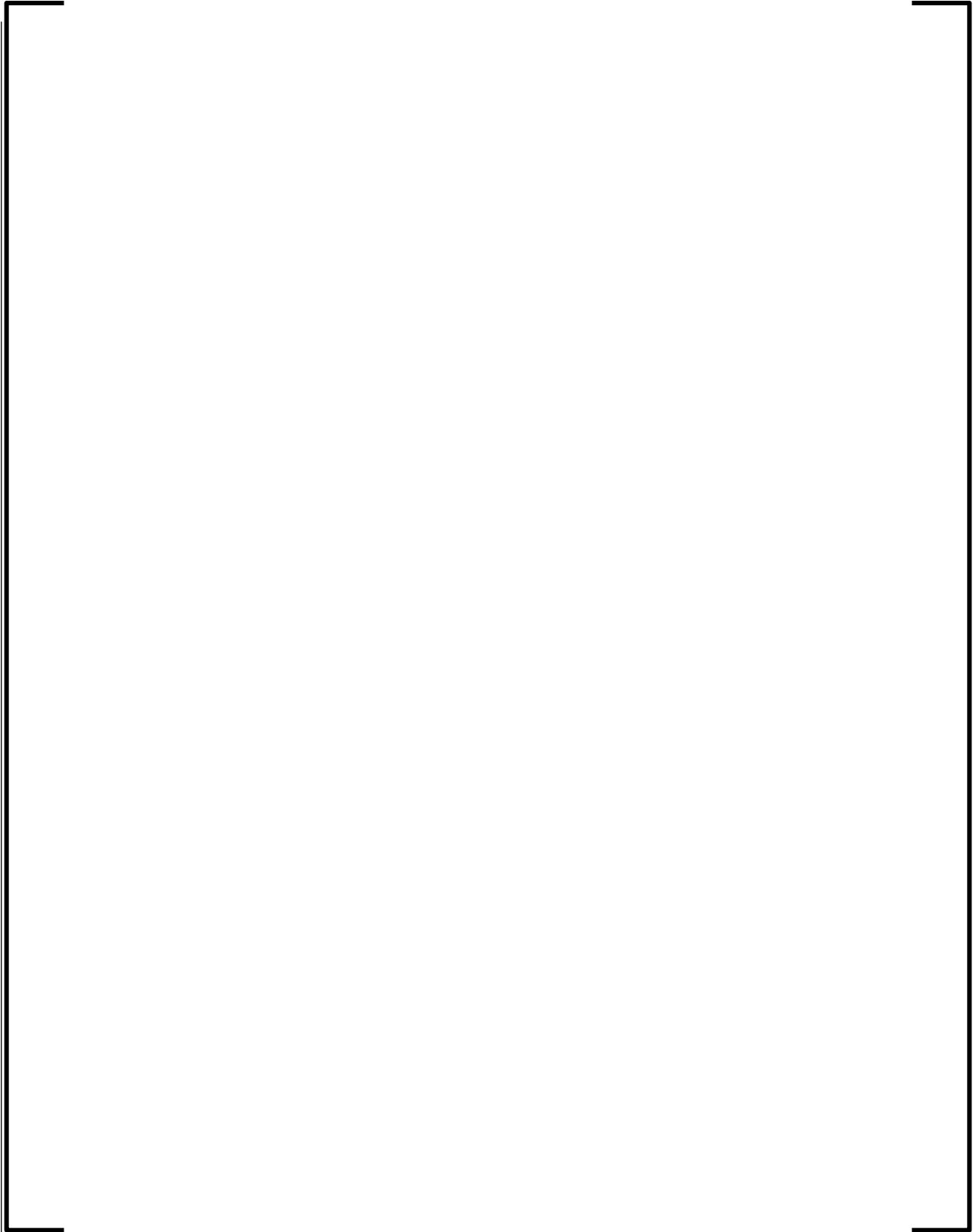
The AS containment wall model Pi groups are summarized in Table 12-9.

Table 12-9—Pi Groups for the AS Containment Wall Model

Pi Group	Algebraic Expression	Definition
$\Pi_{6,1}$		

Pi Group	Algebraic Expression	Definition
$\Pi_{10,1}$		

12.4.8   Containment Scaling Model for Post-HL Injection Phase

The ER and AS mass and energy conservation equations for the Post-HL Injection phase are derived in the following sections.

12.4.8.1   Assumptions

Additional assumptions for the long-term cooling phase are:

12.4.8.2   EB/AS Loop Momentum Model for Post-HL Injection Phase

12.4.8.3   Reduced-Order ER Model for Post-HL Injection Phase

12.4.8.3.1   Reduced-Order ER Mass Conservation Equations

AREVA NP Inc.

ANP-10299NP

Applicability of AREVA NP Containment Response Evaluation Methodology to the

Revision 2

U.S. EPR™ for Large Break LOCA Analysis

Technical Report

Page 12-61

12.4.8.3.2   Reduced-Order ER Mixture Energy Conservation Equations

)

The ER model Pi groups for the post-hot leg injection phase are summarized in Table 12-10.

AREVA NP Inc.

Applicability of AREVA NP Containment Response Evaluation Methodology to the
U.S. EPR™ for Large Break LOCA Analysis

Technical Report

ANP-10299NP
Revision 2

Page 12-63

Table 12-10—ER Model Pi Groups for the Post-HL Injection Phase

Pi Group	Algebraic Expression	Definition
$\Pi_{2,1}$		
$\Pi_{2,5}$		
$\Pi_{2,6}$		
$\Pi_{2,9}$	)	
$\Pi_{2,11}$		
$\Pi_{2,12}$		

12.4.8.4   Reduced-Order AS Model for Post-HL Injection Phase

12.4.8.4.1   Reduced-Order AS Mass Conservation Equations

12.4.8.4.2   Reduced-Order AS Energy Conservation Equations

The AS model Pi groups for the post-hot leg injection phase are summarized in
Table 12-11.

AREVA NP Inc.

ANP-10299NP

Applicability of AREVA NP Containment Response Evaluation Methodology to the
U.S. EPR™ for Large Break LOCA Analysis

Revision 2

Technical Report

Page 12-66

Table 12-11—AS Model Pi Groups for the Post-HL Injection Phase

Pi Group	Algebraic Expression	Definition
$\Pi_{7,5}$		
$\Pi_{7,9}$		
$\Pi_{7,13}$		
$\Pi_{7,14}$		

12.4.8.4.3   Reduced-Order ER and AS Structure Conservation Equations

12.4.9   IRWST Scaling Model

Figure 12-2 illustrates the interactions of the IRWST component with neighboring components. The water collected in the IRWST at the bottom of the containment is pumped by the LHSI pumps through the LHSIHX heat exchangers, and injected back into the RCS.

12.4.9.1   Assumptions

The main assumptions for the IRWST water model are:

12.4.9.2   IRWST Water Volume Model for Blowdown and Pre-HL Injection Phase
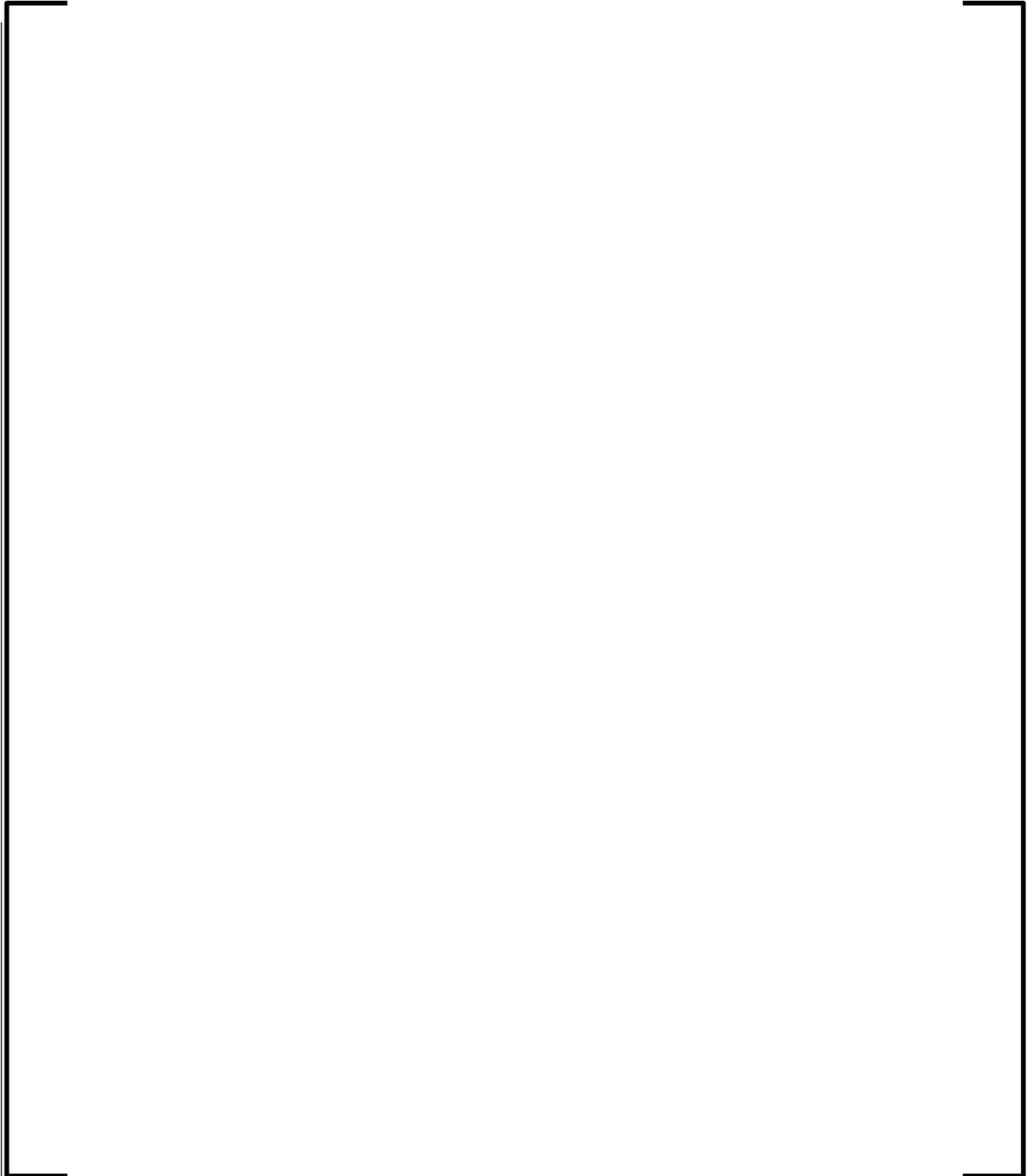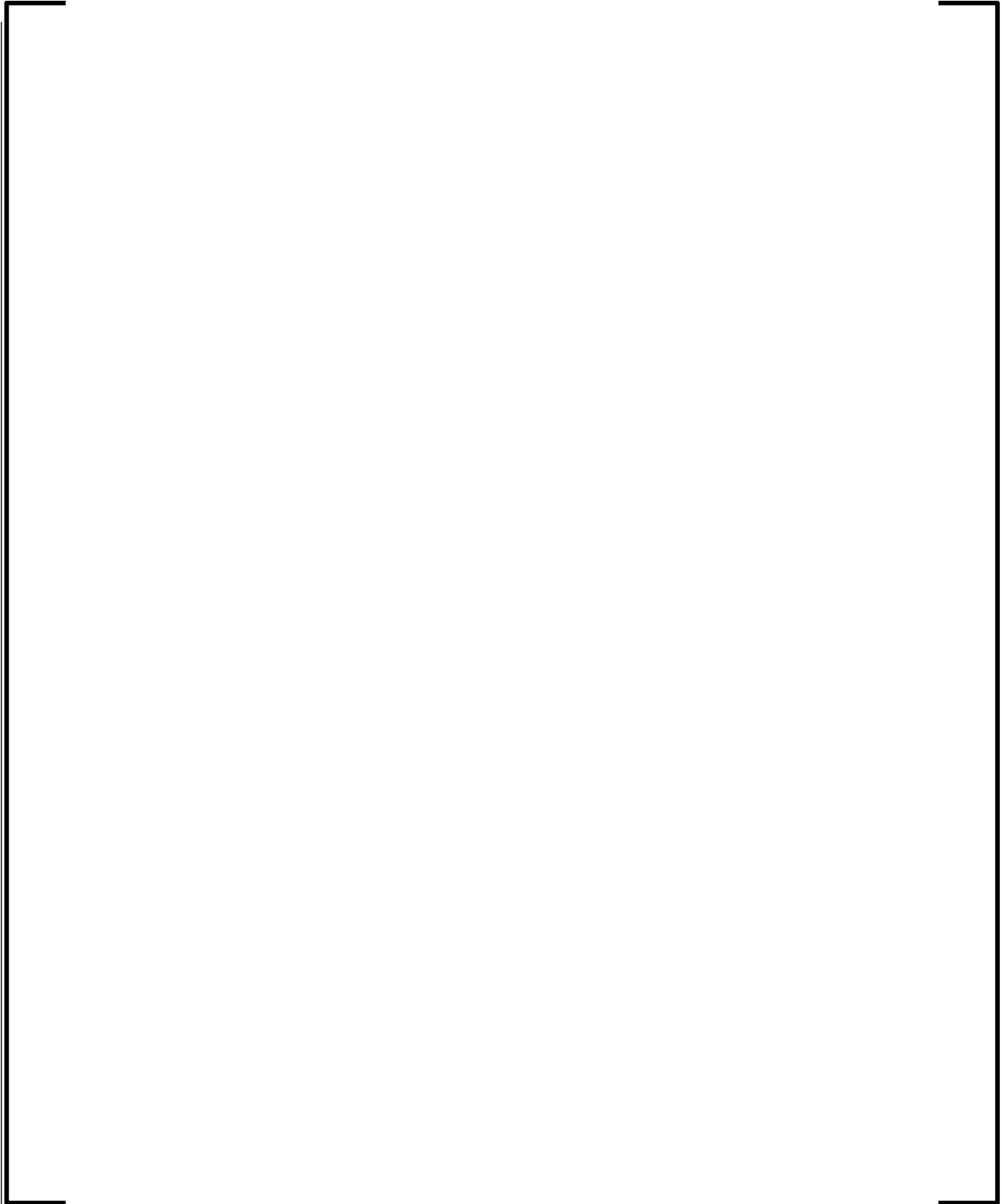
AREVA NP Inc.

Applicability of AREVA NP Containment Response Evaluation Methodology to the
U.S. EPR™ for Large Break LOCA Analysis
Technical Report

ANP-10299NP
Revision 2

Page 12-69

AREVA NP Inc.

ANP-10299NP

Applicability of AREVA NP Containment Response Evaluation Methodology to the
U.S. EPR™ for Large Break LOCA Analysis

Revision 2

Technical Report

Page 12-70

The IRWST model Pi groups for the blowdown and pre-hot leg injection phases are summarized in Table 12-12.

Table 12-12—IRWST Model Pi Groups for the Blowdown and Pre-HL Injection Phases

Pi Group	Algebraic Expression	Definition
$\Pi_{8,1}$		
$\Pi_{8,2}$		
$\Pi_{8,3}$		
$\Pi_{8,4}$		
$\Pi_{8,5}$		
$\Pi_{8,6}$		
$\Pi_{8,7}$		

Pi Group	Algebraic Expression	Definition
$\Pi_{8,8}$		
$\Pi_{8,9}$		
$\Pi_{8,10}$		

12.4.9.3   IRWST Model for Post-HL Injection Phase

)

The IRWST model Pi groups for the post-hot leg injection phase are developed analogously to Section 12.4.9.2 in Table 12-13.

Table 12-13—IRWST Model Pi Groups for the Post-HL Injection Phase

Pi Group	Algebraic Expression	Definition
$\Pi_{8,1}$		
$\Pi_{8,6}$		
$\Pi_{8,9}$		
$\Pi_{8,10}$		

12.4.9.4   IRWST Containment Wall Heat Transfer Model

The IRWST containment wall (component #14) heat transfer conduction equation, assuming it is in contact with the IRWST water only and at the adiabatic boundary condition, is given by:

AREVA NP Inc.   ANP-10299NP
Applicability of AREVA NP Containment Response Evaluation Methodology to the Revision 2
U.S. EPR™ for Large Break LOCA Analysis
Technical Report   Page 12-74

–
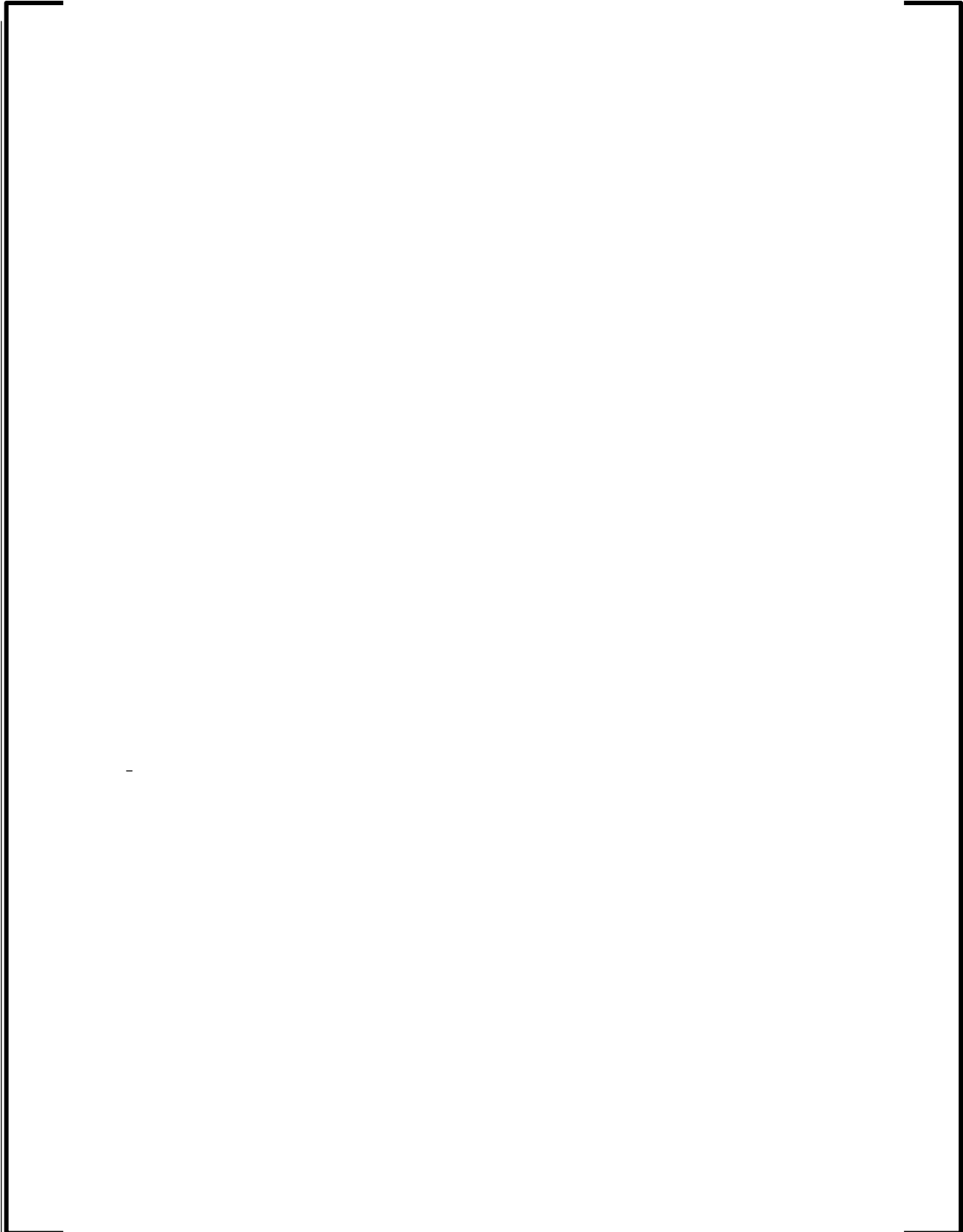
The IRWST model Pi groups for containment wall heat transfer model are summarized in Table 12-14.

Table 12-14— IRWST Pi Groups for the Containment Wall Heat Transfer Model

Pi Group	Algebraic Expression	Definition
$\Pi_{14,1}$		

12.5   U.S. EPR LBLOCA Containment PIRT Ranking Validations and Reconciliations

12.5.1   Selection of Reference Parameters
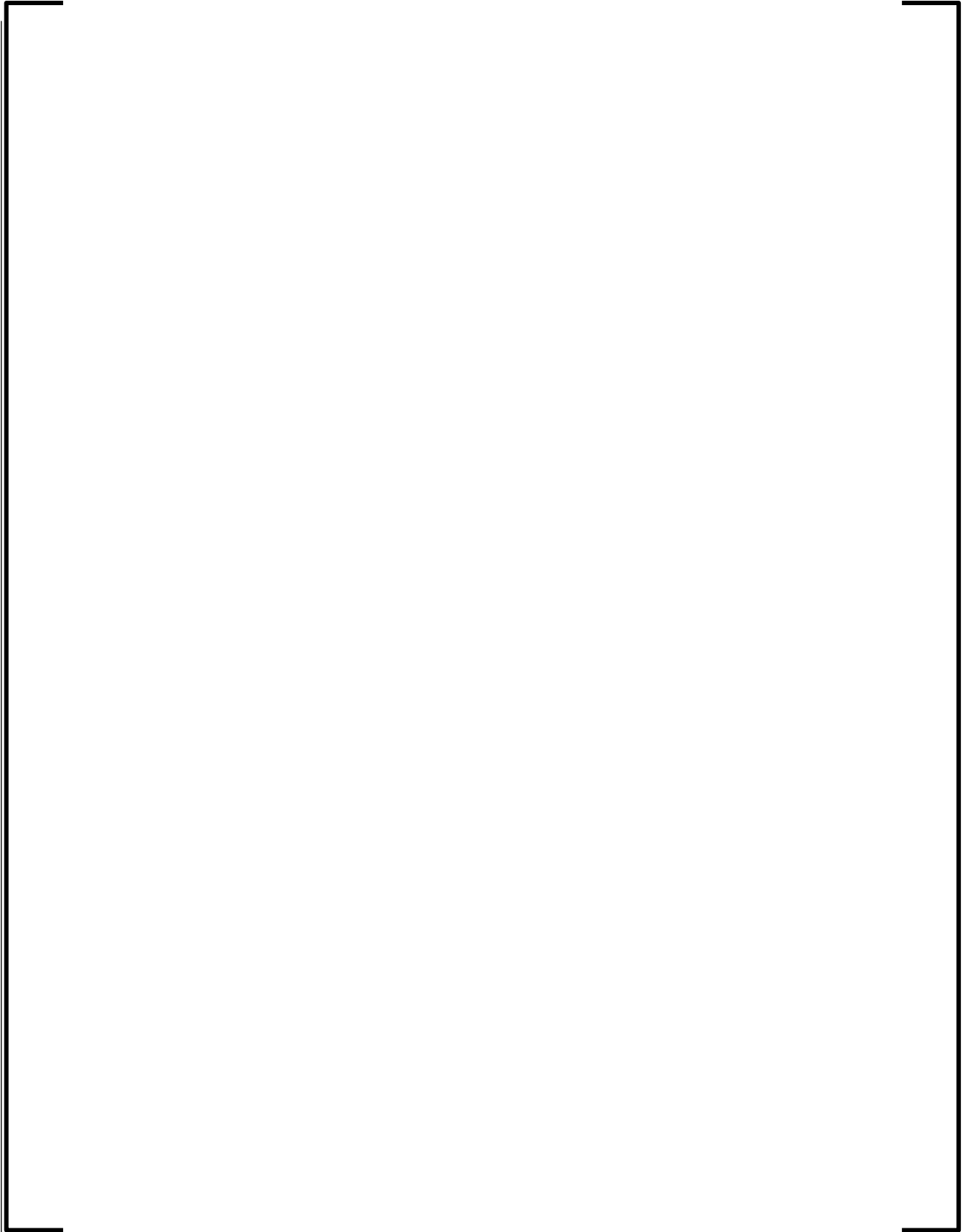
12.5.1.1   RCS Component Pi Group Rankings

12.5.1.2   ER Component Pi Group Rankings

Table 12-15—U.S. EPR RCS Component Pi Group Rankings

Pi Group	Relevant PIRT Parameter	Blowdown Value	Blowdown Ranking	Pre-HLInj Value	Pre-HL Inj Ranking	Post-HL Inj Value	Post-HL Inj Ranking
$\Pi_{1,1}$							
$\Pi_{1,2}$							
$\Pi_{1,3}$							
$\Pi_{1,4}$							
$\Pi_{1,5}$							
$\Pi_{1,6}$							
$\Pi_{1,7}$							
$\Pi_{1,8}$							

Pi Group	Relevant PIRT Parameter	Blowdown Value	Blowdown Ranking	Pre-HLInj Value	Pre-HL Inj Ranking	Post-HL Inj Value	Post-HL Inj Ranking
$\Pi_{1,9}$							
$\Pi_{1,11}$							
$\Pi_{1,12}$							
$\Pi_{1,13}$							
$\Pi_{1,14}$							

Table 12-16—U.S. EPR ER Component Pi Group Rankings

Pi Group	Relevant PIRT Parameter	PIRT Ranking	Reconciled PIRT Ranking (B/Pre/Post)	Blow-down Value	Blow-down Ranking	Pre-HL Inj Value	Pre-HL Inj Ranking	Post-HL Inj Value	Post-HL Inj Ranking
$\Pi_{2,1}$									
$\Pi_{2,1}$									
$\Pi_{2,2}$									
$\Pi_{2,2}$									
$\Pi_{2,3}$									

---

[3] The 0.0 value is assigned due to model assumptions.

Pi Group	Relevant PIRT Parameter	PIRT Ranking	Reconciled PIRT Ranking (B/Pre/Post)	Blow-down Value	Blow-down Ranking	Pre-HL Inj Value	Pre-HL Inj Ranking	Post-HL Inj Value	Post-HL Inj Ranking
$\Pi_{2,3}$									
$\Pi_{2,4}$									
$\Pi_{2,4}$									
$\Pi_{2,5}$									
$\Pi_{2,5}$									
$\Pi_{2,6}$									
$\Pi_{2,6}$									
$\Pi_{2,7}$									
$\Pi_{2,7}$									
$\Pi_{2,8}$									
$\Pi_{2,8}$									
$\Pi_{2,9}$									
$\Pi_{2,9}$									
$\Pi_{2,10}$									
$\Pi_{2,11}$									

Pi Group	Relevant PIRT Parameter	PIRT Ranking	Reconciled PIRT Ranking (B/Pre/Post)	Blow-down Value	Blow-down Ranking	Pre-HL Inj Value	Pre-HL Inj Ranking	Post-HL Inj Value	Post-HL Inj Ranking
$\Pi_{2,11}$									
$\Pi_{2,12}$									
$\Pi_{2,12}$									
$\Pi_{2,13}$									

12.5.1.3   AS Component Pi Group Rankings

The non-dimensional Pi group values of the AS component for all three phases are

summarized in Table 12-17. [

]

Table 12-17—U.S. EPR AS Component Pi Group Rankings

Pi Group	Relevant PIRT Parameter	PIRT Ranking	Reconciled PIRT Ranking (B/Pre/Post)	Blow-down Value	Blow-down Rank-ing	Pre-HL Inj Value	Pre-HL Inj Rank-ing	Post-HLInj Value	Post-HL Inj Rank-ing
$\Pi_{7,1}$									

---

[4] The 0.0 value is assigned due to model assumptions.

Pi Group	Relevant PIRT Parameter	PIRT Ranking	Reconciled PIRT Ranking (B/Pre/Post)	Blow-down Value	Blow-down Rank-ing	Pre-HL Inj Value	Pre-HL Inj Rank-ing	Post-HLInj Value	Post-HL Inj Rank-ing
$\Pi_{7,1}$									
$\Pi_{7,2}$									
$\Pi_{7,2}$									
$\Pi_{7,3}$									
$\Pi_{7,3}$									
$\Pi_{7,4}$									
$\Pi_{7,4}$									
$\Pi_{7,5}$									
$\Pi_{7,5}$									
$\Pi_{7,6}$									
$\Pi_{7,6}$									
$\Pi_{7,7}$									
$\Pi_{7,7}$									
$\Pi_{7,8}$									
$\Pi_{7,8}$									

[5] The 0.0 value is assigned due to model assumptions.

Pi Group	Relevant PIRT Parameter	PIRT Ranking	Reconciled PIRT Ranking (B/Pre/Post)	Blow-down Value	Blow-down Rank-ing	Pre-HL Inj Value	Pre-HL Inj Rank-ing	Post-HLInj Value	Post-HL Inj Rank-ing
$\Pi_{7,9}$									
$\Pi_{7,9}$									
$\Pi_{7,10}$									
$\Pi_{7,11}$									
$\Pi_{7,12}$									
$\Pi_{7,13}$									
$\Pi_{7,13}$									
$\Pi_{7,14}$									
$\Pi_{7,14}$									

12.5.1.4   ER/AS Natural Circulation Flow Component Pi Group Rankings

The non-dimensional Pi group values of the ER/AS natural circulation flow component

for all three phases are summarized in Table 12-18. [

]

[

]

Table 12-18—U.S. EPR ER /AS Natural Circulation Flow Component Pi Group Rankings

Pi Group	Relevant PIRT Parameter	PIRT Rank-ing	Recon-ciled PIRT Ranking (B/Pre/Post)	Blow-down Value	Blow-down Rank-ing	Pre-HL Inj Value	Pre-HL Inj Rank-ing	Post-HL Inj Value	Post-HL Inj Rank-ing
$\Pi_{11,1}$									
$\Pi_{11,1}$									
$\Pi_{11,2}$									
$\Pi_{11,2}$									
$\Pi_{11,3}$									
$\Pi_{11,4}$									
$\Pi_{11,4}$									
$\Pi_{11,5}$									
$\Pi_{11,5}$									
$\Pi_{11,6}$									

---

[6] The 0.0 value is assigned due to model assumptions.

12.5.1.5 IRWST Component Pi Group Rankings

The non-dimensional Pi group values of the IRWST component for all three phases are

summarized in Table 12-19. [   ]

Table 12-19—U.S. EPR IRWST Component Pi Group Rankings

Pi Group	Relevant PIRT Parameter	PIRT Ranking	Reconciled PIRT Ranking (B/Pre/Post)	Blowdown Value	Blowdown Ranking	Pre-HL Inj Value	Pre-HL Inj Ranking	Post-HL Inj Value	Post-HL Inj Ranking
$\Pi_{8,1}$									
$\Pi_{8,2}$									
$\Pi_{8,3}$									
$\Pi_{8,4}$									
$\Pi_{8,5}$									
$\Pi_{8,6}$									
$\Pi_{8,7}$									
$\Pi_{8,8}$									
$\Pi_{8,9}$									
$\Pi_{8,10}$									

AREVA NP Inc.
ANP-10299NP
Applicability of AREVA NP Containment Response Evaluation Methodology to the
Revision 2
U.S. EPR™ for Large Break LOCA Analysis
Technical Report
Page 12-86

12.5.1.6   Structure Wall Components Pi Group Rankings

The non-dimensional Pi group values of the structure wall components for all three

phases are summarized in Table 12-20. [

]

Table 12-20—U.S. EPR Structure Wall Component PI Group Rankings

Pi Group	Relevant PIRT Parameter	PIRT Ranking	Recon-ciled PIRT Ranking (B/Pre/Post)	Blow-down Value	Blow-down Ranking	Pre-HL Inj Value	Pre-HL Inj Ranking	Post-HL Inj Value	Post-HL Inj Ranking
$\Pi_{4,1}$									
$\Pi_{5,1}$									
$\Pi_{6,1}$									
$\Pi_{10,1}$									
$\Pi_{14,1}$									

AREVA NP Inc.

Applicability of AREVA NP Containment Response Evaluation Methodology to the
U.S. EPR™ for Large Break LOCA Analysis
Technical Report

ANP-10299NP
Revision 2

Page 12-87

12.5.2 PIRT Reconciliation

Table 12-21—U.S. EPR PIRT Reconciliation for Containment Pressure Following an LBLOCA

Component	Process	Phenomena	Blow-down Rank	Pre-HL-Injection Rank	Post-HL Injection Rank
Atmosphere					
Structure Interior					
Structure: Surface (solid and film)					

Pool:
Interior

Pool:
Surface

12.6 Integral Effects Test (ISP-23 HDR/T31.5) Assessment and Evaluation

12.6.1 Scaling Criteria for Test Facility (HDR)

AREVA NP Inc.

Applicability of AREVA NP Containment Response Evaluation Methodology to the
U.S. EPR™ for Large Break LOCA Analysis
Technical Report

ANP-10299NP
Revision 2

Page 12-92

AREVA NP Inc.   ANP-10299NP
Applicability of AREVA NP Containment Response Evaluation Methodology to the   Revision 2
U.S. EPR™ for Large Break LOCA Analysis
Technical Report   Page 12-93
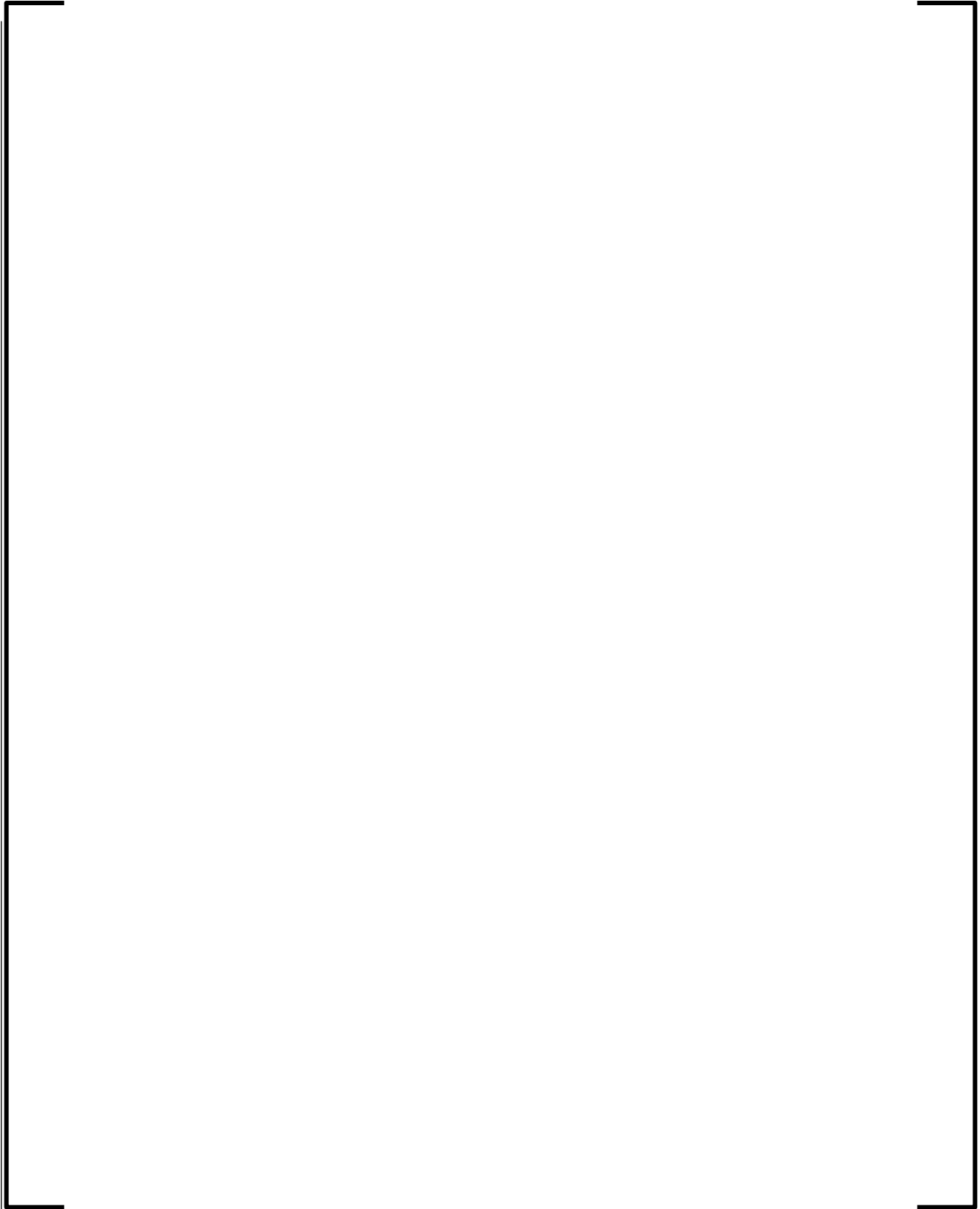
12.6.2   *IET (HDR vs. U.S. EPR) Scaling Ratio Comparisons*

Table 12-22—Scaling Ratios between HDR and U.S. EPR Design Parameters

Parameter	HDR Value	U.S. EPR Value	Ratio (HDR/ U.S. EPR)	
Primary System				
Initial pressure (pa)				
Volume (m^3)				
Break area (m^2)				
Initial core power (MW)				
Containment				
Height (m)				
Total structural mass (kg)				
Free volume (m^3)				
Structural mass/volume (kg/m^3)				
Initial pressure (pa)				
Surface area/ volume (m^{-1})				
ER				
Total structural mass (kg)				

Parameter	HDR Value	U.S. EPR Value	Ratio (HDR/ U.S. EPR)	
Free volume (m^3)				
Volume (%)				
Structural mass/volume (kg/m^3)				
Surface area (m^2)				
Surface area/ volume (m^{-1})				
AS				
Total structural mass (kg)				
Free volume (m^3)				
Volume (%)				
Structural mass/volume (kg/m^3)				
Surface area (m^2)				
Surface area/ volume (m^{-1})				

12.6.3   Evaluation of Impact of HDR IET Distortions Based on Figure of Merit

The figure of merit of the IET is containment pressure response. The relevant phenomena associated with the U.S. EPR containment pressure have been identified and qualified by the PIRT and are presented in Table 12-21.

The Pi groups were evaluated using GOTHIC results for both the HDR and U.S. EPR models. The results of the distortion analysis are presented in this section.
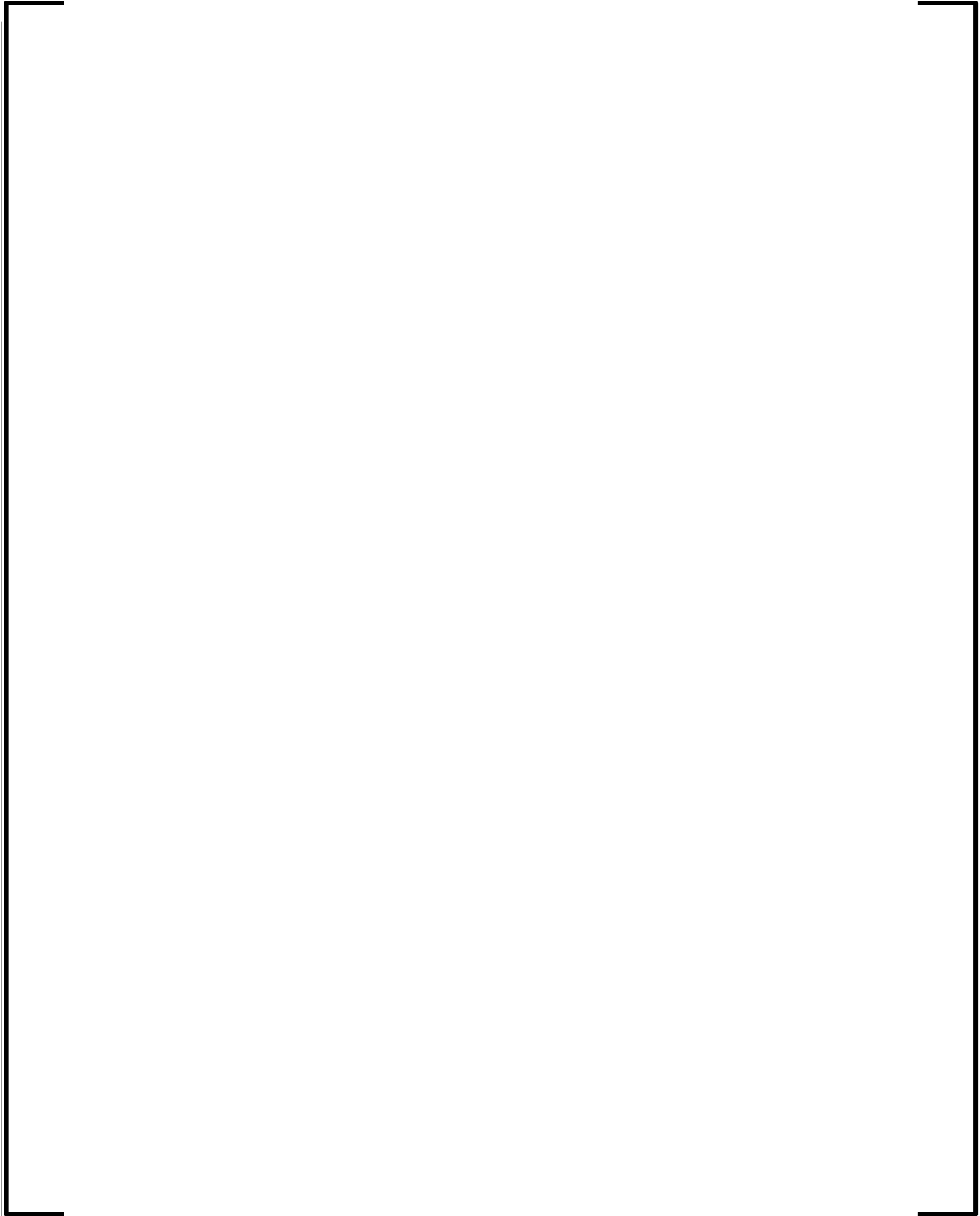
12.6.3.1   HDR Test Distortion Analysis (Blowdown Phase)

12.6.3.2   RCS Component Distortion Analysis

Figure 12-6—RCS Component PI Groups Comparisons (Blowdown)

Table 12-23—RCS Component PI Groups and Distortions (Blowdown)

∏ Values for the Blowdown Phase RCS Pressure						
∏	U.S. EPR	Importance	HDR	Importance	DF	Distortion
$\prod_{1,3}$						
$\prod_{1,4}$						
$\prod_{1,5}$						
$\prod_{1,6}$						
$\prod_{1,7}$						
$\prod_{1,8}$						
$\prod_{1,9}$						

12.6.3.2.1   ER Component Distortion Analysis

Figure 12-7 shows comparisons for the ER total and steam mass Pi groups between the HDR and U.S. EPR design. The distortion levels are given in Table 12-24.

Figure 12-7—ER Total and Steam Mass PI Groups Comparisons (Blowdown)

Table 12-24—ER Total and Steam Mass PI Groups and Distortions (Blowdown)

∏ Values for the Blowdown Phase ER Total and Steam Mass							
∏	**U.S. EPR**	Import-ance	**HDR**	Import-ance	**DF**	Distor-tion	**PIRT**	Signif-icance
∏$_{2,1}$								
∏$_{2,2}$								
∏$_{2,3}$								

$\prod_{2,4}$							
$\prod_{2,5}$							
$\prod_{2,6}$							
$\prod_{2,7}$							
$\prod_{2,8}$							

Figure 12-8 shows comparisons for the ER pressure (or pressure rate of change) Pi groups between the HDR and U.S. EPR design. The distortion levels are given in Table 12-25.

Figure 12-8—ER Pressure PI Groups Comparisons (Blowdown)

Table 12-25—ER Pressure PI Groups and Distortions (Blowdown)

$\prod$ Values for the Blowdown Phase ER Pressure								
$\prod$	U.S. EPR	Import-ance	HDR	Import-ance	DF	Distor-tion	PIRT	Signif-icance
$\prod_{2,9}$								
$\prod_{2,10}$								
$\prod_{2,11}$								
$\prod_{2,12}$								
$\prod_{2,13}$								

12.6.3.2.2   ER/AS Recirculation Flow Component Distortion Analysis

Figure 12-9 shows comparisons for the ER/AS recirculation flow Pi groups between the HDR and U.S. EPR design. The distortion levels are given in Table 12-26.

AREVA NP Inc.

Applicability of AREVA NP Containment Response Evaluation Methodology to the
U.S. EPR™ for Large Break LOCA Analysis
Technical Report

ANP-10299NP
Revision 2

Page 12-101

Figure 12-9—ER/AS Recirculation Flow PI Groups Comparisons (Blowdown)

Table 12-26—ER-to-AS Recirculation Flow PI Groups and Distortions (Blowdown)

Π Values for the Blowdown Phase ER/AS Mass Recirculation Flow								
Π	**U.S. EPR**	**Import-ance**	**HDR**	**Import-ance**	**DF**	**Distor-tion**	**PIRT**	**Signif-icance**
$\Pi_{11,1}$								
$\Pi_{11,2}$								
$\Pi_{11,3}$								
$\Pi_{11,4}$								
$\Pi_{11,5}$								
$\Pi_{11,6}$								

12.6.3.2.3   AS Component Distortion Analysis

Figure 12-10 shows comparisons for the AS total and steam mass Pi groups between

the HDR and U.S. EPR design. The distortion levels are given in Table 12-27. [

]

AREVA NP Inc.

Applicability of AREVA NP Containment Response Evaluation Methodology to the
U.S. EPR™ for Large Break LOCA Analysis
Technical Report

ANP-10299NP
Revision 2

Page 12-102

Figure 12-10—AS Total and Steam Mass PI Groups Comparisons (Blowdown)

Table 12-27—AS Total and Steam Mass PI Groups and Distortions (Blowdown)

Π Values for the Blowdown Phase AS Total and Steam Mass								
Π	U.S. EPR	Import-ance	HDR	Import-ance	DF	Distor-tion	PIRT	Signif-icance
$\Pi_{7,1}$								
$\Pi_{7,2}$								
$\Pi_{7,3}$								
$\Pi_{7,4}$								
$\Pi_{7,5}$								
$\Pi_{7,6}$								
$\Pi_{7,7}$								
$\Pi_{7,8}$								

Figure 12-11 shows comparisons for the AS pressure Pi groups between the HDR and

U.S. EPR design. The distortion levels are given in Table 12-28. [

]

AREVA NP Inc.

ANP-10299NP

Applicability of AREVA NP Containment Response Evaluation Methodology to the
U.S. EPR™ for Large Break LOCA Analysis

Revision 2

Technical Report

Page 12-103

Figure 12-11—AS Pressure PI Groups Comparisons (Blowdown)

Table 12-28—AS Pressure PI Groups and Distortions (Blowdown)

$\prod$ Values for the Blowdown Phase AS Pressure								
$\prod$	U.S. EPR	Import-ance	HDR	Import-ance	DF	Distor-tion	PIRT	Signif-icance
$\prod_{7,9}$								
$\prod_{7,10}$								
$\prod_{7,11}$								
$\prod_{7,12}$								
$\prod_{7,13}$								
$\prod_{7,14}$								

12.6.3.2.4   Structure Wall Components Distortion Analysis

Figure 12-12 shows comparisons for the structure wall components Pi groups between the HDR and U.S. EPR design. The distortion levels are given in Table 12-29.

Figure 12-12—Structure Wall Components PI Groups Comparisons (Blowdown)

Table 12-29—Structure Wall Components PI Groups and Distortions (Blowdown)

$\prod$	U.S. EPR	Import-ance	HDR	Import-ance	DF	Distor-tion	PIRT	Signif-icance
$\prod_{4,1}$								
$\prod_{5,1}$								
$\prod_{6,1}$								
$\prod_{10,1}$								
$\prod_{14,1}$								

Values for the Blowdown Phase Structure

12.6.3.3   HDR Test Distortion Analysis (Pre-HL Injection Phase)

12.6.3.3.1   RCS Component Distortion Analysis

Figure 12-13 shows comparisons for the RCS component Pi groups between the HDR and U.S. EPR design. The distortion levels are given in Table 12-30.

AREVA NP Inc.   ANP-10299NP
Applicability of AREVA NP Containment Response Evaluation Methodology to the   Revision 2
U.S. EPR™ for Large Break LOCA Analysis
Technical Report   Page 12-106

Figure 12-13—RCS Component PI Groups Comparisons (Pre-HL Injection

Table 12-30—RCS Component PI Groups and Distortions (Pre-HL Injection)

$\prod$ Values for the Pre-HL Injection Phase RCS Pressure						
$\prod$	U.S. EPR	Importance	HDR	Importance	DF	Distortion
$\prod_{1,3}$						
$\prod_{1,4}$						
$\prod_{1,5}$						
$\prod_{1,6}$						
$\prod_{1,7}$						
$\prod_{1,8}$						
$\prod_{1,9}$						

12.6.3.3.2   *ER Component Distortion Analysis*

Figure 12-14 shows comparisons for the ER total gas mass balance Pi groups between the HDR and U.S. EPR design. The distortion levels are given in Table 12-31.

AREVA NP Inc.

Applicability of AREVA NP Containment Response Evaluation Methodology to the
U.S. EPR™ for Large Break LOCA Analysis

Technical Report

ANP-10299NP
Revision 2

Page 12-107

Figure 12-14—ER Total and Steam Mass PI Groups Comparisons (Pre-HL Injection)

Table 12-31—ER Total and Steam Mass PI Groups and Distortions (Pre-HL Injection)

∏ Values for the Pre-HL Injection Phase ER Total Mass							
∏	U.S. EPR	Import-ance	HDR	Import-ance	DF	Distor-tion	PIRT	Signif-icance
∏$_{2,1}$								
∏$_{2,2}$								
∏$_{2,3}$								
∏$_{2,4}$								

AREVA NP Inc.

ANP-10299NP

Applicability of AREVA NP Containment Response Evaluation Methodology to the

Revision 2

U.S. EPR™ for Large Break LOCA Analysis

Technical Report

Page 12-108

∏ Values for the Pre-HL Injection Phase ER Total Mass							
∏	U.S. EPR	Import-ance	HDR	Import-ance	DF	Distor-tion	PIRT	Signif-icance
∏$_{2,5}$								
∏$_{2,6}$								
∏$_{2,7}$								
∏$_{2,8}$								

Figure 12-15 shows comparisons for the ER energy balance Pi groups between the HDR and U.S. EPR design. The distortion levels are given in Table 12-32.

Figure 12-15—ER Energy Pi Groups Comparisons (Pre-HL Injection)

Table 12-32—ER Energy PI Groups and Distortions (Pre-HL Injection)

∏ Values for the Pre-HL Injection Phase ER Pressure							
∏	U.S. EPR	Import-ance	HDR	Import-ance	DF	Distor-tion	PIRT	Signif-icance
$\prod_{2,9}$								
$\prod_{2,10}$								
$\prod_{2,11}$								
$\prod_{2,12}$								
$\prod_{2,13}$								

12.6.3.3.3   ER/AS Recirculation Flow Component Distortion Analysis

Figure 12-16 show comparisons for the ER/AS Recirculation Flow Pi groups between the HDR and U.S. EPR design. The distortion levels are given in Table 12-33.

Figure 12-16—ER/AS Recirculation Flow PI Groups Comparisons (Pre-HL Injection)

Table 12-33—ER-to-AS Recirculation Flow PI Groups and Distortions (Pre-HL Injection)

∏ Values for the Pre-HL Injection Phase ER Mass Outflow							
∏	U.S. EPR	Import-ance	HDR	Import-ance	DF	Distor-tion	PIRT	Signif-icance
∏₁₁,₁								
∏₁₁,₂								
∏₁₁,₃								
∏₁₁,₄								
∏₁₁,₅								
∏₁₁,₆								

12.6.3.3.4   AS Component Distortion Analysis

Figure 12-17 shows comparisons for the AS total and steam mass balance Pi groups between the HDR and U.S. EPR design. The distortion levels are given in Table 12-34.

Figure 12-17—AS Total and Steam Mass PI Groups Comparisons (Pre-HL Injection)

Table 12-34—AS Total and Steam Mass PI Groups and Distortions (Pre-HL Injection)

∏ Values for the Pre-HL Injection Phase AS total and Steam Mass							
∏	U.S. EPR	Import-ance	HDR	Import-ance	DF	Distor-tion	PIRT	Signif-icance
∏$_{7,1}$								
∏$_{7,2}$								
∏$_{7,3}$								
∏$_{7,4}$								
∏$_{7,5}$								
∏$_{7,6}$								
∏$_{7,7}$								
∏$_{7,8}$								

Figure 12-18 shows comparisons for the AS pressure Pi groups between the HDR and U.S. EPR design. The distortion levels are presented in Table 12-35.
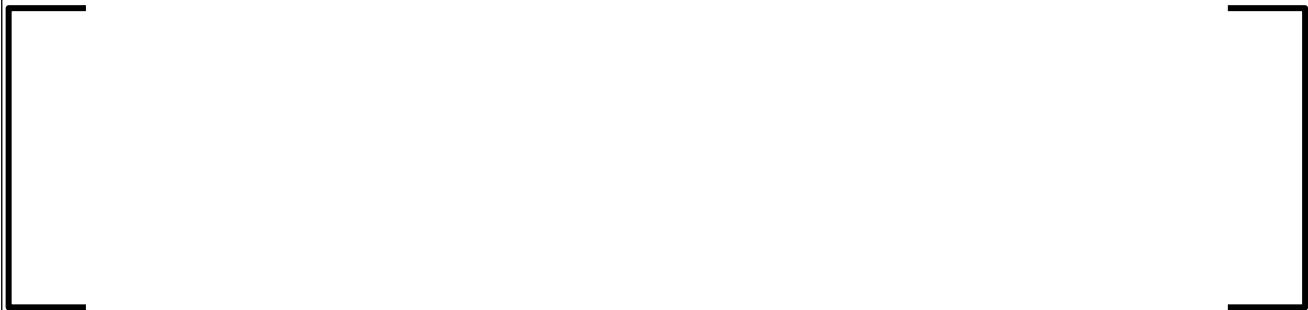
Figure 12-18—AS Pressure PI Groups Comparisons (Pre-HL Injection)

Table 12-35—AS Pressure PI Groups and Distortions (Pre-HL Injection)

∏ Values for the Pre-HL Injection Phase AS Pressure							
∏	U.S. EPR	Import-ance	HDR	Import-ance	DF	Distor-tion	PIRT	Signif-icance
∏$_{7,9}$								
∏$_{7,10}$								
∏$_{7,11}$								
∏$_{7,12}$								
∏$_{7,13}$								
∏$_{7,14}$								

12.6.3.3.5   *Structure Wall Component Distortion Analysis*

Figure 12-19 shows comparisons for the structure wall components Pi groups between the HDR and U.S. EPR design. The distortion levels are given in Table 12-36.

Figure 12-19—Structure Wall PI Groups Comparisons (Pre-HL Injection)

Table 12-36—Structure Wall PI Groups and Distortions (Pre-HL Injection)

∏	Values for the Pre-HL Injection Phase Structure							
∏	U.S. EPR	Import-ance	HDR	Import-ance	DF	Distor-tion	PIRT	Signif-icance
$\prod_{4,1}$								
$\prod_{5,1}$								
$\prod_{6,1}$								
$\prod_{10,1}$								
$\prod_{14,1}$								

12.6.3.4   HDR Test Distortion Analysis (Post-HL Injection Phase)

12.6.3.4.1   ER Component Distortion Analysis

Figure 12-20 shows comparisons for the ER pressure Pi groups between the HDR and U.S. EPR design. The distortion levels are given in Table 12-37.

AREVA NP Inc.

Applicability of AREVA NP Containment Response Evaluation Methodology to the
U.S. EPR™ for Large Break LOCA Analysis
Technical Report

ANP-10299NP
Revision 2

Page 12-115

Figure 12-20—ER Pressure PI Groups Comparisons (Post-HL Injection)

Table 12-37—ER Pressure PI Groups and Distortions (Post-HL Injection)

∏ Values for the Post-HL Injection Phase ER Pressure								
∏	U.S. EPR	Import-ance	HDR	Import-ance	DF	Distor-tion	PIRT	Signif-icance
∏2,6								
∏2,11								
∏2,12								

12.6.3.4.2   AS Component Distortion Analysis

Figure 12-21 shows comparisons for the AS pressure Pi groups between the HDR and

U.S. EPR design. The distortion levels are given in Table 12-38.

[

]

Figure 12-21—AS Pressure PI Groups Comparisons (Post-HL Injection)

Table 12-38—AS Pressure PI Groups and Distortions (Post-HL Injection)

∏ Values for the Post-HL Injection Phase AS Pressure							
∏	U.S. EPR	Import-ance	HDR	Import-ance	DF	Distor-tion	PIRT	Signif-icance
$\prod_{7,5}$								
$\prod_{7,9}$								
$\prod_{7,13}$								
$\prod_{7,14}$								

12.6.3.4.3   Structure Wall Component Distortion Analysis

Figure 12-22 shows comparisons for the structure wall Pi groups between the HDR and U.S. EPR design. The distortion levels are given in Table 12-39.

[   ]

AREVA NP Inc.

Applicability of AREVA NP Containment Response Evaluation Methodology to the
U.S. EPR™ for Large Break LOCA Analysis
Technical Report

ANP-10299NP
Revision 2

Page 12-117
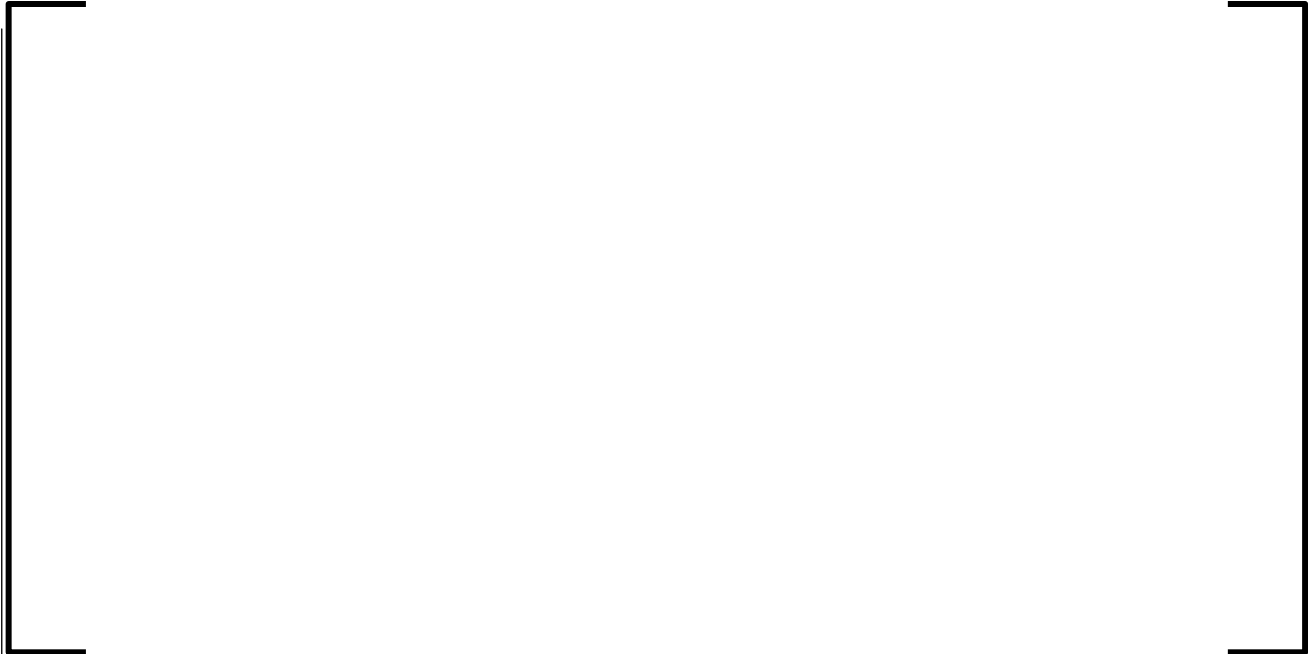
Figure 12-22—Structure Wall PI Groups Comparisons (Post-HL Injection)

Table 12-39—Structure Wall PI Groups and Distortions (Post-HL Injection)

∏ Values for the Post-HL Injection Phase Structure								
∏	U.S. EPR	Import-ance	HDR	Import-ance	DF	Distor-tion	PIRT	Signif-icance
∏5,1								
∏6,1								
∏10,1								

12.6.3.5   HDR IET Distortion Analysis Summary

Table 12-40—HDT T31.5 Distortion Significance Summary

Phase	# of Pi Groups	# High	# Medium	# Low
Blowdown				
Pre-HL Injection				
Post-HL Injection				

12.6.3.6   Figure of Merit Confirmatory Scaling Analysis

Table 12-41—Scaling Analysis Residence Time Ratio Comparisons

Phase	HDR t_0 (s)	U.S. EPR t_0 (s)	Ratio (HDR/ U.S. EPR)
Blowdown			
Pre-HL Injection			
Post-HL Injection			

12.6.3.6.1   Blowdown Phase

The non-dimensional comparisons of HDR versus U.S. EPR pressure behaviors in the ER, AS, and RCS components for the Blowdown phase are shown in Figure 12-23, Figure 12-24, and Figure 12-25, respectively.

Figure 12-23—Comparison of Non-Dimensional EB Break Room Pressure vs. Time (Blowdown)

**Figure 12-24—Comparison of Non-Dimensional AS Dome Pressure vs. Time
(Blowdown)**

**Figure 12-25—Comparison of Non-Dimensional RCS Pressure vs. Time
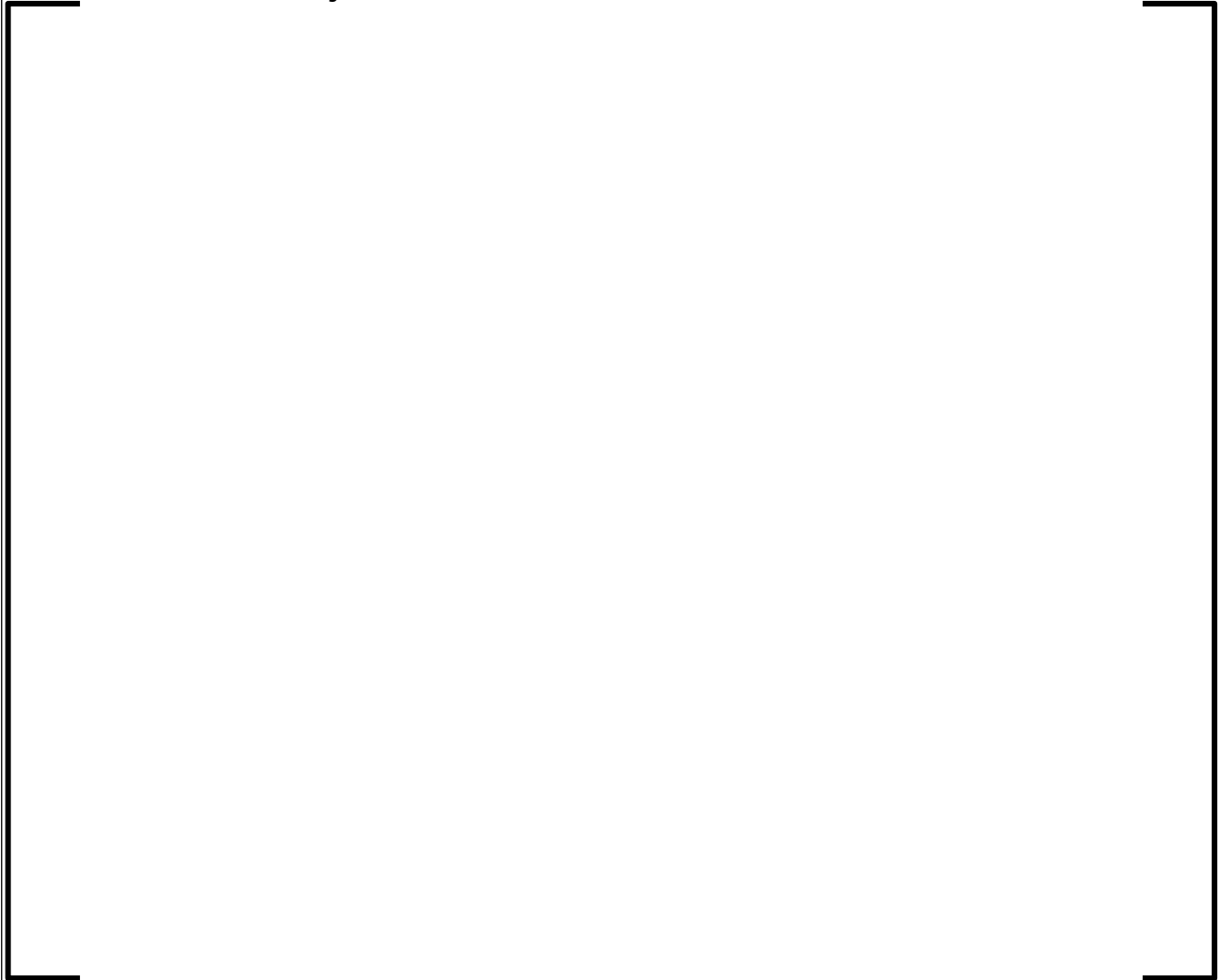(Blowdown)**

12.6.3.6.2   Pre-HL Injection Phase

Figure 12-26—Comparison of Non-Dimensional AS Dome Pressure vs. Time (Pre-HL Injection)

12.6.3.6.3   Post-HL Injection Phase

Figure 12-27—Comparison of Non-Dimensional AS Dome Pressure vs. Time

(Post-HL-Injection)

12.7   APPENDIX B REFERENCES

12.1.   S. Banerjee, M.G. Ortiz, T.K. Larson, and D.L. Reeder, "Top-Down Scaling Analyses Methodology for AP600 Integral Tests," INEL-96/0040, Lockheed Martin, May 1997.

12.2.   S. Banerjee, M.G. Ortiz, T.K. Larson, D.L. Reeder, "Scaling in the Safety of Next Generation Reactors," Nuclear Engineering and Design, **186** (1998) 111–133.

12.3.   N. Zuber, et al., "An Integrated Structure and Scaling Methodology for Severe Accident Technical Issue Resolution: Development of Methodology," Nuclear Engineering and Design, **186** (1998) 1-21.

12.4.   OECD/NEA Group of Experts, "SOAR on Containment Thermal-Hydraulics and Hydrogen Distribution," NEA/CSNI(1999)(16), 1999.

12.5.   J. Hawkins, Engineering Thermodynamics, John Wiley & Sons, 1960.

12.6.   M.J. Moran and H.N. Shapiro, Fundamentals of Engineering Thermodynamics, 5th Ed., John Wiley & Sons, 2004.

12.7.   D.P. Jordan and M.D. Mintz, Air Tables, McGraw-Hill, 1965.

AREVA NP Inc.

Applicability of AREVA NP Containment Response Evaluation Methodology to the
U.S. EPR™ for Large Break LOCA Analysis
Technical Report

ANP-10299NP
Revision 2

Page 12-124

12.8. H.M. Kim and M.L. Corradini, "Modeling of Condensation Heat Transfer in Reactor Containment," Nuclear Engineering and Design, 118, (1990) 193-211.

12.9. EPRI, "GOTHIC Containment Analysis Package Technical Manual," Version 7.2b(QA), NAI 8907-06 Rev 17, March 2009.

12.10. J. N. Reyes Jr. and L. Hochreiter, "Scaling Analysis for the OSU AP600 Test Facility (APEX)," Nuclear Engineering and Design 186 (1998) 53-109.

12.11. CSNI, "CSNI International Standard Problems (ISP) Brief Descriptions (1975-1999),"NEA/CSNI/R(2005), March 2000.

12.12. W. Wulf, U.S. Rohatgi, "System Scaling for the Westinghouse AP600 Pressurized Water Reactor and Related Test Facilities," NUREG/CR-5541, January 1998.

13.0   APPENDIX C – DEVELOPMENT OF THE DYNAMIC PRESSURE EQUATION

Figure 13-1 depicts the single-node control volume of the RCS model (component #1). As shown, no work is done on or by the system, energy is convected in and out of the system across its boundaries, and heat is also transferred in and out across the system through its boundaries. E, the total energy content of this system, is the sum of its kinetic energy, potential energy, and internal energy (Reference 13.1, Appendix A).

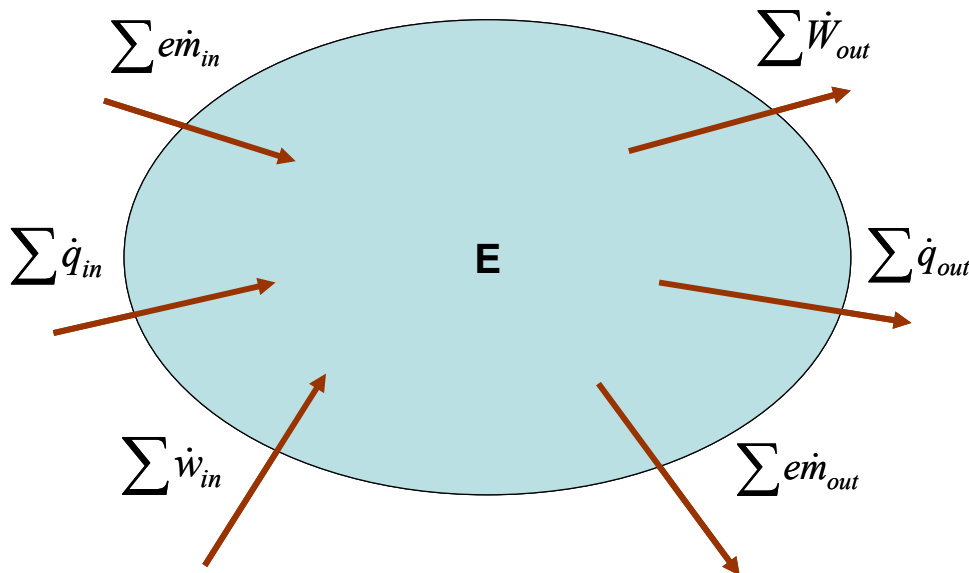**Figure 13-1—RCS Lumped Parameter Model**

Defining ε as the energy per unit mass in the system, and the system's mass is M, then:

$$E = \varepsilon M \tag{13.1}$$

It follows that

$$\varepsilon \equiv \frac{u^2}{2} + gz + \mu \tag{13.2}$$

Mass flows across system boundaries carry energy in the convected mass and carry energy by flow work. The energy transferred due to mass flow across a boundary is:

$$\dot{m}(\varepsilon + pv) = \dot{m}\left(\frac{u^2}{2} + gz + \mu + pv\right)$$ (13.3)

The last two terms inside the parenthesis on the right are the definition of enthalpy, h:

$$h = \mu + pv$$ (13.4)

Substituting Eq. (13.4) into Eq. (13.3) yields an expression for the energy convected per unit mass, e

$$e = h + \frac{u^2}{2} + gz$$ (13.5)

With the definitions above, an energy balance on the control volume is:

$$\frac{dE}{dt} = \left(\sum \dot{W}_{in} - \sum \dot{W}_{out}\right) + \left(\sum \dot{q}_{in} - \sum \dot{q}_{out}\right) + \left(\sum e\dot{m}_{in} - \sum e\dot{m}_{out}\right)$$ (13.6)

A mass balance on the same control volume yields:

$$\frac{dM}{dt} = \sum \dot{m}_{in} - \sum \dot{m}_{out}$$ (13.7)

A state equation for the control volume can now be written, wherein the pressure is a function of the specific internal energy and the specific volume:

$$p = p(\mu, v) \equiv p\left(\frac{U}{M}, \frac{V}{M}\right)$$ (13.8)

Equation (13.8) can be differentiated with time to get Eq. (13.9), below

$$\frac{dp}{dt} = \frac{\partial p}{\partial \mu}\bigg|_v \frac{d\mu}{dt} + \frac{\partial p}{\partial v}\bigg|_\mu \frac{dv}{dt}$$ (13.9)

or

AREVA NP Inc.

ANP-10299NP

Applicability of AREVA NP Containment Response Evaluation Methodology to the

Revision 2

U.S. EPR™ for Large Break LOCA Analysis

Technical Report

Page 13-3

$$\frac{dp}{dt} = \frac{\partial p}{\partial\left(\frac{U}{M}\right)}\Bigg|_{\left(\frac{V}{M}\right)} \frac{d\left(\frac{U}{M}\right)}{dt} + \frac{\partial p}{\partial\left(\frac{V}{M}\right)}\Bigg|_{\left(\frac{U}{M}\right)} \frac{d\left(\frac{V}{M}\right)}{dt} \qquad (13.10)$$

The following working assumptions can now be introduced:

1. The control volume is fixed

2. Thermodynamic equilibrium is assumed

3. No work is done on or by the system

4. Kinetic and potential energy changes are negligible

5. The control volume is filled with a homogeneous and saturated mixture

6. Outflows have control volume properties

7. No energy is generated in the control volume (though net heat flow occurs)

Based on assumption #4, the total energy in the control volume is:

$$E \approx U \text{ and } \varepsilon M = \mu M \qquad (13.11)$$

Differentiating Eq. (13.11) with respect to time yields:

$$\frac{dE}{dt} = \frac{d(\mu M)}{dt} = \mu\frac{dM}{dt} + M\frac{d\mu}{dt} \qquad (13.12)$$

Substitute Eq. (13.7) into (13.12) to obtain:

$$\frac{dE}{dt} = \frac{d(\mu M)}{dt} = \mu\left(\sum \dot{m}_{in} - \sum \dot{m}_{out}\right) + M\frac{d\mu}{dt} \qquad (13.13)$$

Substituting Eq. (13.13) in the energy balance Eq. (13.6) and using assumption #3:

$$\left(\sum \dot{q}_{in} - \sum \dot{q}_{out}\right) + \left(\sum e\dot{m}_{in} - \sum e\dot{m}_{out}\right) = \mu\left(\sum \dot{m}_{in} - \sum \dot{m}_{out}\right) + M\frac{d\mu}{dt} \qquad (13.14)$$

Collecting terms:

AREVA NP Inc.
Applicability of AREVA NP Containment Response Evaluation Methodology to the
U.S. EPR™ for Large Break LOCA Analysis
Technical Report

ANP-10299NP
Revision 2

Page 13-4

$$M \frac{d\mu}{dt} = \left(\sum \dot{q}_{in} - \sum \dot{q}_{out} \right) + \sum \dot{m}_{in} \left(e_{in} - \mu \right) - \sum \dot{m}_{out} \left(e_{out} - \mu \right) \tag{13.15}$$

Equation (13.9) can be rearranged to get an expression for $\frac{d\mu}{dt}$:

$$\frac{d\mu}{dt} = \left[\frac{dp}{dt} - \left. \frac{\partial p}{\partial v} \right|_{\mu} \frac{dv}{dt} \right] \left(\frac{1}{\left. \frac{\partial p}{\partial \mu} \right|_{v}} \right) \tag{13.16}$$

Substitute Eq. (13.16) into Eq. (13.15) to obtain:

$$\left[\frac{dp}{dt} - \left. \frac{\partial p}{\partial v} \right|_{\mu} \frac{dv}{dt} \right] \left(\frac{M}{\left. \frac{\partial p}{\partial \mu} \right|_{v}} \right) = \left(\sum \dot{q}_{in} - \sum \dot{q}_{out} \right) + \sum \dot{m}_{in} \left(e_{in} - \mu \right) - \sum \dot{m}_{out} \left(e_{out} - \mu \right) \tag{13.17}$$

Solving for the pressure rate term yields:

$$\frac{dp}{dt} = \left(\frac{\left. \frac{\partial p}{\partial \mu} \right|_{v}}{M} \right) \left[\left(\sum \dot{q}_{in} - \sum \dot{q}_{out} \right) + \sum \dot{m}_{in} \left(e_{in} - \mu \right) - \sum \dot{m}_{out} \left(e_{out} - \mu \right) \right] + \left. \frac{\partial p}{\partial v} \right|_{\mu} \frac{dv}{dt} \tag{13.18}$$

Expanding the specific volume differential in the last term of Eq.(13.18) yields:

$$\frac{dv}{dt} = \frac{d\left(\frac{V}{M} \right)}{dt} = \frac{1}{M} \frac{dV}{dt} - \frac{V}{M^2} \frac{dM}{dt} \tag{13.19}$$

$$\frac{dv}{dt} = \frac{1}{M} \frac{dV}{dt} - \frac{v}{M} \frac{dM}{dt} \tag{13.20}$$

Since the volume is fixed:

AREVA NP Inc.
ANP-10299NP
Applicability of AREVA NP Containment Response Evaluation Methodology to the
Revision 2
U.S. EPR™ for Large Break LOCA Analysis
Technical Report
Page 13-5

$$\frac{dv}{dt} = -\frac{v}{M}\left(\sum \dot{m}_{in} - \sum \dot{m}_{out}\right) \tag{13.21}$$

Define $\dot{q}_{net} = \sum \dot{q}_{in} - \sum \dot{q}_{out}$ and substitute Eq. (13.21) into Eq. (13.20) to obtain:

$$\frac{dp}{dt} = \frac{1}{M}\frac{\partial p}{\partial \mu}\bigg|_{v}\left[\dot{q}_{net} + \sum \dot{m}_{in}\left(e_{in} - \mu\right) - \sum \dot{m}_{out}\left(e_{out} - \mu\right)\right] - \frac{\partial p}{\partial v}\bigg|_{\mu}\frac{v}{M}\left(\sum \dot{m}_{in} - \sum \dot{m}_{out}\right) \tag{13.22}$$

Once again, invoking assumption # 4 that kinetic and potential energy changes are negligible, and that $e \approx h$, Eq. (13.22) becomes Eq. 13.23:

$$\frac{dp}{dt} = \frac{1}{M}\frac{\partial p}{\partial \mu}\bigg|_{v}\left[\dot{q}_{net} + \sum \dot{m}_{in}\left(h_{in} - \mu\right) - \sum \dot{m}_{out}\left(h_{out} - \mu\right)\right] - \frac{\partial p}{\partial v}\bigg|_{\mu}\frac{v}{M}\left(\sum \dot{m}_{in} - \sum \dot{m}_{out}\right) \tag{13.23}$$

The expression above contains the derivative of pressure with respect to internal energy at constant specific volume, and the derivative of pressure with respect to specific volume at constant internal energy. Since the interest is in a saturated mix, it is convenient to write the derivative of pressure with respect to specific volume at constant specific internal energy in terms of the derivative of pressure with respect to specific internal energy at constant specific volume using the triple product rule, or:

$$\frac{\partial p}{\partial v}\bigg|_{\mu} = \frac{-\dfrac{\partial p}{\partial \mu}\bigg|_{v}}{\dfrac{\partial v}{\partial \mu}\bigg|_{p}} \tag{13.24}$$

The specific internal energy and volume can be defined in terms of the equilibrium quality as:

$$\left.\begin{array}{l}\mu = \mu_f + x\mu_{fg} \\ v = v_f + xv_{fg}\end{array}\right\} \tag{13.25}$$

Using these relations in Eq. (13.25), the specific internal energy can be written as:

AREVA NP Inc.

Applicability of AREVA NP Containment Response Evaluation Methodology to the
U.S. EPR™ for Large Break LOCA Analysis
Technical Report

ANP-10299NP
Revision 2

Page 13-6

$$\mu = \mu_f + \left(v - v_f\right)\frac{\mu_{fg}}{v_{fg}} \tag{13.26}$$

Along the saturation line, μ_f, v_f, μ_{fg} and v_{fg} are functions of pressure only, so that the derivative of Eq. (13.26), with respect to specific volume at constant pressure yields:

$$\left.\frac{\partial \mu}{\partial v}\right|_p = \left.\frac{\partial \mu_f}{\partial v}\right|_p + \left.\frac{\partial \left(v \dfrac{\mu_{fg}}{v_{fg}}\right)}{\partial v}\right|_p - \left.\frac{\partial \left(v_f \dfrac{\mu_{fg}}{v_{fg}}\right)}{\partial v}\right|_p = \frac{\mu_{fg}}{v_{fg}}\left.\frac{\partial v}{\partial v}\right|_p = \frac{\mu_{fg}}{v_{fg}} \tag{13.27}$$

Substitute Eqs. (13.24) and (13.27) into Eq. (13.23), and regroup terms to obtain:

$$\frac{dp}{dt} = \frac{1}{M}\frac{1}{\left.\dfrac{\partial \mu}{\partial p}\right|_v}\left[\sum \dot{m}_{in}\left(h_{in} - \mu + v\frac{\mu_{fg}}{v_{fg}}\right) - \sum \dot{m}_{out}\left(h_{out} - \mu + v\frac{\mu_{fg}}{v_{fg}}\right) + \dot{q}_{net}\right] \tag{13.28}$$

Reference:

13.1. S. Banerjee, M.G. Ortiz, T.K. Larson, and D.L. Reeder, "Top-Down Scaling Analyses Methodology for AP600 Integral Tests," INEL-96/0040, Lockheed Martin, May 1997.